

# **Book of Abstracts**

## **14<sup>th</sup> International Conference Advanced Carbon Nanostructures ACNS'2019**

July 1-5, 2019

Saint-Petersburg, Russia

St. Petersburg, 2019

**Book of Abstracts of 14<sup>th</sup> International Conference  
“Advanced Carbon Nanostructures” (ACNS’2019)  
Saint-Petersburg, July 1-5, 2019**

ISBN 978-5-93634-060-4

Scientific editors: Artur Dideikin, Aleksandr Meilakhs

Layout: Larisa Zaitseva

Design: Vadim Siklitsky

## Organizers

- Ioffe Institute, St. Petersburg, Russia
- National Research Centre "Kurchatov Institute", Moscow, Russia
- Petersburg Nuclear Physics Institute named by B.P. Konstantinov of National Research Centre "Kurchatov Institute", Gatchina, Russia
- Saint-Petersburg State Institute of Technology, St. Petersburg, Russia

## Official Partners

- Fund for Infrastructure and Educational Programs, RUSNANO Group
- SOL instruments Ltd.

## International Advisory Committee

<b>Banhart F.</b>	Strasbourg University, France
<b>Cataldo F.</b>	Taylor & Francis, USA
<b>Echegoyen L.</b>	University of Texas at El Paso, USA
<b>Enoki T.</b>	Tokyo Institute of Technology, Japan
<b>Gogotsi Yu.</b>	Drexel University, USA
<b>Gruen D.</b>	Argonne National Laboratory, USA
<b>Kalish R.</b>	Israel Institute of Technology, Technion, Israel
<b>Kraetschmer W.</b>	Max-Planck Institute, Germany
<b>Murayama H.</b>	The KAITEKI Institute Inc., Japan
<b>Osawa E.</b>	Nanocarbon Research Institute Ltd., Japan
<b>Shinohara H.</b>	Nagoya University, Japan
<b>Williams O.</b>	Cardiff University, UK

## International Programme Committee

<b>Dideikin A.T.</b>	<b>Chair</b> , Ioffe Institute, St. Petersburg, Russia
<b>Meilakhs A.P.</b>	<b>Secretary</b> , Ioffe Institute, St. Petersburg, Russia
<b>Shnitov V.V.</b>	<b>Secretary</b> , Ioffe Institute, St. Petersburg, Russia
<b>Aksenov V.L.</b>	Joint Institute for Nuclear Research, Dubna, Russia
<b>Aleksensky A.E.</b>	Ioffe Institute, St. Petersburg, Russia
<b>Artjomov A.S.</b>	Prokhorov General Physics Institute, Moscow, Russia
<b>Baidakova M.V.</b>	Ioffe Institute, St. Petersburg, Russia

<b>Dolmatov V.Yu.</b>	Special Design and Technological Office "Technolog", St. Petersburg, Russia
<b>Eletskii A.V.</b>	National Research Center "Kurchatov Institute", Russia
<b>Korobov M.V.</b>	Moscow State University, Russia
<b>Kozyrev S.V.</b>	Peter the Great St. Petersburg Polytechnic University, Russia
<b>Krashennnikov A.</b>	Helmholtz-Zentrum Dresden-Rossendorf, Germany
<b>Krestinin A.V.</b>	Institute of Problems of Chemical Physics, Russia
<b>Kulakova I.I.</b>	Lomonosov Moscow State University, Russia
<b>Murin I.V.</b>	St. Petersburg State University, Russia
<b>Okotrub A.V.</b>	Nikolaev Institute of Inorganic Chemistry, Novosibirsk, Russia
<b>Piotrovskiy L.B.</b>	Institute of Experimental Medicine, St. Petersburg, Russia
<b>Shenderova O.A.</b>	Adamas Nanotechnologies, USA
<b>Shikin A.M.</b>	St. Petersburg State University, Russia
<b>Sokolov V.I.</b>	Institute of Organoelement Compounds, Moscow, Russia
<b>Titov V.M.</b>	Institute of Hydrodynamics, Novosibirsk, Russia
<b>Voznyakovskii A.P.</b>	Lebedev Research Institute for Synthetic Rubber, St. Petersburg, Russia
<b>Vul' A.Ya.</b>	Ioffe Institute, St. Petersburg, Russia

### **Organizing Committee**

<b>Vul' A.Ya.</b>	<b>Conference Chair</b> , Ioffe Institute, Russia
<b>Vorobyova I.V.</b>	<b>Secretary</b> , Ioffe Institute, Russia
<b>Chaivanov B.B.</b>	National Research Center "Kurchatov Institute", Russia
<b>Eremenko I.L.</b>	Kurnakov Institute of General and Inorganic Chemistry, Russia
<b>Kop'ev P.S.</b>	Ioffe Institute, Russia
<b>Kveder V.V.</b>	Institute of Solid State Physics, Russia
<b>Reich K.V.</b>	Ioffe Institute, Russia
<b>Sarantseva S.V.</b>	Petersburg Nuclear Physics Institute named by B.P. Konstantinov of National Research Centre "Kurchatov Institute", Russia
<b>Siklitsky V.I.</b>	Ioffe Institute, Russia
<b>Shevchik A.P.</b>	Saint-Petersburg State Institute of Technology, Russia

# **Invited Lectures**

## Dipole polarizability of fullerene compounds: Numerical estimates and their applications

*Sabirov Denis*<sup>1</sup>

*diozno@mail.ru*

<sup>1</sup> Institute of Petrochemistry and Catalysis of RAS, Ufa, Russia

As fullerenes is the only molecular form of carbon, describing their chemical behavior and related physicochemical processes demands knowledge of the molecular properties. Among the latter, we focus on their dipole polarizability ( $\alpha$ ) [1]. In this report, we generalize experimental and theoretical data on  $\alpha$  values of fullerenes and their derivatives and make a snapshot of current applications of polarizability to fullerene chemistry and materials science.

Polarizability of fullerenes and their derivatives (mainly of  $C_{60}$  and  $C_{70}$ ) has been studied with different theoretical methodologies (semiempirical methods, DFT, perturbation theory, coupled clusters theory *etc.*) and experimental techniques (ellipsometry, electron energy-loss spectroscopy, molecular beam deflection, and near-field interferometry; see, *e.g.* [2-4]). All these studies consider that fullerenes are the molecules with very high polarizability (ca. 80 and 100  $\text{\AA}^3$  for  $C_{60}$  and  $C_{70}$ , respectively). The measured  $\alpha$  values increase from the isolated molecules to fullerene clusters and solid state (fullerite) in contrast to "common" molecules. We discuss the non-coinciding size-dependences of fullerene static and dynamic polarizabilities; effect of mechanical deformations and charging of the fullerene core on  $\alpha$ ; dipole polarizability of the main classes of fullerene compounds (exohedral one-cage adducts, multi-cage compounds and endohedral complexes).

The numerical estimates of  $\alpha$  are used in the fullerene chemistry and materials science. We primarily point here the application of polarizability to anion- $\pi$  catalysis with fullerenes [5], organic photovoltaics [6], dynamics of molecules inside the fullerene cages [7], chromatographic behavior [8], theoretical astrochemistry of  $C_{60}$  [9]. These works stress the crucial role of polarizability in the mentioned processes.

The work is currently supported by the Russian Foundation for Basic Research (project number 19-03-00716).

### References

1. D. Sh. Sabirov, *RSC. Adv.* (2014) **4**, 44996.
2. C. Eklund, A. M. Rao, Y. Wang, P. Zhou, K. A. Wang, J. M. Holden, M. S. Dresselhaus, G. Dresselhaus, *Thin Solid Films* (1995) **257**, 211.
3. I. Compagnon, R. Antoine, M. Broyer, P. Dugourd, J. Lermé, D. Rayane, *Phys. Rev. A.* (2001) **64**, 025201
4. K. Hornberger, S. Gerlich, H. Ulbricht, L. Hackermüller, S. Nimmrichter, I. V. Goldt, O. Boltalina, M. Arndt, *New J. Phys.* (2009) **11**, 043032.
5. J. Lopez-Andarias, A. Bauza, N. Sakai, A. Frontera, S. Matile, *Angew. Chem.* (2018) **130**, 11049.
6. D. Sh. Sabirov, *J. Phys. Chem. C* (2016) **120**, 24667.
7. L. Liu, L. Li, Q. Zeng, *Phys. Chem. Chem. Phys.* (2017) **19**, 4751.
8. X. Liu, T. Zuo, H. C. Dorn, *J. Phys. Chem. C* (2017) **121**, 4045.
9. D. Sh. Sabirov, R. R. Garipova, F. Cataldo, *Mol. Astrophys.* (2018) **12**, 10.

## Spectroscopic insights on the nanocarbon-water interface

*Tristan Petit*<sup>1</sup>

*tristan.petit@helmholtz-berlin.de*

<sup>1</sup> Helmholtz-Zentrum Berlin fuer Materialien und Energie, Berlin, Germany

Many applications of nanocarbons, especially in medicine, biosensing and energy conversion, involves chemical and electronic processes in aqueous medium. As a result, an in-depth characterization of the nanocarbon-water interface is essential for the understanding of nanocarbon properties in aqueous environment. Probing *in situ* the nanocarbon-water interface with vibrational and electronic spectroscopies remains however an experimentally challenging task.

In this presentation, I will present our latest work on the characterization of the interface between nanodiamonds (NDs) with water using infrared and X-ray absorption spectroscopy methods. In particular, the effect of NDs surface chemistry on their hydration properties will be highlighted [1]. Infrared spectroscopy, applied during exposure of NDs to water molecules, can provide information on the changes of vibrational bonds of surface functional groups and water molecules upon adsorption on the carbon surfaces. Different water adsorption profiles are clearly observed depending on the NDs surface chemistry. *In situ* Soft X-ray absorption spectroscopy, applied directly on colloidal dispersions, can be used to selectively probe the carbon or oxygen atoms and elucidate changes upon solvation of either the NDs or water molecules electronic structure. We found that the water hydrogen bonding environment is strongly impacted by the NDs, especially when the NDs surface is hydrogenated [1,2].

Recent measurements on carbon dots will also be presented and compared to NDs [3]. Our results highlight that the surface chemistry of nanocarbons plays a significant role on their hydration properties.

### References

- [1] T. Petit, L. Puskar, T.A. Dolenko, S. Choudhury, E. Ritter, S. Burikov, K. Laptinskiy, Q. Brzustowski, U. Schade, H. Yuzawa, M. Nagasaka, N. Kosugi, M. Kurzyp, A. Venerosy, H.A. Girard, J.-C. Arnault, E. Osawa, N. Nunn, O. Shenderova, E.F. Aziz, Unusual Water Hydrogen Bond Network around Hydrogenated Nanodiamonds, *J. Phys. Chem. C*. 121 (2017) 5185–5194. doi:10.1021/acs.jpcc.7b00721.
- [2] T. Petit, H. Yuzawa, M. Nagasaka, R. Yamanoi, E. Osawa, N. Kosugi, E.F. Aziz, Probing Interfacial Water on Nanodiamonds in Colloidal Dispersion, *J. Phys. Chem. Lett.* 6 (2015). doi:10.1021/acs.jpcllett.5b00820.
- [3] J. Ren, F. Weber, F. Weigert, Y. Wang, S. Choudhury, J. Xiao, I. Lauermann, U. Resch-Genger, A. Bande, T. Petit, Influence of surface chemistry on optical, chemical and electronic properties of blue luminescent carbon dots, *Nanoscale*. 11 (2019) 2056–2064. doi:10.1039/C8NR08595A.

## Fluorescent Diamond Particles: Synthesis, Properties, and Applications

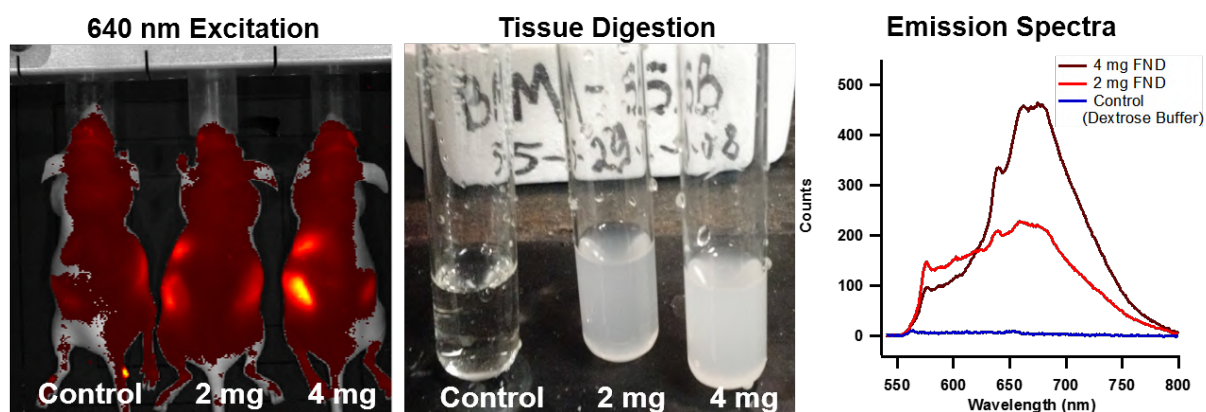
*Shenderova O.A.*<sup>1</sup>

*oshenderova@adamasnano.com*

<sup>1</sup> Adamas Nanotechnologies, Inc., Raleigh, North Carolina, USA

Diamond particles containing color centers, the crystallographic defects embedded within the diamond lattice, outperform other classes of fluorophores by providing a combination of outstanding photostability, magneto-optical properties and intrinsic biocompatibility. Within the N-related family of optical defects, the nitrogen-vacancy defect (NV) has received the greatest consideration due to numerous applications in both emerging and mature technologies: background-free and long-term cell imaging in the red/near infrared spectral region, super-resolution imaging, correlative and multiphoton microscopy. The spin properties of NV centers in nanodiamonds promise exciting applications in ultrasensitive metrology at the nanoscale detecting changes in magnetic and electric fields, temperature and pressure. A breakthrough recent discovery that <sup>13</sup>C polarization can be strongly enhanced in diamond at room temperature based on optical pumping of NV centers advocates nanodiamonds as a new paradigm for optical hyperpolarization in magnetic resonance (MRI) clinical imaging. Recently, our group succeeded in large-scale production of fluorescent diamond particles (FDP) containing NV centers in hundred-gram per batch scales using irradiation with 2-3 MeV electrons. Major factors influencing the efficiency of color centers production in diamond particles as well as compromises between brightness and particles size will be discussed. One limitation in FND production has been the narrow fluorescent color palette while one of the important requirements for fluorescent bioprobes is multicolor emission for multiplexed imaging of few markers in a single study. Our recent achievements in production of multicolor diamonds (from blue to NIR emission) will be reported as well as our efforts toward their adaptation for use in the biomedical science community will be reviewed.

Acknowledgment: NIH NHLBI SBIR Phase I and Phase II Contract HHSN268201500010C; NIH NCI Phase I SBIR grant R43CA232901.



Whole-body IVIS imaging. a) Images of three mice, administered either 0, 2, or 4 mg/mL nanodiamond in 5% dextrose buffer. (courtesy of Ashlyn Rickard, Palmer group, Department of Radiation Oncology, Duke University). b) Spleens after piranha acid digestion, showing contrast of accumulated particles. c) Bulk spectra of samples in 3 indicating dose-dependent recovery and validation of FND presence.



---

## **Lateral Diamond Nanowires with exceptionally high current density; properties and applications**

*Pakpour-tabrizi A.C.*<sup>1</sup>, *Jackman R.B.*<sup>1</sup>

*r.jackman@ucl.ac.uk*

<sup>1</sup> University College London, UK

This paper reviews recent work at UCL regarding novel nanoscale electrically addressable diamond devices. Based on extremely high-quality boron-doped diamond  $\delta$ -layers ( $\delta$ -BDD), this technology provides an exciting playground for exotic physics and traditional electronic engineering. Moreover, these NWs have great promise in the field of molecular sensing. Lateral Nano-Wires (L-BDD-NW) are defined in very thin heavily boron doped diamond epi layers. For the results reported here, the delta layer is on the surface of a [100] single crystal diamond. Electrical isolation is possible due to the very low defect and high quality 'intrinsic' CVD buffer layer grown on the HPHT substrate before the  $\delta$ -layer is grown. The resultant nanowires are some 2nm deep and 10-20nm wide, and show current densities surpassing 300A/mm<sup>2</sup>. After etching the L-BDD-NW the spatial confinement and electrical properties of the wire can be further engineered using electrostatic side and top gating. We report exceptional current densities indicative of ballistic transport and preliminary results from the first ever fabricated diamond-FinFET type device. A range of other exciting and novel device structures will be mentioned, and applications identified.

---

## **Synthesis, Structure and Novel Applications of Heteroatoms-Doped Carbon Quantum Dots**

*Bi Hong*<sup>1</sup>

*bihong@ahu.edu.cn*

<sup>1</sup> School of Chemistry and Chemical Engineering, Anhui University, Hefei, China

Carbon quantum dots (CQDs) are a new class of carbon nanomaterials with size below 10 nm, usually consisting of sp<sup>2</sup>-hybridized carbon core and an amorphous shell comprised of abundant organic groups. CQDs show various fascinating properties, such as tunable excitation/emission, high fluorescence, chemical inertness, photostability, extremely low toxicity, good biocompatibility and eco-friendliness. Due to the anomalous optical and chemical properties of the CQDs, they have a wide range of applications in the fields of bio-imaging, biosensor, photocatalysis, optoelectronics, and etc. In this presentation, I will talk about recent progress on synthesis, optical property studies and biomedical applications of heteroatoms-doped CQDs (e.g., non-metal and metal-doped CQDs) in my lab. Particularly, near infrared (NIR) fluorescence of heteroatoms-doped CQDs and their potential applications in fluorescence imaging/magnetic resonance imaging (MRI) both *in vitro* and *in vivo*, as well as photodynamic therapy (PDT) of tumors will be highlighted.

## **Sugar Chain Modified Graphene FET for High Sensitive & Selective detection of Influenza Virus**

*Matsumoto K.*<sup>1</sup>

*k-matsumoto@sanken.osaka-u.ac.jp*

<sup>1</sup> Institute of Scientific & Industrial Research, Osaka University, Osaka, Japan

The avian influenza virus and the human influenza virus are selectively detected with high sensitivity using the sugar chain functionalized graphene FET.

The avian influenza virus which can infect to human has the highly pathogenic and quite dangerous. So, we should know whether the avian virus has the human infection or not. So far, however, it takes more than one weeks to know whether the virus can infect to human or not to increase the number of the virus up to  $10^6$ . In the present study, we have succeeded in detecting the human infection within 20minutes with  $\sim 100$  virus using the high sensitive graphene FET.

The surface of the cell for human and avian is covered by the sugar chain. The structure of the sugar chain for human and avian which cover the cell has the difference at the end of their structures, i.e., for the human sugar chain, sialic acid is connected to thea2-6 galactose, and for the avian sugar chain, to the a2-3 galactose. Influenza virus recognize this structural difference and the human influenza virus connects to only to human sugar chain and avian influenza virus connects to only avian sugar chain, and there is no cross contamination. When the avian flu virus changes its structure and get the human infection, it can connect both the avian and the human sugar chains. In order to selectively detect the human infection, the surface of graphene FET was modified by the human sugar chain which can selectively combine to the human virus and not combine to avian virus.

Using the sugar chain modified graphene FET, the real human and avian influenza viruses were detected. The sugar chain modified graphene FET was in the phosphoric buffer solution and the human influenza virus was introduced. Before and after the introduction of the virus, the I-V characteristics of graphene FET was measured and the shift of the Dirac point of 32.6mV was observed. This is because the virus has a minus charge which induce the positive charge on the graphene surface and the positive current of graphene FET increases and then the Dirac point shifts to the right hand side. This means the detection of the virus using the graphene FET was succeeded in. Figure shows the selective detection of the human influenza virus. By increasing the concentration of human virus, human virus which has minus charge connects to the human sugar chain, and the shift of the Dirac point of the graphene FET increases. At the concentration of virus up to 256HAU, the shift of the Dirac point reaches as large as 44.3mV. On the other hand, avian influenza virus could not connect to the human sugar chain and does not cause the Dirac point shift. Thus, we have succeeded in the selective detection of human type and avian type influenza virus by the sugar chain modified graphene FET.

Using the sugar chain modified graphene FET, we have succeeded in selectively detects the human infective influenza virus within 20 minutes.

## Graphene-on-surfaces: structural design and multifunctional applications

Zhu H.W.<sup>1</sup>

*hongweizhu@tsinghua.edu.cn*

<sup>1</sup> School of Materials Science and Engineering, Tsinghua University, Beijing, China

Graphene has the potential for creating thin film devices, owing to its two-dimensionality and structural flatness. Assembling graphene-based building blocks into hybrid structures or composites with diverse targeted structures has attracted considerable interests for generating new properties and expanding its potential applications [1]. This presentation will focus on three "graphene-on-surfaces" hybrid structures (Fig.1) [2]: I) Graphene-on-semiconductor: Graphene-on-Si can function as a quality Schottky junction with high photoelectric conversion [3,4]. Graphene serves multiple functions as transparent electrode, active junction layer, hole collector and anti-reflection layer in graphene-on-semiconductor heterojunction photo-devices, such as solar cells and photodetectors, and could be extended to other optoelectronics; II) Graphene-on-polymer: Tiling structures are designed in graphene, composing overlapped graphene plates and realize high sensitivity strain sensing, which can measure either tiny or large strains with record high gauge factors [5]. By combining artificial intelligence with digital signal processing, the graphene based sensing system represents a new smart tool to classify and analyze signals in fields of vital signs monitoring, robotics, fatigue detection, and in vitro diagnostics; III) Graphene-on-ceramic: Graphene oxide (GO)-based membranes are developed for highly efficient ion separation and water desalination [6]. Due to the narrow dimension of nano-capillaries and the co-existence of sp<sup>2</sup> aromatic channels with various oxygen functionalities, GO membranes can afford excellent selectivity towards various ions based on molecular sieving effect and diverse chemical interactions, showing promises in filtration and separation for water treatment applications.

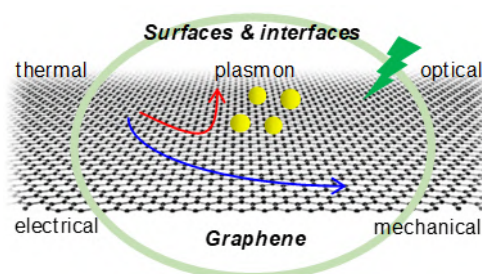


Fig.1. "graphene-on-surface" system.

### References

1. C. L. Li, Q. Cao, F. Z. Wang, Y. Q. Xiao, Y. B. Li, J. J. Delaunay, and H. W. Zhu, *Chem. Soc. Rev.* (2018) **47**, 4981.
2. G. K. Zhao, X. M. Li, M. R. Huang, Z. Zhen, Y. J. Zhong, Q. Chen, X. L. Zhao, Y. J. He, R. R. Hu, T. T. Yang, R. J. Zhang, C. L. Li, J. Kong, J. -B. Xu, R. S. Ruoff, and H. W. Zhu, *Chem. Soc. Rev.* (2017) **46**, 4417.
3. X. M. Li, L. Tao, Z. F. Chen, H. Fang, X. S. Li, X. R. Wang, J. -B. Xu, and H. W. Zhu, *Appl. Phys. Rev.* (2017) **4**, 021306.
4. X. M. Li, and H. W. Zhu, *Phys. Today* (2016) **69**, 46.
5. T. T. Yang, D. Xie, Z. H. Li, and H. W. Zhu, *Mater. Sci. Engin. R - Rep.* (2017) **115**, 1.
6. P. Z. Sun, K. L. Wang, and H. W. Zhu, *Adv. Mater.* (2016) **28**, 2287.

## Graphene-based low-dimensional hybrid heterostructures and device applications

Choi Suk-Ho<sup>1</sup>

sukho@khu.ac.kr

<sup>1</sup> Kyung Hee University, Yongin, Korea

A wide variety of optoelectronic devices based on graphene has been and are still being studied, and some of them have already reached a level of competitiveness comparable to conventional semiconductor devices [1,2]. However, single-layer graphene has low light absorbance (only 2.3%) in the ultraviolet to near infrared region, short light-matter interaction length, and high sheet resistance, unfavourable for light harvesting applications [3,4]. In addition, the ultra-short lifetime of excitons in pure graphene resulting from its gapless nature also leads to fast carrier recombination, which limits the efficient production of photocurrent or photovoltage. However, graphene transparent conductive electrodes are highly attractive for optoelectronic device applications due to their extremely-high carrier mobilities, almost-perfect transmittance, and high flexibility, and the sheet resistance can be lowered by a simple doping technique. The emergence of graphene/low-dimensional-nanomaterials-based hybrid heterostructures provides a platform useful for fabricating high-performance optoelectronic devices such as photodetectors (PDs), solar cells, and light-emitting diodes, thereby overcoming the inherent limitations of graphene. Here, I report our recent studies of optoelectronic devices based on graphene-based low-dimensional hybrid heterostructures, composed of graphene, graphene quantum dots (GQDs), Si quantum dots/nanowires, porous Si, and two-dimensional (2D) perovskites, with being assisted by doping of graphene.

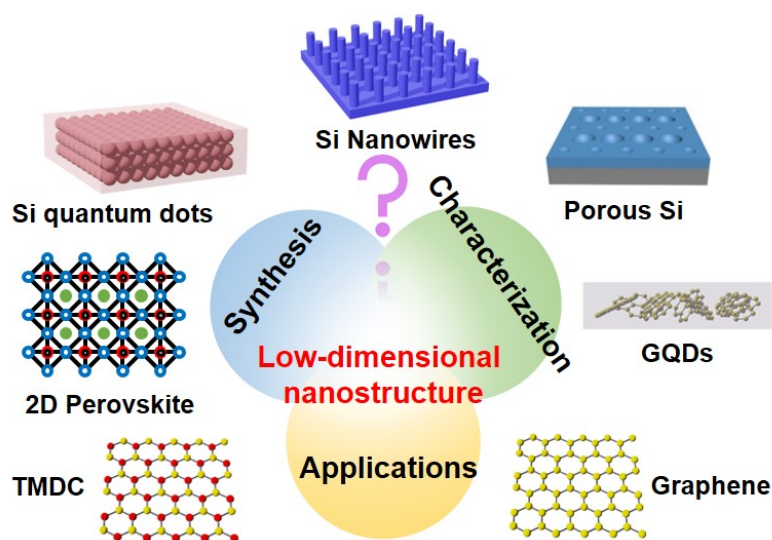


Fig.1. Synthesis, characterization, and device application of graphene-based low-dimensional hybrid heterostructures.

### References

1. Z. Liu, S.P. Lau, and F. Yan, *Chem. Soc. Rev.* (2015) **44**, 5638.
2. F.H.L. Koppens, T. Mueller, Ph. Avouris, A.C. Ferrari, M.S. Vitiello, and M. Polini. *Nature Nanotech.* (2014) **9**, 780.
3. Z. Sun and H. Chang, *ACS Nano* (2014) **8**, 4133.
4. C. Xie, C. Mak, X. Tao, and F. Yan, *Adv. Funct. Mater.* (2017) **27**, 1603886.

## Electrochemically exfoliated graphene: strategies to avoid graphene oxidation

Munuera J.M.<sup>1</sup>, Paredes J.I.<sup>1</sup>, Villar-Rodil S.<sup>1</sup>, Martínez-Alonso A.<sup>1</sup>, Tascon J.M.D.<sup>1</sup>

tascon@incar.csic.es

<sup>1</sup> Instituto Nacional del Carbon, INCAR-CSIC, F. Pintado Fe 26, 33011 Oviedo, Spain

Electrochemical exfoliation is a promising method to produce graphene materials. It relies on the delamination of graphite electrodes in proper electrolytes [1]. A limitation of this procedure is its tendency to yield substantially oxidized nanosheets, particularly under anodic conditions. Here, we discuss several strategies to reduce the oxygen content of anodically exfoliated graphene.

Graphite powder (Sigma Aldrich), flakes (Mersen), foil (Mersen) and highly oriented pyrolytic graphite (HOPG, Advanced Ceramics) were used as anode in anodic exfoliation treatments, which were carried out in the setup shown schematically on Fig. 1. Small-particle graphites yielded poorly exfoliated graphene, while graphite foil and HOPG afforded thinner, but more oxidized nanosheets. The oxidation degree was higher for HOPG due to its dense structure. Unlike this, in the case of graphite foil the wrinkled and void-rich morphology made the delamination process more efficient without requiring extensive oxidation.

Two strategies were explored to decrease the O/C ratio of anodic graphene: i, replacing the commonly used sulfate anions by sacrificial (oxidizable) electrolytes, and ii, using antioxidants as electrolyte additives [2]. Results from the former approach indicated that some aromatic sulfonates got oxidized while avoiding oxidation in the nanosheets (XPS O/C ratio as low as ~0.02). Using sodium halides as electrolytes, a proper choice of both anode material (graphite foil) and sodium halide concentration led to graphenes with a relatively low O/C ratio (0.06). Finally, when chloride anions (as NaCl or KCl) were used as an additive of sulfate-based electrolytes in optimal quantities, they prevented graphene oxidation without negatively interfering with the ability of the sulfate anion to induce delamination, affording graphene nanosheets with an O/C ratio down to 0.02.

In summary, we have demonstrated several successful strategies for the preparation of anodically exfoliated graphene that avoid nanosheet oxidation. They rely on the use of proper electrolytes and/or electrolyte additives that act as sacrificial agents in anodic oxidation. This finding can have practical applications in the large-scale production of graphene nanosheets, as only simple, cheap and abundant chemical species (e.g., sulfate salts and NaCl) are required.

We acknowledge funding through grant MAT2015-69844-R (Spanish MINECO and ERDF) and pre-doctoral contract FPU14/00792 (Spanish MECED). We also acknowledge partial funding from Principado de Asturias and ERDF through grant IDI-2018-000233.

### References

1. J.M. Munuera, J.I. Paredes, S. Villar-Rodil, M. Ayán-Varela, A. Martínez-Alonso and J.M.D. Tascón, *Nanoscale* (2016) **8**, 2982.
2. J.M. Munuera, J.I. Paredes, S. Villar-Rodil, A. Castro-Muñiz, A. Martínez-Alonso and J.M.D. Tascón, *Appl. Mater. Today* (2018) **11**, 246.

## Formation of carbon nanotubes from graphite

Peter J.F. Harris<sup>1</sup>

*p.j.f.harris@reading.ac.uk*

<sup>1</sup> Electron Microscopy Laboratory, University of Reading, Reading, RG6 6AF, UK

Multi-walled carbon nanotubes (MWCNTs) produced by arc-discharge have superior properties to those made by any other technique [1], and yet the mechanism of the growth process is still a matter of debate. Part of the problem is that it is difficult to study the growth process of the nanotubes in a controlled way. In this paper, I describe transmission electron microscopy (TEM) studies of graphite which has undergone a structural transformation as a result of the passage of an electric current. Importantly, the graphite is exposed to the current for a much shorter period than that normally used to produce carbon nanotubes, so the structures observed may represent the precursors to nanotube formation.

A commercial arc-evaporator was employed to pass a current through graphite rods which were held together by a spring mechanism. One of the rods was thinned to a diameter of 1 mm. The chamber was pumped to a pressure of approximately  $3 \times 10^{-4}$  mbar and a current of 75 A was passed for 5 seconds. These conditions are similar to those used in the "classic" method of nanotube synthesis in the arc [2], but in the latter case the current is passed for several minutes rather than a few seconds. Following evaporation, the thinned carbon rod was found to have slightly shortened, and a small deposit was formed in the area where the two rods made contact. This was collected and examined by TEM. The collected carbon contained some "normal" graphite, but this was accompanied by many regions which had a very different appearance [3]. Micrographs of such areas, at intermediate and high magnifications, are shown in Fig. 1. Here, the outline of the structure is much more irregular than in the fresh graphite, with many curved and unusually-shaped features. The material is decorated with numerous short nanotubes and nanoparticles. In some areas, nanotubes are observed to be seamlessly joined to the larger regions. It is suggested that this material represents the early stages of the formation of multiwalled carbon nanotubes, and that the mechanism involves a direct transformation of graphite into carbon nanotubes, rather than a two-stage process as envisaged in some previous models. A better understanding of the growth process might help in developing ways of producing high-quality MWCNTs in bulk.

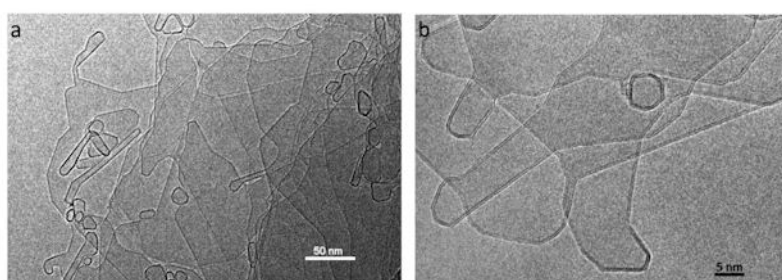


Fig.1. TEM images of carbon structures produced by passing current through graphite, (a) intermediate magnification (b) high magnification.

### References

1. P.J.F. Harris, *Carbon Nanotube Science*, Cambridge University Press, 2009.
2. T.W. Ebbesen, P.M. Ajayan, *Nature* (1992) **358**, 220.
3. P.J.F. Harris, *Phil. Mag.* (2011) **91**, 2355.

## Carbon Nanotubes: From Synthesis to Applications

*Nasibulin Albert G.*<sup>1,2</sup>

*a.nasibulin@skoltech.ru*

<sup>1</sup> Skolkovo Institute of Science and Technology, Nobel str. 3, Moscow, Russia 143026

<sup>2</sup> Department of Applied Physics, Aalto University School of Science, Espoo, Finland

The unique properties of single-walled carbon nanotube (SWNT) films, such as high porosity and specific surface area, low density, high ratio of optical transmittance to sheet resistance, high thermal conductivity and chemical sensitivity, and tunable metallic and semiconducting properties, open up avenues for a wide range of applications.

Direct integration of the CNTs produced by the aerosol methods into different applications, especially for high-performance flexible and stretchable electronics, is discussed. Produced SWCNT/polymer composite films have exhibited excellent optical and electrical properties as well as high mechanical flexibility. Wide variety of potential application of these networks has been already successfully demonstrated.

Transparent, stretchable and flexible energy storage devices have gathered great interest due to their suitability for display, sensor and photovoltaic applications. In this paper, we report the application of aerosol synthesized SWCNT thin films as electrodes for electrochemical double-layer capacitor (EDLC). SWCNT films exhibit extremely large specific capacitance ( $178 \text{ F g}^{-1}$  or  $552 \mu\text{F cm}^{-2}$ ), high optical transparency (92%) and stability for 10000 charge/discharge cycles. A transparent and flexible EDLC prototype is constructed with a polyethylene casing and a gel electrolyte.

Stretchable all-solid supercapacitors based on aerosol synthesized single-walled carbon nanotubes (SWCNTs) have been also successfully fabricated and tested. High quality SWCNT films with excellent optoelectrical and mechanical properties were used as the current collectors and active electrodes of the stretchable supercapacitors. A transmittance up to 75% was achieved for the supercapacitors made from the assembly of two PDMS/SWCNT electrodes and a gel electrolyte in between. The transparent supercapacitor has a specific capacitance of  $17.5 \text{ F g}^{-1}$  and can be stretched up to 120% elongation with practically no variation in the electrochemical performance during 1000 stretching cycles.

This research was supported by the Russian Science Foundation (project № 17-19-01787).



## **Highly-stretchable carbon nanotube devices for wearable electronics applications**

*Ohno Y.*<sup>1</sup>

*yohno@nagoya-u.jp*

<sup>1</sup> Nagoya University, Nagoya, Japan

Wearable electronics have the potential to revolutionize preventive medical care and health promotion technologies. Carbon nanotube thin films are promising electronic materials for transistors and integrated circuits, biosensors, and other passive components to build stretchable devices with excellent wearability and performance because of the high-carrier mobility, mechanical flexibility, and biocompatibility. In the presentation, after reviewing recent progresses of wearable electronics, our recent works on highly-stretchable devices based on carbon nanotube thin film are introduced. The low-voltage operable, highly-stretchable, and robust carbon nanotube thin film transistors have been realized by controlling the strain applied to the device. Stretchable energy harvesting devices based on triboelectric generation, will also be presented.

## Fluorinated nanodiamond as unique neutron reflector

*Nesvizhevsky V V*<sup>1</sup>

*nesvizhevsky@ill.eu*

<sup>1</sup> Institut Laue-Langevin, Grenoble, France

*This talk is given on behalf of Cardiff Univ./Clermont-Ferrand Univ./ESRF/ILL/Ioffe Inst./JINR+ collaboration.*

With the pronounced worldwide trend of increasing the range of useful neutrons towards smaller energies, driven in particular by large-scale structure diffractometers, reflectometers, time-of-flight and spin-echo techniques as well by particle physics, the progress is limited by low fluxes of the less energetic part of the cold neutron spectrum. The drop in flux is caused by a fundamental reason: independently of a choice of materials for neutron reflectors, they are composed of atoms. Atoms in solids and liquids are separated by distances of a few tenth of nm. If the neutron wavelength is larger than that, neutrons are weakly scattered by atoms/nuclei, and the diffraction is limited by the interplanar distances available.

For fabrication of efficient neutron reflectors, currently there is no alternative to the mimicking of conventional reflectors by means of replacing atoms/nuclei with nanoparticles of low-absorbing highly-scattering materials - thus changing the characteristic scale of neutron wavelengths [1]. Nanodiamonds is an evident choice for the material of such reflectors. The reflectivity of available nanodiamonds was measured to be much higher than that for any alternative reflector [2]. However, it remained low for neutron velocities above 160 m/s mainly because of the high content of hydrogen impurities.

We overcome this principle difficulty using fluorinated nanodiamonds [3]. We performed a detailed analysis of samples of this material using several complementary techniques including prompt- $\gamma$  neutron analysis, neutron activation analysis, small-angle neutron scattering, neutron diffraction, X-ray diffraction, Raman scattering, infrared absorption, multinuclear solid-state NMR. We concluded that diamond cores ( $sp^3$ ) of nanoparticles remain unaffected upon fluorination,  $sp^2$  carbon disappeared, and the hydrogen content in nanodiamonds is drastically reduced by the fluorination achieving a level 35-60 times lower; metallic impurities stayed essentially unaffected.

Using this information, we showed that this new class of reflectors can provide a reflectivity curve with high albedo thus minimizing the existing "leak" of neutrons through the so-called reflectivity spectral gap. The high diffusive and quasi-specular reflection will allow improving dramatically the performance of neutron sources, the efficiency of neutron delivery, and thus fluxes of slow neutrons at neutron instruments. It might also allow designing a new generation of neutron sources and experiments.

Even further major improvement of properties of nanodiamonds for such neutron reflectors is going to be achieved in the future due to a reduction of neutron-absorbing impurities, due to an optimized selection of nanoparticle sizes, due to a proper control of nanodiamond clustering, due to an optimization of properties of nanodiamonds for particular types of neutron reflectors, etc; for easier handling, nanodiamonds have to be purified from impurities that are activated in neutron fluxes. These works are in progress.

### References

1. V. Nesvizhevsky, Phys. At. Nucl. (2002) **65**, 400.
2. V. Lychagin, A.Yu. Muzychka, V.V. Nesvizhevsky, G. Pignol, K.V. Protasov, A.V. Strelkov, Phys. Lett. B (2009) **679**, 186.
3. V. Nesvizhevsky, U. Köster, M. Dubois, N. Batisse, L. Frezet, A.B. Bosak, L. Gines, O. Williams, Carbon (2018) **130**, 799.

## **CVD diamond: technology, properties and applications**

*Vikharev A.L.*<sup>1</sup>

*val@appl.sci-nnov.ru*

<sup>1</sup> Institute of Applied Physics RAS, Nizhny Novgorod, Russia

Currently single crystal diamonds and polycrystalline diamond films are being grown by the chemical vapor deposition (CVD) technology. For this purpose microwave plasma-assisted CVD reactors are most widely used. The interest to microwave frequency band is connected with the opportunity to generate plasma away from walls or electrodes having high electron concentration and to obtain high power density determining the rate of gas mixture activation (radicals generation) in the reactor. As a result, the microwave plasma-assisted CVD method allows to grow high-quality (with a low level of impurities and high crystalline perfection) diamond. The report describes all stages of the process of obtaining diamond in the CVD reactor from the preparation of substrates to the analysis of the films obtained.

To obtain semiconductor diamond with a given concentration of impurities, the technology of doping single-crystal diamond is being developed in the process of its growth. Doped CVD diamond is a wide-gap semiconductor and, due to its unique physical properties (high breakdown fields, high thermal conductivity, high carrier saturation velocity), is a promising material for creating new generation electronic devices. A major obstacle to the realization of the potential of diamond is the problem of creation of the charge carriers (electrons or holes) in the diamond. Due to the high activation energy of an acceptor impurity in diamond (the lowest activation energy of 0.37 eV is boron impurity), to obtain sufficient conductivity, high concentrations of boron are required, at which carrier mobility is significantly reduced. The solution to this problem is the development of technology for creating delta-doped layers in CVD diamond, which are very thin (several nanometers) layers with a high concentration of boron. The report presents the results of experiments on the growth of delta layers doped with boron in a single-crystal diamond and discusses the possibilities of creating unipolar electronic devices.

The doping of a diamond with a donor impurity (phosphorus) is also being actively investigated. Phosphorus creates n-type conductivity and has an activation energy of 0.57 eV. Doping a diamond with phosphorus turned out to be a technologically complex process, which does not allow creating a sufficient concentration of conduction electrons in the crystal. Obtaining a CVD diamond with electronic conductivity type would significantly expand the range of electronic devices created on diamond. The basis for diamond electronics can already be p-n junctions, as is the case in conventional semiconductor electronics. The report discusses the possibilities of creating bipolar electronic devices on diamond.

The unique physical properties of diamond make it possible to create different color centers in diamond. Color centers in diamond (e.g. NV, SiV, GeV centers) attract much interest for many modern applications, including quantum information processing, quantum communication and ultrasensitive magnetometry. The most intensively studied color center in diamond is nitrogen-vacancy center. NV-center is an attractive system because of the unique properties of its electronic transitions, which allow initialization and read-out of NV-center state using optical pumping and the fluorescence signal measurement. In this report we will discuss the method of controlled creation of NV-centers in diamond using delta-doping, which in contrast to the method of ion implantation does not produce lattice defects and allows controlling the depth of the NV-center to within a few nanometers.

---

## **RAMAN SPECTROSCOPY AS A BASIC TECHNIQUE FOR IDENTIFICATION OF VARIOUS MODIFICATIONS OF CARBON**

*Bukalov S. Sergey*<sup>1</sup>

*buklei@ineos.ac.ru*

<sup>1</sup> Scientific and Technical Center on Raman Spectroscopy, A.N. Nesmeyanov Institute of Organoelement Compounds, Russian Academy of Sciences, Moscow, Russia

Materials and composites based on various carbonaceous compounds are widespread in nature and widely used in modern industry and nanotechnology. These species contain carbon atoms in  $sp^3$  and  $sp^2$  hybridization and their various combinations. Their macroscopic properties are determined by the details of their structure, that is, crystallite size, shape, ordering, and packing. All this information can be acquired from the Raman spectra because each carbon modification exhibits its very own Raman spectrum characterized by a given number of Raman lines with their particular parameters (frequency, intensity, half-width, contour). That is why this non-destructive method which does not need special preparation of the sample is of major interest. Laser Raman micro-spectroscopy on its modern level exemplified by Raman spectrometers of last generation, such as T64000, LabRAM HR Horiba-Jobin Yvon equipped by high-sensitive CCD detectors and microscopes, allows one to identify various carbon modifications and gives a unique possibility of sample Raman micro-mapping, that is, obtaining information about sample homogeneity/heterogeneity. This study presents the results of Raman investigations of vast variety of carbonaceous compounds. These are carbonaceous materials of natural origin (graphites of various genesis, shungites, meteorites, Lunar soil, living matter), as well as of industrial origin, such as turbostratic graphite, glassy carbon, carbon fibers, diamond-like carbon, nanotubes, etc).

## Synchrotron based study of advanced carbon nanostructures

*Brzhezinskaya M.*<sup>1</sup>

*maria.brzhezinskaya@helmholtz-berlin.de*

<sup>1</sup> Helmholtz-Zentrum Berlin fuer Materialien und Energie, Berlin, Germany

By accelerating electrons to near-light speed, radiation sources like synchrotron light sources generate brilliant beams of light from infra-red to X-rays. Synchrotron radiation is one of the most powerful tools for investigation in a wide range of disciplines including nanoscience, electronics, structural biology, health and medicine, solid-state physics, materials and magnetism, earth and environmental sciences, chemistry, cultural heritage, energy and engineering. Synchrotrons are versatile facilities that can be used for many different techniques, major of them diffraction/scattering, image, spectroscopy, polarimetry.

Therefore, synchrotron is the power tool for investigation of advanced carbon nanostructures. Image techniques ensure their visualization, x-ray diffraction methods characterizing the degree of crystallinity, spectroscopy provides information on the nature of chemical bonding.

As Prof. Kroto predicted, "21<sup>st</sup> century will be the carbon age". This is greatly due to the diverse structural forms and functions of carbons. Tailoring of carbon structure, that is, controlling the physicochemical properties of carbon materials on the nanometer scale (nanocarbons) will be core technology for obtaining novel carbons with new and extraordinary functions [1]. Nanocarbons include various forms of carbon in the range from graphene to nanoporous materials. Among them, carbon nanotubes (CNTs) have attracted a wide range of scientists due to their unique morphology and nanosized scale. At present, it was accepted that chemical functionalization of carbon nanotubes (CNTs), i.e., attachment of individual atoms/molecules or their aggregates to CNTs, can extend the field of application of these nanosystems in nanoelectronics, sensorics, hydrogen power engineering, bioengineering, medicine, etc.

In this lecture will be presented results of combined investigations of atomic structure and electronic properties of functionalized carbon nanotubes and their derivatives for different applications, among them, for nanoelectronics as logical elements, memory and data transmission devices [2]; energetics, as hydrogen storage media [3]; aerospace as coating with high resistivity to complicated external effects, e.g. ionizing radiation. Major attention will be paid to discussion of changes appeared in atomic and electronic structure of CNTs under functionalization, the nature of chemical bonding between CNT and atoms/molecules or their ensembles during and after functionalization of CNTs, new details on mechanism of CNT functionalization, the chemical state of atoms used for functionalization.

### References

1. Nanoscale phenomena: basic science to device applications, ed. Z. Tang, P. Sheng, (Springer Science+Business Media, New York, 2008), 250 p.
2. A. Eliseev, L.V. Yashina, N.I. Verbitsky, M.M. Brzhezinskaya, M.V. Kharlamova, M.V. Chernysheva, A.V. Lukashin, N.A. Kiselev, A.S. Kumskov, B. Freitag, A.V. Generalov, A.S. Vinogradov, Y. Zubavichus, E. Kleimenov, and M. Nachttegaal, Carbon (2012) 50, 4021.
3. M. Brzhezinskaya, G. Yalovega, V. Shmatko, A. Krestinin, I. Bashkin, and E. Bogoslavskaja, J. Electron Spectros. Relat. Phenomena (2014) 196, 99.

## **Analysis of nanoparticles sizes in sols by dynamic light scattering (DLS) technique**

*Shvidchenko A.V.*<sup>1</sup>

*avshvid@mail.ioffe.ru*

<sup>1</sup> Ioffe Institute, St.Petersburg, Russia

The method of dynamic light scattering (DLS) is one of the most common methods for analysis of particle size in sols [1]. It is widely used in the fields of chemistry, physics, and biomedicine. Such a prevalence of DLS is due to the following features: speed of analysis (measurement takes several minutes), a small volume of the sample under study (from 1 ml of sol), sample preservation (it is a non-destructive method), a wide range of determined sizes (from nanometers to microns).

The DLS is based on the analysis of occurring in time fluctuations of the radiation intensity scattered on colloidal particles, macromolecules or polymers in liquid media [2]. The cause of fluctuations is the interference of scattered light from individual particles, the relative position and mutual orientation of which changes with time as a result of their Brownian motion. The relaxation time of the intensity fluctuations of the scattered light is the decay time of the exponential time correlation function of the scattered light, which is measured using the digital correlator. The relaxation time depends on the speed of particles movement. In turn, the speed of particles movement (or rather, their translational diffusion coefficient) depends on their hydrodynamic diameter, according to the Einstein-Stokes equation. Thus, the analysis of the intensity fluctuations of the scattered radiation makes it possible to obtain information on the hydrodynamic diameters of particles in sols.

Despite all the convenience and ease to use of DLS analyzers, the method has some weak points. Firstly, the particles should not have a dedicated direction of motion which due to deposition of particles. Secondly, the size is calculated in the approximation of spherical particles. Thirdly, the particles should not be polydisperse in sol, otherwise the measurement results may be incorrect. It is very important when particles smaller than 10 nm are investigated [3].

Based on the above, we can say that DLS is an effective method for particle size analysis, which requires a very careful approach.

### **References**

1. Yan Y.D., Clarke J.H.R. *Advances in Colloid and Interface Science* (1989), **29**, pp 277-318.
2. Berne B.J., Pecora R. *Dynamic Light Scattering*, John Wiley, New York, (1976), pp. 376.
3. Aleksenskii A.E., Shvidchenko A.V., Eidel'man E.D. *Tech. Phys. Lett.* (2012), **38**, pp 1049-1052.

## **NMR spectroscopy of weakly ordered nanostructures: capabilities, techniques, examples**

*P.M. Tolstoy*<sup>1</sup>, *A.S. Mazur*<sup>2</sup>, *M.A. Vovk*<sup>2</sup>

*peter.tolstoy@spbu.ru*

<sup>1</sup> Institute of Chemistry, St. Petersburg State University, Russia

<sup>2</sup> Center for Magnetic Resonance, St. Petersburg State University, Russia

In this introductory presentation we discuss the main approaches used in Nuclear Magnetic Resonance (NMR) spectroscopy for the study of weakly ordered systems. This broad class of structures lacking a long-distance order (sometimes called “soft matter”) includes polymers, glasses, films, complex mixtures of organic molecules, pharmaceutical preparations, metal-organic frameworks, mesoporous materials, and such carbon nanostructures as nanodiamonds and modified fullerenes.

NMR has a number of disadvantages: low sensitivity, long characteristic time scales and being applicable only to nuclei with non-zero spin. However, these disadvantages are turned into advantages upon a closer inspection: in each NMR spectrum one focuses exclusively on a specific isotope of a particular element (selectivity) and the spectral information is averaged over molecular motions which might be non-essential to the studied phenomenon, thus significantly simplifying the spectrum. One of the most important NMR spectral observable is the chemical shift – a measure of the resonance frequency and a property of the electron shell surrounding the observed nucleus and its vicinity. The chemical shift values are local and sensitive markers for the electronic structure which makes them indispensable when studying weakly ordered systems. Basically, the interpretation of the chemical shift values is an attempt to solve the reverse spectroscopic problem: finding the structure that would correspond to the observed spectrum. Technically speaking, this problem is poorly formulated and thus its solution heavily relies on previously established robust spectrum-structure correlations and/or quantum-chemical computations. Luckily, a number of such correlations is safely established or could be tailored for the problem at hand, thus allowing one to analyze NMR spectra in a predictive manner. A couple of examples of the NMR spectral analysis of carbon nanostructures will be given.

In the presentation we also discuss several major techniques employed in the high resolution solid-state NMR spectroscopy of organic and organometallic compounds, such as Magic Angle Spinning (MAS), Cross-Polarization (CP) Nuclear Overhauser Effect (NOE), and Diffusion Ordered Spectroscopy (DOSY) and present some examples of their use.

## **Secondary Ion Mass Spectrometry (SIMS) and its Applications for the Characterization of Carbon-Based Material**

*Ber Boris*<sup>1,2</sup>

*boris.ber@mail.ioffe.ru*

<sup>1</sup> Ioffe Institute, Saint Petersburg, Russia

<sup>2</sup> The Center of Multi-User Equipment "Material Science and Characterization for Advanced Technologies", Saint Petersburg, Russia

Secondary Ion Mass Spectrometry (SIMS) is a well approved surface analysis technique. By now SIMS is used for over fifty years. Its development was mainly fueled by semiconductor industry, where it is one of the key characterization technique used for R&D, for monitoring of technological processes during production (so called in-line SIMS), for reengineering of the device structures, and for failure analysis.

In the field of the physics of semiconductor devices and solid state multilayered structures SIMS analysis is one of the most important characterization techniques, too. The importance of SIMS is motivated by the following characteristics of this technique. SIMS can be used to measure all elements in the Periodic Table and their isotopes. SIMS has a high trace sensitivity down to ppb levels, that makes possible to measure the concentrations of impurities, including intentional and unintentional doping in semiconductor structures. SIMS is capable to perform accurate in-depth profiling of multilayered heterostructures and ultra-shallow implanted structures with nanometer-scale depth resolution. Valuable information about two-dimensional distribution of elements can be obtained by SIMS imaging. SIMS in-depth profiling and imaging may be combined to yield a three-dimensional SIMS chemical maps of materials and heterostructures.

In this presentation basic phenomenon of SIMS process is described, and the issue of SIMS quantification for the concentrations of impurities is addressed. The technique of in-depth SIMS analysis, its strengths and limitations are considered focusing on the challenge of accurate analysis of near-surface and interface regions. The information of state-of-the art tools for SIMS analysis of nano-scaled heterostructures is presented.

The case studies shown illustrate the application of SIMS to the in-depth characterization of the carbon-based structures. Fundamental and instrumental effects limiting the depth resolution, the sensitivity and the accuracy of SIMS analysis are discussed.



# **Oral Presentations**

**Fullerene stability. A topological approach***ORI Ottorino*<sup>1</sup>*ottorino.ori@alice.it*<sup>1</sup> Actinium Chemical Research Institute

Still, stability of fullerene isomers under the arc-discharge synthesis conditions poses many open questions. Different approaches operate with energetic, structural, and topological parameters of the fullerene molecules to explain why some fullerene isomers are more preferable than the others. In the talk we show examples in which topological roundness plays a role when predictions are compared to experimental data on the C<sub>50</sub>, C<sub>84</sub>, I<sub>h</sub> family. We have found that the molecules of most stable fullerene IPR isomers have the minimal extremal roundness. These results and the method may be applied to other fullerene isomeric sets and contribute to the understanding of the grounds of the interconnection “topology - structure - energy” underlying structural chemistry.

## Intershell correlations in endohedral atoms

Amusia M.Ya.<sup>1,2</sup>, Chernysheva L.V.<sup>2</sup>

amusia@012.net.il

<sup>1</sup> Racah Institute of Physics, the Hebrew University, Jerusalem, Israel

<sup>2</sup> A. F. Ioffe Physical-Technical Institute, St. Petersburg, Russian Federation

We have calculated partial contributions of different atomic and fullerenes subshells to the total dipole sum rule in the frame of the random phase approximation with exchange (RPAE) and found that they are essentially different from the numbers of electrons in respective subshells. This difference manifests the strength of the intershell interaction. Concrete calculations were performed for a number of endohedrals, e.g. Xe and Xe@C<sub>60</sub>.

Sum rules are relations that connect oscillator strengths of discrete  $f_k$  transitions, dipole non-relativistic photoabsorption cross-section as a function of incoming photon frequency  $\sigma(\omega)$  and the number of electrons  $N$  in the system. In atomic system of units one has

$$\sum_{\text{All } k} f_k + (c/2\pi^2) \int_0^\infty \sigma(\omega) d\omega \quad (1)$$

It existed a believe that a similar approximate equation is valid for subshell contributions of the considered system, that is incorrect, as illustrates the table:

Partial and total sums  $S_{i,HF}^L$ ,  $S_{i,HF}^\nabla$ ,  $S_{i,RP}$ ,  $\Delta_i \equiv S_{i,RP} \cdot N_i$ ,  $\sum_{j \leq i} S_{j,RP}$  of Xe;  $\sum_{j \leq i} S_{j,RP}^\circ$  - Xe@C<sub>60</sub>

Xe, N= Z=54	Subshell <i>i</i>	$N_i$	$S_{i,HF}^L$	$S_{i,HF}^\nabla$	$S_{i,RP}$	$\Delta_i$	$\sum_{j \leq i} S_{j,RP}$	$\sum_{j \leq i} S_{j,RP}^\circ$
1	1s	2	0.50	0.50	0.50	-1.50	0.50	0.57
2	2s	2	0.98	0.97	0.93	-1.07	1.43	1.36
3	2p	6	3.59	3.45	3.57	-2.43	5.00	4.63
4	3s	2	1.05	1.01	0.92	-1.08	5.92	5.58
5	3p	6	4.34	4.15	4.17	-1.83	10.09	10.00
6	3d	10	13.30	11.3	12.31	+2.31	22.40	24.20
7	4s	2	0.75	0.66	0.68	-1.32	23.08	24.88
8	4p	6	2.35	2.07	2.28	-3.72	25.36	26.10
79	4d	10	18.56	11.9	14.82	+4.82	40.18	36.49
10	5s	2	0.33	0.26	0.53	-1.47	40.71	37.06
11	5p	6	12.65	6.18	8.73	+2.73	<b><math>S_{RP}</math> =49.44</b>	<b><math>S_{RP}^\circ = 73.67</math></b>

Here  $N_i$  is the number of electrons in  $i$ -subshell,  $S_i$  is the partial sum (1), indexes  $L, \nabla$  denote results of Hartree-Fock (HF), index RP means RPAE calculations for subshell  $i$  of Xe; @ marks results for endohedral Xe@C<sub>60</sub>. Note that  $S_{RP}^\circ = 73.67 > 54$  in Xe@C<sub>60</sub>, the outer subshell takes much of its oscillator strength from C<sub>60</sub>. It would be very interesting to perform experimental investigation aiming to demonstrate the prominent violation of the partial sum rules. This is not a simple task, having in mind that for each subshell  $i$  the measurements must be performed in a broad region in coincidence with creation of only  $i$  vacancy. However, such an experiment would be of great importance for the understanding of electronic structure of atoms and atom-like formations. For more details see [1].

### References

1. M.Ya. Amusia and L.V. Chernysheva, JETP Letters (2018), **108**, 435.

## Magnetic studies of endohedral fullerenes

Krylov D.S.<sup>1</sup>, Popov A.A.<sup>2</sup>

*dskrylov@gmail.com*

<sup>1</sup> Center for Quantum Nanoscience, Institute for Basic Science (IBS), Seoul, Republic of Korea

<sup>2</sup> Leibniz Institute for Solid State and Materials Research, Helmholtzstrasse 20, 01069 Dresden, Germany

Since the discovery of first manganese clusters that retain their magnetisation for months at low temperatures, there has been intense interest in single-molecule magnets because of potential applications in data storage, spintronics, quantum computing, and magnetocaloric cooling. Endohedral clusterfullerenes exhibit outstanding magnetic properties due to lanthanide ions encapsulated inside the carbon cage providing large magnetic moments and anisotropies.

The nitride clusterfullerene family and specifically DySc<sub>2</sub>N@C<sub>80</sub> [1] and Dy<sub>2</sub>ScN@C<sub>80</sub> fullerenes were pioneer fullerene single-molecule magnets. Recently the magnetic properties of Dy-nitride clusterfullerenes were investigated explicitly in a broad range of temperatures. For DySc<sub>2</sub>N@C<sub>80</sub>, the intriguing process of quantum tunneling of magnetization was studied in detail for powder and single-crystal samples with different dilution methods [2]. For Dy<sub>2</sub>ScN@C<sub>80</sub>, the coupling between two Dy ion was of the main interest. Magnetic studies of this compound revealed: that the quantum tunneling process is effectively suppressed due to exchange interactions in the cluster; that above 60 K, thermally-activated relaxation proceeds via the fifth-excited Kramers doublet with the energy of 1735±21 K [3].

An ultimate case of magnetic coupling inside the fullerene cage was recently found in Dy<sub>2</sub>@C<sub>80</sub>(CH<sub>2</sub>Ph) [4] and Tb<sub>2</sub>@C<sub>80</sub>(CH<sub>2</sub>Ph) [5], members of a new di-metal endohedral fullerene family with a single-electron lanthanide-lanthanide bond. Giant exchange interactions between lanthanide ions and the unpaired electron result in the single-molecule magnetism with a high 100-s blocking temperature of 18 K and 25.2 K respectively for Dy<sub>2</sub>@C<sub>80</sub>(CH<sub>2</sub>Ph) and Tb<sub>2</sub>@C<sub>80</sub>(CH<sub>2</sub>Ph).

### References

1. Westerström, J. Dreiser, C. Piamonteze, M. Muntwiler, S. Weyeneth, H. Brune, S. Rusponi, F. Nolting, A.A. Popov, S. Yang, L. Dunsch, T. Greber, *Journal of the American Chemical Society*, 2012, **134**(24): p. 9840-9843.
2. S. Krylov, F. Liu, A. Brandenburg, L. Spree, V. Bon, S. Kaskel, A.U.B. Wolter, B. Büchner, S.M. Avdoshenko, A.A. Popov, *Phys.Chem.Chem.Phys.*, 2018, **20**, 11656.
3. S. Krylov, F. Liu, S.M. Avdoshenko, L. Spree, B. Weise, A. Waske, A.U.B. Wolter, B. Büchner, A. A. Popov, *Chem.Comm.*, 2017, **53**, 7901.
4. Liu, D.S. Krylov, L. Spree, S.M. Avdoshenko, N.A. Samoylova, M. Rosenkranz, A. Kostanyan, T. Greber, A.U.B. Wolter, B. Büchner, A. A. Popov, *Nature Communications*, 2017, **8**, Article number: 16098.
5. Liu, G. Velkos, D.S. Krylov, L. Spree, M. Zalibera, R. Ray, N.A. Samoylova, C. Chen, M. Rosenkranz, S. Schiemenz, F. Ziegls, K. Nenkov, A. Kostanyan, T. Greber, A.U.B. Wolter, M. Richter, B. Büchner, S.M. Avdoshenko, A.A. Popov, *Nature Communications*, 2019, **10**, Article number: 571.

## DETONATION NANODIAMOND HYDROSOLS: RHEOLOGY AND STRUCTURE

*Kuznetsov N.M.*<sup>1</sup>, *Belousov S.I.*<sup>1</sup>, *Chvalun S.N.*<sup>1,2</sup>, *Eidelman E.D.*<sup>3,4</sup>, *Shvidchenko A.V.*<sup>3</sup>, *Yudina E.B.*<sup>3</sup>, *Vul' A.Ya.*<sup>3</sup>

*kyz993@yandex.ru*

<sup>1</sup> National Research Center "Kurchatov Institute", Moscow, Russia

<sup>2</sup> Enikolopov Institute of Synthetic Polymeric Materials of the Russian Academy of Sciences, Moscow, Russia

<sup>3</sup> Ioffe Institute, St. Petersburg, Russia

<sup>4</sup> St. Petersburg State Chemical Pharmaceutical University, St. Petersburg, Russia

Nanodiamonds produced by detonation (DND) is one of attractive advanced carbon nanostructures [1]. The interest in DND increases rapidly due to their unique properties, such as nanosize, thermal conductivity, biocompatibility, high surface area, various surface modifications etc. Pristine commercial DND tend to form clusters and aggregates with sizes about hundreds of nanometers. The most of practical applications require DND to be purified and deagglomerated [2]. The temperature annealing method [2] allows to produce individual DND particles of 4-5 nm [3]. This particles form unusually high stable hydrosols and show sol-gel transition at really low particles concentration (about 5-6 wt%) [4]. Even more suspensions reveal the yield at concentration less than 1 wt% [5]. Such behavior of low filled suspensions is typical for fillers with high aspect ratio and cannot be easy comprehended for DNDs. To explain the observed effects it was suggested the formation of chains and fractal structures of diamond nanoparticles in an aqueous medium leading to an increase in aspect ratio, "spongy" percolation network formation and appearance of the yield stress. Such interactions are possible, due to non-symmetric shape of individual particle and electrical double layer.

In this study the structural organization of particles in an aqueous medium is considered, a pronounced thixotropic behavior of suspensions, which is qualitatively similar for particles with negative and positive electrokinetic potentials, is found as well. The structure of hydrosols studied by various methods such as rheology, X-ray analysis, dynamic light scattering, transmission electron microscopy and cryo-electron tomography. The rheological behavior and possible mechanisms of sol-gel transition depending on surface of DND particles is discussed.

This work partially supported by Russian Foundation for Basic Researches, project 18-29-19117 mk.

### References

1. V.N. Mochalin, O. Shenderova, D. Ho, Y. Gogotsi. *Nature Nanotechnology*, (2012), **7**, 11.
2. *Detonation Nanodiamonds - Science and Applications*. ed. A. Ya. Vul', O. A. Shenderova, Pan Stanford Publishing, (2013).
3. A.T. Dideikin, A.E. Aleksenskii, M.V. Baidakova, P.N. Brunkov, M. Brzhezinskaya, V. Yu. Davydov, V.S. Levitskii, S.V. Kidalov, Yu. A. Kukushkina, D.A. Kirilenko, V.V. Shnitov, A.V. Shvidchenko, B.V. Senkovskiy, M.S. Shestakov, A. Ya. Vul'. *Carbon*, (2017), **122**, 737.
4. A.Ya. Vul', E.D. Eidelman, A.E. Aleksenskiy, A.V. Shvidchenko, A.T. Dideikin, V.S. Yuferev, V.T. Lebedev, Yu.V. Kul'velis, M.V. Avdeev. *Carbon*, (2017), **114**, 242.
5. N.M. Kuznetsov, S.I. Belousov, D.Yu. Stolyarova, A.V. Bakirov, S.N. Chvalun, A.V. Shvidchenko, E.D. Eidelman, A.Ya. Vul'. *Diamond & Related Materials*, (2018), **83**, 141.

## Thermal conductivity of nanodiamond aqueous dispersions by thermal lensing and heat flow techniques

*Usoltseva L.O.<sup>1</sup>, Volkov D.S.<sup>1</sup>, Avramenko N.V.<sup>1</sup>, Korobov M.V.<sup>1</sup>, Proskurnin M.A.<sup>1</sup>*

*usoltsevalilya@gmail.com*

<sup>1</sup> Department of Chemistry, M.V. Lomonosov Moscow State University, Moscow, Russia

Cooling is one of the most significant and challenging heat-transfer applications. Conventional heat transfer fluids such as water, lubricant oils and glycols have low thermal conductivities compared to metal and metal oxides. Efforts are made to improve the performance of heat transfer systems by adding nano-sized solid particles with high thermal conductivity to base fluids [1-3]. From the practical viewpoint, it is important to get a stable, chemically inert, and environment-friendly dispersion (nanofluid). As the latter, nanodiamond (ND) aqueous dispersions can be used, whose thermophysical properties should be elucidated.

Accurate measurements of the fundamental transport property, thermal conductivity, of nanofluids is still a problem. The most commonly used, the hot-wire transient method needs a large liquid volume and the accuracy of experimental data suffers from convective effects and possible presence of ions of conducting fluids. To overcome these limitations, a remote optical photothermal detection approach can be used, namely, thermal-lens spectrometry (TLS). It is based on the formation of a lenslike element (refractive-index field) while heating a light-absorbing sample by a focused laser beam. TLS evaluates thermal diffusivity from the transient curve, and then thermal conductivity is assessed using the data on volume specific heat, which is readily obtained by DSC and densitometry. TLS may provide the data for both the dispersed phase and the dispersion medium, simultaneously. This method of thermal-diffusivity determination based on finding transient characteristic time of thermal lensing was used for estimating thermal diffusivities of ND dispersions. Thermal conductivity was also obtained directly by a more common heat flow steady-state technique (a Fox 50 instrument).

Three different trademarks of ND (RUDDM, RDDM, and SDND) were selected as those forming concentrated aqueous dispersions (up to 20%). Thermal diffusivity (by TLS), heat capacities, densities, and thermal conductivities were determined. We observed a linear dependence of density on concentration and a decrease of specific heat of aqueous ND nanofluids, the latter can be linearly correlated as a concentration function regardless of ND type. An increase (up to 3%) in thermal conductivity of RUDDM samples was observed. The differences and advantages of simultaneous use of heat-flow and photothermal techniques will be discussed.

This work was supported by the RFBR grant 18-33-00586 mol\_a.

### References

1. D.K. Devendiran, V.A. Amirtham, *Renewable and Sustainable Energy Reviews* (2016) **60**, 21.
2. C. Pang, J.W. Lee, Y.T. Kang, *International Journal of Thermal Sciences* (2015) **87**, 49.
3. M. Raja, R.Vijayana, P.Dineshkumar, M.Venkatesan, *Renewable and Sustainable Energy Reviews* (2016) **64**, 163.

## Luminescent properties of Si- and N-doped nanodiamonds synthesized from adamantane

*Kudryavtsev O.S.*<sup>1</sup>, *Ekimov E.A.*<sup>2</sup>, *Romshin A.M.*<sup>1,3</sup>, *Pasternak D.G.*<sup>1,3</sup>, *Vlasov I.I.*<sup>1</sup>

*leolegk@mail.ru*

<sup>1</sup> Prokhorov General Physics Institute of RAS, Moscow, Russia

<sup>2</sup> Institute for High Pressure Physics of RAS, Troitsk, Moscow, Russia

<sup>3</sup> Moscow State University, Moscow, Russia

The methods of controllable and uniform formation of luminescent centers in nanodiamonds, particularly nitrogen-vacancy (NV) and silicon-vacancy (SiV), are of current interest in relation of potential application of emitting nanodiamonds as optical markers, electric and magnetic sensors, single-photon emitters. For this purpose, we have developed HPHT synthesis of nanodiamonds from its molecular analogue adamantane, controlling the size of crystallites in a wide range by changing a temperature of the synthesis [1]. For NV and SiV formation in such nanodiamonds the mixtures of adamantane (C<sub>10</sub>H<sub>16</sub>) with, respectively, adamantanecarbonitrile (C<sub>11</sub>H<sub>15</sub>N) and tetraphenylsilane (C<sub>24</sub>H<sub>20</sub>Si) have been used as precursors. In the present work, the luminescent properties of two samples synthesized at the N/C = at.0.1% and Si/C = at.0,0007% in the precursors were investigated. The produced nanodiamonds were dispersed on glass substrates and individual crystals were studied using atomic-force, confocal luminescence and scanning electron microscopes, as well as the Henbury-Brown-Twiss interferometer. It was found that nitrogen and silicon are fairly evenly distributed throughout the sample volume, luminescence was observed from all crystallites, and its intensity increased with crystallite size. Measurement of the second-order correlation function  $g^{(2)}$  for the luminescence intensity of the smallest diamond crystallites (100–200 nm) showed that nitrogen-doped nanodiamonds contain typically 1-2 color centers, and silicon-doped ones - about 10 centers. The prospects for creating single photon emitters based on “organic” nanodiamonds are discussed.

This work was supported by the Russian Science Foundation (grant number 14-12-01329).

### References

1. A. Ekimov, O. S. Kudryavtsev, N. E. Mordvinova, O. I. Lebedev, I. I. Vlasov, *Chemnanomat* (2018) 4, 269.

## Photoluminescence from NV centers in 5 nm detonation nanodiamonds: identification and large sensitivity to magnetic field

*Osipov V.Yu.*<sup>1</sup>, *Treussart F.*<sup>2</sup>, *Abbasi Zargaleh S.*<sup>2</sup>, *Takai K.*<sup>3</sup>, *Shakhov F.M.*<sup>1</sup>, *Hogan B.T.*<sup>4</sup>, *Baldycheva A.*<sup>4</sup>

*osipov@mail.ioffe.ru*

<sup>1</sup> Ioffe Institute, St.Petersburg, Russia

<sup>2</sup> Laboratoire Aime Cotton, CNRS, Université Paris-Sud, ENS Paris-Saclay, Orsay, France

<sup>3</sup> Department of Chemical Science and Technology, Hosei University, Koganei, Tokyo, Japan

<sup>4</sup> College of Engineering Mathematics and Physical Sciences, University of Exeter, Exeter, UK

We show that the content of nitrogen-vacancy (NV) colour centers in the nanodiamonds (DNDs) produced during the detonation of nitrogen-containing explosives is  $2.4 \pm 0.3$  ppm. This concentration is the largest known for nanodiamonds of size  $< 10$  nm with artificially created NV centers. The concentration was estimated from the electron paramagnetic resonance (EPR) as determined from the integrated intensity of the  $g=4.27$  line. This EPR line is related with “forbidden”  $\Delta m_s = 2$  transitions between the Zeeman levels of a NV centre’s ground triplet state.

Confocal fluorescence microscopy enables detection of the broadband, structureless, red photoluminescence (PL) of the NV colour centers in nanoscale DND aggregates formed from the individual 5 nm nanoparticles. We have further confirmed the detection of the triplet NV centers through the observation of an abrupt drop in the PL intensity when an external magnetic field is applied. When an external magnetic field is switched “ON” and “OFF”, an accompanying variation of the PL intensity is observed (Fig.1), which results from the sensitivity of the NV triplet ground state to magnetic field and from the optically detectable magnetic resonance characteristic of the negative NV charge state only. This effect is a unique feature of NV centers, which cannot be observed for other light-emitting colour centers, in the visible domain, in diamond. The application of this effect to discriminate ultra-small DND (size  $< 10$  nm) in biological environment with large autofluorescence background is promising [1]. Such DND could also be used as point optical probes of high-resolution nanoscale magnetic field sensing and all-optical magnetic imaging [2].

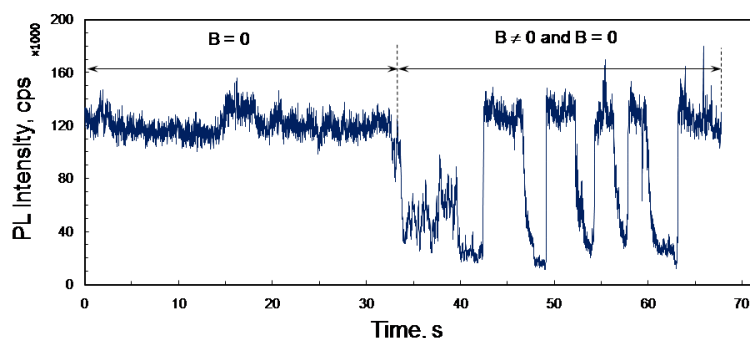


Fig.1. Photoluminescence intensity versus time of NV centers in a single DND aggregate spincoated on a glass coverslip in the presence or absence of an external magnetic field. Excitation laser wavelength: 532 nm. In absence of external magnetic field ( $B=0$ ) we observe only small changes of intensity, that might be due to the blinking of some of the NV color centers close to DND surface. When we apply a magnetic field we observe a large decrease of the PL intensity.

### References

1. R. Chapman and T. Plakhoitnik, *Optics Letters* (2013) **38** (11), 1847-1849.
2. J.-P. Tetienne, L. Rondin, P. Spinicelli, M. Chipaux, T. Debuisschert, J.-F. Roch and V. Jacques, *New Journal of Physics* (2012) **14**, 103033.



## Relationship between the type of hybridization of carbon nanoparticles and their fluorescence.

*Vervald A.*<sup>1</sup>, *Lachko A.*<sup>1</sup>, *Kudryavtsev O.*<sup>2</sup>, *Vlasov I.*<sup>2</sup>, *Shenderova O.*<sup>3</sup>, *Dolenko T.*<sup>1</sup>

*alexey.vervald@physics.msu.ru*

<sup>1</sup> Faculty of Physics, M.V. Lomonosov Moscow State University, Moscow, Russia

<sup>2</sup> General Physics Institute, Russian Academy of Sciences, Moscow, Russia

<sup>3</sup> Adamas Nanotechnologies, Inc., Raleigh, USA

Carbon nanoparticles (CNPs) – nanodiamonds (NDs) and carbon dots (CDs), particularly their subspecies graphene oxides – have a characteristic broadband fluorescence. Due to this fluorescence coupled with mechanical stability, non-toxicity, and easily modifiable surface, CNPs can be used as fluorescent biomarkers, drugs carriers, and adsorbents for biomedicine [1]. Results of many studies indicate the surface origin of CNPs' fluorescence, but the mechanisms of which yet is not fully known. For both types of nanoparticles – NDs and CDs – the dependence on surface functionalization [2,3], “red edge” effect [4] and pH-dependence [5,6] of their fluorescence was shown. Based on the similarity of the mentioned characteristic and the fact that on the surfaces of NDs some sp<sup>2</sup>-hybridized carbon is almost always present, it has been suggested that this non-diamond phase of carbon is the source of surface fluorescence of NDs. However, the clear connection between the carbon phase and fluorescence of carbon nanoparticles has not been established.

The aim of this work was the verification of the theory of the surface-“graphite” origin of the nanodiamonds' fluorescence. To do this, the fluorescence of the aqueous suspensions of the following carbon nanoparticles with different sp<sup>2</sup>/sp<sup>3</sup> carbon hybridization ratio were studied:

- Carbon dots (graphene oxides) (CD);
- Nanodiamonds decorated with carbon dots (CDND);
- CDNDs purified from sp<sup>2</sup>-hybridized carbons by different methods;
- NDs as much as possible cleared of graphite carbon.

The surface properties of CNPs and their relations with fluorescence were studied by the methods of vibrational spectroscopy – confocal Raman and IR adsorption spectroscopies. The changes of the fluorescence of CNPs with the change of the pH of the suspensions were observed, the quantum yields of their fluorescence were calculated. The obtained results support the proposed hypothesis.

This study has been performed at the expense of the Russian Science Foundation (grant number 17-12-01481) (A.L., T.D. – data acquisition, data analysis), Basis Foundation (A.V. – data processing).

### References

1. K. Turcheniuk and V.N. Mochalin, *Nanotechnology* (2017) **252001**, 1.
2. J. Xiao, P. Liu, L. Li, and G. Yang, *J Phys Chem C* (2015) **119**, 2239.
3. J. Shang, L. Ma, J. Li, W. Ai, T. Yu, and G. G. Gurzadyan, *Sci Rep* (2012) **2**, 792.
4. T. A. Dolenko, S. A. Burikov, A. M. Vervald, A. A. Khomich, O. S. Kudryavtsev, O. A. Shenderova, and I. I. Vlasov, *J Appl Spectrosc* (2016) **83**, 294.
5. C. Galande, A. D. Mohite, A. V. Naumov, W. Gao, L. Ci, A. Ajayan, H. Gao, A. Srivastava, R. B. Weisman, and P. M. Ajayan, *Sci Rep* (2011) **1**, 85. <https://doi.org/10.1038/srep00085>
6. P. Reineck, D. W. M. Lau, E. R. Wilson, N. Nunn, O. A. Shenderova, and B. C. Gibson, *Sci Rep* (2018) **8(1)**, 2.

## Paramagnetic defects in e-beam irradiated Ib type HPHT micro- and nano-diamonds: effects of variable fluence and annealing

*Shames A.I.*<sup>1</sup>, *Smirnov A.I.*<sup>2</sup>, *Milikisiyants S.*<sup>2</sup>, *Nunn N.*<sup>3</sup>, *Torelli M.D.*<sup>3</sup>, *Shenderova O.*<sup>3</sup>

*sham@bgu.ac.il*

<sup>1</sup> Ben-Gurion University of the Negev, Beer-Sheva, Israel

<sup>2</sup> Department of Chemistry, North Carolina State University, Raleigh, NC, USA

<sup>3</sup> Adamas Nanotechnologies, Inc., Raleigh, NC, USA

Paramagnetic defects induced by e-beam irradiation in synthetic Ib type high-pressure high-temperature (HPHT) micro- and nano-diamonds were studied by continuous wave (CW) electron paramagnetic resonance (EPR) spectroscopy at X-band (9.4 GHz), pulsed EPR at X- and Q-bands (34 GHz) and photoluminescence (PL) spectroscopies as a function of radiation fluences (up to  $5 \times 10^{19}$  e<sup>-</sup>/cm<sup>2</sup>) and post-irradiation thermal annealing. Increasing fluence causes a reduction in the initial content of substitutional nitrogen (P1 centers) accompanying by a progressive formation of paramagnetic negatively charged vacancies (V) as well as spin-triplet interstitials (R1/R2). On annealing of all the irradiated samples at 850 °C the contents of both V and R/R2 drastically diminish. In contrast, the contents of, mainly, the negatively charged nitrogen vacancy spin-triplet centers NV (W15) as well as secondary spin-triplet centers (identified as W16, W17, W18, and W33) progressively grow (*cf.* Fig. 1). For the annealed samples EPR spectra of so-called “forbidden”  $\Delta M_s = 2$  electronic spin transitions observed at  $g \approx 4$  (“half-field” EPR spectra) allow for quantification of NV centers providing contents from 4 ppm for the fluence to  $5 \times 10^{18}$  e<sup>-</sup>/cm<sup>2</sup> to 12 ppm ( $5 \times 10^{19}$  e<sup>-</sup>/cm<sup>2</sup>). Further annealing at 1400 °C significantly reduces the content of W17, W18, and W33 but not W15 and W16 defects. The efficacy of NV center fabrication and resulting “brightness” as a function of the e-beam radiation fluence are also reported. Analysis of PL spectra provides for identification of color centers in the irradiated diamond samples and tracking their evolution on annealing. The data help in understanding the role of different factors affecting the formation of color centers in diamond toward optimization of the fabrication protocols.

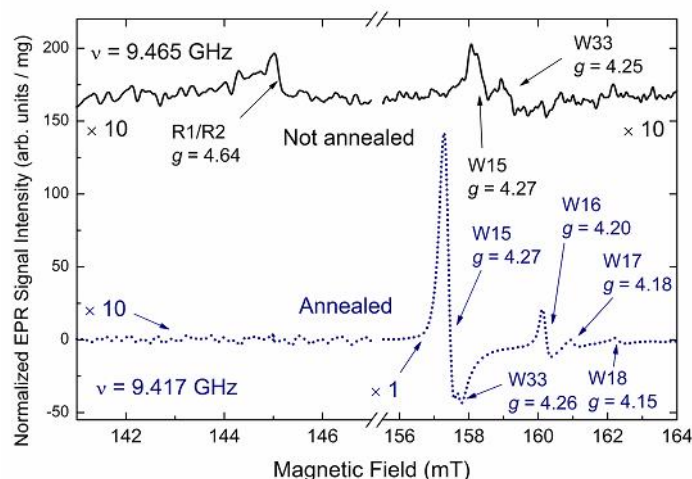


Fig.1. Half-field CW EPR spectra of  $5 \times 10^{19}$  e<sup>-</sup>/cm<sup>2</sup> electron irradiated samples before (black line) and after annealing at 850 °C (red line). All spectra were recorded at room temperature ( $T = 295$  K),  $P_{MW} = 100$  mW,  $A_m = 0.1$  mT,  $RG = 2 \times 10^5$ ,  $n_{acq} = 25$ ,  $\nu = 9.465$  GHz (not annealed) and  $\nu = 9.417$  GHz (annealed). Arrows point to “forbidden” lines attributed to R1/R2 interstitial triplet centers ( $g = 4.64 \pm 0.01$ ) as well as W15 ( $g = 4.27 \pm 0.01$ ), W33 ( $g = 4.25 \pm 0.01$ ), W16 ( $g = 4.20 \pm 0.01$ ), W17 ( $g = 4.18 \pm 0.01$ ) and W18 ( $g = 4.15 \pm 0.01$ ) centers.

## **Gold and nanodiamond: new jewels for sensing, imaging, diagnostic and drug delivery.**

*Orlanducci Silvia*<sup>1</sup>

*silvia.orlanducci@uniroma2.it*

<sup>1</sup> Dept. of Chemical Science and Technology, University of Rome Tor Vergata, Rome, Italy

Gold decorated nanodiamond could find numerous applications in the biological field. Thanks to the combination of the astonishing properties of both components, applications may range from optical labeling and imaging to molecular and drugs delivery and biosensing.

The use of AuNP-ND hybrid system was proven to be very effective in photoacoustic tomography. Similarly, to the graphene energy absorbing capability, nanodiamond can amplify the photoacoustic signal of the gold. Moreover, the quenching of the ND fluorescence creates an energy transfer mechanism between the excited nanodiamond and the gold NP, capable to support this remarkable amplification.

Gold decorated nanodiamond was successfully used as Surface Enhanced Raman Spectroscopy (SERS) substrate showing excellent SERS activity mainly based on the charge transfer process.

This process is particularly advantageous in all cases of fluorescent substrates since the charge or energy transfer turns off the fluorescence allowing the acquisition of the Raman signal. Furthermore, as in the case of the photoacoustic signal, diamond can easily dissipate the heat developed by the irradiated metal, increasing the durability of the SERS substrate.

Another application of nanodiamond-gold hybrid system could be found in the delivery and label of hydrophobic substances, mainly drugs. The diamond allows the transport of insoluble substances in an aqueous environment, thus avoiding the use of potentially toxic solvents or surfactants. Moreover, the Au strongly improve the contrast in electron microscopy images allowing better detection of nanoparticles inside the cellular system.

This review describes the techniques used for the synthesis of these materials and a critical discussion of some recent results on their application will be done. As examined, the synergy between the two particles is particularly evident in the improvement of the plasmonic and photoacoustic properties of the gold. In addition, the catalytic and sensor activity of the hybrid system show peculiarities not found in the individual components alone.

### **References**

S. Orlanducci, *European Journal of Inorganic Chemistry* 2018(48), pp. 5138-5145

## Composite proton-conducting membranes with nanodiamonds

*Kulvelis Yu.V.*<sup>1</sup>, *Primachenko O.N.*<sup>2</sup>, *Odinokov A.S.*<sup>2</sup>, *Shvidchenko A.V.*<sup>3</sup>, *Bayramukov V.Yu.*<sup>1</sup>, *Gofman I.V.*<sup>2</sup>, *Lebedev V.T.*<sup>1</sup>, *Ivanchev S.S.*<sup>2</sup>, *Vul A.Ya.*<sup>3</sup>, *Kuklin A.I.*<sup>4</sup>, *Wu B.*<sup>5</sup>

*kulvelis\_yv@pnpi.nrcki.ru*

<sup>1</sup> B.P. Konstantinov Petersburg Nuclear Physics Institute, NRC "Kurchatov Institute", Gatchina, Russia

<sup>2</sup> Institute of Macromolecular Compounds, Saint Petersburg, Russia

<sup>3</sup> Ioffe Institute, Saint Petersburg, Russia

<sup>4</sup> Joint Institute for Nuclear Research, Dubna, Russia

<sup>5</sup> Heinz Maier-Leibnitz Zentrum, Garching, Germany

Perfluorinated proton-conducting membranes have great opportunities for the use in hydrogen fuel cells. Short side chain membranes are of special interest due to their high performance in wide temperature range. Various types of modifications are also being applied to improve the membranes properties [1].

The development of new type of composite membranes based on a polymer matrix modified by particles of functionalized detonation nanodiamond (DND) will provide an increase in proton conductivity in combination with greater strength and temperature stability of the membrane characteristics (the key problems of membrane materials). The authors have developed methods for preparing nanodiamonds as perfect crystals (sp<sup>3</sup>-hybridization) with negative  $\zeta$ -potential in hydrosols, without surface regions with sp<sup>2</sup>-hybridized carbon atoms. This makes possible to regulate the ordering of nanodiamond ensembles in the resulting polymer matrix during the sublimation of the solvent from the layers of the solution with the polymer and diamond components during the preparation of membrane films by casting from solution.

The experimental results obtained by proton conductivity and mechanical strength measurements, small and very small neutron scattering (SANS and VSANS), atomic force microscopy are discussed.

The work was supported by Russian Foundation for Basic Research (grant No 19-03-00249).

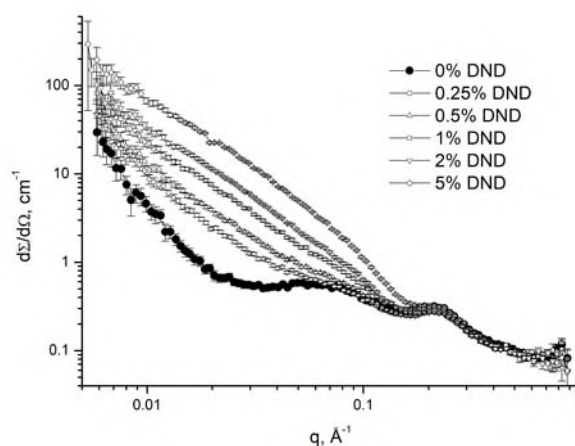


Fig.1. SANS on dry membranes with incorporated DND particles.

### References

1. Yu.V. Kulvelis, S.S. Ivanchev, O.N. Primachenko et al. // RSC Adv. 2016. V. 6. P. 108864.

## Lateral boron doped diamond nanowires, properties, performance and prospects for quantum technologies.

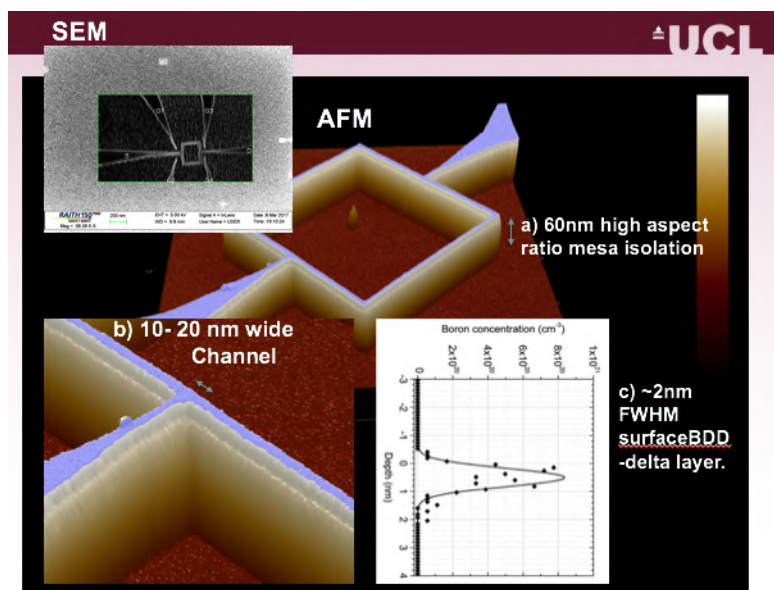
Alexander C Pakpour-Tabrizi<sup>1</sup>, R B Jackman<sup>1</sup>

Alexander.pakpour-tabrizi11@ucl.ac.uk

<sup>1</sup> University College London

Electronically active low dimensional structures have been made in a variety of material systems, while quantum dot like defects in diamond are a huge field of study, lateral nanowire structures are yet to draw such attention. Nanowires in other material systems have been investigated in applications as varied as quantum computing, chemical or optical sensing and power electronics to name but a few.

By utilising a mix of additive and subtractive processing a novel lateral diamond nanowire is fabricated and characterised. The substrate and foundation for this nanowire is a highly boron doped diamond epilayer ( $10^{20}$  boron/cm<sup>3</sup>), grown on high purity insulating single crystal CVD diamond epi layer. The dopants are confined spatially in a 1-2nm region, this delta function like distribution can be shown to have similar electronic properties to a bulk doped. The  $\delta$ -doped epi-layer is then patterned and etched to leave wires with width dimensions on the order 15nm and arbitrary controllable lengths. In this talk we will discuss the transport mechanisms and phenomena observed, as well as showing novel field effect transistors utilising a varying number of these wires to achieve high current handling and demonstrate the scalability of this unique technology.



SEM, AFM and SIMS profiles of nanoscale boron doped diamond processed into novel low dimensional structures for advanced technology.

## Microcapacitors based on fluorinated graphene films

*Okotrub A.V.*<sup>1</sup>, *Sysoev V.I.*<sup>1</sup>, *Gorodetskii D.V.*<sup>1</sup>, *Bulusheva L.G.*<sup>1</sup>

*spectrum@niic.nsc.ru*

<sup>1</sup> Nikolaev Institute of Inorganic Chemistry SB RAS, Novosibirsk, Russia

Graphene materials have been ideal material platform for constructing flexible electronic; its 2D structure, high specific area and good conductivity are attractive for energy storage devices. The fluorinated graphenes with composition  $C_2F$  were synthesized using low temperature fluorination by  $BrF_3$  from natural graphite. Suspension of fluorinated graphite in toluene was used to produce films having a thickness of 1 - 10  $\mu m$ . The UV radiation treatment of film surface performed local conversion of fluorinated graphene to graphene. Depending on irradiation conditions, it is possible to vary functionalization degree of the resulted graphene material. The almost complete removal of fluorine atoms of surface layer of films was achieved using focusing radiation of low power laser ( $\lambda = 380$  nm). Produced electrode material with high electrical conductivity and flexibility is useful for energy storage devices without binders or conductive additives. We reveal an influence of structural features and functional composition of graphene material on electrochemical performance of in-plane supercapacitors. Pattern of microelectrodes was drawing by UV laser and supercapacitors properties of these elements were measured for different acid electrolytes. Obtained materials showed tunable electrochemical performance, which reaches 1.5  $mF/cm^2$  at rate 0.8 mV/s. The change of chemical states of capacitor surface under electrical charging was controlled by XPS and NEXAFS *in situ* measurements. We reveal an influence of structural features and functional composition of graphene material on electrochemical performance of in-plane micro supercapacitors.

## Carbon-metal endohedral structures synthesized by pyrolysis

*Bairamukov V.Yu.<sup>1</sup>, Lebedev V.T.<sup>1</sup>*

*vbayramukov@gmail.com*

<sup>1</sup> B.P.Konstantinov Petersburg Nuclear Physics Institute, NRC Kurchatov Institute, 188300 Gatchina, Leningrad dist., Russia

Prospects of creation of new type materials composed of endohedral molecular cells which provide saving native physical and chemical properties of encapsulated metal atoms of rare earth elements are discussed. In connection with this, recent results concerning synthesis, functionalization and structural features and behaviors of endofullerenes and derivatives in solutions are presented as well as the data of physical-chemical researches and neutron scattering experiments showed self-assembly phenomena of endohedral molecular objects. In comparison to aforesaid material, the alternative metal-carbon systems prepared from metal-organic compounds by pyrolysis should be considered as evolved from molecular crystals to delicate matrices incorporating metal atoms or groups along with a formation of local atomic graphite-like order at the level of tiny globular structures observed by transmission electron microscopy and X-ray diffraction (Fig. 1). Forthcoming principles of preset designing of endohedral materials are under development and application for some model systems.

The work was supported by Russian Foundation for Basic Researches (grant № 18-29-19008, 18-32-00500)

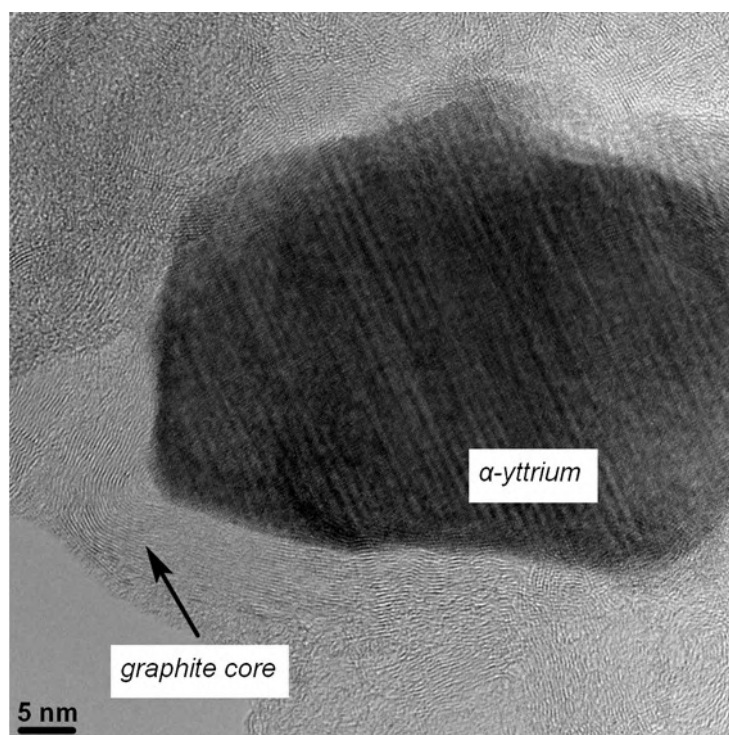


Fig. 1. High-resolution TEM image of core-shell structure prepared by pyrolysis of yttrium bis-phthalocyanine

### References

1. V.I. Tikhonov, V.K. Kapustin, V.T. Lebedev, A.E. Sovestnov, V.Yu. Bairamukov, K.Ya. Mishin. *Radiochemistry* (2016), 58, 545.

## Two photon fluorescence of the hollow spherical carbon nitride nanostructures

Zinin P. V.<sup>1</sup>, Acosta T.<sup>2</sup>, Misra A.<sup>2</sup>, Sharma S.<sup>2</sup>, Khabashesku V.<sup>3</sup>, Bogomolov A.<sup>1</sup>

zosimpvz@mail.ru

<sup>1</sup> Scientific-Technological Center of Instrumentation, Russian Academy of Sciences, Moscow, Russia

<sup>2</sup> Hawaii Institute of Geophysics and Planetology, University of Hawaii, Honolulu, Hawaii, USA

<sup>3</sup> Department of Chemical and Biomolecular Engineering, University of Houston, Houston, Texas, USA

Recently graphitic C-N materials, including graphitic  $C_3N_4$  ( $g-C_3N_4$ ), has become the hotspot in the materials science for its unique electronic structure. With medium band gap as well as thermal and chemical stability in ambient environment, it becomes one of the most promising photocatalytic materials [1]. In addition, considerable attention has been paid on its photoelectronic application, such as light emitting device, photocathode, optical sensor, etc. [2]. Later it was found some times ago that graphitic modifications of  $C_3N_4$  were extremely fluorescent under laser irradiation [3, 4]. It was demonstrated that the intensity of the fluorescence depends on the nanostructure of the carbon nitrides: at the maximum it is more than *two orders* as high for carbon nitride spheres as for graphitic carbon nitride particles [5]. The record high value of the fluorescence quantum yield (QY), up to 32% at excitation 532 nm and 38% at excitation 633 nm. was attributed to the spherical shape of this form of carbon nitride ( $s-C_3N_4$  structures) [5]. It was also found that fluorescence excited in  $s-C_3N_4$  has the high intensity of the anti-Stokes fluorescence.

The aims of this report is to study non-linear effect of the pulsed laser excitation with different graphitic  $C_3N_4$  structures including  $s-C_3N_4$  structures and disordered graphitic  $C_3N_4$  ( $g-C_3N_4$ ) on the anti-Stokes fluorescence. In summary, experimental studies, conducted recently, demonstrated that a difference of the fluorescence intensity of different modifications of  $g-C_3N_4$  materials could be more *than two orders*. Physics of these phenomena is not understood. Because of extremely high fluorescence and a high two-dimensional rigidity of carbon nitride materials studying effect of the crystal structure, nano and bonding on the optical properties of these materials should result in finding novel photonic materials with highest three or two-dimensional elastic moduli and extremely high fluorescence.

### References

- [1] X. C. Wang, K. Maeda, A. Thomas, K. Takanabe, G. Xin, J. M. Carlsson, K. Domen, M. Antonietti, Nat. Mater. 8 (2009) 76-80.
- [2] G. P. Dong, Y. H. Zhang, Q. W. Pan, J. R. Qiu, J. Photochem. Photobiol. C-Photochem. Rev. 20 (2014) 33-50.
- [3] P. V. Zinin, L. C. Ming, S. K. Sharma, V. N. Khabashesku, X. R. Liu, S. M. Hong, S. Endo, T. Acosta, Chem. Phys. Lett. 472 (2009) 69-73.
- [4] L. C. Chen, D. J. Huang, S. Y. Ren, T. Q. Dong, Y. W. Chi, G. N. Chen, Nanoscale 5 (2013) 225-230.
- [5] P. V. Zinin, A. V. Ryabova, V. A. Davydov, V. Khabashesku, S. Boritko, S. K. Sharma, D. V. Pominova, V. Loshenov, Chem. Phys. Lett. 633 (2015) 95-98.



## Charge transport in composites with 2D, 1D and 0D carbon nanostructure fillers

*Forro Laszlo*<sup>1</sup>

*laszlo.forro@epfl.ch*

<sup>1</sup> Ecole Polytechnique Federale de Lausanne, Lausanne, Switzerland

One of the great achievements of nanoscale science is the development of large scale synthesis of 2D (graphene), 1D (carbon nanotubes) and 0D (fullerenes and nanodiamonds) carbon-based nanostructures (CBNs). The CBNs as fillers allow the synthesis of composites with various matrices improving their electrical, mechanical and thermal properties.

In this presentation, the analysis of the electrical conductivity of composites (preferentially using SU-8 negative photoresist as matrix) with 2D, 1D and 0D CBN fillers is studied both experimentally and theoretically. The charge transport was investigated as a function of filling factor, temperature, size distribution of CBNs and hydrostatic pressure.

In all cases, it is primordial to closely control the distribution of the CBNs in the matrix, in order to properly describe the charge transport from tunneling processes to percolation, from hopping to power-law behavior. Especially is interesting the effect of applied pressure on the composites where the increase of the effective dielectric permittivity improves the screening of the Coulomb interaction and reduces the optimal hopping distance of the electrons[1-4].

The advancement in the development of these exceptional functional composites with CBNs will be illustrated by macroscopic or lithographically defined structures.

Acknowledgment. This work was performed in collaboration with Claudio Grimaldi, Maryam Majidian, Peter Matus, Arnaud Magrez, Vladimir Kuznetsov and many others. The financial support of the Swiss National Science Foundation is acknowledged.

### References

1. M. Majidian, C. Grimaldi, A. Pisoni, L. Forro and A. Magrez, *Scientific Reports*, 8, 7495 (2018)
2. C. Grimaldi, M. Mionic, R. Gaal, L. Forro, and A. Magrez, *Appl. Phys. Lett.* 102, 223114 (2013).
3. M. Majidian, C. Grimaldi, A. Pisoni, L. Forro and A. Magrez, *Carbon* 80, 364 (2014).
4. C. Grimaldi et al, *Appl. Phys. Lett.*, submitted

## Percolation phenomena in nanocarbon composites

Bocharov G.S.<sup>1</sup>, Eletskii A.V.<sup>1</sup>

eletskii@mail.ru

<sup>1</sup> National Research University Moscow Power Engineering Institute, Moscow, Russia

Nanocarbon composites present a new type of nanomaterials consisted of electric conducting carbon nanoparticles and a non-conducting matrix. A typical example of such composites is a polymer matrix doped with carbon nanotubes (CNT) [1]. Due to a high aspect ratio of nanotubes insertion of very small quantity of CNT (on the level of 0.01%) promotes the percolation transition resulting in an enhancement of the conductivity of the material by 10 - 12 orders of magnitude. Another type of nanocarbon composite is a film consisted of partially reduced graphene oxide produced as a result of thermal reduction of graphite oxide material [2 - 4]. Distinctive peculiarity of both types of nanocomposites relates to the dependence of the specific resistivity of the materials on the applied voltage [4 - 6]. Such a behavior caused by non-ideal contacts between neighboring carbon particles involving into the composite. The resistance of this contact depends drastically on the intra-contact field, which promotes the dependence of the material resistivity on the applied voltage. The model description of such a non-linear dependence has been presented. The calculation results are compared with both literature data and the measured data obtained for reduced graphene oxide thermally treated at various temperatures.

This work is supported by the state tasks No..3.1414.2017/4.6 and 3.7131.2017/6.7.

### References

1. Eletskii A.V., Knizhnik A.A., Potapkin B. V., Kenny J. M. "Electrical characteristics of carbon nanotube-doped polymer composites" *Physics-Uspechi* **50** 209 (2015)
2. Huh S.H. Thermal Reduction of Graphene Oxide. In: *Physics and Applications of GrapheneExperiments*, 2011. URL: [https://www.intechopen.com/books/physics and applications of graphene experiments/ thermal reduction of graphene oxide](https://www.intechopen.com/books/physics_and_applications_of_graphene_experiments/thermal_reduction_of_graphene_oxide).
3. Shulga Y.M., Martynenko V.M., Muradyan V.E., Baskakov S.A., Smirnov V.A., Gutsev G.L. Gaseous products of thermos and photo reduction of graphite oxide. *Chem. Phys. Lett.*, 2010, 498, P. 287-291.
4. S. Bocharov, A.V. Eletskii, V.P. Mel'nikov "Electrical properties of thermally reduced graphene oxide" *Nanosystems: Physics, Chemistry, Mathematics* **9**(1) 96 2018.
5. S. Bocharov, A. V. Eletskii, A. A. Knizhnik "Nonlinear Resistance of Polymer Composites with Carbon Nanotube Additives in the Percolation State" *Technical Physics* **61** 1506 (2016).
6. S. Bocharov, A. V. Eletskii. "Percolation transition under thermal reduction of graphene oxide" *J. Structural Chemistry* **59** 806 (2018).

## Raman study of gradient polypropylene composites filled with carbon black

*Yablokov M.Yu.*<sup>1</sup>, *Shchegolikhin A.N.*<sup>2</sup>, *Lebedev O.V.*<sup>1,3,4</sup>, *Mukhortov L.A.*<sup>3</sup>, *Ozerin A.N.*<sup>1</sup>

*yabl1@yandex.ru*

<sup>1</sup> Enikolopov Institute of Synthetic Polymer Materials, Russian Academy of Sciences, Moscow, Russia

<sup>2</sup> Institute for Biochemical Physics, Russian Academy of Sciences, Moscow, Russia

<sup>3</sup> Moscow Institute of Physics and Technology (State University), Moscow Region, Russia

<sup>4</sup> Center for Design, Manufacturing and Materials, Skolkovo Institute of Science and Technology, Moscow, Russia

Functionally graded materials are currently in the focus of multidisciplinary research in materials science [1-4].

In the present work, gradient composites of polypropylene (PP) filled with 7.5-15 wt.% of CB have been studied. The composites were prepared by a special procedure providing the enrichment of surface with conducting CB particles.

The effect of surface layer enrichment of polymer composites with CB has been investigated with the aid of Raman spectroscopy ( $\lambda_{\text{exc}} = 785 \text{ nm}$ ). The Raman spectra of studied samples were completely dominated by the bands G and D of the filler CB particles over PP bands. The increase of the incident laser power above 10 mW has led to corresponding growth in the temperature of the composite resulting in the melting of PP matrix, since CB particles strongly absorb in the NIR spectral region. Therefore only laser powers below 10 mW with laser focusing on the very surface of the sample have been employed during Raman measurements.

For Raman study small-sized samples were cut out from hot-pressed composites normally to the pressing surface and flattened using sledge microtome. This geometry of samples gives the possibility to characterize concentration gradient of carbon filler in polymer matrix while scanning of laser beam in the direction, perpendicular to pressing surface. The spectra were run in multiple points with an incremental step of 5-10 mcm. It has been found that integral intensity of G and D Raman bands of CB was relatively constant and low in points situated far from the sample surface but showed a gradual increase and growth in close proximity to the surface layer. Thus the growth of CB concentration in the vicinity of the composite surface has been confirmed. Surface concentration of CB was estimated on the basis of calibration dependence. The linear dependence of Raman integral intensity of CB signal on filler concentration was obtained for the samples with constant filler concentration in polymer matrix. The reproducibility of data obtained was due to uniform samples surfaces, prepared with the help of sledge microtome, and constancy of all the parameters for Raman spectra measurements.

Other peculiarities of Raman measurements on carbon/PP gradient composites will be reported and discussed.

This work was supported by RFBR grant № 18-29-19112

### References

1. M. Naebe, K. Shirvanimoghaddam, *Applied Materials Today* (2016) **5**, 223.
2. K. Claussen, T. Scheibel, H-W. Schmidt, R. Giesa, *Macromol. Mater. Eng.* (2012) **297**, 938.
3. Almasi, M. Sadeghi, W. Lau, F. Roozbahani, N. Iqbal, *Mater. Sci. Eng. C.* (2016) **64**, 102.
4. R. Parihar, S. Setti, G. Srinivasu R.Sahu, *Sci. Eng. Compos. Mater.* (2018) **25**, 309.

## The biodegradation of fullerene C<sub>60</sub> by human enzyme myeloperoxidase

*Piotrovskiy L.B.*<sup>1</sup>, *Litasova E.V.*<sup>1</sup>, *Sokolov A.V.*<sup>1</sup>, *Utsal V.A.*<sup>2</sup>, *Zhurkovich I.K.*<sup>2</sup>

*levon-piotrovsky@yandex.ru*

<sup>1</sup> Institute of Experimental Medicine, Saint-Petersburg, Russia

<sup>2</sup> Institute of Toxicology, Saint-Petersburg, Russia

The drug without the knowledge of its fate in the organism is nothing. Although fullerene C<sub>60</sub> is of particular interest among other carbon nanostructure's, data on its transformations in mammals are virtually absent. Attempting to find the possibility of degradation of fullerene C<sub>60</sub> by mammalian enzymes, we have selected myeloperoxidase (MPO), which is one of the key components of the innate immune system of mammals and ensures neutrophil activity against foreign agents. Fullerene (Neotec Product, Russia, 99%) was used as nanoC60 prepared by the solvent-exchange method (a light yellow solution with a particle size ranging from 130 to 390 nm and a zeta potential of -30 mV). MPO was isolated from the extract of frozen HL-60 cells and purified by affinity chromatography's, and this allowed to obtain a homogeneous product with a high specific activity. The nanoC60 solution was incubated at 37°C in the presence of 100 nM MPO in 150 mM NaCl, adding hydrogen peroxide daily to a final concentration of 50 μM. The selected time and concentration mode of adding hydrogen peroxide does not inactivate the enzyme, i.e., provided a stable formation of HOCl. The monitoring of changes of the reaction mixture showed that, during the first two days of incubation in the presence of MPO the yellow solution became colorless. In the UV spectra of the reaction mixture, the intensity of the peak at 333-335 nm decreases over time until the complete disappearance. The IR spectroscopy data showed that the signals characteristic of the unsubstituted fullerene core C<sub>60</sub> disappeared 3 days after the addition of hydrogen peroxide. The mass-spectra of the reaction mixture on the 5-6 days contained no fragments with the molecular weights of 720 and above, which, in turn, indicates the degradation of core [1]. In the methyl *tert*-butyl ether extract of reaction mixture of the 5<sup>th</sup> day by chromat-mass-spectrometry were detected the present, among others, of the following compounds, namely 4-methylheptan-2-on, 3-methylbenzaldehyde, 4-ethyl-1,3-benzenediol, 4-hydroxy-4-methylpentan-2-on and 2,2,4,4-tetramethyltetrahydrifuran. Thus, we for the first time demonstrated the principal possibility of biodegradation of fullerene C<sub>60</sub> molecule using the human neutrophil enzyme MPO. This process, unlike other examples of the biological modification of fullerenes, leads to a complete loss of the fullerene molecule topology.

### References

Litasova E.V., Iljin V.V., Sokolov A.V., Vasilyev V.B., Dumpis M.A., Piotrovskiy L.B. The biodegradation of fullerene C<sub>60</sub> by myeloperoxidase. Doklady Biochem. Biophys. 2016, Vol. 471, pp. 417-420.

## Carbon nanoparticles as carriers for medical radionuclides

*Garashchenko B.L.*<sup>1</sup>, *Yakovlev R.Y.*<sup>1</sup>

*yarules@yandex.ru*

<sup>1</sup>Vernadsky Institute of Geochemistry and Analytical Chemistry of Russian Academy of Sciences, Moscow, Russia

Due to the distinctive physicochemical and biological properties that arise at the nanoscale, as well as a unique set of properties with respect to other nanoparticles, nano-diamonds (ND), multi-walled nanotubes (MWNT) and graphene oxide (GO) can be used as carriers of radionuclides in radiopharmaceuticals (RP). The creation of RP based on ND, MWNT and GO particles with a modified surface implies the possibility of obtaining nanoparticles with adjustable size and controllable rate of desorption of a radionuclide in the body, sorption of radionuclides in various chemical states, keeping them on the surface and ensuring targeted delivery [1].

<sup>99m</sup>Tc, <sup>223</sup>Ra, <sup>213</sup>Bi and <sup>211</sup>Pb are ones of the most widely used and researched radionuclides in the SPECT-diagnosis and alpha-therapy of cancer, cardiovascular and many other diseases [2, 3].

The samples of carbon nanoparticles obtained in the work were characterized by the methods of transmission electron microscopy, infrared spectroscopy, X-ray photoelectron spectroscopy, Raman and dynamic light scattering. The sorption properties of the obtained samples of carbon nanomaterials with respect to <sup>99m</sup>Tc, <sup>223</sup>Ra, <sup>213</sup>Bi, and <sup>211</sup>Pb on various types of ND, MWNT and GO surfaces were studied. Complete extraction of <sup>99m</sup>Tc, <sup>213</sup>Bi, and <sup>211</sup>Pb from an aqueous solution in a physiologically acceptable pH 6-7.4 within 5-30 minutes was established [4]. Several samples with adsorbed radionuclides washed in saline were found to be stable during the day.

The results show the promise of using carbon nanoparticles as radionuclide carriers in composition of modern radiopharmaceuticals.

This work is supported by the Russian Science Foundation (project № 18-13-00413).

### References

1. K. Chow, X.-Q. Zhang, M. Chen, R. Lam, E. Robinson, H. Huang, D. Schaffer, E. Osawa, A. Goga, D. Ho, Nanodiamond Therapeutic Delivery Agents Mediate Enhanced Chemoresistant Tumor Treatment, *Sc. Transl Med* (2011) **3**, p. 73ra21.
2. Banerjee, M.R.A. Pillai, N. Ramamoorthy, Evolution of Tc-99m in diagnostic radiopharmaceuticals, *Seminars in nuclear medicine*(2001) **31**(4), p. 260.
3. L. Garashchenko, V.A. Korsakova, R.Y. Yakovlev, Radiopharmaceuticals based on alpha emitters: preparation, properties, and application, *Physics of Atomic Nuclei* (2018) **81**(10), p. 1515.
4. L. Garashchenko, N.N. Dogadkin, N.E. Borisova, R.Y. Yakovlev, Sorption of <sup>223</sup>Ra and <sup>211</sup>Pb on modified nanodiamonds for potential application in radiotherapy, *J Radioanal Nucl Chem* (2018)**318**(3), p. 2415.

## **Nanodiamond and cellulose: a technological liaison for restoration methodologies**

*Palmieri Elena*<sup>1</sup>, *Cicero Cristina*<sup>2</sup>, *Mercuri Fulvio*<sup>2</sup>, *Zammit Ugo*<sup>2</sup>, *Orlanducci Silvia*<sup>1</sup>

*palmieri.ele@hotmail.it*

<sup>1</sup> Department of Chemistry Sciences, Univ. degli Studi di Roma Tor Vergata, Rome, Italy

<sup>2</sup> Department of Industrial Engineering, Univ. degli Studi di Roma Tor Vergata, Rome, Italy

The interest of the scientific community in nanodiamond is related to its many features, which mainly derive from its structure and composition, explaining its possible employment in the Restoration and Conservation of Cultural Heritage.

The conservation science requires expertise ranging from the humanities, to the physics and chemistry. The composition of the artwork as well as its preservation state determine the protocol to be followed and the materials to be used for an effective restoration treatment. Amongst the nanomaterials that have been proposed, in the form of dispersions of nanoparticles, micellar solutions, microemulsions and gels, nanodiamond (ND) represent nowadays one of the most exciting material to be used in the field of cultural heritage. The use of nanocomposites diminishes the impact on both the operators and the environment because of a reduced use of chemicals with respect to the materials traditionally employed. At present, the ND obtained by detonation of explosive material constitutes the most interesting and studied form of nanodiamond, also thanks to the low-cost process of production that leads to a high-quality material. ND are structured in a core-shell configuration, being composed by a diamond core with a rigid lattice structure surrounded by an amorphous sp<sup>2</sup> carbon shell composed by one or more layers of fullerene. The unique surface chemistry is the peculiarity that characterizes the ND with respect to other carbon nanostructures, making it possible to perform chemical manipulation, without compromising the properties of the diamond core, thus explaining their application in many fields among which for instance cultural heritage.

The application of nanodiamond composites and dispersions as consolidating agents for parchment substrates has been studied. Different nanocomposites and dispersions based on ND have been tested showing very promising results and making ND a high-performance additive in the field of restoration. The short- and long-term effect of ND treatment on parchment has been evaluated by analysing the collagen denaturation temperature, measured by the Light Transmitted Analysis (LTA), compared to the one observed in non-ND-treated parchment. ND composites, at certain concentrations, seem to improve the structural stability of the collagen networking, slowing down the effects of ageing.

The use of nanodiamond dispersions has shown to be effective in contrasting the thermo-hygrometrically induced ageing and in reducing the negative effects promoted by employment of traditional materials for consolidating purpose, such as Klucel G. (hydroxy propyl cellulose). Therefore, nanodiamond has confirmed itself to be a promising material to be applied to the Restoration and Conservation of Cultural Heritage.

## Hybrid molecular structures with nanodiamonds for biomedicine

*Lebedev V.T.*<sup>1</sup>, *Kulvelis Yu. V.*<sup>1</sup>, *Kizima E.A.*<sup>2</sup>, *Tropin T.V.*<sup>2</sup>, *Trofimuk A.D.*<sup>3</sup>, *Shestakov M.S.*<sup>3</sup>

*lebedev\_vt@pnpi.nrcki.ru*

<sup>1</sup> B.P.Konstantinov Petersburg Nuclear Physics Institute, NRC, Kurchatov Institute, Gatchina, Leningrad distr., Russia

<sup>2</sup> Joint Institute for Nuclear Researches, Dubna, Moscow distr., Russia

<sup>3</sup> Ioffe Institute, St.Petersburg, Russia

Review of the development of molecular design and the results of studies of hybrid structures of nanodiamonds associated with molecular objects (polymers, fullerenes, diphthalocyanines of rare earth elements) has been presented to demonstrate a variety of new hybrid molecular structures to be introduced in biomedicine for diagnostics and therapy of socially significant diseases. It seems very attractable and profitable in practice to apply paramagnetic rare earth atoms (Gd, Ho, Pr etc.) integrated into endofullerenes and diphthalocyanines to accelerate strongly a transversal spin relaxation of surrounding protons in biological tissues. This may be promising to create effective prototypes of contrasting agents for Magneto-Resonance Imaging when these nanostructures are modified with hydrophilic groups to get a good solubility in aqueous biological media. Along with a substantial enhancement of the relaxivity by one order in magnitude these substances allow minimize the risks of hazardous pollution of biological medium by heavy toxic atoms from the complexes during medical tests. It is achieved by means of the encapsulation of magnetic atoms into durable carbon cage of fullerene being resistant to chemical attacks in processes of metabolism of living organisms. On the other hand, the other kind of new structures based on nanodiamonds modified by rare earth elements have been tested to observe a luminescence induced by X-ray exposing. The latter is considered as a way to enhance greatly the abilities of photodynamic therapy. In this method a photosensitizer is excited by laser to generate very cytotoxic singlet oxygen breaking the tumor cells. The proposed X-ray luminescent structures are considered as very important to realize a desirable application of photodynamic therapy for deep lying tissues that remains still not possible or complicated for standard method based on laser excitation of photosensitizers. The designed composites have been studied by Dynamic Light Scattering and Neutron Small-Angle Scattering to analyze their structures and self-assembly in aqueous solutions.

The work was supported by Russian Foundation for Basic Researches (grant No 18-29-19008).

### References

1. Yu.V. Kulvelis, A.V. Shvidchenko, A.E. Aleksenskii, E.B. Yudina, V.T. Lebedev, M.S. Shestakov, A.T. Dideikin, L.O. Khozyaeva, A.I. Kuklin, Gy. Török, M.I. Rulev, A.Ya.Vul // *Diamond & Related Materials*. 2018. V. 87. P. 78.
2. V. T. Lebedev, A. A. Szhogina, M. V. Suyasova // *IOP Conf. Series: Journal of Physics: Conf. Series*. 2018. V.994. P. 012005.

## Complex conductivity of monolayer graphene and zitterbewegung

*Firsova N.E*<sup>1,2</sup>, *Ktitorov S.A.*<sup>1,3</sup>

*ktitorov@mail.ioffe.ru*

<sup>1</sup> Ioffe Institute, St. Petersburg, Russia

<sup>2</sup> Peter the Great St. Petersburg Polytechnic University, St. Petersburg, Russia

<sup>3</sup> St. Petersburg Electrotechnical University, St. Petersburg, Russia

A formula for complex conductivity of monolayer graphene was derived in [1]. The graphene membrane irradiated by the weak time-periodic electric field in the terahertz range was considered there to this aim. The method of the proof was based on the study of the time-dependent density matrix. The exact solution of the von Neumann equation for density matrix was found within the linear approximation on external field. The induced current was calculated and then the formula for quantum complex conductivity as a function of the external field frequency, Fermi energy and temperature was derived. The found formula for quantum complex conductivity allowed us to obtain also the formulae for inductance  $L$  and capacitance  $C$  and to show that the graphene membrane was a kind of the resonant circuit near the Dirac point. We show that the found in [1] real and imaginary parts of complex conductivity obey the Kramers-Kronig (KK) dispersion relations. We find a deep relation between the graphene optical conductivity peculiarities and Zitterbewegung (ZB). ZB ("trembling motion" from German) is a fast oscillating motion of elementary particles, in particular electrons that obeys the Dirac equation. ZB phenomenon was first predicted by Erwin Schrödinger in 1930 [2] as a result of his analysis of the wave packet solutions of the Dirac equation for electrons in free space. He concluded that the interference between positive and negative energy states produced what appeared to be a fluctuation (at the speed of light) of the position of an electron around the mean value with an angular frequency of  $2mc^2/\hbar$ . ZB of a free relativistic particle has never been observed because of the huge value of the trembling frequency. However, graphene with its Dirac states near the  $K$  and  $K'$  critical points is an ideal test area to simulate many of the quantum electrodynamics phenomena. In particular, ZB was shown in [3] to exist in graphene with the trembling frequency realistic to be measured. Also we see that the complex conductivity obtained in [1] has a resonance at the frequency, which coincides with the ZB one calculated in [3] for monolayer graphene. On the other hand we show that the resonance frequency can be expressed through the introduced in [1] values for the graphene inductance and capacitance. So we see that it is just ZB, which determines conductivity dynamics in the vicinity of the Dirac point. So we can say that the main sense of the formula for complex conductivity in the vicinity of the Dirac point is ZB. We see also that the value of ZB frequency is related with the found magnitudes of the inductance and capacitance by Thomson's formula i.e.  $\omega_{\text{BZ}} = (LC)^{-1/2}$ .

### References

- E.Firsova, Photonics and Nanostructures - Fundamentals and Applications, (2017) **26**, 8-14.
- Schrödinger, Berliner Ber. (1930) 418; Berliner Ber, (1931) 63.
- I. Katsnelson, The European Physical Journal B (2006) **51**, 157.



---

## **On the mechanism of the oxygen reduction reaction at graphene surfaces: insights from computational quantum chemistry**

*Radovic L.R.*<sup>1</sup>

*lradovic@udec.cl*

<sup>1</sup> Penn State University (USA) and University of Concepcion (Chile)

At the heart of the controversy-plagued discussions of the mechanism and efficiency of the oxygen reduction reaction is the identification of the active sites in electrocatalysts ranging from carbon blacks to graphene nanoribbons and heat-treated phthalocyanines. The symptomatic distinction between the two-electron and the four-electron process points to the dissociation of O<sub>2</sub> as the central issue. Here we use the heretofore unrecognized resolution of this dichotomy in gas-phase oxidation of graphene-based materials (e.g., coal combustion) - where the production of CO<sub>2</sub> or CO has long been of both practical and fundamental importance - to identify the electrocatalytically active sites. Our computational results, using density functional theory, are presented and compared with abundant experimental evidence on the behavior of pristine graphene as well as its N-, B- and transition-metal-doped counterparts. Electron transfer readily occurs through a carbene-type site upon O<sub>2</sub> chemisorption on the zigzag edge. Whether dissociation occurs hinges on proton transfer occurring either before or after the triplet-to-singlet stabilization of a peroxy-type surface intermediate.

## Graphene on the (001) Surface of Cubic-SiC Epilayers: Growth Mechanism and Electronic Properties

*Aristov V.Yu.*<sup>1,2</sup>, *Chaika A.N.*<sup>1</sup>, *Molodtsova O.V.*<sup>2,3</sup>, *Babekov S.V.*<sup>2,4</sup>, *Locatelli A.*<sup>5</sup>, *Mentes T.O.*<sup>5</sup>, *Sala A.*<sup>5,6</sup>, *Marchenko D.*<sup>7</sup>, *Potorochin D.*<sup>2,3,8</sup>

v.yu.aristov@mail.ru

<sup>1</sup> Institute of Solid State Physics of the Russian Academy of Sciences, Chernogolovka, Russia

<sup>2</sup> Deutsches Elektronen-Synchrotron DESY, Hamburg, Germany

<sup>3</sup> ITMO University, Saint Petersburg, Russia

<sup>4</sup> Johannes Gutenberg - Universitet, Mainz, Germany

<sup>5</sup> Elettra-Sincrotrone Trieste S.C.p.A., Trieste, Italy

<sup>6</sup> University of Trieste and IOM-CNR, Trieste, Italy

<sup>7</sup> Helmholtz - Zentrum Berlin für Materialien und Energie, Berlin, Germany

<sup>8</sup> TU Bergakademie Freiberg, Freiberg, Germany

The graphene synthesis on low-cost cubic-SiC/Si(001) wafers represents a realistic method for mass production of graphene layers suitable for electronic applications and compatible with existing silicon technologies. The graphene grown on such substrate typically exhibits nanometer-sized domains with different lattice orientations [1]. Here we present the in-situ investigation of layer-by-layer graphene growth on the cubic-SiC/Si(001) wafers. The measurements were performed by means of a number of methods: scanning tunneling microscopy with atomic resolution, low-energy electron microscopy (LEEM), high-resolution laterally-resolved X-ray photoelectron spectroscopy ( $\mu$ -XPS), angle-resolved photoelectron spectroscopy ( $\mu$ -ARPES), and micro low-energy electron diffraction ( $\mu$ -LEED) [2]. The experimental data evidence the opportunity to control the local thickness of the graphene overlayer on the silicon carbide substrate in-situ during UHV synthesis. Significantly, presented data disclose the mechanisms of the surface transformation and layer-by-layer graphene growth on cubic-SiC/Si(001) in UHV at high temperatures. Finally, we will briefly report the electronic structure, transport and magnetic properties of such continuous and uniform nanostructured few-layer graphene with self-aligned nano-domain boundaries synthesized by the method above [1-3].

This work was carried out within the state task of ISSP RAS and supported by the Russian Foundation for Basic Research (Grant Nos. 17-02-01139, 17-02-01291).

### References

1. A.N. Chaika, V.Yu. Aristov, O.V. Molodtsova, *Prog. Mater. Sci.* (2017) **89**, 1.
2. V.Yu. Aristov, A.N. Chaika, O.V. Molodtsova, S.V. Babekov, A. Locatelli, T.O. Mentès, A. Sala, D. Potorochin, D. Marchenko, B. Murphy, B. Walls, K. Zhussupbekov, and I.V. Shvets, *ACS Nano* (2019) **13**, 526.
3. H.-C. Wu, A.N. Chaika, M.-C. Hsu, T.-W. Huang, Mour. Abid, Moh. Abid, V.Yu. Aristov, O.V. Molodtsova, S.V. Babekov, Y. Niu, B.E. Murphy, S.A. Krasnikov, O. Lubben, H. Liu, B.S. Chun, Y.T. Janabi, S.N. Molotkov, I.V. Shvets, A.I. Lichtenstein, M.I. Katsnelson, C.-R. Chang, *Nature Commun.* (2017) **8**, 14453.

## Functionalized graphenes: from synthesis to applications

*Rabchinskii M.K.<sup>1</sup>, Ryzhkov S.A.<sup>1</sup>, Baidakova M.V.<sup>1,2</sup>, Shnitov V.V.<sup>1</sup>, Kirilenko D.A.<sup>1,2</sup>, Pavlov S.I.<sup>1</sup>, Chumakov R.G.<sup>3</sup>, Dideikin A.T.<sup>1</sup>, Besedina N.A.<sup>4</sup>, Vul A.Ya.<sup>1</sup>*

*rabchinskii@mail.ioffe.ru*

<sup>1</sup> Ioffe Institute, St.Petersburg, Russia

<sup>2</sup> ITMO University, Saint-Petersburg, Russia

<sup>3</sup> NRC Kurchatov Institute, Moscow, Russia

<sup>4</sup> St. Petersburg Academic University, St. Petersburg, Russia.

The increasing progress in the study of pristine and chemically derived graphenes led to arising of new subclass of graphene materials, functionalized graphenes (FGs). These are the conductive graphene layers decorated with the certain types and amounts of functional groups. Owing to the presence of these functionalities, FGs exhibit new electronic properties and can be easily grafted with various moieties. All this makes FGs to be perfect candidates for a large field of applications: gas sensing, biosensing, formation of photovoltaic and optoelectronic devices.

In this study we present our results on the synthesis, physical properties and application of three different FGs. Carboxylated (C-xy) graphene was synthesized via photochemical modification of graphene oxide (GO) films [1]. By the means of various spectroscopy methods and electron microscopy it is demonstrated that C-xy graphene is presented by perforated graphene layers grafted with up to 11 at.% of carboxyl groups [2]. The valence band structure and work function of C-xy graphene is determined to significantly differ from the ones in pristine graphene. Further studies has shown that grafting of C-xy graphene with aptamers can be performed, allowing manufacturing of viral biosensors. The second FG, carbonylated (C-ny) graphene with up to 11 at.% of carbonyl groups was synthesized via wet-chemistry GO modification [3]. This FG exhibits low conductivity and highly defective structure. Nevertheless, C-ny graphene is determined to be an efficient frame for obtaining luminescent films by non-covalent bonding with lanthanide  $\beta$ -diketonate complexes. Aminated graphene (Am) with up to 5 at.% of amine groups is a third member of CFs family obtained via the two-step liquid phase GO reduction. The presence of amines is shown to allow Am graphene grafting with fullerenes or dyes. Considering high conductivity of up to 280 S/m this makes Am graphene to be a perfect candidate for formation of various optoelectronic devices and photovoltaic systems.

Thus, FGs appears to be a versatile platform for the formation of graphene-based structures and rigorous study of graphene physical properties. At the same time, only the initial steps are done in this field and synthesis of new types of FGs is of a high interest nowadays.

The presented work was financially supported by the Russian Foundation for Basic Research (grant no. 18-29-19172). The experiments were carried out on the equipment of the Joint Research Center "Materials science and characterization in advanced technology" and the Unique Scientific Equipment "Kurchatov Synchrotron Radiation Source".

### References

1. A. E. Aleksenskii, S. P. Vul', A. T. Dideikin, V. I. Sakharov, I. T. Serenkov, M. K. Rabchinskii, V. V. Afrosimov. *Nanosyst.: Phys., Chem., Math.* (2016) 7, 81–86.
2. M. K. Rabchinskii, V. V. Shnitov, A.T. Dideikin, A. E. Aleksenskii, S. P. Vul', M. V. Baidakova, I. I. Pronin, D. A. Kirilenko, P. N. Brunkov, J. Weise, and S. L. Molodtsov. *J. Phys. Chem. C* (2016) 120, 28261-28269.
3. M. K. Rabchinskii, A. T. Dideikin, D. A. Kirilenko, M. V. Baidakova, V. V. Shnitov, F. Roth, S. V. Konyakhin, N. A. Besedina, S. I. Pavlov, R. A. Kuricyn, N. M. Lebedeva, P. N. Brunkov and Al. Ya. Vul'. *Scientific Reports* (2018), 8, 14154.

## Nitrogen incorporation in carbon structures by plasma post treatment.

*Stanislav A. Evlashin*<sup>1</sup>, *Yurii M. Maksimov*<sup>2</sup>, *Pavel V. Dyakonov*<sup>3</sup>, *Konstantin I. Maslakov*<sup>2</sup>, *Yuri A. Mankelevich*<sup>3</sup>, *Ekaterina N. Voronina*<sup>3,4</sup>, *Sergei V. Vavilov*<sup>5,6</sup>, *Alexander A. Pavlov*<sup>7</sup>, *Elena V. Zenova*<sup>7</sup>, *Iskander S. Akhatov*<sup>1</sup>, *Nikolay V. Suetin*<sup>3</sup>

*s.evlashin@skoltech.ru*

<sup>1</sup> Center for Design, Manufacturing & Materials, Skolkovo Institute of Science and Technology, Moscow, Russia

<sup>2</sup> Department of Chemistry, Lomonosov Moscow State University, Moscow, Russia

<sup>3</sup> Skobeltsyn Institute of Nuclear Physics, Lomonosov Moscow State University, Moscow, Russia

<sup>4</sup> Faculty of Physics, Lomonosov Moscow State University, Moscow, Russia

<sup>5</sup> Center for Electrochemical Energy Storage, Skolkovo Institute of Science and Technology, Moscow, Russia

<sup>6</sup> Moscow Institute of Physics and Technology, Moscow, Russia

<sup>7</sup> Institute of microelectronics and nanotechnology, Russian Academy of Science, Moscow, Russia

Each year demand for stable and powerful electrochemical sources is growing rapidly. New materials are being developed to increase stability and specific capacitance of electrochemical resources. Doping electrodes with other during fabrication or as a post treatment can become an alternative to existing techniques. In this study, we investigate incorporation of nitrogen and oxygen atoms inside graphene and highly oriented pyrolytic graphite. For doping we use DC plasma in various atmospheres. Structural characteristics of the samples were analyzed by Raman and X-ray photoluminescence spectroscopies. The obtained data demonstrate incorporation of about 3 at, % nitrogen in carbon lattice. These values influence the capacitance of energy sources dramatically. The capacitance of the sample has increased by the order of 6 and reached 600 F/g. These values are close to the best-achieved results. Incorporation of nitrogen and oxygen has been explained by DFT numerical simulation[1]. They were performed in VASP (Vienna Ab initio Simulation Package) code and ORCA software. DFT simulation results are in a good agreement with experimental data. DC Plasma post treatment of carbon-based structures can be used for improvement of the specific capacitances of electrodes. Scalability of the process allows mass production of electrodes for supercapacitors.

This work was supported by Russian Foundation for Basic Research 17-08-01414 A.

### References

1. Evlashin, S. et. al. N-Doped Carbon NanoWalls for Power Sources. *Scientific reports*, 2019, In Progress

## **Influence of molecular oxygen on oriented and mismatched graphene on Co(0001)**

*Shevelev V.O.<sup>1</sup>, Bokai K. A.<sup>1</sup>, Vilkov O. Yu.<sup>1</sup>, Usachov D. Yu.<sup>1</sup>*

*victorshevelev@yandex.ru*

<sup>1</sup> Saint Petersburg State University, Saint Petersburg, Russia

One of the most used method of epitaxial growth of graphene on transition metal surfaces is a chemical vapor deposition (CVD). It allows to product highly uniform films with large area. The interface of graphene with metals has a huge potential to realize spin-polarizing device contacts, magnetism and superconductivity. Though, the strong interaction in most graphene-metal interfaces breaks the characteristic linear  $\pi$  bands of graphene that give rise to high-mobility massless Dirac quasiparticles. Intercalation of atoms or molecules in between graphene-metal interfaces can decrease this interaction and still remains in focus of research. There are a number of works dedicated to investigation of oxygen intercalations in the cases of graphene on Ru, Cu, and Ir substrates, characterized by weak interaction between graphene and substrate. The other notable interface is graphene/Ni(111). Recent findings showed that oxygen intercalation of this interface clarify the role of rotated domains in intercalation process [1]. Likewise, intriguing interface for spin-based devices is graphene/Co(0001) [2]. Here oriented graphene, in contrast to one on Ni(111) surface, possess strong sublattice asymmetry [3] which may affect the adsorption and intercalation of oxygen. Nevertheless, this topic has not received any attention yet.

Herein, we demonstrate comprehensive study of intercalation of oriented and misoriented graphene on Co(0001) with molecular oxygen. We have found, that in both cases annealing of samples in oxygen atmosphere leads to intercalation of oxygen atoms under graphene which results in notable weakening of the interaction between graphene and substrate. In the case of misoriented graphene oxygen intercalation was accompanied by termination of graphene domain boundaries by oxygen atoms. In the case of well oriented graphene termination of boundaries was not detected, pointing to preserve the integrity of most graphene layer. In the both cases prolonged annealing led to partial etching of graphene, that results in formation of carbonates. Besides that XPS and PEEM studies demonstrated appearance of stoichiometric and non-stoichiometric Co oxides, the latter were formed in the areas of Co, not covered by graphene. Moreover, micro-NEXAFS has shown an absence of detectable amount of oxygen under graphene. These facts allow us to conclude that in the case of Co surface, covered by graphene, the latter is able to efficiently prevent the formation of bulk Co oxides even during annealing of the sample in oxygen atmosphere.

This work was supported by Saint Petersburg State University Grant 11.65.42.2017 and RFBR Grant No. 17-02-00427 A.

### **References**

1. Bignardi, P. Lacovig, M. Dalmiglio, F. Orlando, A. Ghafari, L. Petaccia, A. Baraldi, R. Larciprete, and S. Lizzit, *2D Mater.* 4, 025106 (2017)
2. V. Kamalakar, A. Dankert, J. Bergsten, T. Ive, and S. P. Dash, *Sci. Rep.* 4, 1 (2014)
3. Y. Usachov, A. V. Fedorov, O. Y. Vilkov, A. E. Petukhov, A. G. Rybkin, A. Ernst, M. M. Otrokov, E. V. Chulkov, I. I. Ogorodnikov, M. V. Kuznetsov, L. V. Yashina, E. Y. Kataev, A. V. Erofeevskaya, V. Y. Voroshnin, V. K. Adamchuk, C. Laubschat, and D. V. Vyalikh, *16*, 4535 (2016)

## Swelling of graphene oxide membranes in alcohols: effects of molecule size and ageing.

Iakunkov A.<sup>1</sup>, Sun Jinhua<sup>1</sup>, Boulanger Nicolas<sup>1</sup>, Rebrikova Anastasia<sup>2</sup>, Korobov Mikhail<sup>2</sup>, Talyzin Alexandr V.<sup>1</sup>

alexandr.talyzin@physics.umu.se

<sup>1</sup> Department of Physics, Umea University, Umea, SE-901 87, Sweden

<sup>2</sup> Department of Chemistry, Moscow State University, Leninskie Gory 1-3, Moscow 119991, Russia

Swelling of multilayered graphene oxide (GO) membranes is directly related to the size of “permeation channels” which enable diffusion of solvents and solutions. As demonstrated in earlier studies the interlayer distance of Brodie graphite oxides immersed in liquid alcohols increases proportionally to the length of molecules providing multilayered intercalation<sup>1</sup> with interlayer distances up to  $\sim 50\text{\AA}$ .<sup>2</sup> However, GO membranes and graphite oxides are materials with different swelling properties.<sup>3</sup> Therefore, we performed XRD study of swelling for Hummers graphite oxides and graphene oxide (HGO) membranes in a set of progressively longer liquid alcohols (methanol to 1-nonanol). Both precursor graphite oxides and freshly prepared HGO membranes were found to swell in the whole set of liquid alcohols with increase of interlayer spacing from  $\sim 7\text{\AA}$  (solvent free) up to  $\sim 26\text{\AA}$  (in 1-nonanol). Pronounced ageing effects were observed for membranes stored on air for periods over 3-6 months with significant sample to sample variations. The HGO membranes and thin films stored at ambient conditions for 5 years showed nearly complete absence of swelling in all alcohols but preserved swelling in water. In contrast, graphite oxide powders showed unmodified swelling in alcohols even after 4 years of air storage. Ageing of GO membranes during on air storage can be one of reasons for strong scatter of permeation properties reported over past years. Standardization of drying and storage conditions is required for better reproducibility of experiments with GO membranes.

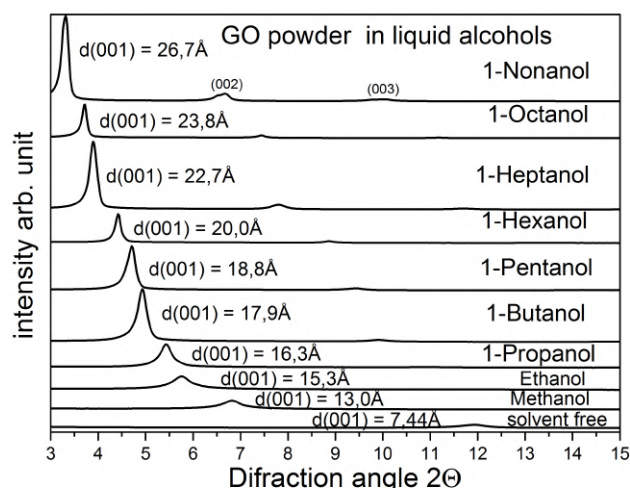


Fig.1. XRD patterns recorded from of GO powder immersed in excess of liquid alcohols (CuKalfa radiation)

### References

1. Klechikov, A.; Sun, J. H.; Baburin, I. A.; Seifert, G.; Rebrikova, A. T.; Avramenko, N. V.; Korobov, M. V.; Talyzin, A.V., *Nanoscale* 2017, 9 (20), 6929-6936.
2. Garcia, A. R.; Canoruiz, J.; Macewan, D. M. C., *Nature* 1964, 203 (494), 1063-1064.
3. Talyzin, A. V.; Hausmaninger, T.; You, S. J.; Szabo, T., *Nanoscale* 2014, 6 (1), 272-281

## **Harnessing the Mechanism of Graphene Oxide Formation. The Role of Water.**

*Dimiev Ayrat*<sup>1</sup>, *Shukhina Ksenia*<sup>1</sup>, *Khannanov Artur*<sup>1</sup>

AMDimiev@kpfu.ru

<sup>1</sup> Kazan Federal University, Kazan, Russia

Graphene Oxide (GO) has become one of the most studied materials of the last decade, being successfully tested for numerous applications. GO is formed by oxidizing graphite by potassium permanganate in concentrated sulfuric acid media. Recently we demonstrated that conversion of graphite to GO involves three distinct steps: formation of stage-1 graphite intercalation compound (GIC), conversion of stage-1 GIC to pristine graphite oxide, and delamination of PGO with its conversion to GO upon exposure to water.<sup>1,2</sup> The most intriguing and most elusive step in this process is the second one, resulting in formation of the covalent C-O bonds. In this study, we investigate the role of water in this process by monitoring the reaction in-situ by optical and Raman microscopy. We demonstrate that the rate of reaction, and the structure of GO product highly depend on the concentration of sulfuric acid. The rate of the reaction is the highest in the range of the sulfuric acid concentrations 88-92%. At the acid concentrations <80%, graphite is not oxidized because the stage-1 GIC condition is not attained due to the low Red-Ox potential of the acid. At the same time, reaction does not proceed at all at the acid concentrations >100%, elucidation the important role of water in the process. Finally, we arrive to conclusion that the actual oxidizing agent species, attacking carbon atoms, are not derivatives of permanganate anion in sulfuric acid, as it is commonly believed, but water molecules. Moreover, we demonstrate that the step of covalent oxidation is reversible: the as-formed C-O bonds can be easily cleaved with reinstating the original intact graphene structure.

### **References**

1. Dimiev, A.M.; Tour, J.M. Mechanism of graphene oxide formation. *ACS Nano*, 2014, 8, 3060.
2. Dimiev A.M. Mechanism of Formation and Chemical Structure of Graphene Oxide, in *Graphene Oxide. Fundamental and Applications* edited by Dimiev, A.M.; Eigler, S. Wiley and Sons, London, 2016.

## Hot pressing synthesis of MoS<sub>2</sub>/perforated graphene materials for efficient Li-ion batteries

*Stolyarova S.G.<sup>1</sup>, Koroteev V.O.<sup>2</sup>, Okotrub A.V.<sup>1,3</sup>, Bulusheva L.G.<sup>1,3</sup>*

*stolyarova@niic.nsc.ru*

<sup>1</sup> Nikolaev Institute of Inorganic Chemistry SB RAS, Novosibirsk, Russia

<sup>2</sup> CIC nanoGUNE Consolider, Donostia-San Sebastian, Spain

<sup>3</sup> Novosibirsk State University, Russia

Lithium-ion batteries (LIB) are widely used as power sources for portable devices due to the small size of lithium ion and the higher voltage of these batteries as compared to lead and nickel batteries. To ensure a lasting operation of modern devices and to supply new, more powerful devices, electrode materials with high capacities and energy densities are required. The generation of electrical energy in LIB occurs because of extraction of lithium ions from the anode material, and this process determines the characteristics of the battery. MoS<sub>2</sub>/C composites are most promising as an anode material due to the high capacity of the sulfide component and its stabilization on the surface of conductive carbon component (C). The interface between MoS<sub>2</sub> and carbon plays an important role in the operation of the hybrid material as the LIB anode. The interface must provide stability, conductivity, and electroactivity of the anode material.

To improve these parameters, we have proposed to strengthen the interfacial interactions between carbon and MoS<sub>2</sub> components by using perforated graphene material (HG) [1] as electrically conductive support for MoS<sub>2</sub> and applying temperature along with reaction components compression during the synthesis [2]. The initial composites obtained by precipitation of MoS<sub>3</sub> on the HG surface were annealed in a pressing mould at 400-600 ° C and 100 bar. A study of the products of the synthesis revealed the formation of covalent C - Mo bonds, which lead to the stabilization of MoS<sub>2</sub> nanoparticles at the boundaries of nanoscale holes present in graphene layers. Compression of the reagents contributes to the formation of a thinner MoS<sub>2</sub> coating, compared with the samples synthesized without mechanical pressure. The number of layers and the lateral size of MoS<sub>2</sub> crystals depend on the synthesis temperature. Tests of hybrid materials in Li-ion half-cells revealed the higher values of the specific capacity of MoS<sub>2</sub>/HG synthesized under pressure. A strong interaction between the components prevents destruction of MoS<sub>2</sub> during the discharge/charge of electrodes and leads to an increase in the specific capacity up to 900 mAh/g at a current density of 0.1 A/g.

*The work was conducted with financial support from the Russian Science Foundation (Grant 16-13-00016)*

### References

1. G. Bulusheva, S.G. Stolyarova, A.L. Chuvilin, Y. V. Shubin, I.P. Asanov, A.M. Sorokin, M.S. Mel'gunov, S. Zhang, Y. Dong, X. Chen, H. Song, A.V. Okotrub, Creation of nanosized holes in graphene planes for improvement of rate capability of lithium-ion batteries, *Nanotechnology* 29 (2018) 134001.
2. S.G. Stolyarova, A. V. Okotrub, Y. V. Shubin, I.P. Asanov, A.A. Galitsky, L.G. Bulusheva, Effect of Hot-Pressing on the Electrochemical Performance of Multilayer Holey Graphene Materials in Li-ion Batteries, *Phys. Status Solidi B* 255 (2018) 1700262. doi:10.1002/pssb.201800202.



## Impact structure of carbon nanotubes on their electrochemical properties

*Kuznetsova V.R.*<sup>1,2</sup>, *Lobiak E.V.*<sup>1</sup>, *Bulusheva L.G.*<sup>1,3</sup>, *Okotrub A.V.*<sup>1,3</sup>

*kuznetsova.viktoriya.98@mail.ru*

<sup>1</sup> Nikolaev Institute of Inorganic Chemistry of the Siberian Branch of the Russian Academy of Sciences, Novosibirsk, Russia

<sup>2</sup> Novosibirsk State Technical University, Novosibirsk, Russia

<sup>3</sup> Novosibirsk State University, Novosibirsk, Russia

Carbon nanotubes (CNT) have exceptional mechanical, thermal and electronic properties. The application of CNTs most widely employed so far has been the construction of various detection devices, such as gas sensors, electrochemical detectors and biosensors with immobilized biomolecules [1]. Properties and specification of such devices are defined by the structure of the CNT, of which they are made.

Unique properties of carbon nanotubes (CNTs) such as high conductivity, nanotexture, and resiliency are very beneficial for electrochemical applications where pure CNTs and/or their composites play the role of electrode material [2]. Depending on the type of CNT, their properties and application differ. Single-wall carbon nanotubes (SWCNTs) have peculiar electronic transport, high current-carrying capability, small intrinsic capacitance, and extraordinary thermal and mechanical properties. Therefore, SWCNT use as material for electronics and lithium ion batteries [3]. Multi-wall carbon nanotubes (MWCNTs) have employed as conductive additive for the layer-structured compound that has been widely used as very effective cathode material. MWCNTs reduce the resistance and improving the electrochemical performance of the composite cathode [4].

In the present research, MgO supported e-Keggin type polyoxomolybdate clusters were used as a catalyst precursor for the CCVD synthesis of CNTs. The advantages of these catalysts is that, there have molecular clusters structure for the formation of discrete catalyst particles with a controlled size [5].

The influence of temperature, gas flow rates and gas ratio on structure of CNT were discovered in the present work. The materials were tested as electrode materials for a supercapacitor performance. The deformation leads to significant changes in electrical conductivity: with an increasing deformation of CNT, its conductivity decreases.

The work was partially supported by the Russian Foundation for Basic Research (grant № 18-33-01053).

### References

- [1] P.C. Matter, *Physics Condensed Matter*, **15** (2003), p. 3011-3035
- [2] G. Lota, K. Fic, E. Frackowiak, *Energy and Environ. Sci.*, **4** (2011), p. 1592-1605
- [3] M. Trojanowicz, *TrAC*, **25** (2006), p. 480-489
- [4] X. Liu, Z. Huang, S. Oh, B. Zhang, P. Ma, M. Yuen, J. Kim, *Composites Science and Technology* **72** (2012), p. 121-144
- [5] E.V. Lobiak, E.V. Shlyakhova, L.G. Bulusheva, P.E. Plyusnin, Y.V. Shubin, A.V. Okotrub, *J. Alloys Compd.*, **621** (2015), p.351-356.

## Thermoelectric properties of single-wall carbon nanotube thin films obtained by vacuum filtration

*Tambasov I.A.*<sup>1</sup>, *Voronin A.S.*<sup>2</sup>, *Evsevskaya N.P.*<sup>1,3</sup>, *Tambasova E.V.*<sup>4</sup>

*tambasov\_igor@mail.ru*

<sup>1</sup> Kirensky Institute of Physics, Federal Research Center KSC Siberian Branch of Russian Academy of Sciences, Krasnoyarsk, Russia

<sup>2</sup> Krasnoyarsk Scientific Center, Federal Research Center KSC Siberian Branch of Russian Academy of Sciences, Krasnoyarsk, Russia

<sup>3</sup> Institute of Chemistry and Chemical Technology, Federal Research Center KSC Siberian Branch of Russian Academy of Sciences, Krasnoyarsk, Russia

<sup>4</sup> Reshetnev Siberian State University of Sciences and Technologies, Krasnoyarsk, Russia

The nanostructured materials based on single-wall carbon nanotubes (SWCNTs) and nanocomposites based on them are very promising for thermoelectric applications. This is because a high value of Seebeck coefficient was found for semiconducting single-walled carbon nanotubes.

In the present study, we have separated industrially accessible SWCNTs into semiconducting and metallic fractions by using aqueous two-phase extraction. In addition, thin films based on unseparated, semiconducting and metallic SWCNTs were obtained by vacuum filtration. The microstructure, optical transmittance and thermoelectric properties of thin films were investigated.

Fig. 1 shows the method for preparing thin SWCNT films and the temperature dependence of the thin SWCNT film power factor.

It was found that the largest Seebeck coefficient was observed for thin films based on semiconducting SWCNTs. The maximum Seebeck coefficient was 98  $\mu\text{V}/\text{K}$  at the temperature of 170 C. The power factor for a thin *un*-SWCNT film was 213  $\mu\text{W}\cdot\text{m}^{-1}\cdot\text{K}^{-2}$  at room temperature. However, as the temperature increased, the power factor decreased down to 54  $\mu\text{W}\cdot\text{m}^{-1}\cdot\text{K}^{-2}$  at the temperature of 200 C. The power factor for thin *m*-SWCNT film was 47 and 74  $\mu\text{W}\cdot\text{m}^{-1}\cdot\text{K}^{-2}$  at room temperature and 200 C, respectively. The maximum power factor for a thin *sc*-SWCNT film was 2.8  $\mu\text{W}\cdot\text{m}^{-1}\cdot\text{K}^{-2}$  at 160 C. We believe that the thin films obtained from industrially available SWCNTs might become the basis for the manufacture of highly efficient thermoelectric nanocomposite materials.

### Acknowledgements

The study was carried out by a grant of Russian Science Foundation (project No. 17-72-10079).

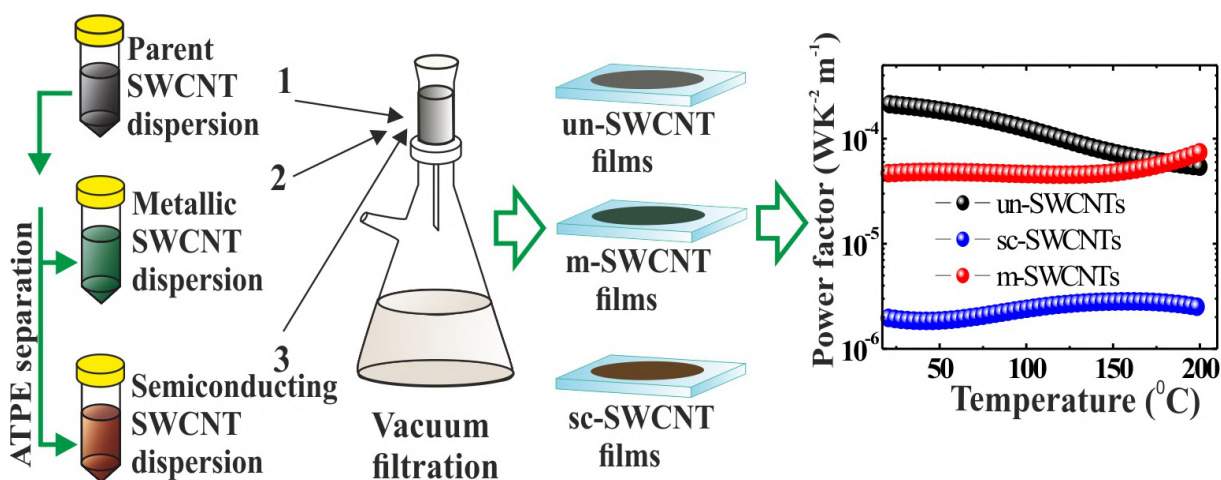


Fig. 1. A block diagram of the process of thin SWCNT film formation and the temperature dependence of the thin SWCNT film power factor.

## AFM Ultradensification of SWCNT network. Optical and mechanical properties.

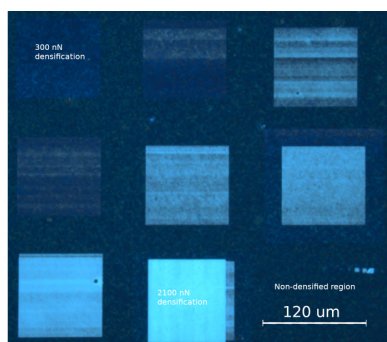
*Grebenko A.K.*<sup>1</sup>, *Zhukov S.V.*<sup>2</sup>, *Nasibulin A.G.*<sup>1</sup>

*artem.grebenko@skoltech.ru*

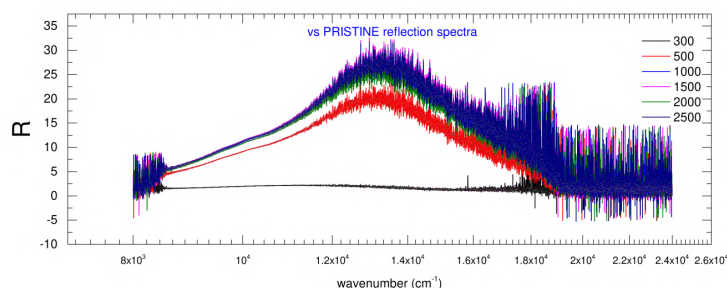
<sup>1</sup> Laboratory of Nanomaterials, Center for Photonics and Quantum Materials, Skolkovo Institute of Science and Technology, Moscow, Russia

<sup>2</sup> Terahertz Laboratory, Moscow Institute of Physics and Technologies, Dolgoprudniy, Russia

We report novel and unique method of the localized modification of SWCNT film by the means of Atomic Force Microscope (AFM) force lithography. By controlling the tip-film interaction force it is possible to create regions with highly increased reflective properties both in visible and infrared regions, keeping at the same time transmittance and conductivity of the film on the roughly same level as before modification. Such modification can be utilized for the creation of all-carbon static holograms, diffraction lattices and photonic crystals. We report the detailed spectroscopic analysis of the tubes modification in infrared, visible and THz ranges and structural data from the neutron scattering. We demonstrate the possible structures, that can be created by such modification and prove, that after the modification no extra phase appears in the matter of the film. The authors acknowledge Skoltech NGP Program (Skoltech-MIT joint project)



a



b

a) Photograph illustrating several ~90 μm squares pressed by AFM with different cantilever pressure in the 60% (transparency) SWCNT film. b) Reflectance spectra of densified regions in dependence of the modification force level.

## Electronic properties of filled single-walled carbon nanotubes

*Kharlamova M.V.<sup>1</sup>, Kramberger C.<sup>2</sup>, Eder D.<sup>1</sup>*

*mv.kharlamova@gmail.com*

<sup>1</sup> Institute of Materials Chemistry, Vienna University of Technology, Vienna, Austria

<sup>2</sup> Faculty of Physics, University of Vienna, Vienna, Austria

Single-walled carbon nanotubes (SWCNTs) possess outstanding chemical, physical and mechanical properties, which can find applications in different fields, for instance, nanoelectronics. The properties of SWCNTs are completely dependent on their atomic structure. As-synthesized nanotube samples usually contain mixtures of nanotubes with different atomic structure and electronic properties. This causes inhomogeneity of their properties and limits their applications.

Several methods have been established for the controllable modification of the electronic properties of SWCNTs. They include chemisorption and physisorption on the outer surface of SWCNTs, substitution of atoms in walls of SWCNTs, intercalation of SWCNT bundles and filling of internal channels of SWCNTs. Among these methods, the filling of nanotube channels is a very promising method for tailoring the electronic properties of SWCNTs, because a variety of substances with appropriate properties can be encapsulated inside nanotubes [1].

In this work, we perform the filling of metallicity mixed and sorted SWCNTs with d-metal halogenides by a capillary technique using the melts of the salts. We study the influence of the encapsulated compounds on the electronic properties of SWCNTs [2, 3]. High-resolution transmission electron microscopy proves the high-yield filling of SWCNTs and formation of one-dimensional nanocrystals of the salts. X-ray photoelectron spectroscopy (XPS) confirms the chemical composition of the introduced compounds. We show that the filling of SWCNTs leads to the modification of Raman modes of nanotubes. The shifts of the peaks and alteration of the profile of radial breathing mode and G-band of Raman spectra testify to a strong doping of SWCNTs. XPS proves that the encapsulated salts lead to p-doping of SWCNTs accompanied by the downshift of their Fermi level and the charge transfer from nanotubes to the encapsulated compound.

The obtained information about the influence of the filler on the electronic properties of SWCNTs is elemental for applications of nanotubes in nanoelectronic devices.

### References

1. M.V. Kharlamova, *Prog. Mater. Sci.* (2016) **77**, 125.
2. M.V. Kharlamova, C. Kramberger, O. Domanov, A. Mittelberger, K. Yanagi, T. Pichler, D. Eder, *J. Mater. Sci.* (2018) **53**, 13018.
3. M.V. Kharlamova, C. Kramberger, A. Mittelberger, K. Yanagi, T. Pichler, D. Eder, *J. Spectrosc.* (2018) **2018**, 5987428.

## Multiregime pulse fiber laser based on electrochemically gated carbon nanotube saturable absorber

*Mkrtchyan A. A.*<sup>1</sup>, *Gladush Y. G.*<sup>1</sup>, *Kopylova D. S.*<sup>1</sup>, *Khabushev E. M.*<sup>1</sup>, *Ivanenko A. V.*<sup>2</sup>, *Nyushkov B. N.*<sup>2</sup>, *Kokhanovskiy A. Y.*<sup>2</sup>, *Kobtsev S. M.*<sup>2</sup>, *Nasibulin A. G.*<sup>1,3</sup>

*aram.mkrtchyan@skoltech.ru*

<sup>1</sup> Skolkovo Institute of Science and Technology, 121205 Moscow, Russia

<sup>2</sup> Novosibirsk State University, 630090 Novosibirsk, Russia

<sup>3</sup> Aalto University, 02150 Espoo, Finland

Pulse lasing driven by a real saturable absorber (SA) in a fibre laser cavity is conditional on modulation characteristics determined by the nonlinear material and implementation geometry of the SA. Generally, these parameters can be only preset during the SA fabrication. For instance, modulation depth of a single-wall carbon nanotube saturable absorber (SWCNT-SA) transferred on a D-shape fiber is governed by its thickness and length [1]. Here we demonstrate electronic control of pulse lasing regimes in an all-PM fibre laser by using an original electrochemically gated in-line SWCNT-SA.

To prepare a SWCNT-based electrochemical cell we used high quality aerosol synthesized SWCNTs collected on the cellulose filter directly from the reactor zone. SWCNTs were dry-transferred on a polarization maintaining side-polished fiber, then covered by ionic liquid, encapsulated and implemented it into the fiber laser (Fig. 1a). By applying the voltage on the SWCNT-SA we were able to switch the laser operation between the sub-picosecond mode-lock and microsecond Q-switch regimes [2]. In Fig. 1b shown the optical spectra of these regimes. A transmittance-correlated map of the voltage-induced switching between the pulse lasing regimes is shown in Fig. 1c. Thus, effective electronic control of pulse lasing in fibre lasers with the gated SWCNT-SA was established.

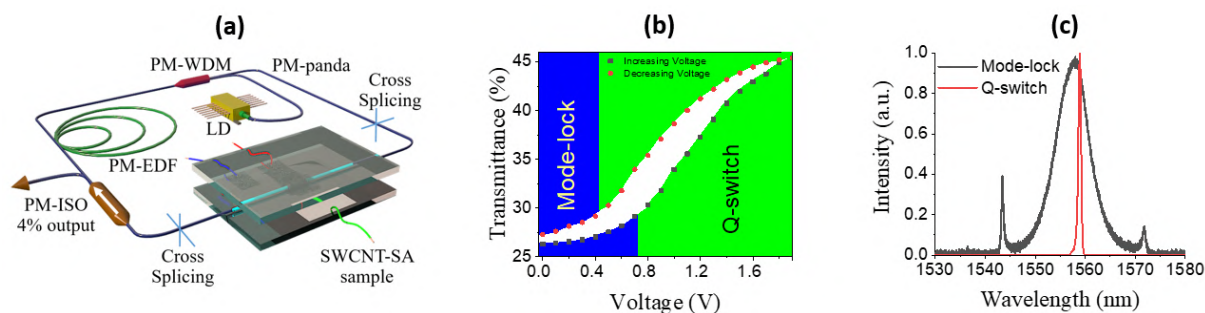


Figure 1. (a) Scheme of the fiber laser with a gated SWCNT-SA; (b) SWCNT-SA sample linear transmittance depending on the voltage. Colour corresponds to the generation regime depending on the voltage; (c) Optical spectra measured both in Mode-lock and Q-switch regimes

### References

1. Aram A. Mkrtchyan, Yuriy G. Gladush, Diana Galiakhmetova, Vsevolod Yakovlev, Vadim T. Ahtyamov, and Albert G. Nasibulin, *Opt. Mater. Express* (2019) **9**, 1551
2. Eun Jung Lee, Sun Young Choi, Hwanseong Jeong, Nam Hun Park, Woongbin Yim, Mi Hye Kim, Jae-Ku Park, Suyeon Son, Sukang Bae, Sang Jin Kim, Kwanil Lee, Yeong Hwan Ahn, Kwang Jun Ahn, Byung Hee Hong, Ji-Yong Park, Fabian Rotermund, Dong-Il Yeom, *Nat. Commun.* (2015), **6**, 6851

---

## **New Frontiers in Single-walled Carbon Nanotubes Applications**

*Bezrodny A.E.*<sup>1</sup>, *Predtechensky M.R.*<sup>1,2</sup>

*bezrodny.ae@ocsial.com*

<sup>1</sup> OCSiAl Group, Novosibirsk, Russia

<sup>2</sup> Institute of Thermophysics SB RAS, Novosibirsk, Russia

Despite the rich history and the outstanding mechanical and electrical properties of SWCNT, their commercialization has been quite slow, mainly because of the prohibitively high cost and poor quality of SWCNT materials with scantily defined standards and their control. Besides, the challenge of introducing SWCNTs into different systems has not been commercially addressed. Untreated SWCNTs represent themselves as the entangled mesh of interbound bundles and the task of their efficient dispersion into polymer matrices requires special approaches.

In this presentation, we demonstrate that the recent developments in synthesis of high quality SWCNT and their processing into intermediate products, including purification, dispersion in liquids, polymers, and various special matrices offer a broad spectrum of their application. We illustrate a few successful examples of such applications: dramatic improvement of electrical properties, enhancement mechanical properties, batteries performance etc. We believe that the affordability of SWCNTs and the intermediate products should ensure market acceptance and stimulate further scientific research leading to novel applications.

## Characterization of Carbon Materials with Confotec® MR200 Confocal Raman Microscop

*Kopachevsky V.D.<sup>1</sup>, Kudryakov A.V.<sup>1</sup>, Grigorenko A.M.<sup>1</sup>, Gvozdev A. A.<sup>1</sup>, Shashkov S.N.<sup>1</sup>*

*sales@solinstruments.com*

<sup>1</sup> SOL instruments Ltd., Minsk, Belarus

Confocal Raman microscopy is one of the most fundamental tools of the scientific lab. It is a very powerful analytical technique that can be of great benefit to characterization of carbon materials. Raman instruments are very fast, non-destructive and provide a great deal of flexibility in samples.

We describe in this paper a new Raman microscopy approach (Fig.1), specially developed scanning confocal Raman Microscope Confotec® MR200, which is very compact, (fully integrated with a standard optical microscope) and powerful tool. With a newly designed spectrograph and the recent optical technologies, Confotec® MR200 sensitivity, spatial resolution and spectral calibration accuracy have been highly improved, making it the optimal solution for carbon applications. Confotec® MR200 is the best Raman microscope in its class that deserves the maximum score for the price/quality criterion.

Every lab that is characterizing carbon materials will benefit from having access to such Raman tool.

Fig.1. Scanning Confocal Raman Microscopes Confotec® MR200.



## Studying the effect of weight concentration of CNTs on the heat release mode in self-regulating heaters

*Yagubov V.S.<sup>1</sup>, Shchegolkov A.V.<sup>1</sup>*

*vitya-y@mail.ru*

<sup>1</sup> Tambov State Technical University, Tambov, Russia

Smart materials possessing different functional properties can be widely used in the development of new-generation devices that work without special elements of automatic control. The whole class of such devices can be attributed to electric heaters (heat fans, electrical inventories, electrical heating cables, etc). For them, the property of temperature self-regulation is of special significance.

As the basis of such functional materials, various polymeric matrices modified with carbon nanomaterials (CNMs) are most often used. For instance, in [1], a film heater made of carbon nanotubes (CNTs) is described; it can be used as anti-slip coatings for aviation. In [2], the development of mesoporous and macroporous paper made of a CNTs-modified polymer composite is presented. To obtain heating paper a "Triton X-100" surfactant was used as a binder. In [3], a technique for manufacturing a heating element based on a fluoroplastic modified with a 20- and 35-wt.% paste containing a graphene-like material is reported. In our previously published paper [4], we describe a method for producing a nano-modified composite based on silicone rubber, from which heating element samples having a self-regulation effect were made.

In the present paper, we consider the effect of different concentrations of CNTs, synthesized over different catalysts, on changes in the specific volume and surface resistance. In the course of the research, the regularity of the effect of CNTs weight contents in an elastomer on the change in its electrical resistance was established. A methodology for manufacturing experimental samples based on nano-modified elastomers was developed, as a result of which tests were carried out by applying a constant voltage from two electrodes. Besides, the temperature field was studied at different DC supply voltage on the surface of heating elements made of elastomers containing different CNTs amounts. It was found that the power and heat release of the self-regulating heater increase when increasing the CNTs weight content.

Moreover, it was experimentally proved that when the nanomodified heaters are connected to a DC source, the effect of self-regulation of the temperature on their surface can be observed due to the stabilization of the electric current value.

### References

1. D. Janas and K.K. Koziol, *Carbon* (2013) **59**, 457.
2. H. Chu, Z. Zhang, Y. Liu and J. Leng, *Carbon* (2014) **66**, 154.
3. A. Shchegolkov, N. Paramonova, A. Hrobak, A. Shchegolkov, and A. Tkachev, *AIP Conference Proceedings* (2018), **2041**, 020025
4. V.S Yagubov and A.V. Shchegolkov, *Proceedings of the Voronezh State University of Engineering Technologies* (2018), **80**, 341



## Carbon adsorbents of high density with precision nanoporous structure for adsorption storage systems of methane

*Men'shchikov I.E.<sup>1</sup>, Fomkin A.A.<sup>1</sup>, Shkolin A.V.<sup>1</sup>, Shiryayev A.A.<sup>1</sup>, Petukhova G.A.<sup>1</sup>*

*i.menshchikov@phych.e.ac.ru*

<sup>1</sup> A.N. Frumkin Institute of physical chemistry and electrochemistry of Russian academy of sciences (IPCE), Moscow, Russia

Nanoporous material (adsorbent) with specially adjusted porous structure and surface chemistry demonstrating high activity to methane provided by the principle of volume filling of its micropores by gas molecules is the basis of adsorption storage systems of natural gas, which represent an alternative to known technologies of compressed and liquefied natural gas. The most promising adsorbents today are nanoporous carbon adsorbents of different origin [1]. Bulk (packing) density of an adsorbent, the increase of which provides high volumetric storage capacity of adsorption system, is one of the most important parameters besides main structural-energy properties of porous material [1].

In this work, several samples of nanoporous carbon adsorbents of different genesis (derived from thermosetting plastics, wood, peat, natural coal and silicon carbide) have been synthesized using different activation methods. "Tuning" of nanoporous structure parameters was being performed using data of XRD, SAXS and SEM investigations on each stage of synthesis. Such parameters as effective width ( $X_0$ ) and volume ( $W_0$ ) of micropores, characteristic energy of adsorption ( $E_0$ ) determined on the basis of the Dubinin Theory of volume filling of micropores [1,2] using experimental data of  $N_2$  adsorption at 77 K were used as well. Obtained values of these parameters varied in wide ranges:  $X_0 = 0.8-1.84$  nm,  $W_0 = 0.8-1.8$  cm<sup>3</sup>/g,  $E_0 = 13-30$  kJ/mol. Methane adsorption was measured in the pressure range from 0 to 30 MPa and temperatures from 177 to 360 K on a special volume-gravimetric high-pressure adsorption unit. Samples with the highest adsorption activity to methane were selected for further development of the technology of increasing of their bulk density and obtaining of shaped samples, which were further studied in terms of specific volume capacity, adsorption cyclic stability and mechanical strength.

It was shown, that the most effective adsorbents for methane storage were the materials derived from wood and peat and activated by thermochemical method with further densification under pressure. Specific volumetric storage capacity for methane of the best samples exceeded 220 nm<sup>3</sup>(methane)/m<sup>3</sup>(storage system) at pressures up to 8 MPa and temperature of 273 K. Produced shaped materials (Fig.1) of advanced packing density and specific storage capacity were used for filling of the prototypes of storage systems with further tests [1].

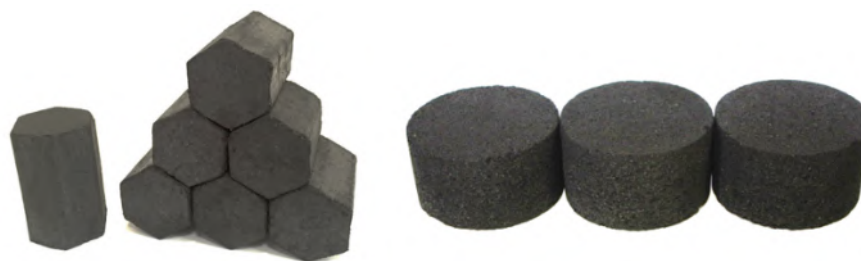


Fig.1. Shaped nanoporous carbon materials of advanced packing density and specific storage capacity.

### References

1. E. Men'shchikov, A. A. Fomkin, A. Yu. Tsvadze, A. V. Shkolin, E. M. Strizhenov and E.V. Khozina, Adsorption, April (2017), **Volume 23**, Issue 2, 327.
2. M. Dubinin, Progress in Surface and Membrane Science (1975), **Volume 9**, 1-70.

## CARBON NANOMATERIALS BASED ON PLANT BIOPOLYMERS AS SORBENTS OF RADIONUCLIDES

Kidalov S.V.<sup>1</sup>, Vozniakovskii A.A.<sup>1</sup>, Vozniakovskii A.P.<sup>2</sup>, Karmanov A.P.<sup>3</sup>, Kocheva L.S.<sup>3</sup>, Rachkova N.G.<sup>3</sup>

voznap@mail.ru

<sup>1</sup> Ioffe Institute, St.Petersburg, Russia

<sup>2</sup> Institute of Synthetic Rubber, Saint-Petersburg, Russia

<sup>3</sup> Institute of Biology of Komi Scientific Centre of the Ural Branch of the Russian Academy of Sciences, Syktyvkar, Russia

The intensive development of nuclear power has led to a sharp increase in the volume of radioactive waste and the pollution of huge amounts of water. For the purification of water from various radionuclides, highly porous carbon sorbents, including graphene materials, are widely used. However, the use of graphene materials for water purification from radionuclides is hampered by the imperfection of the technologies for their production, which do not allow obtaining more material at an affordable price.

The purpose of this study was to study the sorption properties of graphene nanoplatelets (GNP) synthesized by the method of self-propagating high-temperature synthesis (SHS) concerning long-lived heavy radionuclides ( $U^{238}$  and  $Th^{232}$ ). Figure 1 shows the sorption index  $C$  for samples of GNPs obtained from lignin (Clg), starch (CSt) and bark (CB) by the SHS method in relation to heavy  $U^{238}$  and  $Th^{232}$  radionuclides. As can be seen from Figure 1, the use of GNP is the sorption rate  $S$  for these samples is not less than 97% of uranium and thorium, which shows the promise of using the GNP obtained by the SHS method as a sorbent of radionuclides.

This work was supported by the RFBR grant №18-29-24129.

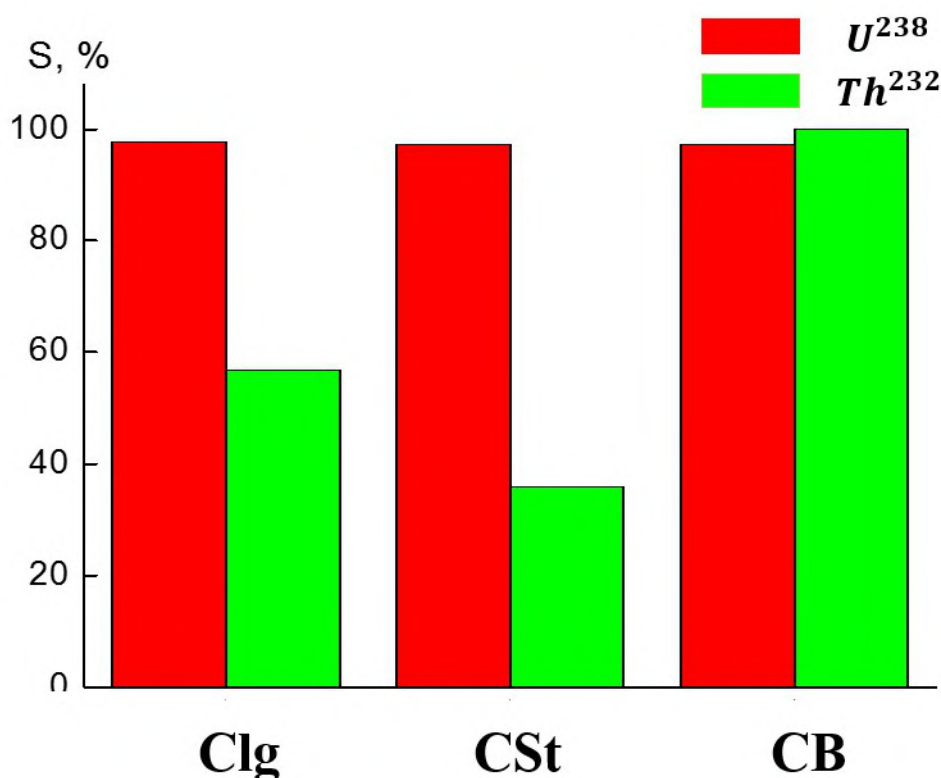


Figure 1. Adsorption index  $S$  for samples CL, CS and CB in relation to  $U^{238}$  and  $Th^{232}$  radionuclides.

**Poster session 1:  
Fullerenes.  
Nanodiamond Particles.**

## Electrophilic trifluoromethylation of fullerene anions: simple, selective, efficient.

*Bogdanov V.P.*<sup>1</sup>, *Dmitrieva V.A.*<sup>1</sup>

*vb@thermo.chem.msu.ru*

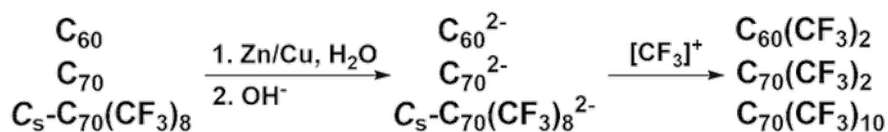
<sup>1</sup> Moscow State University, Moscow, Russia

Trifluoromethylfullerenes (TFMFs) is a vast class of fullerene-based materials with more than 100 characterized compounds only for C<sub>60</sub> and C<sub>70</sub>. However, the synthetic availability of most of them is relatively poor which significantly limits the number of explored applications.

Up until now all of the TFMFs were synthesized in radical reactions with fullerenes, which is a great method for the research on the influence of the CF<sub>3</sub> groups arrangement on the molecule structure, stability and electronic properties but not so much for the production of the particular TFMFs themselves in sufficient quantities. [1] The most popular method of ampoule trifluoromethylation applied to C<sub>70</sub> leads to only several major products such as some isomers of C<sub>70</sub>(CF<sub>3</sub>)<sub>8</sub> and C<sub>70</sub>(CF<sub>3</sub>)<sub>10</sub>, none of which have particularly remarkable properties on their own. [1]

Here we report a new trifluoromethylation method suitable for fullerene anions. The method is based on several electrophilic trifluoromethylation agents such as Togni and Umemoto reagents applied towards C<sub>60</sub>, C<sub>70</sub> and C<sub>s</sub>-C<sub>70</sub>(CF<sub>3</sub>)<sub>8</sub> anions generated from their dihydrides. The patterns of trifluoromethylation are explored and the outlook on the kind of TFMFs becoming accessible by the combination of the nucleophilic and electrophilic trifluoromethylation methods is presented.

*This work was supported by RFBR (grant № 18-33-01192).*



### References

1. O. V. Boltalina, A.A. Popov, I.V. Kuvychko, N.B. Shustova, & S.H. Strauss, *Chemical reviews* (2015), **115(2)**, 1051-1105

## Selective synthesis of dioxane monoadducts of the C<sub>60</sub> and C<sub>70</sub> fullerenes with $\alpha$ -diols in heterogeneous conditions under ultrasonication

*Kinzyabaeva Zemfira S.*<sup>1</sup>, *Sharipov Glus L.*<sup>1</sup>

*zefa5@rambler.ru*

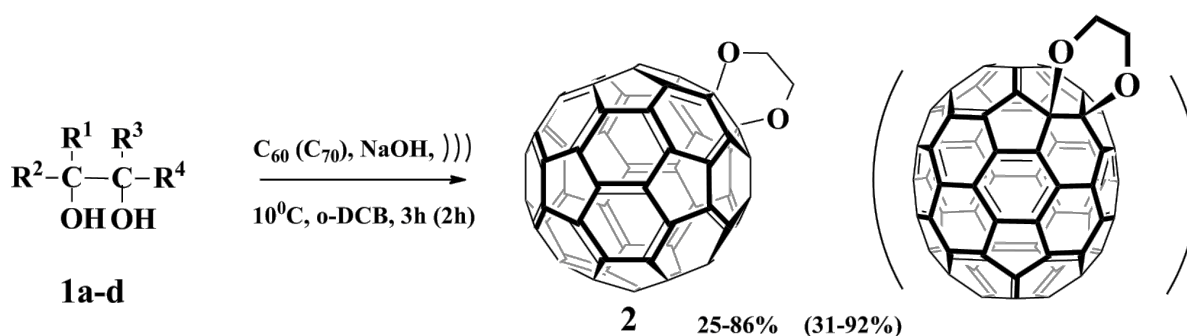
<sup>1</sup> Institute of Petrochemistry and Catalysis, UFRC RAS

Syntheses of the C<sub>60</sub> derivatives containing dioxane moieties are poorly presented in periodicals and there are no works using the ultrasound for the production of such compounds [1-3]. Herewith, the dioxane derivatives of C<sub>70</sub> have not been currently obtained. We have developed a selective and efficient method for the synthesis of 1,9-dihydro[C<sub>60</sub>-I<sub>h</sub>][5,6](1,4-dioxano)fullerene and 5,6-dihydro[C<sub>70</sub>-D<sub>5h(6)</sub>][5,6](1,4-dioxano)fullerene. Our method is based on the heterogeneous reaction of C<sub>60</sub> or C<sub>70</sub> with  $\alpha$ -diols in the presence of solid NaOH under ultrasonication (Scheme).

The use of ultrasound allows the selective addition of the dioxane addend to the fullerene cages with the quantitative yields in heterogeneous media without phase transfer catalysts. The highest yields of compound **2** (86 and 92% for C<sub>60</sub> and C<sub>70</sub>, respectively) are achieved for the ratio of the reactants fullerene:**1a-d**:NaOH = 1:10<sup>3</sup>:62.5. All synthesized compounds have been identified with a set of spectroscopic techniques (MALDI TOF/TOF, one- and two-dimensional <sup>1</sup>H and <sup>13</sup>C NMR, IR, UV-Vis). Based on the <sup>1</sup>H and <sup>13</sup>C NMR and UV-Vis data, we have concluded that the C<sub>70</sub>-dioxane adduct is a 5,6-isomer. If C<sub>60</sub> and **1a** are involved in the sonochemical reaction in *o*-dichlorobenzene without NaOH, we observe the formation of polyadduct C<sub>60</sub>(CH<sub>2</sub>OH)<sub>6</sub> instead of compound **2**. The ultrasonication under room temperature results in a decrease in selectivity of the product **2** formation. When using the substituted diols **1b-1d**, compound **2** is formed with lower yields as compared to the case of **1a**. We explain this fact with the break of the  $\alpha$ -C-C bonds in **1b-1d** when ultrasonicated with the subsequent formation of ethylene glycol **1a**, which is further added to the C<sub>60</sub> or C<sub>70</sub> cages.

Currently, we scrutinize the mechanism of this reaction with EPR and UV spectroscopic methods.

The work was supported with the Russian Foundation for Basic Research (project number 19-03-00716).



**R**<sup>1</sup>, **R**<sup>2</sup>, **R**<sup>3</sup>, **R**<sup>4</sup> = H (**Ia**); **R**<sup>1</sup> = Me, **R**<sup>2</sup>, **R**<sup>3</sup>, **R**<sup>4</sup> = H (**Ib**); **R**<sup>1</sup>, **R**<sup>3</sup> = Me, **R**<sup>2</sup>, **R**<sup>4</sup> = H (**Ic**); **R**<sup>1</sup>, **R**<sup>2</sup>, **R**<sup>3</sup>, **R**<sup>4</sup> = Me (**Id**)

### References

- [1] F. B. Li, X. You, T. X. Liu, G.-W. Wang, *Org. Lett.* 14 (2012) 1800.
- [2] J. Wu, F. B. Li, X. F. Zhang, J. L. Shi, L. Liu, *RSC Adv.* 5 (2015) 30549.
- [3] X.F. Zhang, F.B. Li, J. Wu, J.L. Shi, Z. Liu, L. Liu, *J. Org. Chem.* 80 (2015) 6037.

## Aromatic conjugated fullerenes for organic electronics

*Okolzina A.I.*<sup>1</sup>, *Tulyabaev A.R.*<sup>1</sup>, *Tuktarov A.R.*<sup>1</sup>, *Khalilov L.M.*<sup>1</sup>

*anzhelika\_ok@bk.ru*

<sup>1</sup> Institute of Petrochemistry and Catalysis RAS, Ufa, Russia

Organic solar cells (OSC) with bulk heterojunction (BHJ), which involve donor polymers and acceptor fullerene derivatives, are widely used, because they possess mechanical mobility, low weight, and ease of preparation [1]. A [6,6]-phenyl- $C_{61}$ -butyric acid methyl ester (PCBM) that has enhanced acceptor properties compared to that of initial  $C_{60}$  and proved to be a reference compound in current-voltage measurements was one of the first acceptor fullerene derivatives [2]. Currently, the developed PCBM-poly-3-hexylthiophene system in OSC-BHJ has reached its maximum. Considering that the modification of donor polymers is a rather complex and time-consuming problem, one of the ways to rise the power conversion efficiency (PCE) of OSCs is an increase in energy of LUMO of an acceptor fullerene derivative.

The LUMO energy of new 1,2-dihydrofullerenes **1-8**, bearing aromatic fragments bound to a fullerene core through a double or triple bond, is theoretically assessed in this work with the PBEPBE/6-311G(d,2p) quantum chemical approach to obtain OSC-BHJ with high PCE. We assumed that the addition of an aromatic fragment to a fullerene core through a double or triple bond will lead to a conjugated system of  $\pi$ -orbitals, which will contribute to a better migration of electrons inside it during the conversion of solar energy compared to that of PCBM and its derivatives. The theoretical results obtained in this work will be used in the purposeful synthesis of new promising 1,2-dihydrofullerenes and subsequent current-voltage measurements for their inclusion in the composition of promising OSCs with BHJ.

This work was financially supported by the Russian Foundation for Basic Research (project no. 18-03-00092 A).

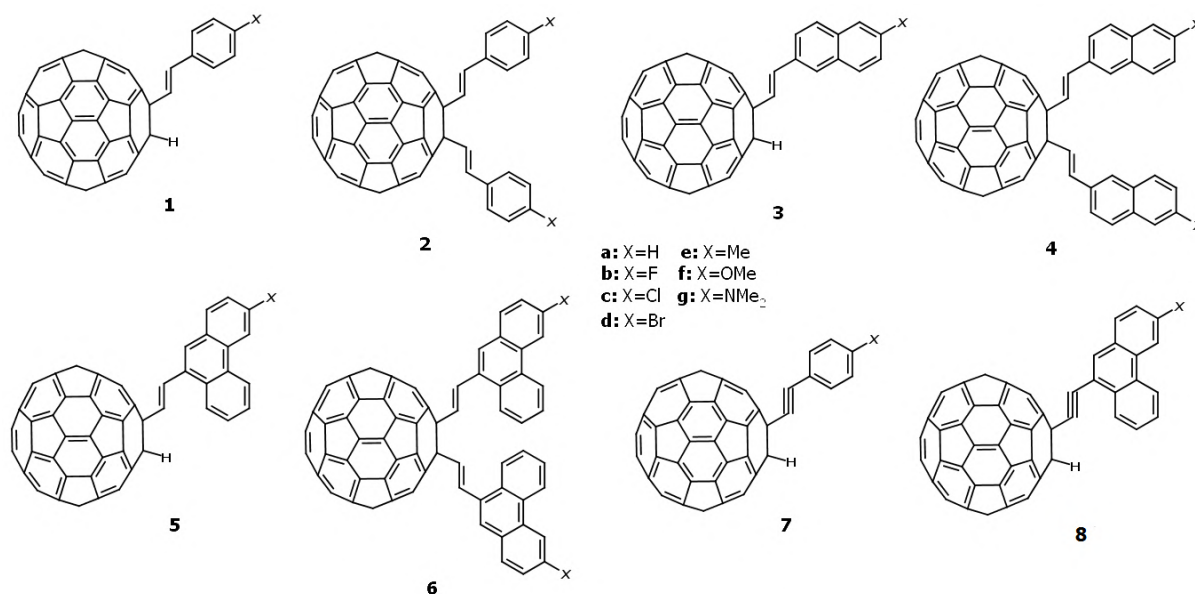


Fig.1. The structure of 1,2-dihydrofullerenes 1-8.

### References

1. R. Ganesamoorthy, G. Sathiyam, and P. Sakthivel, *Sol. Energ. Mat. Sol. C* (2017) **161**, 102.
2. C. Hummelen, B. W. Knight, F. LePeq, F. Wudl, J. Yao, and C. L. Wilkins, *J. Org. Chem.* (1995) **60**, 532.

## Superconductivity in Alkali-Doped Fullerenes with Wood's metal and heterofullerenes with two different alkali metals $A^{(1)}A^{(2)}MC_{60}$

*Kulbachinskii V.A.*<sup>1,2</sup>, *Ezhikov N.S.*<sup>1</sup>, *Lunin R.A.*<sup>1</sup>, *Bulychev B.M.*<sup>3</sup>

*kulb@mig.phys.msu.ru*

<sup>1</sup> M.V. Lomonosov Moscow State University, Low Temperature Physics and Superconductivity Department, 119991, GSP-1, Moscow, Russia

<sup>2</sup> Russia Moscow Institute of Physics and Technology (State University), 141700 Dolgoprudny, Moscow Region, Russia

<sup>3</sup> M.V. Lomonosov Moscow State University, Department of Chemistry, 119991, GSP-1, Moscow, Russia

Alkali-doped fullerenes  $A^{(1)}A^{(2)}A^{(3)}C_{60}$  ( $A^{(i)} = K, Rb, Cs$ ) are superconductors, having the highest superconducting transition temperature  $T_c$  among molecular solids. In potassium-doped  $K_3C_{60}$   $T_c=18$  K,  $T_c=29$  K in  $Rb_3C_{60}$ ,  $T_c$  is 33 K for  $RbCs_2C_{60}$ , and for  $Cs_3C_{60}$  under pressure  $T_c=40$  K has been reported [1]. Substitution one or two alkali atoms in  $A_3C_{60}$  gives possibility to get superconductors with lower or even with higher  $T_c$  as compared with the host fullerene. For example, in fullerene  $K_2LuC_{60}$   $T_c=20$  K [2], that is higher than in the host fullerene  $K_3C_{60}$ . There are a lot of different methods for synthesis of fullerenes. We developed a method of reactions of the liquid gallams (eutectic alloys Ga:In, Ga:Sn, Ga:Bi) with a solution of fullerene in the organic solvents for synthesis the heterofullerenes with one or two alkali metal atoms [3]. Also synthesis is available in the organic solvent from amalgams [4]. The intercalation reaction between the amalgam of intercalated metal run in the organic solvent like toluene or tetrahydrofuran (THF). Heterofullerene  $K_2Hg_xC_{60}$  synthesized by with method is a superconductor with  $T_c=22$  K (higher than for the host  $K_3C_{60}$  [4]).

Here we report our experimental data on the synthesis and investigation of superconductivity in fullerenes and heterofullerenes doped by Wood's metal (W - Sn,Pb,Bi,Cd, melting temperature  $T_m=65^\circ C$ ), alloy Y (Y - Bi,Sn,Pb,In,Cd,Tl -  $T_m=41.5^\circ C$ ) and Tl doped heterofullerenes with two different alkali metals -  $ACsTiC_{60}$  ( $A=K, Rb$ ) Synthesis was carried out in a vacuum full-glass system at  $T=110^\circ C$  in toluene [3] with contact of fullerene solution with liquid metals. Tl participated in the reaction in a form of alloy with alkali metals. All reagents were liquid to allow executing a reaction at reduced temperature. Homogeneity of the composition of obtained compounds is close to the ideal that is especially important for the complicated compounds. Synthesis of the initial alkali metal fullerenes, partial removal of toluene, blending of fullerene suspension with suspension of heterometal halogenide was done in absolute toluene or THF. Drying of products of reaction and packaging in ampoules for measurements were carried out in vacuum. We found superconductivity in heterofullerenes  $K_2W_1C_{60}$  ( $T_c=16$  K),  $Rb_2W_1C_{60}$  ( $T_c=8$  K) and  $K_2Y_1C_{60}$  ( $T_c=8$  K). Also synthesized heterofullerenes with Cesium  $KCsTiC_{60}$  ( $T_c=21.7$  K) and  $RbCsTiC_{60}$  ( $T_c=26.4$  K) are superconductors.

### References

1. Gunnarsson, Reviews of Modern Physics. (1997) **69**, 575.
2. Bulychev B.M., Lunin R.A., Kul'bachinskii V.A., Shpanchenko R.V., Privalov V.I., Russ. Chem. Bull., Int. Ed. (2004) **53**, 1686.
3. Lunin R.A., Velikodny Y.A., Bulychev B.M., Kulbachinskii V.A., Polyhedron. (2015) **102**, 664.
4. Bulychev B.M., Kulbachinskii V.A., Lunin R.A., Kytin V.G., Velikodny Yu.A., Fullerenes, Nanotubes and Carbon Nanostructures, (2010) **18**, 381.

## The photopolymerization rate and activation energy of $C_{60}$ rotations in fullerene and its molecular complexes.

*K. P. Meletov*<sup>1</sup>

*mele@issp.ac.ru*

<sup>1</sup> Institute of Solid State Physics RAS, Chernogolovka, Moscow region 142432, Russia

We have studied the temperature dependence of the photopolymerization rate in pristine  $C_{60}$  and molecular complexes  $\{Pt(dbdtc)_2\}_2 \cdot C_{60}$  and  $\{Pt(nPr_2dtc)_2\} \cdot (C_{60})_2$  by Raman spectroscopy at temperatures 190–330K. The Raman spectra were measured under continuous illumination by 100  $\mu$ W laser power at  $\lambda_{exc}=532$  nm by means of consequent scans with 60 seconds duration. The measurements exhibit an intensity increase of the dimer-related  $A_g(2)$  mode of the  $C_{60}$  molecule and a decrease of the monomer's one. The photopolymer content grows exponentially with the exposure time while the time constant increases with the decrease of temperature. Since the fullerene polymerization related to the 2+2 cycloaddition reaction needs the parallel orientations of double C=C bonds of neighboring molecules, the temperature induced activation of the  $C_{60}$  rotations substantially affects the photopolymerization rate under fixed conditions of laser power, excitation wavelength and beam focusing. Thus, the photopolymerization rate exhibits an activation type temperature dependence. The activation energy  $E_A$  of the photopolymerization time constant, obtained from the Arrhenius dependence of the time constant on the temperature, is found to be  $(0.24 \pm 0.04)$  eV for pristine  $C_{60}$ ,  $(0.13 \pm 0.01)$  eV and  $(0.18 \pm 0.01)$  eV for  $\{Pt(nPr_2dtc)_2\} \cdot (C_{60})_2$  and  $\{Pt(dbdtc)_2\}_2 \cdot C_{60}$  molecular complexes, respectively. The activation energy for pristine  $C_{60}$  is consistent with the energy barrier 0.3 eV between various equilibrium molecular orientations [1], while the decrease of the activation energy for the  $C_{60}$  complexes agrees well with higher stability of the pristine  $C_{60}$  photopolymer [2,3]. **Acknowledgments.** The research is carried out within the state task of ISSP RAS and partial support of the RAS Presidium Program "Physics of condensed matter and new generation materials"

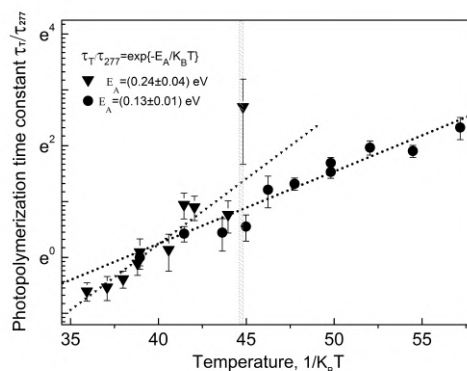


Fig.1 Arrhenius dependence of the photopolymerization time constant  $\tau_T/\tau_{277}$  on the temperature for the pristine  $C_{60}$  (triangles) and  $\{Pt(nPr_2dtc)_2\} \cdot (C_{60})_2$  complex (circles), dot lines – linear approximation of experimental data. Shaded area shows the phase transition fcc-sc near 260 K.

### References

1. J. P. Lu, X.-P. li, R. M. Martin, PRL, v.68, 1551-1554, 1992.
2. K. P. Meletov, J. Arvanitidis, D. Christofilos, G. Kourouklis, V. A. Davydov, Nanosystems:Physics, Chemistry, Mathematics, v. 9 (1), 29-32, 2018.
3. K. P. Meletov, Physics os Solid State, v. 60, 2103-2108, 2018.



## Investigations of polystyrene-fullerene nanocomposites by neutron and X-ray reflectometry

*Tropin T.V.*<sup>1</sup>, *Karpets M.L.*<sup>1,2</sup>, *Kosiachkin Ye.M.*<sup>1,2</sup>, *Gapon I.V.*<sup>1,2</sup>, *Gorshkova Yu.E.*<sup>1</sup>, *Avdeev M.V.*<sup>1</sup>, *Schick C.*<sup>3,4</sup>, *Schmelzer J.W.P.*<sup>3</sup>, *Askenov V.L.*<sup>1,5</sup>

*ttv@jinr.ru*

<sup>1</sup> Frank Laboratory of Neutron Physics, Joint Institute for Nuclear Research, Dubna, Russia

<sup>2</sup> Taras Shevchenko National University of Kyiv, Kyiv, Ukraine

<sup>3</sup> Institute of Physics, University of Rostock, Rostock, Germany

<sup>4</sup> Butlerov Institute of Chemistry, Kazan Federal University, Kazan, Russia

<sup>5</sup> National Research Center Kurchatov Institute, Moscow, Russia

Glass transition in different materials remains is one of the most exciting phenomena for research in both experimental and theoretical investigations in the area of condensed matter physics. A particularly interesting field in this respect is investigation of polymers glass transition [1]. Different polymers are applied in modern technologies and new fields of application are emerging. One of the most actively evolving research fields involves study of thin polymer films.

Neutron and X-ray scattering studies of polymers structure in glassy and liquid state have been performed during last 30 years and have proven to be very supportive [2]. Recently performed investigations of polymer thin films and glass transition of bulk polymer systems gave new insights. Presently, the most interesting topic is the study of polymer nanocomposites, and their glass transition, as new materials for technological applications[3].

We report the reflectometry investigations of structural organization and glass transition of thin films of polymer nanocomposites. Neutron reflectometry was performed at the GRAINS instrument of the IBR-2 reactor (Dubna). X-ray reflectometry was also performed in Dubna. Specular reflectivity was measured and analysed for free surface of different nanocomposites consisting of *d*PS/PS as a matrix and C<sub>60</sub>/C<sub>70</sub> as nanofillers. For neutrons scattering, the temperature range covering the transitional region between molten and amorphous glassy states (40-135 °C) was investigated. Initial modelling results allowed clarifying the nanoparticles concentrations that could be distinguished by the method [4]. The influence of nanoparticles on glass transition temperature of thin films, as well as the internal structure of these thin films, a highly debated subject in the literature at present, were investigated.

### References

1. S. Napolitano, E. Glynos, N.B. Tito, Rep. Progr. Phys. (2017) **80**(3), 036602.
2. R. Inoue, K. Kawashima, K. Matsui, M. Nakamura, K. Nishida, T. Kanaya, N.L. Yamada, Phys. Rev. E (2011) **84**, 031802.
3. D. Cangialosi, V.M. Boucher, A. Alegria, J. Colmenero, Soft Matter (2013) **9**(36), 8619.
4. M.L. Karpets, T.V. Tropin, L.A. Bulavin, J.W.P. Schmelzer, Nucl. Phys. At. Energy, (2018) **19**(4), 376.

## Mechanisms of supramolecular ordering of water-soluble derivatives of fullerenes in aqueous media

*Lebedev V.T.*<sup>1</sup>, *Kulvelis Yu. V.*<sup>1</sup>, *Voronin A.S.*<sup>2</sup>, *Komolkin A.V.*<sup>2</sup>, *Kyzyma E.A.*<sup>3,4</sup>, *Tropin T.V.*<sup>3</sup>, *Garamus V. M.*<sup>5</sup>

*lebedev\_vt@pnpi.nrcki.ru*

<sup>1</sup> B.P.Konstantinov Petersburg Nuclear Physics Institute, NRC, Kurchatov Institute, Gatchina, Leningrad distr., Russia

<sup>2</sup> Saint Petersburg State University, Saint Petersburg, Russia

<sup>3</sup> Joint Institute for Nuclear Research, Dubna, Russia

<sup>4</sup> Taras Shevchenko National University of Kyiv, Kyiv, Ukraine

<sup>5</sup> Helmholtz-Zentrum Geesthacht, Centre for Materials and Coastal Research, Geesthacht, Germany

Comprehensive analysis of the mechanisms determining the ordering of hydroxylated fullerenes, fullereneols  $C_{60}(OH)_x$  and  $C_{70}(OH)_x$  ( $X \sim 30$ ), in aqueous solutions has been performed using modeling the arrangement of hydroxyl groups on the surface of fullerenes and a set of experimental data obtained in X-ray and neutron scattering experiments. The fractal type structures of fullereneols [1] organized at the scales of several tens of molecular diameters are described by means of scattering data complementary combined treatment in direct and reciprocal space. This allowed evaluate correctly the subtle features of fullereneols mutual arrangement defined by fine balance of hydrophobic and hydrophilic interaction of molecules with non uniform distributions of hydroxyls. The modeling was computed with the use of quantum chemistry methods by minimizing molecular energy for different configurations of OH-groups by their attachment to the surfaces of carbon cages. It was shown the preferred localization of hydroxyls at the opposite poles while equatorial zone becomes depleted with the groups and become hydrophobic. As a result fullereneols' agglutinating happens in aqueous solutions via hydrophobic areas at carbon cages. This fact regulates the active growth of supramolecular structures in fullereneol's solutions at three spatial scales covering the distances from a few up to hundred molecular radii. A self-similar nature of these structures was established. Initially fullereneols have built primary groups (several molecules) then joint into intermediate clusters integrated within large-scale aggregates  $\sim 100$  nm. Structural peculiarities of fullereneols' ordering have been studied as dependent on their concentration which range covers a variety of systems from highly diluted solutions to concentrated gel-like systems. The presented results enable to generalise the basic principles of fullereneols' behaviour in aqueous media that is necessary for real progress of carbon materials applications in biomedicine and advanced chemical technologies.

The work was supported by Russian Foundation for Basic Researches (grant No 18-29-19008).

### References

1. V. T. Lebedev, A. A. Szhogina, M. V. Suyasova // IOP Conf. Series: Journal of Physics: Conf. Series. 2018. V.994. P. 012005.

## Superconducting properties of nanostructure based on $C_{60}/YBCO$ .

Faradzheva M.P.<sup>1</sup>, Prikhodko A.V.<sup>2</sup>, Konkov O.I.<sup>3</sup>

faradzheva\_mp@spbstu.ru

<sup>1</sup> Department of Experimental Physics, Peter the Great St. Petersburg Polytechnic University, St.Petersburg, Russia

<sup>2</sup> Department of Experimental Physics, Peter the Great St. Petersburg Polytechnic University, St.Petersburg, Russia

<sup>3</sup> Physicochemical Properties of Semiconductors, Ioffe Institute, St.Petersburg, Russia

Microwave studies of copper-based structures based on  $C_{60}$  have shown the superconducting properties of these materials at nitrogen temperatures [1]. This paper presents the results of studying the microwave properties (45GHz) of nanostructures based on  $C_{60}/YBa_2Cu_3O_{7.6}$  (YBCO) using the original technique described in [2]. Figure 1 illustrates the temperature dependence of the amplitude of the reflected signal for thin samples with dimensions 10x10 mm: 1 - Cu, 2- synthesized nanopowder YBCO, 3- YBCO nanopowder aged for 4 hours at temperature of 600C, 4- the nanostructure ( $C_{60}/YBCO$ ) which is obtained by mixing the powder of fullerene  $C_{60}$  in a mass ratio of 6:1 with the synthesized nano YBCO and aged for 4 hours at a temperature of 600 °C. When the critical transition temperature ( $T_c$ ) in the superconducting state is reached, the amplitude of the reflected signal increases sharply. As shown in Figure 1 (curve 4) for sample  $C_{60}/YBCO$ ,  $T_c$  is shifted to the low-temperature area ( $T_c=80,2$  K). Such a shift may be due to the appearance of additional Josephson junctions due to the interaction of  $C_{60}$  and YBCO. In this case, the transition width decreases 2 times. This is probably due to the formation of additional  $C_{60}$ -CuO bonds, which led to a more abrupt transition, as observed earlier [1]. Studies of new structures based on  $C_{60}/YBCO$  are mostly used when creating superconducting reflective surfaces for the radar stealth of objects.

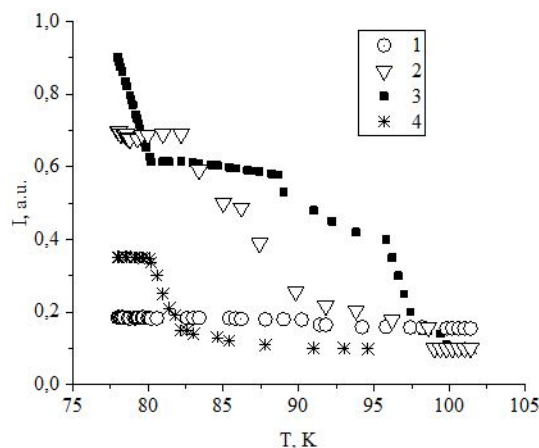


Fig. 1 The temperature dependence of the amplitude of the reflected signal: 1-Cu, 2- nanoYBCO, 3—nanoYBCO (600°C), 4-  $C_{60}/YBCO$

### References

1. F. Masterov, A.V. Prikhodko, O.I. Konkov, Fullerene Science and Technology. (1998) **6** (3), 481.
2. P. Faradzheva, A.V. Prikhod'ko, O.I. Kon'kov, St. Petersburg Polytechnical State University Journal. Physics and Mathematics (2018), **11** (4), 7.

## Time delay in electron-fullerene elastic scattering

Amusia M.Ya.<sup>1,2</sup>, Baltenkov A.S.<sup>3</sup>

amusia@012.net.il

<sup>1</sup> A. F. Ioffe Physical-Technical Institute, St. Petersburg, Russian Federation

<sup>2</sup> Racah Institute of Physics, the Hebrew University, Jerusalem, Israel

<sup>3</sup> Arifov Institute of Ion-Plasma and Laser Technologies, Tashkent, Uzbekistan

The time-picture of collisions of microscopic particles was suggested relatively long ago [1], being a natural continuation of the classical description. However since then it existed in a dormant state. Only recently it became clear that temporal picture can play a very important role in analyses of interaction between very short high intensity laser pulses with atoms and molecules [2]. The collisions with electrons were almost completely left out.

In this talk we discuss the temporal picture of electron collisions with fullerene. Within the framework of a Dirac bubble potential model for the fullerene shell, we calculated the time delay in slow-electron elastic scattering by it. It appeared that the time of transmission of an electron wave packet through the Dirac bubble potential sphere that simulates a real potential of the C<sub>60</sub> cage exceeds by more than an order of magnitude the transmission time via a single atomic core. Resonances in the time delays are due to the temporary trapping of electron into quasi-bound states before it leaves the interaction region.

The simplicity of the model that represents the fullerene, namely infinitely thin potential, permits to perform calculation pure analytic. The partial time-delay  $\tau_l(E)$  as a function of incoming electron energy  $E$  is connected to the partial  $l$ -wave scattering phase shift  $\delta_l$  by the following formula

$$\tau_l(E) = 2(d\delta_l(E)/dE) \quad (1).$$

The sign and magnitude of the time delay depends upon presence or absence of bound levels with a given scattering phase. Since C<sub>60</sub> has a bound negative ion  $s$ -state, close to zero  $E$  the phase shift behaves as  $\sim(-\pi-E^{1/2})$  that leads to time delay  $\sim-E^{-1/2}$  that goes to  $-\infty$ . Note that appearance of the  $s$ -level leads to a jump in times delay - from  $+\infty$  to  $-\infty$  at  $E=0$ . The time delay reaches its maximum for  $f$ -wave at  $E=0.94$  eV and is as big as about 500 atomic units or  $1.3 \times 10^4$  attoseconds. The calculations demonstrate that the C<sub>60</sub> time delay exceeds that for an isolated atom by more than an order of magnitude. Entirely, for small  $E$  the time delay averaged over angular momenta increases from  $-125$  to  $+280$  at. un. with  $E$  increase from 0.01 to 0.04, with subsequent abrupt decrease followed by oscillations while  $E$  grow.

For more details see [3].

It is of interest to study time delays in elastic scattering processes experimentally. However, one should keep in mind that the duration of a quantum-mechanical process determined by (1) differs from respective value in classical physics, since uncertainty principle puts its limitation upon accuracy of definition of both duration  $\tau(E)$  and energy  $E$ , since  $\Delta\tau \times \Delta E > 1$  at. un.

### References

1. P. Wigner, Phys. Rev. (1955) **98** 145.
2. Pazourek, S. Nagele, and J. Burgdörfer, Rev. Mod. Phys. (2015) **87** 765.
3. Ya. Amusia and A.S. Baltenkov, J. of Phys. B (2018) **52** (1) 015101

## Double-caged fullerene derivatives with long alkyl moiety for solar cells

*Kosaya M.P.*<sup>1</sup>, *Vysochanskaya O.N.*<sup>1</sup>, *Brotsman V.A.*<sup>1</sup>, *Goryunkov A.A.*<sup>1</sup>

*maria.cosaya@yandex.ru*

<sup>1</sup> Lomonosov Moscow State University, Moscow, Russia

Highly soluble fullerene derivatives with two or more fullerene cages are of particular interest as prospective acceptor materials for design of stable photovoltaic devices with improved morphology and charge transport properties. Recently it was demonstrated that photoelectric characteristics of *n*-alkyl ethers of double-caged fullerene derivatives nonmonotonically correlates with alkyl chain length [1]. Highest photovoltaic performance was found for solar cells based on the C<sub>9</sub> and C<sub>10</sub>-alkyl ethers whereas the devices based on C<sub>8</sub> and C<sub>18</sub>-alkyl ethers unexpectedly revealed two-fold PCE drop. However, the photovoltaic properties of C<sub>7</sub>, C<sub>11</sub>-C<sub>17</sub> alkyl ethers have not been studied.

Here we report a series of novel highly soluble double-caged fullerene derivatives with C<sub>7</sub>, C<sub>11</sub>, C<sub>13</sub>, C<sub>14</sub>, and C<sub>15</sub>-alkyl groups in the ester function and their effect on photovoltaic performance of solar cells based thereon.

Novel double-caged fullerene derivatives have been prepared through lithium salt-assisted [2+3]-cycloaddition of azomethine ylides generated from glycine esters and paraformaldehyde [1]. Synthesized compounds were LC isolated as individual compounds with 95+% purity and characterized by MALDI mass-spectrometry and NMR spectroscopy. Optical and electronic properties of novel double-caged fullerene derivatives have been studied by UV/Vis-spectroscopy and cyclic voltammetry. The effect of alkyl moiety on solubilities of double-caged fullerene derivatives is discussed.

Novel double-caged fullerene derivatives were tested as an acceptor material in P3HT-based organic solar cells and demonstrated strong dependence of PCE on the length of the alkyl moiety. The morphology of the active layer was studied by microscopy methods. The effect of alkyl chain length in double-caged fullerene derivatives on their solubility, morphology and photoelectric characteristics (series and shunt resistances and short-circuit current density) is discussed.

*This work was supported by RFBR (project № 17-03-00488).*

### References

1. A. Brotsman, A.V. Rybalchenko, D.N. Zubov, D.Yu. Paraschuk, A.A. Goryunkov., *J. Mater. Chem. C.* (2019) **7**, 3278.

## Difluoromethylation of trimetallic nitride endohedral fullerenes

*Pykhova A.D.*<sup>1</sup>, *Semivrazhskaya O.O.*<sup>1</sup>, *Ioffe I.N.*<sup>1</sup>

*a.d.pykhova@gmail.com*

<sup>1</sup> Moscow State University, Moscow, Russia

Encapsulated metal atoms or clusters considerably affect the electronic and chemical properties of the endohedral fullerenes. They donate electrons to the carbon cage, and metal-based frontier orbitals, occupied or vacant depending on the metal, can be implicated in the redox processes. The effect of the endohedral moieties on the chemical behavior is of particular importance since virtually any practical application of fullerenes requires their chemical derivatization in order to increase solubility, create a linker, or to tune certain electronic characteristics. Of interest are not only the general trends in reactivity but also the regiochemical implications due to the orienting effects of the exohedral atoms.

Insertion of a CF<sub>2</sub> bridge into a C-C bond via reaction with CF<sub>2</sub>ClCOONa provides an interesting test case for both experimental and theoretical studies of reactivity. There are two possible alternative mechanisms: the carbene pathway and the intramolecular nucleophilic substitution upon attachment of CF<sub>2</sub>Cl. The present study addresses CF<sub>2</sub> addition to the trimetallic nitride endohedral metallofullerenes (EMF) and its effect on the structural and electronic properties. We consider the two major Sc<sub>3</sub>N EMFs - Sc<sub>3</sub>N@I<sub>h</sub>-C<sub>80</sub> and Sc<sub>3</sub>N@D<sub>3h</sub>-C<sub>78</sub>. Despite general similarity, the two molecules have a number of differences both in the shape and topology of the carbon cage and in the dynamics of the endohedral cluster. The endohedral molecules were found to be less reactive than the pristine fullerenes, and the reaction regioselectively affords the [6,6]-open isomers where the inserted CF<sub>2</sub> group cleaves the [6,6]-bond to 2,2-2,3 Å. Analyzed against the experimental observations, the computational results corroborate the CF<sub>2</sub>Cl pathway rather than the previously suggested carbene mechanism.

The reported study was funded by RFBR according to the research project № 18-33-00896. The research is carried out using the equipment of the shared research facilities of HPC computing resources at the Lomonosov Moscow State University.

## Process control of fullerene synthesis by the influence of a magnetic field on the plasma of a high-frequency carbon arc

*Dudnik A.I.*<sup>1,2</sup>, *Osipova I.V.*<sup>1</sup>, *Nikolaev N.S.*<sup>1,2</sup>, *Churilov G.N.*<sup>1,2</sup>

*heavenrise@yandex.ru*

<sup>1</sup> Kirensky Institute of Physics, Federal Research Center KSC SB RAS, Krasnoyarsk, Russia

<sup>2</sup> Siberian Federal University, Krasnoyarsk, Russia

Theoretical estimates, and then quantum chemical calculations, confirmed that fullerene formation rate in plasma depends on the values of temperature and electron density [1, 2]. The helium pressure increase in the chamber was also shown to lead to an increase in the temperature gradient and the electron density in the arc - discharge plasma, with the higher fullerene content in the resulting fullerene mixture increasing significantly [3]. As above, it can be assumed that the arc plasma, being in a magnetic field, and therefore under its pressure, will form a fullerene composition upon cooling, depending on the pressure.

Studies of the effect on the fullerene composition and yield in an HF arc discharge plasma in case when the discharge current vector and magnetic field direction vector were collinear have been carried out. In a fullerene mixture formed without a magnetic field, the amount of higher fullerenes ( $C_n$ , where  $n > 70$ ) was 8.7 wt.%. In case of a phase shift between the discharge current and the magnetic field strength of  $\pi/2$ , the number of higher fullerenes is up to 9.8 wt.%. The field synthesis cophased with the discharge current results in the higher fullerene formation in amounts of 12 wt.%. For both cases, the field influence leads to a decrease in the fullerene content by 2-3 wt.%.

Thus, the study results of the influence of the magnetic field on the composition and number of the formed fullerenes correspond to the pressure effect of the buffer gas, helium, in the chamber. Not only will collinear magnetic fields, but also perpendicular ones to the discharge current be presented in current work in the research results.

The reported study was funded by RFBR according to the research project № 18-32-20011.

### References

1. G.N. Churilov, P.V. Novikov, V.E. Tarabanko, V.A. Lopatin, N.G. Vnukova, N.V. Bulina, Carbon (2002) **40**, P.891-896.
2. G.N. Churilov, A.S. Fedorov, P.V. Novikov, Carbon (2003) **41**, P. 173-178.
3. G.N. Churilov, W. Kratschmer, I.V. Osipova, G.A. Glushenko, N.G. Vnukova, A.L. Kolonenko, A.I. Dudnik, Carbon (2013) **62**, P. 389-392.

## Stability of small nitrogen clusters inside the carbon cage: Molecular dynamic study

*Gimaldinova M.A.*<sup>1,2</sup>, *Katin K.P.*<sup>1,2</sup>, *Grishakov K.S.*<sup>1,2</sup>, *Maslov M.M.*<sup>1,2</sup>

*margaritagimaldinova@gmail.com*

<sup>1</sup> Nanoengineering in Electronics, Spintronics and Photonics Institute, National Research Nuclear University MEPhI, Moscow 115409, Russia

<sup>2</sup> Laboratory of Computational Design of Nanostructures, Nanodevices, and Nanotechnologies, Research Institute for the Development of Scientific and Educational Potential of Youth, Moscow 119620, Russia

Non-molecular forms of nitrogen are regarded as promising high-energy materials. They are metastable compounds, which can transform into the molecular nitrogen with a significant energy release. Many all-nitrogen clusters and crystals were theoretically predicted [1], and some of them were experimentally synthesized under the extreme conditions (see, for example, [2]).

Here we consider two small nitrogen clusters: tetrahedral  $N_4$  and cubic  $N_8$ . Their geometries correspond to the local minima at the potential energy landscape [1]. Even at room temperatures, they decompose due to their thermal vibrations. Therefore, pristine  $N_4$  and  $N_8$  clusters are not suitable for practical applications. There are many ways to stabilize them - chemical passivation, space confinement, the introduction of carbon atoms into their skeleton [3], etc. In particular, encapsulation of nitrogen system inside the  $C_{60}$  carbon cage can result in the significant increase of kinetic stability of the former. Such effect was previously reported for the  $N_3$ ,  $N_5$ , and  $C_4H_4$  molecules, encapsulated inside the  $C_{60}$  [4-5].

To find the influence of outer  $C_{60}$  cage on the stability of small nitrogen clusters, we performed comparative molecular dynamics study of  $N_4$  and  $N_8$  clusters as well as  $N_4@C_{60}$  and  $N_8@C_{60}$  endohedral complexes. We apply non-orthogonal tight-binding interatomic potential [6], which combines acceptable accuracy and high performance. More rigorous density functional approach was also used for some sensitive calculations. Specially prepared initial configurations with randomly distributed atomic velocities evolve in time according to Newton's equations of motions. The time evolution of heated atomic systems until decomposition of nitrogen clusters was visualized. Decomposition channels were studied in detail. Activation energies and frequency factors of corresponding processes were derived from the temperature dependence of the lifetimes of nitrogen clusters. According to our calculations, the presence of  $C_{60}$  leads to increasing of  $N_4$  and  $N_8$  lifetimes. We assume that carbon cages can be regarded as efficient containers for high-energy all-nitrogen clusters.

The reported study was funded by RFBR according to the research project No. 18-32-20139 mol\_a\_ved.

### References

1. X. Silva, F.T. Silva, B.R.L. Galvao, J.P. Braga, J.C. Belchior, *J. Mol. Model.* (2018) **24**, 196.
2. I. Eremets, R.J. Hemley, H.-K. Mao, E. Gregoryanz, *Nature* (2001) **411**, 170.
3. Zhang, G. Chen, X. Gong, *Mol. Simul.* (2019) **45**, 129.
4. Liang, X. Gao, X. Zhang, *J. Mol. Model.* (2015) **21**, 265.
5. M. Maslov, K.P. Katin, *Fuller. Nanot. Car. N.* (2014) **22**, 560.
6. M. Maslov, A.I. Podlivaev, K.P. Katin, *Mol. Simul.* (2016) **42**, 305.



## Fullerene formation in plasma at different rates of temperature and electron concentration change

*Dudnik A.I.*<sup>1,2</sup>, *Osipova I.V.*<sup>1</sup>, *Novikov P.V.*<sup>3</sup>, *Churilov G.N.*<sup>1,2</sup>

*heavenrise@yandex.ru*

<sup>1</sup> Kirensky Institute of Physics, Federal Research Center KSC SB RAS, Krasnoyarsk, Russia

<sup>2</sup> Siberian Federal University, Krasnoyarsk, Russia

<sup>3</sup> Krasnoyarsk Institute of Railway Transport, Krasnoyarsk, Russia

There are various models of the formation of fullerenes, based both on the idea of assembling fullerenes from small clusters [1] and on annealing large clusters with the emission of carbon dimers [2]. These models reveal important aspects of the phenomenon of spontaneous transformation of carbon vapor into stable fullerene molecules. From a practical point of view, a model that takes into account the rate of change of temperature and electron concentration in plasma along the arc discharge radius may be of great interest.

Earlier, we proposed a model [3, 4] of the formation of fullerenes accounting the charges of carbon clusters in a plasma. Then it was improved [5]. The model takes into account the cluster heating and cooling. In addition, the heating and cooling of the carbon clusters by buffer gas is considered. The calculations give the qualitatively correct correlation between fullerene yields in helium and argon.

In this work, in the model the data obtained on the temperature distribution and electron concentration in a carbon-helium plasma [6] were taken into account. The results of calculations carried out for different pressures of the buffer gas correlate with the results of experiments [6] and will be used in the future to improve the technique of controlled fullerene synthesis.

The reported study was funded by RFBR according to the research project № 18-32-20011.

### References

1. I. Alekseev, G.A. Dyuzhev. *Tech. Phys.* (2002) **47**, 634.
2. G. Zheng, Z. Wang, S. Irle, K. Morokuma. *J. Nanosci. Nanotech.* (2007) **7**, 1662.
3. A. Fedorov, P.V. Novikov, G.N. Churilov. *Chem. Phys.* (2003) **293**, 253.
4. L. Stepanov, Yu.A. Stankevich, L.K. Stanchits, G.N. Churilov, A.S. Fedorov, P.V. Novikov. *Tech. Phys. Lett.* (2003) **29**, 927.
5. S. Fedorov, P.V. Novikov, Yu.S. Martinez, G.N. Churilov. *J. Nanosci. Nanotech.* (2007) **7**, 1315.
6. N. Churilov, W. Krätschmer, I.V. Osipova, G.A. Glushenko, N.G. Vnukova, A.L. Kolonenko, A.I. Dudnik. *Carbon* (2013) **62**, 389.

## Aggregation of $C_{70}$ fullerene in an *o*-xylol solution. The features revealed by the dynamic light scattering methods

Arutyunyan A.V.<sup>1</sup>, Kozlov V.S.<sup>1</sup>, Zavatskii E.I.<sup>1</sup>, Kulvelis Yu.V.<sup>1</sup>

arut61@mail.ru

<sup>1</sup> National Research Center Kurchatov Institute B.P. Konstantinov Petersburg Nuclear Physics Institute, Gatchina, Russia

By means of the dynamic light scattering methods ( optical heterodyne scheme), the appearance of large aggregates of fullerene  $C_{70}$  (with the diameter 570–600 nm) and the further sharp increase in their concentrations within 2, 3 days with no visible change in their size have been revealed. This is evidenced by the centering at the same frequency of Doppler shifts in the scattering spectra of aggregates (Fig.1A, B).

It is also shown that the directional motion of the aggregates and accordingly Doppler shifts in the spectra are associated with the light pressure, with the entrainment of formed aggregates by the laser beam (a light power of about 15 mW) and are not associated with convection, i.e. with heating caused by the same beam (Fig.1C, D).

The work was supported by Russian Foundation for Basic Researches (grant No 18-29-19008).

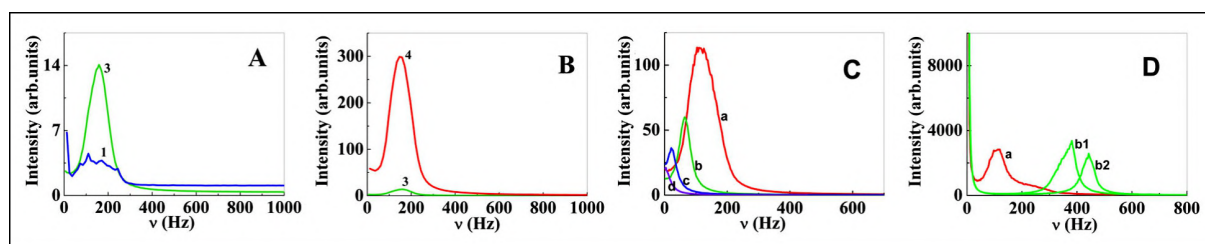


Fig.1. Spectra of light scattered by the  $C_{70}$  fullerene sample. (A) on the first and third days of observation, (B) on the third and fourth days of observation. (C) with the successive weakening of the scattering beam entering the sample by double damping filters (a) without the weakening of the scattering beam, (b) in the presence of a double damping filter, (c) at the fourfold weakening of the scattering beam, and (d) at the eightfold weakening of the scattering beam. (D) spectra of light scattered by the  $C_{60}$  fullerene sample at a scattering angle of  $90^\circ$  for (a) scattering from two counterpropagating joined beams simultaneously and (b1 and b2) the case where one of the counterpropagating scattering beams is blocked.

### References

A.V. Arutyunyan, E.I. Zavatskii, V.S. Kozlov, and M.V. Suyasova, JETP Letters (2018) Vol. 108, No. 10, p. 680.

## Cryometry data and excess thermodynamic functions in the binary systems: adduct of fullerene C<sub>60</sub>, fullerene C<sub>70</sub> - H<sub>2</sub>O

Keskinova M.V.<sup>1,2</sup>, Charykov N.A.<sup>3,1</sup>, Semenov K.N.<sup>3,4</sup>, Keskinov V.A.<sup>3</sup>, Safyannikov N.M.<sup>1</sup>, Shaimardanov Z.K.<sup>5</sup>, Shaimardanova B.K.<sup>5</sup>, Kulenova N.A.<sup>5</sup>, Tyurin D.P.<sup>3</sup>

safyannikov\_nm@systan.ru

<sup>1</sup> S-Petersburg Electrotechnical University "LETI", ul. Prof. Popova 5, 197376, St. Petersburg, Russia

<sup>2</sup> Ltd. "TONSPRING", Saint-Petersburg, Russia

<sup>3</sup> S-Petersburg State Technological Institute (Technical University), Moskovsky pr. 26, 190013, St. Petersburg, Russia

<sup>4</sup> S-Petersburg State University, Universitetskaya emb. 7/9, 199034, St. Petersburg, Russia

<sup>5</sup> D. Serikbayev East Kazakhstan state technical university, A.K. Protozanov St. 69, 070004, Ust-Kamenogorsk, The Republic of Kazakhstan

Using a Beckman thermometer, the concentration dependence of water crystallization temperatures was investigated for C<sub>60</sub>(OH)<sub>22-24</sub> - H<sub>2</sub>O, C<sub>70</sub>(OH)<sub>12</sub> - H<sub>2</sub>O, C<sub>70</sub>[C(COOH)<sub>2</sub>]<sub>3</sub> - H<sub>2</sub>O, C<sub>60</sub>(C<sub>5</sub>H<sub>9</sub>NO<sub>3</sub>)<sub>2</sub> - H<sub>2</sub>O, C<sub>60</sub>(C<sub>6</sub>H<sub>14</sub>N<sub>2</sub>O<sub>2</sub>)<sub>2</sub> - H<sub>2</sub>O, C<sub>60</sub>(C<sub>6</sub>H<sub>13</sub>N<sub>2</sub>O<sub>2</sub>)<sub>2</sub> - H<sub>2</sub>O, C<sub>60</sub>(C<sub>4</sub>H<sub>8</sub>NO<sub>3</sub>)<sub>2</sub>-H<sub>2</sub>O binary systems at 273.15 - 272.50 K.

The semi-empirical Virial Decomposition Asymmetric Model of virial expansion of the excess Gibbs energy of the light fullerene derivatives solutions was applied. On the basis of the proposed model, partial and average molar thermodynamic functions of binary solutions as well as the conditions of stability against phase separation were determined.

All systems demonstrate gigantic positive deviations from the ideality and have micro-heterogeneous behavior in the concentration in molar fraction scale higher than  $3 \div 5 \cdot 10^{-5}$  a.u.

This work was supported by Russian Foundation of Fundamental Investigations - RFBR (Projects №№ 18-08-00143 A, 19-015-00469 A, 19-016-00003 A), as well in the framework of the state assignment of the Ministry of Science and Higher Education of the Russian Federation (Project № 8.2080.2017 / 4.6).

### Literature.

1. Nikolay A. Charykov, Konstantin N. Semenov, Enriqueta R. López, Josefa Fernández, Evgeny B. Serebryakov, Viktor A. Keskinov, Igor V. Murin. Excess thermodynamic functions in aqueous systems containing soluble fullerene derivatives. *J. of Molecule Liquids*. 2018. Vol.256. P. 305-311. <https://doi.org/10.1016/j.molliq.2018.01.177>
2. N.M. Safyannikov, N.A. Charykov, P.V. Garamova, K.N. Semenov, V.A. Keskinov, A.V. Kurilenko, I.A. Cherepcova, D.P. Tyurin, V.V. Klepikov, M.Yu. Matuzenko, N.A. Kulenova, A.A. Zolotarev. Cryometry data in the binary systems bis-adduct of C<sub>60</sub> and indispensable aminoacids - lysine, threonine, oxyproline. *Nanosystems: Phys., Chem., Math.* 2018. V. 9 N1. P. 46-49. DOI 10.17586/2220-8054-2018-9-1-46-48.
3. Matuzenko M.Yu., Tyurin D.P., et al. Cryometry and excess functions of fullerenols and trismalonates of light fullerenes - C<sub>60</sub>(OH)<sub>24</sub> and C<sub>70</sub>[C(COOH)<sub>2</sub>]<sub>3</sub> aqueous solutions. *Nanosystems: Phys., Chem., Math.*, 2015, 6 (4), P. 704-714.
4. Matuzenko M.Yu., Shestopalova A.A., et al. Cryometry and excess functions of the adduct of light fullerene C<sub>60</sub> and arginine - C<sub>60</sub>(C<sub>6</sub>H<sub>12</sub>NaN<sub>4</sub>O<sub>2</sub>)<sub>8</sub>H<sub>8</sub> aqueous solutions. *Nanosystems: Phys., Chem., Math.*, 2015, 6 (5), P. 715-725.

## Skeletal transformations of buckminsterfullerene upon chlorination

*Vysochanskaya O.N.*<sup>1</sup>, *Brotsman V.A.*<sup>1</sup>, *Troyanov S.I.*<sup>1</sup>

*olja.vysochanskaya@gmail.com*

<sup>1</sup> Department of Chemistry, Lomonosov Moscow State University, Moscow, Russia

In recent decade, it has been established that many higher fullerenes obeying the isolated pentagon rule (IPR) were susceptible to skeletal transformations forming structures with fused pentagons or even with heptagon in the carbon skeleton upon chlorination [1-2]. It was assumed that the chlorination of the most common fullerenes  $C_{60}$  and  $C_{70}$  leads to the formation of exclusively IPR-chlorides up to  $D_{3d}$ - $C_{60}Cl_{30}$  and  $C_{70}Cl_{28}$ , respectively. However, the possibility of Stone-Wales rearrangements and the formation of non-IPR structures of fullerene  $C_{60}$  under harsh chlorination conditions was shown in [3]. Single crystal X-ray diffraction revealed three chlorides with non-IPR frameworks:  $D_{2d}$ - $^{1805}C_{60}Cl_{24}$ ,  $C_{2v}$ - $^{1810}C_{60}Cl_{24}$ , and  $D_5$ - $^{1794}C_{60}Cl_{20}$ .

In this work, optimization of the synthesis of non-IPR derivatives of  $C_{60}$  was carried out under chlorination with  $SbCl_5$ . The impact of initial substrates, time of synthesis, and temperature on chlorination products was studied. After HPLC separation of the products, the crystals of two non-IPR isomers  $C_{60}Cl_{24}$  and non-IPR chloride  $^{1809}C_{60}Cl_{16}$  (Fig. 1, a) were investigated by single crystal X-ray diffraction. Both non-IPR  $C_{60}Cl_{24}$  (Fig. 1, b and c) isomers were further characterized by IR spectroscopy. To receive more information on the products of the syntheses, high-temperature trifluoromethylation of the chlorination products was applied followed by HPLC separation. In this way,  $^{1810}C_{60}(CF_3)_{14}$  (Fig. 1, d) was isolated and studied by X-ray diffraction and IR spectroscopy. Molecular structures as well as chlorination and trifluoromethylation patterns of the isolated compounds are discussed in more detail.

This study was supported by the RFBR, grant № 19-03-00733.

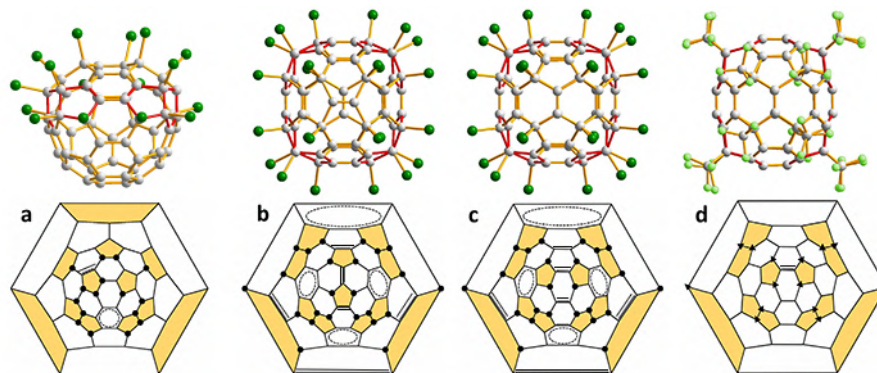


Fig.1. Molecular structures and Schlegel diagrams of non-IPR chlorides  $^{1809}C_{60}Cl_{16}$  (a),  $^{1805}C_{60}Cl_{24}$  (b),  $^{1810}C_{60}Cl_{24}$  (c) and  $^{1810}C_{60}(CF_3)_{14}$  (d).

### References

1. N. Ioffe, A.A. Goryunkov, N.B. Tamm, L.N. Sidorov, E. Kemnitz, S.I. Troyanov, *Angew. Chem. Int. Ed.* (2009) **48**, 5904.
2. N. Ioffe, Ch. Chen, S. Yang, L.N. Sidorov, E. Kemnitz, S.I. Troyanov, *Angew. Chem. Int. Ed.* (2010) **49**, 4784.
3. A. Brotsman, N.B. Tamm, V.Yu. Markov, I.N. Ioffe, A.A. Goryunkov, E. Kemnitz, S.I. Troyanov, *Inorg. Chem.* (2018) **57**, 8325.

## Fullerenes for medical purposes: from active bioagent to drug-delivery system

*Kuzmenko M.O.*<sup>1,2</sup>, *Kyzyma O.A.*<sup>1,2</sup>, *Tropin T.V.*<sup>1</sup>, *Ivankov O.I.*<sup>1,3</sup>

*kuzjamaryna@gmail.com*

<sup>1</sup> Joint Institute for Nuclear Research, Dubna, Russia

<sup>2</sup> Taras Shevchenko National University of Kyiv, Ukraine

<sup>3</sup> Institute for Safety Problems of Nuclear Power Plants, NAS Ukraine, Kyiv, Ukraine

Fullerenes due to pleiotropic activity are promising agent for different medical applications. They are used as a separate active component and as a carrier of medications in targeted delivery and/or prolonged therapy. The fullerenes water solutions, which were prepared by extraction from C60/NMP, characterized by the unique small cluster sizes (~ 10 nm) and the acceptable middle size cluster for nanomedicine (~60 nm) of fullerenes that lead to improved biocompatibility of fullerenes. We assume that fullerene interacts with NMP via a charge transfer mechanism. Stabilization of fullerenes in water solutions due H-bonding between water and NMP. The evidence of the type of the molecular interaction we found from the quantum-chemical calculation's results in the density functional theory with long-range separated hybrid functional and subsequent analysis: wave functions, PES, the charge transfer transition density matrix from time dependent DFT calculations of 100 excited states( $f > 0.001$ ).

Based on the aqueous dispersions of fullerene, it was designed a number of drug delivery system as fullerenes-polyphenols, fullerenes-alkaloids, polysaccharides-fullerenes. We presented crucial information about each active component of the drug-delivery systems, below in this narrative.

Oxyresveratrol is a polyphenols compound, well-known representative of stilbene, found in the roots, leaves, stem and fruit of many widely distributed plants. It possesses antitumor activity. As a bioactive compound oxyresveratrol has demonstrated strong antioxidant activity, effectively scavenge free radicals. Oxyresveratrol exhibited a wider effective dosage range as an intracellular antioxidant for reducing oxidative stress. The molecules of oxyresveratrol aggregates under the influence of additive fullerene as a result of supramolecular self-organization.

Berberine is alkaloids found in such plants as Berberis. It can reduce the growth and spread of various different types of cancer, and a inhibit cell proliferation and to be cytotoxic towards cancer cells. Nevertheless, the bioavailability of Berberine is low. In this reason, we proposed the fullerenes like a berberine's carrier to improve his bioavailability and selectivity.

Pectins, as a compound, are linear polysaccharides composed primarily of D-galacturonic acids. Pectin has the anti-adhesive apoptosis-promoting, apoptosis -inducing properties and can increase apoptotic responses of tumor cells to chemotherapy. Pectin can increase the bioavailability of the drug in oncology treatment because of similar structure of pectin to glucose, and the increased cancer cellular uptake of glucose on compare to healthy cell. So, if we will proved the existence of pectin's shell around fullerenes in water solutions we can say that we create the carrier-drug systems for active targeting with high selectivity and a wide set of bioactivity.

Small-angle neutron scattering, dynamic light scattering, and UV-Vis spectroscopy investigated the undermentioned systems. In addition, a computer model of carrier-drug interaction was proposed based on quantum chemical calculations.

## Chromatography-free synthesis of mono-adducts of fullerene C<sub>60</sub>.

*Nikolaev D.N.<sup>1</sup>, Piotrovskiy L.B.<sup>1</sup>*

*pp225@yandex.ru*

<sup>1</sup> Institute of Experimental Medicine, St. Petersburg, Russia

The majority of chemical transformations involving the addition of addends to C<sub>60</sub> core have two main disadvantages: the formation of poly-adducts along with the target mono-adduct and, consequently, the need for the target mono-adduct purification by column chromatography. This is also true for the synthesis of 3'H-cyclopropa[1,9](C<sub>60</sub>-I<sub>h</sub>)[5,6]fullerene-3'-carboxylic acid (FCA) previously reported by our group [1].

According to our recent results, decreasing the molar equivalent of cyclopropanation agent from 1.8 eq to 0.3 eq in relation to C<sub>60</sub> leads to benzhydryl ester FCA being the only product along with unreacted C<sub>60</sub>. The ester can be separated in 30% yield based on total C<sub>60</sub> (100% based on reacted C<sub>60</sub>), which is higher than previously reported (55% based on reacted C<sub>60</sub>). In order to prepare the target FCA from the mixture of its benzhydryl ester and C<sub>60</sub> we removed benzhydryl protecting group directly from the mixture under the conditions we reported previously. The isolation of FCA from the mixture with C<sub>60</sub> involved esterification of FCA with 2-chlorotriyl chloride resin with the subsequent washing of FCA-linked resin from unreacted C<sub>60</sub>. Cleavage of FCA from the resin can be done by standard reagents which are used in solid phase peptide synthesis. The synthesis of other mono-adducts of C<sub>60</sub> (for example, with amine group) can be performed in a similar way using the same resin.

### References

D. N. Nikolaev, P. B. Davidovich, L. B. Piotrovskii, *Russ. J. Org. Chem.* (2016) 52, 1050–1053.

## Possible role of sp-defect migration in an odd fullerene shell in selection of abundant isomers of fullerenes

*Sinitsa A. S.*<sup>1</sup>, *Lebedeva I. V.*<sup>2</sup>, *Popov A. M.*<sup>3</sup>, *Knizhnik A. A.*<sup>1</sup>

*alexsinitsa91@gmail.com*

<sup>1</sup> National Research Centre Kurchatov Institute, Moscow, Russia

<sup>2</sup> CIC nanoGUNE, San Sebastian, Spain

<sup>3</sup> Institute for Spectroscopy of Russian Academy of Sciences, Troitsk, Moscow, Russia

It is commonly accepted that fullerene formation occurs via self-organization of initially chaotic carbon system without precursors of certain structure. The detailed arguments in favor of this route have been brought forward in reviews [1,2]. However, after more than thirty years since the discovery of fullerenes, the puzzle of the high yield of certain abundant isomers of fullerenes (like a C<sub>60</sub> fullerene) is not yet solved. Numerous molecular dynamics (MD) studies show that just after formation a fullerene shell contains structural defects (such as 7-, 8-rings and other rings, sp-hybridized atoms). Thus annealing of these defects is necessary for the formation of the "perfect" fullerene shell containing an even number of sp<sup>2</sup> atoms. To explain this annealing of defects of the fullerene structure and the abundance of certain isomers of fullerenes it is necessary to fully understand the reactions of structure transformation after fullerene shell formation.

Here we perform reactive MD simulations of dynamical behavior of a fullerene shell with an odd number of atoms. Namely, the stochastic migration of two-coordinated atom position (or sp-defect) is observed. The schemes of bond rearrangements during the migration events are presented. The performed analysis of the correlation between the fullerene energy and number of 7- and 8-rings allows us to conclude that such a migration can lead to formation of the perfect fullerene shell and thus contributes to selection of abundant isomers of fullerenes. The conclusion drawn from the MD simulations is confirmed by density functional theory calculations of barriers of migration events that change the number and configuration of the different rings. Based on these results, we propose a possible atomistic mechanism of annealing of fullerene defects caused by the migration of the sp-defect in a fullerene shell with an odd number of atoms at intermediate stages of fullerene synthesis.

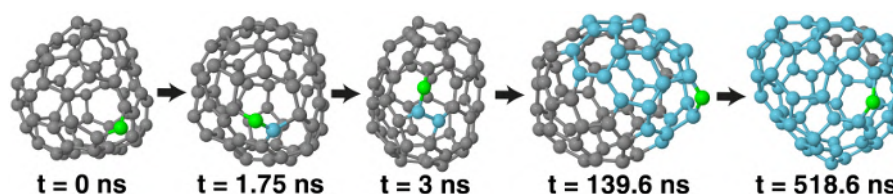


Fig.1. Simulated structure evolution showing the sp-defect migration in the C<sub>69</sub> fullerene at temperature of 3000 K. Current and former sp atoms are colored in green and blue, respectively.

### References

1. Lozovik, Y. E.; Popov, A.M. Formation and Growth of Carbon Nanostructures: Fullerenes, Nanoparticles, Nanotubes and Cones. *Physics Uspekhi* 1997, **40**, 717.
2. Irle, S.; Zheng, G.S.; Wang, Z.; Morokuma, K. The C<sub>60</sub> Formation Puzzle "Solved": QM/MD Simulations Reveal the Shrinking Hot Giant Road of The Dynamic Fullerene Self-Assembly Mechanism. *J. Phys. Chem. B* 2006, **110**, 14531.

## Comparative study of endofullerenols with magnetic atoms in aqueous solutions by neutron scattering and NMR

*Kulvelis Yu.V.*<sup>1</sup>, *Lebedev V.T.*<sup>1</sup>, *Ievlev A.V.*<sup>2</sup>, *Chizhik V.I.*<sup>2</sup>, *Artemiev A.N.*<sup>3</sup>, *Belyaev A.D.*<sup>3</sup>, *Knyazev G.A.*<sup>3</sup>

*lebedev\_vt@pnpi.nrcki.ru*

<sup>1</sup> B.P. Konstantinov Petersburg Nuclear Physics Institute, NRC "Kurchatov Institute", Gatchina, Russia

<sup>2</sup> Saint Petersburg State University, Saint Petersburg, Russia

<sup>3</sup> National Research Centre "Kurchatov Institute", Moscow, Russia

Crucial problems of aqueous solutions stability of water-soluble forms of fullerenes and endofullerenes are of great importance for their biomedical applications, which progress strongly depends on the knowledge of the interactions between these molecules especially in the case of magnetic atoms (Gd, Fe) inside carbon cages [1,2]. Hydroxyls on the surface of cages make very difficult to predict a preferable way of fullerenols' mutual arrangement in aqueous media as defined by a competition between hydrophobic and hydrophilic interactions, electric and magnetic dipolar forces between molecules. The cages may also carry magnetic moments due to known phenomena of spin leakage from encapsulated metal atom to surrounding carbon shell. The EXAFS measurements have proved the endohedral structures of these metal-carbon complexes and given necessary structural parameters defining coordination geometry and the distances between metal atom and surrounding carbons.

The experimental results are devoted to comparative studies of endofullerenols with 4f- and 3d-metal atoms having magnetic moments stimulating molecular ordering in aqueous medium when a significant screening of electrostatic dipolar interactions occurs due to very high polarity of water. A comprehensive analysis of neutron scattering data for the solutions of different fullerenols has enabled to treat the relaxivity effects from encapsulated atoms creating randomly varying magnetic fields. The protons spins interact with these fields making precessions under the applied fields in NMR experiments. Thus, the modelling of Magneto-Resonance Imaging (MRI) technique was realized, widely used in modern diagnostics. The performed experiments serve to provide a basement for design of new contrasting agents for MRI as well as elucidated the features of endofullerenols' superstructures in solutions as dependent on their concentrations, pH and temperatures. This should be important for biomedical applications of these new materials.

The work was supported by Russian Foundation for Basic Researches (grant No 18-29-19008).

### References

1. V.T. Lebedev, Yu.V. Kulvelis, V.V. Runov, A.A. Szhogina, M.V. Suyasova // NANOSYSTEMS: PHYSICS, CHEMISTRY, MATHEMATICS. 2016. V. 7 (1). P. 22.
2. V.T. Lebedev, A.A. Szhogina, M.V. Suyasova // IOP Conf. Series: Journal of Physics: Conf. Series. 2018. V.994. P. 012005.



## Characterizing size and composition of fullerene nanoparticles in aqueous dispersions

*Turetskiy E. A.*<sup>1,2</sup>, *Andreev S. M.*<sup>1</sup>, *Shershakova N. N.*<sup>1</sup>, *Shatilov A. A.*<sup>1,2</sup>, *Timofeeva A. V.*<sup>1,2</sup>, *Kozhikhova K. V.*<sup>1</sup>, *Smirnov V. V.*<sup>1,2</sup>, *Khaitov M. R.*<sup>1</sup>

*E.Turetskiy@nrcii.ru*

<sup>1</sup> NRC Institute of Immunology FMBA of Russia

<sup>2</sup> I.M. Sechenov First Moscow State Medical University

Despite being insoluble in most polar solvents[1], fullerene C<sub>60</sub> can form stable colloid dispersions in aqueous media[2]. Such Aqueous Fullerene Dispersions (AFD) have a number of practical applications, including use in biology and medicine as anti-inflammatory agents[3]. For this purpose, AFDs are obtained by dissolution of fullerene C<sub>60</sub> in 1-methylpyrrolidone (MP), mixing it with aqueous solution of appropriate stabilizer and removing MP by dialysis through semi-permeable membrane[4]. This method has recently been improved significantly by substituting dialysis with more efficient process of tangential flow filtration. In this work, a number of physical-chemical characteristics of AFD, obtained by this method, are described.

UV-Vis absorption spectra were recorded on a double beam spectrophotometer in the range of 190-800 nm. Sizes of nanoparticle was measured by dynamic light scattering method and  $\zeta$ -potential was established. Freeze-dried dispersions have been studied using Fourier transformed infrared spectroscopy (FTIR) and elemental composition has been studied using elemental analyzer. Fullerene within AFD has additionally been identified using matrix assisted laser desorption/ionization time-of-flight (MALDI-TOF) mass spectrometry.

UV-Vis spectra showed a wide band of absorption from 550 to 400 nm and 3 peaks at 230, 270 and 340 nm. As with dialysis method, 340 nm peak has shown great linearity of calibration curve and is suggested to be used for quantitative analysis. Number and position of peaks did not depend of the particle size, which varied greatly, depending on stabilizer used. Hydrodynamic radius of particles in unstabilized AFD has been established as roughly 50 nm and two to six times that for AFDs stabilized with different poloxamers and polysorbates.  $\zeta$ -potential was estimated as roughly -15 mV for all dispersions studied. FTIR spectra of freeze-dried samples were compared to spectra obtained from pristine fullerene. While all the major peaks are retained, a number of small emerging peaks is observed. The latter can be attributed to presence of water and MP within the freeze-dried powder. This can be confirmed by elemental analysis, which showed 2.28% nitrogen and 1.11% hydrogen content within fullerene freeze-dried sample. These results indicate water and MP presence within fullerene clusters. The possibility of hydrogen and nitrogen being covalently bound to fullerene within clusters have been excluded by applying MALDI-TOF mass-spectrometry, results of which clearly show a singular peak at  $m/z=720$ .

Results described in this work could be useful to elucidate AFD physical and chemical properties. Fullerene cluster's ability to incorporate light molecules, shown here on example of MP and water, could be used in the future for small molecule drug delivery and controlled release.

### References

1. Marcus Y. [и др.]. Solubility of C<sub>60</sub> Fullerene // The Journal of Physical Chemistry B. 2001. № 13 (105). С. 2499-2506.
2. Chen K.L., Elimelech M. Aggregation and deposition kinetics of fullerene (C<sub>60</sub>) nanoparticles // Langmuir. 2006.
3. Shershakova N. [и др.]. Anti-inflammatory effect of fullerene C<sub>60</sub> in a mice model of atopic dermatitis. // Journal of nanobiotechnology. 2016. (14). С. 8.
4. Andreev S. [и др.]. Study of Fullerene Aqueous Dispersion Prepared by Novel Dialysis Method: Simple Way to Fullerene Aqueous Solution // Fullerenes, Nanotubes and Carbon Nanostructures. 2015. № 9 (23). С. 792-800.

## Fullerene-based colloids for biomedical applications: Structural study by scattering techniques

Tomchuk A.A.<sup>1</sup>, Kyzyma O.A.<sup>1,2</sup>, Andreev S.M.<sup>3</sup>, Shershakova N.N.<sup>3</sup>, Turetskii E.A.<sup>3</sup>, Ivankov O.I.<sup>1</sup>, Tomchuk O.V.<sup>1,2</sup>, Aksenov V.L.<sup>4,1</sup>, Avdeev M.V.<sup>1</sup>

a.a.tomchuk@gmail.com

<sup>1</sup> Frank Laboratory of Neutron Physics, Joint Institute for Nuclear Research, Dubna, Russia

<sup>2</sup> Taras Shevchenko Kyiv National University, Kyiv, Ukraine

<sup>3</sup> National Research Center 'Institute of Immunology', Federal Medical-Biological Agency of Russia, Moscow, Russia

<sup>4</sup> National Research Center 'Kurchatov Institute', Moscow, Russia

Fullerenes show rather strong antioxidant activity, which has much prospects in cosmetic industry and medicine [1]. The experiments on cytotoxicity indicate the absence of significant toxic effects of fullerene solutions, regardless of the fullerene aggregate size [2]. The development of new efficient methods to obtain stable C<sub>60</sub> aqueous solutions is of current interest with respect to practical applications. Thus, it was shown [3] that amino acids and a number of other natural substances have a stabilizing effect on aqueous dispersions of C<sub>60</sub> and in some cases reduce the particle size, which improves membranotropic properties.

In this study, structural characterization of complexes of C<sub>60</sub> with different stabilizers (lysine, arginine, piperazine, etc.) in water were done within a combined approach including small-angle neutron scattering (SANS), small-angle X-ray scattering (SAXS), dynamic light scattering (DLS) and UV-Vis absorption spectroscopy. Structural changes of the aggregates were observed depending on the type of the stabilizer used. A stabilization mechanism of the systems at nanolevel is discussed.

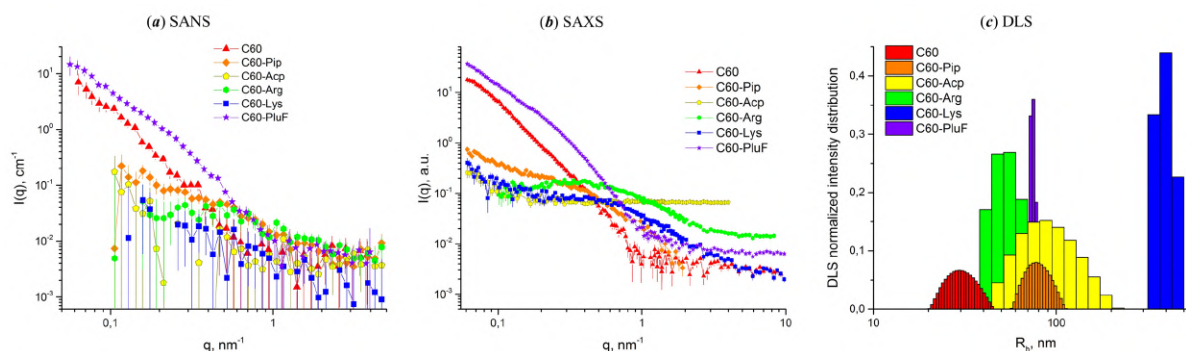


Fig.1. Experimental data on scattering of neutrons (a), X-rays (b) and light (c) by aqueous colloidal solutions of fullerenes C<sub>60</sub> with different stabilizing agents.

### References

1. Shershakova N., Baraboshkina E., Andreev S., Purgina D., Struchkova I., Kamyschnikov O., Nikonova A., Khaitov M. *Journal of Nanobiotechnology* (2016) **14**, 1483.
2. Kyzyma E.A., Tomchuk A.A., Bulavin L.A., Petrenko V.I., Almasy L., Korobov M.V., Volkov D.S., Mikheev I.V., Koshlan I.V., Koshlan N.A., Bláha P., Avdeev M.V., Aksenov V.L. *Journal of Surface Investigation* (2015) **9**, 1.
3. Andreev S.M., Purgina D.D., Bashkatova E.N., Garshev A.V., Maerle A.V., Khaitov M.R. *Nanotechnologies in Russia* (2014) **9**, 369.

## High pressure behavior of the crystal structure of the fullerene molecular complex with ferrocene $C_{60}^*\{Fe(C_5H_5)_2\}_2$ .

*Kuzmin A. V.*<sup>1</sup>, *Khasanov S. S.*<sup>1</sup>, *Meletov K. P.*<sup>1</sup>, *Konarev D. V.*<sup>2</sup>

*kuzminav@issp.ac.ru*

<sup>1</sup> Institute of Solid State Physics RAS, Chernogolovka, Moscow region 142432, Russia

<sup>2</sup> Institute of Problems of Chemical Physics RAS, Chernogolovka, Moscow region 142432, Russia

We have studied the crystal structure of the molecular complex  $C_{60}^*\{Fe(C_5H_5)_2\}_2$  by X-ray diffraction analysis at pressures up to 50 kbar using the diamond anvil cell (DAC) technique. In a parallel way, the pressure dependence of the phonon modes in the Raman spectra of  $C_{60}(Fc)_2$  were acquired up to 100 kbar. The structural data were collected for the high quality single crystals of typical size  $\sim 200 \mu$  using the four-circle Oxford Diffraction diffractometer equipped with two-dimensional CCD Atlas S2 and DAC with Boehler type Ia anvils. The Raman spectra were recorded in the back-scattering geometry using spectrograph Acton SpectraPro-2500i with Peltier cooled CCD. The right part of Fig.1 shows the pressure dependence of the unit cell volume  $V/V_0$  fitted by the Murnaghan equation of state  $(V/V_0)^B = 1/\{1 + P \cdot (B'/B)\}$  (dashed line). The dependence is smooth and monotonous, the bulk modulus and its derivative  $B=8.485 \text{ GPa}$  and  $B'=10.36$  are close to those of other  $C_{60}$  complexes. The left side of Fig.1 emphasizes the pressure dependence of the shortest distance  $L$  between the donor Fc and acceptor  $C_{60}$  molecules. The data clearly demonstrate two regions fitted by independent linear dependence with different pressure coefficients (dashed lines). This peculiarity is an indicator of the intermolecular interactions crossover, probably due to partial charge transfer between the donor and acceptor molecules starting at this point. **Acknowledgments.** The research is carried out within the state task of ISSP RAS and partial support of the RAS Presidium Program "Physics of condensed matter and new generation materials".

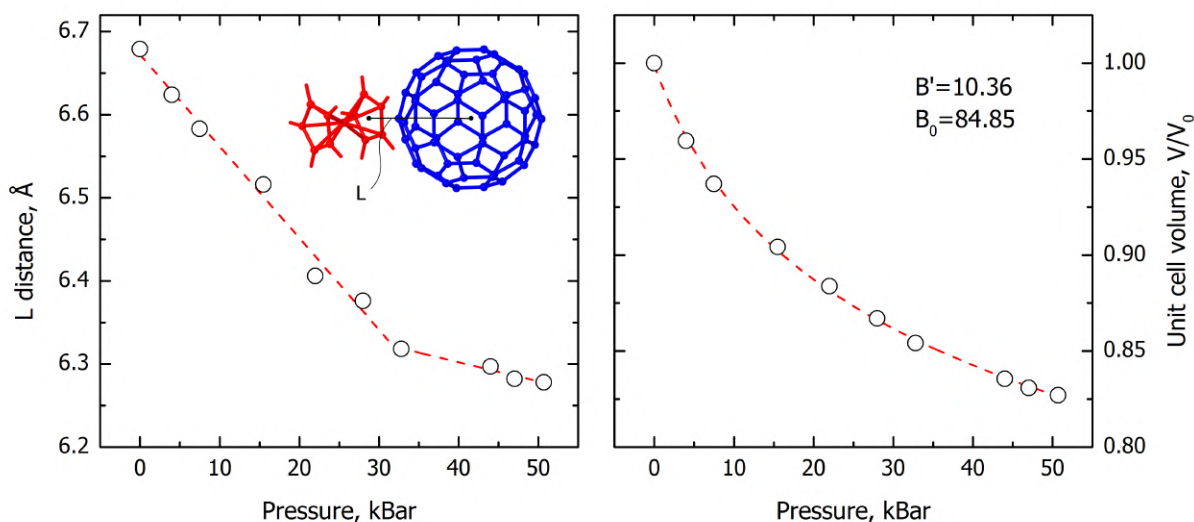


Figure 1. Pressure dependence of the unit cell volume  $V/V_0$  and the shortest distance between the donor and acceptor molecules  $L$  for the  $C_{60}(Fc)_2$  molecular complex.

## Luminescence switching properties of fullerene[60]-containing spiropyrans, a promising light-controlled molecular switches

*Galimov D.I.*<sup>1</sup>, *Kinzyabaeva Z.S.*<sup>1</sup>, *Sabirov D.Sh.*<sup>1</sup>, *Tuktarov A.R.*<sup>1</sup>, *Khuzin A.A.*<sup>1</sup>, *Dzhemilev U.M.*<sup>1</sup>

*galimovdi@mail.ru*

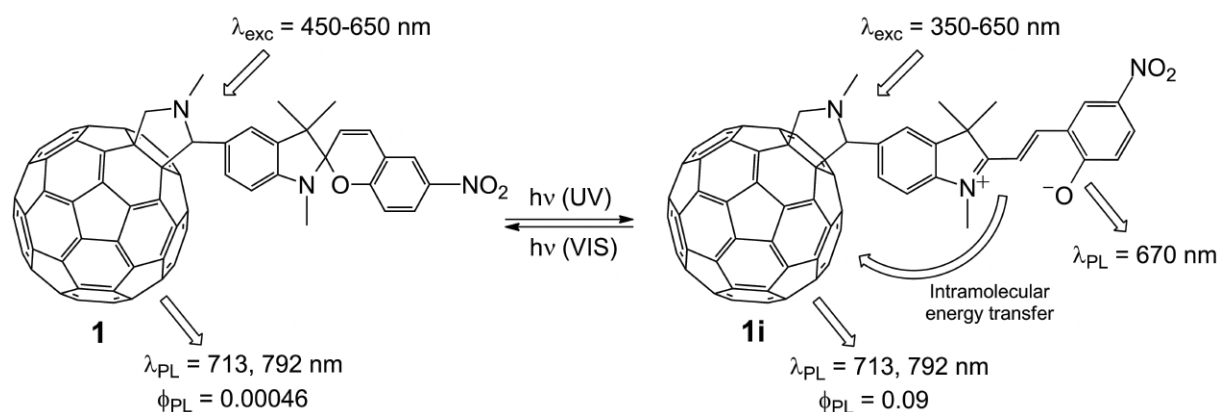
<sup>1</sup> Institute of Petrochemistry and Catalysis RAS, Ufa, Russia

Switching luminescence, one of the promising ways of current photochromic techniques, was primarily demonstrated on benzospiropyrans [1]. Introducing of diverse functional groups, metals or even large molecular moieties to the spiropyran structure allows producing a large set of hybrid photochromic systems. Recently [2], the first photochromic fullerene-spiropyran adduct (**1**) has been synthesized via the 1,3-dipolar cycloaddition of azomethyne ylide to C<sub>60</sub>.

In the present work, we report on the results of spectrophotometric and luminescence studies of fulleropyrrolidine **1**. We have obtained the absorption and photoluminescence (PL) spectra, lifetimes of the excited states, concentration and temperature dependences, quantum yields of PL ( $\phi_{PL}$ ) of fulleropyrrolidine in its spirocyclic (closed) **1** and merocyanine (open) forms. As a result, the first example of fullerene-containing photochromic compounds have been found due to photoisomerization **1** → **1i** [3]. The **1i** form has the PL yield one order larger than pristine spiropyrans and with  $\phi_{PL} = 0.09$  seems to have the highest luminescence among the fullerene monoadducts. The calculated thermodynamic parameters of photoisomerization **1** → **1i**, dipole moments and mean polarizabilities of **1**, **1i** and parent spiropyrans (the PBE/3 $\zeta$  method, Priroda 11.0 program) suggest that the introducing the fullerene core to the photochromic system leads to the enhancement of the efficacy of the switch.

The reversible luminescent switching upon transits **1** ↔ **1i** and the higher photostability of compound **1** make the photochromic fullerene derivatives promising for new molecular devices and related nano-applications.

The work was supported by the Russian Foundation for Basic Research (project No 19-03-00716).



### References

1. A. Parthenopoulos, P.M. Rentzepis, *Science* (1989) **245**, 843.
2. A.R. Tuktarov, A.A. Khuzin, A.R. Tulyabaev, O.V. Venidictova, T.M. Valova, V.A. Barachevsky, L.M. Khalilov, U.M. Dzhemilev, *RSC Adv.* (2016) **6**, 71151.
3. D.I. Galimov, A.R. Tuktarov, D.Sh. Sabirov, A.A. Khuzin, U.M. Dzhemilev, *J. Photochem. Photobiol. A - Chem.*, (2019) **375**, 64.

## Magnetic properties of a fullerene composite

Berezkin V.I.<sup>1</sup>, Kidalov S.V.<sup>2</sup>, Popov V.V.<sup>2</sup>, N.V.Sharenkova<sup>2</sup>

13745pop@mail.ru

<sup>1</sup> Research Center for Ecological Safety, Russian Academy of Sciences, Saint Petersburg, Russia

<sup>2</sup> Ioffe Institute, St. Petersburg, Russia

Recently, special attention is drawn to the magnetic properties of materials, in which there are no magnetic atoms of transition elements. Thus, in a number of pure carbon structures, as well as in some organic substances, ferromagnetic hysteresis is observed, which persists to high temperatures. The most interesting results on the magnetic properties of carbon objects were obtained in the study of structures based on fullerenes, graphene and nanotubes. Typically, fullerenes are combined into a molecular lattice of the face-centered cube (FCC) type. There are various methods to modify such fullerenes, allowing to change the symmetry and transform the molecular lattice. It is, for example, polymerization. The most complete polymerization, up to partially three-dimensional one, is realized when fullerenes are exposed to high pressures and high temperatures (HPHT). In this case, the initial molecular FCC lattice can be transformed into a covalent tetragonal, orthorhombic or rhombohedral one. With this technology, as temperature and pressure increase, the degree of disorder in the arrangement of molecules can increase, and molecules themselves begin to collapse. As a result, amorphized graphite-like ( $sp^2$ ) and diamond-like ( $sp^3$ ) carbon structures are obtained, which are accompanied by an increase of the magnetic centers concentration [1].

In this paper, we study the magnetic properties of a doped with Na composite where fullerenes  $C_{60}$  are placed in the carbon matrix based on exfoliated graphite (EG, [2]). The mixture of  $C_{60}$ , EG, and  $NaN_3$ , which is decomposed into Na and  $N_2$  at 275 °C, was processed by HPHT technology at the pressure of 7 GPa and the temperature of 600 °C. The X-ray diffraction analysis of the samples shows that  $C_{60}$  molecules under these conditions remain mostly undisturbed. Measurements of the magnetic moment in the obtained samples were performed by the vibration method in the PPMS QD apparatus.

The total magnetic moment,  $M$ , of all samples turned out to consist of a sum of dia-(D), ferro-(FM), and paramagnetic (PM) contributions:  $M = M_D + M_{FM} + M_{PM}$ . The magnetic susceptibility weakly depends on the temperature down to  $T=50$  K, and the positive PM contribution to it significantly increases at  $T<50$  K. In samples where  $C_{60}$  prevails over EG, the  $M_{PM}(H)$  curves at  $T=3$  K can be well reproduced by a Brillouin-type function using  $g$ -factor  $g=2$  and a total angular momentum  $J=1$ , which corresponds to magnetic moment equal to  $2m_B$  per a magnetic center ( $m_B$  is the Bohr magneton).

The concentration of PM centers,  $N_{PM}$ , obtained from the data on paramagnetic properties of samples predominantly consisting of fullerenes, lies within  $(3-5) \cdot 10^{18} \text{ g}^{-1}$ , which is a typical value for magnetic centers in defective carbon structures [3]. As the concentration of EG in the samples increases, the value of  $N_{PM}$  also increases significantly. The contribution of the impurity of sodium in the magnetic properties of the material is not essential.

### References

1. R. A. Wood, M. H. Lewis, M. R. Lees, S. M. Bennington, M. G. Cain, and N. Kitamura. *J. Phys.: Condens. Matter.* (2002) **14**, L385.
2. D. D. L. Chung. *Mater. Sci.* (2016) **51**, 554.
3. P. Esquinazi and R. Hohn. *J. Magn. Magn. Mater.* (2005) **290-291**, 20.

## Comparative thin-layer chromatographic profile of water dispersions of C<sub>60</sub>

*Andreev S.M.*<sup>1</sup>, *Stepanova E.A.*<sup>1</sup>, *Turetskiy E.A.*<sup>1,2</sup>, *Shershakova N.N.*<sup>1</sup>, *Semenkin A.*<sup>3</sup>, *Kozhikhova K.V.*<sup>1</sup>

*sm.andreev@nrcii.ru*

<sup>1</sup> NRC Institute of Immunology FMBA, Moscow, Russian Federation

<sup>2</sup> Sechenov First Moscow State Medical University, Moscow, Russian Federation

<sup>3</sup> Drugs Technology LLC, Khimki, Moscow Region, Russian Federation

**Background.** Aqueous dispersion/solution of fullerene C<sub>60</sub> (AFS) obtained by the biocompatible diafiltration method [1] have previously been shown to have interesting biological properties, including antiviral action against the herpes simplex virus types 1 and 2 and anti-inflammatory - in the murine model of atopic dermatitis with very low toxicity [2]. AFS nanoparticles contain, in addition to C<sub>60</sub>, N-methylpyrrolidone (MP) molecules in the form of a charge transfer complex and water, although their spatial distribution in the particle is not yet known. It is obvious that the properties of C<sub>60</sub> solution (single molecules) in toluene and AFS (clusters) should be significantly different. The purpose of the present study was to compare a chromatographic behavior of AFS and C<sub>60</sub> in toluene using thin-layer chromatography (TLC).

**Methods.** The AFS (1 mg C<sub>60</sub>/ml, particles size ~200 nm, z-potential -24.2 mV) was prepared as described in [1] and contained pluronic F-127 (stabilizer). Chromatographic experiments were performed at room temperature on glass-based plates with silica gel without fluorescent indicator (Merck, Darmstadt) cut into 50x100 mm. Samples were: AFS, fullerene C<sub>60</sub> solution in toluene (1 mg/ml), nC<sub>60</sub> (~100 µg/ml, dispersion obtained by conventional ultrasonic method), MP (10 mg/ml), pluronic F-127 and fullerenol. Mixture of toluene and dimethylformamide (1:1) was used as the mobile phase. The fullerene was visually detectable as brown spots on a white background of TLC plate, while iodine fumes increased the contrast of the spots. The visualized spots on the plate (for AFS) were neatly cut out, extracted with the same mobile phase and their contents were analyzed by MALDI-TOF mass spectrometry.

**Results.** TLC analysis of C<sub>60</sub>/toluene solution showed only one brown spot near the front. The AFS sample demonstrated 4 spots: 1<sup>st</sup> near the front, 2<sup>nd</sup> just below (Rf ~0.92), 3<sup>rd</sup> with Rf ~0.46 and 4<sup>th</sup> at the start. In relation to nC<sub>60</sub> was detected 2 spots: very weak on the front and noticeable at the start. Fullerenol showed only one spot at the start, while pluronic had a high mobility with a Rf of about 0.9-0.93. Analysis of the cut out spots showed that they contain only C<sub>60</sub> (m/z 720).

**Conclusion.** The results of TLC analysis coupled with mass spectrometry demonstrate the absence of a noticeable chemical modification of fullerene in the process of obtaining a concentrated form of AFS (1 g/L). Moreover, the TLC can serve as a simple express-analysis of the authenticity of AFS. It is important to note that the colloidal status of fullerene particles significantly affects the chromatographic behavior. Although all the spots into which the fullerene dispersions were separated contain the same substance, it is reasonable to assume that the particles retained in these spots should differ in some of their properties, and this requires further study.

### References

1. Andreev S. et al. 2015. Fullerenes, Nanotubes and Carbon Nanostructures, 23(9):792-800; Patent. RU 2679257 (17.01.2018).
2. Shershakova, N. et al. 2016. J. Nanobiotechnology, 14:1483-1493.

## Metallic and antiferromagnetic states with strong spin frustration in fullerene radical-anion salts with triangular lattices

*Konarev D.V.*<sup>1</sup>, *Khasanov S.S.*<sup>2</sup>, *Otsuka A.*<sup>3</sup>, *Yamochi H.*<sup>3</sup>, *Lyubovskaya R.N.*<sup>1</sup>

*konarev3@yandex.ru*

<sup>1</sup> Institute of Problems of Chemical Physics RAS, Chernogolovka, Russia

<sup>2</sup> Institute of Solid State Physics RAS, Chernogolovka, Russia

<sup>3</sup> Graduate School of Science, Kyoto University, Kyoto, Japan

- In this report we discuss our strategies for preparation of fullerene compounds, which can show metallic conductivity or to be Mott insulators with strong magnetic coupling of spins and strong spin frustration.
- For preparation of compounds with triangular lattices from fullerene radical anions we use cations and components having  $C_{3v}$  symmetry. (MDABCO<sup>+</sup>)(C<sub>60</sub><sup>•-</sup>)(TPC) (**1**) (MDABCO<sup>+</sup> is *N*-methyl diazabicyclooctanium, TPC is triptycene) is a rare example of fullerene based quasi-two-dimensional (2D) metal, which contains closely packed hexagonal fullerene layers (Fig. 1a) [1]. Modification of a structure of metal **1** by using substituted triptycenes is discussed. Bulkier MQ<sup>+</sup> cations (*N*-methylquinuclidinium) increase the interfullerene distance in the layered complex (MQ<sup>+</sup>)(C<sub>60</sub><sup>•-</sup>)(TPC) (**2**) and transfer it to the Mott insulator with an antiferromagnetic coupling of spins ( $Q = -27$  K). Variation of the cations used allows to modify properties of fullerene salts. Cryptand(M<sup>+</sup>) cations form air-stable complexes **3** and **4** with partial charge transfer to fullerenes. They have hexagonal packing of fullerenes (Fig. 1b) and show metallic conductivity or charge separation [1]. Tributylmethylphosphonium cations allow one to pack C<sub>60</sub><sup>•-</sup> and endometallofullerene Sc<sub>3</sub>N@C<sub>80</sub><sup>•-</sup> radical anions in (TBMP<sup>+</sup>)(Fullerene<sup>•-</sup>)×0.33C<sub>6</sub>H<sub>4</sub>Cl<sub>2</sub> salts (**6**, **7**) in closely packed Kagome lattices (Fig. 1c) with strong magnetic coupling spins ( $Q = -109$  and  $-43$  K, respectively) without magnetic ordering down to 1.9 K [2]. Salt **6** is a candidate for the observation of a quantum spin liquid state in the C<sub>60</sub><sup>•-</sup> system.
- The work was supported by RSF №18-13-00292 and RFBR №17-53-12017.

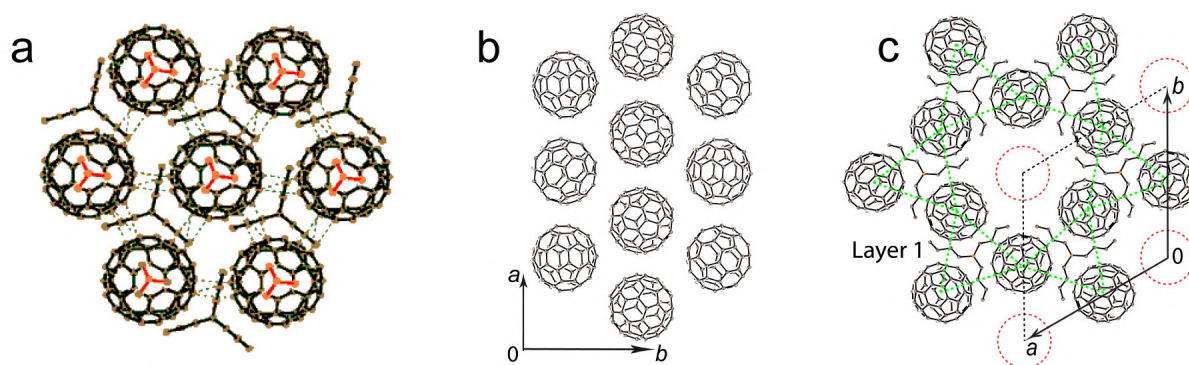


Fig. 1. (a) Projection of organic (MDABCO<sup>+</sup>)(TPC) layers on hexagonal fullerene layers in **1**; (b) view on the fragment of hexagonal fullerene layer in {cryptand[2.2.2](Na<sup>+</sup>)}(C<sub>60</sub>)<sub>3</sub>×2C<sub>6</sub>H<sub>4</sub>Cl<sub>2</sub> (**3**) [1]; view on the Kagome lattice from C<sub>60</sub><sup>•-</sup> in **6** [2].

### References

1. D.V. Konarev, S.S. Khasanov, M. Ishikawa, E.I. Yudanov, A.F. Shevchun, M.S. Mikhailov, A. Stuzhin, A. Otsuka, H. Yamochi, G. Saito, and R.N. Lyubovskaya, *ChemistrySelect* (2016) **1**, 323.
2. D.V. Konarev, S.S. Khasanov, Y. Shimizu, A. Otsuka, H. Yamochi, G. Saito, and R.N. Lyubovskaya, *ChemPhysPhysChem.* (2019) **21**, 1645.

## Electrochemical study of $S_6$ - $C_{60}(CF_3)_{12}$ : a new general methodology for low-soluble fullerene derivatives

*Urintsev D.I.<sup>1</sup>, Kosaya M.P.<sup>1</sup>*

*danil.urintsev@mail.ru*

<sup>1</sup> Chemistry Department of Lomonosov Moscow State University, Moscow, Russia

Inert and non-toxic fluorocarbon compounds are promising as dielectric materials and as constituents of composite materials, providing high thermal, chemical and photostability [1]. Particularly interesting members of the fluorocarbon family are trifluoromethylated fullerenes that additionally feature electron acceptor and fluorophore properties mediated by their fused assemblies of unsaturated five- and six-membered rings. Recently, many trifluoromethylated fullerenes have been found to show a good linear correlation between the first reduction potential and the theoretically calculated LUMO energy [2]. However, a number of trifluoromethylated fullerenes were not to be included in that study because of their low solubility in the commonly used solvents that rendered electrochemical experiments impossible.

In the present work, we report a new general approach that may enable electrochemical investigations of many less-soluble fullerene compounds by utilizing perfluorinated organic solvents. As a test case, we studied the  $S_6$ -symmetric  $C_{60}(CF_3)_{12}$  [3] which is known to form low-soluble crystalline phase. The isolated and comprehensively spectroscopically characterized  $S_6$ - $C_{60}(CF_3)_{12}$  compound was subjected to cyclic voltammetry (CVA). The use of the perfluorinated solvents afforded, for the first time, sufficient room-temperature solubility of  $S_6$ - $C_{60}(CF_3)_{12}$  and enabled optimization of the CVA conditions for its study.  $S_6$ - $C_{60}(CF_3)_{12}$  was observed to undergo reversible reduction at -0.8 V with respect to the  $C_{60}^{0/-}$  potential, indicative of weaker acceptor properties of its triphenylene-like conjugated substructures. To further test the potential of the perfluorinated solvents, we plan to perform a broader electrochemical survey of various types of poorly soluble fullerene derivatives.

### References

1. Lemal D.M. Perspective on Fluorocarbon Chemistry // *J. Org. Chem.* 2004. Vol. 69, № 1. P. 1-11.
2. Kosaya M.P. et al. Facile separation, spectroscopic identification, and electrochemical properties of higher trifluoromethylated derivatives of the [70]fullerene // *Chem. - Asian J.* 2018. Vol. 13, № 15. P. 1920-1931.
3. Troyanov S.I., Dimitrov A., Kemnitz E. Selective Synthesis of a Trifluoromethylated Fullerene and the Crystal Structure of  $C_{60}(CF_3)_{12}$  // *Angew Chem Int Ed.* 2006. Vol. 45. P. 1971-1974.



## Luminescence properties of fullerene C<sub>60</sub> in aqueous media

*Pirogova M.O.*<sup>1</sup>, *Mikheev I.V.*<sup>1</sup>, *Korobov M.V.*<sup>1</sup>, *Volkov D.S.*<sup>1</sup>, *Proskurnin M.A.*<sup>1</sup>

*mariy7991@yandex.ru*

<sup>1</sup> Chemistry Department, Lomonosov Moscow State University, Moscow, Russia

During the last decade, the production and determination of fullerenes in aqueous dispersions (AFDs) has been showed an upward trend. The main areas of application of AFDs are medicine and pharmacology. AFDs of unmodified fullerenes (having no addends) can be introduced into human body as anticancer or antiviral drugs. However, the chemistry of fullerene compounds and AFD properties still should be fully unraveled. Fluorescence spectroscopy is a rather sensitive method, occupies a special place in research of biological objects and can be used for low concentrations of AFDs.

Luminescence properties of pristine fullerenes and their derivatives in nonpolar solvents, especially peculiarities of C<sub>60</sub> in organic solutions under different conditions and state, have been previously investigated. However, much less data are known for AFDs. Thus, the aim of this study is to estimate luminescence properties of aqueous fullerene C<sub>60</sub> dispersions.

AFDs were obtained by the ultrasound-induced solvent-exchange technique from toluene (the ratio of toluene to water is 1:5, within 24 h treating time). UV/vis/NIR, total organic carbon analysis, HPLC-UV, and headspace gas chromatography/mass spectrometry were used to characterize the obtained AFDs and showed the dissolved organic substances akin benzene, toluene, etc. at lower than ppb-levels.

Excitation-emission map (EEM) fluorescence spectra of AFDs were obtained (Fig. 1). A band was found in the photoluminescence spectra of AFD C<sub>60</sub> with a maximum at 350–430 nm at excitation wavelengths of 280–350 nm. In toluene solutions, the characteristic regions are red-shifted (*ca.* 200 nm at emission). The red shift proves a different type of interaction (fullerene-polar/nonpolar solvent) in molecular solutions in toluene compared to colloidal solutions in water. There are peculiarities in the electronic structure of the EEM, in toluene solutions there are three characteristic peaks maxima; although in aqueous, only one peak is manifested.

The optimum conditions for registration of spectra were selected (exciting/emission slit range, detector voltage, and integration time). Limits of detection for fullerenes in aqueous dispersions are estimated as *ca.*  $n \times 10^{-7}$  M ( $\lambda_{\text{Ex}} = 349$  nm) that would allow the use of the technique at the level of concentrations of AFDs in medicine. The influence of highly saline media based on buffer solutions, phosphate buffer saline (PBS), and sodium chloride on the change of fullerene EEM spectra were studied. After analyzing the obtained EEM spectra of AFDs, no significant difference was found, which proves very similar intermolecular interactions in AFDs under different conditions. With fluorescence spectroscopy, the spectra of formation of hydrogen bonds in existing systems for further use of AFDs as antiviral and antitumor drugs were studied. The results will be presented in more detail in the presentation. In the future, AFDs should be checked for the interaction with proteins, lipids, and other biomolecules to understand the possible behavior of AFDs in human body.

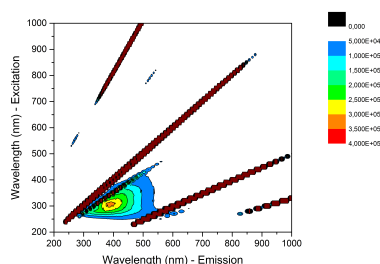


Fig. 1. Luminescence spectra of an aqueous fullerene C<sub>60</sub> dispersion, 10 ppm.

## Adsorption of alkyltrimethylammonium bromides on nanodiamonds

*Badun G.A.<sup>1</sup>, Chernysheva M.G.<sup>1</sup>, Gus'kov A.V.<sup>1</sup>, Sinolits A.V.<sup>1</sup>, Popov A.G.<sup>1</sup>, Egorov A.V.<sup>1</sup>, Egorova T.B.<sup>1</sup>, Kulakova I.I.<sup>1</sup>, Lisichkin G.V.<sup>1</sup>*

*badunga@yandex.ru*

<sup>1</sup> Lomonosov Moscow State University, Moscow, Russia

High specific surface area and functional surface composition of detonation nanodiamonds allow the modification of nanodiamonds surface with different compounds either by chemical synthesis or adsorption [1]. Pretreatment of nanodiamonds sets the functional composition of the surface and provides its positive or negative zeta potential in the aqueous suspension. Previously, we have shown that being quaternary ammonium base the surface active drug (Myramistin) can adsorb on both positively and negatively charged nanodiamonds [2,3]. To reveal the mechanism of the adsorption process we studied the adsorption of three representatives of a homologous series of alkyltrimethylammonium bromides (dodecyl, tetradecyl and hexadecyl) on nanodiamonds of positive and negative zeta potential. The amount of the surfactant on nanodiamond surface was determined using tritium labeled compounds that were obtained by means of tritium thermal activation method [4].

Nanodiamonds produced by PlasmaChem were used in this study. Nanodiamond powder was used as received as well as subjected to air annealing at 450°C during 1 hour. The suspension of single-digit nanodiamond (SDND, PlasmaChem) was used as received. Nanodiamond powder was suspended in water as it was described in ref [2]. Nanodiamonds were characterized by means of FTIR, BET and TEM. The suspensions were also characterized by DLS. It was found that nanodiamond subjected to air annealing and SDND possess negative value of zeta potential as well as its functional composition was very close.

The adsorption experiments were carried out according to the procedure described previously [2,3]. For all types nanodiamonds we obtained adsorption isotherms of alkyltrimethylammonium bromides of Langmuir type. It reached plateau region at concentration value close to critical micelle concentration. However, the value of maximum adsorption was decrease with molecular weight growth. For nanodiamonds that were subjected to air annealing and SDND the isotherms were identical and maximum adsorption obtained for these samples was as much as 30 times higher than maximum adsorption on nanodiamonds of positive zeta potential. The reversibility of adsorption of alkyltrimethylammonium bromides was determined in water and in 0.9% NaCl. For all samples it was found that desorption in water is negligible while in presence of salt the desorption reached 57% suggesting the dominant role of electrostatic interactions in the adsorption process. We also control value of zeta potential as a function of surface concentration of alkyltrimethylammonium bromides surface concentration. We have found that all types of nanodiamonds are stabilized in the aqueous suspension when the adsorption reaches plateau region.

This work was supported by Russian Foundation for Basic Research (grant # 17-03-00985).

### References

1. Neburkova J., Vavra J., Cigler P. *Current Opinion Solid State Mater. Sci.* (2017) **21**, 43.
2. Chernysheva M.G., Popov A.G., Tashlitsky V.N., Badun G.A. *Colloids Surface A.* (2019), **565**, 25.
3. Chernysheva M.G., Alexeev M.E., Myasnikov I.Yu, Popov A.G., Badun G.A. *Abstr. 13th Int. Conf. Advanced Carbon Nanostructures (ACNS'2017)*, p. 42.
4. Badun G.A., Chernysheva M.G., Ksenofontov A.L. *Radiochimica Acta.* (2012), **100**, 401.

## **Application of aluminum oxide nanofibers as a carrier for nanodiamonds.**

Ronzhin N.O.<sup>1</sup>, Posokhina E.D.<sup>1,2</sup>, Mikhлина E.V.<sup>3</sup>, Simunin M.M.<sup>2</sup>, Bondar V.S.<sup>1</sup>, Ryzhkov I.I.<sup>4</sup>

*michanel@mail.ru*

<sup>1</sup> Institute of Biophysics SB RAS, Akademgorodok 50/50, 660036 Krasnoyarsk, Russia

<sup>2</sup> Siberian Federal University, Svobodny 79, 660041 Krasnoyarsk, Russia

<sup>3</sup> 3Institute of Computational Modelling SB RAS, Akademgorodok 50/44, 660036 Krasnoyarsk, Russia

<sup>4</sup> Institute of Computational Modelling SB RAS, Akademgorodok 50/44, 660036 Krasnoyarsk, Russia

Surface properties of detonation nanodiamonds such as large specific area, the abundance of different chemically active groups and traces of metals [1] make this nanomaterial applicable as a catalyst for the development of new analytical sensors, for example, for phenol detection [2,3]. In this regard, a fixation of the nanoparticles on a solid matrix will facilitate further practical adaptation of nanodiamond-based sensors for environmental monitoring. To achieve this goal, in the present study we used Nafen™ alumina nanofibers [4] as a solid matrix and nanodiamonds possessing high colloidal stability in hydrosol [1] to fabricate the Nafen-nanodiamond composite material.

For binding of nanodiamonds with Nafen nanofibers, the colloidal solutions with certain concentrations of the nanomaterials were directly mixed with each other in aqueous medium while stirring continuously. The composite was made by filtration deposition [5] of alumina nanofibers with nanodiamonds and then sintered at 300 °C to ensure its structural stability in aqueous solutions.

A study on the SEM morphology of the obtained samples showed that the mixing led to spontaneous deposition of nanodiamonds on the surface of alumina nanofibers. The zeta-potential measurement of nanodiamonds colloidal solution and Nafen colloidal solution showed that nanodiamonds are negatively charged, while the Nafen nanofibers are positively charged. Thus, the electrostatic attraction is responsible for deposition of nanodiamonds on the nanofibers. The surface charge on the nanodiamonds is caused by the presence of carboxyl and ketone functional groups, while the alumina nanofibers exhibit amphoteric dissociation reactions of aluminum hydroxide. It is confirmed by the sample analysis with the help of XPS method.

In conclusion, it should be added that the nanodiamonds incorporated into the alumina matrix retained their reactive surface. It was shown that due to nanodiamonds, the obtained composite exhibited catalytic activity in oxidative azo coupling reaction (phenol - 4-aminoantipyrine - hydrogen peroxide) and was able to detect phenol in aqueous medium.

The work is supported by the Russian Foundation for Basic Research Grant № 18-29-19078.

### **References**

1. N. Gibson, O. Shenderova, T.J.M. Luo et al. // *Diam. Relat. Mater.* 18 (2009) 620–626.
2. N. Ronzhin, A. Puzyr, A. Burov et al. // *J. Biomater. Nanobiotech.* 5 (2014) 173–178.
3. N. Ronzhin, A. Puzyr, V. Bondar // *J. Nanosci. Nanotechnol.* 18 (2018) 5448–5453.
4. Features of Nafen alumina nanofibers, <http://www.anftechnology.com/nafen/>
5. Solodovnichenko V.S., Lebedev D.V. et al. // *Adv. Eng. Materials*, 2017, V. 19, 1700244.

## Obtaining of diamonds from detonation of individual explosives.

*Dolmatov V. Yu.*<sup>1,2</sup>, *Dorokhov A.O.*<sup>3</sup>, *Kislelev M. N.*<sup>3</sup>, *Kozlov A.S.*<sup>1,2</sup>, *Myllymaki V.*<sup>4</sup>, *Vehanen A.*<sup>4</sup>

*diamondcentre@mail.ru*

<sup>1</sup> FSUE "SCTB "Technolog", St.Petersburg, Russia

<sup>2</sup> St. Petersburg State Institute of Technology (Technical University), St.Petersburg, Russia

<sup>3</sup> JSC Plant "Plastmass", Kopeisk, Russia

<sup>4</sup> Carbodeon Ltd. Oy, Vantaa, Finland

To obtain detonation nanodiamonds (DNDs), mixed charges are used, as a rule, tetryl with hexogen (RDX), in which optimal parameters are selected for power density, oxygen balance, charge density and armor. However, from a technological and economic point of view, the use of an individual explosive would be optimal: the dangerous and time-consuming stage of mixing different explosives is eliminated, the use of expensive and deficient RDX is excluded. In addition, it is desirable to use recycled explosives with sufficiently high power and sensitivity to the initiating pulse and giving a significant DNDs yield. Recyclable tetryl (N-methyl-2,4,6-trinitrophenylnitramine) responds to all these qualities.

The study of the detonation synthesis process was carried out in an explosion chamber (EC) "Alpha-2M", with a capacity of 2.14 m<sup>3</sup>. Undermining was carried out in water reservation (shell), sometimes using an aqueous solution of urotropin. The diameter of the cylindrical charge is 60 mm, the length is ~ 120 mm. EC gas environment is previous explosion gaseous products (PD - products of detonation).

The previously used individual explosives either provide extremely low DND yield (proportion of percent) or there is no industrial production of explosives.

DND obtaining process from industrially produced picric acid (PC) was studied for the first time. Despite the presence of water armoring, the DND yield from the PC is small - no more than 1.2% wt. Thus, the use of PC for industrial production of DND is not economically efficient.

Detonation of tetryl without a shell in a gaseous environment gave a negligible yield - 0.37% wt. and unsuitable for industrial production.

On the contrary, only the use of water or water-urotropin solution armoring increased the DND yield by ~ 20 times - up to 6.3-7.05% by weight with a minimum amount of non-combustible impurities in DND - 0.36-0.94% wt.

Taking into account the large reserves of tetryl, our method allows us to recommend it for industrial production of DNDs.

A new industrial method has been developed for obtaining DND from an individual explosive - tetryl with a high yield (6-7% wt.) and a high DND content in the diamond blend (DB) (51-63% wt.), which significantly simplifies the chemical cleaning of DNDs. In addition, DND enriched with DB can be used in polymer chemistry, electroplating, oils and lubricants without additional processing.

## **Influence of physico-chemical environment to get nano-size surface roughness in machining of diamond single crystals**

*Nozhkina A.V.*<sup>1</sup>, *Ramazanova S.A.*<sup>2</sup>, *Vlasov I.I.*<sup>3</sup>, *Razbegayev A.Y.*<sup>2</sup>, *Katayeva E.R.*<sup>2</sup>, *Zavedeyev Y.A.*<sup>3</sup>

*nojkina@inbox.ru*

<sup>1</sup> VNIIMALMAZ, NUST "MISiS", Moscow

<sup>2</sup> NUST "MISiS", Moscow

<sup>3</sup> IOF RAN, Moscow

The work represents the study results of mechanical treatment of synthetic crystals of a diamond in order to manufacture polished diamond pieces. Polishing of the studied diamonds was done with the use of diamond micropowders with a coating that is chemically active towards silicon-based alloy based upon carbon as well as diamond micropowders and uncoated nanodiamonds.

The theoretical calculation of yield ratio is given based upon the analysis of the morphological characteristics of the crystal and the assessment of its purity while computer simulating on the Sarin machine.

The mass losses in various technological operations are experimentally determined. The correspondence of the actual mass losses with the theoretical calculations is established.

The analysis of the obtained data shows that the use of coated diamond powders doubles the treatment speed of single crystals of the synthetic diamond due to the effect of the physicochemical environment on this process. Graphitization of diamond occurs on the surface of the processed crystal, which significantly simplifies the process of material removal during its machining.

Using optical interference microscope "Zygo 5000" the study of relief and roughness of the surface of the single crystal before treatment and the surface of the diamond after its mechanical treatment with diamond micropowders of different granularity sizes, as well as nanodiamond powders was conducted. The measurement results show that the roughness of the crystal at each technological operation decreases with the reduction in the granularity size of the diamond micropowder from 2822 nm to 7.322 nm when polishing with micropowders without the coating and to 5.350 nm when polishing with micropowders with the coating. With further polishing using nanodiamond powders, the roughness of the treated surface reached 2.2 nm on the single crystal of the synthetic diamond which contains impurity of single nitrogen (C centers).

The roughness value is 1.04 nm on a polished surface of synthetic diamonds type IIa measured by an optical interference microscope "Zygo 5000».

Consequently, the manufacture of polished diamond pieces from synthetic diamonds by mechanical treatment with the use of micropowders with the coating that is chemically active towards carbon allows doubling the productivity of the treatment process and reducing the roughness of the treated surface.

The use of nanodiamonds while mechanical treatment with the use of micropowders reduces the roughness of the treated surface and improves its quality.

Keywords: synthetic diamond, mechanical treatment, roughness.

### **References**

1. Belimenko L.D., Laptev V.A., Klyuyev Y.A., Naletov A.M., Nepsha V.I., Samoylovich M.I. «Vliyaniye otzhiga monokristallov almaza v usloviyakh ikh termodinamicheskoy stabil'nosti na obrazovaniye i prevrashcheniye strukturnykh defektov», DAN SSSR tom 259, № 6, pp. 1360-1363, 1981;
2. Nozhkina A.V. «Fiziko-khimicheskiye protsessy vzaimodeystviya almaza s obrabatyvayemym materialom» v sbornike «Khudozhestvennoye materialovedeniye prirodnyy kamen'. Dizayn. Tekhnologii.», pp. 47-60, Moscow, 2010;

## Influence of explosives power density the yield of detonation nanodiamonds.

*Dolmatov V. Yu.*<sup>1,2</sup>, *Dorokhov A.O.*<sup>3</sup>, *Kislelev M. N.*<sup>3</sup>, *Kozlov A.S.*<sup>1,2</sup>, *Myllymaki V.*<sup>4</sup>, *Vehanen A.*<sup>4</sup>, *Ponyaev A.I.*<sup>2</sup>

*diamondcentre@mail.ru*

<sup>1</sup> FSUE "SCTB "Technolog", St.Petersburg, Russia

<sup>2</sup> St. Petersburg State Institute of Technology (Technical University), St.Petersburg, Russia

<sup>3</sup> JSC Plant "Plastmass", Kopeisk, Russia

<sup>4</sup> Carbodeon Ltd. Oy, Vantaa, Finland

In order to optimize the process of obtaining detonation nanodiamonds a new concept is introduced - the power density of explosives, equal to the ratio of the heat of explosion to the unit of mass (1 kg) and the unit of time (1  $\mu$ s). 1  $\mu$ s is commensurate with the time course of processes in the zone of chemical reaction of explosives. Thus,

$$W=Q/\tau,$$

where W - explosive power kJ / kg \*  $\mu$ s;

Q - heat of explosion, kJ / kg;

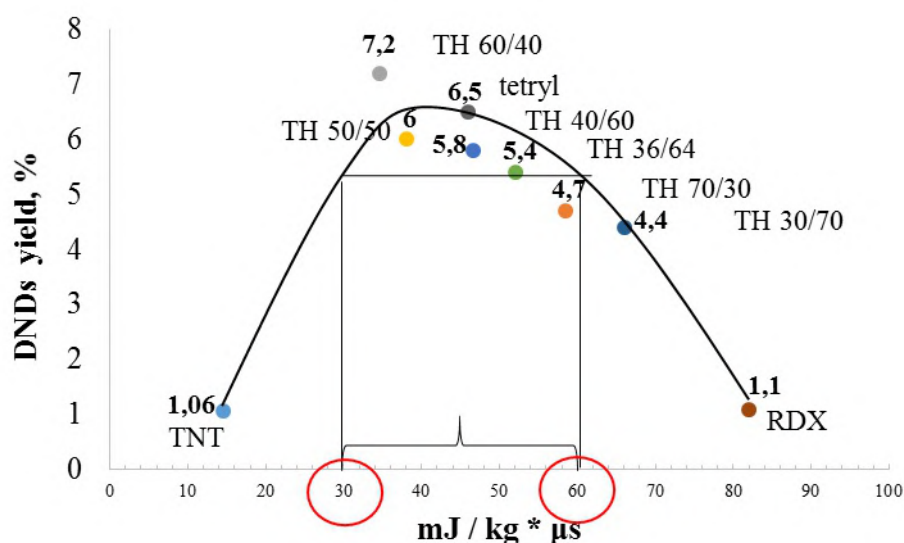
$\tau$  - time of energy release,  $\mu$ s.

The time of a chemical reaction is the time required for a substance to move from the detonation wave front to the Chapman-Jouget plane, where chemical reactions end. The detonation velocity of explosives and the pressure of gases in the Chapman-Jouget plane are related to the power density of explosives. The dependence of detonation nanodiamonds yield on the detonation velocity and pressure in the Chapman-Jouget plane is found. The optimum yield of detonation nanodiamonds (> 5% wt.) falls on the power density of explosives from 30 to 60 mJ / (kg ·  $\mu$ s), the detonation velocity from 7250 to 8000 m / s and the pressure in the Chapman-Jouget plane from 21 to 28 GPa.

Thus, a new unit for measuring the performance of explosives in the synthesis of detonation nanodiamonds has been proposed, which allows a priori to predict the yield of marketable products.

Figure. The dependence of DND yield on the explosive power density, where:

(TNT - trinitrotoluene, RDX - hexogen, TH - alloys of TNT and RDX of different concentrations, Tetryl - N-methyl-2,4,6-trinitrophenyl nitramine).



## **Formulation and properties of a novel perfluoropolyether based fluid containing nanodiamonds**

*Ivanov M.G.<sup>1,2</sup>, Shenderova O.A.<sup>2</sup>, D.M.Ivanov<sup>3</sup>*

*m.g.ivanov@urfu.ru*

<sup>1</sup> Ural State Technical University, Yekaterinburg, Russia

<sup>2</sup> Adamas Nanotechnologies, Raleigh, NC, USA

<sup>3</sup> Ural Federal University, Yekaterinburg, Russia

Perfluoropolyether (PFPE) fluids are perfluorinated polymeric compounds commonly used as lubricants in aerospace, automotive, industrial, and semiconductor applications. Fluorinated synthetic fluids exhibit exceptional thermo-oxidative stability and chemical resistance, low surface energy, good lubricity characteristics, and extended bioinertness. With a goal of further enhancing lubricating properties of fluorinated fluids in heavy duty applications, in the current study we performed developments of PFPE-based nanofluid containing DND additives. In our earlier studies it was demonstrated that lubricating compositions containing detonation nanodiamond (DND) particles with small aggregate sizes significantly reduce friction and wear of sliding surfaces due to a fine polishing effect of DND [1].

Colloidal stability of DND particles in nanolubricants is the key requirement for development of lubricants with significantly enhanced properties [1]. In this study, perfluoropolyether based fluid containing DND was synthesized by high energy ball milling. Preparation routes of PFPE-DND fluid consisted of the steps of modification of DND surface using surfactants and formulation of nanodiamond containing fluid using sonication. As a result, a dark brown transparent fluid containing DND with aggregate size of 20-30 nm in perfluoropolyether was obtained, demonstrating excellent resistance to agglomeration and sedimentation during storage for five years. The FTIR and XPS characterization analysis proved that perfluoropolyether carboxylic acid surfactant successfully decorated nanodiamond surface.

Viscosity and rheological behavior of the formulated perfluoropolyether-DND fluid can be adjusted depending on the intended applications. For example, we will discuss formulation and properties of novel greases based on PFPE, DND and polytetrafluoroethylene (PTFE).

### **References**

1. G. Ivanov, S. V. Pavlyshko, D. M. Ivanov, I. Petrov, O. Shenderova, *JVST B*, 28, 4, 869-876 (2010).

## The new method of purification of detonation nanodiamond and obtaining its stable aqueous suspensions

*Savin S.S.*<sup>1</sup>, *Vozniakowski A.A.*<sup>2</sup>, *Kidalov S.V.*<sup>2</sup>, *Vozniakowski A.P.*<sup>3</sup>, *Ovchinnikov E.V.*<sup>4</sup>, *Liopo V.A.*<sup>4</sup>

*Savin.S.97@mail.ru*

<sup>1</sup> Saint-Petersburg State Institute of Technology, St.Petersburg, Russia

<sup>2</sup> Ioffe Institute, St.Petersburg, Russia

<sup>3</sup> Institute of Synthetic Rubber, St.Petersburg, Russia

<sup>4</sup> Institute of Biology of Komi Scientific Centre of the Ural Branch of the Russian Academy of Sciences, Syktyvkar, Russia

The chemical purity of carbon nanomaterials (CNM), in particular, detonation nanodiamonds (DND), has a strong influence on their final properties. However, the classical methods of purification CNM, for example, by purification of DND in acids and alkalis produce a large quantity of chemical waste that requires special recycling.

In this paper, we proposed an alternative method for the purification of DND, based on the decomposition of nitrate salts into strong oxidant gases that form during their thermal decomposition of salts.

Oxidizing gases allow you to transfer impurities in the gas or water-soluble form, which facilitates their removal. After heating the mixture DND with ammonium nitrate salt, the product was washed with water and isopropyl alcohol and then dried. Figure 1 presents the results of a study of the dispersion of particles of the initial DND (unstable suspension, Fig. A) and a stable aqueous suspension of purified DND (Fig. B). The concentration of DND was 0.1 mass. %

As can be seen from Figure 1, we managed to get a stable aqueous suspension with an average particle size of 40 nm, i. e. The dispersion of DND in a stable suspension is significantly higher than in an unstable suspension, which is due to the removal of impurities, such as metals and their oxides.

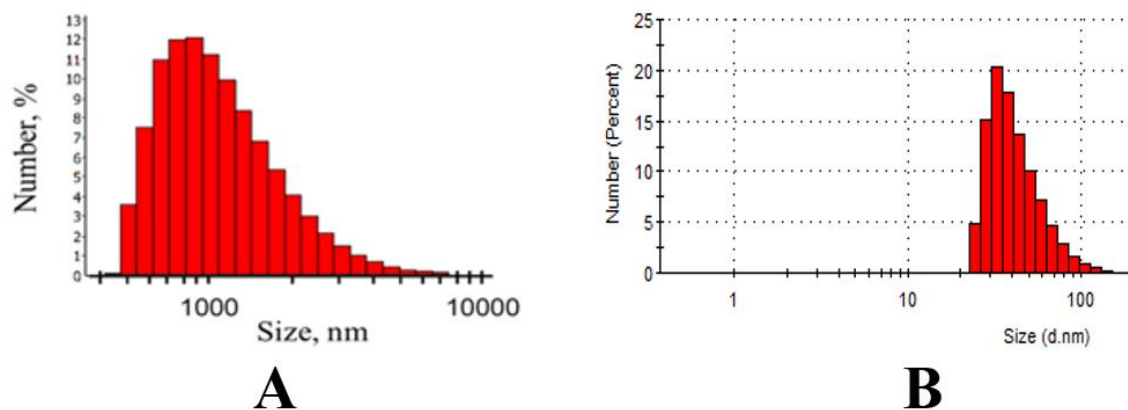


Figure 1. Results of the investigation of the dispersity of the initial DND (A) and DND after purification (B).



## Sensitivity analysis of gas-phase chemistry leading to the formation of carbon nanoparticles

*Leshchev D.V.*<sup>1</sup>

*dimvovich@narod.ru*

<sup>1</sup> Center for Advanced Studies of Peter The Great Saint-Petersburg Polytechnic University, Saint-Petersburg, Russia

Diamond and diamond-like carbon (DLC) have been announced as the 21st-century material [1]. The main method for producing these materials is the chemical vapor deposition (CVD), and its most popular modifications are hot-filament HF CVD (HF-CVD) and microwave plasma enhanced CVD (MWCVD) techniques [1-3]. Those techniques continue to develop actively. Recently, prospects of growing the diamond films by HF-CVD, operating with the use of the heterogeneous dissociation of molecular hydrogen on the catalyst surface were demonstrated [4]. The distinctive feature of that approach consists in a high-speed gas flow, allowing fast delivery of the active particles to the substrate before recombination. It is believed that a high concentration of the atomic hydrogen above growing diamond surface is the main condition of the successful growth of diamond and DLC [5]. Moreover, a high ratio of hydrogen to hydrocarbon radicals is a necessary condition for a stable growth of diamond crystals [6]. Even minor changes in geometry and composition can lead to dramatic fall of diamond growth [6]. Therefore, to optimize existing techniques it is necessary to simulate gas dynamics and chemical reactions occurring in the chamber. A lot of corresponding papers contain either only the gas-phase reactions or only the surface ones.

We started developing a chemical model which include both gas-phase and surface reactions. Despite the in-depth study of practically all corresponding gas-phase reactions [7], rather large discrepancies in the values of pre-exponential factors do exist, not to mention the surface reactions which rates depend on the properties of a specific surface. In this paper an analysis of the sensitivity of the diamond deposition to the values of the pre-exponents of the main chemical reactions, based on the gas-dynamic calculations of the reactor described in [2] is proposed.

Acknowledgements. This work was partially financially supported by Ministry of Science and Education of Russian Federation within the framework of the basic part of state tasks of Peter The Great Saint-Petersburg Polytechnic University (project code 16.7002.2017/8.9) and by the Russian Foundation for Basic Research (grant № 19-08-00533).

### References

1. W. May, *Philos. Trans.R. Soc. (2000) A* **358**, 473.
2. A Rebrov, M Plotnikov, Y Mankelevich, I Yudin, *Phys. Fluids* (2018) **30**, 016106.
3. K. Rebrov, M. V. Isupov. A. Yu. Litvintsev, and V. F. Burov, *Journal of Applied Mechanics and Technical Physics.* (2018) **59**, 771
4. Rebrov A K, Andreev M N, Bieiadovskii T T and Kubrak K V *Coat. Tech.* (2017) **325**, 210
5. Gicquel, K.Hassouni, F.Silva, J.Achard, *Current Applied Physics* (2001) **1**, 479.
6. Mankelevich Yu A and May P W 2008 *Rel. Mat.* **17** 1021
7. Baulch, C. T. Bowman, J. Cobosm R. A. Cox J. A. Kerr, M. J. Pilling, D. Stocker, J. Troe, W. Tsang, R. W. Walker, J. Warnatz, *Journal of physical and chemical reference data* 34.3 (2005): 757-1397.

## **Autoradiography study of nanodiamonds distribution in the composite polymeric films**

*Soboleva O.A.*<sup>1</sup>, *Myasnikov I.Yu.*<sup>2</sup>, *Chernysheva M.G.*<sup>1</sup>, *Korobkov V.I.*<sup>1</sup>, *Badun G.A.*<sup>1</sup>

*Oxana\_Soboleva@mail.ru*

<sup>1</sup> M.V.Lomonosov Moscow State University, Chemistry Department, Moscow, Russia

<sup>2</sup> Vernadsky Institute of Geochemistry and Analytical Chemistry of Russian Academy of Sciences, Moscow, Russia

Composite materials based on detonation nanodiamonds (NDs) and different polymers (epoxy resin, polysulfone, polyacrylonitrile, fluoroelastomers etc.) have a noticeably greater modulus of elasticity and tensile strength compared to the materials without NDs. Surface functionalization of NDs allows controlling interactions between NDs and polymeric matrix and the distribution of the nanoparticles in composite polymeric films. This work aimed to investigate the effect of a surface modification of the NDs on their surface concentration in composite films based on polyvinyl alcohol (PVA) and polyacrylonitrile (PAN).

NDs produced by special designing and technological bureau «Technolog» (St.Petersburg, Russia) and subjected to air annealing were used in the experiments. NDs were modified with adsorption layers of oleylamine and characterised by FTIR, TGA, DLS, Boehm titration techniques. Composite films based on PVA and NDs were prepared from an aqueous dispersion [1]. Composite films based on PAN and NDs were prepared from a dispersion in dimethylsulfoxide. In the last case NDs were modified with perfluorononanic acid. The total concentration of NDs in the composite films was 1 %, weight fraction of modified NDs was 0.2, 0.5, 0.8 and 1.0.

Tritium labelled NDs obtained by tritium thermal activation method [2] and autoradiography were used to study the surface distribution of NDs in the composite films [1, 3]. Two series of experiments were carried out, in which tritium label contained either initial or modified NDs. After processing the autoradiograms distribution patterns of the NDs on the both sides of the films were obtained, the total amount of NDs and fracture of modified nanoparticles in the surface layers were calculated. It was demonstrated that oxidized NDs distribute uniformly in the both composite films. Modification of NDs surface promotes coagulation of the particles at the stage of film formation, sedimentation of the aggregates and non-uniform distribution of the NDs in the films. As a result surface layers at the bottom side of the films are enriched by modified particles. The cellular pattern of NDs distribution in PAN-modified NDs film was observed.

This work was financially supported by RFBR (grant № 17-03-00985-a).

### **References**

1. Soboleva O.A., Chernysheva M.G., Myasnikov I.Yu., Porodenko E.V., Badun G.A. *Colloid Polymer Sci.* (2019) DOI 10.1007/s00396-018-4453-1.
2. Badun G.A., Chernysheva M.G., Yakovlev R.Yu., Leonidov N.B., Semenenko M.N., Lisichkin G.V. *Radiochimica Acta.* (2014) **102**, 941.
3. Soboleva O.A., Porodenko E.V., Chernysheva M.G., Korobkov V.I., Myasnikov I.Yu., Badun G.A. *Materials Today: Proceedings* (2018) **5**, 25907.

## **Mechanical properties of the composite films based on nanodiamonds and polyvinyl alcohol: influence of nanoparticle modification, thermal annulations, and liquid media**

*Porodenko E.V.*<sup>1</sup>, *Golovina E.*<sup>1</sup>, *Soboleva O.A.*<sup>1</sup>

*Oxana\_Soboleva@mail.ru*

<sup>1</sup> M.V.Lomonosov Moscow State University, Chemistry Department, Moscow, Russia

Detonation nanodiamonds (NDs) can serve as a valuable filler of polymer materials due to their high dispersity, chemical resistance, mechanical strength of the particle core and reactivity of the particle shell. The filling is mainly aimed on improving the mechanical strength of the polymer material at a low content of the additive. The aim of our investigation is to study the effect of NDs type, concentration, surface treatment, films manufacturing procedure and liquid media on modulus of elasticity and tensile strength of composite films on the base of NDs and polyvinyl alcohol (PVA). Surface oxidation of the NDs and heat treatment of the composite film may strengthen interactions between NDs and PVA and cause hardening of the film. Surface functionalization of NDs with oleylamine can influence on the surface concentration of the nanoparticles in composite films.

Two types of NDs obtained from a) trinitrotoluene and hexagen (type 1) and b) from tetrayl (type 2) (SKTB "Technolog", Russia) were used. NDs were oxidized at 420°C under air condition for 2 h. NDs were modified with oleylamine. Oxidized and modified NDs were characterized by IR spectroscopy, Boehm titration, TGA and DLS techniques. Composite films were prepared from dispersion of NDs in aqueous solution of PVA. Films were dried at 40°C till constant mass. Mechanical tests in the uniaxial tension mode were carried out, and the Young's modulus, tensile strength and films' elongation before break were determined. Mechanical behaviour of initial films was compared with the same characteristics of the films additionally heat treated (at 150°C for 3 h). The influence of liquid media (water, salt solutions) on mechanical behavior was revealed.

It was demonstrated that NDs type 1 increased films' strength, but NDs type 2- didn't due to coagulation at the stage of film formation. While increasing the fraction of NDs modified with oleylamine in the filler, the strength and Young's modulus of the composite films decreased to the values obtained in the absence of NDs. Heat treatment didn't influence on tensile strength and Young's modulus; the mechanical behavior of the films becomes brittle. In order to expand practical application of the composite films, the mechanical properties have been studied not only in the air but also in aqueous solutions. It was shown that PVA films without heat treatment dissolved in water, NDs addition slightly slowed down this process only. After heat treatment the films became insoluble in aqueous solutions; its plasticity and elongation before break increased dramatically (up to 400 %).

The work was supported in the framework of the state budget topic № AAAA-A16-116030250108-3 (Colloid chemistry and physicochemical mechanics as a basis for the creation of advanced materials and nanostructured systems with controlled properties).

## Regularities of the detonation nanodiamond surface chlorination

*I.I. Kulakova*<sup>1</sup>

*inna-kulakova@yandex.ru*

<sup>1</sup> Chemistry Department, Lomonosov Moscow State University, Moscow, Russia

Recently, the interest in detonation nanodiamond (DNA) use is increasingly shifting to the field of biology and medicine. One of the promising rapidly developing areas in pharmacology is the use of DND as a carrier of biologically active substances (BAS), including drugs, in delivery systems. To create such systems, it is necessary to use DND with predetermined and reproducible properties. This is achieved by the use of chemical modification of its surface, such as chlorination, which activates diamond surface in relation to various nucleophilic reagents. Literature data on the chlorination of diamond surface are ambiguous and do not allow to conclude about the advantages of a particular method of chlorination of DNA. Therefore, the aim of this work was to identify the optimal conditions for the chlorination process of detonation nanodiamond surface for its further use in Biomedicine.

The results of chlorination of DND of one brand with molecular chlorine in the liquid and gas phase, as well as with Thionyl chloride and Sulfuryl chloride were compared. Chlorine content was determined by microanalysis, x-ray fluorescence and x-ray spectroscopy.

The following is established:

□ when using Sulfuryl chloride or Thionyl chloride, samples of DND-Cl contain a significant amounts of sulfur, which is unacceptable for further use of these samples as carriers of BAS;

□ the method of chlorination with molecular chlorine in the gas phase at elevated temperatures is most attractive for the functionalization of DND for biomedical applications; the optimum temperatures of the chlorination are 320-350 °C;

□ liquid -phase bottom chlorination does not provide sufficient chlorine content;

□ the chlorination of DND with molecular chlorine in the liquid phase does not provide sufficient chlorine content in the final product;

□ the gas-phase chlorination can reduce the content of metal impurities in DND samples;

□ chlorinated nanodiamond samples are hydrolytically stable in air for several hours, allowing the use of DNA-Cl in further modification processes without loss of chlorine.

**Acknowledgement.** The authors thank the colleagues from the chemical faculty of Moscow state University A. Egorov and K. Maslakov for their help in the research of physical and chemical properties of DND. The work was supported by RFBR (grant 16-08-01156). The equipment was acquired from the funds of the Moscow State University Development Program

## ODMR study in diamonds microcrystals synthesized from detonation nanodiamonds under HPHT conditions without metal catalyst.

*Breev I.D.*<sup>1</sup>, *Anisimov A.N.*<sup>1</sup>, *Kidalov S.V.*<sup>1</sup>, *Vul' A.Ya.*<sup>1</sup>, *Baranov P.G.*<sup>1</sup>

*breev.ilia.d@mail.ioffe.ru*

<sup>1</sup> Ioffe Institute, St.Petersburg, Russia

Here we present the results from our investigation of the structure and composition of microcrystalline diamonds obtained by sintering at high pressures and at high temperatures of detonation nanodiamond particles. Using optically detected magnetic resonance (ODMR) and photoluminescence (PL) spectroscopy under ambient conditions, we found that such synthesized diamonds has negatively charged nitrogen-vacancy centers (NV<sup>-</sup> centers). Significantly, this type of defects was obtained without any irradiation and annealing. Moreover, defects structure of microcrystalline diamonds strongly differs from the initial detonation nanodiamonds (DND). This indicates the essential transformation of structure and composition of initial detonation nanodiamonds particles during the formation of single crystals at high pressure and temperature. It is assumed that diamond single crystals of size between 500 nm and 15 μm are formed directly from 4 - 5 nm sized diamond nanoparticles under conditions of high pressure and high temperature (HPHT) (P = 7 GPa, T = 1300 - 1700 C°) [1].

For comparison with previous achievements in diamond growth, we obtained ODMR and PL spectra of samples of diamonds crystals under review and initial DND sample. Considering the PL spectra, we concluded that new samples can exhibit NV<sup>-</sup> centers characteristic radiation three times brighter than that of DND sample. Furthermore, ODMR spectra show that the splitting of the resonance line of HPHT DND samples is smaller than that of the detonation one and is approximately equal to the splitting of the resonance in an artificially grown single crystal diamond subjected to irradiation and annealing. It evidence that crystal lattice relaxes during sintering resulting in the decrease of spin Hamiltonian parameter **E** responsible for internal crystal stresses leading to the decrease of the splitting of ODMR resonance line [2].

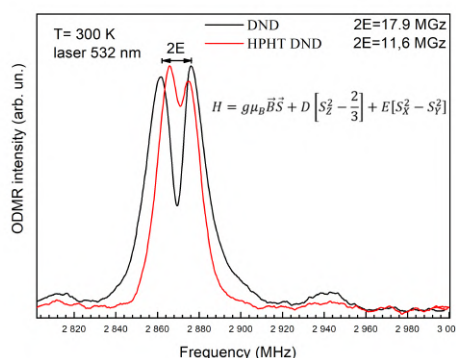


Fig.1. ODMR spectra of NV centers in a diamond of DND and HPHT DND samples.

### References

1. V. Kidalov, M.V. Zamoryanskaya, V. A. Kravez, L.V. Sharonova, F. M. Shakhov, E. B. Yudina, T. O. Artamonova, M. A. Khodorkovskii, A.Ya. Vul', Photo and cathodoluminescence spectra of diamond single crystals formed by sintering of detonation nanodiamond, NANOSYSTEMS: PHYSICS, CHEMISTRY, MATHEMATICS (2019), **10** (1), P. 12-17.
2. J. Rogers, M. W. Doherty, M. S. J. Barson, S. Onoda, T. Ohshima and N. B. Manson, Singlet levels of the NV<sup>-</sup> centre in diamond, New J. Phys. **17** 013048 (2015)

## Nanodiamond cellulose composites for printed energy storage devices on paper substrates

*Palmieri Elena*<sup>1</sup>, *Polino Giuseppina*<sup>2</sup>, *Tamburri Emanuela*<sup>1</sup>, *Lanuti Alessandro*<sup>2</sup>, *Brunetti Francesca*<sup>2</sup>, *Orlanducci Silvia*<sup>1</sup>

*palmieri.ele@hotmail.it*

<sup>1</sup> Department of Chemistry Sciences, University of Rome Tor Vergata, Rome, Italy

<sup>2</sup> CHOSE (Centre for Hybrid and Organic Solar Energy), Department of Electronic Engineering, University of Rome Tor Vergata, Rome, Italy

In recent years, there has been growing interest in using paper or paper-like substrates for batteries and other energy storage devices [1]. Paper can be used simply as the flexible substrate or, exploiting its porous fiber-like nature, as an active film by infiltration or co-preparation with electronic materials. In this work, white paper, electronic paper and cellulose-based substrate (membranes) have been used to fabricate devices with different layouts and, a new polymer electrolyte based on nanodiamond was tested and compared with sodium sulphate liquid electrolyte.

Poly(3,4-ethylenedioxythiophene)-poly(styrenesulfonate) (PEDOT:PSS) was employed to realize anode and cathode electrodes and separators based on hydroxypropyl cellulose (HPC) loaded with different concentration of detonation nanodiamonds (NDs) were used. The energy storage devices were realized using large area techniques like spray coating for the deposition of high conductive PEDOT:PSS electrodes and blade coating for the deposition of electrolytic separator. In order to develop a green solvent free methodology to prepare devices, all components were chosen or formulated in water-based dispersions.

Structural and morphological characterization of nanocomposites were performed by microRaman spectroscopy. Electrochemical characterization of the devices was carried out by cyclic voltammetry, charge/discharge and electrochemical impedance spectroscopy. Different nanocomposites based on ND shown very promising results in terms of stability, mechanical properties and specific capacitance making ND a high-performance additive in the field of green polymer electrolyte for printed energy storage devices on paper.

### References

[1] Brunetti, F., Operamolla, A., Castro-Hermosa, S., Lucarelli, G., Manca, V., Farinola, G. M., Brown, T. M., *Adv. Funct. Mater.* 2019, 1806798. <https://doi.org/10.1002/adfm.201806798>

## To the diamond nanooctahedra thermochemistry

*Spitsyn B.V.*<sup>1</sup>, *Zhevnenko S.N.*<sup>2</sup>, *Ovchinnikov-Lazarev M.A.*<sup>3</sup>

*bvspitsyn@gmail.com*

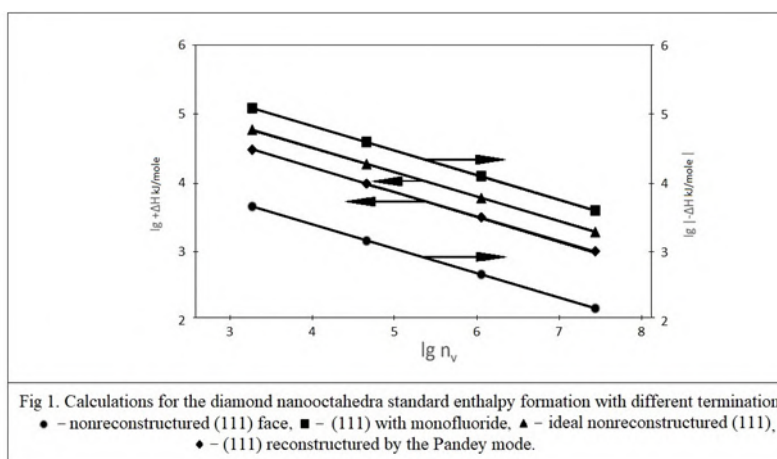
<sup>1</sup> A.N. Frumkin Institute of Physical Chemistry and Electrochemistry. RAS Moscow, Russia

<sup>2</sup> A.N. Frumkin Institute of Physical Chemistry and Electrochemistry. RAS Moscow, Russia

<sup>3</sup> A.N. Frumkin Institute of Physical Chemistry and Electrochemistry. RAS Moscow, Russia

To the nanodiamond thermochemistry quite a number paper chined (e.g. [1]), however only in some ones have been taking in the account a special energetic and chemical states of the surface atoms of the diamond nanocrystals. Let us to consider the regular diamond nanooctahedra with edge in the 3 to 100 nm range with four basic their surfaces states, i.e.: ideal (111) nonreconstructed, (111), but reconstructed by the Pandey mode (i.e. by single and double carbon-carbon bonds alternation), and finally, nonreconstructed (111) faces, covered by monohydride and monofluoride. The calculations was performed on base rupture and formation of chemical bond energies : H-H 435.1, C-C 355.6, C=C 569, C-H 403.8, F-F 159 and C-F 490 kJ/mole, respectively and setuped in bilogarithms at Fig 1.

The calculation results demonstrates an enhanced thermal stability of the diamond nanooctahedra with monofluoride termination.



### References

#### REFERENCES

1. Winter N.S. and Ree F.H.. Carbon particle phase stability as a function of size. Journal of Computer-Aided Materials Design, 5: 279-294, 1998.

## Electronic effects on the interface “nanodiamond surface groups - water molecules”

*Laptinskiy K.A.*<sup>1</sup>, *Bokarev A.N.*<sup>2</sup>, *Burikov S.A.*<sup>3</sup>, *Dolenko S.A.*<sup>1</sup>, *Plastun I.L.*<sup>2</sup>, *Dolenko T.A.*<sup>3</sup>

*laptinskiy@physics.msu.ru*

<sup>1</sup> D.V. Skobeltsyn Institute of Nuclear Physics, M. V. Lomonosov Moscow State University, Moscow, Russia

<sup>2</sup> Department of Applied Information Technology and Communication, Yuri Gagarin State Technical University of Saratov, Saratov, Russia

<sup>3</sup> Physical Department, M. V. Lomonosov Moscow State University, Moscow, Russia

Detonation nanodiamonds (DND) have a unique combination of properties, such as biocompatibility, ability of targeted surface modification, ability to fluorescence which provides the prospects of its use in different applications, primarily in biomedicine. It is already established that surface functionalization plays a key role in DND fluorescence in suspensions, in keeping drugs on the surface and many others [1-3]. However, the mechanisms of interactions of DND surface groups and molecules of the environment are still not clear.

In this study the experimental and theoretical estimations of the interactions on the interface “DND’s surface functional groups - water molecules” were made for DND with different functional surface groups (-COOH, -OH, -H and -polyfunctional) using vibrational spectroscopy and DFT (Fig. 1). The obtained results showed different effect of different surface functionalization on the molecules of the solvent in aqueous suspensions. We proposed an explanation of the observed phenomenon based on manifestation of electronic effects (inductive and mesomeric) on the surface of DND in water. The obtained results demonstrated the essential role of the surface chemistry of DND in studying the processes occurring in their suspensions.

This study has been performed at the expense of the grant of Russian Science Foundation (project No 17-12-01481) (K.A.L., T.A.D. - conducting experiment) and RFBR (project №19-01-00738) (S.A.D. - spectrum analysis using adaptive methods).

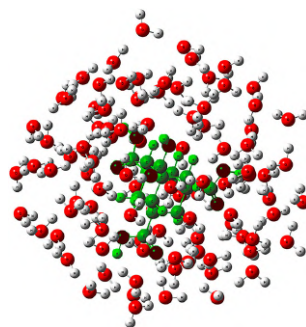


Fig. 1. Structure of the molecular complex of DND with 100 water molecules.

### References

- Reineck, D. Lau, E. Wilson, K. Fox, M. Field, C. Deeleepojananan, V. Mochalin, B. Gibson, *ACS Nano* (2018) **11**(11), 10924.
- Petit, L. Puskar, T. Dolenko, S. Choudhury, E. Ritter, S. Burikov, K. Laptinskiy, Q. Brzustowski, U. Schade, H. Yuzawa, M. Nagasaka, N. Kosugi, M. Kurzyp, A. Venerosy, H. Girard, J-Ch. Arnault, E. Osawa, N. Nunn, O. Shenderova, and E.F. Aziz, *Journal of Physical Chemistry C* (2017), **121**, 5185.
- Krueger, D. Lang, *Advanced Functional Materials* (2012), **22**(5), 890.



## Luminescence of detonation nanodiamonds with different functionalization in ordinary and heavy water

*Laptinskiy K.A.*<sup>1,2</sup>, *Burikov S.A.*<sup>1</sup>, *Vervalde A.M.*<sup>1</sup>, *Shenderova O.A.*<sup>3</sup>, *Vlasov I.I.*<sup>4</sup>, *Dolenko T.A.*<sup>1</sup>

*laptinskiy@physics.msu.ru*

<sup>1</sup> Physical Department, M. V. Lomonosov Moscow State University, Moscow, Russia

<sup>2</sup> D.V. Skobeltsyn Institute of Nuclear Physics, M. V. Lomonosov Moscow State University, Moscow, Russia

<sup>3</sup> Adamas Nanotechnologies, Inc., 8100 Brownleigh Dr, Suit 120, Raleigh, NC 27617, USA

<sup>4</sup> A.M. Prokhorov General Physics Institute, Russian Academy of Sciences, Moscow, Russia

Nanodiamonds (NDs) are found to be a very prospective material in a variety of different applications [1]. However, the lack of knowledge about the origin of NDs luminescence prevents its use as an effective versatile tool in many applications. It is well known that the change of pH value of nanoparticle's environment [2], as well as the change of the environment itself [3] may change the luminescence of NDs. This study is devoted to the investigation of the influence of isotopic exchange of the solvent on the luminescence of the detonation NDs with different surface groups. It was found that as a result of the isotopic exchange of the solvent, the ND's luminescence intensity changes in accordance with the strength of the hydrogen bonds formed by surface groups with surrounding molecules of ordinary or deuterium water (Fig. 1): the bonds between the hydrogen of surface groups and oxygen of deuterium are weaker than the same bonds with the oxygen of ordinary water molecule. A hypothesis about the effect of electron transfer from the ND's surface to the solvent and back on the formation of ND's luminescence was proposed.

This study has been supported by of Russian Foundation for Basic Research (project No. 18-32-00779\_mol\_a).

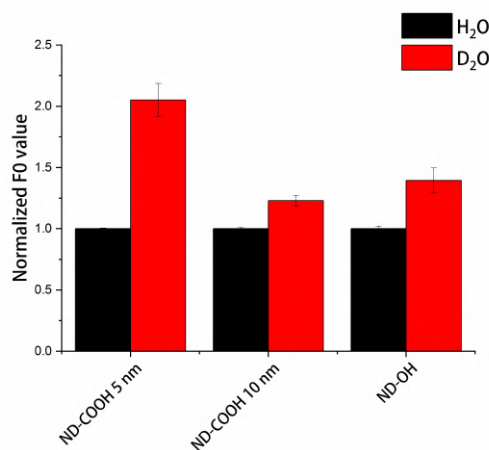


Fig.1. The change of luminescence intensity of NDs with different surface functionalizations with the isotopic change of the solvent (H<sub>2</sub>O-D<sub>2</sub>O).

### References

1. Mochalin, O. Shenderova, D. Ho, Y. Gogotsi. *Nat. Nanotechnol.* (2011) **7**, 11.
2. Reineck, D. Lau, E. Wilson, N. Nunn, O. Shenderova, B. Gibson. *Scientific Reports* (2018) **8**, 2.
3. Dolenko, S. Burikov, K. Laptinskiy, J.M. Rosenholm, O. Shenderova, I. Vlasov. *Physica Status Solidi a* (2015) **212**, 2512.

## **The influence of surfactants on the fluorescence of nanodiamonds**

*Vervald A.<sup>1</sup>, Plastinin I.<sup>1</sup>, Dolenko T.<sup>1</sup>*

*alexey.vervald@physics.msu.ru*

<sup>1</sup> Faculty of Physics, M.V. Lomonosov Moscow State University, Russia

Nanodiamonds are known for their multifunctional easily modifiable surface that is the origin of both their strong sides as well as their biggest downside within the framework of biomedical applications. Due to the surface, nanodiamonds can be used as a base of bioconjugates and drug carriers, or undergo aggregation into big, hard to pull apart clusters. While the exact mechanism of detonation nanodiamonds' fluorescence is not known, many authors argue that the fluorescence as well originates from their surface.

The popular way to aid nanodiamonds disaggregation is the addition of surfactants to the suspensions. On the other hand, in the biomedical applications the interaction of nanodiamonds with the amphiphilic compounds - close relatives of surfactants - and their micellar structures is unavoidable. The accounting of the influence of such interactions on the fluorescence of nanodiamonds is essential to the proper usage of these nanoparticles in the role of biomarkers.

In this study, the influence of the variety of surfactants with different length of hydrocarbon chains on the fluorescence of detonation nanodiamonds with hydrophobic and hydrophilic surfaces was studied using spectroscopic methods. It was found that in general surfactants enhance the fluorescence of carbon nanoparticles, differently with the respect to micellar properties and the lengths of hydrocarbon chains. The hypothesis about the mechanisms of the observed fluorescent changes caused by the interactions of the surfaces of nanodiamonds with the surrounding surfactants is proposed.

This study has been performed at the expense of the Russian Foundation for Basic Research (grant №18-32-00779) (A.V. - conducting the experiments, spectra processing), Russian Science Foundation (grant number 17-12-01481) (I.V. - spectra processing, data analysis; T.D. - data analysis). The authors are sincerely grateful to O.Shenderova for providing nanodiamonds.

## Quantifying absorption and scattering contributions to light attenuation by nanodiamonds

Koniakhin S.V.<sup>1,2</sup>, Rabchinskii M.K.<sup>3</sup>, Besedina N.A.<sup>1</sup>, Sharonova L.V.<sup>3</sup>, Shvidchenko A.V.<sup>3</sup>, Eidelman E.D.<sup>3,4</sup>

*kon@mail.ioffe.ru*

<sup>1</sup> Nanobiotech lab, St. Petersburg Academic University, St. Petersburg, Russia

<sup>2</sup> Institut Pascal, University Clermont Auvergne, Aubiere Cedex, France

<sup>3</sup> Ioffe Institute, St. Petersburg, Russia

<sup>4</sup> St. Petersburg Chemical Pharmaceutical Academy, St. Petersburg, Russia

Nanodiamonds (ND) are one of the unique nanoparticles being investigated due to their exceptional mechanical, heat and optical properties inherited from the bulk diamond. To better understand the size distribution, structure, and phase composition of ND, the optical experiments including measuring absorbance (Abs) spectra are widely used [1,2].

Here, we show an experimental evidence of the domination of absorption over scattering in Abs spectra of ND. We perform the Abs measurements on the UV-vis spectrophotometer equipped with integrating sphere and compare them with conventional absorbance spectra. Additionally, we measure the scattering light intensity at the cuvette side wall (scattering at 90 degree angle). The obtained experimental data were interpreted using the photon random walk simulations based on the scattering cross sections and indicatrices given by the Mie theory [3].

We conclude that only the agglomerates of approx. 100 nm, remaining in the hydrosols [4], govern the scattering. Their fraction can be effectively controlled by centrifugation [5]. We find that despite being very close to  $\lambda^{-4}$  power law the light extinction by the primary 4 nm crystallites is due to absorption only and scattering can be neglected. Another important result is that the Mie theory is obligatory for the description of the ND hydrosols optical properties. Finally, using the obtained absorbance spectra we estimate the fraction of non-diamond phase.

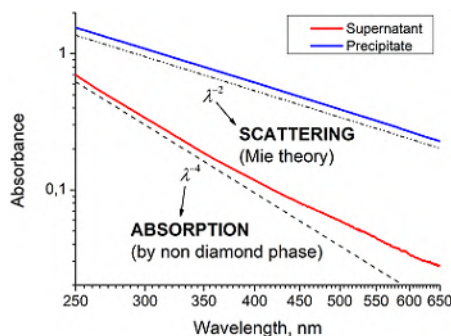


Figure 1 - Detonation ND Absorbance (UV-vis) spectra. Supernatant contains mostly 4 nm primary crystallites and absorbs the light. Precipitate contains a lot of agglomerates and scattering plays a role.

### References

- [1] A.Ya. Vul', E.D. Eydelman, L.V. Sharonova, A.E. Aleksenskiy, and S.V. Konyakhin, *Diamond Relat. Mater* (2011), 20(3), 279.
- [2] S. Tomita, M. Fujii, S. Hayashi, *Physical Review B* (2002) 66(24), 245424.
- [3] C.F. Bohren, D.R. Huffman, *Absorption and scattering of light by small particles*, (John Wiley & Sons, 2008).
- [4] S.V. Koniakhin, M.K. Rabchinskii, N.A. Besedina, L.V. Sharonova, A.V. Shvidchenko, E.D. Eidelman, preprint arXiv:1812.03512, (2018).
- [5] S.V. Koniakhin, N.A. Besedina, D.A. Kirilenko, A.V. Shvidchenko and E.D. Eidelman, *Superlattices and Microstructures* (2018), 113, 204-212.

## Pressure effect on electron-phonon coupling in GeV centres in diamond.

*Razgulov A.A.*<sup>1,2</sup>, *Lyapin S.G.*<sup>1</sup>, *Novikov A.P.*<sup>1</sup>, *Ekimov E.A.*<sup>1</sup>

*aleksandr.razgulov@phystech.edu*

<sup>1</sup> L.F. Vereshchagin Institute for High Pressure Physics, RAS, Troitsk, Moscow, Russia

<sup>2</sup> Moscow Institute of Physics and Technology (State University), Dolgoprudny, Moscow region, Russia

We report low temperature (80K) photoluminescence (PL) studies of microcrystalline diamond with germanium-vacancy (GeV) centres under hydrostatic pressure up to 6 GPa. For the details of diamonds synthesis see ref. [1].

The PL spectrum of GeV centres consists of two main groups of peaks: zero-phonon line (ZPL) and phonon sideband (PSB). Pressure effect on ZPL was reported earlier [2]. Here we report pressure effect on PSB. Due to the high structural quality of the diamond crystal we were able to trace the position and integral intensity of the peak associated with quasi-local vibrational mode (QLVM) of GeV centre up to the highest pressure achieved in the experiment. As the result we managed to determine the pressure effect on the quasi-local phonon energy (the distance between the ZPL peak and the corresponding QLVM peak) and the Huang-Rhys parameter  $S$  characterizing the strength of electron-phonon coupling. The Huang-Rhys parameter  $S$  was defined in following way:  $S = -\ln[I_{ZPL}/(I_{ZPL} + I_{QLVM})]$ , where  $I_{ZPL}$  was integral intensity of ZPL and  $I_{QLVM}$  was an integral intensity of corresponding quasi-local vibrational mode.

The energy of the quasi-local phonon was found to increase linearly ( $dE/dP = 0.24$  meV/GPa) with pressure rise, while the Huang-Rhys parameter was found to decrease linearly ( $dS/dP = -5 \cdot 10^{-3}$  1/GPa). The decrease of  $S$  with increasing pressure indicated a weakening of the electron-phonon coupling. It is worth noting that similar tendencies (increase of phonon energy and decrease of  $S$ ) were found for NV centres [3, 4] with  $dE/dP = 0.9$  meV/GPa and  $dS/dP = -9 \cdot 10^{-2}$  1/GPa. The significant difference between pressure coefficients for GeV and NV centres can be associated with the difference of the structures of these two types of defects in diamond lattice.

Thus we come to the following picture of the hydrostatic pressure effect on the adiabatic potentials and electronic structure of GeV centres in the framework of Frank-Condon approximation. The pressure effect on the harmonic potential of the ground state is manifested in an increase in the phonon energy, or in other words, in increasing the curvature of the potential. The increase of zero-phonon transition energy is caused by the increase of the energy difference between bottoms of the ground and excited states. Finally, the decrease of  $S$  means that the distance between the minima of the adiabatic potentials of the excited and ground states along the configurational coordinate  $Q$  diminishes with pressure.

This work was supported by Russian Science Foundation Grant No. 19-12-00407.

### References

1. E.A. Ekimov, S.G. Lyapin, K.N. Boldyrev, M.V. Kondrin, R. Khmel'nitskiy, V.A. Gavva, T.V. Kotereva, and M.N. Popova, *JETP Lett.* (2015) **102**, 701.
2. S.G. Lyapin, A.A. Razgulov, A.P. Novikov, E.A. Ekimov, and M.V. Kondrin, *Nanosystems: Phys. Chem. Math.* (2018) **9**, 67.
3. B. Deng, R.Q. Zhang, and X.Q. Shi, *Sci Rep* (2014) **4**, 5144.
4. M. Kobayashi and Y. Nisida, *Jpn. J. Appl. Phys.* (1993) **32**, **Supplement 32-1**, 279.

## Non-agglomerated nanodiamonds inside metal matrix

*Popov V.A.*<sup>1</sup>

*popov58@inbox.ru*

<sup>1</sup> National University of Science and Technology MISIS, Moscow, Russia

Primary nanodiamond particles of 5 nanometers in size are united in agglomerates [1-3]. Agglomerate in a metal matrix in composites does not lead to hardening, and can cause destruction of all material as durability of agglomerate is lower than durability of a metal matrix. It means that smashing of agglomerates is an important task. Mechanical alloying allows to shatter agglomerates, but very often there are nanoagglomerates which availability is also undesirable. It is offered to add at a final stage of mechanical alloying to the processed material metal which will form intermetallic compounds with matrix material. The formed intermetallic compounds have various density. It is given to emergence of additional deformations and tension around nanoagglomerates of nanodiamonds. The additional tension and deformations will lead to final destruction of nanoagglomerates. Figure 1 shows the cross section of a metal matrix composite with the strengthening particles which are non-agglomerated nanodiamonds. The matrix contains aluminum and copper. The paper shows that it is possible to reach non-agglomerated condition of the nanodiamond strengthening particles in a metal matrix.

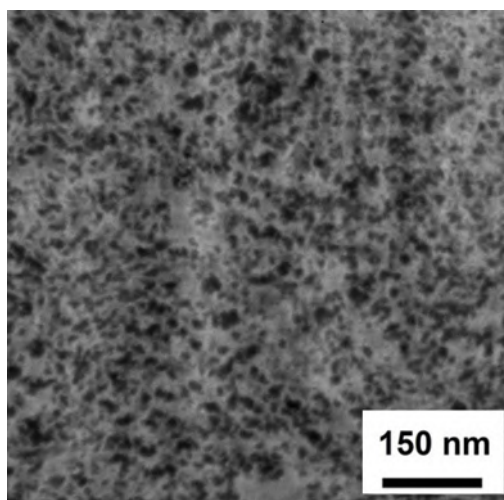


Figure 1. The strengthening particles which are non-agglomerated nanodiamonds in a matrix "aluminum-copper" (SEM, cross section is executed by an ion beam)

### References

1. A.Popov. Surface and Interface Analysis (2018) **v.50**, Is.11, pp. 1106-1109.
2. Popov, M.Burghammer, M.Rosenthal, B.Senatulin, E.Shelekhov, M.Kovalchuk, I.Khodos. Materials Today: Proceedings (2018) **v 5**, Is. 13/P4, pp. 27292-27300.
3. A.Popov, E.V.Shelekhov. J. Surf. Investig.: X-ray, Synchrotron and Neutron Techn. (2017) **v. 11**, Is. 2, pp. 322-325.

## Structural properties of stabilized colloidal nanodiamonds grafted by rare earth metals

*Yudina E.B.*<sup>1</sup>, *Shvidchenko A.V.*<sup>1</sup>, *Aleksenskiy A.E.*<sup>1</sup>, *Kulvelis Yu.V.*<sup>2</sup>, *Vul A.Ya.*<sup>1</sup>

*yudina@mail.ioffe.ru*

<sup>1</sup> Ioffe Institute, Saint-Petersburg, Russia

<sup>2</sup> Petersburg Nuclear Physics Institute, National Research Centre Kurchatov Institute, Gatchina, Russia

Detonation nanodiamond (DND) particles sized 4-5 nm are proved to be a promising material in medicine due to its non-toxicity, relatively small sizes and tunable surface properties. Our recent studies suggest a method for obtaining stable colloids made up of primary DND particles [1]. Polyvinylpyrrolidone (PVP) is revealed to be a biocompatible stabilising agent which prevents DND particles coagulation in isotonic aqueous-saline medium [2]. The high stability of DND particles is due to surface carboxyl groups. The presence of these functional groups allows to graft DND particle by metal ions. The carboxylated DND particles grafted by Gd(III) show significant reduction in spin–lattice ( $T_1$ ) and spin–spin ( $T_2$ ) relaxation times of water protons [3]. This opens new perspectives for using the Gd(III)-grafted DND complexes as novel MRI contrast agents.

Hereby we report on structural characterization of colloidal DND particles grafted by Ln (Ln = Eu, Gd). Both as-prepared and stabilized by PVP samples have been studied by dynamic light scattering (DLS) and small angle neutron scattering (SANS) methods. According to our results presence of Ln leads to close packing of DND particles in branched clusters (Fig.1) with a mean size about 60 nm. Using a contrast variation techniques we have determined the thickness of PVP shell surrounding grafted DND particles in colloids.

**Acknowledgment:** Yudina E.B. thanks the RFBR (project N 18-29-19038 mk) and Kulvelis Yu.V. thanks the RFBR (project N 18-29-19008 mk) for support of this research.

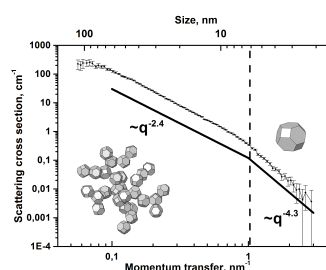


Fig.1. SANS curves of colloidal DND particles grafted by Gd (III).

### References

1. T. Dideikin, A.E. Aleksenskii, M.V. Baidakova, P.N. Brunkov, M. Brzhezinskaya, V.Yu. Davydov, V.S. Levitskii, S.V. Kidalov, Yu.A. Kukushkina, D.A. Kirilenko, V.V. Shnitov, A.V. Shvidchenko, B.V. Senkovskiy, M.S. Shestakov, A.Ya. Vul', *Carbon* (2017) **122**, 737.
2. V. Kulvelis, A.V. Shvidchenko, A.E. Aleksenskii, E.B. Yudina, V.T. Lebedev, M.S. Shestakov, A.T. Dideikin, L.O. Khozyaeva, A.I. Kuklin, Gy. Török, M.I. Rulev, A.Ya. Vul, *Diamond Relat. Mater.* (2018) **87**, 78.
3. M. Panich, M. Salti, S.D. Goren, E.B. Yudina, A.E. Aleksenskii, A.Ya Vul', A.I. Shames, *J. Phys. Chem. C* (2019) **123**, 2627.

## CALORIMETRY OF LOW-TEMPERATURE LIQUID-PHASE OXIDATION OF CARBON NANOPARTICLES

*Vereshchagin A.L.*<sup>1</sup>, *Bychin N.V.*<sup>1</sup>, *Petrov E.A.*<sup>1</sup>

*val@bti.secna.ru*

<sup>1</sup> Biysk Technological Institute (branch) of Altai State Technical University I.I. Polzunova, 659305, Biysk

Traditional methods and approaches to the study of the reactivity of carbon nanoparticles are limited to the use of gas-phase and solid-phase oxidizers. The use of liquid-phase oxidizers is faced with the problem of chemical corrosion of recording devices. To assess the reactivity of carbon nanoparticles, a method of reactive calorimetry with liquid sodium nitrite was proposed. For this purpose, it was studied the possibility of applying the reaction of self-propagating high-temperature synthesis of sodium carbonate between sodium nitrite with carbon nanoparticles to a temperature of 600 °C using method of differential scanning calorimetry (Netzsch DSC 204 01) in nitrogen atmosphere. Sodium nitrite melts at a temperature of 272-275 °C. To exclude gas corrosion of the equipment, urea was added to the reaction mixture to zero oxygen balance. The reaction was carried out in an aluminum cell. The DSC curve of the sample composition with DND is shown in the figure.

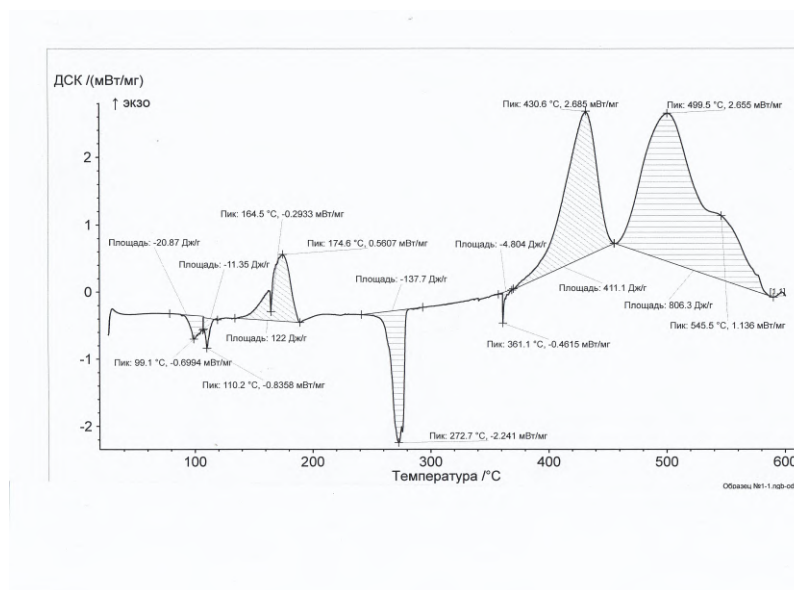
Figure - DSC curve of DND oxidation with liquid sodium nitrite.

The presence of three stages in the oxidation of DND (with maxima at 430 °C, 500 °C and 545 °C), two stages in the oxidation of carbon nanotubes (at 439 °C and 500 °C), and one stage in the oxidation of primary detonation carbon (maximum at 418 °C) and P-803 soot (at 514 °C). The staging of the oxidation of DND can be due to its physical explosion, or the cluster structure of the particles and their heterophase nature.

The heat of oxidation of carbon nanophases by liquid sodium nitrite was: for DND - 1.60; CNT - 0.94; DU - 1.49, soot - 2.17 kJ/g (theoretical heat release - not less than 3.28 kJ/g). The observed heat losses can be attributed to the gas-filled samples of the DND, DU, and CNT and (or) the flow of part of the oxidation reactions in the gas phase.

Differences in the temperature range of oxidation reactions, the heat of reaction and the observed staging allow this method to be used to identify carbon nanoparticles.

The study was carried out with the financial support of the Russian Foundation for Basic Research in the framework of the research project No. 18-29-19070 mk



## Use of nanodiamond for absorption of aerosol particles

*Vereshchagin A.L.*<sup>1</sup>, *Kudryashova O.B.*<sup>2</sup>, *Stepkina M. Yu.*<sup>2</sup>, *Balakhnina A.V.*<sup>1</sup>, *Petrov E.A.*<sup>1</sup>

*val@bti.secna.ru*

<sup>1</sup> BTI AltGTU, Biysk, Russia

<sup>2</sup> IPCET SB RAS, Biysk, Russia

Air pollution is one of the major risk factors for public health. One of the components of air pollution is small particulate matter (PM). Particulate matter with a characteristic size less than 10 microns is especially hazardous to public health. One of the new ways for neutralization of PM10 is spraying in the air of nanostructural sorbent [1]. Nanodiamond can be used as such adsorbent, and electrostatic charging of particles can significantly increase the speed and efficiency of sorption [2].

Proposed mathematical model of coagulation of aerosols is based on the equation of Smolukhovskiy. It allows calculating the speed of coagulation and sedimentation of aerosol. The electrostatic charge of adsorbent particle is shown to lead to a significant acceleration of coagulation processes and to interactions of a sorbent with sorptive (harmful particles).

The theoretical analysis and pilot studies of dynamics of evolution of an aerosol of nanodiamond of two samples (ultradisperse diamond UDD-S and UDDG-S) are carried out at electrostatic spraying of particles. Electrostatic charge of nanodiamond particles was measured to be about  $10^{-19}$  C. It is shown that with an electrostatic charge of particles they quickly (during ~ 45 seconds) coagulate with the fine electroneutral aerosol sprayed in the air. The phenomenon of electrostatic coagulation can be used at the spraying of particles of a nanostructural adsorbent. The high potential of detonation diamond as an adsorbent is known [3]. Use of electrostatic spraying of the nanodiamond in the air containing harmful aerosol pollution is the new way of application of this material proposed by authors.

Comparison of estimated and experimental results of the dynamics of coagulation and sedimentation of electrostatic charged and electroneutral particles of nanodiamond and sorbents was made. The time of sedimentation of an aerosol cloud depending on the size of particles of a sorbent and a method of their spraying is determined. Results of work can be used in the systems of cleaning of the air environment off harmful aerosol emissions.

*The reported study was funded by RFBR according to the research project №18-29-19070 mk*

### References

1. Kudryashova O.B., Stepkina M.Yu., Korovina N.V., Antonnikova A.A., Muravlev E.V., Pavlenko A.A., *Journal of Engineering Physics and Thermophysics* (2015) **88** (4), 833.
2. Kudryashova O.B., Stepkina M.Yu., *Science and Technology of Energetic Materials* (2018) **79** (2), 49.
3. Parkaeva S.A., Belyakova L.D., Larionov O.G., *Sorption and chromatographic processes* (2010), **10** (2), 283.



## Development of technology for producing chromium-diamond coatings using dry diamond-containing compounds.

Burkat G.K.<sup>1</sup>, Dolmatov V.Yu.<sup>2</sup>, Svir K.A.<sup>1</sup>, Dorokhov A.O.<sup>3</sup>, Rudenko D.V.<sup>2</sup>, Myllymaki V.<sup>4</sup>, Vehanen A.<sup>4</sup>

diamondcentre@mail.ru

<sup>1</sup> SPbGTI (TU), St. Petersburg, Russia

<sup>2</sup> FSUE "SCTB "Technolog", St. Petersburg, Russia

<sup>3</sup> JSC Plant "Plastmass", Kopeisk, Russia

<sup>4</sup> Carbodeon Ltd. Oy, Vantaa, Finland

Electrochemical chrome plating is the most popular coating for steel products. The use of detonation nanodiamonds (DND) to enhance the physicomechanical properties of a chrome plating is widely known, and DND is used in the form of low concentrated (~ 5%) aqueous suspensions.

In this paper, we used dry compositions consisting of:

- a mixture of DND (obtained from trotil-hexogen mixture), a surfactant, sodium carbonate, and citric acid (a DND content of 62%);
- diamond blend (DB), obtained by detonating tetryl (N-methyl-2,4,6-trinitrophenylnitramine), the content of the DND is 62%.

Used standard electrolyte chrome plating:  $\text{CrO}_3$  - 250 g / l;  $\text{H}_2\text{SO}_4$  - 2,5 % in the mode of hard and wear-resistant chromium, the concentration of DND and DB in the electrolyte is from 0.1 to 5.0 g / l.

For hard chrome ( $i_k=50, 60, 65, 70 \text{ A/dm}^2$ ,  $t=50^\circ\text{C}$ ), current output increased: when using DND - from 17 to 24%; with DB - from 17 to 20%; microhardness (with DND) - from 9.5 to 17.0 GPa (5 g / l, 70 A /  $\text{dm}^2$ ); with DB, from 9.3 to 14.5 GPa (5 g / l, 60 A /  $\text{dm}^2$ ).

For wear resistant chrome ( $i_k=25, 30, 35, 40 \text{ A/dm}^2$ ,  $t=60^\circ\text{C}$ ), current efficiency increased: when using DND - from 13 to 19%; with DB - from 13 to 18%; microhardness (with DND) - from 8.0 to 13.6 GPa (5 g / l, 40 A /  $\text{dm}^2$ ); wear dropped from 3.0 to 0.8% (DND and DB - 1 g / l, 40 A /  $\text{dm}^2$ ), i.e. 3.8 times.

Thus, for the first time, very high quality indicators of chromium-diamond coatings were achieved with the use of economically preferred dry diamond-containing compounds, and for the first time, DB obtained by undermining tetryl was used.

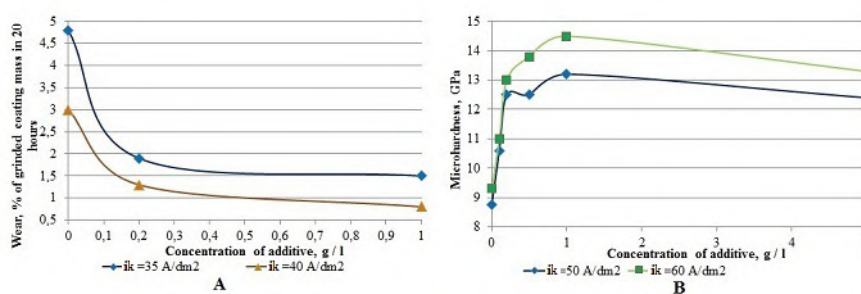


Fig.1 Dependence of wear resistance, % of grinded mass of the coating in 20 hours (DB) for wear-resistant chrome (A) and Dependence of microhardness for hard chromium (DB) (B)

## Nano-diamond powder as reflector for slow neutrons

*Dideikin A.T.*<sup>1</sup>, *Dubois M.*<sup>2</sup>, *Gutfreud Ph.*<sup>3</sup>, *Lychagin E.V.*<sup>4</sup>, *Muzychka A.Yu.*<sup>4</sup>, *Nesvizhevsky V.V.*<sup>3</sup>, *Nezvanov A.Yu.*<sup>4</sup>, *Shakhov F.M.*<sup>1</sup>, *Trofimuk A.D.*<sup>1</sup>, *Zhernenkov K.N.*<sup>4</sup>, *Strelkov A.V.*<sup>4</sup>, *Nekhaev G.V.*<sup>4</sup>

*lychag@nf.jinr.ru*

<sup>1</sup> Ioffe Institute, St. Petersburg 194021, Russia

<sup>2</sup> ICCF, Université Clermont Auvergne, 49 bd. François-Mitterrand, Clermont-Ferrand, France, F-60032

<sup>3</sup> Institut Laue-Langevin, Grenoble, France, 6 rue Jules Horowitz, F-38042

<sup>4</sup> Joint Institute for Nuclear Research, Dubna, Russia, 6 Joliot Curie, R-141980

Efficient neutron reflectors are mandatory for building neutron sources, such as nuclear reactors or spallation neutron sources, also in neutron investigations. For extremely slow, so-called ultracold neutrons (UCN) with the energy of  $<10^{-7}$  eV, neutron optical potential of matter plays a role of nearly ideal reflector. For UCN, the probability of specular elastic reflection from matter is close to unity at any temperature. In order to reflect neutrons with higher energy,  $<10^{-6}$  eV, one uses multi-layer coatings, so-called super-mirrors. The probability of specular elastic reflection of neutrons from good super-mirrors reaches 80-90 %. Until recently, efficient reflectors for neutrons of even higher energy, up to  $10^{-2}$ , had not been known. At even higher energy inelastic processes prevail; they are the basis for reflectors in nuclear reactors.

Recently, the phenomena of efficient diffusive reflection of very cold neutrons (VCN) from nano-structured reflectors at any incidence angle, and quasi-specular reflection of cold neutrons (CN) at small incidence angles were observed for the first time. Nano-structured reflectors bridge nicely the energy gap between reflectors based on two mechanisms mentioned above. In both cases powder of diamond nano-particles was used as a nano-structured matter; in both cases reflection probabilities exceeded by far the characteristics of alternative neutron reflectors.

Further, we assumed that substitution of hydrogen in nanoparticle shells by fluorine would increase the reflection efficiency due to the suppression of neutron losses associated with their travel in powder. In addition, a mean neutron-nuclei potential increases and gets sharper on surface due to the removal of amorphous  $sp^2$  carbon from nanoparticle shells; thus, the neutron scattering probability increases. The last results of experiments with fluorinated powder to illustrate efficiency of such reflector for direct extraction of very cold neutrons and obtained improvement of quasi-specular reflection of cold neutrons will be presented.

Further improvement in the quality of the nano-structured reflector could be associated with the preparing of powders with the necessary properties. Technologies for purification, separation, deagglomeration of nanodiamonds should be developed. The influence of powder parameters (particle size, agglomeration degree, impurity content) on neutron scattering should be investigated to choose optimal powders for specific reflectors construction at different tasks of neutron physic. First steps of this investigation will be presented.

The reported study was funded by RFBR according to the research project № 18-29-19039

## Deagglomeration of shock-compressed synthesis nanodiamond

*Aleksenskii A.E.<sup>1</sup>, Trofimuk A.D.<sup>1</sup>, Shvidchenko A.V.<sup>1</sup>, Yudina E.B.<sup>1</sup>*

*blin@mail.ioffe.ru*

<sup>1</sup> Ioffe Institute

At present time, the detonation nanodiamond is well known material, and its properties are an extensive field for research. But, alternative methods for the synthesis of nanodiamonds, which have been developed to laboratory or even industrial production, are also known. One of such methods is shock compression of graphite in the mass of explosive (RDX) [1]. Nanodiamond obtained in this way differs from detonation nanodiamond in its relatively low nitrogen content [2]. Also the possibility to control the size of the final nanodiamond crystals by changing the composition of the initial explosive is known. It was believed that dynamic synthetic nanodiamond was a polycrystal with significant abrasive properties [1]. From this assumption it was considered that the sols containing individual particles of such nanodiamond could not be obtained.

This report discusses the method for production of hydrosols, containing free particles of nanodiamond synthesized by shock compression of graphite. The first results of the study of the properties of the obtained hydrosol are presented.

The hydrosol, containing the particles of dynamic synthesis nanodiamond was produced by a method similar to that given in [3]. This method has been modified due to the polycrystalline structure of the original product. IR, EPR and other spectra of the obtained product are given. This work was supported by the grant of Russian Foundation for Basic Research No. 17-03-01217 (“Size Effects in Transition from Diamond Nanocrystals to Higher Adamantanes”).

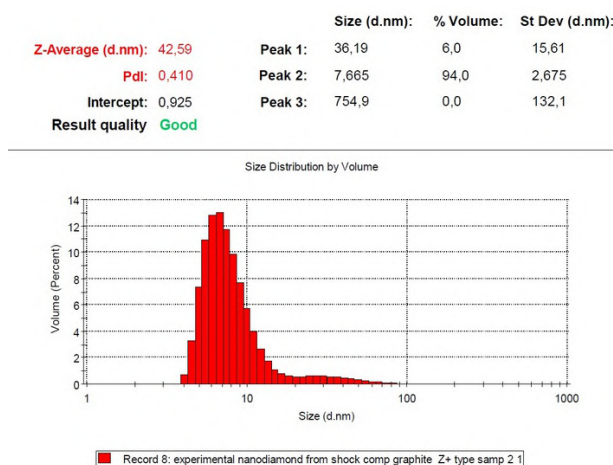


Fig.1. The results of determining the particle size of hydrosol nanodiamond dynamic synthesis using DLS.

### References

1. Tatsii, V. F.; Bochko, A. V.; Oleinik, G. S. Combustion, Explosives, Shock Waves 2009, 45 (1), p.95.
2. O.A. Shenderova, I.I. Vlasov, Stuart Turner, Gustaaf Van Tendeloo, S.B. Orlinskii, A.A. Shiryaev, A.A. Khomich, S.N. Sulyanov, F. Jelezko, Joerg Wrachtrup *The Journal of Physical Chemistry C* (2011) 115, p.14014
3. O.A. Williams, J. Hees, Ch. Dieker, W. Jager, L. Kirste, Ch.E. Nebel *ACS Nano* (2010) 8, p.4824.

## Size effect in the spectra of electron paramagnetic resonance of impurity centers in diamond nanoparticles

G.G.Zegrya<sup>1</sup>, D.M.Samosvat<sup>1</sup>, V.Yu.Osipov<sup>1</sup>, A.Ya.Vul<sup>1</sup>, A.I.Shames<sup>2</sup>

samosvat@yandex.ru

<sup>1</sup> Ioffe Institute, Saint-Petersburg, Russia

<sup>2</sup> Ben-Gurion University of Negev, Beer-Sheva, Israel

This paper considers the influence of the size effect on the spectrum of electron paramagnetic resonance (EPR) of impurity paramagnetic centers in nanoscale diamond particles. It is theoretically shown that with decreasing particle size, the hyperfine structure of the EPR spectrum disappears [1]. The reason for such a change in the spectrum is the delocalization of the wave function of the electron of the surface center over the entire nanoparticle [2], with the result that the electron "feels" the averaged field of all nuclei, which is zero. At the same time, paramagnetic centers located in the bulk of the nanoparticle are also turned off from the hyperfine interaction due to spin diffusion [3]. Thus, with a decrease in size, diamond nanoparticles exhibit characteristic structureless EPR spectra (Fig. 1).

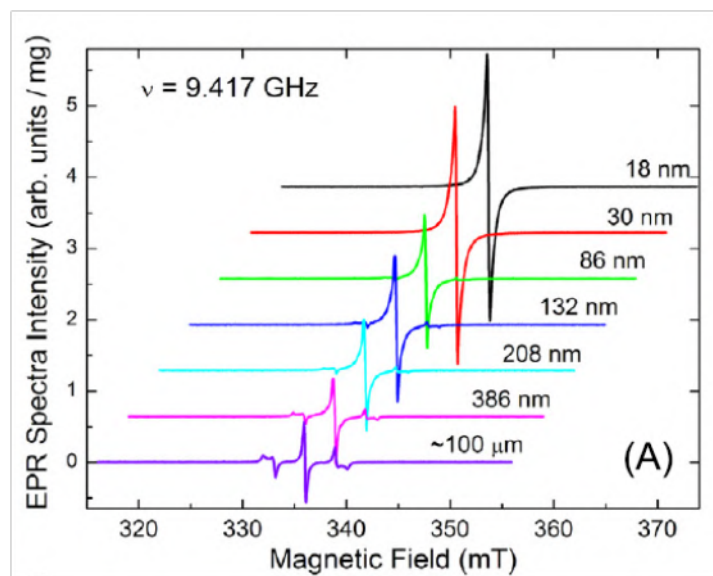


Fig.1. EPR spectrum of nanodiamonds with decreasing it's size [1].

### References

1. Shames A. I., Panich A. M. (2017). Paramagnetic defects in nanodiamonds. *Nanodiamonds*, 131–154. doi:10.1016/b978-0-32-343029-6.00006-4 In: *Nanodiamonds. Advanced Material Analysis, Properties and Applications*. Edited by Jean-Charles Arnault, Chapter 6, Elsevier
2. Abakumov V.N., Perel V.I., Yassievich I.N., Nonradiative recombination in semiconductors, *Modern problems in Cond. Matt. Sci.*, Edited by Agranovich V.M., Maradudin A.A., Volume 33, (1991).
3. Khutsishvili G. R. "Spin diffusion" *Sov. Phys. Usp.* 8 743–769 (1966); DOI: 10.1070/PU1966v008n05ABEH003035

## Dynamic and static investigation of explosion nanodiamonds

*Rubtsov I.A.*<sup>1</sup>, *Ten K.A.*<sup>1</sup>, *Titov V.M.*<sup>1</sup>, *Pruel E.R.*<sup>1</sup>, *Kashkarov A.O.*<sup>1</sup>, *Kremenko S.I.*<sup>2</sup>, *Zubavichus Ya.V.*<sup>3</sup>, *Peters G.S.*<sup>4</sup>, *Veligzhanin A.A.*<sup>4</sup>

*rubtsov@hydro.nsc.ru*

<sup>1</sup> Lavrentyev Institute of Hydrodynamics SB RAS, Novosibirsk, Russia

<sup>2</sup> Novosibirsk State University, Novosibirsk, Russia

<sup>3</sup> Borekov Institute of Catalysis SB RAS, Novosibirsk, Russia

<sup>4</sup> National Research Center "Kurchatov Institute", Moscow, Russia

Nowadays nanodiamonds is widely used in a lot of different areas and its synthesis is one of the necessary and actual questions. The detonation products of high explosives (HEs) with a negative oxygen balance contain a wide phase and morphological variable of carbon forms. This forms of condensed carbon in detonation products depend on the explosion conditions. So that development of the detonation methods for the synthesis of various forms of nanodiamonds is primarily motivated by their commercial and advanced applications. Presently, registration of small-angle x-ray scattering (SAXS) signal is the only way to register experimentally the dynamics of the size of the condensed carbon nanoparticles during detonation of HEs.

This paper presents the experimental results of carbon nanodiamonds synthesis during the detonation of composition TNT/RDX (50/50) and analysis of its saved products.

In this work we used different methods: dynamics registration of SAXS signal during the detonation, static registration of SAXS, high resolution transmission electron microscopy and x-ray diffraction of the recovered carbonaceous residue (soot) of this high explosive.

Comparison and complex analysis of all these methods allowed us to modernize dynamic method for registration formation of nanodiamonds during the explosion.

This work was supported by Russian Foundation for Basic Research (project No. 17-03-00251).

## Hexagonal diamond is in detonation nano and microdiamonds

Shevchenko N.V.<sup>1</sup>, Sigalaev S.K.<sup>2</sup>, Visotina E.A.<sup>3</sup>, Kazakov V.A.<sup>2</sup>, Gorbachev V.A.<sup>1</sup>, Rizakhanov R.N.<sup>2</sup>

nanocentre@kerc.msk.ru

<sup>1</sup> AO "Petrovskiy scientific centre "FUGAS", Moscow, Russia

<sup>2</sup> Keldysh Research Center, Moscow, Russia

<sup>3</sup> NITU "MISIS", Moscow, Russia

The comprehensive studies of the processes of detonation synthesis using mixed explosives have established the presence of a number of allotropic carbon modifications in the composition of the products obtained. The greatest interest among them are nano- and microdiamonds, which have a cubic crystallite structure, as well as graphite with a hexagonal lattice. There is also a possibility of the presence of a hexagonal diamond polytype - lonsdaleite, identified in impact and synthetic diamond-lonsdaleite formations, the manifestation of which is often recorded as packing defects of the crystal structure [1, 2]. The samples of detonation micro- and nano-diamonds, after chemical cleaning with a barothermal method, were studied in the present work in order to study the phase composition and detect the presence of lonsdaleite. The samples were analyzed using high resolution transmission electron microscopy, electron diffraction and Raman scattering with excitation at 244 nm and 514 nm.

Electron-microscopic studies of detonation microdiamonds (Fig. 1a) indicate the presence of a layered diamond-lonsdaleite structure in the sample, mainly represented by a cubic diamond (D) with periodic inclusions of lonsdaleite (L). It is confirmed by electron diffraction recorded during electron microscopic studies. The Raman spectra (RS) registered with excitation at 514 nm showed the presence of a complex maximum at  $1333.4\text{ cm}^{-1}$ , which, after heating the sample up to  $800\text{ }^{\circ}\text{C}$ , splits into two maxima probably related to two carbon phases of cubic nano-D and L. One of them is located at a frequency of  $1316\text{ cm}^{-1}$ . The RS of detonation nano-D with excitation at 244 nm showed the presence of a maximum anomalously offset from the RS peak of micro-D into lower frequencies of the range  $1320\text{ cm}^{-1} \div 1325\text{ cm}^{-1}$  (Fig. 1b). It refers to the characteristic's range of L in the composition of the D-structure [1,2]. The obtained results indicate the possible presence of hexagonal D-phase included in the samples of detonation nano- and micro-D that are not associated with the lattice defects in the cubic packing of detonation diamond structures.

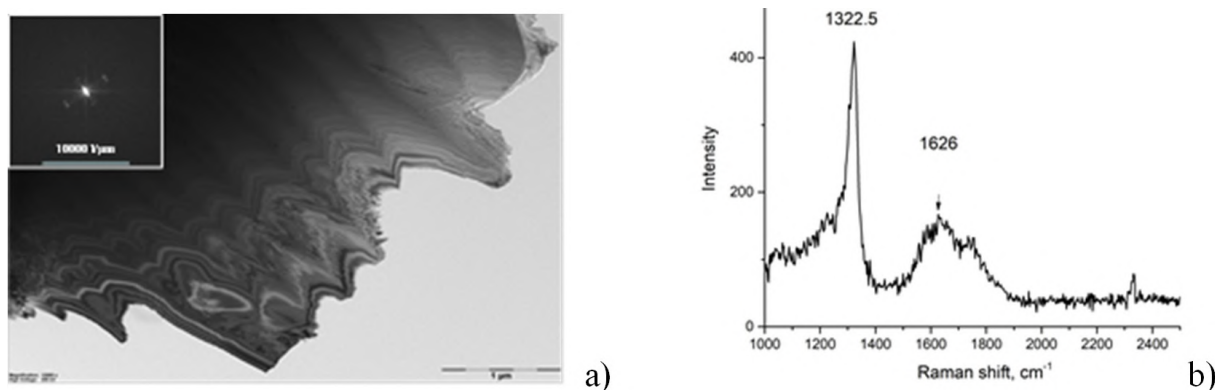


Fig.1 a) Micro-diamond-lonsdaleitic layered structure - microphoto and electron-diffraction pattern; b) the Raman spectrum of detonation bi-phase nanodiamond-lonsdaleite.

### References

1. T.Shumilova, E.Mayer, S.Isaenko. Doklady Earth Sciens, 2011, V 441, P 1552.
2. V.Denisov, B.Martin, N.Sererrynaja, G.Dubinsky, V.Aksenenkov, A.Kirichenko, N.Rumin, I.Perezyogin, V.Blank. Diamond Related Materials, 2011, V 20, P 951.

## Use of nanodiamonds for in situ synthesis of TiC reinforcing nanoparticles in MMC

Popov V.A.<sup>1</sup>, Verшинina E.V.<sup>2</sup>, Popova E.V.<sup>3</sup>

popov58@inbox.ru

<sup>1</sup> National University of Science and Technology MISIS, Moscow, Russia

<sup>2</sup> D.Mendeleev University of Chemical Technology of Russia, Moscow, Russia

<sup>3</sup> Sechenov University, Moscow, Russia

In this work, the research of possibility of in-situ synthesis of TiC nanoparticles in aluminum matrix during mechanical alloying at application as precursors of nanodiamond powders and titanium particles is conducted. Extremely small size of nanodiamond particles and their high hardness are those characteristics of nanodiamonds, which led to the choice them for experiments [1]. High hardness of diamond nanoparticles and their large number lead to an intensification of mechanical alloying process, and the small size positively affects on decrease in the size of synthesizable TiC particles [2].

The optimum composition of initial materials for TiC synthesis in aluminum matrix during mechanical alloying is defined experimentally: Al - 30 g, Ti - 31.98 g; nanodiamonds - 8.02 g. Decrease in amount of aluminum lead to an excessive intensification of synthesis process and (as reaction of synthesis, in this case, starts immediately after the beginning of processing) agglomerates do not manage to be shattered completely; it leads to the fact that a considerable part of synthesized particles have the increased size. At the same time (because of small amount of aluminum), a significant amount of TiC nanoparticles is on a surface of composite granules, and it inevitably leads to material pollution. Increase in amount of aluminum above optimum lead to synthesis process delay. So, at a ratio of mass of aluminum to the sum of mass of the titanium and nanodiamonds equal 35 to 35, creation of TiC nanoparticles is not observed after 6 hours of processing.

At optimum composition, the synthesized TiC particles are nanodimensional and they are evenly distributed in a matrix, there are no defects on interface "matrix - reinforcing particles". The average size of nanoparticles is equal to 30 nanometers. Figure 1 shows TEM image of the synthesized TiC nanoparticles.

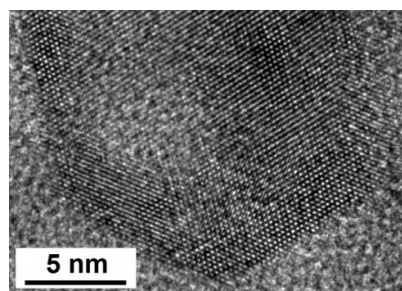


Figure 1. Synthesized TiC nanoparticles inside aluminum matrix (TEM image)

### References

1. Ferreira, P.Egizabal, V.Popov, M.Garcia de Cortazar, A.Irazustabarrena, A.M. Lopez-Sabiron, G.Ferreira. *Diam. Relat. Mat.* (2019) **v.92**, pp.174-186.
2. A.Popov, M.Burghammer, M.Rosenthal, A.Kotov. *Composites. Part B: Engineering* (2018) **v.145**, pp. 57-61

## HPHT synthesis of ultranano-sized diamonds with colour centres

*Davydov V.A.*<sup>1</sup>, *Kulikova L.F.*<sup>1</sup>, *Agafonov V.N.*<sup>2</sup>, *Uzbekov R.E.*<sup>3</sup>

*vdavydov@hppi.troitsk.ru*

<sup>1</sup> L.F. Vereshchagin Institute for High Pressure Physics, RAN, Troitsk, Moscow, Russia

<sup>2</sup> GREMAN, University of Tours, Tours, France

<sup>3</sup> Laboratory of Cell biology and Electron microscopy, University of Tours, Tours, France

Ultra-small, low-strain, artificially produced nanodiamonds (USND) with an internal, active colour centre have substantial potential for quantum information processing applications for bioimaging and biosensing [1]. We demonstrate here the growing of USND (near 92 % from 5 to 13 nm) containing a single or a few bright NV, SiV, and GeV colour centres using the high pressure high temperature (HPHT) method of synthesis based on hydrocarbon growth systems. Previously it was shown that diamond materials obtained in pure hydrocarbon systems are commonly represented mixtures of micro- and submicrometer-size fractions of diamond. Detonation nanodiamonds with the size of 3-4 nm were incorporated in the initial hydrocarbon growth systems for enhancement of the content of nano-size diamond fraction in the products of synthesis. The controlled overgrowing of detonation nanodiamonds in hydrocarbon medium with N, Si or Ge-containing doping components allows to produce ultranano- and nano-size fractions of diamond with different impurity-vacancy color centres. Naphthalene (C<sub>10</sub>H<sub>8</sub>), hexamethylenetetramine (C<sub>6</sub>H<sub>12</sub>N<sub>4</sub>), tetrakis(trimethylsilyl)silane (C<sub>12</sub>H<sub>36</sub>Si<sub>5</sub>) and tetraphenylgermanium (C<sub>24</sub>H<sub>20</sub>Ge) were used as the main hydrocarbon and N, Si, Ge doping components the growth systems. HPHT treatment of the samples was carried out in "Toroid"-type apparatus. The experimental procedure consisted of loading the high pressure apparatus to 8.0 GPa, heating the samples to synthesis temperature and short (1-3 s) isothermal exposure. X-ray diffraction, Raman and PL spectroscopies, SEM and TEM microscopies were used for characterization of synthesized diamond materials. To purify the USND obtained from graphite impurities, we treated them by mixing HNO<sub>3</sub>, HClO<sub>4</sub> and H<sub>2</sub>SO<sub>4</sub> at 250 ° C for 4 h neutralized with NH<sub>4</sub>OH and washed with distilled water. The typical TEM image of USNDs (with SiV centres) and their size histogram is shown in the Fig. 1.

The study was supported by the Russian Foundation for Basic Research (grant 18-03-00936)

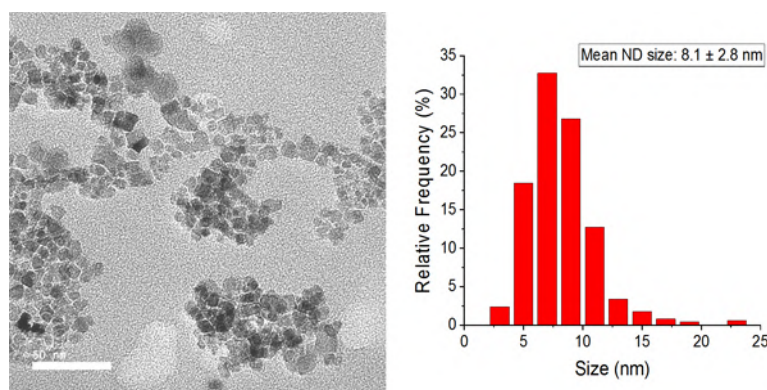


Fig.1. TEM micrograph with the size histogram of USND -Si. Scale bar 50 nm.

### References

1. Jelezko, J. Wrachtrup, Phys. Status Solidi Appl. Mater. Sci. 2006, 203, 3207.



## Ultrafine nanodiamond fractionation by ultracentrifugation

*Besedina N.A.*<sup>1</sup>, *Koniakhin S.V.*<sup>1,2</sup>, *Kirilenko D.A.*<sup>3</sup>, *Shvidchenko A.V.*<sup>3</sup>, *Eidelman E.D.*<sup>3,4</sup>

*besedinadezhda@gmail.com*

<sup>1</sup> Nanobiotech lab, St. Petersburg Academic University, St. Petersburg, Russia

<sup>2</sup> Institut Pascal, University Clermont Auvergne, Aubiere Cedex, France

<sup>3</sup> Ioffe Institute, St. Petersburg, Russia

<sup>4</sup> St. Petersburg Chemical Pharmaceutical Academy, St. Petersburg, Russia

Nanodiamonds (ND) are promising nanoparticles and they are actively investigated for application in advanced materials fabrication, quantum computing, biology and medicine. Most number of ND applications assumes their handling in the form of hydrosols typically containing both individual primary crystallites of about 4-5 nm size and their agglomerates of the size of 100 nm. The presence of agglomerates significantly complicates characterization of nanodiamonds with optical methods [1] and makes it difficult to determine the size of primary nanodiamond crystallites using the Dynamic Light Scattering (DLS) method [2].

In this work we propose a method for ultrafine fractionation of nanodiamonds using the differential centrifugation in the fields up to 215000g. The developed protocols yield 4-6 nm fraction giving main contribution to the light scattering intensity and no agglomerates fingerprints in DLS. The desired 4-6 nm fraction can be obtained from various types of initial nanodiamonds: three types of detonation nanodiamonds (DND) differing in purifying methods [3], laser synthesis nanodiamonds and nanodiamonds made by milling. Zeta potential of nanodiamonds stayed intact during the ultracentrifugation process. According to powder XRD and TEM data ultracentrifugation also leads to a further fractionation of the primary diamond nanocrystallites in the hydrosols from 4 to 2 nm [4].

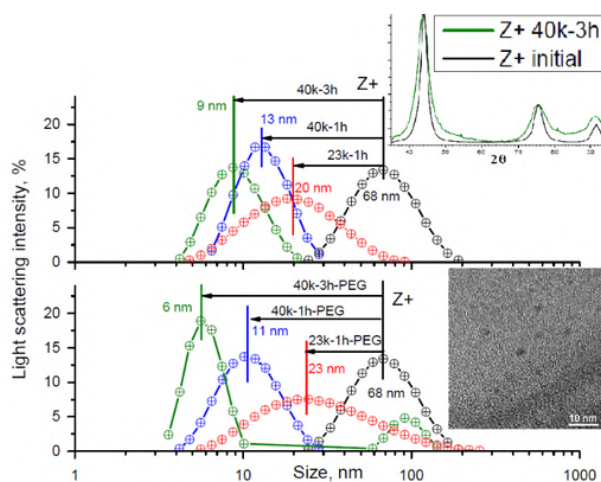


Figure 1 - Results of DND ultracentrifugation for various protocols differing in rotor speed, duration time and presence of viscous PEG layer on the tube bottom. The insets show XRD pattern and TEM data.

### References

1. A.Ya. Vul, E.D. Eydelman, L.V. Sharonova, A.E. Aleksenskiy, and S.V. Konyakhin, *Diamond and Related Materials* (2011), **20(3)**, 279-284.
2. S.V. Koniakhin, I.E. Eliseev, I.N. Terterov, A.V. Shvidchenko, E.D. Eidelman and M.V. Dubina, *Microfluidics and Nanofluidics* (2015), **18(5-6)**, 1189-1194.
3. A.T. Dideikin, A.E. Aleksenskii, M.V. Baidakova, P.N. Brunkov, M. Brzhezinskaya, V.Y. Davydov and V.V. Shnitov, *Carbon* (2017), **122**, 737-745.
4. S.V. Koniakhin, N.A. Besedina, D.A. Kirilenko, A.V. Shvidchenko and E.D. Eidelman, *Superlattices and Microstructures* (2018), **113**, 204-212.

## **Broadband photoluminescence of nanodiamonds: intrinsic feature or another carbon phase?**

*Vlasov I.I.*<sup>1</sup>, *Shenderova O.A.*<sup>2</sup>, *Kudryavtsev O.S.*<sup>1</sup>, *Khomich A.A.*<sup>1</sup>, *Dolenko T.A.*<sup>3</sup>

*vlasov@nsc.gpi.ru*

<sup>1</sup> Prokhorov General Physics Institute of RAS, Moscow, Russia

<sup>2</sup> Adamas Nanotechnologies, Raleigh, USA

<sup>3</sup> Moscow State University, Moscow, Russia

Broadband photoluminescence is observed in purified nanodiamonds (ND) of various origin. In early studies on the optical properties of nanodiamonds, this luminescence was generally associated with a defective diamond surface [1], since its intensity increased with a decrease in nanoparticle size and, therefore, with an increase in the surface / volume ratio of the material under study. In recent years, the assumption about the source of luminescence of nanodiamonds has become more definite; a relationship between luminescence and sp<sup>2</sup>-bonded carbon on the surface of diamond nanoparticles was found [2]. When studying the dependence of luminescence on the degree of chemical purification of detonation ND, we established a relationship between the observed luminescence and oxidized nanographene (nGO) clusters decorated the ND surface [3]. Using transmission electron microscopy, we found that the original (unpurified) diamond grains are mostly covered with multilayer graphene shells and do not exhibit photoluminescent properties. When the amount of graphite is significantly reduced by treatment with acids, and it basically remains in the form of rounded graphene clusters of 1-2 nm in size on a diamond surface, the photoluminescence of the nanomaterial reaches its maximum value. Further acid treatment leads to a decrease in the number of graphene clusters and, accordingly, to a decrease in the luminescence intensity. By choosing an oxidation time of initial detonation nanodiamonds and removing adsorbed water from a ND surface, we managed to increase the luminescence intensity by 2 orders of magnitude compared with the luminescence of well-purified detonation ND. We also found that luminescence of NDs dispersed in water depends on the excitation wavelength and pH value in the same manner as it does for pure nGO. These results testify in favor of the fact that the broadband luminescence observed in various types of nanodiamonds is not their intrinsic feature but is associated with graphene nanostructures adjacent to the diamond surface.

This work was supported by the Russian Science Foundation (grant number 17-12-01481).

### **References**

1. E. Kompan, E. I. Terukov, S. K. Gordeev, S. G. Zhukov, and Yu. A. Nikolaev *Phys. Solid State* (1997) 39, 1928.
2. R. Smith, D. Gruber, T. Plakhotnik, *Diamond & Related Materials* (2010) 19, 314.
3. O. Shenderova, S. Hens, I. Vlasov, S. Turner, Y. Lu, G. Van Tendeloo, A. Schrand, S. Burikov, T. Dolenko, *Particle&Particle Systems Characterization* (2014) 31, 580.

## SANS analysis of aqueous dispersions of Eu- and Gd-grafted nanodiamond particles

Tomchuk O.V.<sup>1</sup>, Avdeev M.V.<sup>1</sup>, Aleksenskii A.E.<sup>2</sup>, Aksenov V.L.<sup>1</sup>, Vul' A.Ya.<sup>2</sup>

tomchuk@jinr.ru

<sup>1</sup> Frank Laboratory of Neutron Physics, Joint Institute for Nuclear Research, Dubna, Russia

<sup>2</sup> Ioffe Physical-Technical Institute, St.Petersburg, Russia

The prospects of nanodiamonds in biomedicine are closely linked with various markers. The chemically active surface of DND enables conjugation with a variety of functional groups that allows preparation of nanoparticles with controlled chemical, electronic and physical properties [1]. The DND surface with negative zeta-potential is mainly functionalized by carboxyl and hydroxyl groups that enable its grafting by metal atoms such as Eu or Gd. There are corresponding indications from the complementary methods that the modification of the DND surface changes the colloidal stability of these particles in water. The discussed modification also resulted in a viscosity growth of the solutions that points to reorganization of the cluster structure in systems under study. Thus, our research aimed at detecting and analyzing changes in the inner structure of DND clusters using small-angle neutron scattering (SANS) [2].

Conventional SANS study did not reveal any significant differences in the structure of modified DND suspensions from previously studied systems (Fig. 1a). The normalized scattering curves repeat each other. However, the neutron scattering in ultra-small range showed a significant difference (Fig. 1b and first few points in Fig. 1a). As before, the initial DND suspension demonstrated the Guinier regime, but for the modified suspension secondary aggregation with a fractal dimension of 2.65 was observed. The observed effect was considered as the basis of the microstructural mechanism for reducing stability during surface grafting.

This work was supported by the Russian Science Foundation (Project No.18-72-00099).

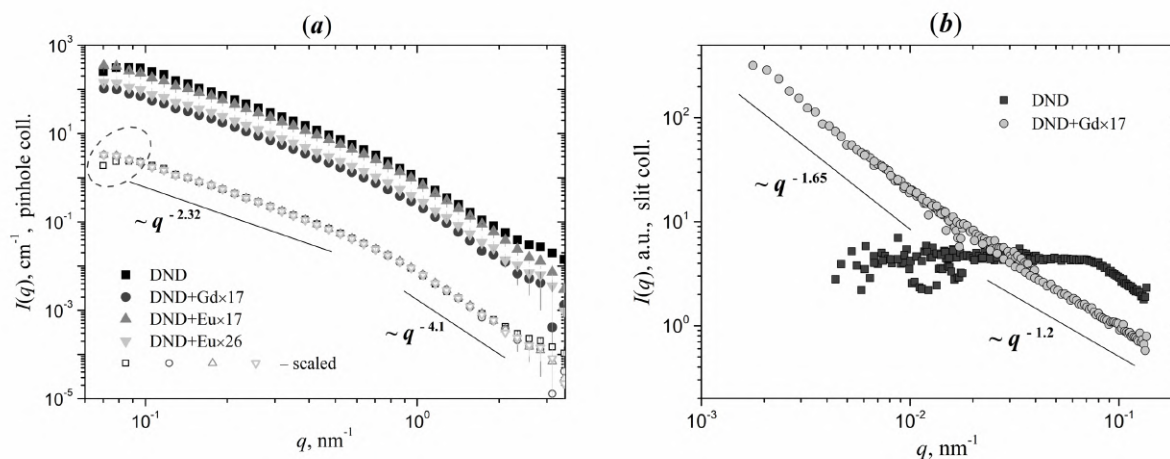


Fig.1. SANS spectra from the aqueous suspensions of DND itself and grafted with corresponding number of lanthanide atoms, obtained at (a) YuMO time-of-flight SANS diffractometer (FLNP JINR, Dubna, Russia) and (b) high-resolution SANS diffractometer MAUD (NPI ASCR, Řež, Czech Republic).

### References

1. M. Panich, M. Salti, S.D. Goren, E.B. Yudina, A.E. Aleksenskii, A.Ya. Vul' and A.I. Shames, J. Phys. Chem. C (2019), **123**, 2627.
2. V. Avdeev, O.V. Tomchuk, O.I. Ivankov, A.E. Alexenskii, A.T. Dideikin, A.Ya. Vul', Chem. Phys. Lett. (2016), **658**, 58.

## DIELECTRIC PROPERTIES OF DETONATION NANODIAMOND SUSPENSIONS IN POLYDIMETHYLSILOXANE

Kuznetsov N.M.<sup>1</sup>, Belousov S.I.<sup>1</sup>, Vdovichenko A.Yu.<sup>1</sup>, Chvalun S.N.<sup>1,2</sup>, Vul' A.Ya.<sup>3</sup>

serbell@gmail.com

<sup>1</sup> Kurchatov Institute, Moscow, Russia

<sup>2</sup> Enikolopov Institute of Synthetic Polymeric Materials of the Russian Academy of Sciences, Moscow, Russia

<sup>3</sup> Ioffe Institute, St. Petersburg, Russia

In recent years, the interest in a various applications of nanodiamonds (DND) produced by detonation synthesis from carbon explosives has increased [1]. An obstacle to use of such DND is their aggregation [2]. The rheological properties of the DND suspensions in silicone oil attract the attention of researchers for the purpose of further applications as new lubricants, due to the improvement in tribological characteristics [3, 4]. Some methods, for example wet ball milling or annealing with following sonication allow to obtain stable DND hydrosols. It is important to note that the agglomeration processes essentially depend on the dielectric characteristics of the medium and the filler. It is obvious that the dielectric properties of water and oil is significantly different. Thus, the sedimentation stability of suspensions and the processes of secondary aggregation of DND become more important aspect in oil media. It is known that the electrophysical characteristics of DND substantially depend on the quality of the particles [5]. So a large amount of sp<sup>2</sup> phase on the particles surface leads to an increase in conductivity.

In the present research the method of broadband impedance spectroscopy was used to study the electrophysical characteristics of DND suspensions in polydimethylsiloxane oil at various concentrations. The frequency dependences of the dielectric constant, conductivity and dielectric loss tangent were obtained in the temperature range from 0 to 50 °C. The differences in electrophysical characteristics depending on the surface chemistry of DND particles were discussed.

This work partially supported by Russian Foundation for Basic Researches, project 18-29-19117 mk.

### References

1. O. A. Shenderova, D. M. Gruen. *Ultrananocrystalline Diamond: Synthesis, Properties and Applications (Second Edition)*, William Andrew Publishing, 2012.
2. A.T. Dideikin, A.E. Aleksenskii, M.V. Baidakova, P.N. Brunkov, M. Brzhezinskaya, V. Yu. Davydov, V.S. Levitskii, S.V. Kidalov, Yu. A. Kukushkina, D.A. Kirilenko, V.V. Shnitov, A.V. Shvidchenko, B.V. Senkovskiy, M.S. Shestakov, A. Ya. Vul'. *Carbon*, (2017), **122**, 737.
3. C.C. Chou, S.H. Lee. *J. Mater. Process. Technol.*, (2008), **201**, 542.
4. O. Shenderova, A. Vargas, S. Turner, D. M. Ivanov, M. G. Ivanov. *Tribol. Trans.* (2014), **57**, 1051.
5. S.S. Batsanov, D.A. Dan'kin. *J. Phys. D: Appl. Phys.* (2016), **49**, 275301.

## Composite aqueous dispersions of graphene oxide - detonation nanodiamond by small-angle scattering

Avdeev M.V.<sup>1</sup>, Tomchuk O.V.<sup>1</sup>, Aksenov V.L.<sup>2,1</sup>, Aleksenskii A.E.<sup>3</sup>, Dideikin A.T.<sup>3</sup>, Vul A.Ya.<sup>3</sup>

avd@nf.jinr.ru

<sup>1</sup> Frank Laboratory of Neutron Physics, Joint Institute for Nuclear Research, Dubna, Moscow Reg., Russia

<sup>2</sup> National Research Center 'Kurchatov Institute', Moscow, Russia

<sup>3</sup> Ioffe Institute, St.Petersburg, Russia

Aqueous dispersions of carbon-based materials such as detonation nanodiamonds (DND) and graphene oxide (GO) are of current interest in view of the growing number of their applications in various areas. Composite systems based on the mixed DND/GO solutions is considered for avoiding the problems of GO wrinkle formation and association.

In the present study, the structural characterization of the partial dispersion of DND particles and clusters, GO sheets and mixed solutions has been performed by scattering techniques including small-angle X-ray (SAXS) and neutron (SANS) scattering following the previously reported approach [1, 2]. The size and fractal character of the aggregates at different scales, as well as the structural features of the particles (size, surface inhomogeneity) are compared for the three types of solutions. The scattering from graphene oxide in water is well described in terms of the model of thin discs with the disc thickness of below 0.5 nm, thus strongly testifying a 2D structure organization of the dispersed associates, as well as the fact that they consist of a single graphene-type layer. With respect to the composite, the binding of individual nanodiamond particles together with their homogeneous and random distribution along the graphene planes has been concluded basing on the analysis of the scattering data.

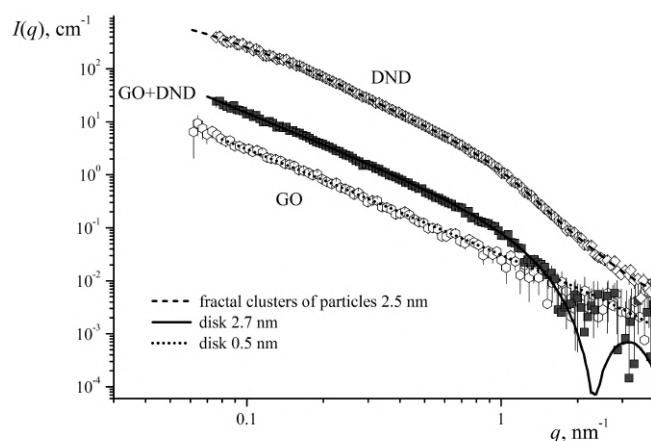


Fig.1. Experimental SANS curves (points) from separate DND and GO aqueous dispersions, as well as from their composite. The lines show the calculated curves corresponding to different structural models.

### References

1. V. Tomchuk, D.S. Volkov, L.A. Bulavin, A.V. Rogachev, M.A. Proskurnin, M.V. Korobov, M.V. Avdeev, *J. Phys. Chem. C* (2015), **119**, 794.
2. V. Avdeev, O.V. Tomchuk, O.I. Ivankov, A.E. Alexenskii, A.T. Dideikin, A.Ya. Vul', *Chem. Phys. Lett.* (2016), **658**, 58.

## Lonsdaleite effect on optical properties of impact diamonds

*Yelisseyev A.P.*<sup>1,2</sup>, *Gromilov S.A.*<sup>2,3</sup>, *Sildos I.*<sup>4</sup>, *Kiisk V.*<sup>4</sup>, *Afanasyev V.P.*<sup>1</sup>

*eliseev.ap@mail.ru*

<sup>1</sup> Sobolev Institute of Geology and Mineralogy SB RAS, Novosibirsk, Russia

<sup>2</sup> Novosibirsk State University, Novosibirsk, Russia

<sup>3</sup> Nikolaev Institute of Inorganic Chemistry SB RAS, Novosibirsk, Russia

<sup>4</sup> Insitute of Physics, University of Tartu, Tartu, Estonia

Impact diamonds are a new nanostructured multiphase carbon mineral formed at extremal P and T-parameters in the shock process when an asteroid meets the Earth. According to electron microscopy the sizes of crystalline pieces (grains) vary from 10 to 100 nm. Optical spectroscopy in different versions was used to study several tens of translucent impact diamonds from the Popigai astrobleme, each ~ 1.5 mm in size. They were mainly thin plates ~100 μm thick, with cubic 3C, hexagonal 2H diamonds and graphite as the dominating carbon phases. Their color varies from colorless to completely opaque as the input of carbon phases with the  $sp^1$ ,  $sp^2$  hybridization increases.

Using Raman spectroscopy and X-rays diffraction, two groups of translucent samples of the impact diamond from the Popigai meteorite crater (PID) were selected: with and without lonsdaleite (L), and the contribution of L was estimated. IR absorption spectroscopy shows the broadening of all features in PIDs with L: both of two-photon diamond absorption and the signal from solid CO<sub>2</sub> inclusions. In the single-phonon region there is no signal from the nitrogen centers, a wide band with a maximum of about 1230 cm<sup>-1</sup> dominates.

In all PIDs, the short-wave absorption edge in the UV region of the spectrum is blurred and described by the Urbach rule as a consequence of electronic transitions between the "tails" of the bands. The absence of temperature dependence in the absorption spectrum indicates a dominant structural disordering in the PID structure. For PIDs composed of grains with a purely cubic structure, transmission in many cases begins at about 225 nm (5.5 eV). For PIDs with a large L contribution the transmission edge is shifted to the long-wave side, the band gap is estimated as  $E_g$  (~3.5÷4 eV) and this value is associated with Lonsdaleite phase. Similar values were obtained earlier in the first principles calculations [1, 2]. The photoluminescence (PL) spectra for PIDs under X-ray and UV (325 nm) excitation are dominated by broad bands with maxima of about 350, 425, 560 nm. In PIDs without L at excitation at 355 nm in addition to wide bands in most diamonds there is a blurred system N3, as well as a set of narrow lines of unknown nature in the range 600-750 nm. In some (rare) PIDs samples with a cubic structure, intense PL is also recorded from nitrogen-vacancy complexes H4, NV, NV, well-known for natural and synthetic diamonds. The corresponding systems are well resolved in the PL spectra at a grain size of more than 50 nm in PIDs, whereas N3, although blurred, is observed in almost all PIDs without lonsdaleite. In PIDs containing L, wide PL bands are shifted to the short-wave side, if present, the lines are weak and broadened, as a result of strong stresses in small-sized grains and difficult migration of defects.

The work was performed on the state assignment of IGM SB RAS and partially supported by RFBR grants № 16-05-00873a and 18-45-140011 p\_a.

### References

1. Wen, J. Zhao, M. Bucknum, P. Yao, T. Li, *Diam. Rel. Mater.*, (2008) **17**, 356.
2. Yelisseyev, G. S. Meng, V. Afanasyev, N. Pokhilenko, V. Pustovarov, A. Isakova, Z. S. Lin, H. Q. Lin, *Diamond & Related Materials* (2013) **37**, 8.

## Thermoluminescence in diamonds of different genesis and types

*Yelisseyev A.P.*<sup>1</sup>, *Vins V.G.*<sup>2</sup>

*eliseev.ap@mail.ru*

<sup>1</sup> Sobolev Institute of Geology and Mineralogy SB RAS, Novosibirsk, Russia

<sup>2</sup> LLC VELMAN, Novosibirsk, Russia

The method of thermally stimulated luminescence (TSL) is a fairly simple method that allows one to obtain information about the centers of capture of charge carriers – shallow states located close to the edges of the permitted bands (VB and CB), and to assess the possibility of using diamonds in dosimeters and other optoelectronic devices.

Natural diamonds of various types within the framework of physical classification (types IaA, IaB, Ib, IIb) as well as impact diamonds from the Popigay meteorite crater (PIDs), synthetic HPHT and CVD diamonds were studied

The characteristic of natural diamonds is shown: well-pronounced peaks of about 400, 580 K are observed for type IaA whereas the others are 105, 145, 210 K (IaB); 290, 380 K (Ib); 150, 260 K (IIb). Parameters of capture centers are calculated. Spontaneous emptying of capture centers with TSL peaks at  $T < 350$  K due to tunnel electronic transitions was recorded. Along with the narrow TSL peaks we observed a continuous TSL glow, especially noticeable at temperatures less than 100 K. This luminescence is rather weak in perfect single crystals, but dominates in IaA-type diamonds with high content of (100) platelets (B2 or B'-centers) and in polycrystalline impact diamonds consisting of nanosized grains. This is the result of strong stresses in the vicinity of extended defects: platelets in IaA-type diamonds and near the surface of nanoscale grains in impact diamonds. In PIDs with a purely cubic structure, three significantly broadened peaks of about 180, 278 and 383 K are discernible in the TSL, while in the presence of hexagonal diamond (lonsdaleite) the peaks are even more broadened and some maxima are difficult to determine.

In HPHT grown diamonds of Ib type the peaks at 250 and 270 K dominate in TSL curves. These centers associated with the manifestation of native defects are absent in natural diamonds. Donor nitrogen demonstrates a quenching effect on the processes of radiative recombination: the intensity of TSL in diamonds with  $N_c$  less than 10 ppm is two to three orders of magnitude higher than in diamonds with  $N_c$  more than 150 ppm. The possibility of controlling the parameters of capture centers in HPHT diamonds by their ionizing irradiation with further annealing is shown. So, irradiation of HPHT synthetic diamond with fast electrons ( $3 \text{ MeV}/10^{18}$

$\text{cm}^{-2}$ ) produces vacancies in their structure. These vacancies become mobile during annealing and NV complexes are formed. These centers operate as effective recombination centers. In diamonds, a pair of deep centers of capture is also generated, and intense peaks of about 470 and 580 K appear in the TSL curves. The low-temperature component in this pair is induced under the action of UV light, while the high-temperature component appears after ionizing irradiation (in particular, by X-rays). It is assumed that such crystals can be used in dosimeters and detectors of UV or ionizing radiation.

This work was performed on state assignment of IGM SBRAS and was partially supported by RFBR grants No. 16-05-00873a and 18-45-140011 p\_a.

## Poole-Frenkel' Effect in Boron-Doped Diamond

Altukhov I.V.<sup>1</sup>, Kagan M.S.<sup>1</sup>, Paprotskiy S.K.<sup>1</sup>, Khvalkovskiy N.A.<sup>1</sup>, Rodionov N.B.<sup>2</sup>, Bolshakov A.P.<sup>3</sup>, Ralchenko V.G.<sup>3</sup>, Khmel'nikskiy R.A.<sup>4</sup>

kagan@cplire.ru

<sup>1</sup> Kotelnikov Institute of Radio Engineering and Electronics of RAS, Moscow, Russia

<sup>2</sup> Institute of Innovative and Thermonuclear Research, Troitsk, Moscow distr., Russia

<sup>3</sup> Prokhorov General Physics Institute of RAS, Moscow, Russia

<sup>4</sup> Lebedev Physical Institute of RAS, Moscow, Russia

Vertical hole transport in diamond films was studied at dc and pulsed electric fields up to  $\sim 5 \cdot 10^5$  V/cm. Basically undoped diamond films CVD grown on diamond substrates heavily doped with boron ( $\sim 2 \cdot 10^{19}$  cm<sup>-3</sup>) have used. The film thickness was  $\sim 10$ -12 nm. The ohmic contacts were made of Ni-W alloy. The dc bias and triangular voltage pulses of 10-100 ms duration were used to record current-voltage (I-V) characteristics.

The I-V characteristics at low fields are linear, which makes it possible to estimate the concentrations of free carriers and acceptors in the material -  $\sim 10^8$  and  $\sim 10^{14}$  cm<sup>-3</sup>, respectively. At fields larger  $\sim 3$  kV/cm, the I-V characteristics are quadratic caused by the linear field dependence of a hole capture rate at ionized boron centres [1]. At higher fields ( $> 30$  kV/cm), the field ionization of the boron acceptors was observed resulted in an exponential rise of current. It was shown that the boron ionization is the result of Poole-Frenkel' effect - the lowering of potential barrier of impurity by an external electric field. This is confirmed by fitting of the experimental dependences of conductivity (free carrier concentration) on electric field by Frenkel's formula  $p \sim \exp[(e^3 E/e)/kT]$  ( $e$  is the elementary charge,  $E$  is the applied electric field,  $\epsilon$  is the permittivity,  $k$  is Boltzmann's constant,  $T$  is the temperature). The field dependence of conductivity at room temperature is shown in Fig. 1.

The work is supported in part by RFBR grant 18-02-01079.

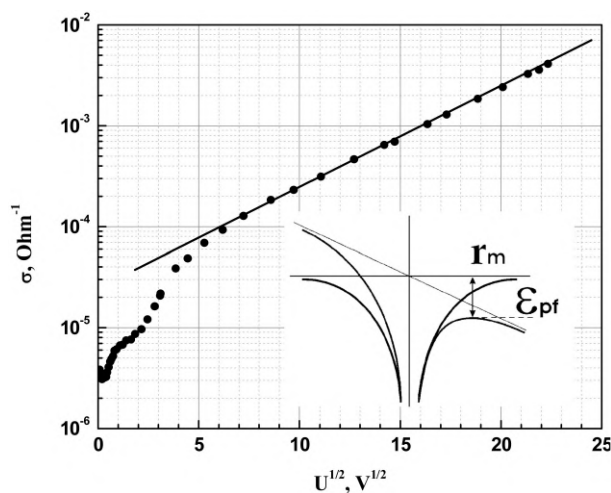


Fig.1. Dependence of conductivity of boron doped diamond on  $U^{1/2}$  showing boron ionization through Poole-Frenkel' effect. Inset - the scheme of the effect.

### References

1. V.N. Abakumov, V.I. Perel, I.N. Yassievich, Nonradiative recombination in semiconductors. Modern Problems in Condensed Matter Sciences, Vol. 33, Amsterdam, North Holland, 1991



## UHT annealing of brown centers and radiation defects in CVD diamond

*Vins V.G.*<sup>1</sup>, *Yelisseyev A.P.*<sup>2</sup>, *Lobarev A.I.*<sup>1</sup>, *Hirani M.*<sup>3</sup>, *Volodin V.V.*<sup>4</sup>, *Blinkov A.E.*<sup>1</sup>, *Faddeenkov V.V.*<sup>1</sup>, *Reznikov E.N.*<sup>1</sup>

*vgvins@gmail.com*

<sup>1</sup> LLC HighTechDiam, Novosibirsk, Russia

<sup>2</sup> Sobolev Institute of Geology and Mineralogy SB RAS, Novosibirsk, Russia;

<sup>3</sup> Soni Tools, Mumbai, India

<sup>4</sup> Novosibirsk State University, Novosibirsk, Russia

The study investigated 10 single crystal of CVD diamond plates of type IIa + Ib. In the initial state the Raman peak at 1332.4 cm<sup>-1</sup> is observed in the Raman spectrum of the plates with an FWHM factor of 4.2-4.5 cm<sup>-1</sup>; in the UV range, the self-absorption edge at 225 nm, the weak absorption band of donor nitrogen is 270 nm (Nc ~ 2 ÷ 3 ppm), and then the monotonically falling absorption, which is responsible for the initial dark brown color of diamonds. Annealing of unirradiated diamonds at T ≥ 1900 ° C leads to the destruction of most brown centers and an increase in transmittance in the visible range by 20-25%. After being irradiated with electrons (RT, 3 MeV / 2 × 10<sup>18</sup> cm<sup>-2</sup>), the plates become almost opaque due to intense absorption in the GR1 system (about 20 cm<sup>-1</sup> at the maximum of the band). In the Raman spectrum in addition to the main peak 1332.4 cm<sup>-1</sup>, three additional low-intensity peaks appear at 1190, 1295, and 1355 ÷ 58 cm<sup>-1</sup>, the last of which is associated with the appearance of sp<sup>2</sup>- hybridized bonds. Peaks of 1190 and 1295 cm<sup>-1</sup>, not previously described in the literature, may be due to the formation during irradiation, in addition to isolated vacancies and interstitial, also their complexes: interstitial-vacancy pairs (IVP). When heated to 300 ° C, simultaneously with a decrease in the concentration of isolated neutral vacancies (V[ppm] = 0.4 × I<sub>693nm</sub> [cm<sup>-1</sup>]) by about 0.5 ppm (corresponding to a decrease in absorption in the GR1 system by 8 ÷ 12%), these lines are annealed, presumably as a result of annihilation of IVP with the formation of a regular lattice site. In the diamonds studied, higher activation energy of annihilation and lower mobility of the interstitials are expected as compared to perfect crystals as a result of strong elastic stresses caused by brown centers. Stepwise, every 100 °, annealing of irradiated diamonds in the range of 300 - 1800 ° C for 30 minutes at each temperature, allowed studying the dynamics of annealing of various defects. So the GR1 system (isolated vacancies) starts to anneal at T ≥ 800 ° C and completely disappears only at 1200 ° C. An intense increase in transmittance in the visible range begins at 1600 ° C, and at 1800 ° C, it is 30% higher than that of the original dark brown plates. Those, enlightenment of diamonds with UHT annealing occur more efficiently if they contain radiation defects. IR absorption also changes regularly: from the original bands: 1130, 1240, 1290, 1332 cm<sup>-1</sup> with absorption intensities ≤ 0.5 cm<sup>-1</sup>, after annealing at 1800 ° C remains only a peak of 1332 cm<sup>-1</sup> with intensity ≤ 0.2 cm<sup>-1</sup>. In the photoluminescence (PL) spectra with UV excitation (365Hg) instead of the original systems 467.5 nm and 575 nm, after the final annealing at 1800 ° C, only H3 is observed, which is responsible for the green PL. This indicates the transformation of donor nitrogen and NV - defects in NVN complexes. The absence of changes in the width of the Raman peak during annealing indicates the preservation of stresses in the diamond structure.

## Novel hybrid nanomaterials based on iron containing diamonds

*Fomina I.G.*<sup>1</sup>, *Korlyukov A.A.*<sup>2</sup>, *Svetogorov R.D.*<sup>3</sup>, *Yakushev I.A.*<sup>1</sup>, *Yudina E.B.*<sup>4</sup>, *Imshennik V.K.*<sup>5</sup>, *Maksimov Yu.V.*<sup>5</sup>, *Goodilin E.A.*<sup>6</sup>, *Eremenko I.L.*<sup>1</sup>

fomina@igic.ras.ru

<sup>1</sup> Kurnakov Institute of General and Inorganic Chemistry RAS, Moscow, Russian Federation

<sup>2</sup> Nesmeyanov Institute of Organoelement Compounds RAS, Moscow, Russian Federation

<sup>3</sup> National Research Center "Kurchatov Institute", Moscow, Russian Federation

<sup>4</sup> Ioffe Institute, St. Petersburg, Russian Federation

<sup>5</sup> Semenov Institute of Chemical Physics RAS, Moscow, Russian Federation

<sup>6</sup> Department of Materials Science, Lomonosov Moscow State University, Moscow, Russian Federation

Functionalization of surface nanoparticle plays an important role in modern nanotechnologies, which are mainly based on bottom-up technology. Diamond nanoparticles are attractive for such technology as a building block for prospective applications as drug delivery and synthesis of various composite materials with unique properties [1, 2]. Developed method of deagglomeration of detonation nanodiamonds (DNDs) and preparation of stable colloids of 4-5 nm DNDs [3] have opened new ways for applications of DNDs in nanotechnologies. It is the surface modification of DNDs, which is the next step in developing of DNDs technology. In the present work, the stable hydrosol of 4-5 nm carboxylated deagglomerated DNDs (DND-COOH) [3] and  $\text{FeCl}_3 \cdot 6\text{H}_2\text{O}$  were used as initial reagents for preparation of novel hybrid magnetoactive nanomaterials based on iron containing DND-COOH. Composition, structure and magnetic behavior of the series samples of the nanodiamonds with the surface modified by the  $\text{Fe}^{3+}$  ions were characterized by powder X-ray diffraction, Mössbauer spectroscopy, and Raman spectroscopy.

This study was supported by the Russian Foundation for Basic Research (Project № 18-29-19038).

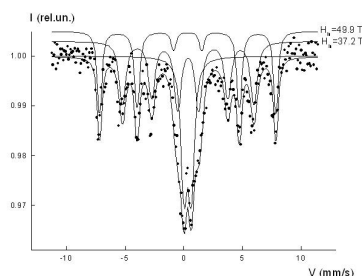


Fig.1. The  $^{57}\text{Fe}$  Mossbauer spectrum at 300K of the nanodiamonds with the surface modified by the  $\text{Fe}^{3+}$  ions shows the existence of two wide sextet lines, that can be attributed to magnetically ordered  $\alpha\text{-Fe}_2\text{O}_3$ ,  $\alpha\text{-FeOOH}$  and narrow paramagnetic doublet of  $\beta$ ,  $\gamma\text{-FeOOH}$ .

### References

1. S. Alwani, R. Kaur, D. Michel, J.M. Chitanda, R.E. Verrall, C. Karunakaran, I. Badea, *Int. J. Nanomedicine* (2016) **11**, 687.
2. L.M. Pastrana-Martínez, S. Morales-Torres, S.A.C. Carabineiro, J.G. Buijnsters, J.L. Figueiredo, A.M.T. Silva, J.L. Faria *Appl. Surf. Sci.* (2018) **458**, 839.
3. A.E. Aleksenskiy, E.D. Eydelman, A.Y. Vul', *Nanosci. Nanotechnol. Lett.* (2012) **4**, 165.

## New theory of crystalline nanoparticles Raman spectra

*Utesov O.I.*<sup>1,2</sup>, *Yashenkin A.G.*<sup>1,3</sup>, *Koniakhin S.V.*<sup>4,2</sup>

*utiosov@gmail.com*

<sup>1</sup>Theory Division, Petersburg Nuclear Physics Institute NRC "Kurchatov Institute", Orlova roshcha, Gatchina, Russia

<sup>2</sup>Nanobiotechnologies Laboratory, St. Petersburg Academic University, St. Petersburg, Russia

<sup>3</sup>Department of Physics, Saint Petersburg State University, St. Petersburg, Russia

<sup>4</sup>Institut Pascal, PHOTON-N2, University Clermont Auvergne, CNRS, Aubiere Cedex, France

Nanoparticles (NP) are intensively studied now for applications in novel materials creation, quantum computing, biology, etc. One of the most important NP characterization methods is Raman spectroscopy. In comparison with bulk material Raman peak of NP is downshifted and asymmetrically broadened. These effects are due to the finite particle size.

To quantify these effects and to connect the peak position with NP size, the phonon confinement model (PCM) is widely used. However, a deeper analysis of the PCM reveals a series of essential problems. Very recently we propose an alternative approach based on the combined use of the dynamical matrix method and bond polarization model (DMM-BPM) [1]. Contrary to the PCM, the DMM-BPM approach allows one to interpret recent experimental data on nanodiamond powders very successfully [1]. The disadvantage of the DMM-BPM is that one of its constituents, the dynamical matrix method, requires diagonalization of huge  $3N \times 3N$  matrices, where  $N$  is the number of atoms in the crystallite. Although this general numerical method inspires the quickly solvable analytical version, this version misses some information about nanoparticle shape.

In the present work, we propose another approach to the Raman spectra (RS) analysis [2]. We substitute the original optical phonon eigenproblem by an effective continuous media problem with the spectrum of optical phonons in the long-wavelength limit. The optical modes were shown to obey the Klein–Fock–Gordon equation with Dirichlet boundary conditions. With the use of continuous reformulation of the BPM, it allows calculating nanoparticle RS. Also, the question of NP shape influence on RS was investigated. We successfully apply our approach for description of experimentally measured RS of nanodiamond powder [3], see Fig. 1.

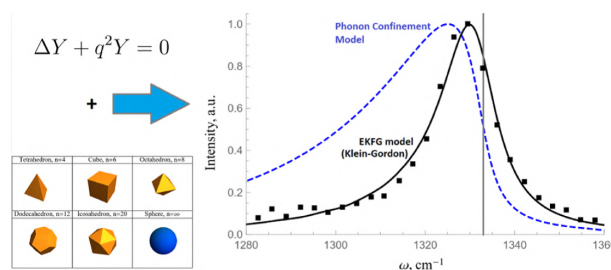


Fig.1. To calculate Raman spectra of arbitrary shaped nanoparticle one can solve Klein-Fock-Gordon-like equation with Dirichlet boundary conditions [2]. RS calculated with the proposed approach successfully interprets the experimental data on nanodiamond powder RS from [3].

### References

1. V. Koniakhin, *et al.*, J. Phys. Chem. C (2018) **122**, 19219.
2. I. Utesov, *et al.*, J. Phys. Chem. C (2018) **122**, 27738.
3. Stehlik, *et al.*, J. Phys. Chem. C (2015) **119**, 27708.

## The effect of the detonation nanodiamond modification on its functional properties

Grechikhina A. M.<sup>1,2</sup>, Abaturov M. A.<sup>1</sup>, Alexenko A. E.<sup>1</sup>, Galushko T. B.<sup>1</sup>, Gorbunov A. M.<sup>1</sup>, Kiselev M.R.<sup>1</sup>, Melnik N.N.<sup>3</sup>, Polushin N. I.<sup>2</sup>, Spitsyn B.V.<sup>1</sup>

*bvspitsyn@gmail.com*

<sup>1</sup> A.N. Frumkin Institute of Physical Chemistry and Electrochemistry, Russian Academy of Sciences, Moscow, Russia

<sup>2</sup> National University of Science and Technology "MISIS", Moscow, Russia

<sup>3</sup> P.N.Lebedev Physical Institute, Russian Academy of Sciences, Moscow, Russia

Detonation nanodiamond (DND) is special nanomaterial because it largely retains the unique mechanical, physical and chemical properties of diamond and, unlike almost all other nano-dispersed materials, there are no foreign phases on its surface, and only a wide range of surface chemicals compounds. In this regard, the surface of an individual nanodiamond crystal can be considered as a subject of a peculiar surface organic chemistry, however, the initial polyfunctionality of individual nanodiamond surface can be changed by carrying out heterogeneous chemical reactions leading either to the removal of surface functional groups or the addition of new ones. Such processes can be considered as a kind of horizontal strategy for modifying nanodispersed diamond [1], in contrast to well-known vertical strategies (bottom-up and top-down). As is known, the duration of the synthesis of DND occurring at the front of the detonation wave is less than 1  $\mu$ s and it requires a considerable lengthy subsequent "upbringing" by chemical and physicochemical methods. Due to fairly strong surface chemical bonds, the DND modification process is usually carried out in chemically active media and / or at elevated temperatures. Oxidative treatment provided by boiling in 72 % HClO<sub>4</sub> at 203 °C for 5 hours. The treatment by hydrogen and deuterium of the surface are provided at atmospheric pressure at 850 °C for 5 hours. The surface chlorination proceeds 6 hours at 450 °C in CCl<sub>4</sub> vapors. According to TGA, the DND modification usually change the polyfunctionality of the surface and stability against oxidation. Moreover the differences of the DND with provided termination in hydrophilicity, IR spectra, photoluminescence and electrophysical properties was measured and discussed.

### References

1. Spitsyn B.V., Davidson J.L., Gradoboev M.N., Galushko T.B., Serebryakova N.V., Karpukhina T.A., Kulakova I.I., Melnik N.N., *Diamond Relat. Mater.*, 2006, Volume 15, 296.

## Green N-V-N luminescence of diamond obtained by sintering of polycrystalline nanodiamonds at high pressure

*Shakhov F.M.*<sup>1</sup>, *Osipov V.Yu.*<sup>1</sup>, *Bogdanov K.V.*<sup>2</sup>, *Jentgens C.*<sup>3</sup>

*fedor.shakhov@mail.ioffe.ru*

<sup>1</sup> Ioffe Institute, Saint-Petersburg, Russia

<sup>2</sup> ITMO University, Saint-Petersburg, Russia

<sup>3</sup> Microdiamant AG, Lengwil, Switzerland

Polycrystalline diamond powder of the dynamic synthesis from graphite with an average size of 25 nm and a crystalline size 7-11 nm [1,2] was treated at 7 GPa and 1300 °C in the presence of 30 wt% C-O-H compound [3].

The synthesized sample was characterized by X-band Electron Paramagnetic Resonance (EPR) and Photoluminescence/Raman (PL) spectroscopy. It is shown that the average size of diamond crystallites after sintering is not less than 70 nm. Powder EPR pattern shows the presence of paramagnetic substitutional nitrogen (P1 centres) at a concentration of less than 200 ppm in a diamond lattice of good crystalline quality. PL spectrum of synthesized diamond is shown in Fig.1 and demonstrates that the main optical centre is nitrogen-vacancy-nitrogen, known as H3.

The formation of large diamond grains from a very tight diamond polycrystalline grains confirms the partial or complete dissolution of the main number of initial diamond crystallites in a C-O-H superfluid, which forms at sintering conditions. Such a dissolution followed by the crystallization of large diamonds from polycrystalline diamonds contradicts to the hypothesis of oriented attachment growth, proposed in [4] for detonation diamonds.

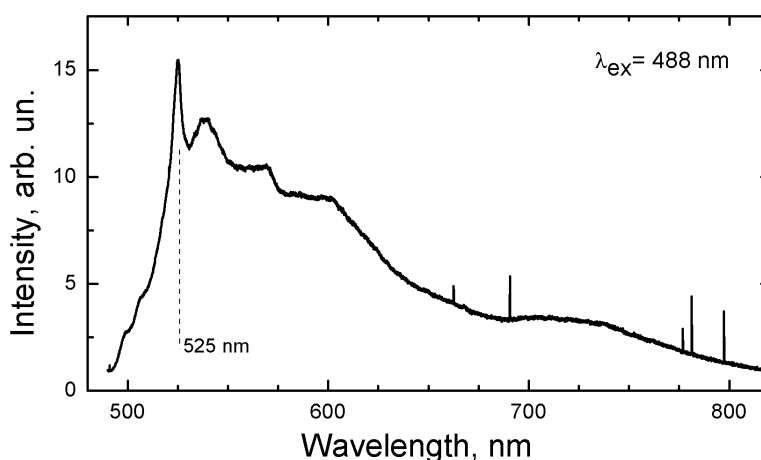


Fig.1. PL of H3-defect in the synthesized diamond

### References

- V. Bogdanov, V.Yu. Osipov, M.V. Zhukovskaya, C. Jentgens, F. Treussart, T. Hayashi, K. Takai, A.V. Fedorov, and A.V. Baranov. *RSC Adv.*, (2016) **6**, 51783-51790.
- I. Shames, D. Mogilyansky, A.M. Panich, N.A. Sergeev, M. Olszewski, J-P. Boudou, and V.Yu. Osipov. *Phys. Status Solidi A.* (2015) **212**, 2400-2409.
- M. Shakhov, A.M. Abyzov, and K. Takai. *J. Solid State Chem.* (2017) **256**, 72-92.
- T. Dideikin, E.D. Eidelman, S.V. Kidalov, D.A. Kirilenko, A.P. Meilakhs, F.M. Shakhov, A.V. Shvidchenko, V.V. Sokolov, R.A. Babunz, and A.Ya. Vul. *Diamond Relat. Mater.* (2017) **75**, 85-90.

## Advanced oxidation process for detonation nanodiamond purification and surface modification

*Shestakov M.S.*<sup>1</sup>, *Besedina N.A.*<sup>2</sup>, *Vul' S.P.*<sup>1</sup>, *Dideikin A.T.*<sup>1</sup>, *Larionova T.V.*<sup>3</sup>, *Shvidchenko A.V.*<sup>1</sup>, *Yudina E.B.*<sup>1</sup>, *Shnitov V.V.*<sup>1</sup>

*mikhail.shestakov@gmail.com*

<sup>1</sup> Ioffe Institute, St.Petersburg, Russia

<sup>2</sup> St Petersburg Academic University, St.Petersburg, Russia

<sup>3</sup> SPbPU, Saint-Petersburg, Russia

An advanced oxidation process has been implemented for detonation nanodiamond purification and surface chemical modification. The treatment intended for chemical oxidation of detonation nanodiamond surface and nondiamond carbon through reactions with hydroxyl radicals ( $\cdot\text{OH}$ ).

A number of detonation nanodiamond samples were processed: detonation carbon, purified industrial grade nanodiamond powder<sup>[1]</sup> and free particle hydrosols of air oxidized<sup>[2]</sup> and hydrogen annealed<sup>[3]</sup> detonation nanodiamonds.

Elemental analysis provided by EDAX. Average size of primary nanodiamonds calculated by XRD data. Carbon sp<sup>2</sup>/sp<sup>3</sup> ratio estimated by Raman. Comparative analysis of surface chemical composition provided by results of XPS and FTIR. Size distribution of detonation nanodiamond hydrosols measured by DLS.

A method for obtaining uniform surface with oxygen-containing functional groups in spite of source of detonation nanodiamond was demonstrated. Limited efficiency approach for purification of detonation soot was developed. Advanced oxidation processing is noted as more convenient for certain tasks than conventional gas-phase methods for surface modification.

*The research was supported by RFBR (Project N 18-29-19125 MK)*



Visit my project page at ResearchGate!

### References

1. V Pichot, M Comet, E Fousson, C Baras, A Senger, F Le Normand, D Spitzer, DRM (2008) **17**, 13.
2. E. Aleksenskiy, E. D. Eydelman, and A. Ya. Vul', NNL (2011) **3**, 68
3. E. Aleksenskii, A. Ya. Vul', S. V. Konyakhin, K. V. Reich, L. V. Sharonova, E. D. Eidel'man, Phys. Solid State (2012) **54**, 578

## Gamma-radiation effect on the photoluminescence of the polymer composite MEH-PPV / detonation nanodiamond

Romanov N.M.<sup>1,2</sup>, Shakhov F.M.<sup>3</sup>, Osipov V.Yu.<sup>3</sup>, Musikhin S.F.<sup>1</sup>

Fedor.Shakhov@mail.ioffe.ru

<sup>1</sup> Peter the Great Polytechnic University, St. Petersburg, Russia

<sup>2</sup> Lappeenranta University of Technology, Lappeenranta, Finland

<sup>3</sup> Ioffe Institute, St. Petersburg, Russia

MEH-PPV is an electrically conductive light-emitting conjugated polymer with a linear formula  $(C_{18}H_{28}O_2)_n$  soluble in toluene, which is widely used as a part of organic light-emitting diodes, perovskite solar cells, organic field-effect transistor (Fig.A.). With the introduction of various nanoscale inclusions into the polymer, such as fullerenes [1], PbS [2] or detonation nanodiamonds charge transfer occurs from the conducting polymer to the dielectric inclusions (bulk heterojunction), which ensures the generation of free charge carriers and their transfer.

The photoluminescence (PL) method was used to investigate MEH-PPV polymer films and films of MEH-PPV/detonation nanodiamond (DND) nanocomposite after irradiation by gamma rays from a <sup>137</sup>Cs source at doses of 0.5–12.2 kGy in the H<sub>2</sub>O equivalent to Fig.A.

Relaxation processes occur during 4 weeks after irradiation in pure MEH-PPV polymer and in nanocomposite MEH-PPV/DND after irradiation with a dose of 12.2 kGy were investigated, Fig.B. It is shown that gamma-irradiation of nanocomposites leads to the formation of structural units similar in structure and composition with structural units of the conductive PPV polymer  $(C_8H_6)_n$ .

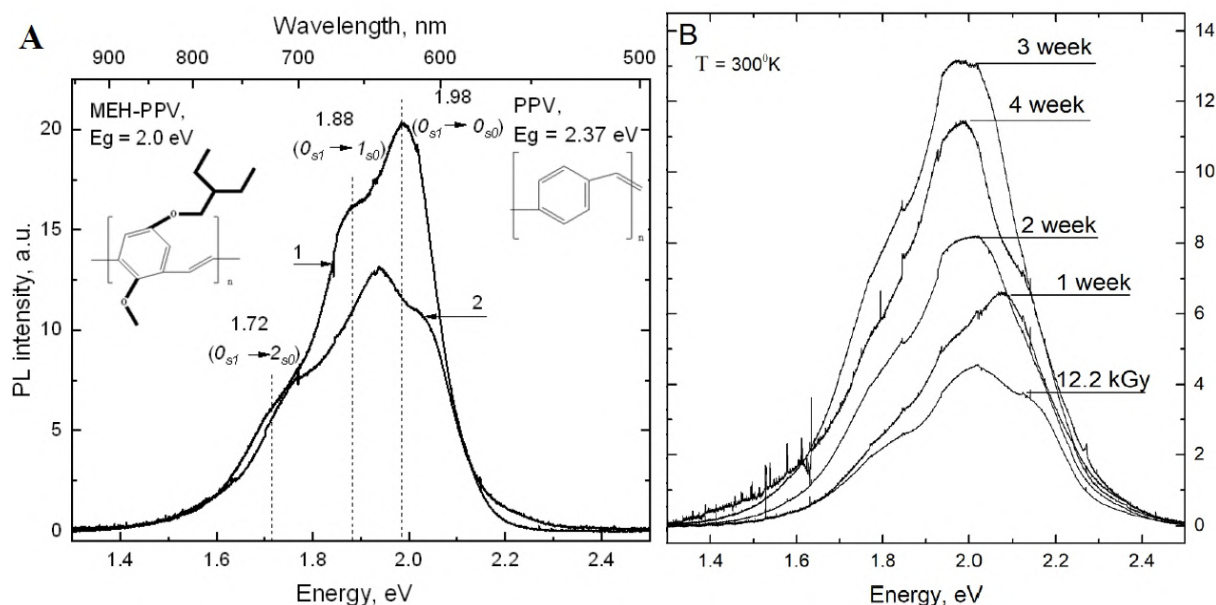


Fig.A. PL spectra before gamma-irradiation: 1 - MEH-PPV; 2 - MEH-PPV/DND. Structural formula of MEH-PPV and PPV polymers. Aliphatic groups are in bold. Fig.B. PL spectra of MEH-PPV/DND composite after gamma-irradiation with 12.2 kGy and after 1-4 weeks of holding at NTP.

### References

1. M. Romanov and S.F. Musikhin. St. Petersburg State Polytechnical University Journal: Physics and Mathematics. (2018) **11**, 41-48.
2. M. Romanov, I.B. Zakharova, M.M. Malova, M.A. Elistratova, S.F. Musikhin. St. Petersburg State Polytechnical University Journal: Physics and Mathematics. (2018) **11**, 22-32.

## Diamond crystals synthesized from graphite with a nickel catalyst and aluminum as a nitrogen getter at HPHT

*Kochetkov F.M.*<sup>1</sup>, *Krasilin A.A.*<sup>1</sup>, *Osipov V.Yu.*<sup>1</sup>, *Shakhov F.M.*<sup>1</sup>

*fedor.shakhov@mail.ioffe.ru*

<sup>1</sup> Ioffe Institute, Saint-Petersburg, Russia

It is known that nitrogen occupies a special place in the research of diamond materials, since it is the main impurity in diamond. Moreover, the form in which nitrogen is contained in diamonds largely determines their properties and serves as the main factor for the classification of diamonds. Nitrogen creates paramagnetic centers in diamond and exists in the form of single nitrogen atoms (P1), as well as in other types of optically detectable centers.

In this work, two samples of microcrystalline diamonds (40-125  $\mu\text{m}$ ) were investigated by the EPR and IR methods for the presence of nitrogen centers, one of which was synthesized in graphite - nickel medium (reference sample D1), and the second (D2) in the same mixture with the addition of aluminum, which serves as a getter of nitrogen, at high pressure (5 GPa) and temperature (1550  $^{\circ}\text{C}$ ).

With the addition of nitrogen getter, a decrease in the amount of nitrogen in the diamond is observed, the crystallinity become more perfect and crystals have fewer centers of P1, C, A and B1 defects.

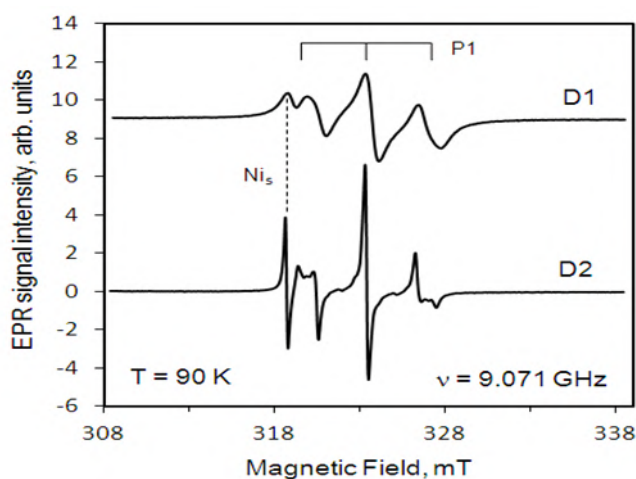


Fig.1. The EPR spectrum of paramagnetic nitrogen centers (P1) in diamonds synthesized without addition of a nitrogen getter (D1) and with its presence (D2).



**Poster session 2:  
Carbon Nanostructures.  
School for Young Scientists.**

## Natural gas partial oxidation process as a way to synthesize graphitized carbon soot

*Lugvishchuk D.S.*<sup>1</sup>, *Mitberg E.B.*<sup>1,2</sup>, *Mordkovich V.Z.*<sup>1,2</sup>

*lugvishchuk.d@tisnum.ru*

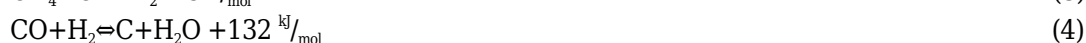
<sup>1</sup> Technological Institute for Superhard and Novel Carbon Materials, Troitsk, Moscow 108840, Russia

<sup>2</sup> INFRA Technology Ltd., Moscow 125009, Russia

Partial oxidation process (POX) is one of the main technologies for natural gas processing:



Although the main product of POX is synthesis gas (a mixture of CO and H<sub>2</sub>), carbon black as a significant by-product (depending on the process conditions) may be formed by the following reactions:



State of the art pilot unit presented in the work [1] makes it possible to produce up to 5 nm<sup>3</sup>/h of syngas and about 50 g/h of graphitized carbon soot as a byproduct, water is also formed in our process. Modernization of the pilot unit allowed us to separate the soot synthesized in the partial oxidation reactor from syngas via scrubber and further collect it in the soot tank. The soot then was dried at room temperature. Obtained carbon soot particles have almost perfect graphitic structure, as TEM analysis indicated, formed at relatively low temperatures (~1070 K) and a fullerene-like cage inside imply that the growth had to be driven by an epitaxial mechanism of a kind which is in good correlation with the work [2]. The time of the transition from a higher temperature zone (1500-1600 K) to the reactor outlet determines the growth duration and hence the spherical particle size. Our process may be considered as a prototype for a production method for graphitized carbon soot. Driven by the need to reduce harmful emissions in the environment, our process allows to utilize and process natural and associated gas to produce syngas with H<sub>2</sub>/CO ratio 1.6-1.8 and valuable graphitized soot as a byproduct.

### References

1. D.S. Lugvishchuk, P.I. Kulchakovsky, E.B. Mitberg, V.Z. Mordkovich, Soot formation in the methane partial oxidation process under conditions of partial saturation with water vapor, *Pet. Chem.* 58 (5) (2018) 427-433.
2. K. Hayashida, S. Nagaoka, H. Ishitani, Growth and oxidation of graphitic crystallites in soot particles within a laminar diffusion flame, / *Fuel* 128 (2014) 148-154

## Structure, properties, and carbon component evolution in nanocomposite TiN-C coating

Dvorak A.<sup>1</sup>, Razanau I.<sup>1,2</sup>, Kazachenko V.<sup>1</sup>

*kvp\_@mail.ru*

<sup>1</sup> State Enterprise "Science and Technology Park of BNTU "Polytechnic", Minsk, Belarus

<sup>2</sup> SSPA "Scientific-Practical Materials Research Centre of NAS of Belarus", Minsk, Belarus

The present report is dedicated to the study of structure, peculiarities of surface layers, structural transformations under laser irradiation as well as mechanical and tribological properties of thin nanocomposite TiN-C coating deposited from the products of a pulsed titanium cathodic arc discharge with carbon ignition in nitrogen atmosphere.

Nanocomposite TiN-C coating was deposited using a modified Maslov-type plasma source. The cathode of the plasma source was made of titanium whereas the ignition system was made of graphite. Thus, each high-current pulse of the cathodic arc between the copper-coated anode and the titanium cathode was ignited in the products of the low-current pulse of the discharge in the graphite ignition system. And hence, each titanium sputtering pulse was accompanied with a lower-intensity graphite sputtering pulse.

Morphology of the coating was studied using scanning electron microscopy (SEM) and atomic-force microscopy (AFM). Chemical composition of the coating was investigated using energy-dispersive X-ray spectroscopy (EDS) and X-ray photoelectron spectroscopy (XPS). Structure of the coating was studied using X-ray diffraction (XRD) and Raman spectroscopy. Mechanical properties of the coating were measured by nanoindentation. Tribological properties were studied using the sphere-on-plane reciprocating dry friction scheme.

Composite TiN-C coating on a silicon monocrystal substrate is characterized by a smooth surface of sub-micron waviness without distinct columnar structure. It is shown that although the content of carbon in the coating lies within an approximate range of 5-15 atomic %, neither XRD reflection peaks of graphite or diamond nor Raman bands characteristic of C-C bond vibrations can be found in the corresponding spectra of the coating in its pristine state.

At the same time, the TiN [111] XRD reflection is shifted by 0.4° to lower angles and the C 1s core level spectrum peak at 282 eV is slightly shifted to higher energy in comparison with the position of the C 1s peak of C-Ti bond in titanium carbide, indicating the increase of the interplanar distance of the titanium nitride structure owing to interstitial carbon atoms implantation.

The Raman spectra of the coating change drastically upon the increase of the excitation laser irradiation power: characteristic C-C bond vibration D and G-peaks appear in the spectra, moreover the peaks remain in the spectra measured under low-power conditions in the previously high-power irradiated spots. The analysis of the peculiarities of Raman spectra measured under various conditions shows that upon heating up by a high-power laser irradiation, carbon of the coating undergoes structural evolution through the formation of nano-size amorphous carbon clusters.

Described structural evolution of the carbon component of the coating leads to adaptive tribological behavior of the coating under heavy friction conditions: upon heating up during friction, the coefficient of friction of the coating against steel counterbody demonstrates distinct working-in peak with following stabilization at lower levels.

## Characterization of graphitized carbon formed as a byproduct of partial oxidation of natural gas

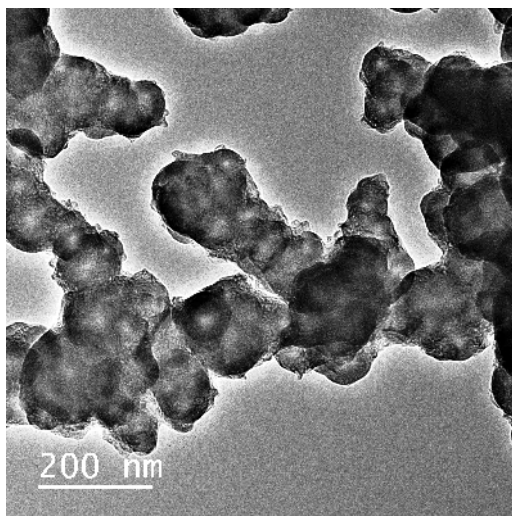
Lugvishchuk D.S.<sup>1</sup>, Mitberg E.B.<sup>1,2</sup>, Karaeva A.R.<sup>1</sup>, Kirichenko A.N.<sup>1</sup>, Kulnitskiy B.A.<sup>1</sup>, Mordkovich V.Z.<sup>1,2</sup>

mitbergeb@tisnum.ru

<sup>1</sup> Technological Institute for Superhard and Novel Carbon Materials, Troitsk, Moscow 108840, Russia

<sup>2</sup> INFRA Technology Ltd., Moscow 125009, Russia

Graphitized carbon nanoparticles of spherical morphology and regular onion-like structure were produced as a byproduct of thermal homogeneous partial oxidation of natural gas in the Pilot Unit presented in the work [1]. The concentric graphitic structure and spherical symmetry along with the absence of amorphous carbon were confirmed by transmission electron microscopy (TEM), electron diffraction, EDX spectroscopy, and Raman investigation. The particles are unusually big for carbon onions and have an outer diameter of 10–50 nm while the inner cage is rather typical for onions and has a diameter below 1 nm. It is worth notice that unlike literature reports on giant onions, the carbon deposit was dominated by these giant spheres. In addition, our process allows producing regular giant onion-like particles from oxygen-containing feedstock despite claims by the work [2]. It is interesting that unlike observations of works [3, 4] there are no low fullerenes or small onions in the deposit. Raman spectra show the ratio of the intensities of D and G peaks that can be used to estimate the degree of perfection of graphitic layers. In our work we achieved  $I_D/I_G = 0.981$ , which is in good correlation with regular onion like carbon properties.



### References

- [1] D.S. Lugvishchuk, P.I. Kulchakovskiy, E.B. Mitberg, V.Z. Mordkovich, Soot formation in the methane partial oxidation process under conditions of partial saturation with water vapor, *Pet. Chem.* 58 (5) (2018) 427–433.
- [2] L. Jiang, Z. Wang, D. Geng, Y. Lin, Y. Wang, J. An, J. He, D. Li, W. Liu, Z. Zhang, Structure and electromagnetic properties of both regular and defective onion-like carbon nanoparticles, *Carbon* (2015).
- [3] V.Z. Mordkovich, The observation of large concentric shell fullerenes and fullerene-like nanoparticles in laser pyrolysis carbon blacks, *Chem. Mater.* 12 (9) (2000) 2813–2818.
- [4] V.Z. Mordkovich, A.G. Umnov, T. Inoshita, Nanostructure of laser pyrolysis carbon blacks: observation of multiwall fullerenes, *Int. J. Inorg. Mater.* 2 (4) (2000) 347–353.

## On the N<sub>2</sub> and NH<sub>3</sub> adsorption on silicon carbide

Davydov S.Yu.<sup>1</sup>, Posrednik O.V.<sup>2</sup>

posrednik1009@gmail.com

<sup>1</sup> Ioffe Institute, Russian Academy of Sciences, St.-Petersburg, Russia

<sup>2</sup> St.-Petersburg Electrotechnical University (LETI), St.-Petersburg, Russia

Silicon carbide is in the focus of research since wide band-gap material with high stability to the temperature, mechanical and radiation actions which permit to use it for devices working at extreme conditions [1]. In the last decade, silicon carbide finds a new area as an object for carbon nanostructures formation [2,3]. Recently, the original method of SiC production from silicon was proposed [4]. Thus, it is of interest to study the adsorption properties of SiC. In this report, we give theoretical estimations for the binding energy of N<sub>2</sub> and NH<sub>3</sub> molecules with the silicon carbide surface. Note, that the problem of N<sub>2</sub> and NH<sub>3</sub> interaction with SiC was firstly arisen from the study of SiO<sub>2</sub>/SiC interface [5].

Here we use a theoretical scheme based on the Anderson Hamiltonian and Haldane-Anderson density of states model [6] for the 4H and 6H silicon carbide polytypes. Estimations for the nitrogen molecule show that the charge transfer between N<sub>2</sub> and SiC can be neglected and the ionic contribution to the adsorption energy  $E_{ads}^{ion} \approx 0$ . Thus, adsorption energy is equal to metallic contribution, which is equal to  $E_{ads}^{met} \sim -3eV$ . Underline, that the difference between adsorption on the Si- and C-faces of SiC manifests itself only through the parameter describing the width of the molecule quasilevels [6]. If consider adsorption bond lengths for Si- and C-faces as equal, such a difference is absent.

As opposed to the system N<sub>2</sub>/SiC, ammonia molecule dissociates on Si(100) [7]. Then hydrogen atoms passivate sp<sup>3</sup>-orbitals of silicon terminated the reaction. It is beyond reason to suppose that this situation does not occur on Si- and C-faces of SiC. Thus, ammonia molecules do not adsorb on silicon carbide.

### References

- [1] A.A. Lebedev. *Semicond. Sci. Technol.*, **21**, R17 (2006).
- [2] Y.H. Woo, T. Yu, Z.X. Chen. *Appl. Phys. Rev.*, **108**, 071301 (2010).
- [3] G.V. Benemanskaya, P.A. Dementiev, S.A. Kukushkin, F.V. Osipov, S.N. Timoshnev. *Pisma v ZhTF*, **45** (5), 17 (2019).
- [4] S.A. Kukushkin, A.V. Osipov, N.A. Feoktistov. *Phys. Solid State*, **56**, 1507 (2014).
- [5] E. Pitthan, A.L. Gobbi, H.I. Boudinov, F.C. Stedile. *J. Electronic Mater.*, **44**, 2823 (2015).
- [6] S.Yu Davydov, A.A. Lebedev, O.V. Posrednik. *Elementary introduction to the theory of nanosystems*. St.-Petersburg, "Lan", 2014. 192 p. [In Russian].
- [7] M.D. Ramsier, J.T. Yates, Jr. *Surf. Sci. Rep.*, **12**, 243 (1991).

## Extended structures of detonation soot of HEs

Satonkina N. P.<sup>1,2</sup>, Ershov A. P.<sup>1,2</sup>, Kashkarov A. O.<sup>1,2</sup>, Rubtsov I. A.<sup>1,2</sup>

snp@hydro.nsc.ru

<sup>1</sup> Lavrentyev Institute of Hydrodynamics SB RAS, Novosibirsk, Russia

<sup>2</sup> Novosibirsk State University, Novosibirsk, Russia

In the case of detonation of condensed explosives of  $C_aH_bN_cO_d$  type, there is a correlation of the electrical conductivity with the carbon content [1,2]. Therewith, the high values of electrical conductivity can be explained by contact conductivity through extended conductive structures.

The development of research technologies does not allow observation this “carbon wires” directly during the detonation yet, but such structures are present in detonation soot. Nano-objects have sufficient strength for their safety in the aggressive background behind the detonation front.

Transmission electron microscope images show (Fig.1) that the detonation soot of carbon-rich explosives contain fibrous structures [3-5], and the distance between the lines is 0.33 nm (on the right image), which corresponds to the conductive form of carbon — graphite. The existence of such carbon structures, in our view, confirms the availability of contact conductivity behind the detonation front.

The work was funded by RFBR according to the research project N 18-03-00227, and partially by RFBR under grant N 18-03-00441.

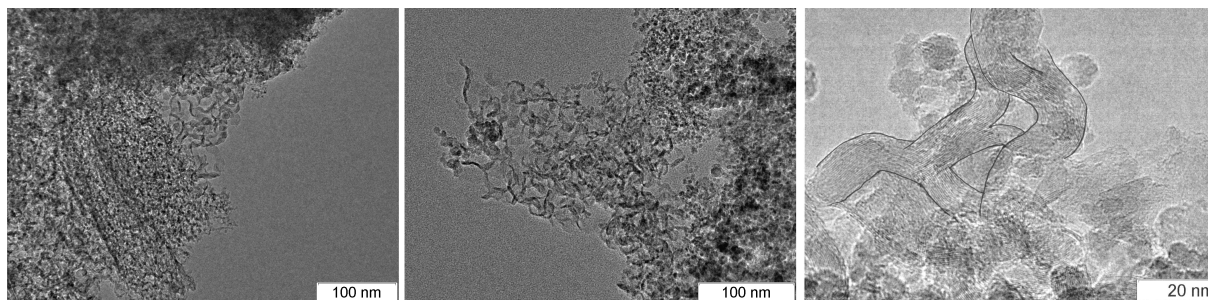


Fig.1. TEM micrographs of detonation soot (TATB, TNT/RDX, TNT from left to right).

### References

1. N. P. Satonkina, The dynamics of carbon nanostructures at detonation of condensed high explosives, *Journal of applied physics* (2015) **118**, p. 245901.
2. N. P. Satonkina, Correlation of Electrical Conductivity in the Detonation of Condensed Explosives with Their Carbon Content, *Combustion, Explosion, and Shock Waves* (2016) **52(4)**, p. 488.
3. N. Roy Greiner, D. S. Phyllips, J. D. Johnson, Fred Volk, Diamonds in detonation soot, *Nature* (1988) **333**, p. 440.
4. Xu Tao, Xu Kang, Zhao Jiazheng, TEM and HREM studies on ultradispersed diamonds containing soot formed by explosive detonation, *Materials Science and Engineering B* (1996) **38**, p. L1.
5. A. O. Kashkarov, E. R. Pruel, K. A. Ten, I. A. Rubtsov, E. Yu. Gerasimov, P. I. Zubkov, Transmission electron microscopy and x-ray diffraction studies of the detonation soot of high explosives, *Journal of Physics: Conference Series* (2016) **774**, p. 012072.

## Nickel nanoparticles - biomorphic carbon composite for energy storage devices

*Orlova T.S.*<sup>1,2</sup>, *Spitsyn A.A.*<sup>3</sup>, *Ponomarev D.A.*<sup>3</sup>, *Kirilenko D.A.*<sup>1</sup>

*orlova.t@mail.ioffe.ru*

<sup>1</sup> Ioffe Institute, St. Petersburg, Russia

<sup>2</sup> National Research University of Information Technologies, Mechanics and Optics, St. Petersburg, Russia

<sup>3</sup> St. Petersburg State Forest Technical University, St. Petersburg, Russia

Energy storage and conversion materials play an essential role in efficient, environmentally friendly use of energy and in the development of renewable sources of energy [1,2].

A facile and low-cost method has been used to fabricate nickel/bioC nanocomposite for applying as binder-free electrodes for supercapacitors. Monolithic partially graphitized porous biocarbons (bioC) with Ni nanoparticles (NiNPs) were obtained through pyrolysis of birch-wood precursors using nickel(II) nitrate as a graphitization catalyst. Oven dried (105–110 °C) birch wood were immersed in 1 M solution of nickel(II) nitrate in water for 120 h. Pyrolysis of the dried impregnated wood was performed in an atmosphere of self-generated gases in a stainless steel reactor with a ramp rate of 2 °C/min up to 970 °C. Then cooling was carried out with the oven. The above high temperature process also resulted in the formation of NiNPs due to the reduction of Ni(NO<sub>3</sub>)<sub>2</sub>. The gravimetric concentration of Ni in the obtained bioC/ NiNPs composite was estimated to be 13.2%. Structural and microstructural characterization was performed by means of x-ray diffraction and transition electron microscopy.

The composite presents highly porous material with pores of about 5 nm in size, which are covered by onion-like carbon. Ni nanoparticles with size of 5-70 nm were uniformly distributed within the three dimensional structure of the carbon matrix (Fig.1a,b). Smaller NiNPs occupied part of the pores surrounded by onion-like carbon (Fig.1c). Along with the onion-like carbon, amorphous carbon, graphite globules with size up to 150 nm are also present. The composite material was used for electrochemical testing as a working electrode in 3M KOH electrolyte. The composite material exhibited enhanced electrochemical behavior, achieving a capacitance of 415 F/g for the total composite material and 3140 F/g for Ni nanoparticles with good cyclic stability. These results demonstrated a high potential of the NiNPs/bioC composites for application as binder-free electrodes for supercapacitors.

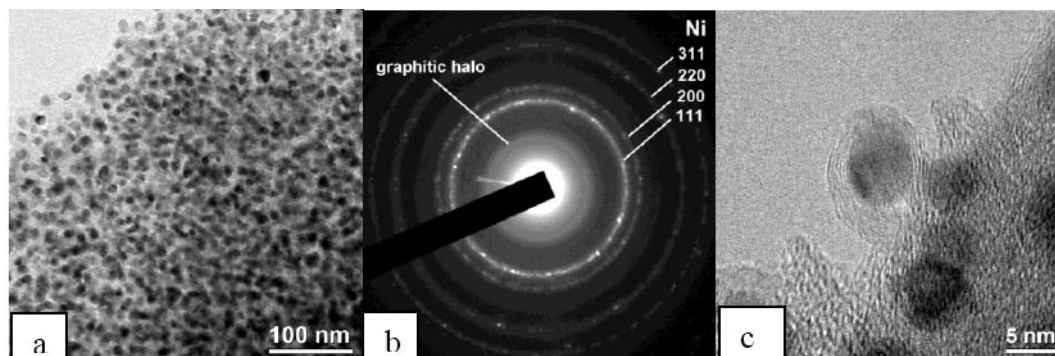


Fig.1. TEM image (a) and corresponding electron diffraction pattern (b) of Ni-nanoparticles supported on porous biocarbon matrix. Ni nanoparticles surrounded by onion-like carbon (c).

### References

1. C. Liu, F. Li, L.-P. Ma, H.-M. Cheng, *Adv. Mater.* (2010) **22**, E28.
2. A. S. Arico, P. Bruce, B. Scrosati, J.-M. Tarascon, W. van Schalkwijk, *Nat. Mater.* (2005) **4**, 366.

## Periodically Ordered Opal Nano-Structures Embedded in Single Crystal Diamond: a route to 2D and 3D photonic crystals

Sovyk D.N.<sup>1,2</sup>, Ralchenko V.G.<sup>1,2,3</sup>, Bolshakov A.P.<sup>1,2</sup>, Dyakov S.A.<sup>4</sup>, Tikhodeev S.G.<sup>1</sup>, Khomich A.A.<sup>1,5</sup>, Kurdyukov D.A.<sup>6</sup>, Shu Guoyang<sup>1,3</sup>, Dai Bing<sup>3</sup>, Zhu Jiaqi<sup>3</sup>

sovyk@inbox.ru

<sup>1</sup> Prokhorov General Physics Institute RAS, Moscow, Russia

<sup>2</sup> National Research Nuclear University MEPhI, Moscow, Russia

<sup>3</sup> Harbin Institute of Technology, Harbin, P.R. China

<sup>4</sup> Skolkovo Institute of Science and Technology, Moscow, Russia

<sup>5</sup> Institute of Radio Engineering and Electronics RAS, Fryazino, Russia

<sup>6</sup> Ioffe Physical Technical Institute Russian RAS, St. Petersburg, Russia

Diamond nanostructures, in view of excellent optical, thermal and mechanical properties, are of increasing interest, for optical applications such as antireflection surfaces, photon emitters based on color centers, and photonic crystals. Porous bulk opal structures (ordered SiO<sub>2</sub> spheres) were used previously [1] as templates to grow photonic crystal based on diamond inverted opal (DIO) by seeding the template with nanodiamond particles, followed by a CVD diamond growth inside the pores. This process, however, principally results in nanocrystalline diamond structures with high amount of defects. Here we describe a new approach to prepare opal-diamond monoliths with *single crystalline* (SC) diamond component.

The process is based on epitaxial diamond growth through nanoscale pores between densely packed SiO<sub>2</sub> nanospheres placed on a SC diamond substrate (Fig.1). Monolayers and multilayers of the ordered silica spheres of ~230 nm in diameter were deposited on HPHT diamond surfaces. Diamond growth then started from the bottom through narrow gaps between the spheres, using a microwave plasma CVD. The opal layers were gradually imbedded in SC diamond, forming an ordered diamond composite. Finally, the SiO<sub>2</sub> spheres were removed by acid etching to obtain the SC diamond inverse opal structures [2]. The approach works for epitaxy on polycrystalline substrates as well. The produced structures were characterized with optical transmission, Raman and photoluminescence spectra. Calculations of the reflection spectra by scattering matrix method were performed which predict the Bragg peak position and intensity as a function of number of buried layers, and indicate that already 8-10 layers are equivalent to bulk DIO.

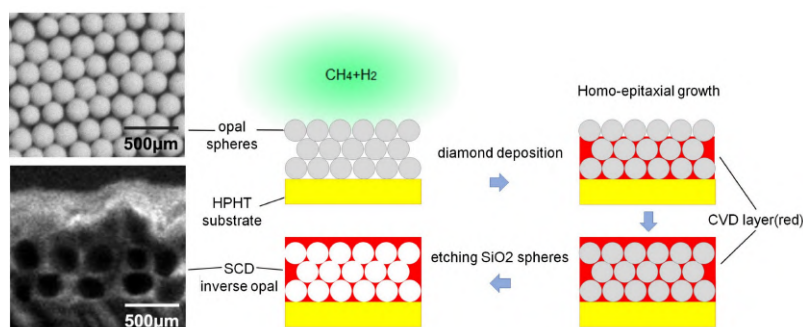


Fig.1. Schematics of preparation of periodical single crystalline diamond inverse opal nanostructure.

### References

1. A. Zakhidov, R.H. Baughman, Z. Iqbal, C. Cui, et al. Science (1998) **282**, 897.
2. B. Dai, G. Shu, V. Ralchenko, A. Bolshakov, et al. Diam. Relat. Mater. (2017) **73**, 204.



## Structural investigation of aluminum-carbon nanocomposite

Torok Gy.<sup>1</sup>, Varga L.K.<sup>1</sup>

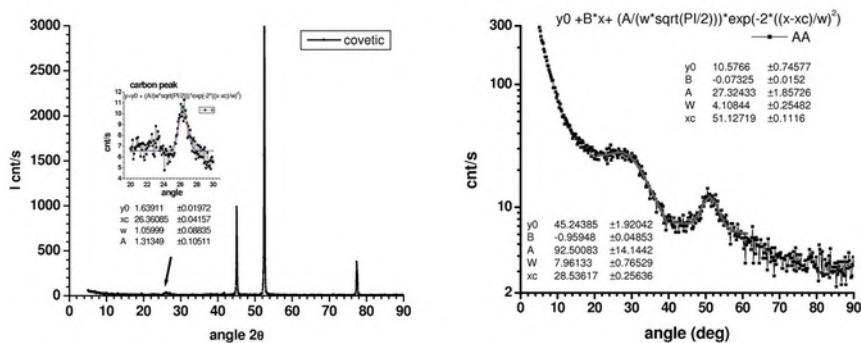
torok.gyula@wigner.mta.hu

<sup>1</sup>Wigner Research Centre for Physics Institute, Budapest, Hungary

Covetic alloys represent a new family of the metal matrix –carbon nanocomposites [1], where the matrix metal solves only ppm amounts of carbon. The carbon nanoparticles are bonded to the metallic matrix by a novel type of a **covalent –metallic** (covetic) bond. Considering the structure of covetic material there were reported globular nanoparticle between 5-200 nm [3] and graphene –like nanoribbons in Al based [2] covetics. In order to understand the nature of this novel type of metal carbon nanocomposite, investigations by X-ray, and Small angle neutron scattering were undertaken.

The base material was industrial 6061 type Al alloy. Two kinds of activated carbon were used: activated carbon (AA) from Alpha Aesar (Johnson Matthey) and (RH) from Reanal, Hungary. In addition ball milled graphite powder was used also having a grain size below 45  $\mu\text{m}$  (340 mesh). Out of these three different carbon powders only the AA type was suitable for infiltration into Al6061.

XRD revealed the presence of the infiltrated, nanosized carbon and its diffraction line was compared with that of the starting activated carbon. The SANS experiment performed at Budapest Neutron Center was data processed using the generalised Beaucage model.[4]. Carbon inclusions of 15 nm average diameter were found having more smooth surface region than the alloying inclusions of the starting Al6061 industrial alloy. The summarized results are presented.



The diffraction pattern of covetic and the starting amorphous carbon pattern (Alpha Aesar)

### References

#### References

1. Bakir M., Jasiuk I. „ Novel metal-carbon nanomaterials: A review on covetics”. *Advanced Materials Letters*. 2017;8(9):884-890
2. M. Iftexhar Jaim, Romaine A. Isaacs, Sergey N. Rashkeev, Maija Kuklja, Daniel P. Cole, Melbourne C. LeMieux, Iwona Jasiuk, Sabrina Nilufar, Lourdes G. Salamanca-Riba „Sp<sup>2</sup> carbon embedded in Al-6061 and Al-7075 alloys in the form of crystalline graphene nanoribbons” *Carbon*, Volume 107, October 2016, Pages 56-66
3. Salamanca-Riba L. A New Type of Carbon Nanostructure Formed Within a Metal-Matrix. *Tech Connect World*. 2012;1:278-281
4. Beaucage, „Approximations Leading to a Unified Exponential/Power-Law Approach to Small-Angle Scattering”, *Appl. C~st.* (1995). 28, 717-728

## Biomodification of natural nanostructured shungite carbon and related electrophysical properties

*Moshnikov I.A.<sup>1</sup>, Kovalevski V.V.<sup>1</sup>, Tovpenec T.Yu.<sup>1</sup>*

*igorm@krc.karelia.ru*

<sup>1</sup>Institute of Geology, Karelian Research Center, RAS, Petrozavodsk, Russia

Shungite rocks are natural composite materials including nanostructured carbon - shungite [1] and mineral components in the form of microcrystals, nanocrystals, as well as layers and clusters intercalating carbon [2]. Shungite rocks can be used in various technologies, in particular as an active filler of composite materials to give them electrical conductivity that is determined by the properties of carbon and its distribution. There are several ways to change the electrophysical properties of carbon based on chemical and thermal treatments that, however, are very costly and energy-intensive. Recently, methods of biological processing of mineral raw materials have been intensively developed. It is characterized by the use of a small amount of technological equipment, high yield of finished raw materials and environmental safety. Bioleaching involves the use of chemolithotrophic microorganisms, the energy source of which is inorganic compounds [3].

Electron microscopy and Raman spectroscopy studies of various shungite rocks subjected to leaching processes under the influence of microorganisms inherent in shungite rocks in laboratory conditions were carried out. Bioleaching leads to the removal of sulfide components of shungite rocks and changes both intralayer and interlayer ordering of shungites. This can be caused by the removal of non-carbon cluster impurities from the intralayer and interlayer space of carbon (the reverse process of graphite intercalation). The assessment of electrical conductivity showed that for all selected samples of shungite rocks there is an increase in electrical conductivity. The maximum increase in electrical conductivity (~20%) was observed for shungite rock with the most noticeable change in the structural ordering of shungite (fig.1). At the same time, different changes in the structural ordering are observed for different shungites. Minimal changes are remarkable for shungite with the least changes in intralayer and interlayer ordering.

Thus, in the course of bioleaching not only sulfide components are removed, but also the structural ordering of shungite carbon and the electrical conductivity of shungite rocks change.

The work is performed in the framework of the PFNI GAN research of IG KarRC RAS and RFBR (17-05-01160).

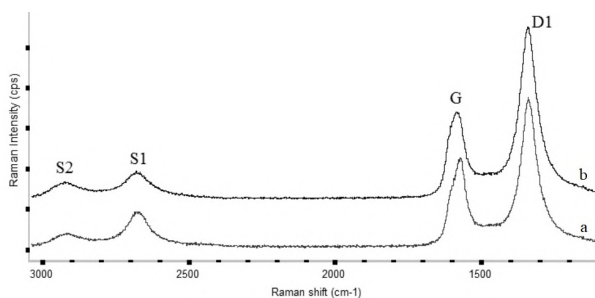


Fig.1 Raman spectra of shungite carbon: a) initial sample, b) processed by microorganisms.

### References

1. Konchits A.A., Shanina B.D., Valakh M.Y., Yanchuk I.B., Yukhymchuk V.O., Yefanov A.V., Krasnovyd S.V., Skoryk M.A. *Functional Materials* (2014) 21(3), p. 260.
2. V.V. Kovalevski, I.A. Moshnikov. *Nanosystems: physics, chemistry, mathematics* (2016)7(1), p. 210.
3. V.M. Gavrish, Yu.O. Shagova. *Power plants and technologies* (2017) 3(4), p. 89.

## Synthesis of metal-decorated micro- and nanoporous carbons via pyrolysis of ZIF- and HKUST-type MOFs.

Oliva Gonzalez Cesar Maximo<sup>1</sup>, Navarro Tellez Ana de Monserrat<sup>1</sup>, Kharisov Boris Ildusovich<sup>1</sup>, Kharissova Oxana Vasilievna<sup>1</sup>, Serrano Quezada Thelma Elizabeth<sup>1</sup>, Pena Mendez Yolanda<sup>1</sup>

bkhariss@hotmail.com

<sup>1</sup> Universidad Autonoma de Nuevo Leon, Monterrey, Mexico

The large number of morphologies, formed by metal-organic frameworks (MOFs), their high porosity and stability make them promising precursors for the synthesis of cost-effective micro- and nanoporous carbon materials. In this work, several MOF-derived carbons [1], decorated with cobalt and nickel nanoparticles, were prepared by pyrolysis of the metal-organic frameworks, based on the ZIF- (“zeolitic imidazolate frameworks”) and HKUST- (“Hong Kong University of Science and Technology”) structural types. The synthesis was carried out at 300, 500 and 800°C in a nitrogen atmosphere, using 1-methylimidazole as binders for the ZIF and trimesic acid (H<sub>3</sub>BTC) for the HKUST type structures. The obtained materials were characterized by X-ray powder diffraction (XRD), Fourier transform infrared spectrometry (FT-IR), X-ray dispersive energy spectroscopy (EDS) and scanning electron microscopy (SEM). The micro- and nanoporous carbons, obtained from these MOFs as precursors, possess significant variations in their morphologies (from spherical particles to fibers and needles) and sizes (from 50 nm to several hundreds nm), forming, in particular, flower-like microstructures covered with elemental metal nanoparticles (Fig. 1). On the other hand, in all prepared MOF-derived carbons, the appearance of metallic nanoparticles on their surface with sizes smaller than 60 nm, is maintained constant. These materials could have potential applications in organic catalysis, adsorption and remediation of heavy metals from contaminated wastewater and petroleum impurities from oil-water mixtures in oil-spill sites.

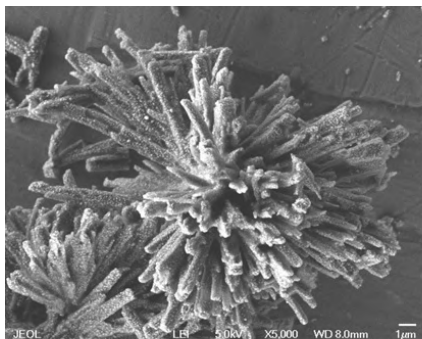


Fig. 1. Ni@C carbon material, containing different needles, converged in a core. The individual needles have an average width starting from 135 nm, while the particles on their surface have an average size of 34 nm.

### References

1. Watcharop Chaikittisilp, Katsuhiko Ariga and Yusuke Yamauchi. J. Mater. Chem. A, 2013, **1**, 14.

## On the kinetic analysis of the hydrogen thermal desorption spectra for graphite and advanced carbon nanomaterials

*Nechaev Yu.S.*<sup>1</sup>, *Alexandrova N.M.*<sup>1</sup>, *Shurygina N.A.*<sup>1</sup>, *Cheretaeva A.O.*<sup>1</sup>, *Pisarev A.A.*<sup>2</sup>

*yuri1939@inbox.ru*

<sup>1</sup> Bardin Central Research Institute for Ferrous Metallurgy, Kurdjumov Institute of Metals Science and Physics, Moscow, Russia

<sup>2</sup> National Research Nuclear University MEPhI (Moscow Engineering Physics Institute), Moscow, Russia

This study is devoted to a further development and applications of results [1-3] on the method of kinetic analysis of the hydrogen thermal desorption spectra (TDS) based (formally) on the first order reactions approach, in materials heated with only one rate. The standard approach of deconvolution of TDS spectra by Gaussian curves was used [1-3]. The method allows to determine values of the activation energy ( $Q$ ) and the pre-exponential factor of the rate constant ( $K$ ) of the processes, along with the identification of them on the basis of results [1-3].

It is worth to note, that usually the kinetic quantities ( $Q$  and  $K$ ) are determined with the help of the Kissinger method, in which several heating rates are used.

In the present study, such an analysis [1-3] has been performed for a number of highly cited data [4-9] on hydrogen TDS spectra for graphite and some advanced carbon nanomaterials.

Some aspects of using the first order reactions approach, especially for the diffusion controlling cases [1-3] are discussed, along with approaches of Polanyi-Wigner equation of the first order process [1-3], the second order process [6, 7], and Gaussian curves approach [10].

Perspectives of further applications of this method [1-3] are considered, as well.

### Acknowledgements

*This work was financially supported by the RFBR (Project # 18-29-19149 mk).*

### References

1. S. Nechaev. Physics – Uspekhi (2006) **49**, 563; Uspekhi Fizicheskikh Nauk (2006) **176**, 581 (www.ufn.ru).
2. S. Nechaev and T.N. Veziroglu. International Journal of Physical Sciences (2015) **10**, 54. <https://doi.org/10.5897/IJPS2014.4212>.
3. S. Nechaev, V.P. Filippova, A. Yurum, Yu. Yurum, T.N. Veziroglu. Journal of Chemical Engineering and Chemical Research (2015) **2**, 421.
4. Rusinov, N. Trifonov, Yu. Gasparyan, B. Khripunov, M. Mayer, J. Roth, A. Pisarev. Journal of Nuclear Materials (2011) **417**, 616.
5. Pisarev, Yu. Gasparyan, A. Rusinov, N. Trifonov, V. Kurnaev, A. Spitsyn, B. Khripunov, T. Schwarz-Selinger, M. Rasinski, K. Sugiyama. J. Nucl. Mater. (2011) **415**, 5785.
6. Hornekaer, Ž. Šljivančanin, W. Xu, R. Otero, E. Rauls, I. Stensgaard, E. Lægsgaard, B. Hammer, F. Besenbacher. Phys. Rev. Lett. (2006) **96**, article # 156104.
7. Zhao, R. A. Outlaw, J. J. Wang, M. Y. Zhu, G. D. Smith, B. C. Holloway. J. Chem. Phys. (2006) **124**, 194704-1.
8. C. Elias, R.R. Nair, T.M. G. Mohiuddin, S.V. Morozov, P. Blake, M.P. Halsall, A.C. Ferrari, D.W. Boukhvalov, M.I. Katsnelson, A.K. Geim, K.S. Novoselov. Science (2009) **323** (5914), 610.
9. Rajasekaran, F. Abild-Pedersen, H. Ogasawara, A. Nilsson, S. Kaya. Phys. Rev. Lett. (2013) **111**, article # 085503
10. Legrand, A. Oudriss, C. Savall, J. Bouhattate, X. Feaugas. Int. J. Hydrogen Energy (2015) **40**, 2871

## Effect of structure and oxidation state of carbon nanomaterials on the conversion of propanol-2

Tveritina E.A.<sup>1</sup>, Zhitnev Yu.N.<sup>1</sup>, Kulakova I.I.<sup>1</sup>, Savilov S.V.<sup>1</sup>, Lunin V.V.<sup>1</sup>

nna-kulakova@yandex.ru

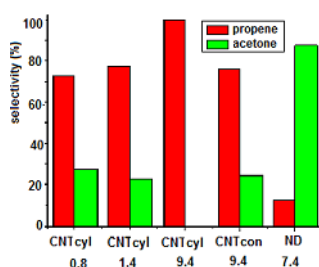
<sup>1</sup> Chemistry Department, Lomonosov Moscow State University, Moscow, Russia

It is known that catalytic dehydration of aliphatic alcohols is carried out on acid Lewis, and dehydrogenation – on basic Lewis centers. It is the catalytic conversion of alcohols that is usually used as a test reaction to the content of acidic and basic Lewis catalyst centers. Oxygen atoms in the composition of carbon nanomaterials (CNM) surface are mainly included in the carbonyl, carboxyl, anhydride, ethereal functional groups, which in catalysis play the role of Lewis acid and basic centers. The aim of this study was to identify the effect of oxidative treatment and the structure of carbon matrix on the formation of acid-base properties of CNM.

We used the following carbon nanomaterials: carbon nanotubes (CNT): cylindrical (CNTcyl) different degrees of oxidation and conical (CNTcon), nanodiamonds of detonation synthesis (ND). The study of the influence of the structure and degree of oxidation of CNM on their catalytic activity was performed by pulsed microcatalytic method. The formation of oxygen-containing surface functional groups occurred during the treatment of CNM with nitric acid for different times (table.) The test reaction was the conversion of propanol-2. The figure shows the obtained data on the selectivity of conversion depending on the nature of the carbon matrix and the oxygen content in the samples of UNM.

It was found that the catalytic activity of CNM (Fig.) is affected by their matrix structure and the content of oxygen surface groups. The conversion of propanol-2 on the way of dehydration goes on ND, whereas the dehydration goes mainly on CNTs. Comparison of the catalytic activity of CNM with approximately the same oxygen content, but with different carbon structure, showed that the activity of cylindrical CNTs (9.35% O<sub>2</sub>) exceeds the activity of conical CNTs (9.4% O<sub>2</sub>) and is significantly higher than the activity of ND (7.40% O<sub>2</sub>). The specific surfaces of cylindrical and conical CNTs are of the same order and equal to 249 and 204 m<sup>2</sup>/g, respectively. This fact indicates that, unlike ND, not only the surface functional groups of CNTs participate in the catalytic process, but also the sp<sup>2</sup>-carbon structure itself in the form of defects due to its curvature.

**Acknowledgement.** The work was done on the subject of chemical faculty “Petrochemistry and catalysis” and was supported by RFBR (grant 16-08-01156). The equipment was acquired from the funds of the Moscow State University Development Program.



Conversion of propanol-2 on samples of CNM (oxygen content, % by weight. indicated on x-axis)

## A X- and W-band EPR study of carbon related dangling bonds in SiCN and SiCN/Fe ceramics

Andronenko S.I.<sup>1</sup>, Misra S.K.<sup>2</sup>

sergey.andronenko@gmail.com

<sup>1</sup> Institute of Physics, Kazan Federal University, Kazan, Russian Federation, 420008

<sup>2</sup> Department of Physics, Concordia University, Montreal, Qc, H3G 1M8, Canada

SiCN is a new class of materials for high-temperature electronics. Magnetic properties of SiCN materials doped with different transition metal ions can vary from paramagnetic to superparamagnetic and to ferromagnetic [1]. Superparamagnetic materials are potentially useful in developing high-temperature sensor devices [2]. Consequently, investigation of SiCN ceramics and its conductive and magnetic derivatives is currently of great interest. The SiCN ceramics consists of SiCN nanoparticles ( $\text{Si}_3\text{N}_4$ -like structure), which are covered with graphene layers [1,2]. Further,  $sp^2$  and  $sp^3$ -carbon related dangling bonds, which are usually formed in this graphene layers [3,4], could be investigated by EPR, a powerful technique to detect various types of paramagnetic defects. The X-band narrow EPR line near  $g = 2.00$  is due to two carbon related dangling bonds [3]. It is structureless at X-band, but at W-band these signals become resolved. The EPR study of SiCN ceramics, annealed at  $1100^\circ\text{C}$  was carried out at 300 K at W-band (93.96 GHz). The two observed W-band EPR lines are due to carbon-related  $sp^2$  and  $sp^3$ -dangling bonds. The EPR line with  $g = 2.0033$  is associated with  $sp^3$ -carbon related dangling bonds in amorphous carbon and the EPR line with  $g = 2.0011$  is associated with  $sp^2$ -carbon related dangling bonds, which are located in broken aromatic rings of graphene layers, similar to that, observed in treated diamond [5]. Relative intensities of these two EPR lines depends on annealing temperature.

This research was supported by the Natural Sciences and Engineering Research Council of Canada (NSERC) (SKM); SIA is grateful for partial support of research project, allocated to Kazan Federal University for the state assignment (#3.2166.2017/4.6).

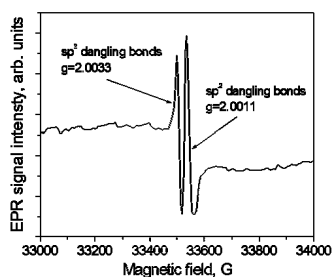


Figure 1. W-band EPR spectrum of SiCN/Fe ceramics in the range 33,000 – 34,000 G.

### References

1. S. K. Misra, S. Andronenko, I. Gilmutdinov, R. Yusupov, Appl. Magn. Reson. (2018) **49**,1397.
2. A. Leo, S. Andronenko, I. Stiharu, R. B. Bhat, Sensors (2010) **10**, 1338.
3. S.I. Andronenko, I. Stiharu, S.K Misra, J. Appl. Phys. (2006) **99**, 113907.
4. S.I. Andronenko, A.A. Rodionov, S.K. Misra, Appl. Magn. Reson. (2018) **49**,335.
5. O.E. Andersson, B.L.V. Prasad, H. Sato, T. Enoki, Y. Hishiyama, Y. Kabaragi, M. Yoshikawa, S. Bandow, Phys. Rev. B (1998) **58**, 16387.

## Spectroscopy and TEM of Fe-carbon nanoclusters synthesized in electric arc

*Kozlov V.S.*<sup>1</sup>, *Lebedev V.T.*<sup>1</sup>, *Balabas O.A.*<sup>2</sup>, *Semenov V.G.*<sup>2</sup>, *Ubeyvovk E.V.*<sup>2</sup>

*kozlov\_vs1@pnpi.nrcki.ru*

<sup>1</sup> B.P.Konstantinov Petersburg Nuclear Physics Institute, NRC, Kurchatov Institute, Gatchina, Leningrad distr., Russia

<sup>2</sup> St.Petersburg State University, St. Petersburg, Russia

Design of carbon endohedrals captured metal atoms (lanthanides, magnetic 3d elements) are in frontiers of fundamental and applied sciences [1]. While, endometallofullerenes  $M@C_{2n}$  (EMF) are poorly synthesized in practice in the amounts which are often not enough even for laboratory experiments. Along with molecular forms, a search of methods to create desirable metal-carbon clusters (like multiwall endofullerenes) should enables to overcome the restrictions in the production of core-shell particles encapsulating metal atoms (groups) which save their properties (magnetic, optical, luminescence etc.) for various applications in biomedicine, chemical technologies, material sciences. Carbon based magnetic materials are promising as effective contrasting agents in Magneto-Resonance Imaging and Hyperthermia methods in medicine. A special interest is attracted to atomic clusters of 3d metals in carbon shells. Saving pristine physicochemical nature, captured atom or metal cluster acquires a complex of new properties conditioned by the core-shell structure (biocompatibility, stability and protection from environmental influences, chemical attacks). As a result of arc combustion of composite electrodes, the encapsulation of metal atoms can occur in a multilayer graphite shell (onions) or carbon nanotubes and eventually molecular structures (EMF). The EMF with 3d metals extremely poorly studied because their producing in macro quantities remains still problematic. It seems important to search the effective ways of synthesis of a variety of different endohedral metal-carbon structures. Here we presented the results devoted to chromatographic analysis, mass spectroscopy, Mössbauer spectroscopy and transmission electron microscopy (TEM) of various forms of Fe-encapsulating carbon nanoclusters produced in electric arc and examined to identify their phases and magnetic states. Samples of soot were prepared by the evaporation of carbon rods with embedded precursors ( $Fe_2O_3$ , iron phthalocyanine pyrolysate). We performed a conventional extraction of metal-carbon products (Sokslet process, ultrasound action) to obtain their condensate in organic solvents of different polarity (o-xylene, aniline, dimethylformamide). According to chromatographic analysis and mass spectroscopy the samples contain fullerenes  $C_{60}$ ,  $C_{70}$ , higher fullerenes  $C_{2n}$  ( $n = 36-70$ ), onion-like structures with Fe and metal Fe clusters incorporated in matrix of non graphitized carbon composed of fullerene-like fragments [1]. We found the average size of various clusters in the range 5-13 nm. The Mössbauer spectra of the samples were measured at 298K with and without an external magnetic field and at 77K. The results showed complex phase composition in different proportions:  $\gamma$ -Fe,  $FeC_2$ ,  $Fe_3C$  and  $\alpha$ -Fe in superparamagnetic state [2].

The work was supported by Russian Foundation for Basic Researches (grant No 18-29-19008).

### References

1. J. F. Harris Peter // J. Mater. Sci. 2013. V. 48. P. 565-577.
2. V.S. Kozlov, V. G. Semenov, and V. V. Panchuk // Journal of Surface Investigation: X-ray, Synchrotron and Neutron Techniques, 2017. Vol. 11. No. 5. P. 908-911.

## Detonation method for synthesis of bimetallic nanoparticles

*Kashkarov A.O.*<sup>1,2</sup>, *Pruuel E.R.*<sup>1,2</sup>, *Gerasimov E.Yu.*<sup>3,2</sup>, *Moroz B.L.*<sup>3,2</sup>, *Kremenko S.I.*<sup>1,2</sup>, *Dashapilov G.R.*<sup>1,2</sup>

*kashkarov@hydro.nsc.ru*

<sup>1</sup> Lavrentyev Institute of Hydrodynamics SB RAS, Novosibirsk, Russia

<sup>2</sup> Novosibirsk State University, Novosibirsk, Russia

<sup>3</sup> Boreskov Institute of Catalysis SB RAS, Novosibirsk, Russia

The use of explosive energy allows us to synthesize metal nanoparticles with simultaneous deposition them on the detonation carbon. In this way, it is possible to produce nanoparticles of various noble metals ranging in size from a few to several hundred nanometers. The average size of the obtained particles can be predetermined by the composition of the initial components. For instance, the authors previously obtained the samples containing palladium nanoparticles with the average number-weighted sizes of 1.5, 2.5, 3.1, and 6.4 nanometers.

The method of synthesis consists in thermal decomposition of a metal-containing precursor upon detonation of the explosive composite containing it. This leads to the release of individual metal atoms, which are then joined into nanoparticles. The support for nanoparticles consisting of detonation carbon is also formed during the explosion. It represents the graphite-like carbon with a sufficiently high surface area and can be used as a support for catalysts. The detonation carbon covers the surface of metal particles and prevents their further growth. Thus, the particle size is controlled by the kinetics of carbon condensation. The limitation of the final particle size is also due to the mechanical expansion of the area occupied by the explosion products, which prevents diffusion and agglomeration of metal atoms. In addition, both the chemical nature of the metal and its content in the precursor affect the particle size. Regulation of these factors allows one to predetermine the average particle sizes.

One of the advantages of this synthetic procedure is the ability to obtain bimetallic catalysts based on noble metals. Behind the detonation front the, the formation of the alloyed particles occurs. Since the process is fast-flowing and essentially non-equilibrium, the fairly uniform mixing of metals inside the alloy particles is observed, and the growth of nanoparticles is limited by the initial conditions of the experiment. This report presents the results of obtaining the bimetallic Pd/Cu and Pd/Ag particles on detonation carbon, which are formed by using the precursor mixtures consisting of the corresponding bimetallic compound and an explosive.



## Features of the use of X-ray diffraction analysis to study the fine structure of carbon fibers

*Fazlitdinova A.G.*<sup>1</sup>, *Tyumentsev V.A.*<sup>1</sup>, *Shayderov A.I.*<sup>1</sup>

*fazlitdinovaag@mail.ru*

<sup>1</sup>Chelyabinsk State University, Chelyabinsk, Russia

X-ray diffraction analysis is one of the most common methods for monitoring the parameters of the structure of materials. However, when it is used to analyze the structure of carbon and polymeric materials, a number of problems arise. The large depth of penetration of X-rays causes participation in the formation of a diffracted beam by the volumes of the test substance located substantially below the Bragg-Brentano self-focusing plane, which leads to a distortion of the diffraction maximum profile. The material may include coherent scattering regions (CSR), the parameters of the crystal structure of which are somewhat different. As a result, the experimentally observed diffraction peaks become asymmetric and are not described by Gauss, Lorentz, or Voigt functions. Therefore, the information obtained by standard methods about the value of the interplanar distance and the size of the CSR does not reflect the real structure of the material. The report analyzes the possibilities and results of applying the method of X-ray analysis to study the fine structure of carbon fibers (CF). A comparison was made of the results of the separation of the experimentally observed asymmetric diffraction peak of 002 CF samples into symmetric ones described by the Gauss, Lorentz, and Voigt functions.

The studies were performed using an X-ray diffractometer D8 ADVANCE. To ensure the condition of self-focusing of the Bragg-Brentano diffracted beam with the entire volume of the substance with which the X-ray beam interacts, the CF was arranged in the form of a thin (~0.1 mm) layer of filaments.  $\text{Cu}_{\text{K}\alpha-2}$  removal was performed using the DIFFRAC plus package. The profiles of the diffraction asymmetric peak of the 002 CF were analyzed using Origin 8.

The influence of the geometry of obtaining X-ray patterns on the profile of diffraction peak was studied. It is shown that when conducting X-ray structural studies of materials characterized by a large depth of penetration of X-rays, it is necessary to strictly ensure the fulfillment of the condition of self-focusing for the entire volume of the sample forming the diffracted beam.

A comparison was made of the results of the separation of the experimentally observed asymmetric diffraction peak of 002 into symmetric ones described by the Gauss, Lorentz, or Voigt functions. It is shown that the asymmetric diffraction peak of the shock wave can be represented as three components - the symmetric peak described by the Gauss, Lorentz, or Voigt functions. The average value of the coefficient  $R^2$ , calculated from the results of the decomposition of the studied samples, turned out to be the highest when using the Voigt and Gauss functions ( $R^2$ , respectively, 0.9994 and 0.9992; when using the Lorentz function,  $R^2 = 0.9975$ ). In the case of using the Gauss and Voigt functions for analyzing the profile of the asymmetric peak 002 under study, the average dimensions of CSR  $L_{002}$  of the selected components turned out to be quite close. When using the Lorentz function, the dimensions  $L_{002}$  of the corresponding components of the decomposition are almost 1.5 times larger, the components of the decomposition also correspond to smaller values of the interplanar distances. The diffraction peak profiles of the 002 CF were analyzed after the removal of the  $\text{Cu}_{\text{K}\alpha-2}$  component. It is shown that this did not affect the values of the average dimensions  $L_{002}$  and the interplanar distances  $d_{002}$  of the decomposition components. It is concluded that the analysis of experimentally observed asymmetric peak of fibrous materials using the Origin 8 program requires the use of the Gauss or Voigt function.

## Photo- and X-ray luminescent diamond composites with embedded nanoparticles of rare-earth element fluorides

*Sedov V.S.<sup>1</sup>, Kuznetsov S.V.<sup>1</sup>, Martyanov A.K.<sup>1</sup>, Ralchenko V.G.<sup>1,2</sup>, Fedorov P.P.<sup>1</sup>*

*sedovvadim@yandex.ru*

<sup>1</sup> Prokhorov General Physics Institute of the Russian Academy of Sciences, Moscow, Russia

<sup>2</sup> Harbin Institute of Technology, Harbin, P.R. China

Free-electron lasers allow the generation of coherent electromagnetic radiation in the X-ray range with very high peak power [1]. Thus, there are new challenges in fabricating detectors and visualizers for the “hard” high-power radiation. Diamond is a perfect candidate for the role of X-ray transparent matrix not only due to low X-ray absorption but also due to its high thermal conductivity and chemical/radiation resistance. To add X-ray luminescence (XRL) properties to such diamond matrix, rare-earth (RE) based  $\text{EuF}_3$  nanoparticles were added in the bulk of polycrystalline diamond films [2].

Photo- and X-ray luminescent composites based on europium fluoride nanoparticles embedded in polycrystalline diamond (PCD) were obtained by CVD overgrowth technique (Fig. 1). Both photoluminescence (PL) and XRL spectra reveal an intensive signal from Eu atoms near 612 nm. The full width at half maximum (FWHM) of the peak is as low as 2 nm and 6.1 nm for PL and XRL, respectively. The use of  $\beta\text{-NaGdF}_4\text{:Eu}$  nanopowders instead of pure europium oxide or europium fluoride allow obtaining a high-intensity luminescence with a rather higher signal-to-noise ratio. PL mapping showed high density of XRL sources, which makes possible using a diamond-fluoride composite as high-resolution luminescent screens.

This work was supported by the Russian Foundation for Basic Research, grant No. 16-29-11784\_ofi.

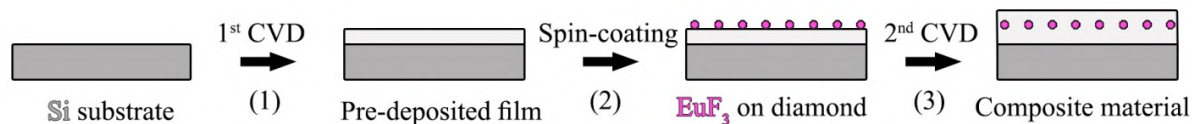


Fig.1. The scheme of diamond composite preparation by imbedding  $\text{EuF}_3$  nanoparticles between two microcrystalline diamond layers on the silicon substrate.

### References

1. K.C. Prince, E. Allaria, C. Callegari, R. Cucini, G. De Ninno, S. Di Mitri, B. Diviacco, E. Ferrari, P. Finetti, D. Gauthier, L. Giannessi, Nat. Photonics (2016) **10**, 176.
2. V.S. Sedov, S.V. Kuznetsov, V.G. Ralchenko, M.N. Mayakova, V.S. Krivobok, S.S. Savin, K.P. Zhuravlev, A.K. Martyanov, I.D. Romanishkin, A.A. Khomich, P.P. Fedorov, Diam. Relat. Mater. (2017) **72**, 47.

**PHASE TRANSITIONS IN CARBON MATERIALS AT HIGH PRESSURES**

*Tikhomirova G.V.*<sup>1</sup>, *Petrosyan T.K.*<sup>1</sup>, *Volkova Ya.Yu.*<sup>1</sup>, *Tebnikov A.V.*<sup>1</sup>

*galina.tikhomirova@urfu.ru*

<sup>1</sup> Ural Federal University, Ekaterinburg, Russia

Transport phenomena in carbon materials (monomeric, rhombohedral and tetragonal phases of fullerene C<sub>60</sub>, single-wall and double-wall carbon nanotubes (SWNT and DWNT), graphene and graphite) have investigated at pressures up to 35 GPa. Relaxation kinetics of these materials at changing pressure was studied. The measurements were performed using the high-pressure chamber with anvils made of synthetic carbonado diamonds.

In the course of treatment by high pressure and temperature, fullerene undergoes consequent phase transformations. These phases have quite different both resistivities (from hundreds Ohm to hundreds MOhm) and their temperature dependences. Resistivity peculiarities were identified with the known phase transitions of fullerene. The scheme of sequence of phase transformations under high pressures is suggested. Resistivity relaxation times for all fullerite phases are determined as more than two hours.

Samples of single-wall carbon nanotubes (SWNT) under study were grown by CVD and cleaned by HiPCO (High pressure CO) method. The SWNT diameters estimated by means of TEM (transmission electron microscope) were 0.8 to 1.2 nm. Strong pressure dependence of the SWNT bundles was found. The complicated pressure dependence of resistivity of double-wall carbon nanotubes (DWNT) is attributed to deformation of their structure. Destruction of DWNT begins at essentially lower pressures than SWNT because of larger diameter of outer tube and respectively larger number of defects. Nevertheless, there is no complete collapse of DWNT up to 30 GPa.

Conductivity, magnetoresistance and thermoelectromotive force of graphite and graphene, as well as their relaxation kinetics, in dependence on pressures were studied. The features observed are attributed to phase transitions.

The possibility of formation of new carbon phases from graphite at continuous exposure (24 hrs) under pressures of 18 GPa to 45 GPa was examined. The features in the pressure dependence of resistance as well as its relaxation times observed in the range 27--35 GPa are connected likely with the inclusion of a new phase, which did not disappear after removal of the load.

## Polarization study of carbon nanodots photoluminescence

*Nelson D.K.<sup>1</sup>, Starukhin A.N.<sup>1</sup>, Reshetov V.I.<sup>1</sup>, Kurdyukov D.A.<sup>1</sup>, Eurov D.A.<sup>1</sup>, Golubev V.G.<sup>1</sup>*

*d.nelson@mail.ioffe.ru*

<sup>1</sup> Ioffe Institute, St. Petersburg, Russia

Carbon nanodots (CDs) represent a new type of luminophore based on carbon nanoparticles with few nanometers in size. The possibility of the functionalization of the surface of CDs with different atomic groups allows the targeted variation of their properties. CDs are easily synthesized, inexpensive, low-toxic, and chemically inert, which favorably distinguishes them from semiconductor quantum dots. Along with applications in optoelectronics, energy storage and conversion, and catalysis, CDs are of particular interest for various biomedical applications. The spectral composition of CD emission allows considering them as possible white-light sources. The basic problem in the investigation of the photophysical properties of CDs is to establish the nature of optical transitions in these objects, which remains unclear. An efficient method of studying the properties of radiative states in various atomic systems is polarized luminescence, which yields information about the structure of elementary emitters and their interaction with each other and the environment. The present report is aimed at investigating polarized luminescence of CDs isolated in glycerol matrices.

Studies of the fluorescence of carbon nanodots in glycerol showed that, under excitation with linearly polarized light, it was predominantly linearly polarized in the same plane as the excitation. The degree of linear polarization is highest at the short-wavelength edge of the emission band and decreases with increasing wavelength [1]. The observed photoinduced linear polarization of the radiation indicates a latent optical anisotropy of the system. The ensemble of photoexcited nanodots can be considered as a system of linear dipole oscillators with random orientation in space. Linearly polarized light excites mainly oscillators whose dipole moments are parallel to the vector  $E$  of the light wave. If during the lifetime of the radiative state the orientations of the dipole moments do not change significantly, the radiation of the oscillator system will be predominantly polarized in the same plane as the exciting light.

An increase of the temperature causes the luminescence depolarization. In dilute solutions, energy migration between different nanodots can be neglected. In this case the main mechanism for the depolarization of colloidal solution emission is the Brownian rotation of particles. The thermal motion of the particles in the solution disrupts the anisotropic distribution of the oscillators, tending to the isotropization of the distribution function and, consequently, to depolarization of radiation. The degree of depolarization is determined by the angle of rotation of the particle during the lifetime of the excited state, which depends on its size, temperature, and viscosity of the medium. Besides thermally induced depolarization of the CD emission, the linear polarization of the emission of CD solutions with different viscosities was studied at fixed temperatures, the dependence of the degree of the polarization on solvent viscosity was established.

The experimental data were analyzed in the framework of Levshin-Perrin model. We have established that the observed behavior of polarization degree of luminescence is described by the Levshin-Perrin equation, which gives evidence of the rotational mechanism of depolarization. By comparing the experimental and theoretical dependences, the size of the rotating elementary emitters was estimated. The results indicate that atomic groups in nanodots responsible for photoluminescence possess a high local mobility.

### References

1. D. K. Nelson, B. S. Razbirin, A. N. Starukhin, D. A. Eurov, D. A. Kurdyukov, E. Yu. Stovpiaga, and V. G. Golubev, *Opt. Mater.* **59**, 28 (2016).

## Synthesis, Characterization of Elastic, Optical and Electrical Properties of Diamond-Like BC<sub>x</sub> Nano-Phases Synthesized under High and Low Pressures

Zinin P. V.<sup>1</sup>, Filonenko V. P.<sup>2</sup>, Fominski V. Y.<sup>3</sup>, Roamov R. I.<sup>3</sup>, Bulatov K. M.<sup>1</sup>, Bykov A. A.<sup>1</sup>, Kutuza I. B.<sup>1</sup>, Leksikov A.<sup>1</sup>, Titov S. A.<sup>1</sup>

zosimpvz@mail.ru

<sup>1</sup> Scientific and Technological Center of Unique Instrumentation, Russian Academy of Sciences, Moscow, Russia

<sup>2</sup> Institute for High Pressure Physics, Russian Academy of Sciences, Troitsk, Russia

<sup>3</sup> National Research Nuclear University MEPhI (Moscow Engineering Physics Institute), Moscow, Russia

We present experimental results on the synthesis of boron rich diamond-like carbon phases (BC<sub>x</sub>) obtained by high pressure synthesis, sintering and pulsed laser deposition.

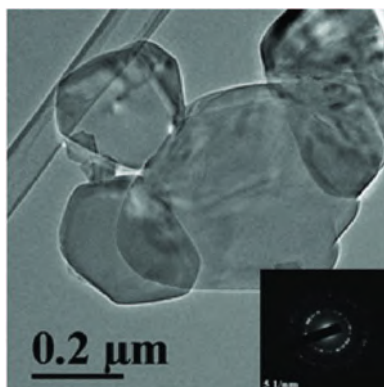
Thermobaric treatment of the diamond-like *dl*-BC<sub>3</sub> phase leads to the formation of BC<sub>3</sub> hetero-nano-diamonds. We found that after laser heating at 1100 K and 25 GPa in a high pressure cell almost all graphitic layers of the *g*-BC<sub>3</sub> transform into a cubic structure. The x-ray diffraction pattern of the cubic BC<sub>3</sub> phase (*c*-BC<sub>3</sub>) can be indexed with a cubic unit cell  $a = 3,6420$  (0,0647) Å. This is in line with the theoretical simulations demonstrating that the total energies of the graphitic BC<sub>3</sub> structure should be higher than that of the equivalent *dl*-BC<sub>3</sub> phase at ambient conditions.

The pulsed laser deposition (PLD-BC<sub>x</sub>) films found to be rigid with the resistivity as low as that of best conductive boron-doped diamond nano-films. It indicates that the presence of B atoms in a laser plasma leads to the formation of sp<sup>3</sup> bonds in the material in the process of PLD. The thickness of the films varies from 10-100 nm. Laser ultrasonics measurements showed that the elastic properties of the *dl*-BC<sub>x</sub> phases depend on the carbon sp<sup>2</sup> versus sp<sup>3</sup> content

We synthesised star-shaped pentagonal microcrystals of boron carbide with extremely low carbon content (~ 5%), from M-carborane under high pressure 7 GPa and high temperature 1370 K. These crystals have five-fold symmetry and grow in the shape of stars. The 5-fold symmetry is a characteristic feature of quasi-crystalline solids. When M-carborane is mixed with lamp soot, two phases are formed under high pressure high temperature conditions: (a) boron carbide phase with a composition of B<sub>4</sub>C; and (b) heavily boron doped diamond microcrystals.

The combination of unique characteristics can be achieved by changing the ratio B/C.

Research funded by Russian Science Foundation grant (RSF 17-12-01535).



Nanodiamonds with high boron content obtained under high pressure and high temperature from the globular carbon 20-40 nm.

## Low-temperature transformations of carbon allotropes in the theraphthal - ascorbic acid system.

*Kharissova Oxana V.*<sup>1</sup>, *Rodriguez Jared*<sup>1</sup>, *Kharisov Boris*<sup>1</sup>

*bkhariss@hotmail.com*

<sup>1</sup> Universidad Autonoma de Nuevo Leon

Multi-wall carbon nanotubes and graphite are relatively stable carbon allotropes, which could be solubilized and/or unfolded by a series of physical and chemical methods. Here, we present a low-temperature formation of several nanocarbons starting from these precursors, such as nano-onions, graphene sheets, and carbon nanoribbons (Fig. 1). The experiments were carried out under ultrasonic treatment of aqueous systems “carbon allotrope - theraphthal [1,2] - ascorbic acid” at various ratios and concentrations. Resulting nanocarbons were studied by scanning electron microscopy, transmission electron microscopy, XPS, FTIR and Raman spectroscopy. Based on the experimental results, the mechanisms for carbon nanotube unfolding and separation of graphite layers were proposed. These reactions are based on the formation of Reactive Oxygen Species (ROS) by theraphthal in ultrasonic conditions and their further interaction with carbon precursors. These transformations can be considered as greener methods for obtaining nanocarbons.

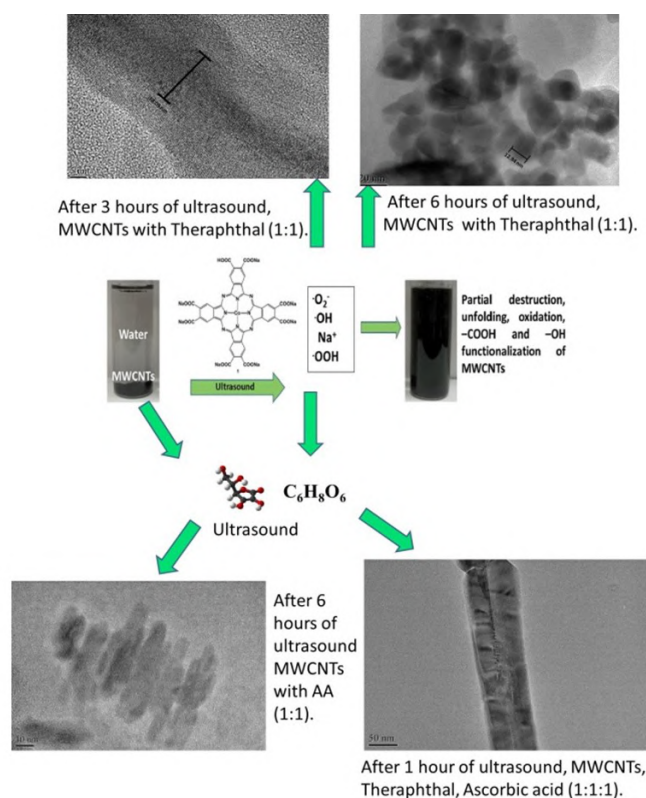


Fig. 1. Generalized scheme of nanoribbons formation from MWCNTs as precursors.

### References

- [1] O.L. Kaliya and E.A. Luk'yanets. On the article about the component composition of teraphthal preparation. *Pharm. Chem. J.* 2009, **43**(10), 587.
- [2] M.S. Goizman, E. V. Degterev, K. F. Turchin, A. P. Arzamastsev. Quality control of teraphthal production. 1. Chemical composition. *Pharm. Chem. J.* 2007, **41**(12), 670.

## Hybrid sp<sup>2</sup>-sp<sup>3</sup> bonds in carbon spiroids: energetical issues

*Siklitskaya A.*<sup>1</sup>, *Yastrebov S.G.*<sup>2</sup>

*asiklit@ichf.edu.pl*

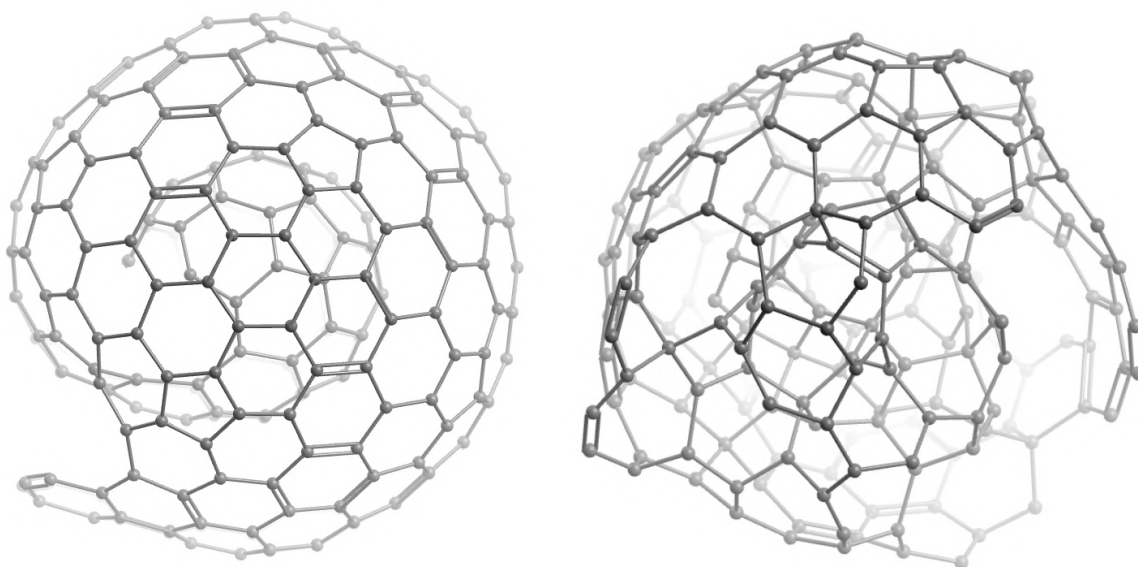
<sup>1</sup> Institute of Chemical Physics PAN, Warsaw, Poland

<sup>2</sup> Ioffe Physical-Technical Institute, St.Petersburg, Russia

Carbon spiroids are the relatively new and one of the least studied carbon allotropes. The perspectives for its use in electrochemical storage were unveiled in paper [1], hydrogen storage [2] and in catalysis.

We studied the differences between the ideal model spiroid [3] and the spiroid from paper [4] within the framework of semiempirical ab-initio approach implied in Gaussian program package[5]. We've found that presence of the hybrid sp<sup>2</sup>-sp<sup>3</sup> bonds may influence positively on the cluster's stability.

We acknowledge the computational grant G60-8 from the Interdisciplinary Center for Mathematical and Computational Modelling(ICM) in Warsaw.



Left picture shows the ideal carbon spiroid C300. Right picture shows the carbon spiroid with hybrid sp<sup>2</sup>-sp<sup>3</sup> bonds.

### References

1. M. Zeiger, N. Jackel, V. N. Mochalin and V. Presser, *J. Mater. Chem. A*, 2016, 4, 3172-3196.
2. Yastrebov, M. Chekulaev, A. Siklitskaya, J. A. Majewski, Fröhlich resonance in carbon nanospiroids and the 2175Å interstellar absorption feature, *Nuclear Instruments and Methods in Physics Research Section B: Beam Interactions with Materials and Atoms* 393 (2017)
3. M. Ozawa, H. Goto, M. Kusunoki, E. Osawa, Continuously Growing Spiral Carbon Nanoparticles as the Intermediates in the Formation of Fullerenes and Nanooxions, *J. Phys. Chem. B.* 106 (2002) 7135-7138, <http://dx.doi.org/10.1021/jp025639z>, past 12
4. S.G. Yastrebov, R. Smith, A.V. Siklitskaya, Evolution of diamond nanoclusters in the interstellar medium, *Mont. Not. R. Astron. Soc.* 409 (2010) 1577
5. M. J. Frisch, G. W. Trucks, H. B. Schlegel, G. E. Scuseria, M. A. Robb et.al. "Gaussian 09, Revision B.01," 2009.

## Detonation synthesis of 2D carbon structures

*Voznyakovsky A.P.*<sup>1</sup>, *Dolmatov V.Yu.*<sup>2</sup>, *Voznyakovsky A.A.*<sup>3</sup>

*voznap@mail.ru*

<sup>1</sup> S.V. Lebedev Research Institute for Synthetic Rubber, St. Petersburg, Russia

<sup>2</sup> FSUE "SCTB"Technolog", St. Petersburg, Russia

<sup>3</sup> Ioffe Institute, St. Petersburg, Russia

Detonation synthesis of nanocarbons is well developed and used to produce 3D nanocarbons - detonation nanodiamonds. The basis of the synthesis is the detonation decomposition of a mixture of 2,4,6-trinitrotoluene (TNT) and 1,3,5-trinitro-1,3,5-triazacyclohexane (RDX) of the composition (TNT / RDX = 60/40). To date, it has been reliably established that, under the detonation synthesis conditions of 3D carbon structures of approximately 95% of the mass are formed from carbon atoms entering the composition of TNT molecules. Thus, the role of RDX in the charge is reduced to the formation of additional energy of explosive decomposition, which is necessary for the formation of highly organized 3D carbon structures by the "bottom up" mechanism. It should be noted that the direct product of detonation synthesis is a physically inseparable mixture of 3D nanocarbon and the so-called "amorphous carbon". Moreover, depending on detonation synthesis specific conditions, the content of "amorphous carbon" in the synthesis product may be 30-60% by weight. Based on the chemistry of the carbon atom, it is natural to assume that the carbon atoms that form the particles of "amorphous carbon" are not clusters of carbon atoms, but are the product of self-organization processes into some simplest structures. It can be assumed that the most thermodynamically advantageous is the process of forming 2D carbon structures with  $sp^2$  organization that goes with the least loss of system entropy. Eliminating RDX from the composition of the charge, you can completely shift the process of detonation synthesis to 2D carbon structures formation. 2D carbon structures, depending on the number of carbon atoms forming them, can form from soot particles to complexly organized sorbents. Such a variant of detonation synthesis can be useful in solving an important environmental problem - the disposal of ammunition with a completed shelf life. Namely, the replacement of their destruction by detonation, the recycling process with the formation of the value-added product.

The paper presents experimental data on the study of 2D carbon structures powders obtained by the explosive TNT decomposition under the conditions of the process of detonation synthesis. Analysis of the complementary data obtained by the combination of spectral and electron microscopy techniques, made it possible to conclude that the obtained powder particles in their structure agree well with the data characteristic of 2D graphene structures. Additionally, the data obtained on the true density of powders ( $\rho = 2.10985 \text{ g / cm}^3$ ) and on their specific surface ( $S = 559 \text{ m}^2 / \text{g}$ ) also confirm the validity of this assumption.



## Stress modulation, graphitic nanoclusters and electronically-active defects in laser irradiated bulk-diamond

*Rossi M.C.*<sup>1</sup>, *Valentini V.*<sup>2</sup>, *Pettinato S.*<sup>3</sup>, *Conte G.*<sup>4</sup>, *Kononenko T.V.*<sup>5,6</sup>, *Ralchenko V.G.*<sup>5,6,7</sup>, *Salvatori S.*<sup>3</sup>

*mcrossi@uniroma3.it*

<sup>1</sup> Università degli Studi Roma Tre, Electronic Engineering Dept., 00146 Rome, Italy

<sup>2</sup> Institute for Structure of Matter, CNR, Monterotondo (Rome), Italy

<sup>3</sup> Università degli Studi Niccolò Cusano, Roma, Engineering Dept. 00166 Rome, Italy

<sup>4</sup> Università degli Studi Roma Tre, Dip. di Scienze Matematiche e Fisiche, 00146 Rome, Italy

<sup>5</sup> General Physics Institute of the Russian Academy Sciences, - 119991 Moscow, Russia

<sup>6</sup> National Research Nuclear University MEPhI, - 15409 Moscow, Russia

<sup>7</sup> Harbin Institute of Technology, 92 Xidazhi Str. - 150001 Harbin, P.R. China

Array of surface connected buried columns contact structures realized by femtosecond pulsed laser irradiation of single-crystal CVD-diamond have been investigated by confocal micro-Raman and photoconductivity (PC) spectroscopy. The latter have been used to assess if and how the site selective graphitization treatment affects the electronic properties in the diamond detection volume. In untreated diamond slab, a sharp PC transition of about five orders of magnitude is observed close to the diamond band gap, whereas a monotonic decrease of the PC signal is detected down to 2 eV, thereby confirming the high crystalline quality of the diamond sample. After buried graphitic contacts formation, the sharp PC rise at the diamond band gap transition is still observed, but a defect related PC band appears above 2.5 eV. Spectral PC measurements have been then performed superimposing a HeNe laser-light bias during the measurements. In this condition, an extra PC contribution is detected at photon energies in the range 4-5 eV. These results have been interpreted in terms of carrier transitions from valence band to vacancy related intragap energy levels at 0.6 or 2.5 eV, depending on their charge states. If this interpretation holds, HeNe biasing at 1.96 eV could increase the higher level occupancy, giving rise to the mentioned additional PC contribution. The formation of defects induced by the irradiation process has been also investigated by micro-Raman spectroscopy measurements. In untreated regions of diamond, the Raman spectrum shows the narrow one-phonon Raman peak at  $1332\text{ cm}^{-1}$  of the perfect diamond lattice, with no significant photoluminescence (PL) background. Upon femtosecond laser irradiation, local graphitization occurs as confirmed by the detection of D and G bands at about  $1360$  and  $1580\text{ cm}^{-1}$ . At the same time, the one-phonon diamond peak broadens and shifts to lower frequencies, owing to disorder and stress related effects. Further, an intense PL background appears, reflecting the induced disorder in the crystalline diamond phase. In order to gain a more insight on these effects, a monitoring of vibrational characteristics has been performed by moving the laser spot in the radial direction from the center of a buried column toward its surrounding untreated diamond region. Close to the pillar core the  $I_D/I_G$  intensity ratio suggests an achieved graphitic nanoparticle size  $L_a$  in the range  $5-8 \pm 1\text{ nm}$ . At the same time, a very broad and downshifted residual diamond peak is detected, suggesting that graphitic nanoparticles are embedded into a highly disorder, strained diamond tissue. According to polarized light images of the pillar cross section, reporting concentric circle structure with different colors, a stress modulation occurs, as reflected by diamond peak splitting. About 10  $\mu\text{m}$  further in the untreated zone, unaltered diamond lineshape peak on a flat PL background is detected, confirming that graphitization process mainly affects the structural characteristics of diamond in the range close to pillar cross section, where formed vacancy defects may give raise to carrier recombination, which could be a detrimental effect for the electronic transport properties of a diamond device based on buried-columns contacts.

## Optical properties of carbon spiroid C<sub>300</sub>

*Chekulaev Maxim*<sup>1</sup>, *Yastrebov Sergey*<sup>2</sup>, *Siklitskaya Alexandra*<sup>3</sup>

*mchs89@gmail.com*

<sup>1</sup> Ioffe Institute, St.Petersburg, Russia

<sup>2</sup> Ioffe Institute, St.Petersburg, Russia

<sup>3</sup> Institute of Chemical Physics PAN, Warsaw, Poland

Spiroidal allotropic modifications of carbon remain excite attention because possibilities of their miscellaneous applications in solving problems of hydrogen energy and catalysis [1,2]. Moreover, using the C<sub>300</sub> spiroid as an example, we will show that the optical properties of spiroids coincide with 217.5 nm absorption band, known from astrophysics. This coincidence allows to extend our knowledge on physics of formation of spiroids to processes operating in the interstellar medium during the irradiation of diamond nanoparticles with stochastic ultraviolet radiation [3]. The problem of calculation of the optical properties was solved step by step. The tight binding model was used to calculate the electron spectrum of the C<sub>300</sub> spiroid. Simultaneously we use the optimization of the C<sub>300</sub> geometry by Car-Parrinello molecular dynamics, we estimate the degree of disorder of skeleton of the spiroid. We discovered some distortion of the skeleton that breaks symmetry selection rules for optical transitions. That allowed us to extend the Tauc model to calculation of the imaginary part of the dielectric function through the sum of combinations of possible optical transitions from the zone of states occupied by electrons to the zone of unoccupied states. Next, the ionization potential of the spiroid was calculated, which attained value of 5 eV. It was implied that for photon energies exceeding the value of the ionization potential, the spiroid turns to a sphere filled with electrons. Applying the electrodynamic sum rules to the imaginary part of the dielectric function, we calculated the plasma frequency dependent on the photon energy, which was used to estimate the spectral dependence of the spiroid scattering cross section. The electron relaxation time was used as the fitting parameter in our model. Excellent agreement was obtained between calculated and astrophysical data.

### References

1. M.Zeiger, N. J"ackel, V. N. Mochalin and V. Presser, J. Mater. Chem. A 2016 **4**, 3172.
2. S.G.Yastrebov, M. Chekulaev, A. Siklitskaya and J. A. Majewski, Instrum. Methods Phys. Res. 2017 **393** 59.
3. S.G. Yastrebov, R. Smith, and A.V. Siklitskaya, Evolution of diamond nanoclusters in the interstellar medium, Mont. Not. R. Astron. Soc. 2010 **409** 1577.

## Characterization of amorphous hydrocarbon $CD_x$ films for energy storage applications

*Brzhezinskaya M.*<sup>1</sup>, *Svechnikov N.Yu.*<sup>2</sup>, *Stankevich V.G.*<sup>2</sup>, *Lebedev A.M.*<sup>2</sup>, *Sukhanov L.P.*<sup>2,3</sup>, *Menshikov K.A.*<sup>2</sup>

*svechnikov47@mail.ru*

<sup>1</sup> Helmholtz-Zentrum Berlin fuer Materialien und Energie, Berlin, Germany

<sup>2</sup> National Research Centre Kurchatov Institute, Moscow, Russia

<sup>3</sup> Moscow Institute of Physics and Technology, Dolgoprudny, Russia

Carbon nanostructured materials such as carbon nanotubes, graphitic nanofibers and mechanically milled graphite, have attracted a large attention over the past decades as hydrogen storage materials [1]. It is also worth mentioning the creation of highly efficient hydrogen energy matrices based on typical tokamak carbon films with high hydrogen (deuterium) content. For example, in the case of amorphous  $CD_x$  films ( $x \sim 0.5$ ) deposited on the vacuum chamber walls at a wall temperature of 300–400 K under the erosion of graphite elements of the T-10 tokamak (NRC Kurchatov Institute) during D-plasma discharges [2]. Here, surface defects formed by exposure to ions, electrons and neutrals act as hydrogen trapping sites. Among the defective states were found iron impurities (<1 at.%) as a result of erosion of the chamber walls, and Fe catalytic effect on “facilitating” the thermal desorption of hydrogen (deuterium) from  $CD_x$  films was observed experimentally and confirmed theoretically [3].

In the present work, the C 1s X-ray absorption spectra were measured for the first time for model  $CD_x$  films using the BESSY II storage ring facility of Helmholtz-Zentrum Berlin (Germany). As a result, the obtained  $CD_x$  spectrum was typical for C K-spectra of  $sp^3+sp^2$  hydrocarbon systems, i.e., consisting of four resonances in the subthreshold region and three  $1s \rightarrow \sigma^*$  transitions in the continual group of unfilled  $\sigma^*$  states with wide bands in the post threshold region. It is important that triple-bond resonances ( $C \equiv C$ )  $\pi^*$  and ( $C \equiv C$ )  $\sigma^*$  were absent. This confirms the absence of  $sp^1$  states which is consistent with the previously measured infrared spectra, and this is typical of such type tokamak films with a high H or D content. Also, an estimate of the relative contribution of the  $sp^2/sp^3$  states showed the values:  $sp^3 \approx 0.63$ ,  $sp^2 \approx 0.37$ , which was close to the measurements using X-ray Auger and photoelectron spectroscopies.

An additional analysis of the experimental Fe K-edge spectrum for iron impurities, including the pre-edge peak, the main absorption peak and the coordination number  $N=6.2$  for the  $FeC_{6.2}$  impurity clusters showed that in addition to impurities with  $N=6$ , there can be elements of Fe-C structures with coordination number  $N=4$ , 5, and, possibly,  $N=8$ . This agrees with a fractal structure of  $CD_x$  films [2] forming a branched and highly cross-linked 3D carbon  $sp^3+sp^2$  network, or matrix, accumulating a large number of H-isotopes. The latter can be more easily desorbed due to iron impurities reducing the threshold of thermal desorption. All these features will contribute to the energy applications of these hydrocarbon systems.

### References

1. H. Atsumi, and K. Tauchi, *J. Alloys Comp.* (2003) **356-357**, 705.
2. N.Yu. Svechnikov, V.G. Stankevich, B.N. Kolbasov, Y.V. Zubavichus, A.A. Veligzhanin, V.A. Somenkov, L.P. Sukhanov, A.M. Lebedev, and K.A. Menshikov, *Journal of Surface Investigation: X-ray, Synchrotron and Neutron Techniques* (2017) **11**, 1208.
3. V.G. Stankevich, L.P. Sukhanov, N.Yu. Svechnikov, A.M. Lebedev, K.A. Menshikov, and B.N. Kolbasov, *Eur. Phys. J. Appl. Phys.* (2017) **80**, 20301.

## The transformation of the structure of nanoscale amorphous carbon during the thermobaric treatment

*Filonenko V.P.*<sup>1</sup>, *Zibrov I.P.*<sup>1</sup>, *Lyapin S.G.*<sup>1</sup>, *Anokhin A.S.*<sup>2</sup>, *Trenikhin M.V.*<sup>3</sup>

*filv@hppi.troitsk.ru*

<sup>1</sup> Institute for High Pressure Physics RAS, Troitsk, Moscow, Russia

<sup>2</sup> Institute of Metallurgy and Materials Science RAS, Moscow, Russia

<sup>3</sup> Institute of Hydrocarbons Processing, Omsk Scientific Center SB RAS, Omsk, Russia

Changes in the structure of amorphous globular carbon during thermobaric treatment were investigated by X-ray, electron microscopy and Raman spectroscopy. Starting carbon particles had average diameter of 25 nm. The toroid-type chamber was used for experiments at a pressure of 8.0 GPa. Carbon exposure at temperature of 1300 °C for tens of seconds led to its transformation into structures with various morphologies and degrees of order. The major morphological species in the samples after processing were slabs of graphene sheets. TEM examination also revealed diamond nano-crystallites with 5–8 nm in size [1]. We observed the formation of structurally ordered graphite-like particles at temperatures of 1500 and 1800 °C. As a result of temperature rise, the size of diamond crystallites increased to tens of nanometers.

We also used mixture of amorphous globular carbon and powder of M-carborane with the formula  $B_{10}C_4H_{16}O_2$ . This mixture was treated at 8.0 GPa and 1700 °C. Graphene layers with boron are formed when ordering of the structure of amorphous carbon in the presence of M-carborane. The transformation of such graphite into diamond was activated by hydrogen. As a result, single crystals of diamond (Fig. 1) with sizes up to 10 microns are formed. X-ray analysis showed two diamond phases with different unit cell parameters. Both phases had an increased unit cell dimension which is typical for boron doped diamonds. Raman spectra of crystals confirmed a high degree of doping. The structure was refined by the Rietveld method. It has been shown that the unit cell parameters of diamonds have two discrete quantities: around 3.570 Å for small concentrations of boron (~ 1-1.5%) and around 3.578 Å for larger concentrations (~ 2-3%). It is also found that the number of vacancies is two to three times greater than the concentration of boron. It is assumed that vacancies can form stable complexes with boron atoms. This fact can play an important role in the structure formation and physical properties of heavily boron doped diamonds.

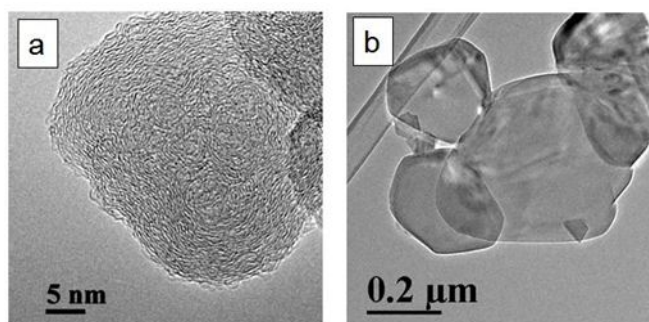


Fig. 1. Morphology of particles: a - globular carbon, b - heavily boron doped diamond

### References

1. V.P. Filonenko, I.P. Zibrov, M.V. Trenikhin etc. *Inorg. Mat.* 2017, 53, 5, 462.
2. I.P. Zibrov, V.P. Filonenko. *Crystals*, 2018, 8, 297

## Physicochemical properties of crystalline carbon/metal nanoflakes

*Proklova A.A.*<sup>1</sup>, *Mamonova D.V.*<sup>1</sup>, *Petrov Yu.V.*<sup>2</sup>, *Manshina A.A.*<sup>1</sup>

*proklova\_97@mail.ru*

<sup>1</sup> Institute of chemistry, Saint-Petersburg State University, Saint-Petersburg, Russia

<sup>2</sup> Physical faculty, Saint-Petersburg State University, Saint-Petersburg, Russia

Carbon/metal hybrid nanostructures are considered to be promising nanomaterials that can be of importance to analytical, biophysical and biomedical applications of Surface-enhanced Raman spectroscopy (SERS) [1]. In recent times synthesis of crystalline carbon/metal hybrids by laser-induced deposition from solution of organometallic supramolecular precursors is regarded as a perspective method [2]. The nanostructures of diverse morphology and size are obtained due to variation of deposition conditions and composition of supramolecular complexes.

In the present work the crystalline carbon/metal hybrids with unique morphology called nanoflakes are reported. They are obtained from acetophenone and aniline solutions of supramolecular complex (SMC)  $[(Au_{13}Ag_{12}(C_2Ph)_{20})(PPh_2(C_6H_4)_3PPh_2)_3](PF_6)$ . It was found that the nanoflakes formed onto substrate/solution interface. As substrates different objects can be used cover glass, glass covered indium tin oxide. The nanoflakes were investigated with various diffraction and optical characterization methods - transmission electron microscopy (TEM), scanning electron microscopy (SEM) and X-ray photoelectron spectroscopy (XPS), absorption, Raman and FTIR spectroscopies. The SEM image of the nanoflakes formed in acetophenone solution is shown in Fig.1.

It was in studies revealing that variation of such deposition parameters as laser radiation intensity, exposure time, and concentration of SMC solution affect only the geometric dimensions, not the chemical composition and structure of nanoflakes. The data obtained with EDX analyses demonstrate that the nanostructure consist only carbon, silver and gold. In consequence of investigation it was found that the nanoflakes are relating to typical carbon/metal hybrids in which the continuous phase is crystalline carbon matrix with metallic nanoparticles incorporated.

### Acknowledgments

This work was supported by the RFBR grant #17-03-01284. Samples' measurements were performed at Research Park of Saint-Petersburg State University at Center for Optical and Laser Materials Research and Nanotechnology.

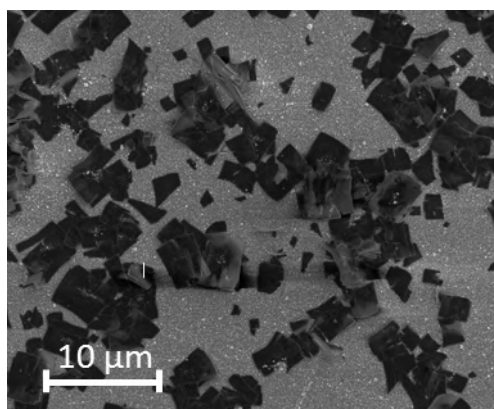


Fig.1. SEM image of nanoflakes obtained from acetophenone solutions of SMC.

### References

1. S. Pruneanu, A. R. Biris, F. Pogacean, D. M. Lazar, S. Ardelean, F. Watanabe, E. Dervishi and A. S. Biris, *ChemPhysChem* (2012) **13**, 3632.
2. A. A. Manshina, E. V. Grachova, A. V. Povolotskiy, A. V. Povolotckaia, Y. V. Petrov, I. O. Koshevoy, A. A. Makarova, D. V. Vyalikh and S. P. Tunik, *Sci. Rep.* (2015) **5**, 12027.

## Emission properties of carbon nanobelts

Tomilin O.B.<sup>1</sup>, Rodionova E.V.<sup>1</sup>, Rodin E.A.<sup>1</sup>, Soldatova V.I.<sup>1</sup>

evg.rodin54@gmail.com

<sup>1</sup> National Research Mordovia State University, Saransk, Russia

Carbon nanobelts were synthesized and studied both theoretical and practical, but emission properties of such molecules had not researched. Essentially carbon nanobelts are ultrashort open single-walled carbon nanotubes (SWCNT). It is shown [1] in cylindrical carbon molecules in-plane p-electron conjugation causes to specific molecular orbitals (EMO) which are characterized by electron localization at the ends of SWCNT, but these EMO are vacant. Is it true for carbon nanobelts? Nowadays it is unknown.

This investigation covers energy spectrum cyclacenes (Fig.1a) and cyclophenacenes (Fig.1b) on the value of electric field strength  $E$  (V/Å) applied along nanobelt axis. Model molecules are cyclacenes ( $n=5-10$ ) and cyclophenacenes ( $n=5-7$ ). The value  $E$  changed from 0.0 to 1.5 V/Å. Electron structure of model molecules was calculated for every  $n$  using DFT 6-31G/B3LYP (Firefly/GAMESS program package).

The results are presented in Fig.1. Summary:

- All researched model molecules possess two EMOs which are characterized by an extreme electron localization at the ends molecules. When value  $E$  is increased, energy of EMO1 is increased too, but energy of EMO2 is decreased and reached the conduction band edge at value  $E=E_{\text{con}}$ . The same behavior is observed for all model molecules SWCNT. It can be supposed that only at values  $E \geq 2.0$  V/Å the coincidence of the EMO2 with the edge of the valence band is possible, thus providing physical conditions for electron emission.
- For model molecules cyclophenacenes  $E_{\text{con}}=0.9$  V/Å, whereas for model molecules cyclacenes  $E_{\text{con}}=1.5$  V/Å.

The reported study was funded by RFBR according to the research project 18-33-00588.

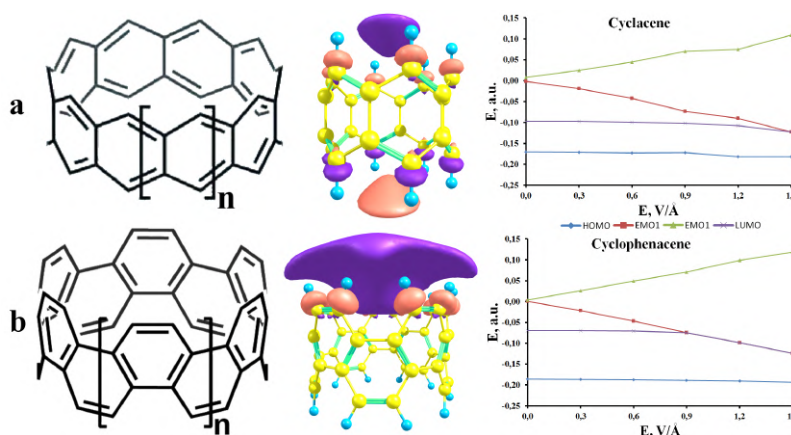


Fig.1. Summary of carbon nanobelts: a) cyclacenes ( $n=5-10$ ) and b) cyclophenacenes ( $n=5-7$ ).

### References

- B. Tomilin, E. V. Rodionova, E. A. Rodin and E. E. Muryumin, *Nanosystems: Physics, Chemistry, Mathematics* (2018) **9**, 70.

## **Low-threshold field emission of electrons and anomalous photosensitivity of carbon quantum dots on the surface of oxidized silicon**

*Zhurkin A.M.*<sup>1</sup>

*aleksey.zhurkin@avalon.ru*

<sup>1</sup> Peter the Great St.Petersburg Polytechnic University (SPbPU), St.Petersburg, Russia

In this paper, we are studying carbon quantum dots on the surface of oxidized silicon. Such structures have unique properties. One of these is the low-threshold field emission of electrons, which occurs when the electric field is about 1 V/ $\mu\text{m}$ . For such structures, the gain parameter of the electric field  $\beta$  must be equal to 1000. Taking into account the sizes of the inhomogeneities on the surface, according to the classical Fowler-Nordheim theory, it is impossible to achieve such a gain parameter for the field emission. In previous works [1], there are theoretical models describing this phenomenon presented. Carbon quantum dots which are capable of low-threshold field emission also have abnormal photosensitivity [2]. It manifests itself in the appearance of an electrical potential difference on the surface of the sample when illuminated by light.

This paper presents new research results of these phenomena. The surface of oxidized silicon consists of carbon quantum dots of ellipsoidal shape with the size of 5-50 nm in diameter and 4-5 nm in height. These data were obtained by atomic force microscopy (AFM) and scanning tunnelling microscopy (STM) and surface topography was studied. While studying the surface scanning by STM detected certain areas of the surface that responded to external radiation. This was detected by a significant excess of the maximum admissible current for the scanning tunnelling microscope. It is found that not all the surface is sensitive to external light. Some of the samples have open circuit voltage of 30 mV, but short-circuit current to 1  $\mu\text{A}$ . The surface resistance of the photosensitive area of the sample is 35 kOhm. There are some explorations of the issues of photoconductivity from the temperature of the sample, the wavelength and intensity of incident radiation.

Low-threshold field emission and abnormal photosensitivity are the two phenomena that are found in carbon quantum dots on the surface of oxidized silicon. The phenomenon of low-threshold field emission makes it possible to create cold field cathodes for electronic devices. Abnormal photosensitivity can be used to create highly sensitive sensors of a certain radiation spectrum. Presently, there is no generally accepted theory of low-threshold field emission and abnormal photosensitivity. Further research will be aimed at explaining two, possibly dependent, phenomena.

### **References**

1. Arkhipov A.V., Zhurkin A.M., Kvashenkina O.E., Osipov V.S., Gabdullin P.G. Electron overheating during field emission from carbon island films due to phonon bottleneck effect. *Nanosystems: physics, chemistry, mathematics.*, 2018, 1.
2. Arkhipov A.V., Gabdullin P.G., Gordeev S.K., Zhurkin A.M., Kvashenkina O.E. Photostimulation of conductivity and electronic properties of field-emission nanocarbon coatings on silicon. *Tech. Phys.*, 2017, 62(1), P. 127-136.

## **Characterization of individual SiV-luminescent nanodiamonds grown by CVD on various seeds.**

*Pasternak D.G.*<sup>1,2</sup>, *Kudryavtsev O.S.*<sup>2,3</sup>, *Romshin A.M.*<sup>1,2</sup>, *Sedov V.S.*<sup>2</sup>, *Vlasov I.I.*<sup>2,3</sup>

*dg.pasternak@physics.msu.ru*

<sup>1</sup> Lomonosov Moscow State University, Moscow, Russia

<sup>2</sup> Prokhorov General Physics Institute of the Russian Academy of Sciences, Moscow, Russia

<sup>3</sup> National Research Nuclear University MEPhI, Moscow, Russia

Currently various methods for producing nanodiamonds with optically active impurities are being actively developed in the world for using them in quantum optics, nanoelectronics and biomedicine. In this work the structure and luminescent properties of individual diamond nanocrystals synthesized by the CVD technique in a methane-hydrogen gas mixture with the addition of silane (SiH<sub>4</sub>) are investigated. Milled HPHT nanodiamonds crystallites with a mean size of 10 nm, detonation nanodiamonds (DNA), and laser-synthesized nanodiamonds with a mean size of 4-6 nm uniformly distributed on a surface of sapphire substrates were used as diamond nuclei. Growth time were 7.5 and 15 min. The sizes of produced crystallites varied in the range of 50-200 nm. Crystal morphology was studied by scanning electron microscope and atomic force microscope (AFM), luminescent properties were studied by confocal luminescent microscope combined with AFM and Henbury-Brown-Twiss interferometer. The uniformity of SiV center distribution over one sample was determined by the ratio of SiV luminescence intensity to the volume of individual crystallites. The number of SiV centers in individual crystallites was estimated by the dip magnitude of correlation function  $g^2$ . It was shown that CVD diamonds grown on HPHT diamond seed contain significantly more isolated single crystals than diamonds grown on other seeds. The interrelation between crystallite size, synthesis time and silane concentration was studied to design single-photon emitters based on SiV centers in individual CVD diamond nanocrystals.



## Modelling of supramolecular structures based on carbon nanotubes and cyclic/aromatic hydrocarbons for methane and hydrogen storage

*Shkolin A.V.*<sup>1</sup>, *Men'shchikov I.E.*<sup>1</sup>, *Fomkin A.A.*<sup>1</sup>

*shkolin@bk.ru*

<sup>1</sup> Frumkin Institute of Physical chemistry and Electrochemistry Russian academy of sciences, Moscow, Russia

Carbon nanotubes (CNT) are promising materials for adsorption storage of methane and hydrogen [1]. At the same time, an arrangement of nanotubes into ordered arrays, such as triangular packages, leads significant increase of adsorption capacity of these materials [2-3].

At the present work a possibility of formation of supramolecular structures from carbon nanotubes (diameter about 1 nm and length about 5 nm) and coordinate molecules - cyclic and aromatic hydrocarbons (cyclopentane C<sub>5</sub>H<sub>10</sub>, cyclohexane C<sub>6</sub>H<sub>12</sub>, ethyl cyclopentane C<sub>7</sub>H<sub>14</sub>, benzene C<sub>6</sub>H<sub>6</sub>, isopropyl benzene C<sub>9</sub>H<sub>12</sub>, naphthalene C<sub>10</sub>H<sub>8</sub>) was studied by numerical simulation based on molecular dynamics method. The simulation was implemented in microcanonical ensemble (N, V, E) at constant temperatures in a range between 200 and 400 K and was based on physicochemical properties of the substance for coordination of nanotubes.

It was shown that the molecules of cyclic and aromatic hydrocarbons separate nanotubes from each other and orient them mainly into triangular array. Such parameters as number of adsorbed substance molecules and temperature of the experiment, required for self-organization of carbon nanotubes into arrays, depend on physicochemical properties of the adsorbate. It was revealed that the molecules of cyclic and aromatic hydrocarbons were arranged primarily perpendicularly to the surface of nanotubes. Consequently, dimensions of hydrocarbon coordinate molecules correlate to distances between nanotubes in array. Created model supramolecular structures possessed following gaps between nanotubes, determined as distances between geometrical centers of nanotubes, nm: CNT/ C<sub>5</sub>H<sub>10</sub> - 1.8, CNT/C<sub>6</sub>H<sub>12</sub> - 2.0, CNT /C<sub>7</sub>H<sub>14</sub> - 1.9, CNT /C<sub>6</sub>H<sub>6</sub> - 1.9(5), CNT /C<sub>9</sub>H<sub>12</sub> - 2.1, CNT /C<sub>10</sub>H<sub>8</sub> - 2.2.

Step by step removal of coordinate molecules from the system by portions from 5 to 50 pcs, depending on overall amount of nanotubes in the array, leads to development of the porosity between nanotubes without destruction of the space structure (fig. 1). This additional nanoporosity can be used storage of such important gases as methane and hydrogen.

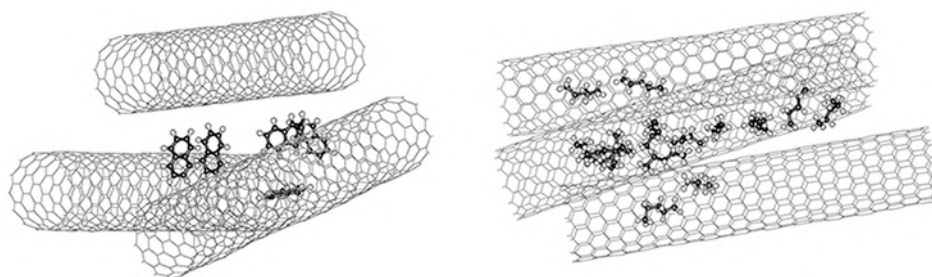


Fig.1. Instant snapshots of molecular dynamics trajectories of supramolecular CNT/C<sub>10</sub>H<sub>8</sub> (left) and CNT/C<sub>5</sub>H<sub>12</sub> (right) structures during porosity formation.

### References

1. Dillon A. C., Gennett T., Alleman J.L., Jones K.M., Parilla P.A., Heben M.J. Carbon nanotube materials for hydrogen storage, Proceedings of the 2000 Hydrogen Program Review NREL/CP-570-28890.
2. Shkolin A.V., Fomkin A.A. // Colloid Journal. 2017. **79**. 701.
3. Mahdizadeh S.J., ayyari S.F. // Theor. Chem. Acc. 2011. **128**. 231.

## Segmented carbon nanofibers: catalytic synthesis, formation mechanism and possible applications

Mishakov I.V.<sup>1,2</sup>, Bauman Y.I.<sup>1</sup>, Wang C.<sup>1</sup>, Korneev D.V.<sup>3</sup>, Rudneva Yu.V.<sup>4</sup>, Plyusnin P.E.<sup>4,2</sup>, Shubin Y.V.<sup>4,2</sup>, Zdanovich A.A.<sup>1</sup>, Matsko M.A.<sup>1</sup>, Vedyagin A.A.<sup>1</sup>

mishakov@catalysis.ru

<sup>1</sup> Borekov Institute of Catalysis, Novosibirsk, Russia

<sup>2</sup> Novosibirsk State University, Novosibirsk, Russia

<sup>3</sup> Monash University, Victoria 3800, Australia

<sup>4</sup> Nikolaev Institute of Inorganic Chemistry, Novosibirsk, Russia

Carbon nanomaterials produced by catalytic CVD of halogenated hydrocarbons now attract much attention due to their particularly unique structure and properties [1]. Here we report on synthesis of carbon nanofibers (CNF) with segmented structure via decomposition of 1,2-dichloroethane (DCE) over Ni-M self-organizing catalysts (SOC).

Series of microdisperse Ni-M alloys (M = Cr, Mo, Pt etc.) was synthesized by specially designed co-precipitation technique. Formation of corresponding Ni-M alloys was confirmed by XRD data. Ni-M alloys were tested as precursors for the SOC during the H<sub>2</sub>-assisted decomposition of DCE at 600°C. Interaction of Ni-M alloys with aggressive medium resulted in their rapid disintegration accompanied by emergence of disperse metallic particles functioning as active centres for CNF production. In all cases the introduction of metal M into Ni-alloy was shown to have positive stabilizing effect on catalytic activity and stability of nickel. The Mo metal in concentration of 8 wt.% was found to have the most significant impact upon catalytic performance of Ni (shortened induction period along with doubled yield of carbon product).

The carbon filaments produced over Ni-M (M = Cr, Mo, Pt) catalysts are characterized with well-expressed segmental structure in which the fragments of densely and loosely packed graphenes are stacked with regular order (Fig.1). The formation mechanism for such structures implies the determining role of chlorine species interacting with metallic active particles. More characteristics of segmented CNF examined by Raman, BET and XPS will be provided in presentation. Also, the possible application of the segmented CNF as a component for the template synthesis of CNF/PE (PE - polyethylene) composites will be discussed in detail.

The work is supported by Russian Foundation for Basic Research (Project 18-29-19053 mk).

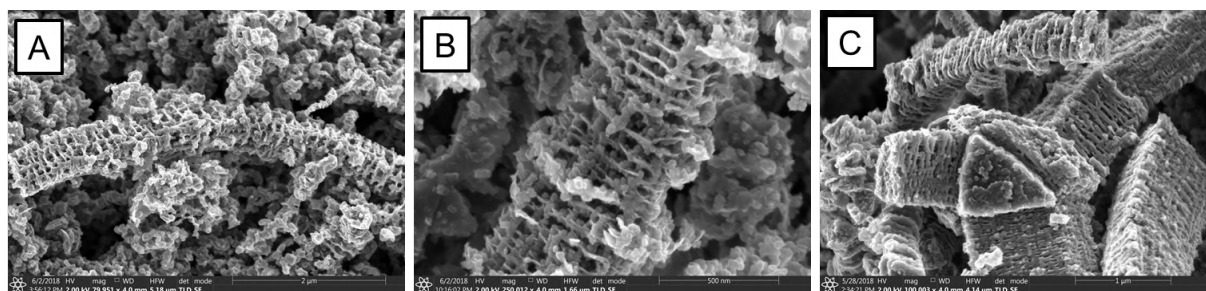


Fig.1. FESEM micrographs of the segmented carbon filaments produced on self-organizing catalysts during H<sub>2</sub>-assisted decomposition of C<sub>2</sub>H<sub>4</sub>Cl<sub>2</sub> at 600°C: A - Ni-Cr(5%); B - Ni-Mo(8%); C - Ni-Pt(5%).

### References

1. Mishakov I.V., Vedyagin A.A., Bauman Y.I., Shubin Y.V., Buyanov R.A. Synthesis of Carbon Nanofibers via Catalytic Chemical Vapor Deposition of Halogenated Hydrocarbons: in book Carbon Nanofibers: Synthesis, Applications and Performance. – Nova Science Publishers, 2018, P.77.

## **A study of process of electroconductive nanofiller particles migration to polymer composite melt boundaries**

*Lebedev O.V.<sup>1,2,3</sup>, Mukhortov L.A.<sup>1,3</sup>, Ozerin A.N.<sup>1</sup>*

*oleg.lebedev@phystech.edu*

<sup>1</sup> Enikolopov Institute of Synthetic Polymer Materials, Russian Academy of Sciences, Moscow, Russia

<sup>2</sup> Center for Design, Manufacturing and Materials, Skolkovo Institute of Science and Technology, Moscow, Russia

<sup>3</sup> Moscow Institute of Physics and Technology, Dolgoprudny, Moscow Region, Russia

In this work, effect of nanoscale filler migration to the surface of the polymer composite in a melted state was investigated. This effect allowed controllably obtaining materials with desired electrophysical characteristics of the composite surface layer. The reasons behind the effect and effective methods of its diagnosis were studied.

The samples of composites based on polypropylene and filled with different types of carbon nanoparticles, particularly single- and multi-walled carbon nanotubes, graphite nanoplatelets, and electroconductive carbon black, were obtained via melt compounding for a wide range of values of the filler content in the composite. The obtained compounds were formed into plate-like samples in a fast-heated press-form at the temperature higher than PP melting temperature with subsequent instant cooling to room temperature. The electrical conductivity of the samples was measured to estimate the percolation threshold value for electrical conductivity in the composite material for each type of the filler.

The samples were melted again in the heated press-form and kept at a given temperature higher than PP melting temperature for a certain amount of time. During their stay in a melted state, their electrical conductance was continuously recorded. Series of kinetic curves were acquired for time-dependent sample electrical conductance for different filler types and filler content. After being held in a melted state, each sample demonstrated electrical conductivity level that was higher than one at the beginning of the heat treatment. Analysis of the filler type influence on the effective time of the melted samples conductance change was performed.

Thin surface layer removal test demonstrated that the high electrical conductance of the samples was provided solely by the surface layer of thickness  $< 10\mu\text{m}$ . That was attributed to the effect of migration of nanoparticles to the composite melt boundaries. Electron microscopy study of the samples structure in a solid phase before and after heat treatment demonstrated additional evidence of that effect.

Further studies of the influence of the melt temperature, matrix type, number of cycles of melting and cooling, etc. were conducted.

A numerical model was proposed to help developing an analytical model describing the process of nanofiller migration to the composite material surface based on the data of electrical conductance measurements.

*The reported study was funded by RFBR according to the research project № 18-29-19112*

## Effect of thermal treatment of reduced graphite oxide on its performance in Li-ion battery.

*Iurchenkova A.A.*<sup>1</sup>, *Fedorovskaya E.O.*<sup>1,2</sup>

*anna.yurchenkova@yandex.ru*

<sup>1</sup> Laboratory of hybrid materials for electrochemical energy storage devices, Novosibirsk State University, 630090, Novosibirsk. 1, Pirogova str., Russia

<sup>2</sup> Physics & Chemistry of nanomaterials laboratory, Nikolaev Institute of Inorganic Chemistry, SB RAS, 630090, Novosibirsk, 3, Acad. Lavrentiev Ave., Russia

Reduced graphite oxide as well as many other carbon nanostructures (carbon nanotubes, graphene, etc.) is promising for production and improvement of electrochemical energy storage devices, such as supercapacitors and Li-ion batteries.

In lithium-ion batteries, carbon nanostructures are used as anode material due to the ability to intercalate and coordinate  $\text{Li}^+$  ions between carbon layers. In this case,  $\text{Li}^+$  ions coordination is made by six carbon atoms of the crystal lattice and the formation of the intercalate with  $\text{LiC}_6$  composition occurs. Materials which are able to intercalate  $\text{Li}^+$  ions between layers are of great interest for Li-ion batteries. That is defined by specific surface area of the material, presence of the functional groups able to coordinate  $\text{Li}^+$  ions and diffusion rate of  $\text{Li}^+$  ions in the anode material. Various organic solvents containing organic salt and Li ions can be used as electrolytes. Li-ion batteries of the above-mentioned structure have the following advantages: high capacities, low self-discharge degree and little explosiveness.

In this work, graphite oxide was synthesized by modified Hummers method as precursor for reduced graphite oxide (RGO) synthesis. Then RGO was synthesized by graphite oxide in sulfuric acid medium within a week. Further, RGO was thermally expanded at  $250^\circ\text{C}$  (RGOTE-250) and thermally treated at  $500^\circ\text{C}$  (RGO-500),  $600^\circ\text{C}$  (RGO-600) and  $700^\circ\text{C}$  (RGO-700) for the selective removal of the oxygen-containing functional groups. Active material with conducting additive and PVDF in N-methylpyrrolidone (NMP) was applied on copper foil and dried in the vacuum oven under  $80^\circ\text{C}$  within 12 hours. The foil was cut to electrodes and models of batteries were made in the argon glovebox. Metallic lithium plates were used as cathode and 1M solution of  $\text{LiPF}_6$  in dimethyl carbonate and ethyl carbonate mixture (1:1) was prepared as electrolyte.

The obtained samples were studied by scanning electron microscopy (SEM), high-resolution transmission electron microscopy (HR TEM), IR-spectroscopy, Raman spectroscopy, charge-discharge cycling, cyclic voltammetry and electrochemical impedance spectroscopy methods. It was shown, that the synthesized materials are a promising for use in Li-ion battery due to the synchronous intercalation and coordination processes proceeding. The work was supported by Russian Federation President Fund (project № MK-712.2019.3).

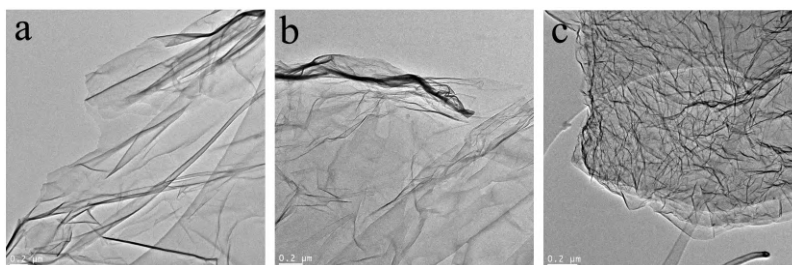


Fig.1.HR TEM images of RGO samples (a) RGOTE-250, (b) RGO-500, (c) RGO-600.

## Hyperbranched polyglycerol modified carbon nanomaterials

*Ivanova M.K.*<sup>1</sup>, *Babenya J.S.*<sup>1,2</sup>, *Garashchenko B.L.*<sup>1</sup>, *Burakova I.V.*<sup>3</sup>, *Burakov A.E.*<sup>3</sup>, *Melezhyk A.V.*<sup>3</sup>, *Yakovlev R.Y.*<sup>1</sup>

yarules@yandex.ru

<sup>1</sup> Vernadsky Institute of Geochemistry and Analytical Chemistry of Russian Academy of Sciences, Moscow, Russia

<sup>2</sup> Dmitry Mendeleev University of Chemical Technology of Russia, Moscow, Russia

<sup>3</sup> Department of Technology and Methods of Nanoproducts Manufacturing, Tambov State Technical University, Tambov, Russia

Modification of the surface of carbon nanomaterials (CN) can directionally change their properties. It is known that the presence of highly biocompatible hydrophilic materials such as glycidol can increase the solubility of CN in water, reduce their hydrophobicity, aggregation, size and make them biocompatibility [1-3]. Modification CN surface hydrophilic with polymer creates adsorption centers for fixing different ligands and radionuclides [1,2]. At the same time, modified nanodiamonds (ND) can stably disperse in the physiological solution that solves the problem of their aggregation and colloidal stability [3].

The purpose of the work was to obtain and characterize hyperbranched polyglycerol modified CN by glycidol (CN-glycidol) suitable for biomedical applications. In this work multi-walled carbon nanotubes (MWNT) and graphene oxide (GO) produced by "NanoTechCenter" Ltd (Tambov), and detonation nanodiamonds (ND) produced by SKTB "Tekhnolog" (St. Petersburg) were used. Modification of CN was carried out at 140 °C in CH<sub>3</sub>OH/glycidol for 6-24 h. For MWNT, carboxylation was carried out (H<sub>2</sub>SO<sub>4</sub>/HNO<sub>3</sub> = 3:1, 100 °C, 6 h). Samples were investigated by FTIR and Raman spectroscopy, TGA/DSC, XRD, XPS, DLS methods.

After modification the amount of oxygen on the ND surface increased from 8 to 33% at., which corresponds to the multilayer coverage of the surface of ND (270 m<sup>2</sup>/g) and creation of hyperbranched structure on its. The size of ND-glycidol in hydrosol is about 20-30 nm. Hydrosol was stable throughout the study period. It was shown that the beginning of decomposition of glycidol on the surface of ND occurs at 200 °C with a 45% weight loss of the sample, which correlated with an increase in the mass of ND after modification by 50%. All the diffractograms of CN-glycidol samples presented a new wide maximum that appeared at 2θ = 21° due to hyperbranched polyglycerol phase. There was a significant increase in oxygen on MWNT-glycidol surface to 22% at. The destruction of the organic layer of MWNT-glycidol similarly with ND started from 200 and ended at 370 °C. The size of the aggregated MWNT-glycidol nanofibers in water increased from 50 (MWNT-COOH) to 150 nm in the presence of a small fraction of micron particles. The oxygen content in GO did not change after modification and remained at a level of 30% at. It was noted that GO-glycidol had a greater thermal stability of the grafted layer compared to other CN and onset temperature of destruction started at 220 °C (mass loss of 59% wt.). GO-glycidol plates size changed from 2 nm to 100 nm, which may be due to the folding of graphene sheets into globules. Synthesised hyperbranched polyglycerol modified carbon nanomaterials can be effective sorbents of radionuclides used in medicine and promising carriers of drugs.

This work is supported by the Russian Science Foundation (project № 18-13-00413).

### References

1. H. Cai, D. Hou, L. Shen, X. Luo, Y. Xue, F. Yu, Functionalization of graphene with hyperbranched polyglycerol for stable aqueous dispersion. *Funct Mater Lett* (2015) 8(06), 1550068.
2. M. Adeli, N. Mirab, M.S. Alavidjeh, Z. Sobhani, F. Atyabi, Carbon nanotubes-graft-polyglycerol: biocompatible hybrid materials for nanomedicine. *Polymer* (2009) 50(15), 3528.
3. J.P. Boudou, M.O. David, V. Joshi, H. Eidi, P.A. Curmi, Hyperbranched polyglycerol modified fluorescent nanodiamond for biomedical research. *Diam Relat Mater* (2013) 38, 131.

## Graphene nanostructures synthesized by self-propagating high-temperature synthesis and their application as an additive in polymer and metal composites.

Kidalov S.V.<sup>1</sup>, Vozniakovskii A.A.<sup>1</sup>, Vozniakovskii A.P.<sup>2</sup>

*alexey\_inform@mail.ru*

<sup>1</sup> Ioffe Institute, St.Petersburg, Russia

<sup>2</sup> Institute of Synthetic Rubber, Saint-Petersburg, Russian Federation

Carbon nanomaterials, in particular, graphene nanostructures (GNS) are actively used by researchers in the creation of metal and polymer composite materials. Using even small (from 0.5 wt.% additive) amounts of GNS, researchers can significantly improve the mechanical and thermal properties of the starting materials. However, the existing methods for the synthesis of GNS are not capable of producing large volumes of material at an affordable price. The high cost of GNS, as well as the dependence of the final properties of the composite on a variety of factors (sample preparation, uniform distribution of the additive), limits the use of GNS in the creation of composites.

In this paper, GNS were synthesized under the conditions of the method of self-propagating high-temperature synthesis. The obtained GNS were used as an additive when creating a composite based on nitrile-butadiene rubber. Figure 1 shows the results of the study of tensile strength and thermal conductivity, depending on the concentration of GNS. As can be seen from Figure 1, the addition of GNS has allowed twisting the ultimate strength and thermal conductivity of rubber up to 2 times. Also, GNS were used as an additive in the creation of an aluminum composite, which also made it possible to improve its strength and thermal properties.

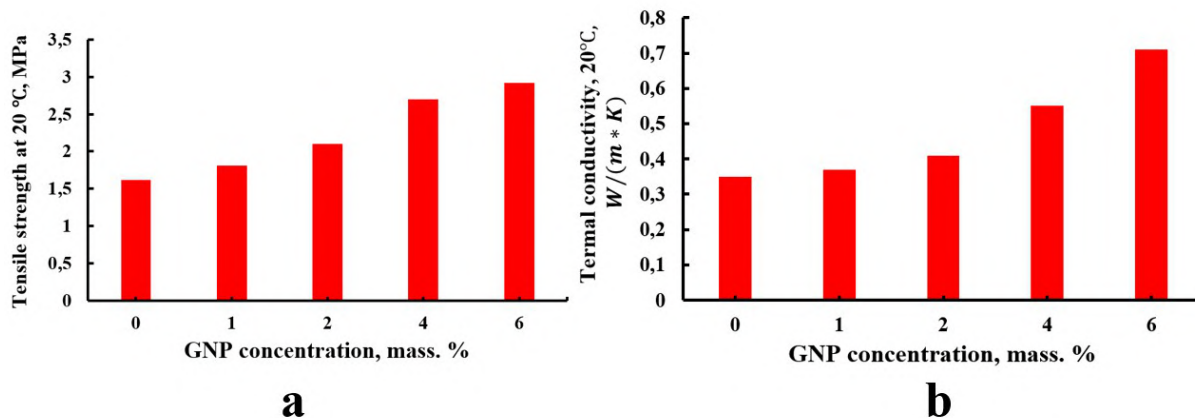


Figure 1. tensile strength (a) and thermal conductivity (b) of the composite material composition of budditadiene-nitrile rubber - GNS.

## On manifestation & physics of the Kurdjumov and spillover effects in carbon nanostructures, under intercalation of high density hydrogen

*Nechaev Yu.S.<sup>1</sup>, Alexandrova N.M.<sup>1</sup>, Shurygina N.A.<sup>1</sup>, Cheretaeva A.O.<sup>1</sup>*

*yuri1939@inbox.ru*

<sup>1</sup> Bardin Central Research Institute for Ferrous Metallurgy, Kurdjumov Institute of Metals Science and Physics, Moscow, Russia

Based on the approaches and results [1-3], experimental evidence and thermodynamics of the self-intercalation of high-density gaseous molecular hydrogen ( $\rho_{\text{H}_2} \approx 0.045 \text{ g/cm}^3$ , at 300 K) into surface nanoclusters in highly oriented pyrolytic graphite and epitaxial graphene, as well as the self-intercalation of high density solid molecular hydrogen into graphite nanofibers (Fig. 1) are considered, with regard to the problem of compact and efficient hydrogen on-board storage [1, 4]. The manifestation and physics of the Kurdjumov and spillover effects in carbon nanostructures, under self-intercalation of high density hydrogen, are discussed.

Perspectives of a further development of results [1-4] are considered, as well.

### Acknowledgements

*This work was financially supported by the RFBR (Project # 18-29-19149 mk).*

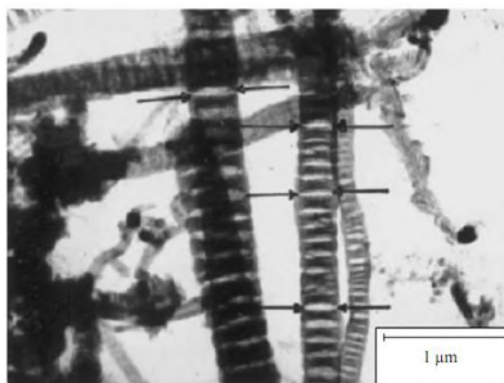


Fig. 1 (from [3]). Micrograph of graphite nanofibers (GNFs) with Pd-catalyst (hydrogenated at 300 K and initial pressure of molecular hydrogen  $P_{\text{H}_2} \approx 8 \text{ MPa}$ ), after release from them of the intercalated solid  $\text{H}_2$  nanophase (17 mass. %) of a high density of  $\rho_{\text{H}_2} \approx 0.5 \text{ g/cm}^3$  (analysis [2, 3]). The arrows in the picture indicate some of the slit-like closed nanopores of the lens shape, where the solid  $\text{H}_2$  intercalated nanophase (under pressure of  $\sim 50 \text{ GPa}$ ) was localized. Such a pressure level can be also evaluated by the consideration of the material deformation and necessary stresses for forming the lens shape nanopores.

### References

1. S. Nechaev, A. Yurum, A. Tekin, N.K. Yavuz, Yu. Yurum, T.N. Veziroglu. *Amer. J. Anal. Chem.* (2014) **5**, 1151.
2. S. Nechaev, T.N. Veziroglu. *Int. J. Chemistry* (2015) **7**, 207.
3. S. Nechaev, T.N. Veziroglu. *Int. J. Phys. Sciences* (2015) **10**, 54.
4. S. Nechaev, V.G. Makotchenko, M.B. Shavelkina, M.Yu. Nechaev, A. Veziroglu, T.N. Veziroglu. *Open J. Energy Efficiency* (2017) **6**, 73.

## Composite material aluminum-carbon nanotubes with high hardness and controllable thermalconductivity.

*Kidalov S.V.*<sup>1</sup>, *Vozniakovskii A.A.*<sup>1</sup>, *Kol'tsova T.S.*<sup>2</sup>, *Tkachev A.G.*<sup>3,4</sup>, *Aladinskii A.A.*<sup>4</sup>

*Kidalov@mail.ioffe.ru*

<sup>1</sup> Ioffe Institute

<sup>2</sup> Peter the Great St. Petersburg Polytechnic University

<sup>3</sup> Tambov State Technical University

<sup>4</sup> NanoTechCenter LTD

Aluminum is widely used in modern industry as a structural material because of its low density. However, it is not without a number of shortcomings such as low hardness and strength. The high thermalconductivity of aluminum can be an advantage (heat sink) and a disadvantage (insulator). In this work, we solve a problem to investigate a possibility to improve the strength properties of aluminum composite with a controllable thermalconductivity while maintaining the low density of aluminum.

To solve these problems, we used an original approach of creating a composite material, namely the growth of carbon nanotubes (CNT) on the surface of the catalyst-coated aluminum particles using catalytic chemical vapor deposition method. CNT concentration was 1 wt. %. The resultant material was sintered at a pressure of 2-5 GPa at a temperature of 600-1500°C and at a processing time of 15-600 seconds.

The resulting samples of composite material aluminum-CNT have a density of 2.7 g/cm<sup>3</sup>, hardness 55-60 HB and controllable thermalconductivity of 50-150 W/(m\*K). We found, that the key parameters affecting the properties of the composite material are the temperature and holding time during hot pressing due to increase/decrease the speed of the chemical reactions between the aluminum and CNT [1].

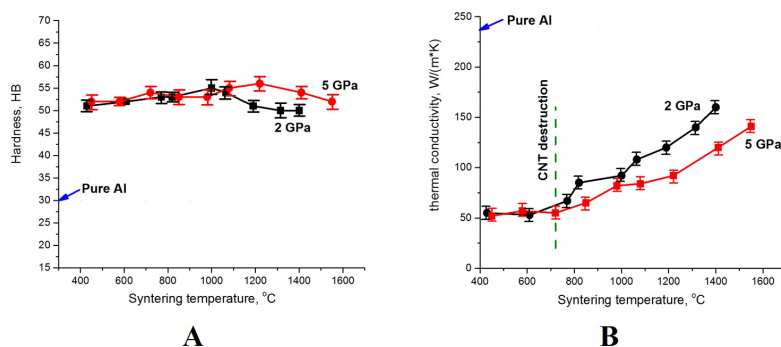


Figure 1. Dependence of the hardness (A) and thermalconductivity (B) of composite materials compacted at pressures of 5 GPa and 2 GPa for 60 s depending on the sintering temperature. The red curve (circles are experimental points) at 5 GPa, the black curve (squares are experimental points) at 2 GPa. The blue arrows show the reference values of the hardness and thermal conductivity of pure aluminum.

### References

1. AA Vozniakovskii, SV Kidalov, TS Kol'tsova, Development of composite material aluminum-carbon nanotubes with high hardness and controlled thermal conductivity, *Journal of Composite Materials*, 2019, <https://doi.org/10.1177/0021998319829894>



## Features of ethanol pyrolysis for synthesis of carbon nanostructures

*Simunin M.M.*<sup>1</sup>, *Minakov A.V.*<sup>2</sup>, *Vyatkin A.S.*<sup>1</sup>, *Mishnev M.O.*<sup>1</sup>, *Ryzhkov I.I.*<sup>2</sup>

*michanel@mail.ru*

<sup>1</sup> Siberian Federal University, Svobodny 79, 660041 Krasnoyarsk, Russia

<sup>2</sup> Institute of Computational Modelling SB RAS, Akademgorodok 50/44, 660036 Krasnoyarsk, Russia

Advanced carbon nanostructures have a great potential in nanotechnology and composite materials. Such structures, in particular, include carbon nanotubes and graphene layers. Either carbon nanotubes or graphene layers can grow on the surface depending on its shape and physical-chemical properties. As a rule, the materials of such surfaces are the most common metals of auxiliary groups [1], in which the carbon is dissolved after chemical deposition from the gas phase. Then, as a result of supersaturation of carbon solution in metal, the carbon precipitates on the surface in the form of graphite islands, which combine into graphene or nanotubes. Besides, the ordered carbon structures can be obtained not only by dissolving carbon in metals, but also by using special surfaces, where the surface diffusion of carbon can occur. Aluminum oxide provides an example of such material [2]. In CVD, it is important to understand by what scheme the pyrolysis reaction of the carbon source will go. This understanding will lead us to the possibility of designing industrial processes, predicting the yield of the main product and the importance of parasitic and side processes.

The work investigates the process of ethanol pyrolysis. In the simulation environment Ansys Fluent, a 2D model of ethanol pyrolysis in a cylindrical furnace was developed on the basis of [3], including the 57 components of the 383 participating reactions accompanying the pyrolysis process in the temperature range from 500 to 1200 °C. The behavior of the main 13 components resulting from the pyrolysis of ethanol was analyzed. It was found that at low temperatures, the amount of aldehydes grows, but after 800 °C their concentration drops sharply and at high temperatures they are no longer observed as pyrolysis products. At low temperatures, carbon monoxide is the most representative source of carbon; however, above 650 °C carbon nanostructures are formed from hydrocarbons. The key role in this process is played by the formation of ethylene [4] during the pyrolysis of ethanol, which itself actively participates in the formation of carbon structures on the surface. At temperatures above 900 °C, the output of methane begins to grow actively, therefore becoming a carbon source. In addition, an increase in the yield of hydrogen with the increase in temperature is found. At temperatures above 1000 °C, it plays the role of an environment that oxidizes methane to a fraction of non-stable carbon fractions in the pyrolysis product.

The data obtained allow us to evaluate the patterns of carbon deposition [5] when compounding nanomaterials, determine the causes and patterns of low-ordered carbon phases removal, and also generally simulate the mass transfer process during ethanol pyrolysis.

The work is supported by the Russian Foundation for Basic Research Grant № 18-29-19078

### References

1. M. Mubarak, E.C. Abdullah, et al // J. of Ind.& Eng. Chem. 20 (2014) 1186-1197
2. Pang J., Bachmatiuk A., Ibrahim I. et al // J Mater Sci. 2016. V. 51. P. 640-667.
3. Marinov, N.M, // Int. J. Chem. Kinet. 31:183-220 (1999)
4. V.Anoshkin; A.G. Nasibulin,; et al // Carbon 2014, 78, 130-136.
5. S. Solodovnichenko, M.M. Simunin et al // Thermochemica Acta, V. 675, 2019. Accepted, in press.

## Highly active, MOF-derived nickel/carbon catalysts for nitroarene reduction

Martin-Jimeno F.J.<sup>1</sup>, Suarez-Garcia F.<sup>1</sup>, Paredes J.I.<sup>1</sup>, Martinez-Alonso A.<sup>1</sup>, Tascon J.M.D.<sup>1</sup>

tascon@incar.csic.es

<sup>1</sup> Instituto Nacional del Carbon, INCAR-CSIC, F. Pintado Fe 26, 33011 Oviedo, Spain

The development of highly active and selective catalysts based on non-noble metals is currently a subject of intense research. In order to achieve a high catalytic activity, very small sizes and a homogeneous dispersion of the metal nanoparticles are needed. The preparation of Ni/carbon hybrid materials with a high catalytic activity is reported here.

The catalysts were obtained by carbonization of an organometallic compound formed by coordination between nickel acetate (Ni(OAc)) and 2-methyl-imidazole (2mIm). This organometallic framework was prepared by reaction between the two precursors at 90 °C. After 30 min of reaction, the solid formed was recovered by centrifugation and carbonized at different temperatures between 400 and 1000 °C under N<sub>2</sub> atmosphere. We tested the catalytic activity of these materials in the reduction reaction of 4-nitrophenol (4-NP) to 4-aminophenol (4-AP) with NaBH<sub>4</sub> as the reducing agent.

As expected, both the size of the Ni nanoparticles and the total metal content increase with increasing carbonization temperature. Thus, Ni content ranges from 35.8 to 75.5 wt.% for samples carbonized at 400 and 1000 °C, respectively. Despite these very high metallic contents, the average particle sizes, determined by measuring more than 1000 particles in TEM images, varied between 4 and 37 nm.

Kinetics of the reduction reaction of 4-NP to 4-AP catalyzed by these Ni/carbon composites exhibited a pseudo-first order behavior and a high apparent reaction rate constant ( $k'$ ). In particular, the sample carbonized at 400 °C exhibited the fastest kinetic behavior [ $k' = 0.186 \text{ L}\cdot\text{g}^{-1}\cdot\text{s}^{-1}$  ( $k'' = 0.521 \text{ L}\cdot\text{g}_{\text{Ni}}^{-1}\cdot\text{s}^{-1}$ )]. Kinetic parameters decreased for samples prepared at 500 and 600 °C. However, they increased for the sample carbonized at 700°C and then decreased again for samples treated at higher temperatures. Thus, two linear trends were noticed for the reaction kinetics as a function of carbonization temperature (from 400 to 600 and from 700 to 1000 °C). Reaction kinetics was affected by the amount of catalyst and the nanoparticle size. Thus, increasing the particle size, the rate constant should decrease due to the lower specific surface area of the catalyst. On the other hand, increasing the amount of Ni, a fastest kinetics should be expected. However, these facts cannot explain the difference in activity between the samples prepared at 400 ( $k'' = 0.521 \text{ L}\cdot\text{g}_{\text{Ni}}^{-1}\cdot\text{s}^{-1}$ ) and 600 °C ( $k'' = 0.153 \text{ L}\cdot\text{g}_{\text{Ni}}^{-1}\cdot\text{s}^{-1}$ ) or between the latter and the sample prepared at 700 °C ( $k'' = 0.295 \text{ L}\cdot\text{g}_{\text{Ni}}^{-1}\cdot\text{s}^{-1}$ ), since Ni content and average particle size are 35.8, 44.2, 50.5 wt.% and 3.8, 7.3 and 7.5 nm for samples prepared at 400, 600 and 700 °C, respectively.

A possible explanation was obtained from X-ray diffraction studies. The sample prepared at 400 °C exhibited a peak at 44.75°, identified as rhombohedral Ni<sub>3</sub>C. Samples prepared at 500 and 600 °C, besides the peaks assigned to the face-centered cubic (fcc) structure of Ni, showed two other peaks centered at 41.90 and 47.60°, which are attributed to an intermediate phase in the decomposition from rhombohedral Ni<sub>3</sub>C to fcc-Ni and identified as a hexagonal close packed (hcp) form. In samples prepared beyond 700°C only the fcc-Ni structure was observed in the diffractograms. Therefore, the two tendencies observed in the reaction kinetics may be due to the different catalytic activities of nickel nanoparticles with different crystalline structures.

We acknowledge funding through grant MAT2015-69844-R (Spanish MINECO and ERDF). We also acknowledge partial funding from Principado de Asturias and ERDF through grant IDI-2018-000233.

## Low-field electron emission from carbon cluster films: combined thermoelectric/hot-electron model of the phenomenon

*Arkhipov A.V.*<sup>1</sup>, *Eidelman E.D.*<sup>1,2,3</sup>, *Zhurkin A.M.*<sup>1</sup>, *Osipov V.S.*<sup>1</sup>, *Gabdullin P.G.*<sup>1</sup>

*arkhipov@rphf.spbstu.ru*

<sup>1</sup> Peter the Great St. Petersburg Polytechnic University, St. Petersburg, Russia

<sup>2</sup> Physics dept., St. Petersburg Chemical Pharmaceutical University, St. Petersburg, Russia

<sup>3</sup> Ioffe Physico-Technical Institute RAS, St. Petersburg, Russia

Various forms of nanostructured carbon are known to possess the capability of cold electron emission in electric field with low macroscopic magnitude ( $\sim 1$  V/mm), even the ones having smooth (or relatively smooth) outer surface [1, 2]. Our previous experiments [3, 4] have demonstrated that, among others, this property is also inherent in one of the simplest form of nanocarbon - thin  $sp^2$ -carbon island (nanocluster) films deposited on Si wafers.

We consider a new model of the phenomenon of low-external-field electron emission by carbon islands (nanoclusters) deposited on crystalline substrates. The model is based on the assumption that, while emission occurs, the film is substantially non-equipotential. Emission centers (ECs) are associated with carbon clusters having the highest potentials, which are surrounded by other islands with potentials lower by a few Volts. Tunneling of charge carriers into the ECs produces there a population of hot electrons capable of overcoming the surface potential barrier. Before emission, these electrons may leave a part of their excessive energy in the ECs in the form of heat. Dissipating into the substrate, this heat produces thermoelectric effect (phonon-induced drag) removing from the EC some number of thermalized electrons. This provides a qualitative explanation to the origin of potential non-uniformity of the emitting surface and the mechanism of its steady-state maintenance.

In this report, we present elements of theoretical description of the considered emission mechanism and its numerical simulations performed for typical experimental conditions. The study has demonstrated that the energy spent in the modelled system for electron emission and EC heating has its eventual source in the external electric field fed by the anode power supply. The requirements to physical characteristics of the system (such as the thermoelectric coefficient, hot-electron relaxation rate, etc.) were determined and found to be plausible. The analysis performed in the framework of the suggested emission model had also showed that the specific electronic structure of  $sp^2$ -carbon probably makes it the most beneficial EC material for achievement of low-field electron emission from cathodes with smooth vacuum boundary.

The study was supported the Russian Science Foundation (project No. 19-19-00631) and by the RF State Assignment in science activity for universities (project No 3.5469.2017).

### References

1. G. Forbes, *Sol. St. Electron.* (2001) **45**, 779.
2. S. Xu, and S. Ejaz Huq, *Mater. Sci. Eng. R-Rep.* (2005) **48**, 47.
3. V. Arkhipov, P. G. Gabdullin, S. K. Gordeev, A. M. Zhurkin, and O. E. Kvashenkina, *Tech. Phys.* (2017) **62**, 127.
4. A. Andronov, E. Budylyna, P. Shkitun, P. Gabdullin, N. Gnuchev, O. Kvashenkina, and A. Arkhipov, *J. Vac. Sci. Technol. B* (2018) **36**, 02C108.

## Study of the surface of polymer composites based on carbon nanostructures using the Raman mapping method

*Dyachkova T.P.*<sup>1</sup>, *Tkachev A.G.*<sup>1</sup>, *Yagubov V.S.*<sup>1</sup>, *Gutnik I.V.*<sup>1</sup>, *Nagdaev V.K.*<sup>1</sup>, *Burakova E.A.*<sup>1</sup>, *Tugolukov E.N.*<sup>1</sup>, *Maksimkin A.V.*<sup>2</sup>

*dyachkova\_tp@mail.ru*

<sup>1</sup> Tambov State Technical University, Tambov, Russia

<sup>2</sup> National University of Science and Technology MISIS, Moscow, Russia

Modifiers based on various polymorphic forms of nanocarbon attract researchers as additives that can improve thermal and electrical conductivity, thermal stability, mechanical and tribological properties of polymer composites. However, the agglomeration phenomena observed with the introduction of carbon nanotubes (CNT) and graphene nanoplates (GNP) into polymer matrices, markedly reduce the efficiency of their application. To solve this problem, at present, various methods of functionalizing the surface of carbon nanostructures are most often used. Another promising direction is the use of the synergy effect observed when CNT, GNP, and carbon black (CB) are used together as part of polymer composites. In any case, the manifestation of one or another effect contributes to the formation of an ordered structure of a nano-modifier in the bulk and surface layer of the composite. One of the tools for establishing the mechanism of the effect of carbon nanomaterials on the mechanical properties and electrical conductivity of polymers is Raman mapping.

The Raman spectra of CNT, GNP, and CB contain characteristic peaks characterizing the presence of an ordered graphene phase (G and 2D) and defects (D). The orientation and location of individual units of a nano-modifier in the surface layer of a composite depend on the nature of the polymer matrix, the method of functionalization and dispersion of the individual or mixed carbon material. By analyzing the Raman maps, one can determine the presence and morphology of the ordered structure of the nano-modifier, the nature of the mutual orientation of the individual components relative to each other.

It was found that polymer composites containing cylindrical CNT and CB with thin linearly parallel ordered structures of carbon nanotubes in the surface layer have the maximum electrical conductivity. At the same time, CB particles obviously perform a stabilizing function.

Composites based on ultrahigh molecular weight polyethylene and functionalized polyaniline GNP with high tensile strength [1] are characterized by the presence of relatively evenly arranged agglomerates in the surface layer. Moreover, the carbon component is practically not manifested. On the Raman spectra with a wavelength of an irradiating laser equal to 633 nm, there are peaks characteristic of the emeraldine salt of polyaniline. It is this component that forms the diffuse structure in the surface layer of the composite. The relationship between the concentration of the nano-modifier, the density of the structure formed in the surface layer of the composite and the manifestation of mechanical properties is established.

Thus, Raman surface mapping allows us to establish the mechanism of interaction of carbon nanomaterials with macromolecules of polymers and to predict the effect of the parameters of the emerging ordered structures on the properties of composites.

The work was funded by the Ministry of Science and Higher Education of the Russian Federation in the framework of the Federal Target Program "Research and Development in Priority Areas of Advancement of the Russian Scientific and Technological Complex for 2014-2020" (Agreement No. 14.577.21.0253, Unique Identification Number: RFMEFI 57717X0253).

### References

1. Dayyoub, A.V. Maksimkin, S. Kaloshkin, E. Kolesnikov, D. Chukov, T. P. Dyachkova, I. Gutnik, *Polymers* (2019) **11**, 23.

## Electrochemical synthesis of graphene in supercritical electrolyte

*Nikiforov A.A.*<sup>1</sup>, *Xu X.*<sup>2</sup>, *Kapitanova O.O.*<sup>2</sup>, *Kondratenko M.S.*<sup>1</sup>

*nikiforov.aa16@physics.msu.ru*

<sup>1</sup> Faculty of Physics, Lomonosov Moscow State University, Moscow, Russia

<sup>2</sup> Faculty of Chemistry, Lomonosov Moscow State University, Moscow, Russia

Graphene attracts enormous research interest because of its exceptional electrical and mechanical properties which can be widely used in electronics and electrochemical energy storage in particular. For graphene production a chemical oxidation by strong inorganic oxidizers is generally used [1]. The technique requires, however, a lot of resources and time, it is not environmentally friendly, and one needs to wash out acids from the product that leads to additional expenses. Electrochemical methods, based on the intercalation of ions from aqueous [2] and non-aqueous [3] electrolytes and the subsequent graphite exfoliation, are cleaner and allow to make the synthesis faster, but they also require washing out the residual electrolytes from the product. To eliminate washing step, a physical way of supercritical exfoliation of graphite (e.g. by rapidly depressurizing) is applied, however this approach usually has a low yield [4]. Thus, there is currently no fast and efficient method for graphene synthesis, and the search of such a method is of a great importance.

We propose to combine physical and electrochemical approaches and try to synthesize graphene using an electrochemical oxidation in a supercritical electrolyte. Due to the synergy of the combined approaches the process of graphene synthesis is expected to become more efficient.

To realize the proposed way, the mechanism of the electrochemical intercalation of ions into graphite from supercritical fluid was studied. For this purpose highly orientated pyrolytic graphite was used as an electrode and tetrabutylammonium tetrafluoroborate in acetonitrile/ $\text{CO}_2$  solution in supercritical state was used as an electrolyte in this work. The intercalation of tetrafluoroborate anion ( $\text{BF}_4^-$ ) was carried out potentiostatically. The degree of intercalation was determined using Raman spectroscopy and X-ray diffraction. The possibility of intercalation of ( $\text{BF}_4^-$ ) anions into graphite from supercritical electrolyte has been shown for the first time.

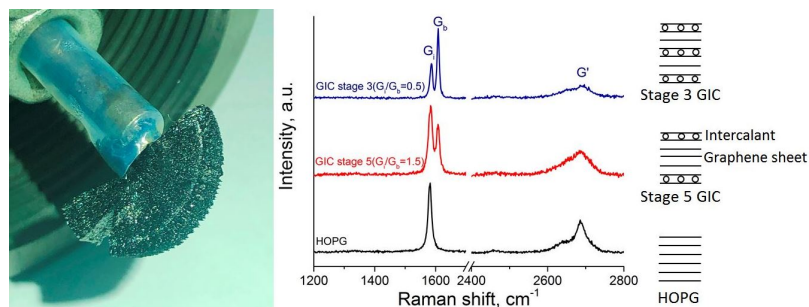


Fig. 1. (left) Optical image of HOPG sample after the intercalation of ( $\text{BF}_4^-$ ) (GIC) and (right) Raman spectra of graphite before and after intercalation at different potentials. Examples of stage 3 and stage 5 GIC structure are shown.

### References

1. He P., Gu H., Wang G., Yang S., Ding G., Liu Z., Xie X. *Chem. Mater* (2017) **29**, № 20. P. 8578.
2. Yu L., Yasuda S., Murakoshi K. *Trans. Mat. Res. Soc. Japan* (2012) **212**. P. 209.
3. Cooper A.J., Wilson N.R., Kinloch I.A., Dryfe R.A.W. *Carbon* N. Y. Elsevier Ltd (2013) **66**. P. 340.
4. Pu N., Wang C., Sung Y., Liu Y., Ger M. *Mater. Lett. Elsevier B.V.* (2009) **63**, № 23. P. 1987.

## **Polymer composites with high electrical conductivity filled by reduced graphene oxide/carbon nanoparticle (CNT, carbon black) blends**

*Shiyanova K.A.*<sup>1</sup>, *Gudkov M.V.*<sup>1</sup>, *Anosov A.A.*<sup>1</sup>, *Koval V.S.*<sup>1</sup>, *Gorenberg A.Ya.*<sup>1</sup>, *Bedin S.A.*<sup>2</sup>, *Melnikov V.P.*<sup>1</sup>

*shyanovakseniya@mail.ru*

<sup>1</sup> Semenov Institute of Chemical Physics of Russian Academy of Sciences, Moscow, Russia

<sup>2</sup> Moscow Pedagogical State University, Moscow, Russia

This work deals with polymeric electroconductive composites with segregated structure, i.e. with wittingly non-uniform distribution of filler, based on the reduced graphene oxide are considered. Interest in such materials is caused by a possibility of achievement of high values of an electrical conductivity with use of low loadings of electroconductive filler. The idea of a composite with the segregated structure is drawing a thin electroconductive layer on powder particles of a polymer with the subsequent hot pressing at which electroconductive layers unite in uniform network [1]. This approach differs from the traditional ones when the electroconductive filler is uniform distributed in a polymer matrix and the conduction of a composite begins to be shown when the filler content is above a percolation threshold which depends on many parameters.

As the graphene oxide (GO) is a good film-former and contains a huge number of the polar oxygen-containing groups promoting good adhesion of GO to a surface of powder particles of polymer on a surface of particles, it is applied on a surface of these particles in the form of a thin covering of nanodimensional thickness. The method which is based on preparation of aqueous-alcoholic dispersion of GO, introduction to this dispersion of powder of polymer and the following evaporation of a liquid phase on the rotor evaporator, was used for covering. This technique allows to easily carry out drawing a filler on polymer particles, to regulate a mass fraction of graphene oxide in total material and also to change covering thickness on each single particle of polymer powder. After covering powder within several hours was processed with vapors of hydrazine at a temperature of 100 °C, which provided transition of graphene oxide to the reduced graphene-like form and gave to a cover on polymer particles an electrical conductivity and it is hot pressed with set pressure value into target material. Carbon nanotubes (CNT) and carbon black (CB) were entered at the stage of preparation of aqueous-alcoholic dispersion together with GO by a dispersion of the described components by means of ultrasonic processing by submersible ultrasonication. Ratios of GO/CNT and GO/CB were regulated by different weigh ratios. The general mass maintenance of excipients in material were changing from 0,1 to 2%.

This method is very attractive for receiving electroconductive polymeric composites as it allows reaching high values of an electrical conductivity of materials at ultra-small filler content. Besides, this method can be easily realized in the industry.

The study was carried out by a grant from the Russian Foundation of Basic Research (Project No. 16-29-06440 ofi\_m).

### **References**

1. Gudkov M.V., Ryvkina N.G., Gorenberg A.Ya., Melnikov V.P., Electroconductive nanocomposites of the segregated structure on the basis of fluoroplastic F-42 and the reduced graphite oxide, Reports of academy of sciences, 2016, volume 466, no. 1, page 1-3

## Morphology of aerogels based on graphene oxide and detonation nanodiamonds composites

*Trofimuk A.D.*<sup>1,2</sup>, *Rabchinskii M.K.*<sup>1</sup>, *Gudkov M.V.*<sup>3</sup>

*trofimuk.ad@mail.ioffe.ru*

<sup>1</sup> Ioffe Institute, St. Petersburg, Russia

<sup>2</sup> St. Petersburg State Institute of Technology, St. Petersburg, Russia

<sup>3</sup> Semenov Institute of Chemical Physics, Moscow, Russia

Supercapacitors are well known devices that are used in high energy density systems. The main advantages of supercapacitors are high energy capacity, high charging and discharging rates, large number of possible recharge cycles and small gabbarts [1]. The increase of the electrodes surface area is the crucial factor in the supercapacitors design. The most common way to reach this goal is obtaining electrodes on the based of high porous systems from nanoscale carbon-based objects [2]. High hopes are attached to supercapacitor electrodes manufactured from graphene-based aerogels because of its large specific surface area and the excellent electric conductivity, as well as chemical inertness. Graphene can be easily obtained from graphene oxide [3]. However, the main problem of the formation of graphene-based electrodes is stacking of graphene layers due to van der Waals forces. Stacking leads to significant surface reduction, which in turn leads to decrease in the capacitance of the supercapacitors [4].

One of the approaches to solve this problem is formation of porous material in which layers of graphene are separated by additional structure - spacer. Weak influence (or its complete absence) of these «pacer on electrical properties of graphene layers is crucial in this case. Furthermore, spacer must be stable in solid state and in solvents exhibit size of 4-10 nm and easy for functionalization. Detonation nanodiamonds (DND) satisfy all these parameters. Of course, study of morphology is the key point for understanding properties of this porous material.

Hereby we present results on our study of the of DND as a spacer for graphene aerogels obtained from graphene oxide. It is demonstrated that GO can be easily grafted with DND nanoparticles with positive zeta potential. Subsequently obtained aerogels form this composite demonstrate higher specific surface area in comparison to pure GO. Furthermore, it is demonstrated that the morphology and specific area value of the obtained aerogels are dependent on the volume of the added DND nanoparticles. Particularly, the increase of the DND fraction results in higher rate of GO layers twisting as is demonstrated by SEM images. Collectively, the obtained results suggest that GO-DND aerogels have high perspectives to be used as supercapacitor electrodes.

The presented work was financially supported by the Russian Foundation for Basic Research (grant no. 18-29-19159).

### References

1. González A., Goikolea E., Barrena J. A., Mysyk R. *Renewable and Sustainable Energy Reviews*, Elsevier (2016) **58 (C)**, p. 1189.
2. Pandolfo A.G., Hollenkamp A.F. *Journal of Power Sources* (2006) **157**, 11.
3. G. Guex, B. Sacchi, K. F. Peuvot, R. L. Andersson, A. M. Pourrahimi, V. Ström, S. Farrisd, R. T. Olsson, *Nanoscale* (2017), **9(27)**, p.9562.
4. Yin Sh., Zhang Ya., Kong J., Zou Ch., Li Ch. M., Lu X., Ma J., Boey F. Y. Ch., Chen X. *ACS Nano* (2011), **5 (5)**, p.3831.

## Electrical resistance analysis of aerogels based on reduced graphene oxide during compression

*Anosov A.A.*<sup>1</sup>, *Koval V.S.*<sup>1</sup>, *Shiyanova K.A.*<sup>1</sup>, *Gudkov M.V.*<sup>1</sup>, *Melnikov V.P.*<sup>1</sup>

*andrew\_anosov.95@mail.ru*

<sup>1</sup> Semenov Institute of Chemical Physics of Russian Academy of Sciences, Moscow, Russia

Modern functional materials used in microelectronics suit a wide list of requirements including low electrical resistance, thermal stability and reproducibility of the functional parameters. It is known that the resistance of porous materials, such as aerogels, is strongly dependent on pressure and on the deformations that can occur when current passes through such materials. Moreover, in the initial state, aerogels are not suitable for use as functional materials, since more than 99% of the volume of material is air. Consequently, the compaction of such materials is inevitable, and therefore there is a need to develop a methodology for assessing changes in the resistance of electrically conductive aerogels in this process in order to study the nature of changes in conductivity and structure of the material. As part of this work, we propose an approach to studying the change in the resistance of a material when it is compacted in a continuously changing volume.

Samples of cylindrical reduced graphene oxide aerogel (height 15 mm, base area 200 mm<sup>2</sup>) were obtained through freeze drying [1]. A polymer cylinder with a polypropylene piston was used to prepare the measuring cell. The role of current collectors was performed by "Wood alloy" inserts, which were obtained by molding at elevated temperatures.

Thus, one of the tasks was to design an instrument that allows to measure sample resistance automatically with high frequency at several measurement ranges and to save information for further processing. Such a device based on an Arduino controller was assembled and programmed. Resistors with nominal values 1, 10, 100, 1 000, 10 000 and 100 000 Ω were chosen as reference resistors. Switching between them was realized due to a magnetic relay. The measurement rate reaches 30-120 times per minute.

As a result of the experiment, it was found that the resistance of the samples varies in a wide range (~ 10 kΩ to ~ 1 Ω). Moreover, it was found that resistance dependence of the selected materials includes several intervals with a fundamentally different nature of changes in the electrical conductivity of the material. This dependency was considered within percolation theory. It has been shown that aerogels can be described as a two-phase (graphene/air) systems. The consideration of more complex systems such as graphene/polymer/air or graphene/metal/air is planned on the future work.

The study was carried out by a grant from the Russian Foundation of Basic Research (Project No. 16-29-06440 ofi\_m).

### References

1. M. V. Gudkov, A. Ya. Gorenberg, A. N. Shchegolikhin, D. P. Shashkin, V. P. Melnikov, Explosive Reduction of Graphite Oxide by Hydrazine Vapor at Room Temperature, *Doklady Akademii Nauk*, 2018, 478 (3), p. 298-301.



## Hydrodynamic behavior of complexes of metallofullerenes Fe @ C60 with biocompatible polymers in aqueous media

*Slyusarenko M.A.*<sup>1</sup>, *Lebedev V.T.*<sup>2</sup>, *Yevlampieva N.P.*<sup>1</sup>

*slusarenko\_masha@mail.ru*

<sup>1</sup> Saint-Petersburg State University, St. Petersburg, Russia

<sup>2</sup> Petersburg Nuclear Physics Institute named by B.P. Konstantinov of NRC Kurchatov Institute, Gatchina, Russia

Contrast agents are very important for modern tomographic analytical methods. Therefore, the search of novel more effective contrast agents continues. Such compounds are intended to improve the resolving power of magnetic resonance methods by orders of magnitude. A demand for being a contrast agent is a high spin density of a compound. Endohedral metallofullerenes meet this requirement [1]. Being hydrophobic, they can be modified with biocompatible polymers in order to obtain the watersoluble complexes [2]. It gives opportunity to use such complexes as new contrast agents for practical magnetic resonance imaging. Application of compounds in medical purposes demands a detailed investigation of their behavior in aqueous solutions. Present study continues previous investigation [3] and is devoted to the hydrodynamic properties of endohedral fullerene Fe@C<sub>60</sub> complexes with the polymers widely used in medicine and pharmacology – dextrin (D) and poly(vinylpyrrolidone) (PVP). The goals of the study were to determine the hydrodynamic dimensions of such complexes in aqueous media at variable conditions. Fe@C<sub>60</sub>-D and Fe@C<sub>60</sub>-PVP complexes and their stability were the objects of the study. The samples of PVP of molecular masses 10x10<sup>3</sup>, 30x10<sup>3</sup> and 50x10<sup>3</sup> g mol<sup>-1</sup> were used for the preparation of the polymer complexes with Fe@C<sub>60</sub>. The average molecular mass of dextrin, which was obtained by a hydrolysis of amylopectin, was (30±2)x10<sup>3</sup> g mol<sup>-1</sup>. The content of bound endohedral metallofullerenes in the hybrid polymer samples investigated was varied in wide range. Present study uses dynamic light scattering (DLS), velocity sedimentation, viscometry and spectrophotometry as the experimental methods. It has been shown that aqueous solutions of Fe@C<sub>60</sub>-PVP samples have a bimodal particle-size distribution. The fast mode has been associated with the PVP molecules, while the slow mode corresponded to the particles whose hydrodynamic sizes were near order of magnitude larger than the molecular radii of PVP. Solutions of the initial dextrin and Fe@C<sub>60</sub>-D samples have the multimodal particle size distributions. It has been estimated that the numerous of polymer molecules may be involved to the interaction with the endohedral metallofullerenes Fe@C<sub>60</sub> in an aqueous media. The acceptable for practical usage variants of complex-particles sizes and conditions of their stability in aqueous solutions have been determined.

This work was supported by the Russian foundation for basic research, project 18-29-19008.

### References

1. Rašović I. (Water-soluble fullerenes for medical applications // *Materials Science and Technology*, 2017. 33:7, P. 777-794
2. Lebedev V.T. et al. Biocompatible water soluble endometallofullerenes // *Nanosystems: physics, chemistry, mathematics*. 2016. V.7, №1. P. 1-7.
3. Yevlampieva N. P., Lebedev V.T., Szhogina A.A., Dubovsky I. M., Slyusarenko M.A. Polymer-endofullerene fe@c60 complexes for biomedical applications // *Vestnik of St. Petersburg State University. Series 4*, 2018. 5, P. 86.

## The role of edge moieties in electronic properties of graphene layers

*Rabchinskii M.K.*<sup>1</sup>, *Shnitov V.V.*<sup>1</sup>, *Baidakova M.V.*<sup>1,2</sup>, *Brunkov P.N.*<sup>1,2</sup>

*rabchinskii@mail.ioffe.ru*

<sup>1</sup> Ioffe Institute, Saint-Petersburg, Russia

<sup>2</sup> ITMO University, Saint-Petersburg, Russia

Tailoring of graphene electronic and optical properties through its functionalization or structural modification is one of the key topics nowadays in nanocarbon science. The main efforts are being made in graphene chemical doping with electron-donating or electron-withdrawing atoms, such as nitrogen, phosphorus or sulfur. The alternative approach is to obtain functionalized graphenes (FGs) – graphene layers decorated with the desired oxygen- or nitrogen-containing functional groups. Significant progress has been made within this field in the last decade, using graphene oxide as a starting material. However, the specific role of oxygen-containing moieties, such as carboxyls, carbonyls, phenols, etc. in FGs electrophysical properties remains to be an open question.

Hereby we present our results on the study of electrophysical properties of various FGs with the desired concentration of carboxyl (C-xy\_Gr) and carbonyl groups (C-ny\_Gr). The studied FGs were obtained via photochemical and wet-chemistry treatment of graphene oxide as is described in our previous works [1-3]. Studies of C-xy\_Gr revealed that the presence of high number of carboxyl groups leads to significant changes in the structure of the valence band with appearance of prominent peaks at 5.1, 13.5 and 25.1 eV. The further studies showed that feature at 5.1 eV is sensitive to the substitution of hydrogen ion in carboxyl groups to earth metal, demonstrating significant increase if sodium cations are introduced. At the same time, the following studies of C-ny\_Gr demonstrated that presence of carbonyl groups also regulates the structure of the valence band around 9.6 eV. Collectively, these results demonstrate the graphene density of states in the valence band is sensitive to the edge-located oxygen-containing functional groups. Moreover, the further study of GO, C-xy\_Gr, C-ny\_Gr and graphene work functions and conductivity measurements also showed dependence of these parameters on the concentration and type of edge moieties. C-xy\_Gr and C-ny\_Gr are determined to exhibit higher work function compared to graphene with its reversible decrease after the elimination of carboxyl and carbonyl groups. Interestingly, the conductivity of C-xy\_Gr appears to be almost the same as in pristine graphene, although it three orders of magnitude lower in C-ny\_Gr.

As a net result, we demonstrate that edge-located oxygen functionalities play significant role in the electrophysical properties of graphene layers, determining the density of states in the valence band, work function and conductivity. Although the detailed mechanisms underlying these effects remains unclear we assume that the obtained results will further expand the opportunities in a controllable modification of graphene electronic properties as well as the use of graphene for gas-sensing and biosensing.

### References

1. A. E. Aleksenskii, S. P. Vul', A. T. Dideikin, V. I. Sakharov, I. T. Serenkov, M. K. Rabchinskii, V. V. Afrosimov. *Nanosyst.: Phys., Chem., Math.* (2016) 7, 81–86.
2. M. K. Rabchinskii, V. V. Shnitov, A. T. Dideikin, A. E. Aleksenskii, S. P. Vul', M. V. Baidakova, I. I. Pronin, D. A. Kirilenko, P. N. Brunkov, J. Weise, and S. L. Molodtsov. *J. Phys. Chem. C* (2016) 120, 28261-28269.
3. M. K. Rabchinskii, A. T. Dideikin, D. A. Kirilenko, M. V. Baidakova, V. V. Shnitov, F. Roth, S. V. Konyakhin, N. A. Besedina, S. I. Pavlov, R. A. Kuricyn, N. M. Lebedeva, P. N. Brunkov and Al. Ya. Vul'. *Scientific Reports* (2018), 8, 14154.

## **Electric arc synthesis and study of mesoporous carbon with packing tin nanoparticles and their use as an anode material in Li-ion batteries**

*Kozlachkov D. V.*<sup>1</sup>, *Zaikovskii A.V.*<sup>2</sup>, *Fedorovskaya E.O.*<sup>1,3</sup>

*d.kozlachkov@g.nsu.ru*

<sup>1</sup> Novosibirsk State University, Novosibirsk, Russia

<sup>2</sup> Kutateladze Institute of Thermophysics, SB RAS, Novosibirsk, Russia

<sup>3</sup> Nikolaev Institute of Inorganic Chemistry, SB RAS Novosibirsk, Russia

Nowadays Li-ion batteries (LIBs) are the most usability for electrical energy storage devices in portable electronics, electro machines and one of the most perspective type of batteries for electrochemistry investigations in the nearest future. Graphite (volume capacity 273 mAh/g) is common anode material in conventional batteries. Due to graphite have low extensive volume expansion (10%), it is stable in the charge-discharge process. In the other hand tin have rather larger theoretical specific capacity (994 mAh/g), but it has huge volume expansion (254%), which leads to bulk tin pulverization and instability of solid electrolyte interface (SEI) film. Therefore usage of tin nanoparticles is perspective for LIBs creation, because they have short diffusion distance for Li ions. In the same time nanoparticles don't distract under volume expansion during charge-discharge process, but they should be isolated to prevent contact and coagulation with each other. Arc discharge synthesis allows to produce uniform metal nanoparticles in the amorphous carbon matrix. [1]

In this study mesoporous carbon materials packing tin nanoparticles were synthesized by the method of arc discharge with DC 150 A and voltage 25 V in helium atmosphere pressure 50 Torr with usage of composite anode consisting of a graphite rod and mixed graphite/tin powder (1:1 weight ratio). In the result the material was synthesized and analysis of TEM images demonstrate it contains tin nanoparticles with 2-30 nm in diameter (10 nm average size) inside amorphous carbon matrix.

The electrochemical properties were performed by cyclic voltammetry, impedance spectroscopy and charge-discharge cycling measurements. For the experiment coin cells were assembled in an argon-filled glove box with lithium cathode and anode prepared from synthesized Sn/C composite as the active material.

It was shown tin nanoparticles are packed inside carbon matrix with 10 nm average diameter as a result of the synthesis. Specific capacity is 1800 mAh/g at the 1<sup>st</sup> cycle, 800 mAh/g at the 2<sup>nd</sup> cycle and nearly 600 mAh/g after 120 cycles Fig. 1. That indicates high efficiently and stable rate of the synthesized material.

This work was supported by grant RSCF №18-79-00038

### **References**

[1] D. V. Smovzh et al. Morphology of aluminium oxide nanostructures after calcination of arc discharge Al-C soot // *Ceramics International* 41 (2015) 8814–8819

## Application of tungsten-cobalt molecular cluster for CCVD synthesis of CNTs

*Kuznetsova V.R.*<sup>1,2</sup>, *Lobiak E.V.*<sup>1</sup>, *Bulusheva L.G.*<sup>1,3</sup>, *Okotrub A.V.*<sup>1,3</sup>

*kuznetsova.viktoriya.98@mail.ru*

<sup>1</sup> Nikolaev Institute of Inorganic Chemistry of the Siberian Branch of the Russian Academy of Sciences, Novosibirsk, Russia

<sup>2</sup> Novosibirsk State Technical University, Novosibirsk, Russia

<sup>3</sup> Novosibirsk State University, Novosibirsk, Russia

Carbon nanotubes (CNTs) are materials that have properties as small dimensions, strength and the remarkable physical properties of these structures make them a very unique material with a whole range of promising applications such as gas sensors, electrochemical detectors, catalytic of organic chemistry and etc. [1].

Catalytic chemical vapor deposition (CCVD) is the most widely used method for the synthesis of carbon nanotubes in industry due to its several advantages as it is the best option for manufacturing high quantity of products at low cost. The choice of optimal parameters for carrying out CCVD synthesis is the main task for controlled growth of CNTs with specified characteristics [2]. The optimal synthesis conditions such as temperature, carbon sources, gas flow rates and gas ratio need to be installed.

In the present research were used molecular clusters  $\text{Na}_{15}[\text{Na}_3\{\text{Co}(\text{H}_2\text{O})_4\}_6\{\text{WO}(\text{H}_2\text{O})\}_3(\text{P}_2\text{W}_{12}\text{O}_{48})_3]\cdot n\text{H}_2\text{O}$  to prepare alloy nanoparticles with specific properties for the CCVD synthesis of CNTs. The advantages of these catalysts are that, they have molecular clusters structure for the formation of discrete catalyst particles with a controlled size [3]. The cluster was mixed with MgO substrate with highly developed specific surface.

In this present study, synthesis of CNTs carried out in a CCVD process at out variation in the rate of flow of gases  $\text{H}_2/\text{CH}_4$ ,  $\text{H}_2/\text{C}_2\text{H}_4$  and  $\text{Ar}/\text{CO}$  and their ratio in the mixture, and changes in the temperature profile. The influence temperature, gas flow rates and gas ration for structure of CNT were discovered.

### References

- [1] J. Heo, H. Cho, J. Lee, et al, *Chemical Engineering Research and Design*, 24 (2014), p. 361-368
- [2] P.C. Matter, *Physics Condensed Matter*, **15** (2003), p. 3011-3035
- [3] J. Wang, F. Ding, D. Luo, D., D. Zhang, X. Wang, J. Yang, X. Bai, F. Peng, Z. Xu, J. Wei, Y. Li, M. Li, R. Li, F. Yang, X. Li, Y. Li, Z. Xu, *Natural*, **510** (2014), p. 522-524

## Electronic structure of cobalt-intercalated graphene on silicon carbide

Lobanova E.Yu.<sup>1,2</sup>, Pronin I.I.<sup>1,2</sup>

elobanova@corp.ifmo.ru

<sup>1</sup> Ioffe Institute, Saint Petersburg, Russia

<sup>2</sup> ITMO University, Saint Petersburg, Russia

Nowadays 2D materials are at the forefront of materials research due to their exceptional electric, optical and mechanical properties. Graphene-based materials hold an important place in this area. In particular, synthesis and study of graphene/ferromagnetic interfaces is of great interest of spintronics. One of common approaches for a graphene synthesis consists of thermal decomposition of silicon carbide [1]. Though it allows obtaining wafer scale high quality graphene, in that case a buffer layer consisting of partially  $sp^3$ -hybridized carbon is formed. The buffer layer negatively affects the electronic properties of graphene. It was previously shown that intercalation of atoms of other substances could reduce the interaction of the buffer layer with SiC and turn the buffer layer into quasi-freestanding graphene [2]. Intercalation of graphene grown on SiC with cobalt atoms is a perspective way of creating ferromagnetic layers under graphene on dielectric substrate. The goal of present study was to investigate the evolution of electronic structure of graphene on SiC during its intercalation with ferromagnetic cobalt atoms.

*Ab initio* calculations were done using Density Functional Theory as implemented in Quantum ESPRESSO package [3]. The generalized gradient approximation (GGA) and PBE pseudopotentials were employed. Kinetic energy cutoffs were set of 200 and 800Ry for the wave functions and for the charge density, respectively. The supercell was constructed periodically translated slab consisted of four SiC bilayers (3 atoms C and 3 atoms Si per layer) covered with the buffer layer (8 atoms) and the graphene (8 atoms) with intercalated Co (4 atoms) placed between the buffer layer and the substrate.  $2 \times 2$  reconstruction of a graphene surface cell was used. A 15Å vacuum layer was introduced to construct the supercell.

At the first stage geometry optimization of the supercell was done taking into account dispersion interaction. Despite for the initial system (graphene/SiC) the buffer layer is corrugated due its interaction with the substrate, after intercalation the buffer layer becomes flat. This evidences that intercalation of graphene with cobalt leads to a relaxation of the system and formation of bilayer graphene on its surface. Optimization has showed that the distance between graphene layers is equal to 3.24 Å, which is close to the case of graphite. The distance between the lower graphene layer and the layer of cobalt atoms is 1.89 Å.

Then self-consistent calculations were carried out for two spin-components. It is shown, that the electronic structure of the intercalated system is strongly modified in comparison with the graphene/SiC(0001) case. Due to proximity of graphene and cobalt the  $p_z$  states of the lower graphene sheet and Co  $3d$  states overlap and become hybridized. Thus, due to the proximity effect electronic structure of upper and lower graphene sheets is different. For the upper layer it is close to the case of quasi-freestanding graphene, while for the lower layer it is similar to the structure of graphene grown on a metal substrate. The presence of magnetic cobalt atoms leads to a spin polarization of the lower graphene sheet.

The work was supported by the Ministry of Education and Science of the Russian Federation (task 3.3161.2017/4.6 of the project part of the State Task).

### References

- [1] V. Yu. Davydov, D.Yu. Usachov, S.P. Lebedev, et al. 2017 *Semiconductors* **51** 1116.
- [2] S. J. Sung, J. W. Yang, P. R. Lee, et al. 2014 *Nanoscale* **6** 382.
- [3] P. Giannozzi, S. Baroni, N. Bonini, et al. 2009 *J. Phys.: Condens. Matter* **21** 395502.

## Heat treatment of the microwave exfoliated graphite oxide (MEGO) by Knudsen Effusion Mass Spectrometry (KEMS)

*Zhirov M.S.*<sup>1</sup>

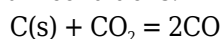
*zhirovmaxim@gmail.com*

<sup>1</sup> Moscow State University, Chemistry Department, Moscow, Russia

The aim of this work was to determine the effect of heat treatment on the composition and structure of microwave exfoliated graphite oxide (MEGO).

Heat treatment was carried out by Knudsen Effusion Mass Spectrometry (KEMS) using nickel effusion cell. Positive ions formed by electron ionization of molecules ( $E_{\text{ion}} = 75$  eV) were analyzed by mass/charge ratio,  $m/e$ , on a MI 1201 magnetic mass spectrometer ( $r = 200$ mm,  $R = 500$ ). At first, a long (~ 5 hour) pumping of the ion source area to a high vacuum was carried out. After the signal at the mass number  $m/e = 18$  ( $\text{H}_2\text{O}^+$ ) reached the level corresponding to the "background" of the device, the cell was gradually heated to the final annealing temperature,  $T_f = 573$  K or  $T_f = 1073$  K. At each intermediate temperature, signals were measured at the mass numbers  $m/e = 18$  ( $\text{H}_2\text{O}^+$ ), 28 ( $\text{CO}^+$ ), 32 ( $\text{O}_2^+$ ), 44 ( $\text{CO}_2^+$ ), 48 ( $\text{SO}^+$ ), and 64 ( $\text{SO}_2^+$ ). As a result of heat treatment, two samples were obtained: low-temperature, MEGO/573, and high-temperature, MEGO/1073. Formation conditions (temperature, K / annealing time, hour) of sample MEGO/573: 523 / 2.5, 573 / 8.0; sample MEGO/1073: 573 / 11.7, 673 / 5.0, 773 / 6.3, 873 / 6.0, 973 / 8.5, 1073 / 23.0. During multi-stage MEGO annealing to final temperature of  $T_f = 1073$  K, the signals at  $m/e = 32$  ( $\text{O}_2^+$ ), 48 ( $\text{SO}^+$ ) and 64 ( $\text{SO}_2^+$ ) remained permanent and low-intensity, weakly dependent on the presence of the sample in cell. Taking into account these features, these signals were considered as "background" for all experiments. On the contrary, for  $m/e = 18$  ( $\text{H}_2\text{O}^+$ ), 28 ( $\text{CO}^+$ ), 44 ( $\text{CO}_2^+$ ) signal intensities in the experiment with the MEGO sample are much higher than without. The formation of the MEGO/573 sample at  $T_f = 573$  K occurred at stationary fluxes of  $\text{H}_2\text{O}$ ,  $\text{CO}$ , and  $\text{CO}_2$ , and the level of these fluxes indicated that their sources remain in the product after the end of the 8-hour annealing. During the formation of the MEGO/1073 sample, the  $\text{H}_2\text{O}$  flux decreased with temperature increasing, and at  $T > 773$  K remained at a level close to the "background". The analysis of  $\text{CO}^+$  and  $\text{CO}_2^+$  signal dependencies on the annealing time showed that the most intense release of carbon oxides occurred in the initial annealing periods (first 5 hours) at temperatures of 873 K, 973 K and 1073 K. After the initial period, the fluxes decreased markedly, and the annealing passed into the stationary state. At  $T_f = 1073$  K the level of stationary flows of  $\text{CO}$  and  $\text{CO}_2$  went beyond the sensitivity limit of the device.

During the annealing of MEGO, no release of oxygen  $\text{O}_2$  and sulfur dioxide  $\text{SO}_2$  was detected. Annealing of MEGO at  $T_f = 573$  K (MEGO/573) is accompanied by the release of  $\text{H}_2\text{O}$ ,  $\text{CO}$ , and  $\text{CO}_2$  molecules, and does not lead to the complete removal of water and oxygen-containing groups from the sample. The release of water molecules reaches a certain minimum level at a temperature of 773 K, and then changes little. Intensive evolution of carbon oxides  $\text{CO}$  and  $\text{CO}_2$  at temperatures of 873–1073 K is completed by reducing their fluxes to a level beyond the sensitivity limits of the mass spectrometer. However, the absence of measurable stationary flows of  $\text{CO}$  and  $\text{CO}_2$  rather indicates the attainment of a certain minimum oxygen content for the given heat treatment conditions in the final product MEGO/1073. The prevalence of  $\text{CO}$  oxide in the gas phase corresponds to the ratio of pressures of carbon oxides under equilibrium conditions:



## NEXAFS study of catalytic system based multiwalled carbon nanotubes

*Mingaleva A.E.*<sup>1</sup>, *Petrova O.V.*<sup>1</sup>, *Nekipelov S.V.*<sup>1,2</sup>, *Sivkov D.V.*<sup>1,3</sup>, *Shomysov N.N.*<sup>1</sup>, *Ob'edkov A.M.*<sup>4</sup>, *Kaverin B.S.*<sup>4</sup>, *Kremlev K.V.*<sup>4</sup>, *Semenov N.M.*<sup>4</sup>, *Kadomtseva A.V.*<sup>5</sup>, *Gusev S.A.*<sup>6</sup>, *Yunin P.A.*<sup>6</sup>, *Tatarskiy D.A.*<sup>6</sup>, *Sivkov V.N.*<sup>1</sup>

*amingaleva@gmail.com*

<sup>1</sup> Institute of Physics and Mathematics FRC Komi SC UB RAS, Syktyvkar, Russia

<sup>2</sup> Pitirim Sorokin Syktyvkar State University, Syktyvkar, Russia

<sup>3</sup> Immanuel Kant Baltic Federal University, Kaliningrad, Russia

<sup>4</sup> Razuvaev Institute of Organometallic Chemistry of RAS, Nizhny Novgorod, Russia

<sup>5</sup> Privolzhsky Research Medical University of the Ministry of Health of the Russian Federation, Nizhny Novgorod, Russia

<sup>6</sup> Institute for Physics of Microstructures RAS, Afonino, Nizhny Novgorod Region, Russia

Hybrid materials based on multi walled carbon nanotubes (MWCNT), which surface is decorated with metals and metal oxides or carbides nanoparticles, have a promising properties in many application. In particular, the composite based on MWCNT modified with copper nanoparticles is used as a catalyst in a germanium tetrachloride reduction process [1].

This work is devoted to the study of catalytic system based on MWCNT decorated with copper nanoparticles (Cu/MWCNT). The Cu/MWCNT composite samples were prepared by pyrolysis of copper formate deposited on the MWCNT surface from an aqueous solution [1]. The pyrolysis was carried out in argon flow at 473 °K. The pristine MWCNT and Cu/MWCNT composite were investigated by Near Edge X-ray Absorption Fine Structure (NEXAFS) spectroscopy [2], X-Ray diffractometry (XRD) and scanning electron microscopy (SEM) techniques.

SEM images show that copper is deposited on the MWCNT surface in the nanoparticles form. According to XRD data it was found that the copper-containing nanoparticles consist of metal copper with cuprous oxide Cu<sub>2</sub>O admixture. The NEXAFS spectra in C1s- and Cu2p-absorption edges energy ranges of the pristine MWCNT and Cu/MWCNT composite were measured using synchrotron radiation of RGLB at BESSY II [3]. The NEXAFS C1s-spectra analysis suggests that nanotubes surface is not destroyed, but modified by the single, double and epoxy carbon-oxygen bonds formation [4]. The NEXAFS Cu2p-spectra show that the copper containing nanoparticles surface is mainly formed by copper oxide CuO.

This work was supported by Bilateral Program of RGLB at BESSY II, Program of UB RAS № 18-10-2-23, Project of RFBR № 19-32-50062\19, the Russian Academic Excellence Project at the Immanuel Kant Baltic Federal University, State assignment of IOMC RAS (topic 45.8), Project of RFBR № 18-33-0077 and Common Research Center "Physics and technology of micro- and nanostructures".

### References

1. V. Kadomtseva, A.V. Vorotyntsev, V.M. Vorotyntsev, A.N. Petukhov, A.M. Ob'edkov, K.V. Kremlev and B.S. Kaverin. Russian J. of Applied Chemistry. (2015). V **88**. 595-602.
2. Stöhr. NEXAFS Spectroscopy (Berlin: Springer Verlag, 1992). 403.
3. I. Fedoseenko, D.V. Vyalikh, I.E. Iossifov et al., Nucl. Instrum. Methods Phys. Res. A. (2003). V **505**. 718.
4. V. Petrova, S.V. Nekipelov, A.E. Mingaleva, V.N. Sivkov, A.M. Obiedkov, B.S. Kaverin, K.V. Kremlev, S.Yu. Ketkov, S.A. Gusev, D.V. Vyalikh, S.L. Molodtsov. J. of Physics: Conference Series. (2016). V **741**. 012038.

## Correlation between gas permeability of graphite foil, microstructure of exfoliated graphite and its preparation conditions

Ivanov A.V.<sup>1</sup>, Maksimova N.V.<sup>1</sup>, Malakho A.P.<sup>1</sup>

key700@mail.ru

<sup>1</sup> Chemistry Department, Lomonosov Moscow State University, Moscow 119991, Russia

Exfoliated graphite (EG) is a carbon material with a crystalline structure of graphite, but which is different from it in morphology, width of graphite crystallites and their arrangement in an individual particle [1]. One of the main industrial applications of exfoliated graphite is the production of flexible graphite foil (GF) by EG compression and the manufacturing of graphite sealing materials. Gas permeability of graphite foil can be used as a measure of media leakage through GF and of its sealability. Quite a large number of research works connect the influence of the EG compaction density with the GF gas permeability [2, 3]. However, the preparation of GF includes a number of steps, which define its structure [4], and the influence of GF preparation conditions on the GF permeability has not been studied.

The aim of the research was to investigate the influence of the stage number of graphite intercalation compound and the EG preparation temperature on the EG structure and gas permeability of GF based on it.

The preparation of graphite foil included the synthesis of graphite intercalation compounds (GIC), which were graphite bisulfate of I, II, III, IV stages, followed by water washing with the formation of expandable graphite, its rapid heating at temperatures of 600, 800, 1000 °C with the formation of exfoliated graphite and the EG compaction to GF. The investigation of the EG structure was performed by SEM, TEM, XRD and Raman spectroscopy. The correlation between the preparation conditions of EG, its matrix dispersity, crystallite size along the c axis and content of amorphous carbon, which influence the GF porous structure, that was investigated by mercury porosimetry and nitrogen adsorption method, and GF gas permeability, was shown.

GF based on EG obtained at 600 °C from GIC of I stage (GF-I-600) had the minimal nitrogen permeance ( $Q(N_2)$ ). The decrease of the GIC stage number up to IV (GF-IV-600) and the increase of the EG preparation temperature up to 1000 °C (GF-I-1000) lead to increase of GF gas permeance (Fig. 1).

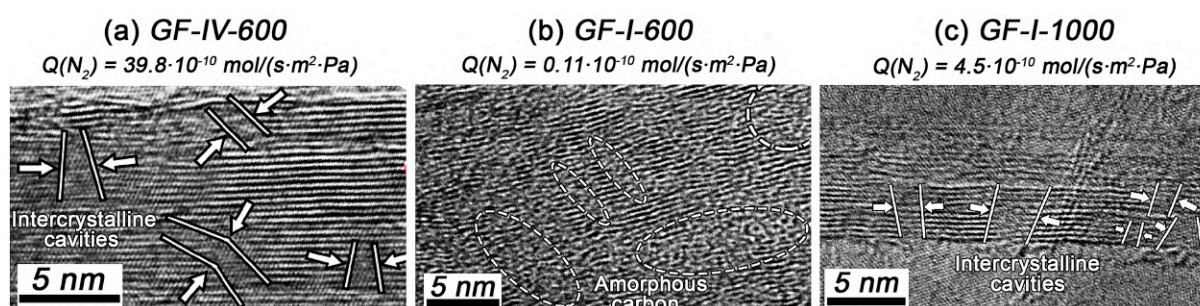


Fig. 1. Values of  $N_2$  permeance and TEM images of GF based on EG obtained at 600 °C from GIC of (a) IV stage and (b) I stage and (c) GF based on EG obtained at 1000 °C from GIC of I stage.

### References

1. D.L. Chung, J. Mater. Sci. (2015) 51, 554.
2. A. Efimova, D.A. Syrtsova, V.V. Teplyakov, Sep. Purif. Technol. (2017) 179, 467.
3. Celzard, J. Mareche, J. Phys. Condens. Matter. (2001) 13, 4387.
4. M. Afanasov, O.N. Shornikova, D.A. Kirilenko, I.I. Vlasov, L. Zhang, J. Verbeeck, V.V. Avdeev, G. Van Tendeloo, Carbon (2010) 48, 1862.



## **Impedance spectroscopy analysis and equivalent circuit modeling of polystyrene composites with carbon nanohorns**

*Baskakova K.I.*<sup>1</sup>, *Sedelnikova O.V.*<sup>1,2</sup>, *Gusel'nikov A.V.*<sup>1</sup>, *Bulusheva L.G.*<sup>1,2</sup>, *Okotrub A.V.*<sup>1,2</sup>

*baskakova@niic.nsc.ru*

<sup>1</sup> Nikolaev Institute of Inorganic Chemistry SB RAS, Novosibirsk, Russia

<sup>2</sup> Novosibirsk State University, Novosibirsk, Russia

The arc discharge method could be used for fabrication of catalyst-free carbon nanostructures with different morphologies depending on synthesis parameters and compositions of electric arc. One of the available products are carbon nanohorns (CNHs), nanotube-like structure with conic tips, which are promising for electromagnetic shielding materials.

In this work, we synthesized CNHs using direct current arc discharge of graphite rod. The synthesis was carried out at a voltage of 60 V, a current of 0.5 kA in a helium atmosphere at a pressure of 0.5 atm. To vary morphology of sample, we add some portions of toluene in helium atmosphere. The obtained samples were characterized using transmission electron microscopy, Raman spectroscopy, X-ray photoelectron spectroscopy, thermogravimetric analysis and elemental CHNS analysis. We found that the addition of toluene results in formation of CNHs of smaller radius, while the defectiveness of samples obtained by the initial and modified methods was unchanged.

Polystyrene composites with different CNHs contents below and above the percolation threshold were obtained by the solution method in chloroform. The real and imaginary parts of composite impedance were measured in the range of 1 kHz - 1 MHz. Modeling of experimental data by different resistor-capacity circuits were done. Above the percolation threshold, the impedance of composites can be described by parallel RC-circuit. When the composite loading is above the percolation threshold, the equivalent circuits contain the additional resistor, which corresponds to formation of conduction path through bulk sample.

This work was partially funded by The RSC project (18-72-00017).

## On the treatment and identification of deuterium thermal desorption spectra for graphite exposed to high flux plasma at high temperatures

*Cheretaeva A.O.*<sup>1</sup>

*alice\_raduga@mail.ru*

<sup>1</sup> Bardin Central Research Institute for Ferrous Metallurgy, Moscow, Russia

This study is devoted to a further development and application of results [1, 2] on the simplified method of kinetic analysis of the hydrogen thermal desorption (TDS) processes, responding to the first-order reactions, in materials heating with only one rate, rather than with several rates, as required by the Kissinger method. It is considered the feasibility and expediency of using such a much less labor-intensive method (in comparison with the Kissinger method) for the kinetic analysis of a number of the known data on hydrogen TDS spectra for advanced carbon nanostructures, including the determination of the rate constants ( $K$ ), activation energies ( $Q$ ) and pre-exponential factors ( $K_0$ ) of the processes, along with the identification of them on the basis of [1, 2].

As an example, such a treatment and identification of data [3] on deuterium TDS spectra for graphite exposed to high flux plasma at high temperatures is performed. Some results of the analysis for graphite are presented in Fig. 1 and Table 1.

**Table 1.** Kinetic characteristics of the deuterium thermal desorption for MPG-8 graphite

Gaussian curve $N_e$	$T_{max}$ , K	$K(T_{max})$ , $s^{-1}$	Temperatures, K	$Q$ , kJ/mol	$K_0$ , $s^{-1}$
1	1040	0.038	950 - 1160	$155 \pm 8$	$3 \cdot 10^6$
2	1120	0.048	1040 - 1215	$243 \pm 10$	$1 \cdot 10^{10}$
3	1230	0.021	1000 - 1390	$146 \pm 3$	$3 \cdot 10^4$

The identification of results of analysis of data [3] has been done by using results [1, 2].

### Acknowledgements

*This work was financially supported by the RFBR (Project # 18-29-19149 mk).*

*The author acknowledges the valuable comments of Prof. Nechaev and Prof. Pisarev.*

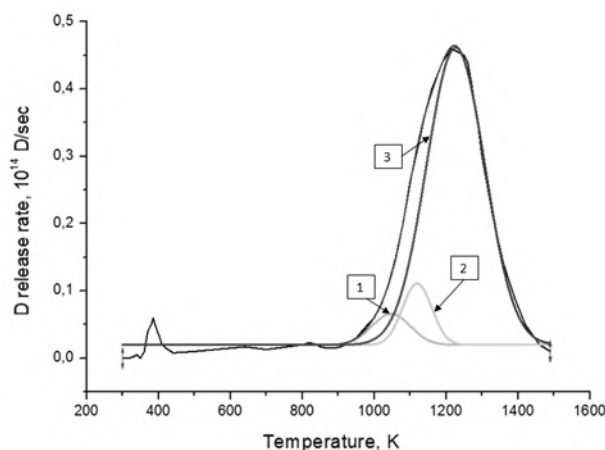


Fig.1. Deuterium TDS spectrum of MPG-8 fine grain graphite exposed to 1 kPa  $D_2$  gas at 873 K for 1 h.

### References

1. S. Nechaev. Physics - Uspekhi (2006) **49**, 563; UFN (2006) **176**, 581.
2. S. Nechaev and T.N. Veziroglu. International Journal of Physical Sciences (2015) **10**, 54.
3. Rusinov, N. Trifonov, Yu. Gasparyan, B. Khripunov, M. Mayer, J. Roth and A. Pisarev. Journal of Nuclear Materials (2011) **417**, 616.

## The impact of graphene-like carbon on the properties of MAO-coatings on the AK5M2 alloy

Zolotaya P.S.<sup>1</sup>, Komarov A.I.<sup>1</sup>, Romanyk A.S.<sup>1</sup>

polina.zolotaya@gmail.com

<sup>1</sup>Joint Institute of Mechanical Engineering of the NAS of Belarus, Minsk, Belarus

The effect of graphene-like carbon on the process of microarc oxidation (MAO), thickness and microhardness of ceramic coatings (CC) created on aluminum alloy AK5M2 was investigated. Microplasma processing of this alloy was carried out in the anodic-cathodic mode in silicate-alkaline electrolyte with the addition of graphene-like carbon (GLC). The method of GLC-obtaining consists in the low-temperature intercalation of graphite in a solution of sodium in liquid ammonia [1]. This GLC doesn't contain structural defects associated with the oxidation of graphite, doesn't contain carboxyl and phenolic groups, but at the same time has a certain amount of amino groups, which make the material alkaline.

According to the research, the introduction of GLC into the electrolyte increases in the thickness of the CC on the AK5M2 alloy (up to 150  $\mu\text{m}$ ) and the microhardness  $H_{\mu}$  by 1.6 times (Fig. 1). The effect of increasing of thickness and physical and mechanical characteristics of the ceramic coatings formed under the influence of a graphene-containing material is also observed in MAO of silumins AK7 [2] and AK12M2MgN [3].

X-ray diffraction analysis determined that the MAO coatings on the alloy AK5M2 consist basically of aluminum oxides:  $\alpha\text{-Al}_2\text{O}_3$  (corundum),  $\gamma\text{-Al}_2\text{O}_3$ , mullite. It has been established that GLC-modification of the coatings leads to an increase in corundum (up to 75-80%) in the composition of a CC, which explains the increase in the microhardness  $H_{\mu}$  of the coating.

As a result of the research it was found that the introduction of graphene-like carbon into the electrolyte leads to an intensification of the process of microarc oxidation and an increase in the strength properties of ceramic coatings. An increase in the thickness of the ceramic coating by 1.5 times and an increase in the microhardness value from 12 GPa for coating without additives to 20 GPa for coating with the addition of GLC were achieved.

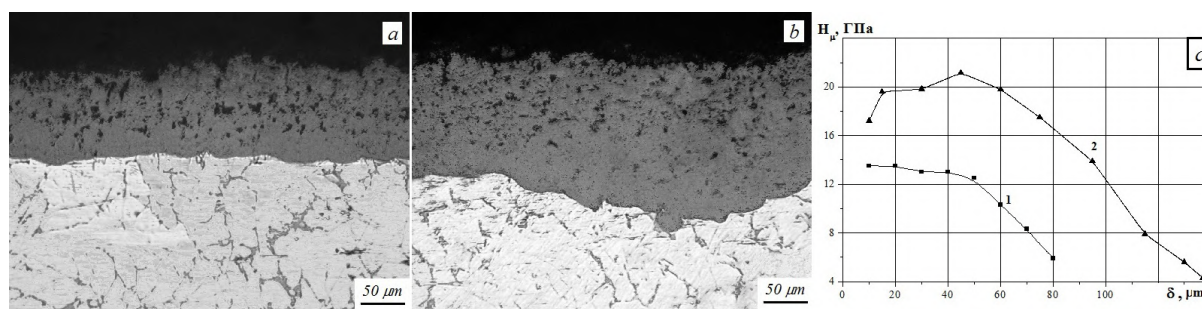


Fig.1. The microstructure of CC AK5M2 without additives (a), with the addition of GLC (b), thickness microhardness distribution (c): (1 - without additives, 2 - with the addition of GLC).

### References

1. V.P. Novikov, S.A. Kirik, Letters to the Journal of Physics and Technology (2011) T. 37 (12), p. 44-49.
2. A.I. Komarov, V.I. Komarova, N.N. Rozhkova, Actual Problems of Mechanical Engineering (2017), p. 366-368.
3. A.I. Komarov, V.I. Komarova, P.S. Zolotaya, Intern. scientific and technical Journal MMMM (2017) №2 (39), p. 39-43.

## Structure formation of AK12M2MgN alloy modified by carbon nanotubes jointly with copper

*Iskandarova D.O.<sup>1</sup>, Komarov A.I.<sup>1</sup>, Orda D.V.<sup>1</sup>, Romanyuk A.S.<sup>1</sup>*

*donata\_i@mail.ru*

<sup>1</sup> Joint Institute of Mechanical Engineering of National Academy of Sciences of Belarus, Minsk, Belarus

The paper presents the results of the impact of carbon nanotubes (CNT), subjected to mechanical activation, on the structure and properties of AK12M2MgN alloy samples containing a different proportion of modifying components (Table 1).

Table 1 - Characteristics of microhardness of AK12M2MgN alloy

Sample	Q <sub>CNT</sub> , %	Q <sub>Cu</sub> , %	H <sub>μ</sub> , MPa α-phase	H <sub>μ</sub> , MPa eutectic	HV, MPa	σ <sub>B</sub> , MPa	δ, %
1	-	-	617	849	883	213	2,5
2	0,05	0,25	600	810	997	300	3,1
3	0,1	0,5	639	859	1040	-	-

Analysis of the modified samples structure showed that the introduction of CNT into the melt jointly with copper ensures the dispersion of the alloy structure: the grain size of the α-phase (Fig. 1) decreases by a factor of 2.5-3, the proportion of thin-needled eutectics with a particle size of Si 5-7 μm increases, and the grinding of intermetallic inclusions occurs by 3-5 times. The complex effect on the structure leads to an increase in the ultimate strength (σ<sub>B</sub>) by 80-90 MPa (Table 1) with a simultaneous increase in the relative elongation (δ).

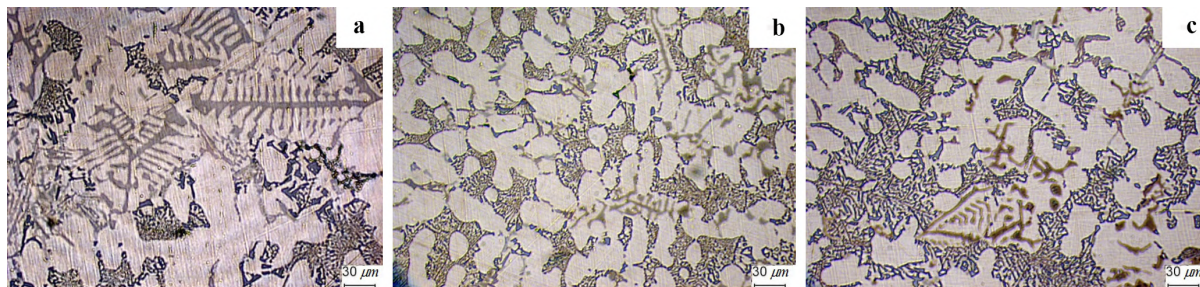


Fig.1. Microstructure of the alloy AK12M2MgN before (a) and after modifying with a complex additive (b - Q<sub>CNT</sub>=0,05%, Q<sub>Cu</sub>=0,25%; c - Q<sub>CNT</sub>=0,1%, Q<sub>Cu</sub>=0,5%).

### References

1. A.I. Komarov, V.I. Komarova, D.O. Iskandarova, D.V. Orda, *Advanced Materials and Technologies* (2017), p. 221-223.
2. A.I. Komarov, V.I. Komarova, D.V. Orda, D.O. Iskandarova, *Mechanical Engineering Issues* (2017) Issue 6, p. 363-365.
3. A.I. Komarov, D.O. Iskandarova, D.V. Orda, *Collection of materials* (2018), p. 156-158.

## Influence of fullerene( $C_{60}$ )-containing star macromolecules on pervaporation efficiency of membranes for fuel desulfurization

*Tataurov M.V.*<sup>1</sup>, *Pulyalina A.Yu.*<sup>1</sup>, *Polotskaya G.I.*<sup>2</sup>, *Vinogradova L.V.*<sup>2</sup>

*maksimuspiter@gmail.com*

<sup>1</sup> Saint-Petersburg State University

<sup>2</sup> Institute of Macromolecular Compounds of Russian Academy of Sciences

The physical and transport properties of membranes based on polyphenylene oxide (PPO) modified by small amounts (5 wt%) of a star-shaped hybrid polymer with polystyrene (PS) arms and poly-(2-vinylpyridine)-*block*-poly-*tert*-(butylmethacrylate) (P2VP-*block*-PTBMA) diblock copolymer arms grafted onto common fullerene  $C_{60}$  branching center were investigated. The efficiency of diffusion membranes modified by fullerene ( $C_{60}$ ) containing macromolecules is demonstrated in pervaporation of thiophene / n-octane mixture. The task was an effective removal of sulfur-containing impurities from n-octane, which is the main component of fuel. The inclusion of star-shaped macromolecules in PPO matrix leads to a change in morphology, physical and transport properties of the membrane. The star-modified membrane exhibits increased productivity and selectivity in the separation of the thiophene / n-octane mixture. The use of polymer hybrid fullerene ( $C_{60}$ )-containing macromolecules as the modifiers of diffusion membranes offers the prospect of the production of highly selective membranes for the separation of liquid and gas mixtures.

### Acknowledgements

Equipment of Resource Centers of Saint Petersburg State University, namely, Interdisciplinary Resource Center "Nanotechnologies", "Thermogravimetric and calorimetric methods of investigation" and Education Resource Centre in the direction of chemistry were used for investigation.

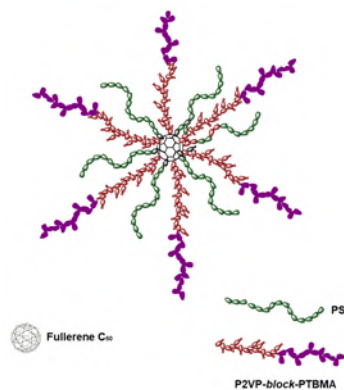


Fig.1. Scheme of star macromolecule with arms of different nature

## Preparation of magnetic sorbent based on exfoliated graphite containing cobalt ferrite for selective sorption of oil from the water surface

*Pavlova J.A.*<sup>1</sup>, *Ivanov A.V.*<sup>1</sup>, *Maksimova N.V.*<sup>1</sup>

*julidev@yandex.ru*

<sup>1</sup> Chemistry Department, Lomonosov Moscow State University, Moscow 119991, Russia

Water pollution, which is mainly caused by oil spills, is one of the major current environmental problems. At present, so-called magnetic sorbents consisting of a porous matrix directly involved in sorption, which modified by a ferrimagnetic or ferromagnetic compound, have proved to be effective in the water purification. The presence of magnetic phase makes it possible to collect sorbent with sorbed oil from the place of oil spill using the magnetic field. Due to its hydrophobic properties and high sorption capacity toward oil, exfoliated graphite (EG), which is a macroporous graphite material, is well suited for using as a sorbent for liquid hydrocarbons [1]. At the same time, the possibility of introducing magnetic iron-containing phases greatly facilitates its collection from the water surface [2, 3]. The aim of this work was to investigate the influence of the EG microstructure on its sorption properties and to obtain the magnetic sorbent based on EG modified by cobalt ferrite with high sorption capacity, hydrophobicity and high saturation magnetization.

Exfoliated graphite containing cobalt ferrite was obtained by impregnation of expandable graphite in mixed solution of iron (III) chloride and cobalt (II) nitrate and the consequent thermal treatment of impregnated expandable graphite at a temperature of 600-1000°C in the air atmosphere. The microstructure and crystalline structure of EG matrix were investigated by SEM, XRD, FTIR spectroscopy and Raman spectroscopy (Fig 1). The ferrite phase was investigated by XRD and Mossbauer spectroscopy (Fig 1). The different preparation conditions (defectiveness of initial expandable graphite and solution concentration) leads to different cobalt ferrite content in exfoliated graphite, which is varied from 7 to 45 wt.%. At the same time, obtained EG is characterized by high sorption capacity toward oil (up to 25 g/g) and low water absorption (up to 2 g/g).

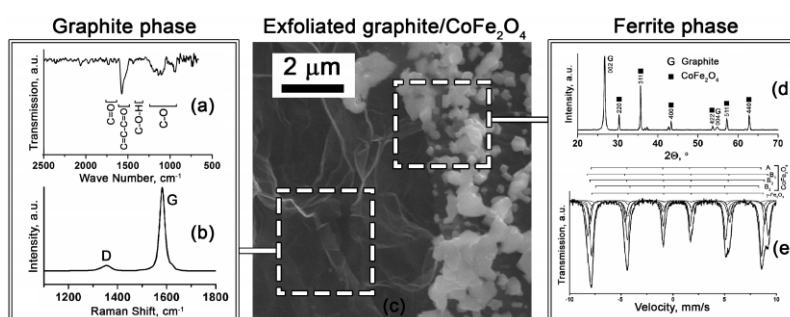


Fig. 1 (a) FTIR and (b) Raman spectra of exfoliated graphite; (c) SEM image, (d) XRD pattern and (e) Mossbauer spectrum of exfoliated graphite containing cobalt ferrite.

### References

1. M. Toyoda, Y. Nishi, N. Iwashita, M. Inagaki, *Desalination* (2002) 151, 139
2. G. Wang, Q. Sun, Y. Zhang, J. Fan, L. Ma, Sorption and regeneration of magnetic exfoliated graphite as a new sorbent for oil pollution, *Desalination*. 263 (2010) 183-188.
3. M.A. Lutfullin, O.N. Shornikova, A.V. Vasiliev, K.V. Pokholok, V.A. Osadchaya, M.I. Saidaminov, N.E. Sorokina, V.V. Avdeev // *Carbon*. 2014 V. 66 P. 417-425.

## Effect of high pressure on the thermoelectrical properties of fullerene $C_{70}$

*Sokolovsky D.N.*<sup>1,2</sup>, *Volkova Ya.Yu.*<sup>2</sup>

*sokolovskyd1@gmail.com*

<sup>1</sup> Ural State Medical University, Ekaterinburg, Russia

<sup>2</sup> Ural Federal University, Ekaterinburg, Russia

The effect of high pressures and temperatures is an effective means for creating metastable carbon phases, strongly dependent on the crystal structure and atomic hybridization. At high pressures in  $C_{60}$  and  $C_{70}$  crystals, the formation of solid carbon structures with covalent bonds between atoms of different fullerene molecules is observed, as is the case in diamond [1, 2].

To study the structural transformations occurring in fullerene  $C_{70}$  crystals at high pressures, the pressure dependences of the Seebeck coefficient ( $S$ ) of sample  $C_{70}$ , as well as the temperature dependences of the electrical resistivity, in the pressure range of 20-46 GPa were investigated.

High pressure has been generated in the diamond anvil cell (DAC) with conductive synthetic diamonds. The resistance of samples was measured in the temperature range of 77-400 K. The temperature of DAC was recorded using a copper/constantan thermocouple. The technique allows studying the sample with a consistent increase and decreasing in pressure, to withstand it under load for a long time [3].

In the pressure range of 20-46 GPa, a weak dependence of the electrical resistance on temperature is observed, and it decreases with increasing pressure. At pressures below 28 GPa, the dependences  $R(T)$  have the form characteristic of nondegenerate semiconductors. When the pressure reaches 34 GPa, the dependences of the electrical resistance on temperature becomes typical for materials with a partially filled conduction band. This may be caused by an increase in the proportion of disordered carbon atoms in the sample, and partial amorphization of fullerenes under pressure, as was previously observed [4].

The sign of the Seebeck coefficient and its value indicate to the electronic type of carrier. In the first cycle of gradual increase in pressure from the minimum (4 GPa) to the maximum value (46 GPa) and back to the minimum (at intervals of 2 GPa), the coefficient  $S$  decreases several times. When removing the load, the value of  $S$  decreases over the entire pressure range. In the two subsequent cycles of increase and removal of the load, there is an increasing dependence of the coefficient  $S$  with increasing pressure, was observed. Such a behavior of the Seebeck coefficient is due to phase transitions induced by high pressure [1, 2, 4].

### References

1. V. Soldatov, G. Roth, A. Dzyabchenko, D. Johnels, S. Lebedkin, C. Meingast, B. Sundqvist, M. Haluska, H. Kuzmany, *Science* (2001) **293**, 680.
2. D. Blank, S.G. Buga, N.R. Serebryanaya, G.A. Dubitsky, B.N. Mavrin, M.Yu. Popov, R.H. Bagramov, V.M. Prokhorov, S.N. Sulyanov, B.A. Kulnitskiy and Ye.V. Tatyatin, *Carbon* (1998) **36**, 319.
3. A. Ignatenko, A.N. Babushkin and V.Yu. Gorlanova, *Physics of The Solid State* (1996) **38**, 130.
4. Liu, M. Yao, L. Wang, Q. Li, W. Cui, B. Liu, R. Liu, B. Zou, T. Cui, B. Liu, J. Liu, B. Sundqvist, and T. Wagberg, *J. Phys. Chem. C* (2011) **115**, 8918.

## **Chitosan adsorption on nanodiamonds: composite stability and mechanism**

*Sinolits A.V.*<sup>1</sup>, *Chernysheva M.G.*<sup>1</sup>, *Popov A.G.*<sup>1</sup>, *Badun G.A.*<sup>1</sup>

*mighty-mouser@yandex.ru*

<sup>1</sup> Lomonosov Moscow State University, Moscow, Russia

Nanodiamonds are considered as a perspective tool in the development of drug delivery platform. Possessing a developed surface containing a large number of functional groups, nanodiamonds are able to adsorb various substances, including polymers. In present work we studied the adsorption of chitosan on nanodiamonds. We used tritium as a tracer of chitosan surface concentration. Tritium label was introduced into the chitosan molecules by means of tritium thermal activation method according to the procedure described in ref [1].

Tritium labeled chitosan was dissolved in 0.02 N HCl, mixed with nanodiamond suspension and incubated during 48 hours at room temperature followed by centrifugation and radioactivity measuring for both supernatant and precipitate [2].

It was found that adsorption isotherm of chitosan is of Langmuir type. The values of maximum adsorption and Langmuir constant are controlled by zeta potential of nanodiamonds. In the cases of negative zeta potential of initial nanodiamonds maximum adsorption was as much as 3 times higher than for positively charged materials indicating the dominant role of electrostatic interactions. Since significant amount of chitosan was irreversibly adsorbed on the surface of positively charged particles we can expect the essential contribution of Van der Waals interaction between chitosan and nanodiamond surface.

Stability of chitosan-nanodiamond composites was analyzed in water, PBS, 0.01 N HCl and serum albumin in PBS (40 g/L) at 37°C during 48 hours. Albumin in PBS was found to be the best desorbing agent for chitosan. Charge compensation by counterion in presence of buffer or HCl results in higher desorption confirmed the dominating ionic mechanism of chitosan binding to nanodiamond surface. Modification of nanodiamonds with chitosan affected its stability in the aqueous suspensions that was controlled by zeta potential measuring as a function of chitosan surface concentration.

Peculiarities of chitosan adsorption on nanodiamonds will be discussed in the presentation.

This work was supported by Russian Foundation for Basic Research (grant № 17-03-00985).

### **References**

1. Gallyamov M.O., Chaschin I.S., Khokhlova M.A., Grigorev T.E., Bakuleva N.P., Lyutova I.G., Kondratenko J.E., Badun G.A., Chernysheva M.G., Khokhlov A.R., *Materials Sci. Eng. C.* (014) **37**, 127.
2. Chernysheva M.G., Popov A.G., Tashlitsky V.N., Badun G.A., *Colloids Surfaces A: Physicochemical and Engineering Aspects* (2019) **565**, 25.



## Structural characterization of carbon nanomaterials by electron microscopy

*Parfimovich I.D.*<sup>1</sup>, *Komarov F.F.*<sup>1</sup>, *Milchanin O.V.*<sup>1</sup>, *Tkachev A.G.*<sup>2</sup>, *Shchegolkov A.V.*<sup>2</sup>

*irongrivus71@gmail.com*

<sup>1</sup> IAPP named after A.N.Sevchenko of BSU, Minsk, Belarus

<sup>2</sup> Tambov State Technical University, Tambov, Russia

Such carbon nanostructures as CNT [1] and graphene [2] discovered at the end of the 20<sup>th</sup> and the beginning of the 21<sup>st</sup> century, due to their unique structural and physical properties have drawn the attention of scientists from around the world. The field of application of such materials is extended a great and is based both on the use of pure nanostructures and as additives in various composites [3]. However, in order for unique materials based on them to possess outstanding properties, it is necessary that the nanotubes and graphene nanoplatelets themselves have the least defective structure.

The present paper is devoted to the study of the structural characteristics of carbon nanomaterials using the combination of methods of transmission (TEM) and scanning electron microscopy (SEM). The objects of the research were industrially manufactured nanostructures produced by "NanoTechCenter", Tambov, Russia.

The studies found that:

- Multi-walled carbon nanotubes are represented by various modifications that differ in length, diameter and degree of entanglement.
- «Taunit» presents of strongly intertwined tubes with a length of about 2  $\mu\text{m}$  and thicknesses in the range from 40 to 70 nm. MWCNT "Taunit-M" is similar in length (2  $\mu\text{m}$ ), however, nanotubes characterized by smaller thicknesses in the range of 10-20 nm. For the «Taunit-MD» material, there are an order of magnitude greater length (20  $\mu\text{m}$ ) and less entanglement of nanotube arrays (Fig. 1 *a*).
- Graphene nanoplates have linear dimensions ranging from 5 to 15  $\mu\text{m}$  and demonstrate a pronounced layered crystal structure, as evidenced by the presence of moire contrast on dark-field micrographs (Fig. 1 *b*), as well as the presence of diffraction rings on the electron diffraction patterns (Fig. 1 *c*).

The results of this study are in good agreement with the structural characteristics presented by the manufacturers of these materials and testify to their high quality.

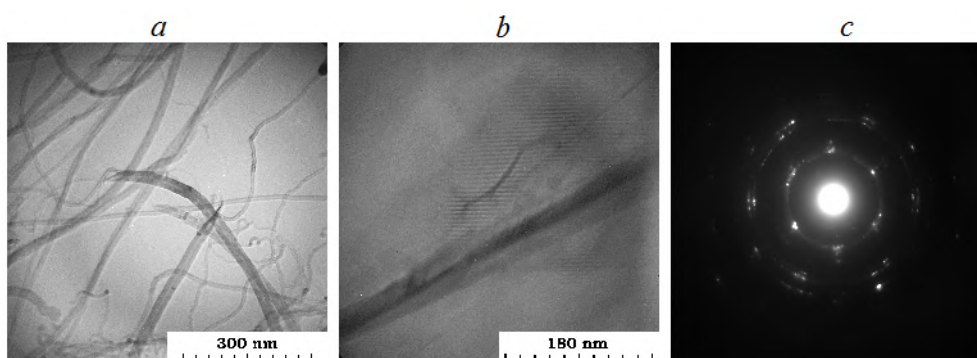


Fig.1. - TEM micrographs of samples of multi-walled nanotubes (a), graphene nanoplatelets (b) and electron diffraction patterns of nanoplatelets (c)

### References

1. Iijima, Nature (1991) **354**, 56.
2. S. Novoselov, A.K. Geim [et. al.] Science (2004) **306**, no. 5698, 666.
3. F.L. De Volder, S.H. Tawfick, R.H. Baughman, A.J. Hart, Science (2013) **339**, no.6119, 535.

## Comparison analysis of graphene oxide reduction methods

*Bunyaev V.A.*<sup>1</sup>, *Chernysheva M.G.*<sup>1</sup>, *Popov A.G.*<sup>1</sup>, *Grigorieva A.V.*<sup>1</sup>, *Badun G.A.*<sup>1</sup>

*vitalii1992@mail.ru*

<sup>1</sup> Lomonosov Moscow State University, Moscow, Russia

Graphene is two-dimensional sheet of sp<sup>2</sup>-hybridized carbon atoms. There are several methods of reduction of graphene oxide using the compounds that not affected the environment. In this context amino acids, plant extracts, carbohydrates, and organic acids should be mentioned. The potential applications of graphene are transport, performing electrodes; bio-, electrochemical, and chemical sensors; hydrogen storage; catalysts and etc. In present work we compared several methods of graphene oxide reduction and used reduced graphene oxide as a platform for radiolabeling peptide with tritium using tritium thermal activation method.

Graphene oxide was purchased from Cheaptubes Ltd. and reduced using several techniques: heating at 90°C in the solution of amino acids, heating at 155°C in water and in the mixture of hydrochloric and trifluoroacetic acids 2:1 with addition of 0.001% of β-mercaptoethanol. Reduced graphene oxide was characterized using Raman and Fourier Transform Infrared spectroscopy. According to Raman spectroscopy analysis quality of reduced graphene oxide obtained in presence of aspartic acid, glycine, valine, lysine, and proline is similar. FTIR spectroscopy analysis indicates the significant reduction and formation of hydrophobic material when graphene oxide was heated in water in comparing with other methods.

In present work graphene oxide and reduced graphene oxide obtained by reduction in aspartic acid, acids mixture and water were subjected to tritium atoms bombardment [1]. Samples of graphene oxide and reduced with the aspartic acid show close values of radioactivity measured directly after tritiation. Higher values of the initial radioactivity were observed for the samples of reduced graphene oxide obtained in acids mixture and in water. However, percentage of tritium in CH-bonds determined after purification from the labile tritium (in the functional groups) was higher for graphene oxide and reduced with the aspartic acid. The reasons of the observed results will be discussed in the presentation.

This work was supported by Russian Foundation for Basic Research (grant № 18-03-20147).

### References

1. A. Badun, M.G. Chernysheva, A.V. Grigorieva, E.A. Eremina, A.V. Egorov. // *Radiochimica Acta* (2016) **104**, 593.

## Hybrid macromolecular fullerene( $C_{60}$ )-containing stars incorporated polyphenyleneisophthalamide membranes for n-butanol dehydration

Larkina A.A.<sup>1</sup>, Polotskaya G.A.<sup>2</sup>, Pulyalina A.Yu.<sup>1</sup>, Vinogradova L.V.<sup>2</sup>

larckina2010@mail.ru

<sup>1</sup> Saint-Petersburg State University, Saint Petersburg, Russia

<sup>2</sup> Institute of macromolecular compounds, RAS, Saint Petersburg, Russia

The relevant problem of development of alternative fuels for internal combustion engines is the production of bio alcohols with high energy value, antiknock properties and low aggressiveness. Among the bioalcohols produced from biomass, n-butanol is the most valuable substitute for gasoline.

This paper is devoted to solve the problem of separation of n-butanol/water mixture to obtain high-purity alcohol due to its dehydration using the pervaporation method. Pervaporation membranes were developed on the basis of polyphenyleneisophthalamide (polyamide) modified with a hybrid macromolecular star-shaped polymer containing arms of polystyrene (PS) and poly-tert-butyl methacrylate (PTBMA) with the fullerene ( $C_{60}$ ) branch center (fig. 1). The effect of various HMS loadings on the performance was evaluated.

The membranes were characterized by a good mechanical strength and heat resistance, and at the same time it had high transport and separation properties. The structure was studied by scanning electron microscopy (SEM), atomic force microscopy (AFM) and X-ray diffraction analysis. Thermal characteristics were obtained during thermogravimetric analysis (TGA) and the method of differentiating scanning calorimetry (DSC). Modification of the membrane with star-shaped fullerene ( $C_{60}$ )-containing polymers led to a sharp increase in the selectivity and permeability of the membrane.

### Acknowledgments

The investigation was carried out with financial support of Russian Science Foundation (RSF), grant 18-79-10116. Equipment of Resource Centers of St. Petersburg State University, namely, "Chemical Analysis and Materials Research Centre", Interdisciplinary Resource Center "Nanotechnologies" and "Thermogravimetric and calorimetric methods of investigation" were used for investigation.

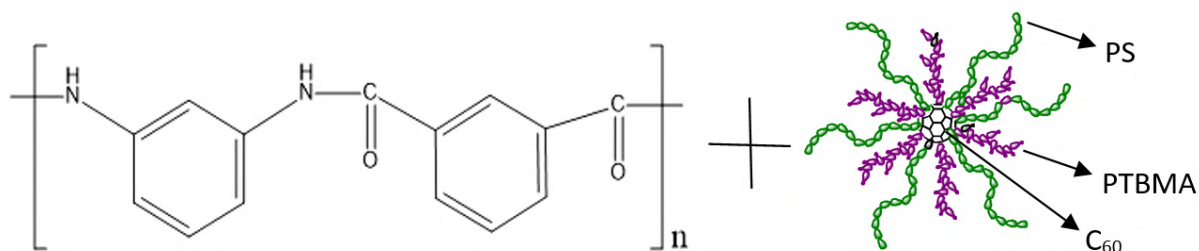


Fig. 1. Chemical structure of polyamide and hybrid macromolecular star

## Colloidosomes with a shell of detonation nanodiamonds

*Palamarchuk K.V.*<sup>1</sup>, *Bukreeva T.V.*<sup>1,2</sup>

*kvp1239@mail.ru*

<sup>1</sup> National Research Center Kurchatov Institute, Moscow, Russia

<sup>2</sup> Shubnikov Institute of Crystallography Federal Scientific Research Center Crystallography and Photonics, Russian Academy of Sciences, Moscow, Russia

In the last decade, development of methods for nanodiamonds synthesis together with the broad range of their possible applications made them one of the most attractive carbon materials for nanotechnology. Nanodiamonds have become a promising object due to inherent fluorescence, excellent biocompatibility, and ease of surface functionalization for biomedicine. Microcapsules have a large functional volume and are able to protect the active ingredient from exposure to the external environment. Encapsulation of the drug reduces side effects of the drug on the body and provides a prolonged effect of the drug. Therefore, promising are microcapsules with a shell consisting of nanodiamonds. This will make it possible to use the advantages of these objects for drug delivery and theranostics. Microcapsules have a large functional volume and are able to protect the active ingredient from exposure to the external environment. Encapsulation of the drug reduces side effects of the drug on the body and provides a prolonged effect of the drug. Therefore, promising are microcapsules with a shell consisting of nanodiamonds. This will make it possible to use the advantages of these objects for drug delivery and theranostics.

In the work, submicron and micron colloidosomes with a shell of detonation nanodiamonds (DND) were obtained by two different methods of emulsion homogenization: in an ultrasonic bath and in an ultrasonic homogenizer. The initial stable hydrosol of DND was prepared at Ioffe Institute according with description in [1]. Self-assembly of DND was carried out on the droplets of the dispersed phase of oil-in-water emulsion. Surfactant ( $10^{-3}$  M) was added to the organic phase for better emulsification. A mixture of dodecane with oleylamine or octadecylamine was added to the sols of positively charged DND. Another mixture, dodecane with stearic acid or oleic acid was added to the sols of negatively charged DND.

Microcapsules obtained in an ultrasonic bath had a submicron size (150-800 nm). This size is suitable for biomedical applications, in particular, for transfer with blood stream. However, capsules yield was less than 5%. The yield of the product prepared by the second method of reached about 90%. Capsules' size was about 2 microns, but a fraction of submicron capsules was also detected. Capsule shells were studied by transmission electron microscopy. Presence of DND was confirmed, their uniform distribution over the shell was also shown.

This work was partially supported by RFBR, project No. 17-53-10013.

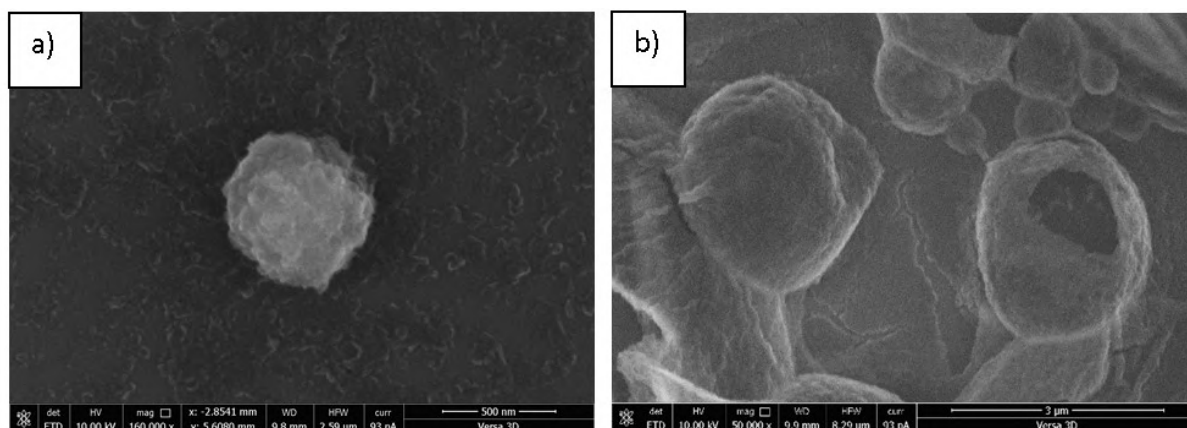


Fig.1. SEM images of colloidosomes obtained: a) in an ultrasonic bath; b) in an ultrasonic homogenizer

## Carbon Nanomaterials Modification by Oxidation and Reduction Reactions

*Babanya J.S.*<sup>1,2</sup>, *Ivanova M.K.*<sup>1</sup>, *Garashchenko B.L.*<sup>1</sup>, *Burakova I.V.*<sup>3</sup>, *Burakov A.E.*<sup>3</sup>, *Melezhyk A.V.*<sup>3</sup>, *Yakovlev R.Y.*<sup>1</sup>

*babanya@geokhi.ru*

<sup>1</sup> Vernadsky Institute of Geochemistry and Analytical Chemistry of RAS, Moscow, Russia

<sup>2</sup> D.Mendeleev University of Chemical Technology of Russia

<sup>3</sup> Department of Technology and Methods of Nanoproducts Manufacturing, Tambov State Technical University, Tambov, Russia

The carbon nanomaterials (CN) have a unique set of physicochemical properties that determine their widespread use in various fields of science and technology. Properties of CN can be changed by modifying their surface and thereby impart high hydrophilicity to CN for their application in biology and medicine. The oxidation of the surface (the formation of -COOH) increases the electrostatic potential of the particles, reduces their size and increases the colloidal stability [1]. Reduction modification allow the decrease number of structures defects in sp<sup>2</sup>-carbon nanomaterials and to reduce its toxicity [2]. The purpose of our work was to obtain and study the physicochemical properties of modified carbon nanomaterials for use in biomedical applications.

The multi-walled carbon nanotubes (MWNT) of the «Taunit M» brand (Nanotechtsentr LLC, Tambov) and the detonation nanodiamonds (ND) (SKTB Technolog, St. Petersburg) were used in this research. Oxidation of CN was carried out in liquid phase (H<sub>2</sub>SO<sub>4</sub>/HNO<sub>3</sub> = 3:1, 100-120 °C, 6-24 h), reduction in hydrogen atmosphere (H<sub>2</sub>, 800 °C, 5 h).

ND have retained their crystalline structure and size (4-6 nm) after oxidation-reduction modification, it was proved by the TEM method. In the reduction process, the surface becomes bifunctional, containing -H and -OH groups; the oxygen content was reduced from 7.7 to 5 at. %. The colloidal stability of hydrosols increased and the size of the aggregates was 50 nm.

Commercial MWCNTs represented curved filamentary multilayer graphene layers of a cylindrical shape with an internal closed cavity with a diameter of up to 30 nm and a wall thickness of 5-10 nm. The oxygen content in the sample decreased from 4 to 10 wt. % (XPS data), the graphene layers were subjected to destruction, about 70% of the MWCNT tips opened up. The formation of carboxyl groups was detected by FTIR spectroscopy by the appearance of a maximum >C=O at 1730 cm<sup>-1</sup>. The hydrodynamic diameter of the rolled MWCNTs decreased to 50 nm according to the data of the DLS. Oxidized MWCNTs practically did not precipitate at 11000 g for 1 h. The content was reduced by oxygen to 0.64 at. % in the recovery process, the reduction led to the stabilization of the MWCNTs in the solution in the form of particles with dimensions of 150 nm and a small amount (up to 5%) of micron-sized particles. Thus, modified CNs were obtained and their stable hydrosols were prepared for further biomedical experiments.

The work was supported by the grant of the President of the Russian Federation MK-4306.2018.3.

### References

1. Thakur V. K., Thakur M. K. (ed.). Chemical functionalization of carbon nanomaterials: Chemistry and applications. CRC Press, (2015), 1102 p.
2. J. Muller, F. Huaux, A. Fonseca, J.B. Nagy, N. Moreau, M. Delos, E. Raymundo-Pinero, F. Beguin, M. Kirsch-Volders, I. Fenoglio, B. Fubini, D. Lison. Structural defects play a major role in the acute lung toxicity of multiwall carbon nanotubes: toxicological aspects. Chemical research in toxicology (2008) 21(9), 1698.

## Using graphene like buffer layer for PA-MBE of III-nitrides on different amorphous substrates

*Borisenko D.P.*<sup>1</sup>, *Gusev A.S.*<sup>1</sup>, *Kargin N.I.*<sup>1</sup>, *Komissarov I.V.*<sup>1,2</sup>, *Labunov V.A.*<sup>1,2</sup>

*DPBorisenko@mephi.ru*

<sup>1</sup> National Research Nuclear University MEPhI, Moscow, Russia

<sup>2</sup> Belarusian State University of Informatics and Radioelectronics, Minsk, Belarus

III-nitride semiconductors and their alloys have attracted considerable attention because of their outstanding properties leading to many applications for light-emitting diodes, laser diodes, high-frequency and high-power transistors. Absolute majority of the GaN-based devices are fabricated on single-crystal sapphire and SiC substrates because of their high crystallinity and lattice parameter compatibility. The main drawback of these substrates - the high cost. Since graphene has a hexagonal lattice, it can be considered as a 2D buffer layer for GaN and AlN epitaxy. Therefore, the purpose of this work was to investigate the possibility of graphene using as a buffer layer for epitaxial growth of III-nitrides (GaN and AlN) by plasma-assisted molecular beam epitaxy (PA-MBE) on amorphous substrates.

In this paper, the multilayer graphene films were grown by chemical vapor deposition on copper using methane as a carbon source and then transferred onto the surface of 2-inch Si wafers with amorphous dielectric layers. (Fig. 1). Then GaN and AlN epilayers were grown by PA-MBE using Veeco GEN 930 setup. The growth of both AlN and GaN layers was started with a high temperature (HT) nucleation of a 20 ÷ 30 nm-thick layer at  $T_s = 710^\circ\text{C}$  under nitrogen-rich mode ( $F_{\text{Al}}/F_{\text{N}} \approx 0,6$ ). After that a 500 nm thick layer of GaN (or AlN) was grown under metal-rich conditions ( $F_{\text{Me}}/F_{\text{N}} > 1,5$ ). Formation of the metal microdroplets under these conditions was avoided by using Ga (or Al) flux interruptions with duration controlled by pyrometry. The nucleation and growth was also monitored in situ by RHEED method.

In the final step, the comparative study of graphene coated parts of the wafers and the parts without graphene was carried out by scanning electron microscopy (SEM) and high-resolution X-ray diffractometry (XRD) including XRD pole figures method. SEM images of the GaN film grown on graphene/dielectric substrate (Fig. 1, c) demonstrate a smooth surface morphology with relatively low density of structural defects. At the same time, SEM image analysis shows that the GaN film on the regions of the substrate without graphene has polycrystalline fine-grained (200 ÷ 300 nm) morphology (Fig. 1, d).

As a conclusion: it was shown that epitaxial GaN and AlN films with close to 2D surface morphology can be obtained by PA-MBE on amorphous substrates with graphene buffer layer using the HT AlN nucleation layer.

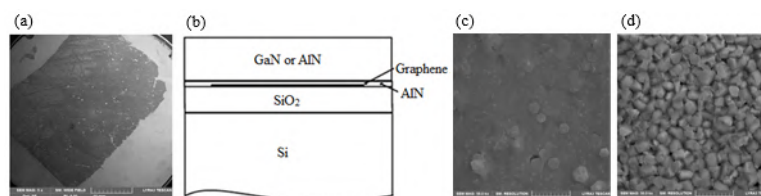


Fig.1. (a) The low-zoom SEM image of the graphene layer on the surface of 2-inch Si wafer before the MBE growth process, (b) cross section scheme of experimental structure. SEM images: (c) - the surface of GaN film on graphene coated part, (d) - the surface of GaN film on amorphous substrates

## Reduced graphite oxide and polypyrrole nanocomposites for supercapacitor applications.

*Iurchenkova A.A.*<sup>1</sup>, *Fedorovskaya E.O.*<sup>1,2</sup>

*anna.yurchenkova@yandex.ru*

<sup>1</sup> Laboratory of hybrid materials for electrochemical energy storage devices, Novosibirsk State University, 630090, Novosibirsk, 1, Pirogova str., Russia

<sup>2</sup> Physics & Chemistry of nanomaterials laboratory, Nikolaev Institute of Inorganic Chemistry, SB RAS, 630090, Novosibirsk, 3, Acad. Lavrentiev Ave., Russia

Supercapacitors are electrochemical energy storage devices with high power, charging-discharging rate, low weight and durability. Charge accumulation in supercapacitors is accounted for two processes: double electric layer formation at electrode surface-electrolyte interface, and redox (reduction - oxidation, so called Faraday) reactions proceeding. Carbon materials mainly accumulate energy due to the double electric layer foundation. Thus, their advantages are large surface area, high conductivity and cycling stability. Conducting polymers and transition metals oxides basically accumulate energy through the Faraday reactions, they possess more capacities, but lower chemical stability in comparison with carbon materials. Thus, derivatization of the composites that combine the carbon template and electrically active conducting polymers properties has shown the promising applications in high-effective electrode supercapacitor materials production.

Reduced graphite oxide (RGO) as well as many other graphene-like materials is promising for production and improvement of supercapacitors. RGO synthesis doesn't require expensive equipment and can be produced in industrial scale. Along with the easier producing it has such characteristics as high specific area and good chemical stability. Polypyrrole is N-heterocyclic conducting polymer with high specific capacity, good electrical and ion-conductivity and chemical stability.

In our work, graphite oxide was synthesized by modified Hummers method as precursor for RGO synthesis. Then RGO was synthesized by graphite oxide ultrasonication in sulfuric acid medium. Further, RGO was thermally expanded at 250°C and then thermally treated at 500°C (RGO-500) for the selective removal of the oxygen-containing groups. The nanocomposites were synthesized by RGO/polypyrrole co-deposition processes. Co-deposition was carried out in acetonitrile media by the action of FeCl<sub>3</sub>.

To study the morphology and functional composition of obtained products SEM, HR TEM, IR-spectroscopy and Raman spectroscopy methods were used. Cyclic voltammetry and electrochemical impedance spectroscopy methods were used to investigate electrochemical behavior of the samples.

It was shown that RGO specific capacity increase after polypyrrole deposition, reaching 200 F/g. Since the materials demonstrated high stability during the cycling process.

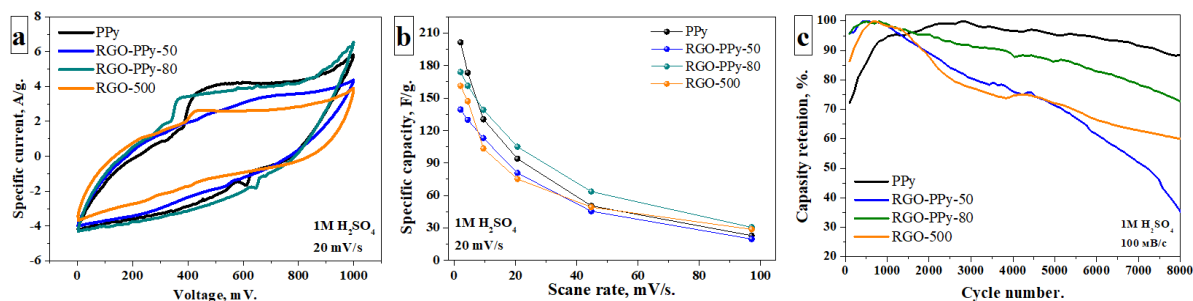


Fig. 1. Samples electrochemical characteristics in 1M H<sub>2</sub>SO<sub>4</sub>: (a) cyclic voltammograms at 20 mV/s; (b) specific capacity in the range of 2-100 mV/s; (c) long-life cycling at 100 mB/c.

## Characterization and purification of phosphorus filled single-wall carbon nanotubes

*Fedosova A.A.*<sup>1,2</sup>, *Stolyarova S.G.*<sup>1</sup>, *Gurova O.A.*<sup>1</sup>, *Koroteev V.O.*<sup>1</sup>, *Bulusheva L.G.*<sup>1,2</sup>, *Okotrub A.V.*<sup>1,2</sup>

*a.fedosova@g.nsu.ru*

<sup>1</sup> Nikolaev Institute of Inorganic Chemistry, SB RAS, Novosibirsk, Russia

<sup>2</sup> Novosibirsk State University, Novosibirsk, Russia

Heteroatom doping of carbon nanotubes (CNTs) is of great interest both from the fundamental point of view to study the effect of alloying impurities on quasi-one-dimensional electrical conductors, and for applications as field cathodes, electrochemical materials, composites, and nanoelectronic devices [1-4]. The first reports demonstrate that in phosphorus-doped CNTs, phosphorus atoms are coordinated by three neighboring carbon atoms, but their content does not exceed 1%.

One of the most effective and simple methods of synthesis of filled single-wall carbon nanotubes (SWCNTs) is ampoule method of synthesis. The filling was carried out in an H-shaped ampoule, in one part of which phosphorus was placed, and in another – SWCNTs. By varying such parameters as the ratio of reagents, synthesis time and synthesis temperature, we achieve 8 at. % of phosphorus content according to XPS. Equally important is the cleaning as the initial SWCNTs and obtained samples. The initial sample contains entangled nanotube bundles and metallic particles of catalyst. To remove residual iron catalyst SWCNTs was stirred in acid in an ultrasonic bath. Acid treatment removes most of the catalyst nanoparticles, however, the samples still contain some residual iron contaminations. To increase the purity of SWCNTs, we used the magnetic separation method, thereby reducing the number of iron nanoparticles to 0.3%. During the synthesis, phosphorus enters into the cavity of the nanotube, but significant part of phosphorus settles on the surface of the nanotube. To remove phosphorus from the surface of the nanotube we used 10 wt. % solution of NaOH and mix it at 60°C. Additional ultrasonic treatment helps to increase the content of phosphorus. Using this method, we able to achieve the phosphorus content 15 at. % according to XPS, while before it was 8 at. %.

### References

1. J.C. Zheng, M.C. Payne, Y.P. Feng, A.T.L. Lim, Stability and electronic properties of carbon phosphide compounds with 1:1 stoichiometry, *Phys. Rev. B - Condens. Matter Mater. Phys.* 67 (2003) 1-4. doi:10.1103/PhysRevB.67.153105.
2. A.T.-L. LIM, J.-C. ZHENG, Y.P. FENG, Stability of Hypothetical Carbon Phosphide Solids, *Int. J. Mod. Phys. B.* 16 (2002) 1101-1104. doi:10.1142/s0217979202010932.
3. F. Claeysens, N.L. Allan, P.W. May, P. Ordejón, J.M. Oliva, Solid phosphorus carbide?, *Chem. Commun.* 8 (2002) 2494-2495. doi:10.1039/b207743b.
4. G. Wang, R. Pandey, S.P. Karna, Carbon phosphide monolayers with superior carrier mobility, *Nanoscale.* 8 (2016) 8819-8825. doi:10.1039/c6nr00498a.



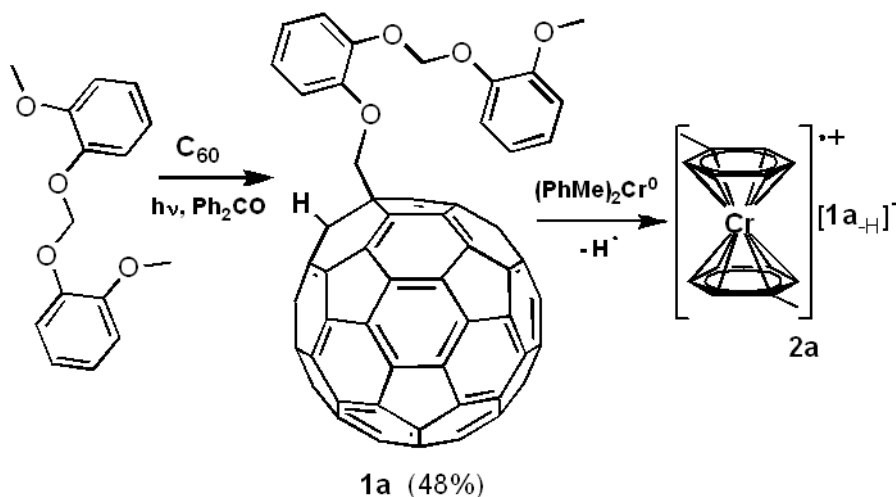
## Bis(arene)chromium 1-((2-((2-methoxyphenoxy)methoxy)phenoxy)methyl)-1,2-dihydrofullerene (**1a**)-1-hydrofulleride (**2a**)

Markin G.V.<sup>1</sup>, Ketkov S.Yu.<sup>1</sup>, Lopatin M.A.<sup>1</sup>, Shavyrin A.S.<sup>1</sup>, Kuropatov V.A.<sup>1</sup>

mag@iomc.ras.ru

<sup>1</sup> G.A. Razuvaev Institute of Organometallic Chemistry, RAS, Nizhny Novgorod, Russia

Bis(toluene)chromium reacts with 1-((2-((2-methoxyphenoxy)methoxy)phenoxy)methyl)-1,2-dihydrofullerene (**1a**), in toluene at 293 K to form salts bis(toluene)chromium 1-((2-((2-methoxyphenoxy)methoxy)phenoxy)methyl)-1-hydrofulleride (**2a**), Fulleride **2a** is stable at 323K. Fulleride **2a** is insoluble in hexane, sparingly soluble in PhMe, soluble in THF. NIR spectrum of fulleride **2a** in THF at 290 K indicates absorption bands in 985 -997 and 645 - 655 nm range typical for anions [**1a<sub>H</sub>**]. Fullerene **1a** was obtained by irradiation of fullerene C<sub>60</sub>, bis(2-methoxyphenoxy)methane and benzophenone in o-dichlorobenzene solution with 1:41:132 molar ratio and 2.8 mg/ml C<sub>60</sub> concentration using luminescent UV lamp 370 nm 10x10w in an evacuated and sealed pyrex ampoule at 313 - 323 K for 450 minutes. After solvent evaporation in vacuo, fullerene **1a** was extracted with CHCl<sub>3</sub>, dried in vacuo, washed by hexane and acetone. Column chromatography over silica gel with toluene as eluent gave first unreacted [60]fullerene, some impurities and then, fullerene **1a** as amorphous brown solid. Fullerene **1a** is insoluble in hexane, soluble in CHCl<sub>3</sub> and THF. The UV/vis spectrum of **1a** in decaline at 290 K show absorption bands typical for 1,2 [60]fullerene derivatives. All reactions were carried out under an inert atmosphere. The work was performed using the instrumental base of the Analytical Center of the G.A. Razuvaev Institute of Organometallic Chemistry, Russian Academy of Sciences and in the framework of the Russian state assignment.



## Colloidal dispersions of nanostructured carbon, silicon and silicon carbide

*Belyavin V.A.*<sup>1,2</sup>, *Kashnik I.V.*<sup>1,2</sup>, *Ivanova M.N.*<sup>2</sup>, *Brylev K.A.*<sup>1,2</sup>, *Nikiforov A.A.*<sup>3</sup>, *Ezdin B.S.*<sup>1</sup>, *Fedorov V.E.*<sup>1,2</sup>

*kozlova@niic.nsc.ru*

<sup>1</sup> Novosibirsk State University, Novosibirsk, Russia

<sup>2</sup> Nikolaev Institute of Inorganic Chemistry, Novosibirsk, Russia

<sup>3</sup> LLC Nikom, Novosibirsk, Russia

- Nowadays, a large variety of methods for preparation of nanomaterials are described in scientific literature. *Top-down* processes, such as liquid phase exfoliation, ablation, etc., as well as *bottom-up* processes, e.g. CVD, wet chemical synthesis, etc., are most widely used. This work reports the development of the relatively less studied method of *bottom-up* nanomaterials synthesis, namely, decomposition of gaseous precursors in a flow-type chemical compression reactor (CCR). This approach of nanopowder production is efficient, relatively low-cost and large-scale.
- CCR is a cyclic heat engine in which the reaction mixture is compressed with a pair of "piston-cylinder" to the temperature and pressure necessary for the rapid course of a chemical reaction. The developed reactor can be used for decomposition of the starting gaseous compounds of different nature. Here, we report the results of decomposition of **carbon**-containing (acetylene, ethylene) and **silicon**-containing (monosilane) precursors, as well as **mixtures** of both carbon and silicon precursors. Depending on the starting compounds, initial loadings, carrier gas, and pressure in the reactor, samples of different structure and chemical composition can be obtained.
- The synthetic conditions were optimized, and the resulting products were investigated by a set of physicochemical methods, such as X-ray diffraction, high-resolution transmission electron microscopy, Raman spectroscopy, thermogravimetric analysis, etc. All samples prepared are well-dispersed and may consist of different phases. If carbon- or silicon-based precursors were used, the samples of nanostructured C and Si, respectively, were obtained. But the most interesting results may be achieved when the mixture of two precursors was used. This approach leads to the formation of binary phase, namely, SiC, that is of great practical interest due to its useful electrophysical properties. Since a limited number of experimental techniques are known for Si or SiC nanoparticle preparation, the presented approach applying the CCR is novel and very promising.
- All samples prepared (C, Si, SiC, and heterogeneous mixtures) are nanostructured powders, therefore, we investigate their ability to form stable colloidal dispersions in polar liquid media under ultrasonic treatment. A wide range of organic solvents were tested. The properties of colloidal dispersions were studied by UV-vis spectra, dynamic light scattering, etc. The prepared colloidal dispersions can be used as inks for 2D printing and as precursors for preparation of thin films and composite materials of different structures.
- This work was supported by Russian Science Foundation (project 19-13-00067).

## Novel fullerene(C<sub>60</sub>)-containing membranes with high selectivity: pervaporation and neutron scattering studies in separation of water-acetic acid mixture

*Rudakova D.A.*<sup>1</sup>, *Polotskaya G.A.*<sup>1,2</sup>, *Pulyalina A. Yu.*<sup>1</sup>, *Lebedev V.T.*<sup>3</sup>, *Torok Gy.*<sup>4</sup>, *Vinogradova L.V.*<sup>2</sup>

*rudakova.gda@gmail.com*

<sup>1</sup> Saint Petersburg State University, Institute of Chemistry, Saint Petersburg, Russia

<sup>2</sup> Institute of Macromolecular Compounds, Russian Academy of Sciences, Saint Petersburg, Russia

<sup>3</sup> Saint Petersburg membrane Nuclear Physics Institute named by B.P. Konstantinov, NRC Kurchatov Institute, Gatchina, Russia

<sup>4</sup> Research Institute for Solid State Physics and Optics, Wigner Research Centre for Physics, Hungarian Academy of Sciences, Budapest, Hungary

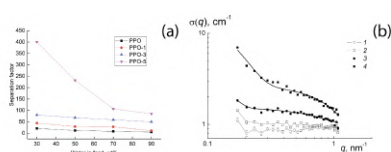
In recent decades, the task of introducing more environmentally friendly and cost-effective technologies stands in the priority areas of the industry. Acetic acid is one of the most important products of commercial organic synthesis. More than half of all acetic acid produced in the world is spent on the manufacture of polymers which are cellulose and vinyl acetate derivatives. Pervaporation is an effective method for obtaining dehydrated acetic acid. The transport properties of membranes based on polyphenylene oxide (PPO) modified with regular star-shaped macromolecules (up to 5 wt.%) containing polar and non-polar arms (polystyrene (PS) and poly-2-vinylpyridine (P2VP)) on a fullerene core were studied during pervaporation separation of acetic acid -water mixtures in a wide range of water concentrations (30-90 wt.%.)

Fig.1. Dependences of separation factor on water concentration in the feed for pervaporation of water – acetic acid mixture (a), cross section  $\sigma(q)$  vs momentum transfer  $q$  for swollen membranes (b).

Sorption experiments were made for mass transfer investigation. Via pervaporation of binary mixture water-acetic acid the transport properties of the membranes were studied. SEM microscopy was employed for morphology characterization. TG and DSC were used for thermal stability estimation. It has been established that the total flux through the membrane increases with an increase in both the content of stars in the membrane and the concentration of water in the initial mixture. The separation coefficient reaches a maximum value when using a membrane containing 5 wt.% star-shaped modifiers. Membranes in the dry and swollen state in deuterated acetic acid were studied by small-angle neutron scattering. It has been established that star-shaped macromolecules are unevenly distributed in the matrix volume and aggregated in the form of supramolecular structures. Such structure creates additional free volume and thus contribute to the formation of diffusion channels, which affects the transport properties of pervaporation membranes.

### Acknowledgements

Equipment of Resource Centers of Saint Petersburg State University, namely, Interdisciplinary Resource Center “Nanotechnologies”, “Thermogravimetric and calorimetric methods of investigation” and Education Resource Centre in the direction of chemistry were used for investigation.



## Temperature dependence of water intercalated graphite oxide at heating

*Grebenkina M.A.*<sup>1,2</sup>, *Gusel'nikov A.V.*<sup>1</sup>, *Stolyarova S.G.*<sup>1</sup>, *Bulusheva L.G.*<sup>1,2</sup>, *Okotrub A.V.*<sup>1,2</sup>

*grmariya@mail.ru*

<sup>1</sup> Nikolaev Institute of Inorganic Chemistry SB RAS, Novosibirsk, Russia

<sup>2</sup> Novosibirsk State University, Novosibirsk, Russia

Graphite oxide (GO) is a hydrophilous graphite derivative with covalent banded oxygen functional groups [1]. GO has potential applications in several fields such as electronics [2], biosensors [3] and filtration of water [4]. Investigation of GO's dielectric properties allows GO to be widely applicable.

In the study we researched temperature dependence of GO's dielectric constant within the temperature range from 25°C to 150°C and the frequency range from 1 Hz to 7 MHz. The dielectric properties of GO synthesized by modified the Hummers method and the Brodie method were compared. Impedance spectroscopy with the method of parallel plates was applied for the measurements. The measuring cell (Fig. 1) for solid samples as well powders was designed. To precise the results the parasitic capacitance was calculated by determination of the empty cell's capacitance with the distance between electrodes equal to the cell with a sample and was subtracted from the capacitance of the sample.

It was observed that intercalated water molecules influence dielectric constant of GO synthesized by the Hummers method at water's phase transition temperature ( $T = 100^{\circ}\text{C}$ ). Despite that GO synthesized by the Brodie method has not the similar feature. The difference was explained by the existence of several interplanar water layers in GO synthesized by the Hummers method.

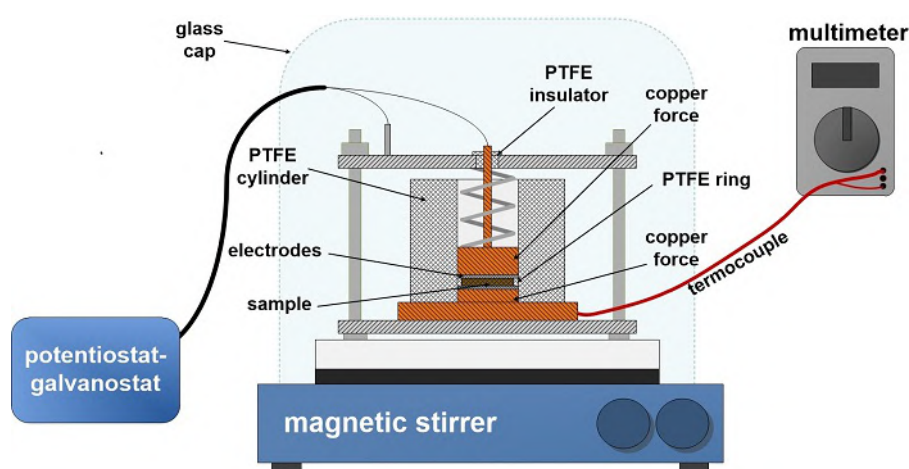


Fig. 1. Scheme of experimental assembly for heating.

### References

1. R. Dreyer, S. Park, C. W. Bielawski, and R. S. Ruoff, *Chem. Soc. Rev.* (2010) **39**, 228.
2. W. Gao, N. Singh, L. Song, Z. Liu, A. L. M. Reddy, L. Ci, R. Vajtai, Q. Zhang, B. Wei, and P. M. Ajayan, *Nature Nanotechnology* (2011) **6(8)**, 496.
3. K. P. Loh, Q. Bao, G. Eda, and M. Chhowalla, *Nature chemistry* (2010) **2(12)**, 1015.
4. R. Devanathan, D. Chase-Woods, Y. Shin, and D. W. Gotthold, *Scientific reports* (2016) **6**, 29484.

## Hot pressing synthesis of P-doped carbon onions as anode material for sodium-ion batteries

*Stolyarova S.G.*<sup>1</sup>, *Fedosova A.A.*<sup>2</sup>, *Okotrub A.V.*<sup>1,2</sup>, *Bulusheva L.G.*<sup>1,2</sup>

*stolyarova@niic.nsc.ru*

<sup>1</sup> Nikolaev Institute of Inorganic Chemistry SB RAS, Novosibirsk, Russia

<sup>2</sup> Novosibirsk State University, Novosibirsk, Russia

Spherical particles with a large interplanar distance have a perspective as an anode material for sodium- and potassium-ion batteries. Replacement of lithium by sodium is expected to reduce the cost of the batteries. Carbon doping by phosphorus allows increasing the capacity of the anode material. Hot pressing allows graphitizing nanodiamond particles with the production of onion-like carbon. Compression of the particles in the presence of the decomposition products of P-containing compounds enables to promote interaction of released phosphorus atoms with defects and edges of graphene-like layers with the formation of P-C bonds [1].

In this work, the syntheses were carried out as follows. Nanodiamonds (NDs) were suspended in ethanol by ultrasound treatment. For phosphorous doping, triphenylphosphine (PPh<sub>3</sub>) was added in the suspension. Then, the powder mixture ND/PPh<sub>3</sub> was pressured at 100 bar and heated at a temperature varied from 1000 and 1500 °C. Characterization of the products by Raman and XPS spectroscopy showed graphitization of NDs at the temperature higher 1000 °C. The electrochemical properties of the materials were examined during the cycling of sodium half-cells and by the method of electrochemical impedance spectroscopy.

*The work was conducted with financial support from the Russian Foundation for Basic Research (Grant 19-53-53020).*

### References

1. A.V. Okotrub, D.V. Gorodetskiy, M.A. Kanygin, L.G. Bulusheva, A. Vyalikh, I.P. Asanov, V.O. Koroteev, S.G. Stolyarova, Y.V. Fedoseeva, Phosphorus incorporation into graphitic material via hot pressing of graphite oxide and triphenylphosphine, *Synth. Met.* (2019) **248**, 53–58.

## **Sulfur filling and structure of TUBALL™ nanotubes**

*Gurova O.A.*<sup>1</sup>, *Sysoev V.I.*<sup>1</sup>, *Lobiak E.V.*<sup>1</sup>, *Sedelnikova O.V.*<sup>1,2</sup>, *Bulusheva L.G.*<sup>1,2</sup>, *Okotrub A.V.*<sup>1,2</sup>

*olga.gurov@gmail.com*

<sup>1</sup> Nikolaev Institute of Inorganic Chemistry SB RAS, Novosibirsk, Russia

<sup>2</sup> Novosibirsk State University, Novosibirsk, Russia

Encapsulation of sulfur inside single-walled carbon nanotubes (SWCNT) could result in new physical properties of nanotubes due to changes in the electronic structure and chemical activity of the material.

Ampoule synthesis is the most effective and simple method for filling of SWCNTs due to its simplicity and wide range of compounds, which could be tried for encapsulation. In this work we used SWCNT (TUBALL™) provided by OCSiAl company. The average tube diameter was 1.7 - 1.9 nm. In order to open carbon «caps», SWCNTs were annealed at 500 °C in open air. To remove residual catalyst, a portion of initial SWCNTs was stirred in HCl acid, followed by washing with distilled water to the neutral pH and drying in muffle furnace. Before filling, nanotube powder with elemental sulfur was ground in an agate mortar. The resulting mixture was poured into a quartz ampoule. The ampoule was sealed in vacuum. Filling of SWCNT was carried out at 700 °C for 15 hours. To remove the sulfure attached to the nanotube surface the as-obtained samples were treated with toluene. The structure of the initial and sulfur-filled SWCNTs was characterized by scanning electron microscopy, optical, Raman and X-ray photoelectron spectroscopies. The electrochemical and gas sensing properties of the SWCNT were measured.

This work was partially supported by and the Russian Science Foundation (Project 18-72-00017).

**Poster session 3:  
Graphene.  
Related Materials + Carbon Nanotubes.  
Biomedical applications.**

## Graphene synthesis in plasma jet with ethanol

*Shavelkina M.B.<sup>1</sup>, Amirov R.H.<sup>1</sup>, Borodina T.I.<sup>1</sup>, Fedyushin N.A.<sup>1</sup>, Yusupov D.I.<sup>1</sup>*

*mshavelkina@gmail.com*

<sup>1</sup>Joint Institute for High Temperatures of Russian Academy of Sciences, Moscow, Russia

The cost of graphene production significantly reduces when using ethanol as a carbon source. Ethanol might be obtained from fermentation of agricultural industries. The process provides an additional benefit due to revalorization of wastes in the graphene production. The method is known of the graphene flakes fabrication via the ethanol decomposition by means of the thermal plasma jet system [1]. The carbon atomic beam is generated by continuous ethanol injection into the argon plasma; the beam then flows through the carbon tube attached to the anode. Graphene is made by epitaxial growth where the proper energy carbon atomic beam collides with the graphite plate.

We develop a new method for the free-standing graphene synthesis. The essence of the method is in the continuous supply of the argon- or nitrogen-ethanol mixture into the direct-current plasma torch with the subsequent strong cooling of the obtained vapor-gas stream. The advantage of the method consists in its simplicity, since it does not require the prior conversion of the liquid alcohol into the gaseous state. This technique provides high-quality powder graphene within just single step, using neither metal catalysts nor specific substrate. We characterized synthesized graphene flakes by means of scanning electron microscopy, simultaneous thermal analysis, and X-ray analysis. We found that the sort of the plasma-forming gas affects the morphology of the final product (Figure ) and its thermal stability. When using argon in the synthesis of graphene, the lateral size of the flakes is within the range of 300–500 nm (Figure (a)). When alcohol is added to nitrogen, the lateral size of the flakes reaches up to 1  $\mu\text{m}$ , but the size dispersion becomes significant (Figure (b)). When heating the samples synthesized in the argon plasma, their mass losses, within the temperature range of 300–1300 K, are not more than 5 wt.%. Graphene produced in the nitrogen plasma is less thermally stable.

Thus, this work demonstrates the features of plasma technology as the low cost, efficient, clean and environmentally friendly route for the high-quality graphene production.

The work is supported by the Russian Foundation for Basic Research, projects nos. 18-08-00040, 19-08-00081, 18-08-00306.

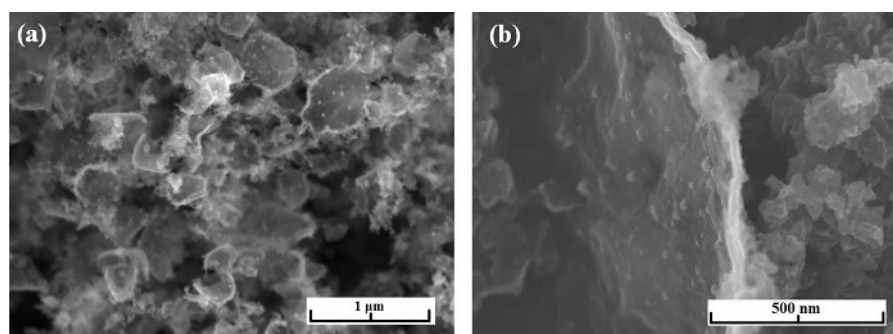


Fig. (a) SEM- image of synthesized graphene in the argon plasma jet, 350 Topp. (b) SEM- image of synthesized graphene in the nitrogen plasma jet, 150 Topp.

### References

1. J. Kim, S.B. Heo, G.H Gu, J.S. Suh, *Nanotechnology* (2010) **21**, 095601 (6pp).



## Nature of paramagnetic centers in graphite oxide according to EPR spectroscopy and DFT calculations

*Vorobiev A.Kh.*<sup>1</sup>, *Astvatsaturov D.A.*<sup>1</sup>

*a.kh.vorobiev@gmail.com*

<sup>1</sup> Moscow State University, Moscow, Russia

Graphite oxide is a non-stoichiometric derivative of graphite prepared by oxidation of pure graphite in acidic conditions. It is known that graphite oxide has a central EPR signal and pair of partially resolved small satellites, which can be observed depending on conditions of spectra recording and sample preparation. There is a widespread supposition that signals in EPR spectra of graphite oxide correspond to localized paramagnetic centers in graphite oxide structure and the satellites are the result of hyperfine interaction of electron spin with hydrogen nucleus. However, nature of paramagnetic centers in graphite oxide has not been studied sufficiently. The aim of this contribution is experimental EPR examination of graphite oxide and quantum-chemical determination of structures conforming to the experimental data.

In our work, the Brodie-type graphite oxide (B-GO) was studied. The samples were degassed in vacuo ( $5 \cdot 10^{-3}$  torr). X-band (3 cm) and Q-band (8 mm) EPR spectra were recorded. Orca (3.0.3) program package was used for quantum-chemical calculations by DFT method.

In our experiments, the EPR spectra of B-GO had an intensive central signal ( $g=2.0030$ ) and contained satellites with distance of  $\sim 10.2$  G. It was found that in course of isotopic exchange (H/D), the satellites vanish and the deuterium hyperfine structure appears. This experiment confirms that the satellites are the result of electron spin coupling with hydrogen. On the other hand, the distance between satellites in the EPR spectra recorded in Q-band was found to be 37 G. This kind of observation is known to be typical to forbidden electron spin transitions accompanied by nuclear spin flips of the hydrogen. The observed distances between satellite signals in X-band and Q-band EPR spectra are in excellent agreement with calculated for these forbidden transitions.

Numerical simulations of experimental spectra were performed for determination of magnetic parameters of paramagnetic centers in B-GO. The simulations show that the EPR spectra of B-GO sample can be described as a sum of central signal and signal with hyperfine splitting with axial tensor of hyperfine constants. Determination of the structures demonstrating the experimentally observed chemical properties and magnetic parameters was performed by DFT calculations. A number of oxygen-centered paramagnetic centers with nearby allocated proton are proposed as potential structures responsible for EPR spectra of graphite oxide.

This work was supported by the Russian Foundation for Basic Research (grant 18-29-19120).

## **Superhydrophobic aerogels based on reduced graphene oxide and ultra-high molecular weight polyethylene**

*Gudkov M.V.*<sup>1</sup>, *Brevnov P.N.*<sup>1</sup>, *Shiyanova K.A.*<sup>1</sup>, *Anosov A.A.*<sup>1</sup>, *Novokshonova L.A.*<sup>1</sup>, *Melnikov V.P.*<sup>1</sup>

*gudkovmv@gmail.com*

<sup>1</sup> Semenov Institute of Chemical Physics of Russian Academy of Sciences, Moscow, Russia

One of the new and quite popular scientific areas is the production of composite materials based on graphene aerogels with a three-dimensional electrically conductive structure, high specific surface and porosity. Materials based on aerogels have relatively high target characteristics, but the authors point out the need for their improvement, which is associated with the fragility of graphene aerogels and materials based on them, as well as the need to modify the surface to control porosity. The problem of obtaining highly filled polymer composites combining high electrical conductivity, the required porosity and mechanical properties is currently under development, and the available literature data show the promise and relevance of the study of new approaches to the creation of electrode materials based on 2D carbon nanostructures.

The task set in the project is inverse to the traditional problem of nanocomposites synthesis - the development of methods for producing highly filled composites based on 2D nanoparticles with a specific architecture. The functional requirements for such materials are the stability of the shape and mechanical properties, the preservation of the nanoscale 2D filler structure, high electrical conductivity and porosity of the composite.

For the first time in world practice, polymerization of ultra-high molecular weight polyethylene on the surface of graphene particles (reduced graphene oxide) has been carried out. Aerogels were synthesized with a polyethylene content of 7, 20, 50, 80, and 93.5 wt. %. It is shown that the "in-situ" polymerization of ethylene on the surface of graphene aerogel significantly decreases the electrical conductivity of the composite and its specific surface even with an insignificant (about 7%) polymer content. However, at high PE contents (more than 20%), the composite material has plasticity, exhibits hydrophobic properties, and ultra-high filling (93.5%) results in a material with superhydrophobic properties.

The study was carried out by a grant from the Russian Foundation of Basic Research (Project No. 16-29-06440 ofi\_m).

---

**Investigation of the mechanical and thermal properties of the composite material of the composition of aluminum-graphene nanoplatelets.**

*Zavarinskii V.I.<sup>1</sup>, Vozniakovskii A.A.<sup>2</sup>, Kidalov S.V.<sup>2</sup>, Ovchinnikov E. V.<sup>3</sup>, Liopo V. A.<sup>3</sup>*

*z1997vova@yandex.ru*

<sup>1</sup> Saint-Petersburg State Institute of Technology, Saint-Petersburg, Russia

<sup>2</sup> Laboratory Physics for Cluster Structures, Ioffe Institute, Saint-Petersburg, Russia

<sup>3</sup> Yanka Kupala State University of Grodno, Belarus

Carbon nanomaterials, in particular, graphene nanoplatelets (GNP) are actively used by researchers as an additive in composite materials (CM) because of their high characteristics, for example, high thermal conductivity and strength. Therefore, researchers around the world are studying the effects of carbon nanomaterials as an additive in CM. However, due to the imperfection of the methods of synthesizing GNP, their cost price remains extremely high, which hampers their introduction into the real industry.

The purpose of this work was to study the mechanical and thermophysical properties of CM aluminum-GNP composition depending on the GNP concentration obtained by the method of selfpropagating high-temperature synthesis (SHS). Cellulose was used as the starting material for GNP. The starting material used was an aluminum powder, grade PA-4, which was mixed with 0.5-5 wt. % GNP by ultrasound treatment. This method allowed us to obtain a uniform distribution of GNP in the aluminum matrix. After mixing, the mixture of aluminum powder with GNP was sintered at high pressure and temperature.

It was found that the addition of GNP improves the mechanical and thermal properties of aluminum.

## Graphene aerogel modification with various polymers and electroconductive fillers

*Koval V.S.*<sup>1</sup>, *Shiyanova K.A.*<sup>1</sup>, *Anosov A.A.*<sup>1</sup>, *Gorenberg A.Ya.*<sup>1</sup>, *Gudkov M.V.*<sup>1</sup>, *Melnikov V.P.*<sup>1</sup>

*tokojami@yandex.ru*

<sup>1</sup> Semenov Institute of Chemical Physics of Russian Academy of Sciences, Moscow, Russia

Graphene is a 2D-structural nanomaterial, that was discovered in the last decade and became an object of great interest. Graphene-like materials can be obtained by chemical reduction or thermal exposure on its main precursor - graphene oxide (GO). But the product received with such methods has numerous disadvantages because of defects occurring due the oxidation process. These deficiencies can be partially fixed by combining graphene-like particles with different materials. For example, modification of the GO surface with alkylamines improve its dispersibility in organic solvents [1]. Besides, since polymers are situated between GO layers, they prevent a sheet stacking.

In this work we study influence of the polymers with different types of binding with GO surface on the surface area of the obtained material. As a polymer component we used sodium polystyrene sulfonate (PSS), polyvinyl alcohol (PVA) and polyethyleneimine (PEI). All of them are soluble in water and can increase dispersibility of final product in water. PEI allows to insert additional components because of covalent binding with the GO surface and branched structure. Besides, polymer additives are capable to improve mechanical properties of obtaining aerogels. Also, graphene materials were modified with electroconductive additives, such as conductive carbon black and carbon nanotubes, with and without PEI. We studied influence of amounts of the additives on the surface area, electrical conductivity and structure of the obtained materials.

The study was carried out by a grant from the Russian Foundation of Basic Research (Project No. 16-29-06440 ofi\_m).

### References

1. Daniel R. Dreyer. "The chemistry of graphene oxide." Chem. Soc. Rev. 2010.

## Extraction of the short-range defect potential parameters from available experimental data on the graphene resistance

*Firsova N.E.*<sup>1,2</sup>, *Ktitorov S.A.*<sup>1,3</sup>

*ktitorov@mail.ioffe.ru*

<sup>1</sup> Ioffe Institute, St. Petersburg, Russia

<sup>2</sup> Peter the Great St. Petersburg Polytechnic University, St. Petersburg, Russia

<sup>3</sup> St. Petersburg Electrotechnical University, St. Petersburg, Russia

We consider a problem of obtaining information about the scattering potentials of the monolayer graphene sample using available experimental data on its resistance. We have in mind a development of the study describing super-high mobility electrons in suspended samples without chemical doping [1]. As far as practical absence of the doping impurities in this case makes Coulomb scattering negligible, we consider models of the short-range scattering potentials. The model of short-range potential is assumed to be supported by the close vicinity of the ring or the circumference of a circle. The diameter of circles is supposed to be of the order of the crystal lattice spacing. The empty core of the model potential guarantees the suppression of nonphysical shortwave modes. Two models are investigated: the delta function on the circumference of a circle and the annual well [2-4]. An advantage of the former is simplicity, while a virtue of the latter is regularity. We consider scattering of electrons by these potentials and obtain exact explicit formulae for the scattering data. We here discuss application of these formulae for calculation of observables. Namely, we analyze the contribution of this scattering into the graphene resistance and plot the resistivity as a function of the Fermi energy according to our theoretical formulae. The obtained results are consistent with experiment [1], where the resistance was measured as a function of the Fermi momentum on the suspended annealed graphene. This fact gives a possibility to find parameters of the modeled potential on the base of the available experimental data on resistance of the suspended graphene sample with the gate voltage controlled Fermi level position. It is clear to be very important for applications.

### References

1. K.I. Bolotin, K.I. Sikes, Z. Jiang et al., *Solid State Communications* (2008) **146**, 351.
2. N.E. Firsova, S.A. Ktitorov, *Phys. Lett. A*, (2010) **374**, 1270.
3. N. E. Firsova, *Nanosystems: Physics, Chemistry, Mathematics* (2013) **4**, 538.
4. S.A. Ktitorov, N.E. Firsova, *Phys. Solid State* (2011) **53**: 411

## Binding of short DNAs to the surface of reduced graphene oxide for electronic applications

*Komarov I.A.*<sup>1</sup>, *Antipova O.M.*<sup>2</sup>, *Kalinnikov A.N.*<sup>1</sup>, *Orlov M.A.*<sup>1</sup>, *Bogachev V.V.*<sup>1</sup>, *Buyanov A.D.*<sup>1</sup>, *Onoprienko E.A.*<sup>1</sup>

ikomarov@emtc.ru

<sup>1</sup> Bauman Moscow State Technical University, Moscow, Russian Federation

<sup>2</sup> Lomonosov Moscow State University, Moscow, Russian Federation

Among the most important trends in device development the creation of flexible devices is on top in 2019. In particular, it is important to develop not only smartphones but set of different sensors that is main paradigm of the 5G networks and IoT. Taking into account that personal healthcare is one of another largest trends it's important to design sensors for such monitoring, especially biosensors for different pathogen detection.

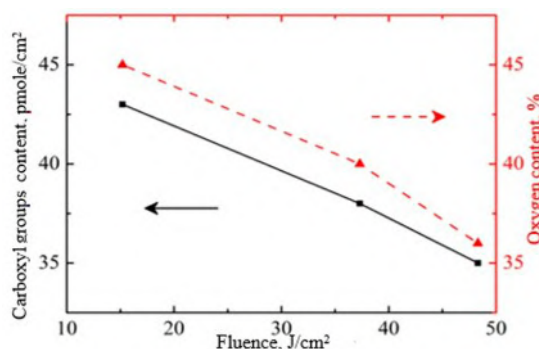
To provide flexibility and acceptable price it's important to use such new and promising material as graphene oxide and its derivatives [1]. Among advantages of graphene oxide are easily processing, relative cheapness and presence of functional groups on the basal plane [2]. The last fact provides us to form transducer film that can be both sensitive and transmitting layer. In this study, the peculiarities of the aptamers interaction with the surface of reduced graphene oxide on flexible substrate were investigated.

Graphene oxide films with different reduction level (reduced with laser fluence range from 15 to 59.4 J/cm<sup>2</sup>), were used for further immobilization of aptamers. The study of the binding of aptamers with graphene oxide films showed that successful conjugation requires the addition of organic solvent to the reaction mixture, carrying out the reaction with ethanol improves the quality of immobilization.

It is shown that the optimal degree of graphene oxide reduction is achieved with the fluence in the range of 15-20 J/cm<sup>2</sup>, that ensures both sufficient conductivity and best conjugation rate due the presence of functional groups.

Thus, the possibility of aptamer based transducer layer formation was shown. Moreover it was shown possibility of control of the aptamers binding degree of to the graphene oxide surface by changing the reduction parameters.

This work is financially supported by the Ministry of the Higher Education and Science of the Russian Federation grant No. 14.574.21.0182 (unique ID: RFMEFI57417X0182).



Dependence of carboxyl groups content and oxygen content on fluence parameter of laser reduced graphene oxide samples.

### References

1. P. Suvarnaphaet and S. Pechprasarn *Sensors* (2017) 17, 2161.
2. B. Gupta, N. Kumar, K. Panda, V. Kanan, S. Joshi & I. Visoly-Fisher (2017) *Scientific Reports* 7, 45030.

## Observation of resonance effects in the Raman spectra of twisted bilayer graphene

*Kononenko O.V.*<sup>1</sup>

*oleg@iptm.ru*

<sup>1</sup> Institute of Microelectronics Technology and High Purity Materials, RAS, Chernogolovka, Moscow Region, Russia

Twisted bilayer graphene attracts a lot of attention due to its angle dependent intriguing electronic and optical properties, such as new Van Hove singularities in the low-energy electronic density of states [1] and strong Raman G band enhancement [2, 3] at specific angles.

Transferred onto oxidized silicon substrate monolayer graphene from Graphene Supermarket was used to obtain folded twisted bilayer graphene. The graphene was scratched with a steel needle to make folded twisted graphene.

The Raman spectroscopy was used for characterization of the graphene. Micro Raman spectra were collected in ambient air and at room temperature with the SENTERRA Bruker Raman microscope at the laser wavelength 532 and 488 nm. A 50x objective lens was used to focus the laser beam to about 1.5 mm spot on the surface of the graphene and to collect the backscattered Raman signal.

G band intensity depending on twisted angle was investigated. A substantial resonance of the G band was found at a twist angle of about 12°. The intensity of the peak G in twisted bilayer graphene was about 30 times higher than the intensity of the peak G in monolayer graphene. In the spectral range of the breathing ZO' modes, a relatively intense band is observed at 95-120 cm<sup>-1</sup>. Corresponding frequencies evidently characterize the fundamental breathing movements between graphene layers, as described for the exfoliated graphene earlier [4].

O.V.K. gratefully acknowledge the financial support of the Russian Foundation for Basic Research (Grant No. 16-29-06306).

### References

1. Li, A. Luican, J. dos Santos, A. Neto, A. Reina, J. Kong, E. Andrei, *Nat. Phys.* (2010) **6**, 109.
2. Carozo, C. M. Almeida, B. Fragneaud, P. M. Bede, M. V. O. Moutinho, J. Ribeiro-Soares, N. F. Andrade, A. G. Souza Filho, M. J. S. Matos, B. Wang, M. Terrones, Rodrigo B. Capaz, A. Jorio, C. A. Achete, L. G. Cancado, *Phys. Rev. B* (2013) **88**, 085401.
3. Yin, H. Wang, H. Peng, Z. Tan, L. Liao, L. Lin, X. Sun, A. L. Koh, Y. Chen, H. Peng, Z. Liu, *Nat. Commun.* (2016) **7**, 10699.
4. H. Lui and T. F. Heinz, *Phys. Rev. B* (2013) **87**, 121404(R)

## Graphene vs. germanene as a sensor material

*Konobeeva N.N.*<sup>1</sup>, *Skvortsov D.S.*<sup>1</sup>, *Belonenko M.B.*<sup>1,2</sup>

*yana\_nn@inbox.ru*

<sup>1</sup> Volgograd State University

<sup>2</sup> Volgograd Institute of Business

Currently, researchers are greatly interested in the choice of material for the detection of impurities. This is due to the large number of possible applications of such sensors in various spheres of human activity. Thus, the works [1, 2] are devoted to the development of sensors based on graphene, silicene [3], and germanene [4]. The last two of the mentioned structures are relatives of graphene, but they have much greater spin-orbit interaction: for silicon - it is 1000 times larger than for graphene, for germanene - it is 10,000 times larger than for graphene.

In this work, we compare two materials (graphene and germanene) in terms of their sensitivity to adsorbed gas molecules. Typically, sensory properties are investigated within the framework of the density functional theory. We use a different approach, which is based on the investigation of the tunneling current flowing in the contact of the material with a metal or superlattice. The main advantage of the proposed approach is the choice of material for contact, which can significantly affect the current-voltage characteristic of the system and improve its response to the existing gas molecules.

A comparison of the tunneling current for the germanene/graphene contact with superlattice is presented in Fig. 1.

This work was supported by Russian Foundation for Basic Research and the government of Volgograd region, grant № 18-42-343002 and the state assignment of the Ministry of Science and Higher Education of the Russian Federation (government task No. 2.852.2017/4.6).

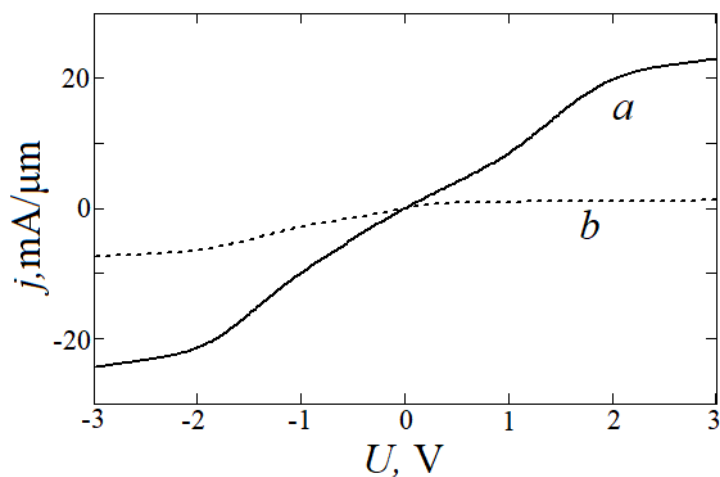


Fig.1. Dependence of the tunneling current density (contact with superlattice) versus the voltage in the case of the one impurity molecule: (a) germanene; (b) graphene.

### References

1. W. Hill, A. Vijayaraghavan and K. Novoselov. IEEE Sensors Journal(2011) **11**, 3161.
2. I.L. Justino, A.R. Gomes, A.C. Freitas, A.C. Duarte and T.A.P. Rocha-Santos. TrAC (2017) **91**, 53.
3. Hu, N. Xia, X. Wu, Z. Li and J. Yang. Phys. Chem. Chem. Phys. (2014) **16**, 6957.
4. K. Gupta, D. Singh, K. Rajput and Y. Sonvane. RSC Advances (2016) **6**, 102264.



## Spin-orbit and exchange coupling induced in graphene under contact with heavy and magnetic metals

*Rybkin A.G.*<sup>1</sup>, *Rybkina A.A.*<sup>1</sup>, *Otrokov M.M.*<sup>2,3,1</sup>, *Vilkov O.Yu.*<sup>1</sup>, *Klimovskikh I.I.*<sup>1</sup>, *Petukhov A.E.*<sup>1</sup>, *Shikin A.M.*<sup>1</sup>, *Chulkov E.V.*<sup>1,2</sup>

*artem.rybkin@spbu.ru*

<sup>1</sup> Saint Petersburg State University, Saint Petersburg, Russia, 198504

<sup>2</sup> Departamento de Física de Materiales UPV/EHU, Centro de Física de Materiales CFM -MPC and Centro Mixto CSIC-UPV/EHU, 20080 San Sebastian/Donostia, 2D Basque Country, Spain

<sup>3</sup> IKERBASQUE, Basque Foundation for Science, 48011 Bilbao, Spain

Graphene being a nonmagnetic material with a weak spin-orbit coupling (SOC) can be considered as a spin transmission element of spintronics, e.g. in a graphene-based spin field-effect transistor or spin valve<sup>1,2</sup>. Additional applications of graphene in spintronics may appear if one changes its properties. Enhancement of SOC in graphene would enable the efficient generation of pure spin currents based on the spin Hall effect and its quantized version. Strong enhancement of SOC has also been observed for Pb-intercalated graphene on Ir(111)<sup>3</sup> and Pt(111)<sup>4</sup>, respectively, both cases pointing toward the quantum-spin-Hall-like state in the carbon honeycomb. A combination of strong spin-orbit coupling (SOC) and robust magnetism could provide a playground for the observation of the quantum anomalous Hall effect (QAHE)<sup>5,6</sup>. The direct contact of graphene with magnetic metals, like Fe, Co or Ni, leads to destruction of the Dirac cone in graphene's electronic structure due to the appearance of hybridization and symmetry-breaking gaps. Thus, special attention should be paid to maintaining intrinsic features of graphene, namely, a linear dispersion of the electronic bands close to the Fermi level and ultrahigh carrier mobility.

In the present talk induced spin-orbit and exchange coupling in graphene under contact with heavy (Au, Pt) and magnetic (Ni, Co, Gd) metals will be addressed. The induced contributions of the intrinsic (internal) and extrinsic (Rashba-like) SOC realized in the studied systems will be analyzed and estimated. The experimental investigation of spin and electronic structure was carried out by spin- and angle-resolved photoemission (SARPES) and crystalline structure - by scanning tunneling microscopy (STM) and low energy electron diffraction (LEED). It will be shown that a quasi-freestanding character, strong exchange splitting and giant spin-orbit coupling are perfectly achievable in graphene at once. SARPES data reveal a giant splitting (up to 0.2 eV) and the appearance of an asymmetric spin structure due to the time reversal symmetry breaking in the system Gr/Au/Co(0001). STM data and DFT calculations suggest that the peculiar reconstruction of the Au/Co(0001) interface is responsible for the exchange field transfer to graphene. The realization of this "magneto-spin-orbit" version of graphene opens new frontiers for both applied and fundamental studies using its unusual electronic band structure.

### References

1. Y.G. Semenov and K.W. Kim, *Appl. Phys. Lett.* (2007) 91, 153105.
2. A.A. Rybkina, A.G. Rybkin, V.K. Adamchuk, D. Marchenko, A. Varykhalov, J. Sánchez-Barriga, and A.M. Shikin, *Nanotechnology* (2013) 24, 295201.
3. M.M. Otrokov, I.I. Klimovskikh, F. Calleja, A.M. Shikin, O. Vilkov, A.G. Rybkin, D. Estyunin, S. Muff, J.H. Dil, A.L. Vázquez de Parga, R. Miranda, H. Ochoa, F. Guinea, J.I. Cerdá, E.V. Chulkov, and A. Arnau, *2D Materials* (2018) 5, 035029.
4. I.I. Klimovskikh, M.M. Otrokov, V.Y. Voroshnin, D. Sostina, L. Petaccia, G. Di Santo, S. Thakur, E.V. Chulkov, A.M. Shikin, *ACS Nano* (2017) 11, 368–374.
5. Z. Qiao, S.A. Yang, W. Feng, W.-K. Tse, J. Ding, Y. Yao, J. Wang, and Q. Niu, *Phys. Rev. B* (2010) 82, 161414.
6. X. Deng, S. Qi, Y. Han, K. Zhang, X. Xu, and Z. Qiao, *Phys. Rev. B* (2017) 95, 121410(R).

## Synthesis, ARPES and STM study of quasi-freestanding graphene on Pt<sub>x</sub>Gd alloy

*Rybkina A.A.*<sup>1</sup>, *Rybkina A.G.*<sup>1</sup>, *Pudikov D.A.*<sup>1</sup>, *Klimovskikh I.I.*<sup>1</sup>, *Estyunin D.A.*<sup>1</sup>, *Shikin A.M.*<sup>1</sup>

*a.rybkina@spbu.ru*

<sup>1</sup> Saint Petersburg State University

Adsorption of rare earth atoms and clusters is an interesting challenge to grow uniform magnetic metal films for use as a part of spin valves or to grow high density of thermally stable magnetic islands for information storage<sup>1-3</sup>. The use of 4f rare earth atoms instead of 3d transition metal atoms has advantage to obtain magnetically stable bits: (i) 4f atoms with larger spin and orbital momenta show larger magnetic anisotropy energy per atom than 3d atoms, (ii) the strong localization of the 4f states leads to less hybridization with the surface, which could increase the lifetimes of the spin states<sup>1</sup>. However, magnetic properties of 4f rare earth atoms and clusters on surfaces were not thoroughly studied. Recently, adsorption and intercalation under graphene of rare earth atoms was investigated<sup>2,3</sup> but investigation of graphene's band structure by angle-resolved photoemission (ARPES) remained out of scope of the studies. The effective way to modify the electronic structure and to shift the Dirac point can be adsorption of Gd adatoms atop of graphene. Among possible adsorbates, rare earth metals and Gd in particular are interesting and unexplored candidates. According to Ref. [4] adsorption of Gd on top of graphene on different metal substrates leads to strong *n*-doping of graphene without modification of the Dirac cone dispersion at the K point in opposite to the case of adsorption of alkali metals followed by their intercalation underneath a graphene with the Dirac point gap opening already at room temperature.

The aim of this work was to study electron energy structure of graphene/Pt(111) upon adsorption and intercalation of Gd atoms. A shift of the Dirac point in graphene below the Fermi level by deposition of Gd atoms with detailed study of the electronic structure of the graphene  $\pi$  states will be shown. Scanning tunneling microscopy (STM) and X-ray photoelectron spectroscopy (XPS) data suggest intercalation of Gd and formation of Pt<sub>x</sub>Gd alloy under graphene after annealing of the system at 1080°C. Pt<sub>x</sub>Gd alloy formation on Pt(111) surface was observed earlier in Ref.[5]. Global gap opening at the Dirac point of graphene was measured by ARPES after intercalation of Gd at lower temperatures that possibly connected with corrugation and AB symmetry breaking. High temperature annealing allows us formation of quasi-freestanding graphene with atomically flat terraces. It was proved that graphene was situated on monolayer of Pt for this case.

### References

1. Schuh, T. Miyamachi, S. Gerstl, M. Geilhufe, M. Hoffmann, S. Ostanin, W. Hergert, A. Ernst, and W. Wulfhekel, *Nano Lett.* (2012) 12, 4805–4809.
2. Liu, C.-Z. Wang, M. Hupalo, H.-Q. Lin, K.-M. Ho, and M.C. Tringides, *Crystals* (2013) 3, 79-111.
3. A. Andersona, M. Hupaloa, D. Keavneyb, M. Tringidesa, D. Vaknin, *J. Magn. Magn. Mater.* (2019), 474, 666-670.
4. Varykhalov, M.R. Scholz, T.K. Kim, and O. Rader, *Phys. Rev. B* (2010) 82, 121101(R).
5. T. Ulrikkeholm, A.F. Pedersen, U.G. Vej-Hansen, M. Escudero-Escribano, I.E.L. Stephens, D. Friebel, A. Mehta, J. Schiøtz, R.K. Feidenhansl', A. Nilsson, I. Chorkendorff, *Surface Science* (2016) 652, 114-122.

## Thermal annealing of defects in graphite nanoplatelets

*Alaferdov A.V.*<sup>1</sup>, *Savu R.*<sup>1</sup>, *Canesqui M. A.*<sup>1</sup>, *Kopelevich Ya. V.*<sup>1</sup>, *Da Silva R. R.*<sup>1</sup>, *Rozhkova N. N.*<sup>2</sup>, *Kompan T. A.*<sup>3</sup>, *Kondratiev S. V.*<sup>3</sup>, *Moshkalev S. A.*<sup>1</sup>

*stanisla@unicamp.br*

<sup>1</sup> UNICAMP, Campinas, Brazil

<sup>2</sup> Institute of Geology, KRS RAS, Petrozavodsk, Russia

<sup>3</sup> VNIIM, St. Petersburg, Russia

Graphite exfoliation in a liquid phase is the main approach used currently for mass production of graphene. Among the methods used for liquid-phase graphite exfoliation, ultrasound processing (sonication) in different solvents is the most popular [1]. The popularity of sonication is due to its low cost, scalability, versatility and ability to produce single layer, a few layer and multilayer graphene sheets or graphite nanoplatelets. Here, the defects produced during ultrasound processing in graphite nanoplatelets with thickness from a few to a few tens of nanometers were studied [2]. It has been shown that due to strong localized energetic impacts produced by cavitation shock waves in graphite, bulk ripplations can be developed inside the samples eventually resulting in formation of large-scale ripples, fracture of layers and formation of multiple localized defects like dislocations. Formation of ripples is more pronounced in large aspect (length/width) ratio platelets or nanobelts that behave as vibrating strings after the energetic impact by shock waves. The height of ripples in some nanobelt samples reached 100 nm evidencing the extremely high intensity of the ripplation process and high energy deposited in samples by shock waves. Further, the samples were thermally treated at temperatures up to 2950 C in inert atmosphere. As confirmed by results of XRD (X-ray diffraction), TEM (transmission electron microscopy) and confocal Raman techniques, fast high-temperature processing successfully anneals most of defects produced by sonication in the nanoplatelets. This is consistent with our observations that the defects associated with ripplations are strongly localized and thus can be fast annealed. The phenomena observed here for thin graphite samples should be valid also for other layered materials processed in liquid phase for exfoliation.

### References

1. A.V. Alaferdov, R.Savu, M.A. Canesqui, Y.V. Kopelevich, R.R. da Silva, N.N. Rozhkova, D.A. Pavlov, Yu.V. Usov, G.M. de Trindade, S.A. Moshkalev. *Carbon* (2018), **129**, 826.
2. A.V. Alaferdov, A. Gholamipour-Shirazi, M.A. Canesqui, Y.A. Danilov, S.A. Moshkalev, *Carbon* (2014), **69**, 525.

## **A Nanostructured Composite Polyhydroquinone/Graphene Oxide Sorbent: Synthesis and Physical-Chemical Properties**

*Babkin A.V.*<sup>1</sup>, *Burakov A.E.*<sup>1</sup>, *Burakova I.V.*<sup>1</sup>, *Neskoromnaya E.A.*<sup>1</sup>, *Kurnosov D.A.*<sup>1</sup>, *Tkachev A.G.*<sup>1</sup>

*Flex\_trol@mail.ru*

<sup>1</sup>Tambov State Technical University, Tambov, Russian

The analysis of scientific works in the field of synthesis of nanostructured composite materials for sorption purification of aqueous media shows that carbon nanomaterials are much more efficient than currently used commercially available sorbents. Besides, they are non-toxic and thermally stable [1]. The prospect of using nanostructured materials in sorption-desorption cycles is substantiated by their unique physical-chemical characteristics determining the performance properties of modern sorbents: specific surface area, presence of chemically active sites, and high potential affinity for components being recovered [2-3].

Functional polymer compounds are increasingly being used as modifying additives to carbon matrices [4]. The main requirements for such materials are as follows: chemical and thermal stability, and ability to ion exchange, complexation and redox reactions for selective extraction of contaminants from aqueous media.

The authors have developed a method for synthesizing an innovative nanocomposite based on 1,4-benzoquinone-modified graphene oxide. The product obtained is technically called "polyhydroquinone/graphene oxide" (PHQ/GO).

Technological parameters of the production of this nanocomposite were comprehensively studied. Quantitative dependences of the effect of the ratio of the initial components participating in the synthesis on the degree of GO surface modification were revealed. It was established that the amount of the modifier grafted nonlinearly depends on the weight of the initial monomer. This is presumably due to concurrent occurrence of several chemical reactions during the 1,4-benzoquinone polymerization. The physical-chemical characteristics of the material synthesized were investigated implementing the following techniques: scanning electron microscopy/energy dispersive X-ray spectroscopy, Raman spectroscopy, and thermogravimetry/differential scanning calorimetry.

The results of studying the structural, physical-chemical and operational properties of the nanostructured composite developed suggest that this material can be used as an efficient universal sorbent for the purification of aqueous media from different contaminants.

### *Acknowledgements.*

*The research was funded by the Ministry of Education and Science of the Russian Federation (Project No.16.1384.2017/PCh).*

### **References**

1. Ge Y., Li Z., Xiao D., Xiong P., Ye N. *Journal of Industrial and Engineering Chemistry* (2014) **20**, 1765-1771.
2. Fialova D., Kremplova M., Melichar L., Kopel P., Hynek D., Adam V., Kizek R. *Materials* (2014), 7(3), 2242 - 2256.
3. Burakov A.E., Babkin A.V., Burakova I.V., Мележик A.V., Kuznetsova T.S., Neskoromnaya E.A., Kurnosov D.A., Mkrtychyan E.S. *Perspective materials* (2019), **2**, 23 - 25.
4. Mukhitdinova B.A., Nikitina A.I. *Asias Journal of Research in Chemistry* (2017), 10, 41-44

## Development of Sorption Materials Based on Iron(III)-Chloride-Modified Graphene oxide for Selective Removal of Organic Pollutants from Aquatic Media

*Neskoromnaya E.A.*<sup>1</sup>, *Burakov A.E.*<sup>1</sup>, *Babkin A.V.*<sup>1</sup>, *Burakova I.V.*<sup>1</sup>, *Melezhik A.V.*<sup>1</sup>, *Mkrtchyan E.S.*<sup>1</sup>

*Lenok.n1992@mail.ru*

<sup>1</sup>Tambov State Technical University, Tambov, Russia

Currently, much attention is being paid to research in the field of graphene structures and functional materials, which are based on studying graphene and its modified forms. This is due to their unique physical-chemical characteristics such as high electrical and thermal conductivity, mechanical strength, thermal stability, *etc.* The works of many research teams convincingly prove the promising use of graphene-based composites as efficient sorption materials [1-2].

Considering the aforementioned, the present research is aimed at developing an effective graphene sorbent for liquid-phase sorption of organic pollutants from aquatic media. The material synthesized in accordance with the method proposed represents a nanostructured composite possessing hydrogel properties: structured three-dimensional carbon skeleton surface-modified with iron nanoparticles (*i.e.*, graphene oxide (GO)/Fe-H<sub>2</sub>O). Within the framework of the research being implemented, the following characteristics of this material were determined: density, specific surface area, porous space parameters. Moreover, the proportion of dry matter in the hydrogel was revealed (by drying to a constant weight at a given temperature (110 °C), the powdery form (GO/Fe-110) of the composite was obtained). Besides, the airgel (GO/Fe-250) of the composite developed was formed, for which the hydrogel synthesized was subjected to hydrothermal drying in isopropanol for 6 h under supercritical conditions, thereby making it possible to get the material with the original volume and porous space structure remained [3].

The sorption capacity of the nanostructured composite, present in various forms (hydrogel and airgel), was estimated for the removal of the model synthetic organic dye, methylene blue, used as a target pollutant. Sorption experiments were carried out under static conditions ("limited volume" method). The following sorption parameters were determined: maximum recovery rate in the selected concentration range, sorption activity of the material, and kinetic characteristics of the target pollutant.

The results of the studies showed that the maximum sorption capacity values obtained under the static conditions for the studied materials are ~2,500, ~1,500 and ~ 2,300 mg/g for the GO/Fe-H<sub>2</sub>O, GO/Fe-110 and GO/Fe-250, respectively. Besides, the high rate of the process of the target pollutant removal from the aquatic media is a distinctive feature of the composites developed herein.

### *Acknowledgements.*

*The research was funded by the Ministry of Education and Science of the Russian Federation (Project No.16.1384.2017/PCh).*

### **References**

1. Li J., Zhang S., Chen Ch., Zhao G., Yang X., Li J., Wang X. ACS Appl. Mater. Interfaces (2012) **4** (9), 4991- 5000.
2. Cong H.-P., Ren X.-C., Wang P., Yu. Sh.-H. ACS Nano (2012) **6** (3), 2693-2703
3. Long Z., Zhan Y., Li, Wan X., He Y., Hou C., Hu H. J Nanopart Res (2017) **19**, 318

## Synthesis of twisted multilayer graphene by the low-pressure chemical vapor deposition with a single injection of acetylene

*Kononenko O.V.*<sup>1</sup>, *Matveev V.N.*<sup>1</sup>, *Levashov V.I.*<sup>1</sup>, *Khodos I.I.*<sup>1</sup>, *Bozhko S.I.*<sup>2</sup>

*oleg@iptm.ru*

<sup>1</sup> Institute of Microelectronics Technology and High Purity Materials, RAS, Chernogolovka, Moscow Region, Russia

<sup>2</sup> Institute of Solid State Physics, RAS, Chernogolovka, Moscow Region, Russia

Mogera et al recently reported on the synthesis of twisted multilayer graphene grown by modified CVD technique [1-3]. The twisted multilayer graphene possesses attractive properties due to high degree of decoupling arising from interlayer twists. Among them, twist-angle-dependent optical absorption in the visible spectral region, semiconducting to metallic transition with increasing of a temperature, photoresponse coinciding with the transition from semiconductor to metallic behavior without a photoresponse at the transition point and others.

The twisted multilayer graphene was synthesized by the low-pressure chemical vapor deposition with a single injection of acetylene on iron film catalyst deposited on oxidized silicon substrate [4]. The structure of the graphene film was investigated depending on the growth time.

The Raman spectroscopy and High Resolution Transmission Electron Microscopy (HRTEM) were used for characterization of the graphene films. Micro Raman spectra were collected in ambient air and at room temperature with the SENTERRA Bruker Raman microscope at the laser wavelength 532. A 50x objective lens was used to focus the laser beam to about 1.5 mm spot on the surface of the graphene and to collect the backscattered Raman signal.

Despite the graphene film thickness of 5-20 nm the Raman spectra collected from the graphene show the symmetric 2D band with a full width at half maximum (FWHM) of 20-35  $\text{cm}^{-1}$ , which can be well fitted by a single Lorentzian curve, and the  $I_{2D}/I_G$  intensity ratio is 2-9. The very low D-band intensity (intensity ratio between D and G peaks smaller than 0.04) indicates a low defect density in the graphene. The spectra are characteristic of monolayer graphene. However, in the majority of these spectra small peaks are observed (R), indicating multilayer graphene with twisted layers.

The features attributed to moiré superlattice which forms due to the rotation of graphene layers were observed in TEM images.

O.V.K. and V.N.M gratefully acknowledge the financial support of the Russian Foundation for Basic Research (Grant No. 16-29-06306).

### References

1. Mogera, R. Dhanya, R. Pujar, C. Narayana and G.U. Kulkarni, *J. Phys. Chem. Lett.* (2015) **6**, 4437.
2. Mogera, N. Kurra, D. Radhakrishnan, C. Narayana, and G.U. Kulkarni, *Carbon* (2014) **78**, 384.
3. Mogera, S. Walia, B. Bannur, M. Gedda, and G.U. Kulkarni, *J. Phys. Chem. C* (2017) **121**, 13938.
4. V. Kononenko, V.N. Matveev, D.P. Field, D.V. Matveev, S.I. Bozhko, D.V. Roshchupkin, E.E. Vdovin, A.N. Baranov, *Nanosystems: Physics, Chemistry, Mathematics*. (2014) **5**, 117.

## The mechanism of spillover of hydrogen on sp<sup>2</sup>-carbon surface

*Leshchev D.V.*<sup>1</sup>

*dimvovich@narod.ru*

<sup>1</sup> Center for Advanced Studies of Peter The Great Saint-Petersburg Polytechnic University, Saint-Petersburg, Russia

Since it was discovered spillover is a real scientific puzzle but at the same time it has found a variety of uses [1]. For example, this is radioactive labeling in biologically active molecules [2-4]. In this case, spillovered hydrogen migrates through both the solid state and the gas phase. Particles of metals of the platinum group deposited on a graphite substrate act as a generator of this active hydrogen.

In the literature, a number of mechanisms have been proposed explaining spillover of hydrogen on carbon surfaces, but all of them contradict the laws of thermodynamics or kinetics [5,6]. In this paper, two mechanisms of hydrogen spillover along the carbon surface are proposed: one is carried through the relay diffusion of atomic hydrogen along graphene planes, the second is carried through the transfer of a carbon radical center along the edge or surface of graphene. Reactions in both mechanisms have low activation energies, which allows them to take place at room temperature and below. Both mechanisms are in agreement with experimental data. Quantum-chemical modeling of elementary chemical acts on model molecular systems has been carried out. Assumptions about how to experimentally confirm or disprove the implementation of these mechanisms in nature have been made.

These spillover mechanisms can also be used in modeling the growth of carbon structures with conjugated bonds and the active participation of hydrogen radicals.

Acknowledgements. This work was partially financially supported by Ministry of Science and Education of Russian Federation within the framework of the basic part of state tasks of Peter The Great Saint-Petersburg Polytechnic University (project code 16.7002.2017/8.9) and by the Russian Foundation for Basic Research (project № 19-08-00533).

### References

1. R. Prins, *Chem. Rev.* (2012) **112**, 2714–2738.
2. Gennadii A. Badun\*, Maria G. Chernysheva, Anastasia V. Grigorieva, Elena A. Eremina, and Alexander V. Egorov *Radiochim. Acta* (2016) **104(8)**, 593.
3. I.A.Razzhivina, G.A.Badun, M.G.Chernysheva, A.V.Garshev, V.P.Shevchenko, K.V.Shevchenko, I.Yu.Nagaev, N.E.Shchepina, *Mendeleev Commun.* (2016), **26**, 59.
4. Razzhivina I.A., Badun G.A., Chernysheva M.G., Korobkov V.I., Zhirnov A.E. *Radiochemistry* (2017) **59**, 284.
5. Yu. A. Zolotarev, A. K. Dadayan, Yu. A. Borisov, V. S. Kozik *Chem. Rev.* (2010) **110**, 5425
6. Hoai T. Nguyen, Lam K. Huynh, Thanh N. Truong, *Carbon* (2017) **121**, 248.

## The influence of adsorbates on edge zero modes in few-layer nanographenes

Ziatdinov A.M.<sup>1</sup>

ziatdinov@ich.dvo.ru

<sup>1</sup> Institute of Chemistry, Far Eastern Branch of the Russian AS, Vladivostok, Russia

According to the data of theoretical and experimental [1-5] studies, near zigzag edges of honeycomb carbon structures the  $\pi$ -electronic states with zero energy (zero modes) stabilize and density of electronic states  $D(E)$  at the Fermi level  $E_F$  tens times exceeds the value of corresponding parameter for macroscopic ordered graphite [6]. Mentioned topological zero modes substantially change known properties of nanosized carbon structures [1-6], but also may initiate essentially new phenomena such as edge magnetism [7] and edge superconductivity [8]. Near armchair edges similar electronic states do not exist [1-6].

In recent years a new field of research in the technology of nanoscale carbon structures has been developed, which is aimed at fine adjustment of their properties with changing chemical state of peripheral atoms. For instance, the emergence of topological zero modes has been established recently at etching graphenic *armchair* edges by hydrogen [9]. However, with appreciating the significance of those works, up to now the problem of influence of adsorbed molecules (adsorbate) on the edge  $\pi$ -electronic band and, thereby, on the properties of nanosized carbon structures, was not treated properly. At the same time, evidently, this information is important for establishing the reasons and mechanisms of changing the properties of carbon nanostructures under the influence of different reagents, for ranking the factors determining their structural organization, electronic structure and chemical reactivity, as well as for solving problems of practical application.

In this work the results of investigations of structure and properties of few-layer nanographenes (nanographites) and their changes under the influence of adsorbed molecules are presented. The presence of specific edge  $\pi$ -electronic states with zero energy (topological zero modes) in nanographites and reversible decrease of  $D(E_F)$  at their interaction with adsorbed molecules of oxygen, chlorine and water have been established. The explanation of discovered effect has been proposed in the terms of model of spin splitting of edge  $\pi$ -electronic states, initiated by transferring small portion of electronic density from nanographites to adsorbed molecules. It has been shown that change in sign of the temperature coefficient of current carrier spin relaxation rate at presence of adsorbate may be accounted for by their interactions with edge spin-split states. The preservation of peripheral  $\pi$ -electronic states of nanographites at saturation of dangling  $\sigma$ -bonds of edge carbon atoms with chlorine has been substantiated.

### References

1. M. Fujita, K. Wakabayashi, K. Nakada, K. Kusakabe, J. Phys. Soc. Jpn. (1996), **65**, 1920.
2. Y. Kobayashi, K. Fukui, T. Enoki, K. Kusakabe, Phys. Rev. B (2005), **71**, 193406.
3. M. Ziatdinov, S. Fujii, K. Kusakabe, T. Mori, T. Enoki, Phys. Rev. B (2013), **87**, 115427.
4. N. Enoki, T. Ando, Physics and chemistry of graphene: graphene to nanographene (Pan Stanford Publishing Pte Ltd., Singapore, 2013), 476 pp.
5. M. Ziatdinov, Russian Chemical Bulletin (2015), **64**, 1.
6. Y. Niimi, T. Matsui, K. Tagami, M. Tsukada, H. Fukuyama, Appl. Surf. Sci. (2005), **241**, 43.
7. Y.-W. Son, M. L. Cohen, S. G. Louie, Nature (2006), **444**, 347.
8. K. Sasaki, J. Jiang, R. Saito, S. Onari, Y. Tanaka, J. Phys. Soc. Jpn. (2007), **76**, 033702.
9. M. Ziatdinov, H. Lim, S. Fujii, K. Kusakabe, M. Kiguchi, T. Enoki and Y. Kim, Phys. Chem. Chem. Phys. (2017), **19**, 5145.



## Quasistatic phenomena in electrical transport in solution gated graphene transistor structures

*Butko A.V.*<sup>1</sup>, *Butko V.Y.*<sup>1,2</sup>, *Lebedev S.P.*<sup>1,3</sup>, *Smirnov A.N.*<sup>1,3</sup>, *Eliseyev I.A.*<sup>1</sup>, *Davydov V.Y.*<sup>1</sup>, *Lebedev A.A.*<sup>1</sup>, *Kumzerov Y.A.*<sup>1</sup>

*russprot@yahoo.com*

<sup>1</sup> Ioffe Institute, St. Petersburg, Russia

<sup>2</sup> St. Petersburg Academic University of Russian Academy of Science, St. Petersburg, Russia

<sup>3</sup> ITMO University, St Petersburg, Russia

Recently proposed sensor applications of graphene transistors in which graphene is exposed directly to the environment without any intervening layers has sparked growing interest to studies of interfacial phenomena in solution gated graphene. For example, it has been shown that graphene interfaced with aqueous solutions is suitable for fabrication of pH sensors [1]. However, there are few studies of hysteretic phenomena in this configuration despite its importance. Among these reports we can mention only a discovery of hysteresis in a scale of seconds in CVD grown graphene at the interface with KCl electrolyte [2].

Therefore, in this work we focus on hysteretic and time dynamic phenomena in transistors based on epitaxial graphene interfaced with a gating solution. We studied [3] electrical transport in transistors fabricated on a surface of high quality epitaxial graphene with density of defects as low as  $5 \cdot 10^{10} \text{ cm}^{-2}$  and observed quasistatic hysteresis with a time constant in a scale of hours. This constant is in a few orders of magnitude greater than the constant previously reported in CVD graphene. The hysteresis observed here can be described as a shift of  $\sim +2\text{V}$  of the Dirac point measured during a gate voltage increase from the position of the Dirac point measured during a gate voltage decrease. This hysteresis can be characterized as a nonvolatile quasistatic state memory effect in which the state of the gated graphene is determined by its initial state prior to entering the hysteretic region. Due to this effect the difference in resistance of the gated graphene measured in the hysteretic region at the same applied voltages can be as high as 70%. The observed effect can be explained by assuming that charge carriers in graphene and oppositely charged molecular ions from the solution form quasistable interfacial complexes at the graphene interface. These complexes likely preserve the initial state by preventing charge carriers in graphene from discharging in the hysteretic region. The observed state memory effect is important for production of graphene based pH and other chemical sensors.

We have also observed that gate voltage dependence of graphene conductivity in transistor structures gated by negatively charged amino acid (aspartic acid) aqueous solutions qualitatively differ from the dependence that was previously observed [1] in graphene gated by the acidic and base aqueous solutions containing small molecular ions. These results demonstrate that graphene transistor structures can potentially be useful for detecting biological markers (molecules) containing negatively charged amino acid tails.

### References

1. P.K. Ang, W. Chen, A.T. Wee, K.P. Loh, J. Am. Chem. Soc. (2008) **130** 14392.
2. H. Wang, Y.H. Wu, C.X. Cong, J.Z. Shang, T. Yu, ACS Nano (2010) **4**, 7221.
3. A.V. Butko, V.Y. Butko, S.P. Lebedev, A.A. Lebedev, V.Y. Davydov, A.N. Smirnov, I.A. Eliseyev, M.S. Dunaevskiy, Y.A. Kumzerov. Applied Surface Science (2018) **444**. 36.

## A new multi-structural approach to photoelectron holography of 2D materials and interfaces

*Tarasov A.V.*<sup>1,2</sup>, *Ogorodnikov I.I.*<sup>2</sup>, *Kuznetsov M.V.*<sup>2</sup>, *Usachov D.Yu.*<sup>1</sup>

*artem.tarasov@spbu.ru*

<sup>1</sup> St. Petersburg State University, St. Petersburg, Russia

<sup>2</sup> Institute of Solid State Chemistry of the Ural Branch of the Russian Academy of Sciences, Ekaterinburg, Russia

X-ray photoelectron holography (XPH) is a powerful and rapidly developing spectroscopic method, which enables direct visualization of atomic structure of single crystal surfaces. This method is based on the photoelectron diffraction (PED) phenomenon that is appearance of photoelectron intensity angular modulations (the PED patterns) caused by interference of photoelectron waves after scattering on ordered atomic structure. PED patterns are uniquely dependent on the atomic positional relationships and can be considered as holograms of atomic arrangement. Nowadays there are the two main implementations for reconstruction of atomic structure from its hologram, namely the approaches based on Fourier transformation (FT) and the SPEA-MEM (Scattering Pattern Extraction Algorithm with Maximum Entropy Method) algorithm [1]. The first group of methods require many holograms that are recorded using multiple energies since FT requires an infinite integral interval. Therefore, such experiments are very time consuming. The second SPEA-MEM method is devoid of this disadvantage and provides possibility to reconstruct an atomic arrangement from a single-energy hologram. However, study of 2D interfaces remains a challenging task for the SPEA-MEM algorithm because of the single-scattering approximation (SSA) implemented in it. The SSA is enough for modelling the forward-scattering and cannot be used for considering the back-scattering which dominates at low kinetic energies and is necessary for investigating adsorbate's position with relation to substrate. Thus, one of ways for further development of the XPH method can be enabling consideration of multiple-scattering events in the prospective MEM algorithm.

In our work we propose a rather straightforward approach for photoelectron holograms reconstruction which includes two steps: multiple scattering calculations of the PED patterns for all expected atomic structures and the MEM algorithm selecting the best combination of structures. This scheme is rather similar to the SPEA-MEM algorithm, but notably differs from it because the latter employs two-atom scattering patterns, while we calculate the multiple-scattering for large clusters. In the case of studying the interface between the 2D crystal and its substrate we calculate a basis set of PED patterns by means of shifting the 2D layer relative to the cluster model of substrate. Thus, the aim of such analysis represents determination of all possible positions of the 2D crystal relative to the substrate and the relative amount of these structures.

Efficiency of applying developed multi-structural approach was demonstrated on structural analysis of the BN/Co system, which structural parameters were determined in good agreement with earlier PED and DFT studies [2]. Then we used our approach for structural investigation of the boron-doped graphene interfaces: B-graphene/Co and B-graphene/Ni. As a result, we have determined possible positions of the graphene layer and boron atoms in it also discovered domination of boron atoms in one of two graphene sublattices. Obtained results may help further development of implementing these interface structures in electronics and spintronics and give us hope that developed algorithm will find its application for wide range of tasks related to studying 2D materials and interfaces.

**Acknowledgments** A.V.T. and D.Yu.U. acknowledge St. Petersburg State University for research Grant No. 11.65.42.2017. A.V.T. and I.I.O. acknowledge the RSF (Grant No. 18-73-00197).

### References

1. M.V. Kuznetsov, I.I. Ogorodnikov and A.S. Vorokh, *Rus. Chem. Rev.* (2014) **83**, 13.
2. D. Yu. Usachov et al., *Phys. Rev. B* (2018) **98**, 195438.

## Low resistance of reduced graphene oxide in polystyrene-based composites with various molecular weights

*Nikolaeva M.N.*<sup>1</sup>, *Bugrov A.N.*<sup>1,2</sup>, *Bezrukova M.A.*<sup>1</sup>, *Rabchinskii M.K.*<sup>3</sup>, *Dideikin A.T.*<sup>3</sup>

*dideikin@mail.ioffe.ru*

<sup>1</sup> Institute of Macromolecular Compounds RAS, Saint-Petersburg, Russia

<sup>2</sup> Saint Petersburg Electrotechnical University "LETI", Saint-Petersburg, Russia

<sup>3</sup> Ioffe Institute, Saint-Petersburg, Russia

UV-perforated flakes of multi-layered reduced graphene oxide (RGO<sub>p</sub>) were functionalized with vinyl groups and copolymerized with polystyrene in toluene. The molecular masses of polystyrene in the composites were 4,000, 6,000, 9,000 and 45,000 Da. In process of precipitation of RGO<sub>p</sub>/polystyrene composite using a mixed solvent (petroleum ether and benzene in a 1:1 ratio), conduction channels were formed in two-dimensional RGO<sub>p</sub> structures.

Despite lateral sizes of separate RGO<sub>p</sub> inclusions are of 10-20 μm [1], precipitation process by petroleum ether described in [2] led to formation of a larger planar structures (up to 1 mm in diameter) of reduced graphene oxide in a non-conductive polystyrene matrix. Since polymer coils become denser during the precipitation some tensions between macromolecules and covalently bonded graphene layers allowed the RGO<sub>p</sub> filler to partially emerge on the surface of polystyrene films being deposited on a glass substrate. Thus, chemical precipitation method of RGO<sub>p</sub> composites was used for the creating of the planar RGO<sub>p</sub> flakes possessing a percolation grid with sufficient areas for electrical measurements on the polystyrene surface. As a result, very low resistances for some flakes precipitated from 15 wt.% composite of 4,500, 6,000 and 9,000 Da molecular masses at the room temperature were obtained. The absolute values of measured resistances turned out to be 1-3 orders lower than resistance of copper. The lowest resistance demonstrated the composite on the base of polystyrene with molecular mass 9,000 Da. Such an extraordinary result allows supposing a presence of superconducting component in the reduced graphene oxide inclusions similar to work [3]. After partial release of separate RGO<sub>p</sub> particles from polymer matrix due to deformation of covalent bonds and possible shift or rotation of RGO<sub>p</sub> layers a superconducting state appears at room temperature, as in [2]. On the contrary, resistance was very high and ranged from semiconductor values to dielectric state in the case of a composite with a molecular weight of 45,000 Da. Possible explanation is in the influence of the large sizes of polystyrene macromolecules bonded with separate RGO<sub>p</sub> particles. Extended polystyrene macromolecules during its precipitation with a mixed solvent prevent the coalescence of RGO<sub>p</sub> particles, due to steric restrictions, which suppress the formation of conduction channels.

1. Rabchinskii M.K., Shnitov V.V., Dideikin A.T. et.al. Nanoscale Perforation of Graphene Oxide during Photoreduction Process in the Argon Atmosphere. *J. Phys. Chem. C*, 2016, **120** (49), P. 28261-28269.
2. Nikolaeva M.N., Bugrov A.N., Anan'eva T.D. et. al. Resistance of reduced graphene oxide on polystyrene surface. *Nanosystems: physics, chemistry, mathematics* 2018, **9**(6), P. 793-797.
3. Saad M., Gilmutdinov I.F., Kiamov A.G. et al. Observation of Persistent Currents in Finely Dispersed Pyrolytic Graphite. *JETP Letters*, 2018, **107** (1), P. 37-41.

## The influence of the copper crystallites orientations on the efficiency of graphene transfer

*Boyko E.V.*<sup>1,2</sup>, *Kostogrud I.A.*<sup>2</sup>, *Smovzh D.V.*<sup>1</sup>

*renboyko@gmail.com*

<sup>1</sup> Physical department, Novosibirsk State University, Novosibirsk, Russia

<sup>2</sup> Kutateladze Institute of Thermophysics, Siberian Branch of the RAS, Novosibirsk, Russia

Graphene - 2-dimensional carbon material attracts the attention of researchers from various scientific fields because of its outstanding properties such as high thermal conductivity (5000 W/(m\*K)) [1], mechanical strength (1 TPa) [2], impermeability for most gases [3], etc. These properties can significantly change when using different kinds of graphene synthesis methods [4], [5]. The CVD method used in this work has several advantages before other synthesis methods: with this method, high quality and large area graphene can be obtained. Scalability of this method has made it one of the most popular methods in the scientific literature.

The CVD method is based on the thermal catalytic decomposition of carbon-containing gas with use of metal catalyst substrate. In this work, the synthesis of graphene was carried out on the copper foil surface. For some practical applications of graphene [6] transfer stage to the target substrate is required. Synthesis and transfer stages play a crucial role in the formation of the graphene structure and characteristics of graphene-based devices.

The work is focused on studying adhesion processes occurred between copper crystallites surfaces and graphene, or in other words, on studying the influence of the copper crystallites orientation on the amount of mechanically transferred graphene.

As a result of the work, it was found out that crystallographic planes of copper - [100], [110] & [111] have the highest adhesion to graphene. Their uniform structure conduces to strong intermolecular interactions between copper and graphene surfaces. In addition, a new quick method measuring the amount of graphene transferred to the target substrate was developed.

### References

1. S. Ghosh, D. L. Nika, E. P. Pokatilov, A. A. Balandin: Heat conduction in graphene: experimental study and theoretical interpretation // *New J. Phys.* - 2009. - Vol. 11. - P. 1
2. C. Lee, X. Wei, J. W. Kysar, J. Hone: Measurement of the elastic properties and intrinsic strength of monolayer graphene // *Science.* - 2008. - Vol. 321. - P. 385
3. Y. Su, V. G. Kravets, S. L. Wong, J. Waters, A. K. Geim & R. R. Nair: Impermeable barrier films and protective coatings based on reduced graphene oxide // *Nature Communications* 5. - 2014. Article number: 4843
4. W.S. Hummers, R.E. Offeman: Preparation of graphitic oxide. // *J. Am. Chem. Soc.* - 1958. - Vol. 80. - P. 1339
5. A. Zurutuza, C. Marinelli: Challenges and opportunities in graphene commercialization // *Nature Nanotechnology.* - 2014. - Vol. 9. - P. 730
6. S. Ren, P. Rong, Q. Yu: Preparations, properties and applications of graphene in functional devices: A concise review // *Ceramics International.* - 2018. - Vol. 44. - P. 11940

## Investigation of the of Graphen films grown on 4H-SiC.

*Alexander A. Lebedev<sup>1</sup>, Pavel V. Bulat<sup>2</sup>, Valerii Yu. Davydov<sup>1</sup>, Sergei P. Lebedev<sup>1</sup>, Alexander N. Smirnov<sup>1</sup>, Nina V. Agrinskaya<sup>1</sup>, Mikhail A. Shakhov<sup>1</sup>*

*shura.lebe@mail.ioffe.ru*

<sup>1</sup> Ioffe Institute, St. Petersburg, 194021 Russia

<sup>2</sup> ITMO University, Kronverkskii av. 49, St. Petersburg, 197101 Russia

One of the most promising technologies for synthesis of graphene, which can produce a high-quality material and, at the same time, be integrated into industrial production process, is the thermal destruction of the surface of silicon carbide (SiC) substrates [1, 2]. Graphene was formed on high-resistivity silicon carbide substrates in order to rule out any influence exerted by the substrate conductivity in transport measurements. The synthesis was performed in a vacuum or in an inert gas (Ar). Prior to growth of graphene, SiC was subjected to sublimation etching to remove the defective layer from its surface. The difference between the techniques used to obtain graphene on SiC in a vacuum and in argon does not consist only in that dissimilar growth media are used. Also different are the growth temperature and the orientation of the substrate surface on which graphene is formed. The following technological parameters were used in the case of growth in a vacuum: residual chamber pressure  $10^{-6}$  Torr, growth temperature 1400–1500°C, growth duration 15 min. The C-face [surface orientation (000)] of the SiC substrate was used to grow graphene. In the case of growth in argon, the growth temperature was raised to 1800–1850°C, the growth duration was 10 min, and the argon pressure in the growth chamber was 760 Torr, with the growth itself performed on the Si-face [surface orientation (0001)] of the substrate. The technological parameters were changed because the growth kinetics was different due to the partial suppression by argon of the sublimation of the silicon carbide components from the substrate surface. As a result, it became possible to use the thermally more stable Si face of the SiC substrate. This, in turn, led to a lower growth rate of graphene and made it possible to obtain homogeneous monolayer graphene films [2].

For the concentration  $1.3 \times 10^{13} \text{ cm}^{-2}$ , the electron mobility in the graphene under study was  $\mu=300\text{--}400 \text{ cm}^2/(\text{V s})$ . In samples of this kind, the magnetoresistance (MR) of the graphene/SiC system exhibited a weak localization in weak magnetic fields and at low temperatures. At higher temperatures, a transition from weak localization to a weak antilocalization (which is a manifestation of the isotopic spin in graphene) was for the first time observed in the magnetoresistance. To the best of the authors' knowledge, this behavior was observed for the first time for graphene on SiC. This effect has been predicted for graphene strongly bound to the substrate, with the spatial scale of scatterers comparable with that of the atomic kind. A clearly pronounced pattern of Shubnikov-de Haas oscillations (Fig.1-4) was observed in measurements at low temperatures (4.2 K) in strong magnetic fields of up to 30 T. This pattern demonstrates that the Berry phase is manifested. These effects are characteristic of graphene and are weakly sensitive to defects on the substrate.

**Acknowledgement.** The study was financially supported by the Ministry of Education and Science of the Russian Federation (contractual agreement no. 14.575.21.0148, unique project identifier RFMEFI57517X0148).

### References

#### References

1. C. Virojanadara, M. Syväjarvi, R. Yakimova, L.I. Johansson, A.A. Zakharov, and T. Balasubramanian, *Phys. Rev. B*, 78, 245403 (2010).
2. V.Yu. Davydov, D.Yu. Usachev, S.P. Lebedev, A.N. Smirnov, V.S. Levitskii, I.A. Eliseev, P.A. Alekseev, M.S. Dunaevskii, O.Yu. Vilkov, A.G. Rybkin, A.A. Lebedev *Semiconductors* 51 (2017) 1072.

## Effect of heat treatment on the composition and structure of the microwave exfoliated graphite oxide

*Skokan E.V.*<sup>1</sup>, *Chilingarov N.S.*<sup>1</sup>, *Knotko A.V.*<sup>1</sup>, *Khavrel P.A.*<sup>1</sup>, *Zhirov M.S.*<sup>1</sup>, *Shulga Y.M.*<sup>2</sup>

*skokan@mail.ru*

<sup>1</sup> Moscow State University, Chemistry Department, Moscow 119991, Russia

<sup>2</sup> National University of Science and Technology MISIS, Leninsky pr. 4, Moscow 119049, Russia

The properties of graphene oxide (for example, high electrical conductivity and mobility of charge carriers after it reducing, a large specific surface area), as well as its comparative cheapness, initiate active searches for the application of this material in applied developments, as well as methods for its chemical modification. Graphene oxide is a promising compound for the production of composite materials. When assessing the possibility of using graphene oxide in this quality, it is necessary to take into account, in particular, the accessibility of areas that are close in composition to graphene and the chemical activity of oxygen-containing groups.

The aim of this work was to determine the effect of heat treatment on the composition and structure of microwave exfoliated graphite oxide (MEGO). Heat treatment included stepwise heating samples of MEGO in a vacuum with mass-spectral monitoring of the composition of the emitted gases. The obtained samples were analyzed by XPS, XRD, IR and Raman spectroscopy, and electron microscopy (SEM and TEM). The complex of these methods made it possible to obtain heat treatment products from MEGO under controlled annealing conditions and determine its effect on various characteristics: morphology, total defectiveness, total oxygen concentration, types of oxygen-containing groups, and sizes of graphene crystallites.

Annealing of MEGO at  $T_f = 573$  K is accompanied by the release of H<sub>2</sub>O, CO, and CO<sub>2</sub> molecules (no release of oxygen O<sub>2</sub> and sulfur dioxide SO<sub>2</sub> was detected), and does not lead to the complete removal of water and oxygen-containing groups from the sample. In the samples MEGO and MEGO / 573 the total oxygen concentration is almost the same, and a similar set of oxygen-containing groups is found.

The release of water molecules reaches a certain minimum level at a temperature of 773 K, and upon further heating changes slowly. Intensive emission of carbon oxides CO and CO<sub>2</sub> at temperatures of 873–1073 K is completed by reducing their fluxes to a level beyond the sensitivity limits of the mass spectrometer.

A 4,4 times decrease in oxygen concentration occurs during high-temperature (1073K) annealing of MEGO. The formation of MEGO/1073 is accompanied not only by the disappearance of quinone fragments and adsorption water, but also by a significant decrease in the content of oxygen-containing groups. The decrease in the content of carbonyl groups is estimated by a factor of 2, and hydroxyl and ether groups - by a factor of 3.

During the high-temperature heat treatment of MEGO, deeper separation of particles occurs with the formation of highly deformed packs with a small number of layers, in which the same wrinkles, folds and twists are present. In addition to the morphological changes, there are numerous holes in the layer structure, which are formed in the areas of active oxygen removal in the form of CO and CO<sub>2</sub> oxides. High-temperature annealing leads to an increase in the concentration of defects by ~20%; at the same time, the average distance between defects is reduced by ~17%. In conclusion, we note that the very small crystal areas distributed by volume, as well as twists, folds, and wrinkles in carbon layers are the “clips” that determine the stability of MEGO and keep them from decay.

## Low-temperature exfoliation/functionalization of graphite using quaternary ammonium cation salts

Novikau U.<sup>1</sup>, Razanau I.<sup>1</sup>, Filipovich S.<sup>1</sup>

ir23.by@gmail.com

<sup>1</sup> Scientific-Practical Materials Research Centre of NAS of Belarus, Minsk, Belarus

In the present report, a method of low-temperature exfoliation of graphite combined with its simultaneous alkylation/hydrogenation is described. The exfoliation of graphite is performed through its intercalation in solution of metallic sodium in liquid ammonia. When alkali metal is dissolved in liquid ammonia, the ion pair of solvated alkali cation  $[\text{Na}(\text{NH}_3)_x]^+$  and solvated electron  $[\text{e}(\text{NH}_3)_y]^-$  is created [1]. Solvated electron gives the solution color ranging from blue to golden depending on the concentration. Upon solvated electron addition to graphite planes, fast intercalation of solvated sodium cation into interplanar space of graphite occurs. The intercalation compound thus produced can also be referred to as "sodium graphenide". After excessive ammonia evaporation, the decomposition of this graphite intercalation compound through its hydrolysis leads to graphite exfoliation into multi-layer flakes [2] with corresponding powder expansion.

To combine the exfoliation with chemical functionalization, salts of quaternary ammonium cation were added to the solution. Tetraethylammonium bromide (TEAB) and ammonium bromide (AB) salts were used in the experiment. Salts were dissolved in liquid ammonia and then added to graphite powder in the sodium solution in liquid ammonia. Upon the reaction proceeding, the solution color changes from intensive blue to transparent. The reaction mixture was mixed for 3 hours, left to dry out under room temperature and then thoroughly washed with distilled water and dried.

FTIR spectra of the synthesized powders have shown the appearance of peaks characteristic of C-H bond vibration in the region of  $2790\text{-}3000\text{ cm}^{-1}$  thus confirming the alkylation/hydrogenation of the exfoliated graphite powder. Thermal stability of the powders was studied using thermal analysis combined with FTIR spectroscopy of the thermal decomposition gaseous products. Molecular structure of the synthesized powders is discussed.

In our opinion, the simplified scheme of the functionalization can be described through the steps of reduction of the quaternary ammonium cation by the solvated electron, its subsequent decomposition into tertiary amine and alkyl radical and following radical grafting onto graphite planes. On the other hand, the radical anions produced by the addition of solvated electrons to graphite planes are thought to play an important role in the functionalization as well similar to Birch reduction mechanism [3]. The functionalization method described in the report is a promising approach for grafting various functional groups/ molecular chains onto graphite and graphene.

### References

1. Jortner, N.R. Kestner, *Electrons in Fluids: The Nature of Metal-Ammonia Solutions* (Springer-Verlag, 1973), p. 31.
2. P. Novikov, S.A. Kirik, *Tech. Phys. Lett.* (2011) **37**, 565.
3. Yang, Y. Sun, L.B. Alemany, W.E. Billups, and T.N. Narayanan, *J. Am. Chem. Soc.* (2012) **134**, 18689.

## Swelling of Graphite oxide in polar liquids: the model to account for sorption and internal structure

*Rebrikova A.T.*<sup>1</sup>, *Avramenko N.V.*<sup>1</sup>, *Talyzin A.*<sup>2</sup>, *Korobov M.V.*<sup>1</sup>

*niccolumtesla@mail.ru*

<sup>1</sup> Department of Chemistry, Moscow state University, Moscow, Russia

<sup>2</sup> Department of physics, Umea University, Umea, Sweden

Graphite oxide (often called graphene oxide) attracts recently wide attention as a material to make membranes for separation/filtration of liquids and gases [1]. Here we present the results of extensive experimental study of interaction of graphite oxides (GO) with a series of polar organic liquids mostly inspired by the interest in properties of GO membranes. Measurements were performed using Differential Scanning Calorimetry (DSC), Thermo gravimetry (TG), isopiestic method and X-ray diffraction (XRD), nuclear magnetic resonance (NMR) and electron spin resonance (ESR). The interaction of GO with polar liquids leads to sorption and formation of saturated swelled GO structures consist of parallel GO planes and layers of organic liquids. The ultimate goal of this study was to come up with a phenomenological model of the GO swelled structures, incorporating data on inter-plane distances, sorption, and number of oxygen containing groups at GO planes. The very concept of "liquid layer" within the GO inter-plane space was carefully examined and the quantitative characteristics of such a "layer" were proposed. The most valuable parameter to describe a "layer" turned out to be a sorbed volume related to a certain increase of the inter-plane distance (2-3Å). The same volume of the "layer" (~0,3-0,5 cm<sup>3</sup>/g GO) was found for liquids with rather different molecular mass. The "layer" covers no more than 50% of the internal GO surface leaving room for bare nano-channels suitable for diffusion through the GO membranes.

No visible correlation of the sorbed volume with the number of oxygen-containing groups was found. This implies that layers of liquid didn't form stable contacts with the GO planes and might have certain translational mobility. Such mobility was confirmed by ESR measurements. Swelled GO structures with 1-5 parallel layers in between two GO planes were detected. Contrary to literature data, no spontaneously formed structures with perpendicular or inclined orientation of sorbed layers were observed. Phase transformations of swelled GO structures were detected at change of pressure or temperature within the system. They were interpreted in terms of incongruent melting - equilibrium desorption of one layer from the swelled structure. Surprisingly only two types of such transitions were detected, namely the transition from two sorbed layers to one and from five layers to four. The systems of Brodie GO with acetonitrile and 1-nonanol, respectively, give the best examples of these two transitions.

This study was supported by the RFBR grants 18-33-00439 mol\_a and 18-29-19120 mk.

### References

1. R. Nair, H.A. Wu, P.N. Jayaram, I.V. Grigorieva, A.K. Geim. *Science* (2012) **335**, 442.



## **h-BN-Graphene lateral heterolayers on lattice-matched surfaces**

*Bokai K.A.*<sup>1</sup>, *Shevelev V.O.*<sup>1</sup>, *Vilkov O.Yu.*<sup>1</sup>, *Marchenko D.E.*<sup>2</sup>, *Makarova A.A.*<sup>3</sup>, *Usachov D.Yu.*<sup>1</sup>

*bokai.kirill@gmail.com*

<sup>1</sup> Saint Petersburg State University, Saint Petersburg, Russia

<sup>2</sup> Helmholtz-Zentrum Berlin für Materialien und Energie, Berlin, Germany

<sup>3</sup> Technische Universität Dresden, Dresden, Germany

During last decades graphene-based systems attract continuous interest and remain a subject of intensive investigations. Graphene, which is a zero-gap semiconductor, and an insulating hexagonal boron nitride (h-BN) are considered as the most promising building blocks for future 2D electronics, but their hybrid structures remain relatively unexplored. Graphene (Gr) and h-BN are isostructural to each other; both possess  $sp^2$ -honeycomb arrangement and nearly the same lattice constant. Their lateral heterostructures are supposed to have novel properties and functionality. Among the unusual physical properties of h-BN-Gr hybrid system are tunable bandgap, magnetism, outstanding thermal transport, etc. [1, 2] However, these properties depend strongly on the stoichiometry, boundary structure (between h-BN and graphene domains) and morphology of a resultant film, and still are not well understood.

One of the most efficient ways to construct the h-BN-Gr lateral heterostructures of high crystalline quality, which provides possibility to study the interplay between atomic scale features and physical properties, is a chemical vapor deposition (CVD) on single-crystal substrates, including Ru(0001), Rh(111), Ir(111), Pt(111), Re(0001) [3-5]. However, these systems are characterized by strong corrugation of h-BN-Gr layer. This corrugation originates from large lattice mismatch between substrates and h-BN-Gr. The corrugation makes analysis of the atomic structure sophisticated. No corrugation was found for the h-BN-Gr grown on matched Ni(111) surface. However, no detailed structural studies of h-BN-Gr/Ni(111) interface were reported. The information on the BN-Gr/Co(0001) system is totally missing.

Here, we report on comprehensive investigation of the h-BN-Gr heterolayers structure formed on the Ni(111) and Co(0001) substrates. A complete layers of Gr and h-BN domains with various B:N:C ratios were obtained in two ways: using a single molecular precursor 1,3,5-trimethylborazine ( $C_3H_{12}B_3N_3$ ) and from mixture of propylene ( $C_3H_6$ ) and borazine ( $N_3B_3H_6$ ) precursors. Given that Ni(111) and Co(0001) substrates possess low lattice constant mismatch (less than 2%) with respect to both h-BN and Gr well-ordered interfaces with (1x1) structure were achieved. Using XPS complemented with DFT study we figured out that formation of zigzag linking edge is more preferred than armchair one. This finding was further confirmed by atomically resolved STM. Photoemission electron microscopy measurements indicate that both Gr and h-BN domains can be as large as a few hundred nm.

This work was supported by Saint Petersburg State University Grant 11.65.42.2017 and RFBR Grant No. 17-02-00427.

### **References**

- [1] R. Zhao, J. Wang, M. Yang, Z. Liu, and Z. Liu, *J. Phys. Chem. C* (2012) **116**, 21098.
- [2] A. Ramasubramaniam and D. Naveh, *Phys. Rev. B* (2011) **84**, 075405.
- [3] M. Iannuzzi and J. Hutter, *Surf. Sci.* (2011) **605**, 1360.
- [4] M. Liu, Y. Li, P. Chen, J. Sun, D. Ma, Q. Li, T. Gao, Y. Gao, Z. Cheng, X. Qiu, Y. Fang, Y. Zhang, and Z. Liu, *Nano Lett.* (2014) **14**, 6342.
- [5] Y. Qi, N. Han, Y. Li, Z. Zhang, X. Zhou, B. Deng, Q. Li, M. Liu, J. Zhao, Z. Liu, and Y. Zhang, *ACS Nano* (2017) **11**, 1807.

## **Influence of defects on heterogeneous electron transfer rate at the basal plane of graphene**

*Kislenko V.A.*<sup>1,2</sup>, *Kislenko S.A.*<sup>2</sup>

*vitaly.kislenko@gmail.com*

<sup>1</sup> Moscow Institute of Physics and Technology, Dolgoprudny, Russia

<sup>2</sup> Joint Institute for High Temperature, Russian Academy of Science, Moscow, Russia

In the field of creating efficient and cheap electrocatalysts for the processes of electrochemical energy conversion, we can highlight the researches of the redox kinetics on the surface of carbon materials containing various defects. There are a new experimental data that indicate the significant change in electron transfer (ET) activity at different types of defects, such as vacancies, graphene edges, impurities and functional groups on the surface.

The local ET rate depends on the geometrical structure of the surface and its composition. The improved electrochemical activity can be explained by the appearance of local electronic states near the Fermi level and, as a result, a larger overlap between the electronic states of graphene and the redox couple.

In this study, the reaction of heterogeneous ET was investigated for the following set of defects: mono vacancy, Stone-Wales defect, double vacancies, substitutional nitrogen atom, epoxy (-O-) and hydroxyl (-OH) functional groups. For these defects the electron density of states (DOS) was calculated using density functional theory (DFT) method. That allowed us to obtain the rate constants of direct and inverse heterogeneous ET in the framework of the Gerischer-Marcus model [1] taking into account the graphene quantum capacitance [2]. This stage provides an opportunity to rank the electrocatalytic efficiency of the defects with respect to various redox couples.

It was shown that defects can lead to catalysis of heterogeneous ET. The range of standard potentials in which this effect is observed depends on the defect type. The most significant result is found for single vacancies. Their presence enhances the electron transfer by an order of magnitude at standard potential from -1 V to 0 V (vs. SHE). Experimental confirmation of the electrocatalytic properties of vacancies was shown in [3], where an increase in the equilibrium rate constant by an order of magnitude at a vacancy density corresponding to the characteristic distance between defects ~2.5 nm was found, which is close to the parameters of our system. For redox couples the standard potential of which lies outside the interval [-1V, 1V], an increase in the rate constant of more than 1.5-2 times in comparison with defect-free graphene is not observed, since a significant relative increase in the DOS far from the Fermi level cannot be provided by presence of studied defects.

The work is supported by grant No. 18-03-00773 from the Russian Foundation for Basic Research.

### **References**

1. R. Memming, *Semiconductor Electrochemistry* (WILEY-VCH, Weinheim, 2015), p. 127.
2. C. Zhan, J. Neal, J. Wu, and D. Jiang, *J. Phys. Chem. C* (2015) 119, p. 22297.
3. J-H. Zhong, J. Zhang, X. Jin, J.-Y. Liu, Q. Li, M.-H. Li, W. Cai, D.-Y. Wu, D. Zhan and B. Ren, *J. Am. Chem. Soc.* (2014) 136, p. 16609.

## EPR and NMR study of molecular mobility of polar liquids in the inter-plane space of graphite oxide

*Chumakova N.A.*<sup>1</sup>, *Rebrikova A.T.*<sup>1</sup>, *Vorobiev A.Kh.*<sup>1</sup>, *Korobov M.V.*<sup>1</sup>, *Tkachev Ya.V.*<sup>2</sup>

*harmonic2011@yandex.ru*

<sup>1</sup> Moscow State University, Russia

<sup>2</sup> Engelhardt Institute of Molecular Biology, Moscow, Russia

Graphite oxide (GO) membranes demonstrate exceptional permeation properties with promise for many applications. Mechanism of such permeation is widely discussed in literature. In the present work we assessed the degree of mobility of polar liquid intercalated in the inter-plane space of graphite oxide. It is known that the polar solvents adsorbed inside the GO powders and membranes do not exhibit freezing/melting phase transition [1, 2]. The data on the molecular mobility of such liquids are incomplete and controversial. The state of the liquid is typically characterized as “strongly bound to the host molecules” [2].

EPR and NMR spectroscopic techniques are very sensitive to rotational and translation mobility of molecules possessing nonzero spin. By means of X-band EPR it was shown that rotation of the stable nitroxide radicals TEMPO in polar liquids (CH<sub>3</sub>OH, H<sub>2</sub>O, CH<sub>3</sub>CN) intercalated in the inter-plane space of GO is almost the same as their rotation in bulk liquids (rotational correlation time is about 10<sup>-10</sup> sec). Figure 1(a) shows EPR spectrum of the spin probe in the system “B-GO - CH<sub>3</sub>CN”. On the other hand, T<sub>2</sub>-filtered <sup>19</sup>F and <sup>1</sup>H NMR using CPMG sequence reveals significantly broader signal in trifluoroethanol (TFE) saturated B-GO sample compared to one obtained for bulk TFE mixed with B-GO (Figure 9(b)). It indicates that diffusion of TFE in the inter-plane space should be somewhat hindered, but it certainly remains in liquid state. It is important to note that experimental techniques used to prepare saturated samples did not allow formation of bulk liquid droplets in the defect areas of GO.

This work was supported by the Russian Foundation for Basic Research (grant 18-29-19120).

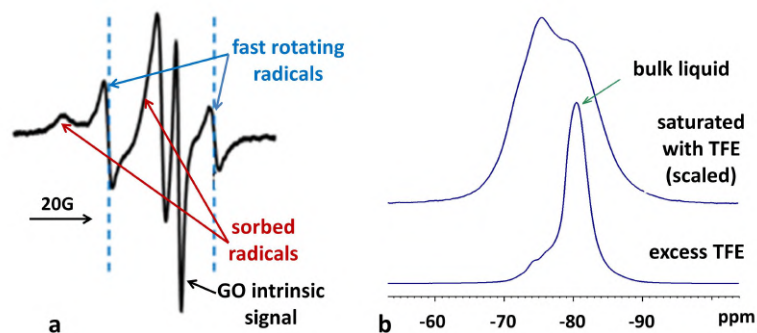


Fig.1. (a, left) EPR spectrum of TEMPO radical in the “B-GO - CH<sub>3</sub>CN” system, dotted lines show the components of rapidly rotating radicals; (b, right) <sup>19</sup>F NMR spectra of the “B-GO - CF<sub>3</sub>CH<sub>2</sub>OH” system, saturated sample (top line), and B-GO mixed with an excess of CF<sub>3</sub>CH<sub>2</sub>OH.

### References

1. Korobov V., Talyzin A. V., Rebrikova A. T., Shilayeva E. A., Avramenko N. V., Gagarin A. N., Ferapontov N. B., Carbon (2016) **102**, 297.
2. Cerveny S., Barroso-Bujans F., Alegri ´a A., Colmenero J., J Phys Chem C (2010) **114**, 2604.

## Terahertz transitions between Landau levels in graphene with different concentrations of electrons

*Baryshnikov K.A.*<sup>1</sup>

*barysh.1989@gmail.com*

<sup>1</sup> Ioffe Institute, St. Petersburg, Russia

The terahertz resonance transitions between Landau levels in graphene are studied theoretically on the basis of technological opportunities to control electronic concentration in it. In an external quantizing magnetic field under the action of unpolarized light incident normally on a graphene monolayer resonant transitions occur between Landau levels (LLs) with a change in the absolute value of their number  $|n|$  by  $\pm 1$  [1,2] ( $n$  is numbered for all integers). LLs in graphene are non-equidistant and demonstrate a root dependence on magnetic field and  $|n|$  [1,2]. The probability of terahertz transitions per unit time as a result of light absorption by graphene is proportional to the degeneracy of the Landau levels (i.e. to the magnitude of the magnetic field), the difference in the population of LLs between which optical transitions are allowed, and the resonant transition frequency factor that has the form of a Lorentzian with an appropriate broadening of the levels. The concentration of carriers sets the Fermi energy that is included in population difference between LLs.

The probability of terahertz transitions between Landau levels for various magnetic fields at 4.2 K is calculated in MATLAB at different positions of Fermi levels corresponding to different concentrations of electrons. A resonant type magnetic field dependence of photoconductivity due to excited by resonant transitions electrons is demonstrated. There is a peak of this dependence at the magnetic field  $B_{\max}$  in a wide range of FEs from 0 upto 400 meV at frequency  $\omega/2\pi=3.3$  THz of the incident beam. This calculation shows that the  $B_{\max}$  increases when FE grows, but there are regions of plateaus resulting in semiladder type of this dependence. The peak values of photoconductivity manifest a periodic dependence on FE with a huge change in value during the period although with the increase in average at high FE. Besides the considered above ideal case of well-defines LLs (small broadening of them), the effects of big broadenings and big fluctuations of FE along the sample are discussed.

The author acknowledges the support from RFBR (Project 18-02-00498).

### References

1. Zheng and T. Ando, Phys. Rev. B (2002) **65**, 245420.
2. L. Sadowski, G. Martinez, M. Potemski, C. Berger, and W. A. de Heer, Phys. Rev. Letters (2006) **97**, 266405.

## Graphene edge as an electrocatalyst for the oxygen reduction reaction.

*Pavlov S.V.*<sup>1,2</sup>, *Kislenko S.A.*<sup>2,3</sup>

*sergey.pavlov@skoltech.ru*

<sup>1</sup> Skolkovo Institute of Science and Technology, Moscow, Russia

<sup>2</sup> Joint Institute for High Temperatures of the Russian Academy of Sciences, Moscow, Russia

<sup>3</sup> Moscow Institute of Physics and Technology, Moscow, Russia

The relevance of this work is due to the fact that the search for cheap and stable catalysts for various redox systems is a significant challenge today. One of the most promising directions in this field is the use of carbon nanomaterials as electrocatalysts. Various defects in such materials are able to create around themselves local electronic states with energies close to the Fermi level, accelerating electron transport across the interface. One of the most common defects is the edge of graphene, the experimental data on the electron transfer kinetics from which is contradictory in the literature. Also, there is a lack of theoretical studies in this area; most of the existing studies published to date are qualitative. In our work, we studied the influence of the graphene edge both from the point of view of the interface structure, which determines the kinetics of the reactants adsorption and from the point of view of the heterogeneous electron transfer kinetics. The method of classical molecular dynamics, as well as density functional theory, was used.

Using the method of classical molecular dynamics, we have obtained the structure of the electrode/electrolyte interface for various types of surface — a single-layer graphene edge, a multilayer graphene edge, a graphene plane [1-3]. Acetonitrile was considered as an electrolyte, as one of the common nonaqueous solvents using in electrochemical systems. We have obtained the distributions of mass and charge densities in the near-electrode layer, the distribution of the electrostatic potential, and the orientational ordering of the solvent. Also, the kinetics of oxygen adsorption to the model surfaces and the corresponding distributions of the equilibrium concentrations were calculated.

Within the framework of the density functional theory, we studied heterogeneous electron transfer from two clusters of graphene with different edge types. Using the Landau-Zener and Marcus theory, the values of electron transfer constants with spatial resolution both along the surface and varying the distance to the surface of the clusters were obtained [4, 5]. The effective electron transfer constants were calculated, taking into account the equilibrium distribution of the oxygen molecules in the near-electrode region, which we have obtained previously by classical molecular dynamics.

The edge of graphene showed a less ordered interface structure with less dense layers of electrolyte compared with the plane of graphite. As a result, the edge of both single and multilayer graphene is an effective surface for adsorption of the oxygen molecules. Also, the accelerated kinetics of the electron transport from the zigzag graphene edge was found in comparison with the graphene plane. At the same time, the armchair graphene edge does not show such electrocatalytic activity.

The work is supported by grant 18-03-00773A of the Russian Foundation for Basic Research.

### References

1. S.V. Pavlov and S.A. Kislenko, *Phys. Chem. Chem. Phys.* (2016) **18**, 30830.
2. S.A. Kislenko and S.V. Pavlov, *High Energy. Chem.* (2017) **51**, 51.
3. S.V. Pavlov and S.A. Kislenko, *J. Phys.: Conf. Ser.* (2018) **946**, 012028.
4. S.V. Pavlov and S.A. Kislenko, *J. Phys.: Conf. Ser.* (2018) **1092**, 012112.
5. S.V. Pavlov, R.R. Nazmutdinov, M.V. Fedorov and S.A. Kislenko, *J. Phys. Chem. C.* (2019). doi:10.1021/acs.jpcc.8b12531.

## Transparent conductive few-layered graphene-based Langmuir-Blodgett films

*Danilov E.A.*<sup>1</sup>, *Samoilov V.M.*<sup>1</sup>

*EgADanilov@rosatom.ru*

<sup>1</sup>JSC "Scientific Research Institute of Graphite-Based Structural Materials "NIIgrazit", Moscow, Russia

Transparent conductive films (TCF) are of crucial importance for modern electronic devices as they are widely used as transparent electrodes in photovoltaics, sensor displays, smart windows, antistatic coatings, OLED technologies. Currently used indium-tin oxide (ITO) films, as well as some alternative materials (conductive polymers, metal nanowires and networks), possess a number of serious drawbacks that hinder their applications in prospective devices.

Graphene films have great potential as TCF material: chemical stability, excellent optical properties and mechanical properties suitable for flexible applications. Unfortunately, scalable large area graphene films have relatively high resistance (over 300  $\Omega$ /sq.) due to high interparticle contact resistance [1]. It has become relatively popular recently to manufacture thin films from graphene-containing suspensions; graphene oxide or partially reduced graphene oxide are normally used in order to provide for better suspension stability and adhesion. Various techniques have been used (Meyer rod, spin coating, spray coating, Langmuir-Blodgett etc.), but no works to date report large area films with desirable level of properties (sheet resistance <100-200  $\Omega$ /sq. at optical transparency over 85%).

In the current study we have successfully applied Langmuir-Blodgett technique to deposit TCFs of few-layered graphene particles on various dielectric, primarily piezoelectric, substrates (glass, quartz, lithium niobite, PVdF, PTFE, PET). Few-layered particles were obtained via direct exfoliation of natural graphite [2] in the presence of surfactants. Aqueous suspensions of few-layered graphene were further centrifuged to remove un-exfoliated graphite and obtain semi-transparent conductive suspensions. Langmuir-Blodgett technique was chosen as it provides considerable pressure as the film is formed which results in high interparticle contact quality. Amphiphility of particle surface is a prerequisite for successful Langmuir-Blodgett deposition, therefore all previous attempts were aimed at graphene oxide-based materials. It was shown that directly exfoliated graphene can also be used as surfactants adsorbed on its surface can also provide sufficient hydrophilicity to form continuous films.

Scanning electron microscopy, Raman spectroscopy, and atomic force microscopy confirmed that films consist of 1-4 layered graphene with no apparent voids across ca. 3'-films, as confirmed by Raman mapping. It was further shown that both hydrophilic and hydrophobic substrates can be efficiently coated with few-layered graphene films having sheet resistance less than 120  $\Omega$ /sq. at average optical transmission 92% by varying surfactant chemical structure (wide variety of non-ionic surfactants including fluorine-containing, polymeric, cholate-based was tested). Number of deposited layers strongly affects electrical and optical properties of the films. One of the advantages of few-layered graphene TCFs is the absence of any specific absorption in the optical region which is very important for sensor applications.

### References

1. J. López-Naranjo, L.J. González-Ortiz, L.M. Apátiga, E.M. Rivera-Muñoz, A. Manzano-Ramírez, J. Nanomaterials (2016), 4928365.
2. V.M. Samoilov, E.A. Danilov, A.V. Nikolaeva, G.A. Yerpuleva, N.N. Trofimova, S.S. Abramchuk, K.V. Ponkratov, Carbon (2015) **84**, 38.

## Cost efficient processing of GO for sensing applications

*Marko Radovic*<sup>1</sup>, *Ivan Bobrinetskiy*<sup>1</sup>, *Nikita Nekrasov*<sup>2</sup>, *Nikolay Struchkov*<sup>2</sup>

*marrad@biosense.rs*

<sup>1</sup> University of Novi Sad, Biosense Institute, Novi Sad, Serbia

<sup>2</sup> National Research University of Electronic Technology, Zelenograd, Russia

Constant scientific and technological advancements have imposed a staggering demand for scalable, robust and low cost solutions for design and fabrication of graphene based devices. Carried out research introduces a bottom-up approach (Figure 1), involving GO ink preparation, optimization of inkjet printing parameters, laser reduction and characterization of GO layer on micron-sized Au electrodes, for application in humidity and gas sensing.

The initial step in the research activities was to optimize the functional dispersion of GO flakes for inkjet printing. Optimization was performed by selection of additives, in order to reduce the surface potential and to obtain printed structures with desired thickness and morphology. Inkjet processing was performed on Fujifilm Dimatix DMP-3000 printer equipped with piezo controlled head, for drop-on-demand operation. Printed layer was incrementally treated by laser radiation for spatial reduction of GO and removal of additives. Main idea behind the laser treatment processing was to obtain gradient in conductivity of the laser reduced GO (LrGO) layer for application in sensing technologies. Raman spectroscopy was utilized as the most powerful probe for investigation of chemical bonding and presence of impurities in the graphene-based samples. From the obtained measurements of D band signature it was established that different levels of laser reduction can be achieved by precise control of the laser power and irradiation time. The resistance of LrGO was measured for each pair of electrodes with different LrGO modified by various duration of laser pulses. The initial resistance of GO channel was about 10 MOhms. Onset of decrease in resistance starts at 80 mW, going down to about 200 kOhms at 130 mW. Varying the time irradiation we demonstrated the decreasing of resistance down to 100 Ohms. For laser powers higher than 200 mW ablation process occurs, as detected by AFM. Investigated device demonstrates good sensitivity to humidity with fast response/recovery times.

From the analysis of obtained results it was established that undertaken approach offers cost-efficient solution to processing of GO nanomaterials for application in advanced technologies.

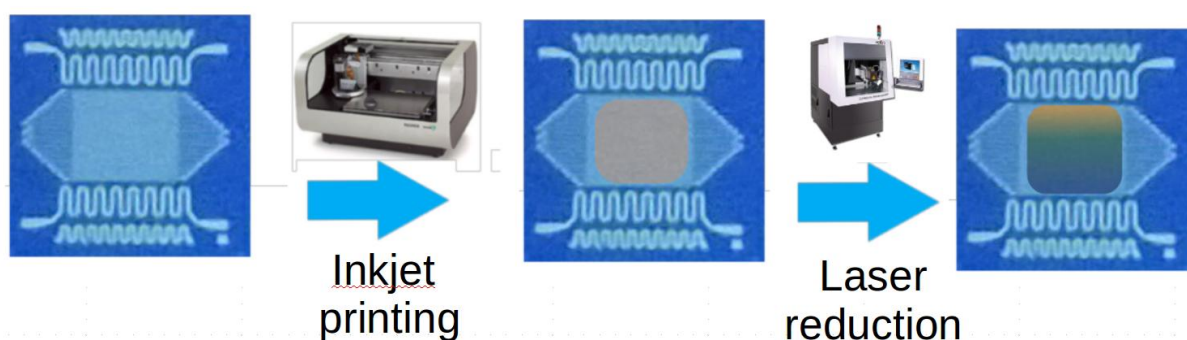


Figure 1. Schematic representation of cost efficient processing of GO on Si chip with interdigitated electrodes and heater elements.

## Shungite carbon nanoparticles as modifiers of ZnS:Cu electrophosphor study based on ESR of Mn impurity ions

Rozhkov S. P.<sup>1</sup>, Talanov A.A.<sup>2</sup>, Rozhkova N.N.<sup>2</sup>

rozhkov@krc.karelia.ru

<sup>1</sup> Institute of biology, Karelian Research Centre RAS, Petrozavodsk, Russia

<sup>2</sup> Institute of geology, Karelian Research Centre RAS, Petrozavodsk, Russia

The spectral-brightness characteristics of ZnS electrophosphors strongly depend on the functional composition of their surface and donor-acceptor (acid-base) properties that affect electronic transitions. An effective way to control microstructural defects distribution in ZnS:Cu particle surface is to record relaxation characteristics of the impurity ions of manganese by electron spin resonance (ESR) technique. This work focuses on clarifying the mechanisms of ZnS:Cu structural defects modification by shungite carbon nanoparticles (ShC).

Aqueous dispersions of ShC nanoparticles [1] were used to modify the surface of the electrophosphor ZnS:Cu particles (commercial electrophosphor E-455). It was found that ShC nanoparticles are effectively fixed on the structural defects of the phosphor, and even small concentration of ShC lead to a significant darkening of the surface of the phosphor and reduce the reflection coefficient at a wavelength of 490 nm [2]. In this case, a nonlinear change in the brightness of the luminescence was observed: decreasing at small concentration of ShC and enhancing in luminescence with higher concentration of nanoparticles.

The ESR spectrum of ZnS:Cu powder contains the components that indicate the presence of paramagnetic Mn centers located in a disordered system. Modification of the surface of the electrophosphor by ShC nanoparticles sufficiently affects the spectrum line width, amplitude and integral intensity. The dependence of the effect on the concentration of ShC nanoparticles is nonmonotonic. This is broadly consistent with the data on the alterations of the electro-luminescence during the modification by ShC nanoparticles.

The dependence of the parameters of the spectral lines on the content of ShC nanoparticles and microwave power saturation can be explained in terms of the formation of extra dislocations with new physicochemical properties in the near-surface layer of electrophosphor during its modification.

### References

1. Rozhkova N.N., Rozhkov S.P., Goryunov A.S. In Carbon Nanomaterials, Sourcebook. Ed. by Sattler K.D. Taylor&Francis Pub, 2016.V1 P. 151-174.
2. Sychev M.M., Myakin S.V., Ogurtsov K.A., Vasina E.S., Matveichikova P.V., Rozhkova N.N., Belyaev V.V. Journal of Optical Technology (2017) **84**, 1, 49.



## Graphene-like film CVD on e-beam exposed SiO<sub>2</sub>/Si by the pyrolysis of different organic precursors

*Sedlovets D. M.*<sup>1</sup>, *Knyazev M.A.*<sup>1</sup>

*sedlovets@iptm.ru*

<sup>1</sup> IMT RAS, Chernogolovka, Russia

Fast, efficient and reproducible manufacturing of graphene-like film (GLF) microstructures on dielectric substrates is of high technological importance for high-capacity storage, photovoltaic devices, sensors, transparent electrodes and defoggers and other applications [1]. GLF in this work are defined as graphene films with the crystallite size of few tens of nm.

Earlier, we reported that pyrolysis of ethanol vapor can yield GLF even without a catalyst. Later, it was shown that the pre-exposure of the substrate by the e-beam can affect the synthesis: the growth rate of the GLF on exposed areas is higher than on unexposed ones [2]. With varying the exposure parameters, this can be used for the controllable growth of thin films and even 3D structures of sp<sup>2</sup> carbon [3]. It was shown in [2] that the exposure-stage carbon contamination is not the factor affecting the deposition. We assume that the main mechanism of this effect is the charge implantation. It is known that charge buildup arises from localization of electrons in trap centers produced under irradiation or preexisting in the dielectric. At the CVD stage, the precursor molecules are attracted by the local electric field from the charge implanted in the dielectric substrate. In this work, we study the deposition of GLFs on pre-exposed SiO<sub>2</sub>/Si from various organic precursors (*i*-C<sub>3</sub>H<sub>7</sub>OH, C<sub>2</sub>H<sub>2</sub>, CH<sub>3</sub>C(O)CH<sub>3</sub>).

The electron beam lithography system used in this work was based on a scanning electron microscope JEOL JSM 840 controlled by Nanomaker hardware-software system. Irradiating electron energy was varied from 1 to 30 keV, the exposure doses were 500-3000 μC/cm<sup>2</sup>. GLFs were grown at 950°C. Carbon structures were grown in a flow-type quartz reactor incorporated in a CVD apparatus, which included a tube furnace, temperature control system, reagent feed system and a vacuum pump. The synthesis was carried out in an inert gas flow at a reduced pressure (~10<sup>3</sup> Pa).

This work was supported by the Russian Foundation for Basic Research (project no. 18-32-00047).

### References

1. H. Wang H, G. Yu, *Advanced Materials* (2016) **28**, 4956.
2. M. Knyazev, D. Sedlovets, O. Trofimov, A. Redkin, *Materials Research Bulletin* (2017) **86**, 322.
3. M. Knyazev, D. Sedlovets, O. Trofimov, *Materials Letters* (2018) **216**, 236.

## Alkaline treatment of reduced graphite oxide

*Kobets A.A.<sup>1</sup>, Fedorovskaya E.O.<sup>1,2</sup>*

*a.a.kobets@mail.ru*

<sup>1</sup> Novosibirsk state university, Novosibirsk, Russia

<sup>2</sup> Nikolaev Institute of Inorganic Chemistry, SB RAS, Novosibirsk, Russia

Carbon nanostructures have high surface area, which can be functionalized with different oxygen-containing groups (hydrogen, carbonyl, carboxyl). This surface modification leads to change in physical and electrochemical properties and still makes it able to covalent or non-covalent functionalization by organic molecules, polymers or biomolecules. Most of the modified materials can be used for electrical application, in particular, as electrodes for supercapacitor. Electrochemical capacitors are devices for accumulation and storage energy with high power, high capacity, long life durability. Cyclic voltammetry allows qualitative analysis of functional composition of the surface at the potential supply. Reduced graphite oxide is an example of carbon nanomaterials with active surface and great opportunities for functionalization and also for study its electrochemical properties.

In this work graphite oxide was synthesized by modified Hummers method from purified graphite. Further, reduced graphite oxide was obtained by treatment of graphite oxide with concentrated sulfuric acid by heating. Functionalization was carried out by hydrothermal alkali treatment, sintering with potassium oxide and potassium hydroxide system, simple treatment with sodium chloroacetate. The morphology and functional composition of all materials were studied by SEM, Raman and FTIR spectroscopy. Also, all of the modified samples were studied by cyclic voltammetry, and the peaks observed on the current-voltage curves were compared with the oxidation-reduction processes occurring on the surface of the carbon matrix at the potential supply.

Thus, it was shown that alkaline treatment led to changes in morphology and functional composition, and also affected the electrochemical properties of the reduced graphite oxide due to the contribution of oxidation-reduction processes.

## Charge pre-modified substrates for graphene-like film CVD

*Sedlovets D.M.*<sup>1</sup>, *Knyazev M.A.*<sup>1</sup>, *Korepanov V.I.*<sup>1</sup>, *Mitina A.A.*<sup>1</sup>

*alena@iptm.ru*

<sup>1</sup> IMT RAS, Chernogolovka, Russia

It is known that the interaction of an electron beam with the silicon oxide results in charge injection into SiO<sub>2</sub>. The charging consists in electron localization in defects in the material [1]. For practical applications, this effect is often undesirable since it can cause high leakage currents or breakdown phenomena. Efforts are applied to eliminate the charging [2]. On the other side, the positive charging effect is utilized to form a useful scanning electron microscope (SEM) contrast for imaging buried microstructures in SiO<sub>2</sub> films [3]. But nobody used this charge as a tool for controllable CVD on an exposed surface. Well-known techniques of electron-beam-induced deposition and etching are not considered because they associated with an electron-mediated decomposition of a precursor molecule and physical restructuring caused by electron bombardment [4], respectively, not with the charge.

Recently we estimated that the exposure of SiO<sub>2</sub>/Si and quartz substrate by electrons affects further CVD of graphene-like film (GLF) [5-6]. We assumed that this influence is caused by charge accumulation. GLFs are nanocrystalline films which can be synthesized without a metal catalyst. Their high transparency combined with a good conductivity provides successful applications in high-capacity storage and photovoltaic devices, sensors, transparent electrodes, field-effect transistor.

In the current work, we aimed to determine the influence of preliminary substrate exposure on the further CVD of GLFs for the case of different dielectric wafers (BN, sapphire). For this purpose, the spectral and electrophysical characteristics were studied for the GLFs grown on pre-exposed substrates. Raman measurements were also carried out for "clean" exposed substrates before synthesis.

The substrates were irradiated by electron beam in a scanning electron microscope JEOL JSM 840. Irradiating electron energies and exposure doses were controlled by Nanomaker hardware-software system. GLFs were grown according to the previously reported procedure [5-6]. Raman spectra of the carbon films were recorded with a Bruker Senterra micro-Raman system equipped with a 532 nm laser in the 300-3700 cm<sup>-1</sup> range. Electrical measurements were carried out by SourceMeter Keithley SMU 2450.

This work was supported by the Russian Foundation for Basic Research (project no. 18-32-00047).

### References

1. J. Vigouroux, J. Duraud, A. Le Moel, C. Le Gressus, D. Griscom, *Journal of Applied Physics* (1985) 57, 5139.
2. M. Touzin, D. Goerriot, C. Guerret-Piecourt, D. Juve, D. Treheux, H.-J. Fitting, *Journal of Applied Physics* (2006) 99, 114110.
3. H.-B. Zhang, R.-J. Feng, K. Ura, *Science progress* (2004) 87, 249.
4. S. Randolph, J. Fowlkes, P. Rack, *Critical reviews in solid state and materials sciences* (2006) 31, 55.
5. M. Knyazev, D. Sedlovets, O. Trofimov, A. Redkin, *Materials Research Bulletin* (2017) 86, 322.
6. M. Knyazev, D. Sedlovets, O. Trofimov, *Materials Letters* (2018) 216, 236.

## Graphene modified BiVO<sub>4</sub> anode material for high-performance lithium-ion batteries.

*Malkin N.A.*<sup>1</sup>

*maalkinn@mail.ru*

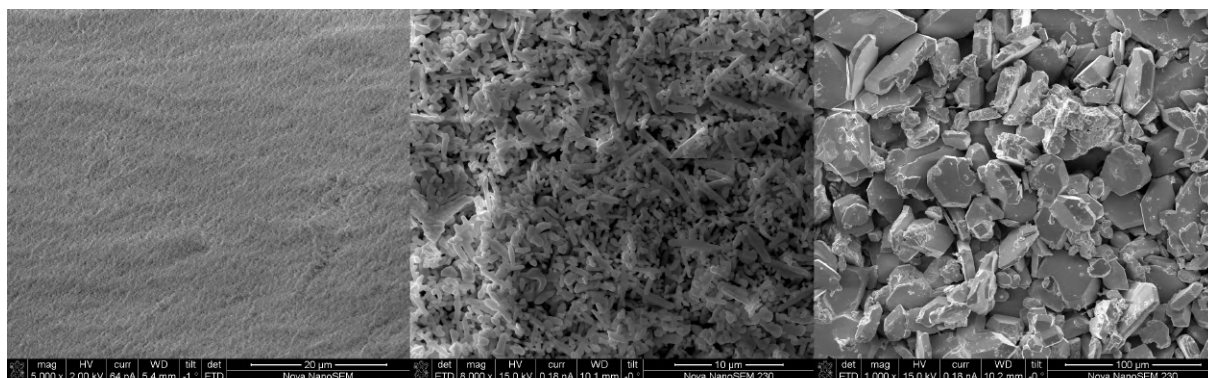
<sup>1</sup>Thermochemistry laboratory, Lomonosov Moscow State University, Moscow, Russia

The search of high-performance anode materials for lithium-ion batteries is currently one of the most important tasks. Battery performance is not only depending on the materials properties of anode and electrodes but also on the interface or surface effects. The development of suitable electrode materials with superior interface or surface properties along with stability and low cost are highly demanded. So, to keep up with recent rapid advancement in cathode materials it is desperately needed to seek for suitable and innovative high-performance anode materials.

Previous research has shown that BiVO<sub>4</sub> is a promising electrode, in particular, anode material for lithium-ion batteries; it shows an excellent reversible capacity of 769 mAh/g at 0.12 A/g with a great capacity retention. [1] The motivation to use this material in this study is its unique layered crystal structure. Varying the conditions of the synthesis makes it possible to easily manage the morphology of the material that can be used to fine tune lithium-ion batteries. The use of graphene can improve material stability and conductivity. [2] That is, the significance of conducting additives in device fabrication will be smaller and therefore the anode of the same size will have more electrode material. This means that capacity of the cell could be increased without changing size, shape and structure of the battery. Also graphene addition can make anode material more durable, because graphene is the strongest material ever produced, it is able to prevent a crystal structure from cracking during cycling.

Graphene modified BiVO<sub>4</sub> were synthesized by hydrothermal method at a temperature 180 °C using bismuth nitrate, ammonium metavanadate, graphene oxide and hydrazine chloride as a reducing agent. Electrochemical properties of initial and graphene modified materials were examined.

The work was supported by RFBR (project 18-53-06009)



BiVO<sub>4</sub>: 1. without hydrothermal treatment, 2. hydrothermal treatment, 3. hydrothermal synthesis with graphene oxide

### References

1. Dubal D., Patil D., Patil S., Munirathnam N. R., Gomez-Romero P. BiVO<sub>4</sub> Fern Architectures: A Competitive Anode for Li-ion Batteries, *ChemSusChem*. 2017. T. 10.
2. Wu H., Liu Q., Guo S. Composites of Graphene and LiFePO<sub>4</sub> as Cathode Materials for Lithium-Ion Battery, *Nano-Micro Letters*. 2014. Vol. 6, № 4, P. 316-326

## Transformation of the buffer layer grown on 4H-SiC to single-layer graphene by hydrogen intercalation

*Eliseyev I.A.*<sup>1</sup>, *Lebedev S.P.*<sup>1</sup>, *Panteleev V.N.*<sup>1</sup>, *Dementev P.A.*<sup>1</sup>

*zoid95@yandex.ru*

<sup>1</sup> Ioffe Institute, St.Petersburg, Russia

One of the most promising growth techniques able to bring graphene-based electronics to mass production is the thermal decomposition of the Si-face of 4H-SiC wafers. Despite its advantages, the electron mobility of such graphene films is limited by the presence of the interface layer between graphene and SiC. However, this layer, also called a buffer layer, is known to be transformable to single-layer graphene by hydrogen intercalation. This process leads to the formation of a quasi-free-standing monolayer graphene (QFSMG) [1]. In the present work, we studied the effect of hydrogen intercalation on the buffer layer by using Raman spectroscopy, atomic force microscopy (AFM) and Kelvin-probe force microscopy (KPFM).

The buffer layer was grown on the Si-face of the semi-insulating 4H-SiC substrate at 1600 °C. After the growth, the resulting buffer layer structures were put into a chamber where they were heated in the H<sub>2</sub> atmosphere at a temperature of 900 °C for 1 hour. The same areas of as-grown and annealed samples were studied by Raman, AFM and KPFM.

According to Raman and KPFM mapping, the as-grown samples were predominantly covered with buffer layer with presence of a small (<10%) fraction of monolayer graphene. Analysis of the 2D-line shift points that the monolayer graphene islands were subjected to relatively high compressive strain ( $\epsilon_{\parallel} \sim 0.3\%$ ), typical for graphene on 4H-SiC.

An analysis of the Raman 2D line FWHM map showed that, after heating in H<sub>2</sub>, the buffer layer was turned into monolayer graphene, and single-layer graphene inclusions became double-layered. The compressive strain values estimated from the 2D line position after H<sub>2</sub> treatment ( $\epsilon_{\parallel} \sim 0.1\%$ ) are significantly lower than the values observed before treatment. These two facts point to the successful intercalation of H<sub>2</sub> under the buffer layer. Appearance of a weak D-line in the QFSMG Raman spectra indicates that a small amount of intercalation-induced point-like defects was introduced. The estimated defect concentration range was within  $10^{10} \dots 10^{11} \text{ cm}^{-2}$ .

Kelvin-probe measurements confirmed the conclusion about the successful conversion of the buffer layer to graphene. KPFM maps demonstrate a transition from the potential contrast value of  $\Delta U_{1LG\text{-}buffer} \sim 1 \text{ V}$  to the value typical for single-double layer graphene pair  $\Delta U_{1LG\text{-}2LG} \sim 100 \text{ mV}$ . The fractions of monolayer and bilayer areas are in a good agreement with the initial fractions of buffer layer and monolayer graphene.

In conclusion, by using Raman spectroscopy and KPFM we have shown that the transformation of the buffer layer to high-quality QFSMG is possible by heating the buffer layer in the H<sub>2</sub> at 900 °C for 1 hour. We expect observation of higher values of electron mobility in these films.

I.A. Eliseyev and S.P. Lebedev acknowledge the support from RFBR (Project 18-02-00498).

### References

1. C. Riedl, C. Coletti, T. Iwasaki, A.A. Zakharov, U. Starke. Phys. Rev. Lett. (2009), **103**, 246804.

## **Influence of functional composition and intercalated water on dielectric properties of graphite oxide**

*Grebenkina M.A.*<sup>1,2</sup>, *Gusel'nikov A.V.*<sup>1</sup>, *Stolyarova S.G.*<sup>1</sup>, *Bulusheva L.G.*<sup>1,2</sup>, *Okotrub A.V.*<sup>1,2</sup>

*grmariya@mail.ru*

<sup>1</sup> Nikolaev Institute of Inorganic Chemistry SB RAS, Novosibirsk, Russia

<sup>2</sup> Novosibirsk State University, Novosibirsk, Russia

Graphite oxide (GO) is a layered structure which is formed by graphene layers modified with different oxygen functional groups and intercalated water molecules in the interlayer space [1]. The composition of GO is influenced by the method of synthesis and it determines the substance's properties [2, 3]. Particularly the degree of graphene layers' oxidation and the concentration of intercalated water molecules formed hydrogen bonds with the layers designate the dielectric properties of GO.

In this study we investigated the frequency and temperature dependence of dielectric constant at water's phase transition temperatures ( $T = 0^{\circ}\text{C}$  and  $T = 100^{\circ}\text{C}$ ). The dielectric properties of GO synthesized by the modified Hummers method and the Brodie method were compared. The method of impedance spectroscopy was applied to measure dielectric constant. The measurements were carried out within the frequency range from 1 Hz to 7 MHz and the temperature range from  $-10^{\circ}\text{C}$  to  $150^{\circ}\text{C}$ . Also the hodographs of GO with valuable humidity were analyzed using electric circuit simulation.

It was indicated that the increase of GO's humidity promotes the appearance of ionic diffusion conductivity for GO synthesized by the Hummers method and the extra mechanism of polarisation for GO synthesized by the Brodie method at low frequencies. The difference was explained by the data of IR spectroscopy which demonstrated the lack of epoxy groups in GO synthesized by the Brodie method. In addition, the origin of water agglomerates in GO synthesized by the Hummers method due to the increase of humidity was detected.

### **References**

1. R. Dreyer, S. Park, C. W. Bielawski, R. S. Ruoff, *Chem. Soc. Rev.* (2010) **39**, 228.
2. K. Chua, M. Pumera, *Chem. Soc. Rev.* (2014) **43**, 291.
3. Barroso-Bujans, S. Cerveny, A. Alegría, J. Colmenero, *Carbon* **48(11)**, 3277.

## Graphene oxide: synthesis, properties and applications

Kapitanova O.O.<sup>1</sup>, Xu X.<sup>1</sup>, Kataev E.Yu.<sup>2</sup>, Zakharchenko T.K.<sup>1</sup>, Belova A.I.<sup>1</sup>, Petukhov D.I.<sup>1</sup>, Eliseev A.A.<sup>1</sup>, Krivchenko V.A.<sup>1</sup>, Panin G.N.<sup>3</sup>, Itkis D.M.<sup>1</sup>, Yashina L.V.<sup>1</sup>, Goodilin E.A.<sup>1</sup>, Korobov M.V.<sup>1</sup>

olesya.kapitanova@gmail.com

<sup>1</sup> Lomonosov Moscow State University, Moscow, Russia

<sup>2</sup> Friedrich-Alexander University Erlangen-Nurnberg, Nurnberg, Germany

<sup>3</sup> Nano Information Technology Academy, Dongguk University, Seoul, Korea

Graphene oxide (GO) is considered as one of the promising derivatives of graphene, in which the ratio of the number of oxidized areas of graphene (sp<sup>3</sup>) and regions where carbon has sp<sup>2</sup>-hybridization can be controlled by varying the conditions of the material synthesis. The control of the degree of oxidation opens up the possibility of obtaining both highly conductive and dielectric materials based on graphene, meanwhile, they can be both hydrophilic and hydrophobic. Numerous studies were focused on the methods of graphene oxidation and types of oxygen groups as well as its stability during thermal treatment under inert atmosphere. At the same time, there are only few studies of redox processes in graphene based materials carried out with spatial resolution.

This talk aims to touch next aspects: 1) a number of synthetic approaches to the production of GO as methods of chemical and electrochemical exfoliation and oxidation of graphite, as well as CVD graphene oxidation by atomic oxygen [1] and photocatalytic oxidation [2], 2) analysis of the type of oxygen groups, along with the morphology of GO using a unique combination of methods of XPS mapping and Raman with spatial resolution [1] and 3) possible application of GO for ultra-high density of storage and computational elements production [2, 3], highly selective membranes for gas dehumidification [4], an effective conductive additive for positive electrodes of Li-V<sub>2</sub>O<sub>5</sub> and Li-S [5] batteries, as well as a model electrode for the study of processes on electrochemical interfaces in the operation of Li-O<sub>2</sub> cells [6].

### References

1. Kapitanova O.O., Kataev E.Yu., Usachov D., Sirotina A.P., Belova A.I., Sezen H., Amati M., Al-Hada M., Gregoratti L., Barinov A., Dong H., Cho H.D., Kang T. W., Panin G.N., Vyalikh D.V., Itkis D.M., Yashina L.V., *J. Phys. Chem. C* (2017) **121(50)**, 27915.
2. Kapitanova, O.O., Panin G.N., Cho H.D., Baranov A.N., Kang T.W. *Nanotechnology* (2017) **28(20)**, 204005.
3. Panin G.N. and Kapitanova O.O., Chapter 4 "Memristive Systems Based on Two-Dimensional Materials" of the Book "Advances in Memristor Neural Networks - Modeling and Applications" (IntechOpen, London, 2018), p. 67.
4. Petukhov D.I., Chernova E.A., Kapitanova O.O., Boytsova O.V., Valeev R.G., Chumakov A.P., Konovalov O.V., Eliseev A.A., *Journal of Membrane Science* (2019) **577**, 184.
5. Kapitanova O.O., Mironovich K.V., Melezhenko D.E., Rokosovina V.V., Ryzhenkova S.Y., Korneev S.V., Shatalova T.B., Xu X., Napol'skiy F.S., Itkis D.M., Krivchenko V.A., *Journal of Materials Research* (2019) **34(4)**, 634.
6. Zakharchenko T.K., Belova A.I., Frolov A.S., Kapitanova O.O., Velasco-Velez J-J., Knop-Gericke A., Vyalikh D.V., Itkis D.M., Yashina L.V., *Topics in Catalysis* (2018) **61(20)**, 2114.

This research was supported by the Russian Foundation of Basic Research (18-29-19120).

## Surface morphology control of the SiC (0001) substrate during the graphene growth by sublimation.

*Amel'chuk D.G.*<sup>1</sup>, *Lebedev S.P.*<sup>1</sup>, *Dementev P.A.*<sup>1</sup>, *Eliseyev I.A.*<sup>1</sup>, *Barash I.S.*<sup>2</sup>, *Lebedev A.A.*<sup>1</sup>

*amelchuk.dmitriy@mail.ioffe.ru*

<sup>1</sup> Ioffe Institute, St.Petersburg, Russia

<sup>2</sup> LLC Gallium-N, St.Petersburg, Russia

One of the most promising technologies of graphene synthesis, which provides the formation of high-quality material and can be integrated into commercial production technology, is the thermal decomposition of the surface of semi-insulating silicon carbide (SiC) substrates. One of the important issues of the technology of graphene growth on silicon carbide is the control of the substrate surface morphology. It is known that during the graphene growth on SiC substrate a stepped surface with atomically flat terraces between steps is formed (step bunching phenomena). In order to make graphene/SiC structure suitable for the creation of various devices, it is necessary to obtain samples with minimal surface roughness, because a decrease in surface roughness leads to a decrease in the anisotropy of the electrical properties. In this work we present studies of the influence of technological parameters of graphene growth on morphology of the substrate surface.

Graphene films were grown by thermal decomposition of the Si (0001) face of single crystalline semi-insulating 4H-SiC substrate in an argon (Ar) ambient. Graphene growth was carried out at a temperature of 1740-1750 °C during 5 min. The growth parameters used to control the morphology of the substrate surface were the heating sample heating rate and the gas pressure in the chamber. Heating rate varied from 100 °C/min to 315 °C/min, gas pressure varied from 700 Torr to 750 Torr. Surface morphology was controlled by atomic force microscopy (AFM). To estimate the surface roughness, we used the root-mean-square (RMS) parameter. The structural quality of graphene was controlled by using Raman spectroscopy and Kelvin-probe force microscopy (KPFM).

The investigations of graphene growth showed the dependence of the surface morphology on the heating rate of the sample. The difference in morphology lies in the different step height and width of the terraces. At low heating rates of the sample, a surface with high steps (>5 nm) and large terraces (2-3 μm) is formed, and the RMS exceeds 1.5 nm. Increasing the heating rate to 250 °C/min and higher leads to a decrease in the height of the step to 0.5-1 nm, the width of the terraces being equal to 100-300 nm, and the RMS value of 0.5-1 nm. In addition, high heating rates make it possible to obtain a more uniform single-layer graphene with a minimum number of bilayer inclusions. At low heating rates, it is much more difficult to achieve the coating of large terraces with monolayer graphene without the inclusions of a bilayer graphene.

Ar pressure in growth chamber also influences the surface roughness. It was found that combination of heating rate about 250 °C/min and the pressure value of 710-720 Torr allow one to get surface roughness with minimal RMS=0.5-0.7 nm. Increasing the pressure to the value of 740-750 Torr during growth leads to an increase of RMS to 0.7-1 nm.

In conclusion, we have shown the way of controlling the morphology of the SiC (0001) substrate surface during the growth of graphene using different combinations of technological parameters.

S.P. Lebedev and I.A. Eliseyev acknowledge the support from RFBR (Project 18-02-00498).



## Dirac cone manipulation by bismuth and oxygen intercalation underneath graphene on Re(0001)

*Gogina A. A.*<sup>1</sup>, *Klimovskikh I. I.*<sup>1</sup>, *Estyunin D. A.*<sup>1</sup>, *Shikin A. M.*<sup>1</sup>

*alevtina\_gogina@mail.ru*

<sup>1</sup> St. Petersburg University, St. Petersburg, Russia

Currently, graphene had been established as the one of the most interesting material for researchers, due to the linear dispersion of electronic states, the so-called Dirac cone. Owing to it is two-dimensional crystal structure, graphene properties strongly depend on the interaction with the various types of substrates. For example graphene on Ir(111) or Pt(111) is quasi-free-standing, while in the case of Re(0001) substrate graphene has a strong interaction with this surface. For such a system the Dirac cone collapses, and dispersion near the high-symmetric K-point is no longer linear, as in the quasi-free-standing graphene. Nevertheless, by intercalation of different atoms under graphene, such as Pb [1], Au, Al or Bi [2, 3] we can detach it from the substrate and reduce the interaction between graphene and the metal surface. The Dirac cone is expected to restore after the intercalation, but the charge transfer and local hybridization effects may still modify the ideal linear Dirac cone structure. Furthermore, the electronic structure of graphene can be changed by oxygen intercalation while exposing the sample in the air. By intercalation of oxygen atoms it is possible to restore linear  $\pi$  bands crossing the Fermi energy and hole doping [4].

This work is devoted to the experimental study of the electronic structure of graphene/Re(0001) after the bismuth and/or oxygen atoms intercalation. The data had been obtained by means of angle-resolved and core-level photoemission spectroscopy. The experiment had been performed at research resource center "Physical methods of surface investigations".

Our results demonstrate that the unique linear dispersion is indeed restored after Bi and O atoms intercalation. Moreover, the Dirac point position is found to be different depending on the intercalated atoms configuration. There are two Dirac cones in the ARPES image and for the first one the charge transfer from the Bi atoms leads to the Dirac point position below the Fermi level, i.e. to the n-doping of graphene. For the second one the Dirac point is located above the Fermi level resulting in p-doping, that is related to the charge transfer to oxygen atoms. Possible reasons of this behavior as well as the perspectives of such graphene p-n junction will be discussed.

### References

1. Estyunin, D. A.; Klimovskikh, I. I.; Voroshnin, V. Yu.; Sostina, D. M.; Petaccia, L. SSN 1063-7761, Journal of Experimental and Theoretical Physics, 2017, Vol. 125, No. 5, pp. 762-767. © Pleiades Publishing, Inc., 2017.
2. Tingwei Hu, Qinglong Fang, Xiaohe Zhang, Xiangtai Liu, Dayan Ma, Ran Wei, Kewei Xu, and Fei Ma. Applied Physics Letters, 113(1), 011602. doi:10.1063/1.5029541
3. Zhizhin, E.V., Varykhalov, A., Rybkin, A.G., Rybkina, A.A., Pudikov, D.A., Marchenko, D., Sánchez-Barriga, J., Klimovskikh, I.I., Vladimirov, G.G., Rader, O., Shikin, A.M. Carbon, 93, 984-996 (2015)
4. Zhang, H.; Fu, Q.; Cui, Y.; Tan, D.; Bao, X. J. Phys. Chem. C 2009, 113, 8296-8301.

## Uniform graphene oxide thin films deposition via spray-coating

*Struchkov N.S.*<sup>1</sup>, *Romashkin A.V.*<sup>1,2</sup>, *Levin D.D.*<sup>1,2</sup>, *Rabchinskii M.K.*<sup>3</sup>

*struchkov.nikolaj@gmail.com*

<sup>1</sup> National Research University of Electronic Technology, Moscow, Russia

<sup>2</sup> Bauman Moscow State Technical University, Moscow, Russia

<sup>3</sup> Ioffe Institute, St. Petersburg, Russia

To realize high potential of the novel 2D carbon material graphene oxide (GO) in the field of optoelectronics, gas- and biosensorics, etc., thin uniform films fabrication techniques are required. Standard methods including dip-coating, drop-casting, layer-by-layer assembly, spin-coating provides high uniformity of the films but have poor manufacturing scalability. Spray-coating is a promising method for GO thin films deposition with well-controllable thickness, compatible with roll-to-roll technology and applicable for a wide range of substrates. Common spraying methods, however, requires high-temperature heating of the substrate which must have high wettability with dispersion medium [1]. This limitation can be partially overcome by deposition of individual microdroplets, without agglomeration on the surface during the evaporation. Microdroplets mode requires optimization of a number of process parameters, determining the average size of the droplets reaching the substrate and the rate of their evaporation from the surface. Both of these factors depends on the vapor pressure of the solvent used and distance between nozzle and substrate. Excessive evaporation during droplets transfer to substrate leads to carrying away of a small droplets with airflow, as well as the GO irreversible crumpling [2]. Dispersion with high boiling point requires high-temperature heating for efficient evaporation during the deposition, as well as post annealing. Optimal composition of high- and low-volatile solvents results in more uniform film deposition due to better self-assembly on the surface [3]. GO with average lateral size  $\sim 20 \mu\text{m}$  dispersed in water and water-NMP mixture with concentration  $60 \mu\text{g/ml}$  was spray-coated at cover-slips heated up to  $80 \text{ }^\circ\text{C}$ , at a flow rate  $0.1 \text{ ml/min}$  and distances  $10$  and  $15 \text{ cm}$ . As a result uniform films were obtained, demonstrating thickness of  $\sim 5 \text{ nm}$  with roughness  $R_a \sim 3 \text{ nm}$  (fig.1). The wrinkles on the surface apparently determined by a large size of GO flakes comparable to the spray droplets.

The presented work was financially supported by the Russian Foundation for Basic Research (grant no. 18-29-19172).

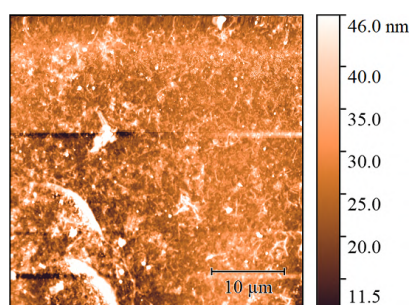


Fig.1. AFM image of thin GO film on glass substrate formed by spray deposition of water solution.

### References

- [1] Y.J. Jeon, J.M. Yun, D.Y. Kim, S.I. Na, and S.S. Kim *Applied Surface Science* (2014) **296**, 140.
- [2] D. Parviz, S.D. Metzler, S. Das, F. Irin, and M.J. Green *Small* (2015) **11**, 2661.
- [3] K.C. Guan, J. Shen, G.P. Liu, J. Zhao, H.L. Zhou, and W.Q. Jin, *Separation and Purification Technology* (2017) **174**, 126.

## Covalent functionalization of graphene by organic dyes via diazonium chemistry approach

*Potorochin D.V.*<sup>1,2,3</sup>, *Molodtsova O.V.*<sup>1,2</sup>, *Aristov V.Yu.*<sup>2,4</sup>, *Chaika A.N.*<sup>4,5</sup>, *Marchenko D.E.*<sup>6</sup>, *Ciobanu A.*<sup>2</sup>, *Walls B.*<sup>5</sup>, *Rabchinskii M.K.*<sup>7</sup>, *Ulin N.V.*<sup>7</sup>, *Baidakova M.V.*<sup>1,7</sup>, *Brunkov P.N.*<sup>1,7</sup>, *Molodtsov S.L.*<sup>1,3,8</sup>

*dm.potorochin@corp.ifmo.ru*

<sup>1</sup> ITMO University, Saint Petersburg, Russia

<sup>2</sup> DESY, Hamburg, Germany

<sup>3</sup> TU Bergakademie Freiberg, Freiberg, Germany

<sup>4</sup> Institute of Solid State Physics RAS, Chernogolovka, Russia

<sup>5</sup> CRANN, Trinity College Dublin, Dublin, Ireland

<sup>6</sup> Helmholtz-Zentrum Berlin, Berlin, Germany

<sup>7</sup> Ioffe Institute RAS, Saint Petersburg, Russia

<sup>8</sup> European XFEL, Schenefeld, Germany

In the current report, a plain method of graphene covalent functionalization by organic dyes, based on the chemistry of diazonium compounds, is presented. The advantages of diazonium chemistry approach are its simplicity, the high degree of functionalization, and the relatively short time that is necessary for the reaction to proceed. For the first time, this method was utilized for the attachment of an organic dye to graphene by Martin et al. [1]; the graphene in the form of nanoplatelets, dispersed in ethanol, was covalently modified by Neutral red dye. Later on, the same procedure was applied to graphene epitaxially grown on cubic-SiC(001) [2]. Such graphene intrinsically exhibits properties of quasi-free-standing graphene due to the mismatch of crystal lattices of cubic silicon carbide and hexagonal graphene and has a size comparable to the size of the initial substrate [3]. It was found by small area STM investigations that phenazine dye molecules are standing up on the graphene surface and exhibit a short-range order with a rectangular unit cell, while STS measurements proved the emergence of a bandgap [2]. Besides, we should emphasize that the grafting procedure of a new type of dye, phenothiazine one, has been conducted for the epitaxial graphene. To get deeper inside of interesting phenomena above we performed vast investigations of the functionalization like XPS, NEXAFS, and UV-PEEM using modern Mega Sciences (a number of European Synchrotron Radiation Facilities). The graphene/dye composites have shown high stability verified by XPS measurements after sonication of them and annealing in ultrahigh vacuum conditions. UV-PEEM imaging with work function contrast proves the homogeneity of the systems on a large scale. STS measurements and secondary electron cutoff confirmed a deep modification of the electronic structure as a result of the functionalization, a wide band gap opening and remarkable change of the work function.

This work was supported by RAS, RFBR (Grant Nos. 17-02-01139, 17-02-01291) and Minobrnauki of Russia (Project 3.3161.2017/4.6).

### References

1. P. Martin, A. Tariq, B.D.O. Richards, G. Jose, S.A. Krasnikov, A. Kulak, N.N. Sergeeva, *Chem. Commun.* (2017) **53**, 10715.
2. N. Sergeeva, A.N. Chaika, B. Walls, B.E. Murphy, K. Walshe, D.P. Martin, B.D.O. Richards, G. Jose, K. Fleischer, V.Yu. Aristov, O.V. Molodtsova, I.V. Shvets, S.A. Krasnikov, *Nanotechnology* (2018) **29**, 275705.
3. N. Chaika, O.V. Molodtsova, A.A. Zakharov, D. Marchenko, J. Sánchez-Barriga, A. Varykhalov, I.V. Shvets, V.Yu. Aristov, *Nano Research* (2013) **6**, 562.

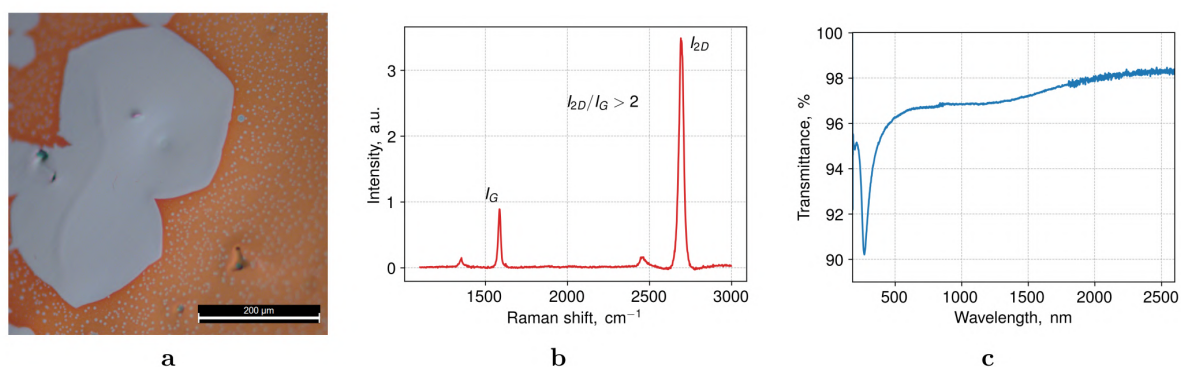
## Self-limiting ambient pressure hydrogen free synthesis of single crystal monolayer graphene.

*Grebenko A.K.<sup>1</sup>, Krasnikov D.V.<sup>1</sup>, Nasibulin A.G.<sup>1</sup>*

*artem.grebenko@skoltech.ru*

<sup>1</sup>Laboratory of Nanomaterials, Center for Photonics and Quantum Materials, Skolkovo Institute of Science and Technology, Moscow, Russia

We report the first self-limiting ambient pressure synthesis of single crystal graphene approach that does not contain hydrogen neither in molecular nor in atomic forms. Regular copper substrates were used both in liquid and solid states and detailed kinetics study were done in order to describe the method and find optimal regime. In comparison to earlier reported hydrocarbon based synthesis[1], the proposed technique demonstrates extremely low nucleation rate wherein the growth rate is rather high (tens of square microns per second). We also present novel dopant-free graphene transfer approach, that utilizes sublimating sacrificial layer. It turned out to be much more convenient and simple in comparison to PMMA or CAT transfer[2]. Finally we demonstrate the adoption of Atomic Force Microscopy capabilities of capturing samples mechanical properties[3] as a facile method for individual grain visualization both on the copper and transfer-target substrates. Such method provides high contrast imaging of the graphene and provide a room for the further improvement by acquiring more sophisticated data out of Force-Distance curves



a Photograph of monolayer graphene grains of sub-millimeter size on copper substrate; b Average Raman spectra of the demonstrated region; c UV-vis transmittance measurements of the large size sample.

### References

1. Cheun Lee, Wei-Wen Liu, Siang-Piao Chai, Abdul Rahman Mohamed, Chin Wei Lai, Cheng-Seong Khe, C.H. Voon, U. Hashim, N.M.S. Hidayah, *Procedia Chemistry*, **19**, 916-921,
2. Mingguang Chen, Robert C. Haddon, Ruoxue Yana and Elena Bekyarova, *Horiz.*, 2017,**4**, 1054-1063.
3. Maugis, *Contact, Adhesion and Rupture of Elastic Solids* (Springer-Verlag, Berlin, 2000).

## Carbon nanotubes as a promising material for nanopiezotronics

*Ilina M.V.<sup>1</sup>, Ilin O.I.<sup>1</sup>, Guryanov A.V.<sup>1</sup>, Ageev O.A.<sup>1</sup>*

*mailina@sfedu.ru*

<sup>1</sup> Southern Federal University, Institute of Nanotechnologies, Electronics and Electronic Equipment Engineering, Taganrog, Russia

The movement of electronics to the nanoscale led to the fact that the flexoelectric effect and the surface piezoelectric effect significantly influence on the electromechanical properties of materials [1]. Nanopiezotronics is studying these effects in nanostructures to develop new devices [2]. The basic element of nanopiezotronics is a two-electrode structure, in which the internal electric field occurring in a nanostructure under strain is used as a voltage controlling the charge carriers transport [2]. The search for such nanostructures continues to date. Our latest research in this area has shown that the strained aligned carbon nanotubes (CNTs) have an internal electric field due to their piezoelectric properties [3, 4]. It is shown that the strained CNTs can be used in the development of nonvolatile memory and nanogenerators [3-5]. The aim is to study the influence of a strain of carbon nanotubes on its electrical properties to develop new nanopiezotronics devices.

As the experimental samples we used vertically aligned CNTs arrays grown by plasma-enhanced chemical vapor deposition. Studies of the experimental samples were carried out by the atomic force microscopy (AFM) using previously developed techniques [3, 4]. The results of experimental studies of a CNT piezoelectric response showed that when the AFM probe is applied to the top of a nanotube the current increases linearly and then goes to saturation. This dependence may be explained by the fact that a CNT predominantly experiences compressive strain and only negative piezoelectric charge is formed at its top when a weak force (up to 200 nN) is applied. Increasing the force further (up to 800 nN), bending strain begins to predominate, which leads to the formation of simultaneously positive and negative charges on the CNT top. As a result, the total piezoelectric charge varies insignificantly and the current dependence saturates when the force is increased.

Studies of the surface potential of strained CNTs confirmed the dependence of the magnitude and sign of the surface potential at the CNT tops on the magnitude of their strain. It was shown that the tops of unstrained CNTs have zero potential. The potential is negative at a compressive strain of the CNTs and is positive at a bending strain of the CNTs. The obtained results can be used in the development of promising nanoelectronics devices based on aligned carbon nanotubes in particular memory elements and high-efficiency nanogenerators. The results were obtained using the equipment of the Research and Education Center and Center of Common Using "Nanotechnologies" of Southern Federal University.

The reported study was funded by RFBR according to the research projects No. 16-29-14023 ofi\_m and No.18-32-00652 mol\_a.

### References

1. J. Zhang, C. Wang, C. Bowen *Nanoscale* (2014) **6**, 13314.
2. Z.L. Wang *Adv. Mater.* (2007) **19**, 889.
3. M.V. Il'ina, O.I. Il'in, Yu.F. Blinov, V.A. Smirnov, A.S. Kolomiitsev, A.A. Fedotov, B.G. Konoplev, O.A. Ageev *Carbon* (2017) **123**, 514.
4. M.V. Il'ina, O.I. Il'in, Yu.F. Blinov, A.A. Konshin, B.G. Konoplev, O.A. Ageev *Materials* (2018) **11**, 638.
5. M.V. Il'ina, A.A. Konshin, E.G. Solomin *Journal of Physics: Conf. Series* (2018) **1124**, 071010.

## **Electrochemical performance of hybrid materials based on carbon nanotubes/porous carbon**

*Lobiak E.V.*<sup>1</sup>, *Kuznetsova V.R.*<sup>1,2</sup>, *Bulusheva L.G.*<sup>1,3</sup>, *Okotrub A.V.*<sup>1,3</sup>

*lobiakev@niic.sbras.ru*

<sup>1</sup> Nikolaev Institute of Inorganic Chemistry SB RAS, Novosibirsk, Russia

<sup>2</sup> Novosibirsk State Technical University, Novosibirsk, Russia

<sup>3</sup> Novosibirsk State University, Novosibirsk, Russia

Carbon nanotubes (CNTs) are one of the most popular material for energy storage devices such as supercapacitors, Li-ion batteries, fuel cells because of their unique physicochemical properties. Typically, due to electrical conductivity and textural properties CNTs are demanded for different electrochemical applications. Besides of CNTs, porous carbon is widely used as in electrochemistry devices because of their easy synthesis, low cost and highly specific surface area. Combination of CNTs and porous carbon in hybrid material allows improving electrochemical properties compared with each of individual component. In addition to this incorporation of nitrogen atoms in CNT structure provides the material wettability by electrolyte thus improving electrochemical properties of hybrid materials.

In the present work, hybrid materials based on CNTs and porous carbon were obtained with different methods. The first one is synthesis of a hybrid material during chemical vapor deposition (CCVD) method with dynamic temperature profile in  $\text{CH}_4/\text{H}_2/(\text{CH}_3\text{CN})$  purging. In this case, CNTs/porous carbon and nitrogen doped CNTs ( $\text{CN}_x$ )/porous carbon hybrids were synthesized. Another method is a mixing of CNTs ( $\text{CN}_x$ ) and porous carbon with a different ratio. Hybrid materials, CNTs and  $\text{CN}_x$  were synthesized using Co-Mo/MgO, Ni-Mo/MgO and Fe-Mo/MgO catalyst while porous carbon were templated by MgO.

Hybrid materials were tested as electrodes for energy storage devices such as supercapacitors, lithium- and sodium-ion batteries. It was determined that the influence of nature of catalyst on the carbon material structures and individual components in hybrid materials as well as the present of incorporated nitrogen on the electrochemical properties of electrodes for electrochemical applications.

The work was supported by the Russian Foundation for Basic Research (grant № 18-33-01053).

## Growth dynamics of inner tubes inside metallocene-filled single-walled carbon nanotubes

*Kharlamova M.V.*<sup>1</sup>, *Kramberger C.*<sup>2</sup>, *Saito T.*<sup>3</sup>, *Shiozawa H.*<sup>2</sup>, *Pichler T.*<sup>2</sup>

*mv.kharlamova@gmail.com*

<sup>1</sup> Institute of Materials Chemistry, Vienna University of Technology, Vienna, Austria

<sup>2</sup> Faculty of Physics, University of Vienna, Vienna, Austria

<sup>3</sup> Nanomaterials Research Institute, National Institute of Advanced Industrial Science and Technology, Tsukuba, Japan

Single-walled carbon nanotubes (SWCNTs) are a fascinating class of carbon nanomaterials possessing exceptional physical, chemical, mechanical and structural properties. The synthesis of SWCNTs with defined properties is required for both fundamental investigations and practical applications. Although the use of SWCNTs in the fields of nanoelectronics has been already realized, the full potential of SWCNTs is still not implemented in applications. This is caused by the fact that as-synthesized SWCNT samples have inhomogeneous properties, and the selective synthesis of SWCNTs with certain conductivity type and structure is elusive. The revealing and thorough understanding of the growth mechanism of SWCNTs is the key to the synthesis of nanotubes with required properties.

This work undertakes the systematic investigation of the influence of synthesis parameters on growth dynamics of nanotubes inside SWCNTs. The study aims at revealing the growth mechanism of inner tubes inside metallocene-filled SWCNTs. The SWCNTs filled with nickelocene (NiCp<sub>2</sub>), cobaltocene (CoCp<sub>2</sub>) and ferrocene (FeCp<sub>2</sub>) molecules serve as a catalyst source and carbon feedstock at the same time, and provide well-controlled conditions for the low-temperature high-yield synthesis of inner tubes.

The growth temperature decreases linearly with decreasing the inner tube diameter. The temperature difference between the largest ( $d_t \sim 1.3$  nm) and the smallest diameter ( $d_t \sim 0.7$  nm) tubes amounts to  $\sim 230^\circ\text{C}$  for the three precursors. The growth temperatures are offset by  $34^\circ\text{C}$  from Ni to Co and another  $28^\circ\text{C}$  from Co to Fe.

By combining in situ annealing and Raman spectroscopy measurements, the monitoring of growth dynamics of nine individual-chirality inner tubes (8,8), (12,3), (13,1), (9,6), (10,4), (11,2), (11,1), (9,3) and (9,2) with the diameters from  $\sim 0.8$  to 1.1 nm has been performed with a time resolution of several minutes [1,2].

The growth mechanism of inner tubes implies two successive stages of the growth on the carburized and purely metallic catalytic particles, respectively. The stages of the tube growth are characterized by the corresponding growth rates and activation energies. The growth rates at both stages are inversely proportional to the inner tube diameter and are also significantly higher for the Ni catalyst. The activation energies of the growth on the carburized Ni and Co catalytic particles decrease monotonically with decreasing the tube diameter, while they show the opposite trend for the purely metallic particles.

### References

1. M.V. Kharlamova, C. Kramberger, T. Saito, Y. Sato, K. Suenaga, T. Picher, H. Shiozawa, *Nanoscale* (2017) **9**, 7998.
2. M.V. Kharlamova, C. Kramberger, Y. Sato, T. Saito, K. Suenaga, T. Pichler, H. Shiozawa, *Carbon* (2018) **133**, 283.

## Carbon nanostructures for drug delivery systems

*Nazarova A.*<sup>1</sup>, *Chudoba D.M.*<sup>1,2,3</sup>, *Jazdzewska M.*<sup>2</sup>, *Woloszczuk S.*<sup>2</sup>

*anazarova@jinr.ru*

<sup>1</sup> Frank Laboratory of Neutron Physics, Joint Institute for Nuclear Research, Dubna, Russia

<sup>2</sup> Adam Mickiewicz University, Poznan, Poland

<sup>3</sup> Saint Petersburg State University, Saint Petersburg, Russia

In the last decade, the most popular type of nanomaterials is carbon nanotubes, which attract the attention of members of various scientific fields. The development of fundamental and applied concepts of carbon nanotubes in the coming years can lead to fundamental changes in materials science, electronics, biology, medicine and ecology.

Carbon nanotubes reveal new opportunities for biological and medical applications: visualization of molecular, cellular and tissue structures; creation of biosensors and electrodes based on them; targeted delivery of various substances; radiation and photothermal therapy. The most promising property of carbon nanotubes in the context of biomedical applications is their ability to penetrate into various tissues of the body and can serve as the basis for targeted drug delivery systems. They are able to transfer large doses of radionuclides and chemotherapeutic agents into tumor cells without destroying normal tissues, significantly reducing the side effects that usually accompany many modern treatments.

Tumor microenvironment is acidic and this property is one of the most important factors, which should be taking into account in drug release. Therefore, a drug delivery system that is responsive in the physiologically acidic pH range (4.5–6.9) is promising for the drug release inside tumor cells.

Here the anticancer drug, Doxorubicin (DOX) was selected, because it possess an amine group in the structure and the physicochemical properties of DOX are highly sensitive to changes in environmental pH. To reduce the undesired effects without reducing drug potency, DOX is usually encapsulated into drug delivery vehicles that have the ability to protect the molecule of interest and selectively target.

Despite the fact that some research works have been done on the effects of in vivo or in vitro antitumor activity but very little is known about the adsorption behavior of anticancer drug on CNTs. Development of the CNT-based drug delivery systems thorough studies of the adsorption and desorption of drugs on CNTs are crucially important. In this work, we prepared MWNTs-nitric acid and evaluated its ability for loading and release pH, loading concentration, time of adsorption and desorption of doxorubicin from CNTs.

### References

1. Riehemann, S. Schneider, T. Luger, Nanomedicine-challenge and perspectives, *Angew. Chem.* 48 (2009) 872–897.
2. S. Cho, Z. Dong, G.M. Pauletti, Fluorescent superparamagnetic nanospheres for drug storage, targeting, and imaging: a multifunctional nanocarriersystem for cancer diagnosis and treatment, *ACS Nano* 4 (2010) 5398–5404.
3. Kruse, S. Rottey, O.D. Backer, Future cancer therapy with molecularlytargeted therapeutics: challenges and strategies, *Biomol. Ther.* 19 (2011)371–389.
4. Mewada, S. Pandey, M. Thakur, Swarming carbon dots for folic acidmediated delivery of doxorubicin and biological imaging, *J. Mater. Chem. B* 2(2013) 698–705.



## Development a complex model of the catalytic centers formation for carbon nanotubes growth

*Ilin O.I.*<sup>1</sup>, *Rudyk N.N.*<sup>2</sup>, *Osotova O.I.*<sup>1</sup>, *Fedotov A.A.*<sup>1,2</sup>

*oiilin@sfedu.ru*

<sup>1</sup> Southern Federal University, Institute of Nanotechnologies, Electronics, and Electronic Equipment Engineering, Taganrog, Russia

<sup>2</sup> Southern Federal University, Laboratory of nanobiotechnologies and new materials, Taganrog, Russia

The practical use of the unique properties of carbon nanotubes (CNT) leads to the need to obtain aligned CNTs located at a given place of the substrate [1]. One of the most promising methods for the synthesis aligned CNTs is plasma enhanced chemical vapor deposition (PECVD). The initial stage of the CNTs synthesis by PECVD is the formation of a continuous catalytic film on the substrate, from which, as a result of annealing, catalytic centers (CC) are formed. Due to the fact that the geometric dimensions, density and composition of CC determine the future properties of CNTs, the actual task is to predict and create arrays of CCs with controlled geometric parameters. To exclude chemical interaction during annealing between the catalytic material layer (Ni, Fe, Co, etc.) and the silicon substrate, is formed barrier layer based on metal films (Cr, V, Ti, etc.).

It was shown that a multilayer structure consisting of two or several contacting materials is initially thermodynamically unstable. Through the contact plane between the layers there will be a continuous process of mutual diffusion accompanied by a decrease in the free energy of the system. It is shown that for a nanoscale thickness of a metal layer, which is much smaller than the diffusion length, the multilayer structure is asymmetric. The most of silicon atoms, passing through diffusion through thin layers of metals, will come out onto the outer surface of the structure and desorb into the vacuum, while chromium atoms saturating the contact area of the substrate will form chromium silicide layer. The intermediate layer of chromium silicide, forms a strong chemical bond and fixes a metal film on a silicon substrate, which will affect on the thermal stress field nature with increasing temperature. The free surface of the film will corrugate. In this case, the steady-state profile will be determined by the equilibrium of the thermal expansion forces and the capillary pressure at each point of the deformed film surface [2]. The resulting drop in the chemical potential ( $\Delta\mu$ ) will initiate of the material diffusion transfer from the inner contact plane to the outer surface of the film:

$$\Delta\mu = ((\alpha_{Si} - \alpha_{Cr}) \cdot E_{Cr} \cdot T - 2 \cdot \gamma \cdot K - n \cdot k \cdot T) \cdot \Omega \quad (1)$$

where  $\alpha_{Si,Cr}$  - coefficient of thermal expansion,  $E_{Cr}$  - Young's modulus,  $T$  - annealing temperature,  $K$  - local curvature of the surface;  $\gamma$  - specific surface energy of chromium;  $n$  - number of atoms per unit volume of the chromium lattice;  $\Omega$  - volume of chromium atom.

It is shown that, after film breaking, surface processes and specific surface energy are the dominant factor controlling the formation of the CC profile. Only after breaking the film into separate fragments can we assume that the process of formation of the CC starts, at the same time, the limiting size factor of the steady segment will be equal to the curvature of the CC surface. At a value of the contact angle  $\varphi=\pi/2$  the steady-state CC is a hemisphere with radius:

$$R = 2 \cdot \gamma / \delta_0 \quad (2)$$

where  $\sigma$  - thermal stress at the metal/substrate interface.

As a result, developed a complex model for the formation of catalytic centers for carbon nanotubes growth from a continuous nanosized catalyst film that allows predicting the dimensions of the CC formation on a silicon substrate. This work is supported by the Russian Science Foundation under grant № 18-79-00176.

### References

1. Il'ina, O. Il'in, Y. Blinov, A. Konshin, B. Konoplev, A. Ageev, *Materials* (2018) **11**, 638.
2. V. Jourdain, C. Bichara, *Carbon* (2013), **58**, 2.

## **Synthesis of new hybrid materials based on multi-walled carbon nanotubes and nanoscale coatings of copper oxide and tungsten oxide**

*Kremlev K.V.*<sup>1</sup>, *Zabrodina G.S.*<sup>1</sup>, *Andreev P.V.*<sup>2</sup>, *Vilkov I.V.*<sup>2</sup>, *Obiedkov A.M.*<sup>1</sup>, *Kaverin B.S.*<sup>1</sup>, *Semenov N.M.*<sup>1</sup>, *Gusev S.A.*<sup>3</sup>, *Tatarsky D.A.*<sup>3</sup>

*kkremlev@mail.ru*

<sup>1</sup> G.A. Razuvaev Institute of Organometallic Chemistry of RAS, Nizhny Novgorod, Russia

<sup>2</sup> Lobachevsky State University, Nizhny Novgorod, Russia

<sup>3</sup> Institute for Physics of Microstructures of RAS, Nizhny Novgorod, Russia

The progress in advanced technologies in various fields of science and industry places high demands on new materials necessary for the implementation of the most modern developments. One of these requirements in the producing new structural materials and catalytic systems is the creation of reinforcing fibers or catalyst carriers with a large specific surface area and mechanical strength. The most effective objects combining these properties are multi-walled carbon nanotubes (MWCNTs). However, for the application of such objects as fillers in any structural material or as a catalyst, it is necessary to modify the surface of the MWCNTs so that they could be effectively used in these areas. Modifying the MWCNTs surface will increase their affinity for the matrix material of the composite when MWCNTs are used as reinforcing fillers in composites or will allow creating a large number of active catalytic centers on the MWCNTs surface when using them as catalyst carriers.

This work proposes a method for the synthesis of new hybrid materials based on MWCNTs and copper oxides or tungsten oxide. Such objects can be used in the catalysis of hydrocarbon pyrolysis, in strong composites or alloys.

The MWCNTs synthesized by the MOCVD method during the pyrolysis of a mixture of toluene and ferrocene were used as the basis for such materials. Next, copper-containing or tungsten-containing coatings were deposited on the surface of the obtained MWCNTs. Hybrid materials based on MWCNTs and nano-sized copper nanoparticles were synthesized according to the developed method using MWCNTs in the form of powder and copper formate as a precursor. In this case, first the precursor itself was deposited on the surface of the MWCNTs, and only after that it decomposed to form copper nanoparticles. The deposition of tungsten-containing particles occurred during the pyrolysis of tungsten carbonyl. Thus, the hybrid materials synthesized were further subjected to oxidation under atmospheric air to obtain copper oxide or tungsten oxide particles on the MWCNTs surface. All synthesized hybrid materials were examined by various physico-chemical methods of analysis to establish their characteristics. The regularities of the formation of these hybrid materials under different initial conditions of synthesis are established, which allows to obtain objects with specified properties.

This work was supported by RFBR (Project 18-33-00776).

## Polymer composites based on epoxy resin with added carbon nanotubes

*Blokhin A.N.*<sup>1</sup>, *Dyachkova T.P.*<sup>1</sup>, *Maksimkin A.A.*<sup>2</sup>, *Stolyarov R.A.*<sup>1</sup>, *Suhorukov A.K.*<sup>1</sup>, *Kharitonov A.P.*<sup>3</sup>

*cha-cha@rambler.ru*

<sup>1</sup> Tambov State Technical University, Tambov, Russia

<sup>2</sup> National University of Science and Technology "MISIS", Moscow, Russia

<sup>3</sup> 1Branch of the Talrose Institute for Energy Problems of Chemical Physics of the Russian Academy of Sciences, Chernogolovka, Russia

Epoxy resin (diglycidyl ether bisphenol-A type) polymer composites with added unmodified and fluorinated carbon nanotubes (CNTs) were studied by FTIR, TGA, DSC and electron microscopy. Composites tensile and flexural strength were measured. CNTs fluorination markedly (by a factor of 2.26) increased its specific surface. Fluorination did not influence CNTs thermal stability below 260°C and did not worsen thermal stability of filled composites. Insertion of 0.1 weight % of CNTs fluorinated at 150°C into polymer matrix resulted in the composite tensile strength increase to 89.6±4.1 MPa (35% increase as compared with unfilled composites). Flexural strength of composite filled with 0.2 weight % fluorinated at 150°C CNTs was increased to 199.7±4.8 MPa (+58% as compared with unfilled composite). Obtained reinforcement values exceeded all the available literature reinforcement data reported for epoxy composites based on epoxy resins similar to used in the current project. Unmodified CNTs were less effective in composite tensile and flexural strength improvement as compared with fluorinated CNTs. Insertion of fluorinated CNTs into a polymer matrix increased glassy temperature and did not influence the composites thermal stability. Surface of composites cuts was studied by electron microscopy technique (fig.1). The reinforced composites can be applied in several industries: aviation, automotive, wind turbine propeller blades, for producing yachts and boats etc.

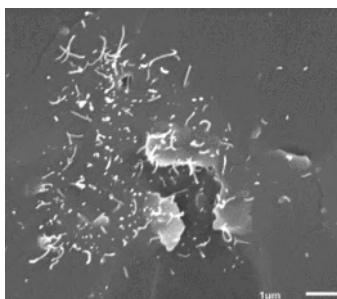


Fig.1. Cut of the polymer composite containing 0.5 weight % of virgin CNTs. Scale 1 μm.

## Carbon vs silicon polyprismanes: A density functional theory study

Maslov M.M.<sup>1,2</sup>, Gimaldinova M.A.<sup>1</sup>, Grishakov K.S.<sup>1</sup>, Katin K.P.<sup>1,2</sup>

Mike.Maslov@gmail.com

<sup>1</sup> Department of Condensed Matter Physics, National Research Nuclear University MEPhI, Moscow, Russia

<sup>2</sup> Laboratory of Computational Design of Nanostructures, Nanodevices and Nanotechnologies, Research Institute for the Development of Scientific and Educational Potential of Youth, Moscow, Russia

We report geometry, energy, and electronic properties of  $[n,5]$ -,  $[n,6]$ -,  $[n,7]$ -, and  $[n,8]$ - carbon and silicon polyprismanes. Polyprismanes or  $[n,m]$ prismanes are the nanotubes of a special type constructed from the dehydrogenated molecules of cycloalkane (carbon rings) or cyclosilanes (silicon rings), where  $m$  is the number of vertices of the closed atomic ring and  $n$  is the number of layers [1]. In this study using density functional theory we have calculated thermodynamic stability, electronic properties, and chemical reactivity of carbon and silicon  $[n,m]$ prismanes with  $m = 5, 6, 7,$  and  $8$  containing from two to ten layers (see Fig.1) by means of calculating frontier molecular orbitals, and some reactivity descriptors. Furthermore, we have performed structural optimization of rather long (“infinite”) polyprismanes taking into account periodic boundary conditions and obtained their band structure, density of electronic states, electronic transmission coefficients, and some mechanical properties to predict their behavior as the part of perspective nanotechnology devices and to illustrate the potential of these systems for the future development of next-gen nanotechnologies. All DFT calculations for the finite  $[n,m]$ prismanes were performed using the TeraChem software, and the calculations under periodic boundary conditions were carried out using the Quantum Espresso package. It is found that the considered polyprismanes become more thermodynamically stable as their effective length increases. However, the character of the energy spectrum and the behavior of transmission function near the Fermi level, illustrate that the silicon polyprismanes exhibit non-typical for the  $sp^3$ -hybridized silicon systems metallic nature, whereas the carbon polyprismanes possess the semiconducting properties in the bulk limit.

The presented study was performed with the financial support of the Russian Science Foundation (Grant No. 18-72-00183).

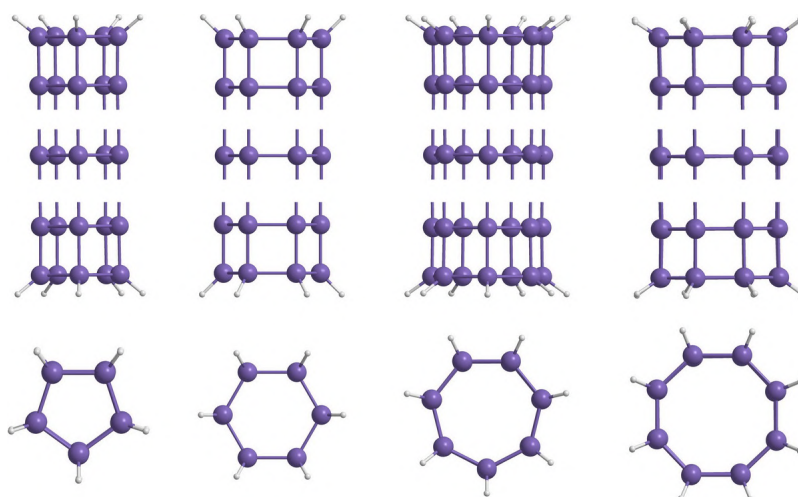


Fig.1. Left to right: Molecular structures of  $[n,5]$ -,  $[n,6]$ -,  $[n,7]$ -, and  $[n,8]$ - carbon and silicon polyprismanes

### References

1. K.P. Katin, S.A. Shostachenko, A.I. Avkhadieva, and M.M. Maslov, Adv. Phys. Chem. (2015) **2015**, 506894.

## Synthesis of pyrocatalysts on the basis of different carbon carriers and their application in the alyumovozdushnykh of EHG

*Revenko V.*<sup>1</sup>

*viktoriaevenko99@mail.ru*

<sup>1</sup> Institute of Fine Chemical Technologies named after M.V.Lomonosov Moscow, Russia

*Revenko V.K, Kiseleva E.A*

*viktoriaevenko99@mail.ru*

*Institute of Fine Chemical Technologies named after M.V.Lomonosov, Moscow, Russia*

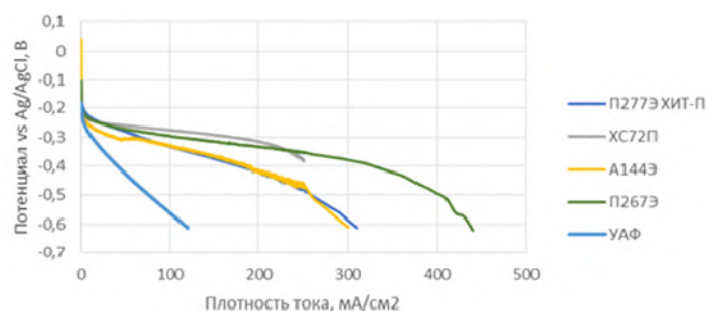
*Joint Institute for High Temperatures of the Russian Academy of Sciences, Moscow, Russia*

An alternative to lithium-ion batteries, widely used as a power source for robotic systems (RTC), can be air-aluminum batteries (PSA), differing by 5-10 times lower cost and 1.5-2 times higher energy intensity. However, they have a low specific power which can be increased due to increase in activity of electrodes and decrease in mass of an element.

Soot is one of the most common carbon carriers of metal catalysts in various applications. Soot doping by heteroatoms, in particular N, allows to increase considerably the polarizing capacity and also activity and selectivity of the considered reaction. For clarification of influence of doping of various types soot, the catalysts used as carriers on the basis of a tetrametoksifenilporfirin of a cobalt (TMFPSO) on electrochemical characteristics (polarizing capacity, activity and selectivity in reaction of restitution of oxygen to water) investigated exemplars: 277HIT;P276E; P277 E-HIT P; HS72P; A114P; P267E; UAF. As an example comparisons used the catalyst synthesized on commercial Vulcan XC72 soot.

The activity of cathodes was significantly increased when replacing the catalyst (UAF absorbite) by the developed pyrocatalyst on the basis of Fe - Co - N - the containing connection (Fig. 1). It is investigated influences of carriers Fe - Co - N - the containing connection on polarizing characteristics of air cathodes. It is shown that on air electrodes with the pyrocatalyst on the basis of P267E diffusion limits start at current density above 350 mA/cm<sup>2</sup>, while on the basis of Vulcan XC72 is more narrow at 200 mA/cm<sup>2</sup>, that is a consequence of influence of a cellular structure, its hydrophylic and hydrophobic properties. (Fig. 1).

Fig.1. Polarizing curves of air cathodes with the UAF catalyst and with the pyrocatalyst on the basis of various technical carbon carriers.



## Effect of heat treatment on the characteristics of the catalyst for the synthesis of carbon nanostructured materials

*Burakova E.A.*<sup>1</sup>, *Dyachkova T.P.*<sup>1</sup>, *Tkachev A.G.*<sup>1</sup>, *Gutnik I.V.*<sup>1</sup>, *Tugolukov E.N.*<sup>1</sup>, *Galunin E.V.*<sup>1</sup>

*elenburakova@yandex.ru*

<sup>1</sup>Tambov State Technical University, Tambov, Russia

Carbon nanotubes (CNTs) are often used as modifiers of various composite materials. Their introduction into the matrix can significantly improve the performance of the composites created. However, nanomaterials with a certain structure and morphology are used as a modifier for each application. It is known that the correctly selected composition of the catalyst and the conditions for the synthesis of nanomaterials make it possible to obtain CNTs with given characteristics. Thus, it is possible to provide a directed synthesis of nanostructures by CVD through metal oxide catalytic systems, on the active centers of which the formation and growth of CNTs take place, so it is important to know the features of obtaining catalysts. The easiest way to obtain a metal oxide catalyst for CNTs synthesis is the wet burning method, in the implementation of which the main stages are the preparation of the pre-catalyst and its heat treatment. Heat treatment is usually carried out in two stages: thermal decomposition of the pre-catalyst and calcination of the resulting metal oxide catalytic system. Since the formation and transformation of the active centers of the catalyst occur at the heat treatment stage, it is important to know how the heat treatment conditions of the pre-catalyst affect the characteristics of the formed system and CNTs synthesized on the obtained catalyst samples. The Co-Mo/Al<sub>2</sub>O<sub>3</sub> catalytic system obtained by wet combustion was chosen as the object of study. In the process of obtaining the catalyst, heat treatment was carried out not in two, but in one stage (there was no calcination stage), while the temperature and duration of the thermal decomposition stage of the pre-catalyst varied. It is revealed that as a result of thermal decomposition of the precursor at 350 °C, catalytic systems with a small specific surface area (~2.0...26.0 m<sup>2</sup>/g), allowing the process gas-phase chemical vapor deposition to synthesize CNTs with a diameter of 5÷30 nm with the degree of deficiency 0,784 (specific output ~0,5..9.4 g<sub>CNT</sub>/g<sub>cat</sub>). Samples of Co-Mo/Al<sub>2</sub>O<sub>3</sub> catalytic system obtained by thermal decomposition at 500 °C and 700 °C have a large specific surface area and are more effective in the synthesis process. The results obtained during the experiment showed that by adjusting the operating parameters of the pre-catalyst heat treatment process, it is possible to control not only the characteristics of the formed catalyst (specific surface area, efficiency), but also CNTs (diameter, degree of defect). The use of Co-Mo/Al<sub>2</sub>O<sub>3</sub> catalytic system obtained without calcination stage in the process of synthesis of carbon nanostructured materials helps to reduce the cost of synthesized nanotubes.

The work was funded by the Ministry of Science and Higher Education of the Russian Federation in the framework of the Federal Target Program "Research and Development in Priority Areas of Advancement of the Russian Scientific and Technological Complex for 2014-2020" (Agreement No. 14.577.21.0253, Unique Identification Number: RFMEFI 57717X0253).

## Investigation of the effect of carbon nanotube surface modification with various functional groups and their use in catalysts for the O<sub>2</sub> electroreduction reaction.

*Kunakovskaya K.D.*<sup>1</sup>, *Kiseleva E.A.*<sup>2</sup>

*kunakovskaja@yandex.ru*

<sup>1</sup> RTU MIREA (MITHT- Institute of Fine Chemical Technologies named after M.V. Lomonosov), Moscow, Russia

<sup>2</sup> JIHT (Joint Institute for High Temperatures of the Russian Academy of Sciences), Moscow, Russia

In fuel cells with proton-conducting (solid) electrolyte and metal-air batteries, the oxygen reduction reaction (MER) is the most difficult because of its low flow rate in comparison with the reactions occurring at the anode or during electro-oxidation of the nanoparticles of the metal phase [1]. Therefore, the development of active and stable electrocatalysts RVC with a lower cost is crucial for the commercial application of TE and metal-air batteries. With the current state of technology, the most practical RVC catalysts are platinum-based materials supported on a carbon carrier (CN) [2]. Platinum (Pt) and alloys based on it are the most common selective in relation to the reduction of oxygen to water, a corrosion-resistant and active catalyst in RVC and used in commercial fuel cells (FC). At the moment, the main strategies that allow to increase the activity and stability of the catalyst based on Pt, aimed at optimizing its composition and structure, for example, alloying with transition metals (Co, Ni, Fe, etc.) [3], as well as the use of new types that are more resistant to the working conditions of fuel cells, carbon materials (PA), with a unique surface morphology (nanotubes, mesoporous carbon, etc.) as catalyst carriers [4]. Studies concerning the optimization of the composition and structure of catalysts have reached a certain level, while the EC characteristics of such systems remain rather low, and the systems themselves are noncommercializable.

Carbon nanotubes have an optimal matrix of physicochemical properties and are promising CNs for RVC catalysts. A distinctive feature of CNTs is their high corrosion resistance, compared with other CMs [5]. The use of CNTs in combination with other strategies (for example, alloying) will significantly increase the commercialization of cathode electrocatalysts [6]. However, due to certain disadvantages of CNTs related to their hydrophobicity and a small number of active centers on the surface, a number of studies are needed regarding the modification of their surface by various functional groups, which, in turn, will create conditions for the uniform distribution of metal nanoparticles over the entire surface. Also, the use of modified CNTs as catalysts carriers will increase the electrochemically active surface area (EAP), the activity in the oxygen reduction reaction (RVC) and the corrosion resistance of the catalysts synthesized on this carrier due to the formation of certain types of bonds between metal nanoparticles and functional groups.

### References

1. Feng L., Suna X., Yao S., Liu C., Xing W., Zhang J. Rotating Electrode Methods and Oxygen Reduction Electrocatalysts, 2014, P. 67
2. Kong J., Cheng W. Chinese Journal of Catalysis. 2017. V. 38. P. 951
3. Martínez-Huerta M.V., Lázaro M.J. Catalysis Today. 2017
4. Bharti A., Cheruvally G. Journal of Power Sources. 2017. V. 360. P. 196
5. Stamatina S. N, Borghei M., Dhiman R., Andersena S. M., Ruiz V., Kauppinen E., Skou E. M. Applied Catalysis B: Environmental. 2015. V. 162. P. 289
6. Vinayan B.P., Jafri R. I. Nagar R., Rajalakshmi N. Sethupathi K., Ramaprabhu S. Int. J. Hydrog. Energy. 2012. V. 37. P. 412

## **Electromagnetic interference shielding of carbon nanotube-fluoropolymer elastomer composites with layered structure**

*Yablokov M.Yu.<sup>1</sup>, Shevchenko V.G.<sup>1</sup>, Mukhortov L.A.<sup>2</sup>, Ozerin A.N.<sup>1</sup>*

*yabl1@yandex.ru*

<sup>1</sup> Enikolopov Institute of Synthetic Polymer Materials, Russian Academy of Sciences, Moscow, Russia

<sup>2</sup> Moscow Institute of Physics and Technology (State University), Moscow Region, Russia

Polymer nanocomposites based on high aspect ratio conductive nanofillers, such as carbon nanotubes, are promising advanced materials for protection from electromagnetic interference (EMI). Due to their low density, design flexibility, ease of processing and high conductivity at low filler loading, polymer composites are attractive materials for use in enclosures for electronic and electrical devices [1-4].

This work is devoted to the development of aerosol method for the deposition of layered carbon nanotubes-containing polymer composite and investigation of its EMI shielding efficiency. Polymer composite films were obtained on metal surface by aerosol spraying of a dispersion of carbon nanotubes in the solution of a copolymer of vinylidene fluoride with hexafluoropropylene SCF 26 (Russia) in acetone. Single-wall TUBALL carbon nanotubes (OksiAl, Russia) were used. Thickness of the coatings was 250-300 mcm. Reflection coefficients of electromagnetic radiation were measured in the range of 20-35 GHz. Three-layer coatings were formed with a concentration of nanotubes decreasing in each subsequent deposited layer. The concentration of nanotubes in the first layer (applied to the metal sample) corresponded to the coating with concentration of nanotubes (0.5% wt.), which had the maximum absorption coefficient. The concentration of nanotubes in the second and third layers was 0.3 and 0.1%, respectively. For effective shielding of electromagnetic radiation, large concentrations of nanotubes are necessary, while maximum of absorption requires concentrations close to the percolation threshold. Gradient samples had significantly better characteristics, (reflection coefficient reached -6dB at 35 GHz) since the outer layer provides a better matching of the wave resistance with free space and a smooth entrance of an electromagnetic wave, and the subsequent layers with an increasing concentration of single-walled carbon nanotubes absorb electromagnetic radiation.

Thus, polymer composite coatings with layered structure and with concentration gradient were obtained. They had shown low reflection coefficient of electromagnetic radiation. The advantage of the proposed aerosol method of applying EMI shielding coatings is in its versatility. Coatings can be applied to the surfaces of any composition and shape.

This work was supported by RFBR grant № 18-29-19112

### **References**

1. Thomassin, C. Jerome, T. Pardoën, C. Bailly, I. Huynen, C. Detrembleur, *Mater. Sci. Eng. R Rep.* (2013) **74**, 211.
2. Al-Saleh, W. Saadeh, U. Sundararaj, *Carbon* (2013) **60**, 146.
3. Kumar, T. Patro, *Mater. Res. Express* (2018) **5**, 115304.
4. Feng, X. Qin, D. Liu, Z. Huang, Y. Zhou, W. Lan, F. Lu, H. Qi, *Macromol. Mater. Eng.* (2018) **303**, 1800377.



## Effect of carbon nanotubes on structure and properties of the antifriction coatings

Kobernik N.V.<sup>1</sup>, Mikheev R.S.<sup>1</sup>, Brzhezinskaya M.<sup>2</sup>

maria.brzhezinskaya@helmholtz-berlin.de

<sup>1</sup> Bauman Moscow State Technical University, Moscow, Russia

<sup>2</sup> Helmholtz-Zentrum Berlin fuer Materialien und Energie, Berlin, Germany

The Sn-Sb-Cu antifriction babbit alloys are widely used in sliding bearings employed in friction units of machines and mechanisms. Babbitts' antifriction characteristics are the highest among those of alloys of this class; however, their fatigue strength is low, which limits the thickness range of babbit-based antifriction coatings and also reduces their wear resistance. Currently more and more attention is paid to using ultradispersed particles, especially nanoparticles, in order to improve characteristics of antifriction materials and coatings based on them. For this purpose, refractory particles (e.g. diamond nanoparticles, WC, SiC) and carbon nanotubes (CNTs) have been already tested. Introduction of nanoparticles results not only in changes in structural-phase components but also in improvement of the antifriction material performance characteristics. Thus, modification of antifriction materials and coatings based on them with nanoparticles may be regarded as a quite topical research direction.

This work is devoted to studying the CNT influence on the tribotechnical characteristics of babbit-based coatings fabricated by cladding. However, it seems impossible to reveal the mechanism of the CNT effect on the babbit alloy performances without detecting them in the antifriction coating structure. Therefore, especial attention was given to searching for and testing of techniques novel for this application. In the framework of this study, the soft x-ray absorption spectroscopy was used to detect CNT within the antifriction coating structure for the first time. Studies of the coatings metal structure by soft x-ray absorption spectroscopy, as well as by the metallographic and fractographic techniques involving electron-microscopy, showed that CNTs remain stable during plasma cladding process and merge into the coating.

In this study, the friction test performed according to the "pin-on-disk" procedure under the dry sliding friction conditions showed that adding to the coating 0.25 %wt of CNTs significantly improves the friction stability (the friction factor scatter coefficient decreases twice with reducing the friction factor and wear resistance by 5% on the average).

## Doping of carbon nanotubes with functional groups

Kapustin S.N<sup>1</sup>, Tsykareva Yu.V<sup>1</sup>

hare22@yandex.ru

<sup>1</sup>Laboratory of Nanotechnology, Northern Arctic Federal University, Arkhangelsk, Russian Federation

Electrophysical properties of CNTs are determined by their chirality, and those of graphene nanotapes - by their size. Industrial production of nanotubes with a preset chirality is not mastered yet, which is why the doping procedure can be used to correct their properties. Doping with functional groups allows to solve several other problems, for example, reduce the tendency towards agglomeration, increase the adhesion to the surrounding substance, add the properties of a chemical sensor. Therefore, the possibility of chemical modification of electrophysical properties of nanoobjects is a subject of interest. Similar methods of doping were considered for some other compounds such as cubane-based chain, graphene, carbon nanotubes [1-3] etc. Understanding the mechanisms of influence of functional groups on the band structure of large molecularly similar formations is also quite important for obtaining conducting polymers.

Information on the influence of purification of CNTs from amorphous carbon, catalyst particles and structure defects on the conductivity as well as temperature and frequency dependences of the conductivity of CNTs for various types and degrees of functionalization will be presented during the speech. A comparative analysis of the influence of the morphology of "matrioshka" and "fish cartilage" CNTs on their properties has been conducted. The non-linear dependence of the degree of functionalization of CNTs on the conductivity presented in Figure 1a is explained.

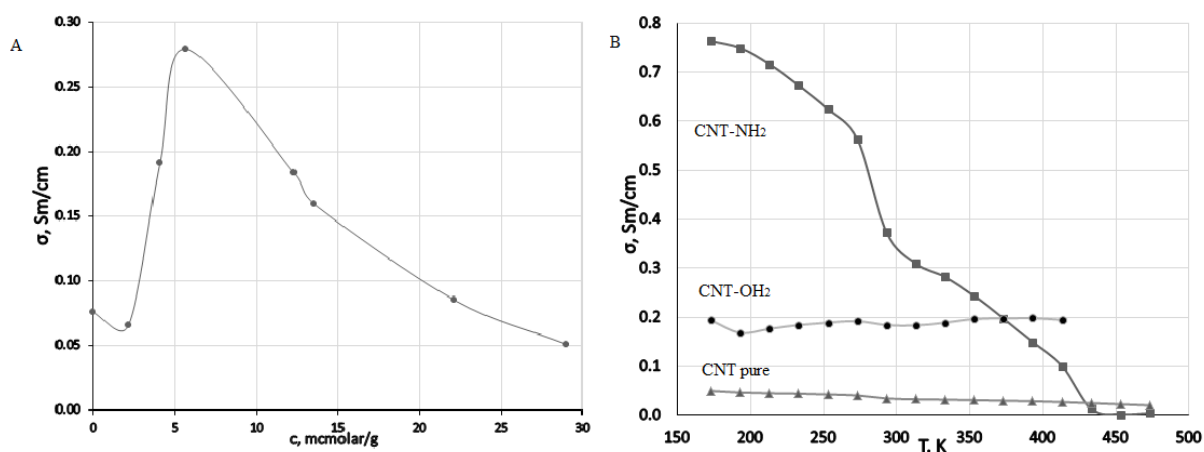


Fig.1. Dependence of the conductivity of "Taunit" f-CNTs on the concentration of carboxile groups (a) and on the temperature for "Taunit-M" f-CNTs with various types of functional groups (b)

### References

1. K.P. Katin and M.M. Maslov, Adv. Condens. Matter Phys. (2015) 2015, 754873.
2. J. Wu, L. Xie, Y. Li, H. Wang, Y. Ouyang, J. Guo, and H. Dai, J. Am. Chem. Soc. (2011) 133 (49), 19668.
3. S.D. Shandakov, A.I. Vershinina, M.V. Lomakin, A.V. Kosobutsky and A.G. Nasibulin, Bulletin of Kemerovo State University, (2015) 5(2), 127.

## On chip carbon nanotube tunnelling spectroscopy

*Matyushkin Y.E.*<sup>1,2,3</sup>, *Kaurova N.S.*<sup>2</sup>, *Voronov B.M.*<sup>2</sup>, *Goltsman G.N.*<sup>1,2</sup>, *Fedorov G.E.*<sup>2,3</sup>

*ya.matyushkin@gmail.com*

<sup>1</sup> National Research University Higher School of Economics, Moscow, Russia

<sup>2</sup> Moscow State University of Education (MSPU), Moscow, Russia

<sup>3</sup> Moscow Institute of Physics and Tehcnology (State University), Dolgoprudniy, Russia

Despite the simplicity of the CNTs band structure within a tight binding approximation, several effects may result in significant modification of electron spectrum in these 1D crystals. Among those are the proximity effect, electron-electron interaction and presence of defects [1-3]. Therefore, it is important to be able to investigate the bandstructure of individual CNTs under different conditions. This work describes an approach allowing for such studies via measurements of the density of states of individual single-walled carbon nanotubes (CNTs) by means of a tunnel contact.

We report on a technology for manufacturing devices in the configuration of field-effect transistors, where the channel of the transistor is an individual single-walled CNT, a tunnel contact is used as a source, and contact to the drain is ohmic (Fig.1). We used silicon substrates (480  $\mu\text{m}$ ) with a thermally grown  $\text{SiO}_2$  film with a thickness of 500 nm. Heavily-doped silicon substrate was used as a back gate. The nanotubes were grown by the CVD method using a three-component catalyst based on iron nitrate [4]. The ohmic contact was made from gold using electron beam deposition (film thickness is 25 nm). The tunnel contact was made using the following method: an aluminium film 2 nm thick was acidified for 1.5 hours at a pressure of  $10^{-3}$  atmospheres, after which a gold film 25 nm thick was deposited *in situ*. We show that by measuring the current-voltage characteristics of our structures between the tunnel and ohmic contacts at a fixed value of the gate voltage at cryogenic temperatures, we actually realize the tunnel spectroscopy of the tube state density on a chip.

### Acknowledgments

This work was supported by the Russian Foundation for Basic Research (№ 19-32-80028 Tunnel Diodes on Single Carbon Nanotubes for Detecting THz Radiation and № 18-29-20116 Infrared active plasmonics based on van der Waals heterostructures).

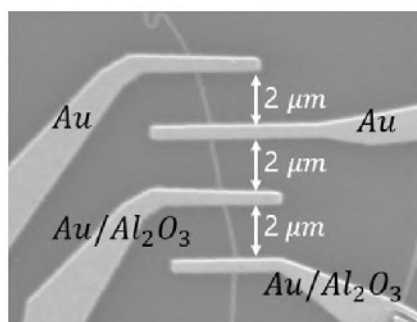


Fig.1. SEM-picture of device.

### References

1. Bronn, Nicholas, and Nadya Mason., *Physical Review B* (2013) **88(16)**, 161409.
2. Aspirtarte, L., McCulley, D. R., Bertoni, A., Island, J. O., Ostermann, M., Rontani, M., ... & Minot, E. D. *Scientific reports* (2017) **7(1)**, 8828.
3. Zhu, C., Liu, Y., Xu, J., Nie, Z., Li, Y., Xu, Y., ... & Wang, F. *Scientific reports* (2017) **7(1)**, 11221.
4. Fedorov, G., Kardakova, A., Gayduchenko, I., Charayev, I., Voronov, B. M., Finkel, M., ... & Ibragimov, R. *Applied Physics Letters* (2013), **103(18)**, 181121.

## Preparation of C-C composites from anthracene

Chichkan A.S.<sup>1</sup>, Chesnokov V.V.<sup>1</sup>

AlexCsh@yandex.ru

<sup>1</sup> Federal Research Center Boreskov Institute of Catalysis, Novosibirsk, Russia

Carbon nanotubes (CNT) are promising carbon materials, because they have unique properties: high strength and electrical conductivity, corrosion resistance, compatibility with living tissues, etc. In this work, it is proposed to use CNT as nucleation of needle coke growth. Needle coke is used in the production of electrodes as its electrical resistivity and thermal expansion coefficient is less than that of spongy coke. Needle coke is produced from highly aromatic raw materials. In this study we investigated the mechanism of coking of anthracene, and the effect of carbon nanotubes (CNTs) on the morphology and crystal structure of the resulting coke.

Anthracene coking was carried out in an autoclave at temperatures of 400–600°C and pressures of 2–4 atm. Anthracene in an amount of 2 g was loaded into an autoclave basket, and the autoclave was placed in an oven to heat the sample to a predetermined temperature. After reaching the set temperature, the sample was held for 2 h.

It was shown that at a temperature of 450°C, intermolecular interaction of two anthracene molecules begins involving the elimination of hydrogen and the formation of a C-C bond between the middle rings [1]. Increasing the coking temperature to 500–600°C leads to the formation of poorly crystallized graphite. In the case of pure anthracene, spherical carbon particles of about a micron in size are produced. The addition of carbon nanotubes leads to the formation of the carbon “coat” covering the surface of CNTs (fig.).

Carbon nanotubes act as nuclei of the new phase. The thickness of the carbon “coat” depends on the temperature of coking. At a temperature of 450°C, an amorphous carbon layer of 1 to 2 nm in thickness is observed on the CNT surface, with the thickness increasing to 10–15 nm at a temperature of 600°C.

This work was supported by the Russian Science Foundation, project no. 17-73-30032.

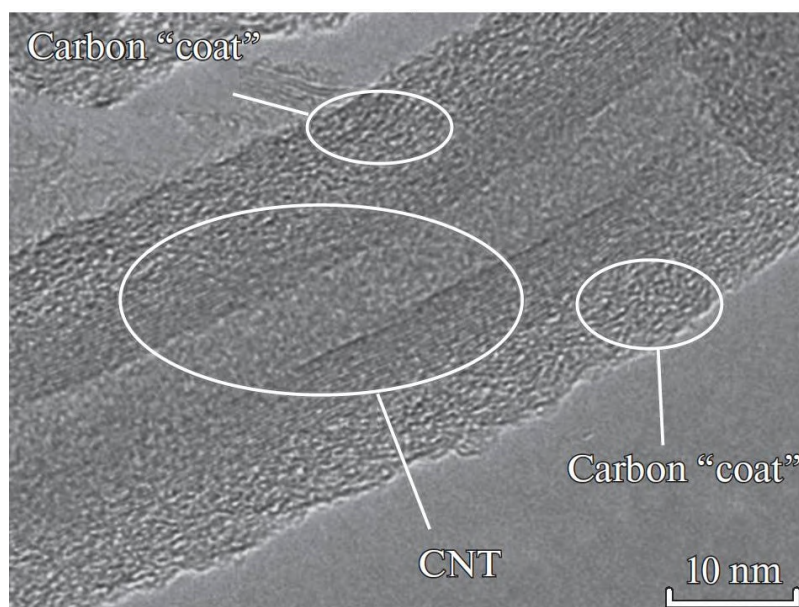


Fig. Electron microscope images of “carbon coat”-covered CNT obtained after coking the CNT-anthracene mixture at a temperature of 600°C.

### References

1. Chesnokov V. V., Chichkan A. S., Paukshtis E. A., *Petroleum Chemistry* (2019) **59**, 186.

## Effect of high pressure on the thermoelectrical properties of carbon nanotubes

*Sokolovsky D.N.*<sup>1,2</sup>, *Volkova Ya.Yu.*<sup>2</sup>

*sokolovskyd1@gmail.com*

<sup>1</sup> Ural State Medical University, Ekaterinburg, Russia

<sup>2</sup> Ural Federal University, Ekaterinburg, Russia

Unique mechanical, thermal and electrical properties of the carbon nanotubes dependences on number of walls (shells), diameter and chirality. Previously, it was shown that carbon nanotubes at pressure undergo a structural phase transitions corresponding to distortion of the nanotube cross-section from circular to oval and flattened form [1-3]. The pressure at which the collapse of carbon nanotubes takes place is inversely proportional to the cube of the diameter of the nanotube [1-2]. Double-walled carbon nanotubes demonstrate a series of structural transitions, like those observed in single-walled nanotubes [2].

At pressures more than 30 GPa, irreversible changes occur with the formation of new 2D, or 3D structural based on nanotubes [1, 3]. Also, the 45–65 GPa compressive stress combined with shear deformation at room temperature results in the joining of carbon nanotubes, and to the formation of some number of graphitic fragments, cross-linked by sp<sup>3</sup>-bonds [4-5]. Many 2D and 3D structures formed by carbon nanotubes are stable after removal of the load [3-5].

Changes in the structure of carbon nanotubes occurs under pressure should be accompanied by the changes of the electrical and thermal properties. Thus, studying effects high pressure on Seebeck coefficient of the carbon nanotubes, can be a complementary tool in characterization structural transitions.

In this work, the studying of effect high pressure on the baric dependences of Seebeck coefficient of the single-walled and double-walled carbon nanotubes in the pressure range 4–46 GP was produced. High pressure has been generated in the diamond anvil cell with conductive synthetic diamonds. We found a strong dependence of the Seebeck coefficient of carbon nanotubes on their structural state, which varies with pressure. The results indicate to certain changes in the structure of carbon nanotubes, induced high pressure. The observed picture can be due to the processes of destruction of the structure of carbon nanotubes.

### References

1. Y. Chen, M. Kim and C.S. Yoo, *Chemical Physics Letters* (2009) **479**, 91.
2. L. Aguiar, E.B. Barros, R.B. Capaz, A.G. Souza Filho, P.T.C. Freire, J. Mendes Filho, D. Machon, Ch. Caillier, Y.A. Kim, H. Muramatsu, M. Endo, and A. San-Miguel, *J. Phys. Chem. C*. (2011) **115**, 5378.
3. S. Zhao, X.F. Zhou, M. Hu, D.L. Yu, J.L. He, H.T. Wang, Y.J. Tian and B. Xu, *Journal of Superhard Materials* (2012) **34**, 371.
4. Y. Pashkin, A.M. Pankov, B.A. Kulnitskiy, I.A. Perezhogin, A.R. Karaeva, V.Z. Mordkovich, M.Y. Popov, P.B. Sorokin and V.D. Blank, *Applied Physics Letters* (2016) **109**, 081904.
5. M. Pankov, A.S. Bredikhina, B.A. Kulnitskiy, I.A. Perezhogin, E.A. Skryleva, Yu.N. Parkhomenko, M.Yu. Popov and V.D. Blank, *AIP Advances* (2017) **7**, 085218.

## **Synthesis of hybrid materials based on multi-walled carbon nanotubes, decorated with nanosized TiC or WC coatings for use as reinforcing fillers in aluminium alloys**

*Kremlev K.V.*<sup>1</sup>, *Aborkin A.V.*<sup>2</sup>, *Zabrodina G.S.*<sup>1</sup>, *Obiedkov A.M.*<sup>1</sup>, *Kaverin B.S.*<sup>1</sup>, *Semenov N.M.*<sup>1</sup>, *Andreev P.V.*<sup>3</sup>, *Vilkov I.V.*<sup>3</sup>, *Babin D.M.*<sup>2</sup>

*kkremlev@mail.ru*

<sup>1</sup> G.A. Razuvaev Institute of Organometallic Chemistry of RAS, Nizhny Novgorod, Russia

<sup>2</sup> Vladimir State University, Vladimir, Russia

<sup>3</sup> Lobachevsky State University, Nizhny Novgorod, Russia

The need to use new durable structural materials leads scientists to look for new opportunities to produce composite materials with hardening additives. One of the most effective reinforcing additives are hybrid materials based on multi-walled carbon nanotubes (MWCNTs), decorated with various nanoscale coatings.

The aim of this work is to create hybrid materials based on MWCNTs and their introduction into Al-Mg alloys as reinforcing components.

The synthesis of MWCNTs was carried out using the MOCVD method in the developed facility using toluene and ferrocene as precursors. The MWCNTs obtained in this way had an outer diameter of about 81 nm on average. Further, to create reinforcing hybrid materials coatings of TiC or WC were deposited on MWCNTs surface using the MOCVD also.  $\text{Cp}_2\text{TiCl}_2$  and  $\text{W}(\text{CO})_6$  were used as precursors of coatings. The hybrid materials thus synthesized were MWCNTs coated with nanoscale continuous layers of TiC or WC nanoparticles. Next, the resulting hybrid materials were used as reinforcing fillers to create new structural nanocomposites based on Al-Mg system alloys. For this, powder metallurgy technologies were used, including preliminary machining of matrix material and filler in high-energy mills and subsequent consolidation of composite powders by thermal deformation methods. An increase in the yield strength of the composites created in comparison with the initial alloys has been established.

This work was supported by the RSF (Project 18-79-10227).

## Double-walled carbon nanotubes with controlled bundle size

*Karaeva A.R.<sup>1</sup>, Kazennov N.V.<sup>1</sup>, Kulnitskiy B.A.<sup>1</sup>, Mordkovich V.Z.<sup>1,2</sup>*

*karaevaar@tisnum.ru*

<sup>1</sup> Technological Institute for Superhard and Novel Carbon Materials, Troitsk, Moscow, Russia

<sup>2</sup> INFRA Technology Ltd., Moscow, Russia

Carbon nanotubes were obtained by the method of gas-phase chemical decomposition of a carbon precursor on the surface of a catalytic particle suspended in a carrier gas stream at a temperature of 1150 °C. Ethanol and ethanol-acetone mixture were used as the carbon precursor, the catalyst was ferrocene, and the growth activator was thiophene.

It was previously shown [1, 2] that the use of ethanol results in aligned bundles of double-walled carbon nanotubes. In this work, a mixture of ethanol and acetone (volume ratio 1:1) was used as a feedstock. The obtained samples were studied by high-resolution electron microscopy. Electrical conductivity was measured by the four-probe method.

Comparative study of the obtained samples showed that the number of walls and the size of the bundles may vary (Fig. 1). In the samples obtained from ethanol only, the bundles consisted of double-walled nanotubes of 8-35 nm in size. In the samples obtained from ethanol - acetone mixture, the bundles of up to 70 nm in size were observed. In the latter case the thin-walled nanotubes (3-7 walls) prevailed, and double-walled nanotubes were very few. Despite these differences, in both cases the oriented bundles of carbon nanotubes of more than 1000 μm in length and with a nanotube diameter of 1.8-15 nm were formed. In addition, the value of electrical conductivity of the purified samples turned out to be rather high and similar for both cases:  $1.4 \cdot 10^5$  -  $9.4 \cdot 10^5$  S/m.

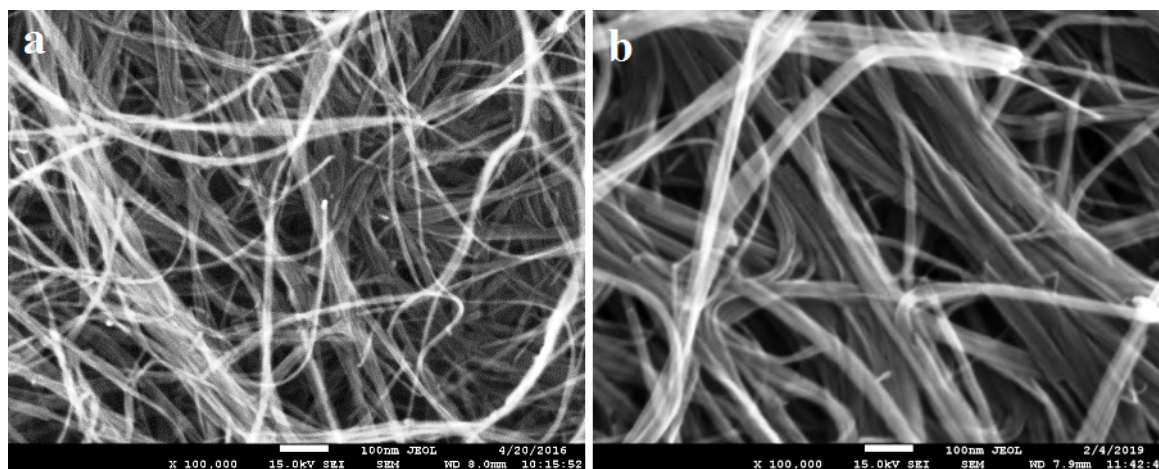


Fig. 1. SEM microphotographs of the bundles of carbon nanotubes obtained from ethanol (a) and from a mixture of ethanol and acetone (b).

### References

1. R. Karaeva, M.A. Khaskov, E.B. Mitberg, B.A. Kulnitskiy, I.A. Perezhogin, L.A. Ivanov, V.N. Denisov, A.N. Kirichenko and V.Z. Mordkovich, Longer Carbon Nanotubes by Controlled Catalytic Growth in the Presence of Water Vapor, *J. Fullerenes, nanotubes and Carbon nanostructures* (2012), 20:4-7, p. 411-418.
2. Z. Mordkovich, N.V. Kazennov, V.S. Ermolaev, E.A. Zhukova, A.R. Karaeva, Scaled-up process for producing longer carbon nanotubes and carbon cotton by macro-spools. *J. Diamond and Related Materials*, 2018, Volume 83, March 2018, p. 15-20.

## Emission properties of carbon nanotubes

Tomilin O.B.<sup>1</sup>, Rodionova E.V.<sup>1</sup>, Rodin E.A.<sup>1</sup>

rodionova\_j87@mail.ru

<sup>1</sup> National Research Mordovia State University, Saransk, Russia

Field electron emission from carbon nanotubes is the theoretical base for creation of new highly useful cathode materials. The mechanism of field electron emission is described by the modified Fowler-Nordheim theory but this approach possesses certain defects [1]. The most important of such defects is the absence of a molecular state that provides electron emission when a constant electric field is applied. It is shown [2] in cylindrical carbon molecules, in-plane p-electron conjugation causes to specific molecular orbitals (EMOs) which are characterized by electron localization at the ends of open single-walled carbon nanotubes (SWCNTs) both chirality (n,0) and (n,n), but these EMOs are vacant. Excitement of electrons to EMOs provides the physical conditions for following electron emission.

The present work studies the dependence of energy spectrum SWCNT, on the value of electric field strength  $E$  (V/Å) applied along SWCNT axis. Model molecules have a length of 6 hexagons are SWCNT fragments of hiralicity (n,0) for  $n=5-7$  and (n,n) for  $n=3-4$ . The value  $E$  changed from 0.0 to 1.5 V/Å. Electron structure of model molecules was calculated for every  $n$  using DFT 6-31G/B3LYP (Firefly/GAMESS program package).

The results of research are presented in Fig.1. Summary:

1. All investigated model molecules formed two EMOs. When value  $E$  is increased, energy of EMO1 is increased too, but energy of EMO2 is decreased and reached the valence band edge at value  $E=E_{cr}$ .
2. For model molecules SWCNTs of hiralicity (n,n)  $E_{cr}=1.2$  V/Å, whereas for model molecules SWCNT of hiralicity (n,0)  $E_{cr}=1.5$  V/Å.

The reported study was funded by RFBR according to the research project 18-33-00588.

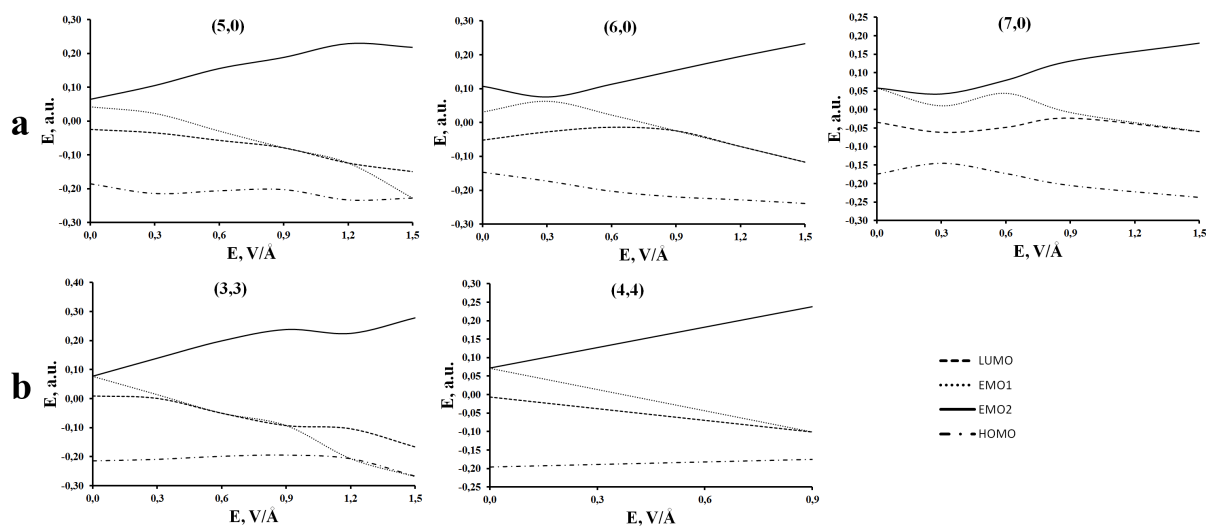


Fig.1. Dependences of values  $E^{EMO}$ ,  $E^{HOMO}$ ,  $E^{LUMO}$  from  $E$  for SWCNT: a-(n,0), b-(n,n).

### References

1. V. Eletsii, Phys. Usp. (2010) **53**, 863.
2. B. Tomilin, E. V. Rodionova, E. A. Rodin and E. E. Muryumin, Nanosystems: Physics, Chemistry, Mathematics (2018) **9**, 70.



## Modification of sealants with long carbon nanotubes

*Khaskov M.A.*<sup>1</sup>, *Chaykun A.M.*<sup>1</sup>, *Karaeva A.R.*<sup>2</sup>, *Kulnitskiy B.A.*<sup>2</sup>, *Mordkovich V.Z.*<sup>2,3</sup>

*khaskov@mail.ru*

<sup>1</sup> All-Russian Scientific Research Institute of Aviation Materials, Moscow, Russia

<sup>2</sup> Technological Institute for Superhard and Novel Carbon Materials, Troitsk, Moscow, Russia

<sup>3</sup> INFRA Technology Ltd., Moscow, Russia

The carbon nanomaterials, especially with ultra-high aspect ratio, give great opportunity to significantly improve many physical chemical and physical mechanical properties of different materials [1], including ones based on organic and inorganic polymers. This work is devoted to modification of the sealants with different chemical nature by the addition of carbon nanotubes with ultra-high aspect ratio.

Long carbon nanotubes were synthesized in specially designed chemical vapour deposition reactor [2] using ethanol, ferrocene and thiophene as the carbon precursors, catalyst and growth activator, respectively. The carbon nanotubes with the length exceeding 1000  $\mu\text{m}$  were used as-obtained and after purification by air annealing with subsequent chemical treatment at hydrochloric acid solution. The SEM images of as-obtained carbon nanotubes cotton (CNT-cotton) and CNT-cotton after purification were presented in Fig.1.

The different composites were obtained by infiltration of carbon nanotubes cotton with the sealants of different chemical nature, including fluorosilicone sealants, polysulfide sealants and siloxane sealants. It was shown that long carbon nanotubes as well as the admixtures change the curing kinetics during vulcanization of the sealants and causes the variation of physical mechanical properties. The influence depends on the chemical nature of the sealants, vulcanization mechanism as well as surface functional groups on CNTs and the content of admixtures.

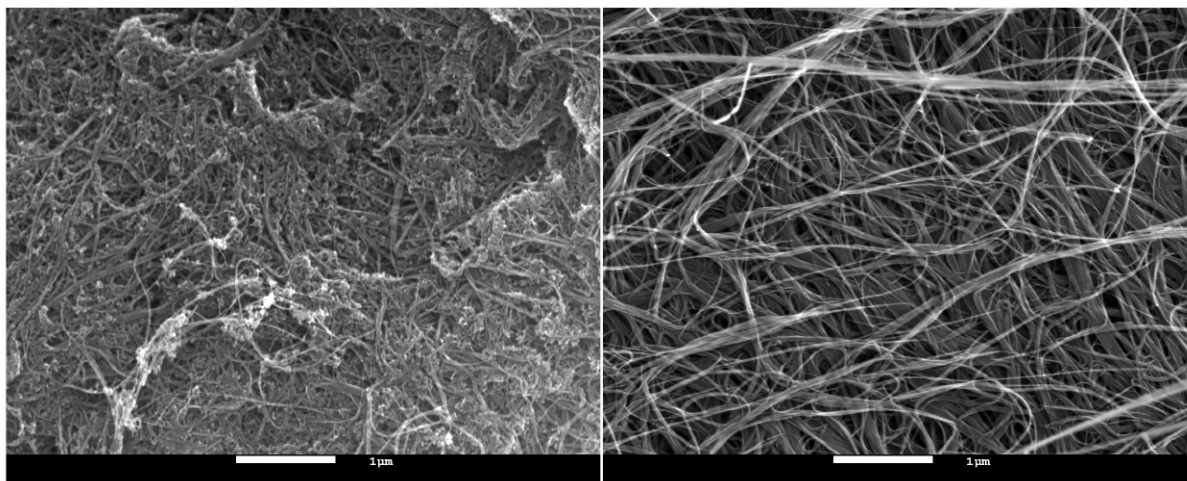


Fig.1. SEM images of CNT-cotton as obtained (left) and after purification (right)

### References

1. A.R. Karaeva, M.A. Khaskov, E.B. Mitberg, B.A. Kulnitskiy, I.A. Perezhogin, L.A. Ivanov, V.N. Denisov, A.N. Kirichenko, V.Z. Mordkovich, J.Fullerenes, Nanotubes and Carbon Nanostructures (2012), **20:4-7**, 411
2. V.Z. Mordkovich , A.R. Karaeva, M.A. Khaskov, E.B. Mitberg, Method and apparatus for producing long carbon nanotubes, Patent WO (2013), 2013/081499 A2

## Investigation of the surface potential of deformed carbon nanotubes

Guryanov A.V.<sup>1</sup>, Ilina M.V.<sup>1</sup>, Osotova O.I.<sup>1</sup>, Ageev O.A.<sup>1</sup>

*guryanov@sfedu.ru*

<sup>1</sup> Southern Federal University, Institute of Nanotechnologies, Electronics and Electronic Equipment Engineering, Taganrog, Russia

The modern development of electronics is associated with the transition to nanostructures that appearance unique properties are not typical for bulk materials. In [1, 2] was shown that carbon nanotubes can appearance piezo- and flexoelectric properties, which opens up wide opportunities for the creation of nanogenerators, memristors, switches and other nanoelectronics devices [1, 3]. The forming bundle carbon nanotubes have elastic nonuniform strain, which results in a non-zero electrical surface potential [2]. The aim of this work is an experimental study of the potential distribution on the bundle surface of vertically aligned carbon nanotubes (CNTs) depending on the bundle diameter.

Study of the surface potential of the aligned CNT bundles were carried out using the Kelvin Probe method of atomic force microscopy (AFM). Scanning of the sample with an area of  $2 \times 2 \mu\text{m}^2$  was carried out at the oscillation amplitude of the AFM probe corresponding to the bias voltages  $U=0.01; 0.1; 0.5$  V. The increase in the oscillation amplitude of the AFM probe led to a greater deviation of a CNT from its axis and, as a consequence, to the formation of bundles with larger diameter. It was shown that both negative and positive values of the potential were observed on the CNT bundle surface. It is associated with various types of CNT deformation: on the one side of a CNT experiences compression deformation, on the other tensile one.

The analysis of the obtained results showed that the minimum and maximum values of the surface potential increase with the increase of the bundle diameters of aligned CNTs. Thus, the maximum positive potential value was 200 mV at a bias voltage  $U=0.01$  V, was 300 mV at  $U=0.1$  V, was 400 mV at  $U=0.5$  V. The CNT bundle diameters were 0.565  $\mu\text{m}$ , 0.61  $\mu\text{m}$  and 0.635  $\mu\text{m}$ , respectively. Studies of the potential distribution along the cross section of the CNT bundle have shown that the potential value tends to zero in the center of the bundle and then increases with displacement to the outer borders of the bundle. This dependence is associated with an increase of the CNT deformation magnitude from the center to borders of the bundle.

Thus, the study of the surface potential of deformed CNTs showed a direct dependence of the potential value on the magnitude and type of the CNT deformation. It is established that the surface potential value increases with increasing a bundle diameter of vertically aligned CNTs. The results can be used to develop nanoelectronics devices based on aligned carbon nanotubes. The results were obtained using the equipment of the Research and Education Center and Center of Common Using "Nanotechnologies" of Southern Federal University.

The reported study was funded by RFBR according to the research project No. 16-29-14023 ofi\_m and Internal grant of the Southern Federal University (project №VnGr-07/2017-26).

### References

1. Kundalwal S.I., Meguid S.A. and Weng G.J. 2017. *Carbon* **117**, 462
2. Il'ina M.V., Il'in O.I., Blinov Y.F., Konshin A.A., Konoplev B.G., Ageev O.A. 2018 *Materials* **11**638
3. Il'ina M.V., Il'in O.I., Blinov Yu.F., Smirnov V.A., Kolomiytsev A.S., Fedotov A.A., Konoplev B.G. and Ageev O.A. .2017 *Carbon* **123**, 514

## Synthesis, characterization and the sensor properties of phosphorus filled single-wall carbon nanotubes

*Fedosova A.A.*<sup>1,2</sup>, *Stolyarova S.G.*<sup>1</sup>, *Sysoev V.I.*<sup>1,2</sup>, *Bulusheva L.G.*<sup>1,2</sup>, *Okotrub A.V.*<sup>1,2</sup>

*a.fedosova@g.nsu.ru*

<sup>1</sup> Nikolaev Institute of Inorganic Chemistry, SB RAS, Novosibirsk, Russia

<sup>2</sup> Novosibirsk State University, Novosibirsk, Russia

Filling single-wall carbon nanotubes (SWCNTs) with various inorganic compounds changes the electronic structure and chemical activity of the material [1,2]. Phosphorus can penetrate into the cavity of the nanotube, forming a different chain structure and nanoclusters, and embed in the graphene lattice with the formation of phosphorus-carbon bonds. Filling nanotubes changes surface properties, which can affect the selectivity and response of sensory materials. For their application, it is important to achieve maximum filling of the nanotube's cavity and minimize the content of impurities, for example, catalyst particles and phosphorus residues on the surface of the nanotube.

One of the most effective and simple methods of synthesis of filled SWCNTs is ampoule method of synthesis. The filling was carried out in an H-shaped ampoule, in one part of which phosphorus was placed, and in the other – SWCNTs. At heating, phosphorus vapors settle both on the surface of the SWCNTs and penetrate into the cavity of the SWCNTs. By varying such parameters as the ratio of reagents, synthesis time and synthesis temperature, it is possible to achieve the best degree of filling with phosphorus. The obtained samples were investigated by Raman spectroscopy, SEM, TEM, AES, and XPS. According to XPS, the sample contains 8 at. % of phosphorus.

A study of the sensing ability showed that the filling of SWCNTs with phosphorus leads to a significant increase in response to electron-acceptor molecules (NO<sub>2</sub>), while the opposite results were observed in the adsorption of electron-donor molecules (NH<sub>3</sub>). The obtained results show that the presence of phosphorus in the inner cavity leads to the p-doping of SWCNTs.

### References

1. J.C. Zheng, M.C. Payne, Y.P. Feng, A.T.L. Lim, Stability and electronic properties of carbon phosphide compounds with 1:1 stoichiometry, *Phys. Rev. B - Condens. Matter Mater. Phys.* 67 (2003) 1–4. doi:10.1103/PhysRevB.67.153105.
2. A.T.-L. LIM, J.-C. ZHENG, Y.P. FENG, Stability of Hypothetical Carbon Phosphide Solids, *Int. J. Mod. Phys. B.* 16 (2002) 1101–1104. doi:10.1142/s0217979202010932.

## Carbon nanotube oxidation in the presence of phase transfer catalyst and qualitative evaluation of the product

*Danilov E.A.*<sup>1</sup>, *Gavrilov Y.V.*<sup>2</sup>

*danilovegor1@gmail.com*

<sup>1</sup> JSC "Scientific Research Institute of Graphite-Based Structural Materials "NIIgrazit", Moscow, Russia

<sup>2</sup> D. Mendeleev University of Chemical Technology of Russia, Moscow, Russia

Functionalized carbon nanotubes (CNT) remain an object of intensive scientific research and industrial interest for over 2 decades as functionalization provides for both controlled regulation of physical (Fermi level, defect concentration) and surface ( $\zeta$ -potential, chemical activity, suspension stability) properties. To date, oxidation remains the most widespread route for surface hydrophilization, as well as a convenient first step for further surface chemistry manipulations. Unfortunately, the most popular protocols for oxidation involve either the use of strong acids (e.g. mixture of nitric and sulfuric acids) which leads to production of considerable amounts of acidic wastewaters and serious damage of nanotube surface, or agents that tend to form disperse deposits upon reduction (e.g. potassium bichromate) that are hard to separate from nanotubes. Characterization of oxidized nanotubes still remains a problem as well.

We report a scalable and controllable way of obtaining oxidized CNT in the powder form via microreactor-based approach in the presence of phase transfer catalyst. Methylene chloride-water binary system was used for performing the process in the presence of triethyl benzyl ammonium chloride (TEBAC) as phase transfer catalyst. Oxidizing agent - potassium permanganate, - was dissolved in the aqueous phase. Reagent concentrations in such quinary system were optimized via optical methods. Phase transfer catalyst conditions provide for controllable oxidation up to very high degrees normally unachievable for potassium permanganate (up to 4 mg-eq./g) without any significant change in morphology as observed via electron microscopy. Moreover, this route allows quantitative regeneration of organic phase (vacuum distillation) as well as simple preparation of powdered highly oxidized CNT via centrifugation. Single-, few- and multilayered CNT, as well as carbon nanofibers were shown to readily undergo controllable oxidation.

Quantitative analysis of the degree of CNT oxidation still remains somewhat controversial topic [1]. For example, early attempts at CNT oxidation in the presence of phase transfer catalyst are known [2], although the product was only characterized via X-ray photoelectron spectroscopy on a semi-qualitative level. In the present work we applied a combination of conductometric Boehm titration, Raman and infrared spectroscopy, as well as energy-dispersive X-ray spectroscopy analysis to develop consistent protocol for quantification of acidic groups.

### References

1. A. Wepasnick, B.A. Smith, K.E. Schrote, H.K. Wilson, S.R. Diegelmann, D.H. Fairbrother. Carbon (2011) **49**, 24.
2. Zhang, J. Xie, V.K Varadan. Smart Mater. Struct. (2002) **11**, 962.

## Carbon nanotubes for stabilization of nitrogen nanostructures

*Grishakov K.S.*<sup>1</sup>, *Maslov M.M.*<sup>1,2</sup>, *Katin K.P.*<sup>1,2</sup>

*kgrishakov@yahoo.com*

<sup>1</sup> Department of Condensed Matter Physics, National Research Nuclear University MEPhI, Moscow, Russia

<sup>2</sup> Laboratory of Computational Design of Nanostructures, Nanodevices and Nanotechnologies, Research Institute for the Development of Scientific and Educational Potential of Youth, Moscow, Russia

Carbon nanotubes (CNTs) have received considerable attention from researchers due to their unique properties and strong potential for applications in various technological areas, such as nanoelectronics, spintronics, etc. There are hollow spaces inside the nanotubes that can hold atoms and molecules. The filling of the medium inside CNT has caused considerable interest, due to the possibility of realizing the capture of unstable and reactive compounds in free space [1,2].

An important class of systems whose stability under normal conditions is of great practical interest are nitrogen nanostructures, in which the nitrogen atoms are connected to each other by single and double bonds. Polymeric nitrogen attracts great interest as a potential high energy density material (HEDM), and it can be decomposed into pure inert gas consisting of N<sub>2</sub> molecules that are environmentally friendly. Polymer nitrogen can release a large amount of energy if it dissociates into N<sub>2</sub> molecules. This is due to the fact that nitrogen has a uniquely large difference between the energy of a single bond (160 kJ/mol) and a triple bond (954 kJ/mol). Over the past years, a number of structures of polymeric nitrogen were theoretically proposed, however, only a few such structures were experimentally found, among which the so-called cubic gauche phase of nitrogen (cg-N), successfully synthesized under extreme conditions (P = 110 GPa, T = 2000K) [3]. However, under normal conditions, these polymeric nitrogen is not yet obtained, therefore the search for an effective method of stabilizing polymeric nitrogen is an actual issue.

Within the non-orthogonal tight-binding model [4,5] and density functional theory in the framework of the code SIESTA 4.01 [6], we considered the encapsulation of various nitrogen systems (nitrogen nanotubes, nitrogen chains, and nitrogen fullerenes) inside zigzag and armchair carbon nanotubes. We found stable configurations, determined the binding energy for different nanotube diameters, and also we investigated the electronic properties of such systems. It has been shown that carbon nanotube is able to stabilize nitrogen nanostructures that are unstable in free space.

The reported study was funded by RFBR according to the research project No. 18-32-20139 mol\_a\_ved.

### References

1. T. Fang, W. Chang, Y. Feng, D. Lu, *Physica E* (2016) **83**, 263.
2. W. Qiao, H. Bai, Y. Huang, *J. Phys. Condens. Matter* (2012) **24**, 185302.
3. M. I. Eremets, A. G. Gavriliuk, I. A. Trojan, D. A. Dzivenko, R. Boehler, *Nature Materials* (2004) **3**, 558-563.
4. M. M. Maslov, A. I. Podlivaev, K. P. Katin, *Molecular Simulation* (2016) **42**, 305-311.
5. M. M. Maslov, A. I. Podlivaev, L. A. Openov, *Physics Letters A* (2009) **373**, 1653-1657.
6. J. M. Soler, E. Artacho, J. D. Gale, A. García, J. Junquera, P. Ordejón, D. Sánchez-Portal, *Journal of Physics: Condensed Matter* (2002) **14**, 2745-2779

## The influence of the way of catalyst preparation on the morphology and properties of carbon nanotubes obtained from ethanol vapor

*Mitina A.A.*<sup>1</sup>, *Redkin A.N.*<sup>1</sup>, *Yakimov E.E.*<sup>1</sup>

*alena@iptm.ru*

<sup>1</sup> IMT RAS, Chernogolovka, Russia

Catalytic pyrolysis of ethanol vapor recognized as a simple relatively low-temperature method for the synthesis of carbon nanotubes (CNT) [1, 2]. CNTs produced at low temperatures have a greater imperfection and, therefore, are easier to undergo oxidative modification (functionalization). Modified CNTs are promising for use as sorbents, electrode material of supercapacitors and fuel cells, catalyst carriers, etc. The prospects for using CNTs as sorbents for solid-phase extraction of heavy metal ions from aqueous media are directly related to the certain requirements. First, the material must have a high capacity for metal ions, which is determined by the degree of functionalization of CNTs. Second, the CNT sorbent should be able to separate well from the solution. The last property depends on the morphology of the material obtained. We have previously shown that synthesis conditions, such as the pyrolysis temperature and the nature of the catalyst, strongly influence the ability of CNTs to oxidative modification. Often, oxidized carbon nanomaterials become pseudo-soluble, due to the solubilization effect. Such materials disperse in the solution in the form of stable colloidal particles, which are almost impossible to separate. To overcome this problem, we carried out work on the study of the effect of preliminary catalyst preparation on the morphology of the obtained CNTs. Nickel nitrate  $\text{Ni}(\text{NO}_3)_2 \cdot 6\text{H}_2\text{O}$  was used as a catalyst precursor. It is established that the conditions for the decomposition of nickel nitrate strongly influence the properties of the synthesized CNTs. When decomposed in air, the catalytic substrate gives CNTs in form of soft "cotton-like" product, which after oxidation tends to "solubilize". Upon decomposition of  $\text{Ni}(\text{NO}_3)_2 \cdot 6\text{H}_2\text{O}$  in an atmosphere of alcohol vapor, a relatively hard brittle nanocarbon material is obtained, which, after functionalization, is easily separated from the solution. The appearance of the materials obtained in different modes of pre-treatment of the catalyst is shown in Fig. 1. In the present work, the obtained materials were studied using electron microscopy, Raman spectroscopy. The kinetic features of the process were also studied for various methods of catalyst preparation. The reasons for the observed differences are discussed.

The work was partially supported by RFBR, grant No 18-03-00473 a.

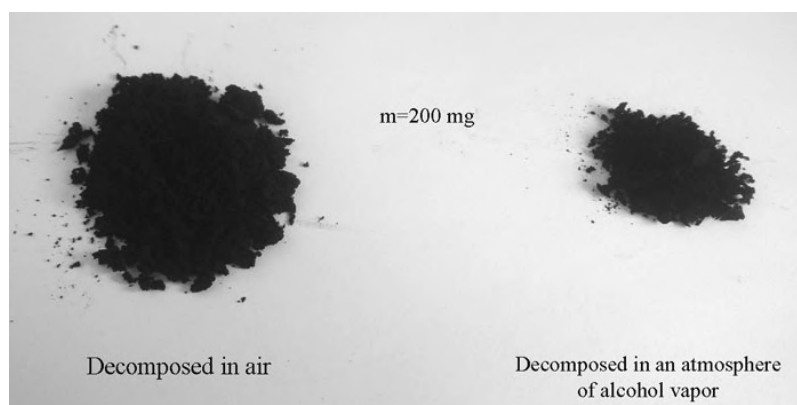


Fig.1. The appearance of the materials obtained in different modes of pre-treatment of the catalyst.

### References

1. S. Maruyama, R. Kojima, Y. Miyauchi, S. Chiashi, V. Kohno, *Chem. Phys. Lett.* 360 (2002), 229-234.
2. A.N. Redkin, V.A. Kipin, L.V. Malyarevich, *Inorg. Mater.*, 42 (2006), 242-245.

## Single-walled carbon nanotubes cleaning via solid-flame combustion process

*Neverovskaya A.Yu.<sup>1</sup>, Voznyakovskii A.P.<sup>1</sup>, Shumilov F.F.<sup>1</sup>, Sukhanova T.E.<sup>1</sup>*

*neverovskaya@yandex.ru*

<sup>1</sup> FSUE S. V. Lebedev Institute of Synthetic Rubber, St.-Petersburg, Russia

Despite the fact that carbon nanotubes (CNTs) have been known for more than twenty years, the problems associated with their practical applications are far from being solved. Depending on the technology of synthesis, both single-walled and multi-walled carbon nanotubes can be obtained (SWCNTs and MWCNTs, correspondently). The choice between SWCNTs and MWCNTs is fundamental, since the structure of CNTs affects their electronic, mechanical and chemical properties. At present, it is still quite difficult to predict which type of nanotubes would be preferable for practical use. The developed high-performance method for preparing of SWCNTs brand TUBALL (OCSiAl, Novosibirsk, Russia) made them available for laboratory research. Accordingly, there is currently a sharp surge in the number of publications on the SWCNTs study.

TUBALL dry powder contains in its composition up to 25 mass% of amorphous carbon and also unwanted inorganic impurities formed during the process. Therefore, cleaning of TUBALL is an obligatory stage of their preparation for practical use. Today, the main approach to the cleaning of SWCNTs is an oxidation by strong acids [1]. At the same time, the number of structural defects of SWCNTs increases and the tubes themselves break up uncontrollably. Also, acidic wastewaters are formed, the disposal of which is a special task, which naturally affects the cost of CNTs for the end user.

The aim of this work was to develop the SWCNTs brand TUBALL cleaning method that meets the current challenges of "green" technologies.

The SWCNTs were cleaned under the conditions of a solid-flame burning process. This ensured the simultaneous effect on the nanotubes of extremely high temperatures and aggressive oxidizing environment. As a result, the complete removal of amorphous carbon and the transfer of inorganic impurities into a water-soluble form followed by their removal with wash water was ensured. The difference between the original and purified SWCNTs is well demonstrated in Fig. 1 (A and B).

Dry powder of purified SWCNTs allowed to obtain stable (during the month of observation) suspensions in various polar solvents without using surfactants, in particular, in ethyl acetate.

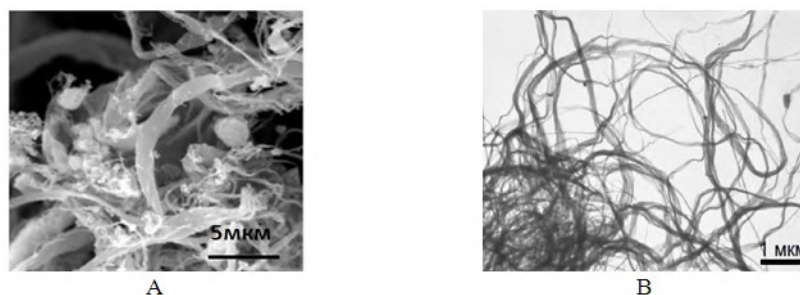


Fig. 1. Electron micrographs of SWCNTs (TUBALL, OCSiAl): A — the original SWCNTs (SEM); B - SWCNTs, purified by the method of solid-flame combustion (TEM).

### References

1. Holzinger M., Hirsch A., Bernier P., Duesberg G.S., Burghard M., *Appl. Phys. A*, (2000) **70**, 599.

## Influence of nonlinear absorption on the ultrashort optical pulse propagation in carbon nanotubes

*Konobeeva N.N.*<sup>1</sup>, *Belonenko M.B.*<sup>1</sup>

*yana\_nn@inbox.ru*

<sup>1</sup>Volgograd State University, Volgograd, Russia

The study of the interaction of electromagnetic field with a medium plays an important role in modern opto- and nano-electronics due to the large number of possible practical applications [1]. In this paper, we investigate the propagation of electromagnetic waves taking into account a pumping and a nonlinear absorption, which is introduced phenomenologically, in a medium with zig-zag carbon nanotubes. Based on Maxwell's equations, an effective equation is obtained for the vector potential of the electromagnetic field, which takes into account the dissipation of the pulse field under the piezoelectric effect associated with the oscillations of the heavy nuclei of the medium [2], the pumping with an external electromagnetic wave and the nonlinear absorption. The possibility of a stable pulse propagation (fig.1) due to the balance of the influence of dissipation and pump field is established. The stability of the steady state form of the electromagnetic pulse at large times is demonstrated when the nonlinear absorption coefficients vary as well as the initial distribution of the field of the pulse entering the system. The stability of a pulse with respect to angular perturbations that violate the cylindrical symmetry of the distribution of its field is substantiated.

This work was supported by the state assignment of the Ministry of Science and Higher Education of the Russian Federation (government task No. 2.852.2017/4.6).

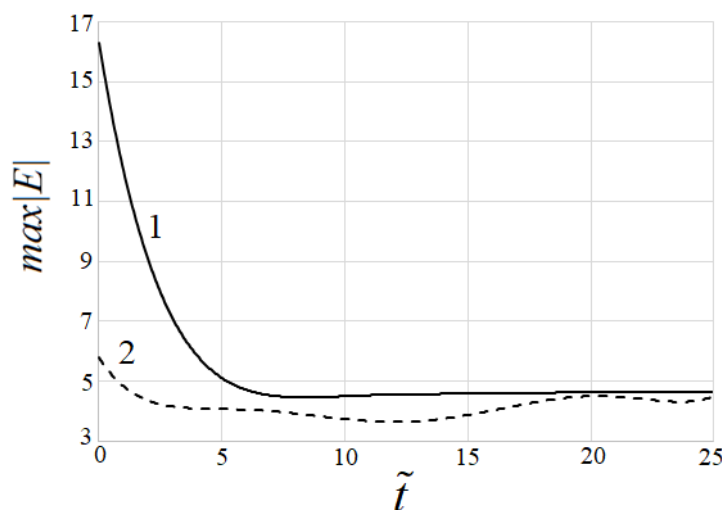


Fig.1. Dependence of the maximum modulus of the pulse amplitude (unit of E is equal to  $10^7$  V/m) on time (in relatively units) for different initial conditions: curve 1 corresponds to one field oscillation; curve 2 corresponds to two field oscillations.

### References

1. A. Mousavi, E. Plum, J. Shi, and N.I. Zheludev, *Sci. Rep.* (2015) **5**(17), 8977.
2. Kim, X. Hong, C. Jin, S.-F. Shi, C.-Y.S. Chang, M.-H. Chiu, L.-J. Li, and F. Wang, *Science*, (2014) **346**, 1205.
3. N.N. Konobeeva, and M.B. Belonenko, *Optics and Spectroscopy* (2018) **125**, 405.



## Purification of carbon nanotubes by acid and magnetic separation combination

*Gurova O.A.*<sup>1</sup>, *Gusel'nikova T.Ya.*<sup>1</sup>, *Arhipov V.E.*<sup>1,2</sup>, *Sedel'nikova O.V.*<sup>1,2</sup>, *Bulusheva L.G.*<sup>1,2</sup>, *Okotrub A.V.*<sup>1,2</sup>

*olga.gurov@gmail.com*

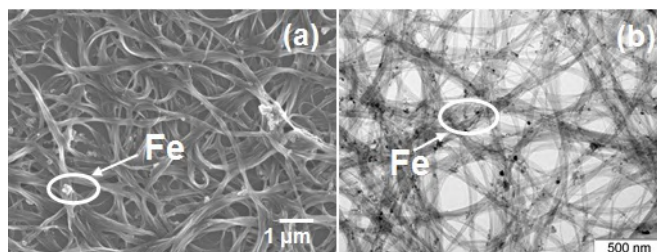
<sup>1</sup> Nikolaev Institute of Inorganic Chemistry SB RAS, Novosibirsk, Russia

<sup>2</sup> Novosibirsk State University, Novosibirsk, Russia

The main impurities of the synthesized carbon nanotubes (CNT) are products such as graphite polyhedrons, amorphous carbon and substrate materials [1]. In addition, SWCNTs contain catalyst particles necessary for the growth of nanotubes [2]. The metal particles can be at the base of the CNT, on its tips or they are incorporated inside the SWCNT [3]. In this work, we offer a combination method of CNTs purification by HCl acid and magnetic separation. We use single-wall carbon nanotubes (SWCNT) provided by OCSiAl company. Tubes average diameter was 1.7 nm. SWCNT had a purity of 75%. According to atomic-absorption spectroscopy, the amount of Fe catalytic particles in the SWCNT data was ~ 7 mass%. In addition, SEM and TEM images confirm a large amount of Fe particles (fig. 1).

In the first stage of purification, SWCNTs were treated with HCl, HNO<sub>3</sub>, H<sub>2</sub>SO<sub>4</sub> and mixture HNO<sub>3</sub>/H<sub>2</sub>SO<sub>4</sub> acids in an ultrasonic bath. After acid treatment, the amount of Fe decreased to 1.8, 3.3, 1.1, 1.2wt%. respectively. SWCNTs dispersion containing surfactant was prepared for the second stage of purification. The SWCNT dispersion was passed through magnetic installation. The magnetic separation was carried out using a silicone tube placed in a magnetic field. SWCNT dispersion was pumped by a slow flow through the tube. It was shown that the amount of iron is reduced to 0.3% for a sample treated HCl and H<sub>2</sub>SO<sub>4</sub>. This method could be combined with other dispersion-based techniques, which allow separation of SWCNT by transport properties and chirality.

This work was partially supported by and the Russian Science Foundation (Project 18-72-00017).



### References

- [1] J Mahalingam, B. Parasuram, T. Maiyalagan, and S. Sundaram, *J. Environ. Nanotechnol.*, 1, 53 (2012).
- [2] N. Dementev, S. Osswald, Yu. Gogotsi and E. Borguet, *J. Mater. Chem.*, 19, 7904 (2009).
- [3] E.V. Lobiak, E.V. Shlyakhova, L.G. Bulusheva, P.E. Plyusnin, Y.V. Shubin and A.V. Okotrub, *J. Alloys Compd.*, 621, 351 (2015)

## Conductivity improvement of spray deposited CNT network

Polikarpov Yu.A.<sup>1</sup>, Alexandrov E.V.<sup>1</sup>, Romashkin A.V.<sup>2</sup>, Levin D.D.<sup>2</sup>

skaldd@yandex.ru

<sup>1</sup> National Research University of Electronic Technology, Moscow, Russia

<sup>2</sup> Bauman Moscow State Technical University, Moscow, Russia

Carbon nanotubes (CNT) thin films show great promise as transparent electrodes and sensing structures. Low cost of CNT based devices can be provided by a solution processes implication. However, strong CNT-solvent interaction, and additionally low volatility of CNT solvents with high stability of colloidal dispersion, complicate residual solvent removal from deposited CNT films. Residual solvent reduces film conductivity and sensory response and degrades stability, which often is characteristic for spray deposition, widely used for scalable, low-temperature and low-cost deposition of high-uniform layers. Post-deposition annealing ineffective for solvent removal at insufficient temperature, which can be limited by process technology. Therefore, the development of residual solvent removal methods is actual problem.

Method of solvent removal by CNT film rinsing in formic acid is purposed. Sparse CNT network formed by spray-coating of 0.2 ml/cm<sup>2</sup> of colloidal dispersions of CNT with a concentration 60 µg/ml in N-methylpyrrolidone (N-CNT) and NMP mixtures with volatile solvents (deionized water (NW-CNT) and cyclohexanone (NC-CNT)) were spray deposited on cover glass (fig. 1a). Networks density was the lower, the more volatile dispersion components were used, due to decrease of transfer efficiency coefficient of NW-CNT and NC-CNT, that was confirmed by the average Raman intensity of G-peak ( $I_G \sim 1590 \text{ cm}^{-1}$ ) of CNT (fig. 1b). The networks resistivity was measured before and after sequential rinsing with formic acid and water to evaluate the treatment efficiency (fig. 1c). As a result, simultaneously both resistivity and Raman intensity decrease was observed, that is probably due to CNT contacts improvement after solvent removal and CNT film became more densely packed so Raman signal is also decreased. Slightly film resistivity increasing after annealing at 160 °C in vacuum after acid treatment allows to disregard any significant contribution of non-covalent doping to a resistivity improvement. So the mechanism of resistivity decrease is removing of residual NMP from CNT surface presumably due to the interaction of NMP with acid molecules and ions, what was described earlier only by modeling and stability of CNT colloidal dispersions investigation [1].

This work was supported by the Ministry of Science and Higher Education of the Russian Federation, agreement №14.574.21.0184 (unique ID RFMEFI57417X0184).

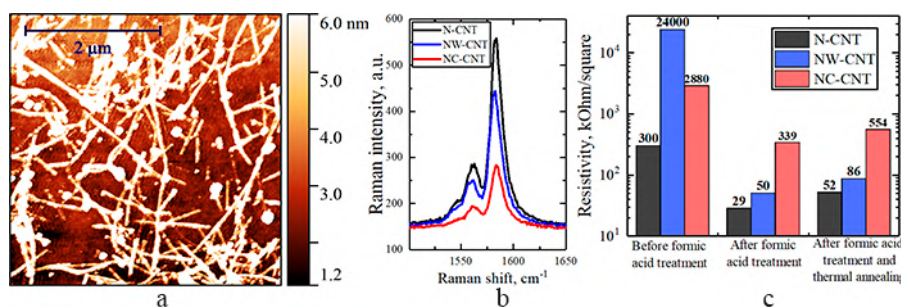


Fig. 1. AFM image of NW-CNT film (a), Raman intensity of G-peak (b), resistivity (c) of N-, NW- and NC-CNT films.

### References

- [1] A.I. Frolov, R.N. Arif, M.Kolar, A.O. Romanova, M.V. Fedorov, and A.G. Rozhin, Chemical science (2012) **3**(2), 541.

## Carbon-based nanomaterials as a support for peptides and proteins tritium labelling

*Badun G.A.<sup>1</sup>, Chernysheva M.G.<sup>1</sup>, Bunyaev V.A.<sup>1</sup>, Ksenofonov A.L.<sup>2</sup>*

*badunga@yandex.ru*

<sup>1</sup> Lomonosov Moscow State University, Moscow, Russia

<sup>2</sup> A.N. Belozersky Institute of Physico-Chemical Biology, MSU, Moscow, Russia

Tritium thermal activation method is a tool for radiolabeling different organic compounds from amino acids [1] to humic substances [2] and carbon-based nanomaterials [3]. The method is based on the short-exposure bombardment of solid compound with tritium atoms that are generated on the surface of tungsten filament at 1700 – 2000 K. The compound is usually adsorbed on the walls of glass reaction flask. However, the application of other substrates can influence on the result of tritium interaction with organic molecules.

In present work we have studied the influence of carbon-based materials (activated carbon, graphene oxide, reduced graphene oxide, nanotubes or nanodiamonds) on the specific radioactivity and intramolecular distribution of tritium in oligopeptide (Dalargin) and bovine serum albumin (BSA).

It was shown that deposition of dalargin on carbon-based substrates significantly changes tritium distribution in the amino acids residues comparing with thick target on the glass surface. When tritium atoms interact with dalargin on the carbon surface the significant increase in the phenylalanine radioactivity indicating that the isotopic exchange occurs by electrophilic mechanism as well as by radical mechanism. Noted that changes in tritium content in glycine, leucine and tyrosine result from different in the structure of the adsorption layers on the carbon surfaces.

In the case of BSA the changes in the intramolecular tritium distribution was not so significant. At the same time, a pronounced effect of increasing the specific radioactivity of the protein was observed comparing with the experiment on the glass surface under the similar conditions. The increase in the specific radioactivity of protein by an order of magnitude is explained by higher availability of protein on carbon surface to the interaction with atomic tritium. The effect of changes of tritium atoms reaction ability on the carbon surface is not evident because of large size of protein globule.

This work was supported by Russian Foundation for Basic Research (grants № 18-03-20147, 17-03-00985).

### References

1. A. Badun, M.G. Chernysheva, A.L. Ksenofontov // *Radiochimica Acta* (2012) **100**, 401.
2. A. Badun, M.G. Chernysheva, Z.A. Tyasto, N.A. Kulikova, A.V. Kudryavtsev, I.V. Perminova // *Radiochimica Acta* (2010), **98**, 161.
3. A. Badun, M.G. Chernysheva, A.V. Grigorieva, E.A. Eremina, A.V. Egorov. // *Radiochimica Acta* (2016), **104**, 593.

## Supramolecular interaction of modified nanodiamonds, biomolecules and drugs: molecular modeling

Plastun I.L.<sup>1</sup>, Bokarev A.N.<sup>1</sup>, Zakharov A.A.<sup>1</sup>, Naumov A.A.<sup>1</sup>

inna\_pls@mail.ru

<sup>1</sup> Yuri Gagarin State Technical University of Saratov, Saratov, Russia

Detonation nanodiamond (ND) is one of most promising materials for targeted drug delivery - one of rapidly developing areas of modern chemistry, pharmacology and medicine [1]. Wide possibilities of surface modification and advantageous dimensions make nanodiamonds very attractive objects for use in the drug delivery process. A number of studies have shown that therapeutic efficacy of drugs is enhanced and their toxicities may be attenuated with immobilization on enriched ND. The one of the simplest immobilization methods is creation of molecular complex due to hydrogen bonds formation that is due to supramolecular interaction. In present work possibility of drug delivery and retention in cells due to hydrogen bonds formation between enriched nanodiamonds and highly toxic drugs on example of doxorubicin and mitoxantrone is investigated by numerical simulation. Using molecular modeling by the density functional theory B3LYP method with 6-31G(d) basic set, we analyze the hydrogen bonds formation and their influence on IR - spectra and structure of molecular complexes which is formed due to interaction between doxorubicin or mitoxantrone and nanodiamonds with different surface functionalization. Molecular modeling of modified nanodiamonds and drugs interaction is based on nanodiamond representation by a diamond-like nanoparticle with simpler structure [2]. Enriched adamantane is used as an example of diamond-like nanoparticle with surface functionalization. As a result of calculations the combined IR spectrum is obtained as imposing of IR spectra for molecular complexes of doxorubicin (or mitoxantrone) and 1,3,5,7-adamantanetetracarboxylic acid in various interaction positions (fig.1). Combined IR spectra for both doxorubicin and mitoxantrone demonstrates a good agreement with experimental data.

Received results demonstrate that there can be strong supramolecular interaction between drugs and modified detonation nanodiamonds. Formed hydrogen bonds can be considered as one of main mechanisms for targeted drug delivery and for drug retention in cells and, thus, for enhancement of anti-cancer therapeutic efficacy.

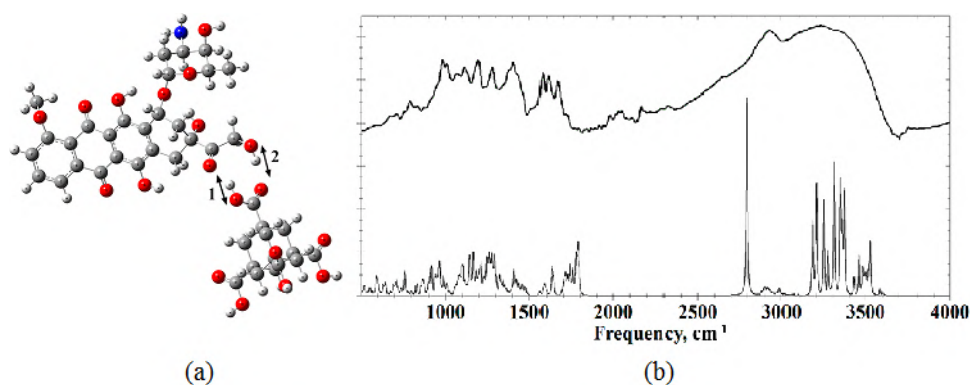


Fig. 1. Molecular complex, formed by 1,3,5,7- adamantanetetracarboxylic acid and doxorubicin: (a) variant of structure and (b) IR spectra: experimental (upper) and calculated combined spectrum (lower)

### References

1. A. Shenderova, G.E. McGuire. *Biointerphases* (2015) **10** (3), p.030802.
2. A.N. Bokarev, I.L. Plastun. *Nanosystems: physics, chemistry, mathematics* (2018) **9**(3), p.370

## Molecular modeling of graphene oxide intermolecular interaction with DNA nitrogenous bases adenine and thymine

*Naumov A.A.<sup>1</sup>, Plastun I.L.<sup>1</sup>, Bokarev A.N.<sup>1</sup>, Zakharov A.A.<sup>1</sup>*

*offhid@mail.ru*

<sup>1</sup> Yuri Gagarin State Technical University of Saratov, Saratov, Russia

In present work the supramolecular interaction of graphene oxide with biomolecules from the DNA composition is investigated. Analysis of intermolecular interaction, structure of graphene oxide and DNA is required for various kinds of biomedical tasks. Graphene oxide is used in areas such as optoelectronics, supercapacitors, memory devices, composite materials, photocatalysis, biomedicine, pharmacology. Graphene oxide can be used in Biomedicine and pharmacology as a delivery system, diagnostic and medicinal products [1].

Graphene oxide (Fig. 1a) is an oxidized form of graphene and consists of carbon, hydrogen, and oxygen in various proportions. It has a hybrid structure consisting of a mixture of sp<sup>2</sup> and sp<sup>3</sup> hybridized carbon atoms [2].

Molecular modeling and calculation of the spectra of molecules and their complexes were carried out on the basis of the density functional theory (DFT) [3] method using the B3LYP [3, 4] functional with the base set 6-31G(d).

The supramolecular interaction involves medium and weak bonds which are created in large quantities in molecular complexes, in particular such bonds include hydrogen bonds. Frequencies in the IR spectrum (Fig. 1c) corresponding to such oscillations lie in the high-frequency region from 1800 cm<sup>-1</sup> and more. Accordingly, in the spectrum of graphene oxide oscillations that will participate in the formation of Oh group bonds are oscillations that have frequencies: 3247 (Fig.1c №1), 3359 (Fig.1c №2), 3385 (Fig. 1c №3), 3419 (Fig. 1c №4).

Active sites in graphene oxide are the nodes with the oxygen that implement connection OH. The oscillations of the active centers are in the range from 3200 to 3500.

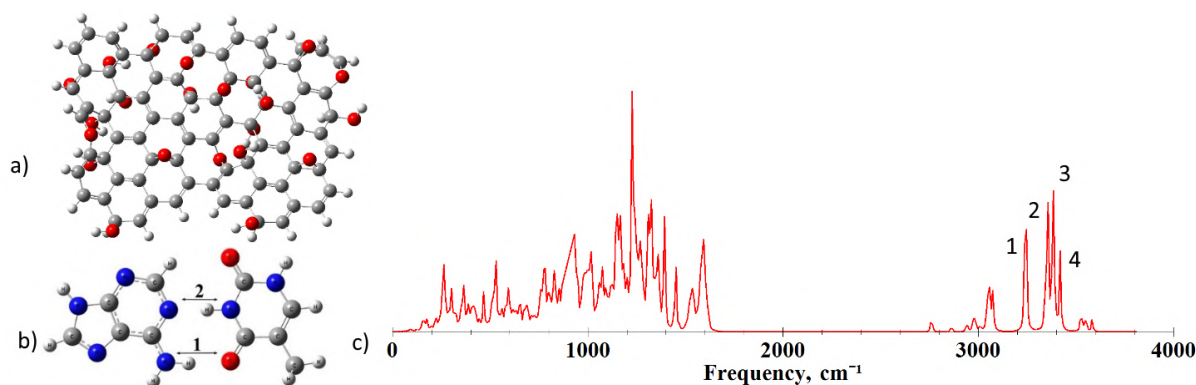


Fig.1 Structures graphene oxide (a), adenine-thymine (b), IR-spectrum of graphene oxide (c)

### References

1. M. Seyyed, A.H. Seyyed, G. Younes, M.A. Ali, B. Aziz, A. Omid, *Drug Metabolism Reviews* 2019, pp. 1-30.
2. A. Dikin, S. Stankovich, E.J. Zimney, R.D. Piner, G.H.B. Dommett, G. Evmenenko, S.T. Nguyen, R.S. Ruoff, *Nature* 2007, pp. 457-460.
3. W. Kohn, the electronic structure of matter: wave functions and density functionals. *Physics-Uspekhi (Advances in Physical Sciences)*, 2002, vol. 172, no. 3, pp. 336-348.
4. J. Pople, *Quantum chemical models. Physics-Uspekhi (Advances in Physical Sciences)*, 2002, vol. 172, no. 3, pp. 349-356.

## Nanosize coatings on the base of diamond-like carbon doped with copper with enhanced antibacterial activity

*Razanau I.*<sup>1,2</sup>, *Kazachenko V.*<sup>1</sup>, *Kai Li*<sup>3</sup>, *Dvorak A.*<sup>1</sup>

*ir23.by@gmail.com*

<sup>1</sup> State Enterprise "Science and Technology Park of BNTU "Polytechnic", Minsk, Belarus

<sup>2</sup> SSPA "Scientific-Practical Materials Research Centre of NAS of Belarus", Minsk, Belarus

<sup>3</sup> Shanghai Institute of Ceramics, Chinese Academy of Sciences, Shanghai, China

Colonization of the surfaces of medical implants inside patient body by bacteria and fungi can lead to complications with subsequent repeated surgical operation for replacement of the implant. Application of antibacterial coatings on the base of antibiotics is limited in the long term by the developing resistance of bacteria and emergence of multi-resistant bacteria. Inorganic antibacterial agents, such as metals, exclude this disadvantage: the mechanism of their bactericidal activity is based upon the disturbance of the cell operation by the biochemically active metal cations that dissolve in the biological medium. At the same time, application of metals for antibacterial purposes is limited by their overall cytotoxicity [1].

The present report is dedicated to the study of nanosize coatings on the basis of diamond-like carbon (DLC) with copper antibacterial agent. DLC is characterized by good biocompatibility and high mechanical and tribological properties. At the same time, copper volumetrically dispersed in DLC allows to implement the mechanism of local dosing release of copper ions into the biological medium.

The coatings were deposited from the products of pulsed cathodic arc discharge with the cathode made of graphite and copper. The coatings were deposited on substrates made of titanium used for medical implant production. Deposition process and structure of the coatings are discussed.

The DLC-Cu coatings were tested for antibacterial activity using E coli strains (Fig.1). The test has shown approximately 25-fold decrease of the surface area colonized by the bacteria. At the same time, the *in vitro* wound healing assay with human HUVEC cells has shown that scratch wound produced in the HUVEC monolayer heals approximately 3.5 times faster on the surface of the DLC-Cu coating in comparison with the pristine titanium substrate. Thus, the biological tests have shown that by combining biocompatible DLC matrix with bactericidal metal agents it is possible to achieve the antibacterial activity and, at the same time, improve the biocompatibility to human cells.

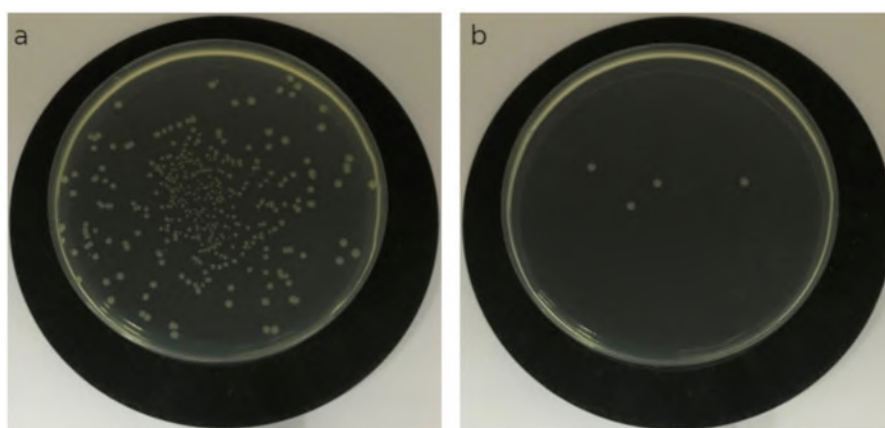


Fig.1. Results of the antibacterial test (E coli strains) for the pristine titanium substrate (a) and the same substrate with nanosize DLC-Cu coating (b).

### References

1. L. Cyphert, H.A. von Recum, *Exp. Biol. Med.* (2017) **242**, 788.

## Multiwall carbon nanotubes based optical biosensor for L-Dopa

Polokhin Aleksandr Alexandrovich <sup>1</sup>, Kharissova Oxana Vasilievna <sup>1</sup>, Selvas Aguilar Romeo de Jesus <sup>1</sup>  
*a.a.polohin@gmail.com*

<sup>1</sup> FCFM, Universidad Autonoma de Nuevo Leon, Monterrey, Mexico

L-dopa is an amino acid which is a precursor of dopamine biosynthesized by humans and some animals. Currently L-Dopa is mainstay of Parkinson's disease treatment as induces the formation of Dopamine [1]. In that case the control of L-Dopa levels during the process of medication is important in order to avoid negative effects [2]. Although a number of electrochemical L-Dopa sensors [3-5], optical methods is also prospective, especially spectrophotometric one. [6]

The working principle of the L-Dopa biosensor describing in this work lays on the use of the specific absorption band of L-dopa - alizarin red reaction. This band is wide with the maximum at the wavelength of the 588 nm [6]. A multimode optical fiber with diameter core was chose as a base of the L-Dopa biosensor. At the first step a polymer jacket of the optical fiber was removed by sulfuric acid (H<sub>2</sub>SO<sub>4</sub>) etch. Then the 5 mm long part of the optical fiber was treated with hydrofluoric acid (HF) in order to etch the cladding which coated the core [7]. At the next stage an array of MWCNT was synthesized by spray pyrolysis chemical vapor deposition (SPCVD) method at the temperature of the 800 C and with the duration of the 10 min. Ferrocene (0,025 wt%) was used as a catalyst and toluene was used as a carbon source (flow rate - 1 ml/min). The scheme of the biosensor is illustrated in Fig. 1. Then the final structure was dived into alizarin red aqueous solution (5 mg/ml) in order to MWCNTs absorb the dye [8].

The optical biosensor transmission spectra in the range of the 200-850 nm without and with L-Dopa molecules were recorded. In order to bound L-Dopa the biosensor had been dived into its solution (20 µg/mL) what resulted in reaction of L-Dopa and alizarin red absorbed with MWNTCs. The absence of optical fiber cladding allowed light to go through CNTs and interact with L-Dopa molecules. The spectrum of the biosensor after the diving demonstrated repeatable absorbance in the range of the 550-620 nm which absented in initial spectra. The described sensor could be used as an instrument of L-Dopa detection.

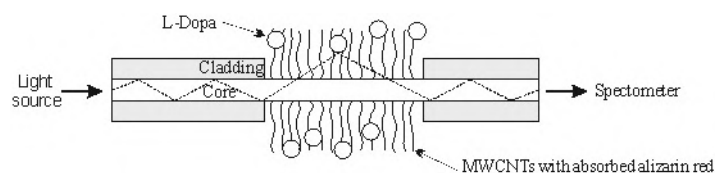


Fig.1. Scheme of the multiwall carbon nanotubes based optical biosensor for L-Dopa

### References

1. Tomlinson, R. Stowe and C. Clarke, *Mov. Disord.* (2010), **25**, 2649.
2. Jubete, E. Ochoteco and G. Linazasoro, *Sensors* (2008), **10**, 239.
3. Teixeira, H. Marcolino and M. Bergamini, *Sens. Actuator B-Chem.* (2007), **122**, 549.
4. Lin, H. Lian and B. Liu, *Anal. Methods* (2015), **7**, 1387.
5. Bergamini, A. Santos and M. Zanoni, *J. Pharm. Biomed. Anal.* (2005), **39**, 54.
6. Basheir, A. Elbashir and H. Aboul-Enein, *Rev. Roum. Chim* (2015), **60**, 555.
7. Zhao, Z. Wu, and X. Zhang, *Frontiers of Optoelectronics in China* (2011), **4**, 338.
8. Machado, S. Carmalin and S. Fagan, *J. Phys. Chem. C* (2016), **120**, 18296.

## **Biodistribution of nanodiamond for potential anti-tuberculosis drug delivery systems**

*Yakovlev R.Y.*<sup>1</sup>, *Bocharova I.V.*<sup>2</sup>, *Lepekha L.N.*<sup>2</sup>

*yarules@yandex.ru*

<sup>1</sup> Vernadsky Institute of Geochemistry and Analytical Chemistry of Russian Academy of Science, Moscow, Russia

<sup>2</sup> Research Central Institute of Tuberculosis, Moscow, Russia

Treatment of tuberculosis (TB) complicated by the need of multi-drug regimens that need to be administered over long periods. To minimise toxicity and improve patients' compliance, extensive progressive efforts have been made to develop various microparticulate- and various other carrier-based drug delivery systems to reduce the dosing frequency. New approaches for treatment have included the development of biodegradable polymeric micro- or nanoparticulate carrier systems to target alveolar macrophages that harbour *M. tuberculosis*. Carbon particles, in particular, nanodiamonds (ND) are extensively studied in biomedical applications, but limitedly used for the development of TB delivery systems.

The focus of the present work was to study *ex vivo* biodistribution of ND particles in different animals and their detailed accumulation in the lung tissue. The radioactive methods was as follows. Tritium label was introduced into ND by the substitution of hydrogen atoms. Tritium labeled nanodiamonds (<sup>3</sup>H-ND) particles biodistribution (the kinetics of accumulation and excretion) was studied in mice during six months using intravenous administration. The time of maximal ND content achievement was shown to depend on the type of organs from which it was gradually excreted. It is necessary to emphasize that <sup>3</sup>H-ND are nanodiamond particles without any chemical surface modifications opposed to articles [1-4]. These studies have revealed sufficiently fast and maximal ND cumulation in lungs of animals. It was found that nanodiamond particles are localized in the form of homogeneous incompact agglomerates in the cytoplasm of histiocytes. There was a lack of pathological changes in the structure of the cells that form the walls of the alveoli. The resulting data allowed to study in details ND biodistribution *ex vivo* for effective development of nanodiamonds-mediated anti-TB drug delivery systems.

This work is supported by the Russian Science Foundation (project № 18-73-00336).

### **References**

1. Y. Yuan, Y. Chen, J.-H. Liu, H. Wang, Y. Liu, Biodistribution and fate of nanodiamonds in vivo, *Diam Rel Mat* (2009) 18, p. 95.
2. X. Zhang, J. Yin, J. Li, Y. Zhu, W. Li, Q. Huang, Z. Zhu, Biodistribution and toxicity of nanodiamonds in mice after intratracheal instillation, *Toxicol Lett* (2010) 198, p. 237.
3. Y. Yuan, X. Wang, G. Jia, T. Wang, Y. Gu, S.-T. Yang, S. Zhen, H. Wang, Y. Liu, Pulmonary toxicity and translocation of nanodiamonds in mice, *Diam Rel Mat* (2010) 19, p. 291.
4. W. Qi, Z. Li, J. Bi, J. Wang, J. Wang, T. Sun, Y. Guo, W. Wu, Biodistribution of co-exposure to multi-walled carbon nanotubes and nanodiamonds in mice, *Nanoscale Res Lett.* (2012) 7, p. 473.



## Hybrid carbon-metal nanoparticles: structure, functions and processing

*Rozhkova N.N.*<sup>1</sup>, *Kovalchuk A.A.*<sup>1</sup>, *Rozhkov S.S.*<sup>1</sup>, *Goryunov A.S.*<sup>2</sup>, *Borisova A.G.*<sup>2</sup>, *Kucherik A.O.*<sup>3</sup>  
 rozhkova@krc.karelia.ru

<sup>1</sup> Institute of geology, Karelian Research Centre RAS, Petrozavodsk, Russia

<sup>2</sup> Institute of biology, Karelian Research Centre RAS, Petrozavodsk, Russia

<sup>3</sup> Stoletovs Vladimir State University, Vladimir, Russia

The ability to integrate metal nanoparticles into biological systems is of special importance for biology and biomedicine. Noble metal nanoparticles attract much interest because of their unique tunability of the plasmon resonance through variation of their size, shape, and composition. These nanoparticles are formed of clustered metal atoms that have to be protected by “capping agents” or stabilized by surface-active substances [1].

The specific characteristics of graphene-metal nanoparticle hybrids are widely used in the production of biosensor systems for detection of allergens, toxins, bioactives and foodborne pathogens [2]. An important aspect in the fabrication of biosensors is the preservation of biological activity of biomolecules while they are immobilized in the nanoparticle microenvironment. Recently it was shown that the interactions with shungite carbon (ShC) nanoparticles affect the native biological state of some blood proteins and the conditions that allow maintaining the biological functionality [3].

Clustering of graphene flakes ~ 1 nm is a key process of a multilevel structural organization scenario and of structural transformations in systems of various physicochemical nature of ShC. Clusterization of graphene flakes in the stable aqueous dispersion of ShC nanoparticles is well reproducible process [4]. The interaction of metal-ShC nanoparticles in aqueous dispersions was a subject of this study. Both dispersions of ShC and metal (Au, Ag) nanoparticles were processed jointly by laser pulses of different durations.

Laser irradiation was highly efficient in producing new types of hybrid ShC-Au and ShC-Ag nanoparticles. Hybrid nanoparticles were stable in water regardless of the laser pulse duration. While the processing parameters turned out to be critical to the structural organization of graphene clusters in the hybrids. They were characterized by using UV-Vis absorption, dynamic light scattering, Raman spectroscopy, and SEM methods.

Comparative study of the hybrids and original ShC nanoparticles in aqueous dispersions and films allows to consider graphene fragments of ShC as stabilizers and “capping agents” of Au- and Ag-nanoparticles in aqueous dispersions.

### References

1. Larginho M., Baptistaa P.V. *Journal of Proteomics*. (2012) **75**, 10, 2811-2823
2. Daniele M.A., Pedrero M., Burrs S., Chaturvedi P., Salim W.W.A., Kuralay F., Campuzano S., McLamore E., Cargill A.A., Ding S., Claussen J.C. In: *Nanobiosensors and Nanobioanalyse* Eds. Vestergaard M., Kerman K., Hsing IM., Tamiya E. Springer 2015. P.137-166.
3. Rozhkova N.N., Rozhkov S.P., Goryunov A.S. In *Carbon Nanomaterials, Sourcebook*. Ed. By Sattler K.D. Taylor&Francis Pub, 2016.V1 P. 151-174
4. Rozhkova N.N., Yemel'yanova G.I., Gorlenko L.E., Griбанov A.V., Lunin V.V/ *Glass Physics and Chemistry* (2011) **37**, 6, 613.

## Synthesis of Fluorine-doped Graphene Quantum Dots with High Singlet Oxygen Production

Li Zhenzhen<sup>1</sup>, Wang Dong<sup>1</sup>, Hu Xiaolong<sup>1</sup>, Bi Hong<sup>1</sup>

bihong@ahu.edu.cn

<sup>1</sup> School of Chemistry and Chemical Engineering, Anhui University, Hefei, China

Recently, graphene quantum dots (GQDs) is extensively applied in biological and medical fields such as bio-imaging, sensing, and image-guided therapy due to its superior optical property, good hydrophilicity, excellent biocompatibility, and extremely low cytotoxicity.<sup>[1,2]</sup> Here, we report the synthesis of a novel kind of fluorine-doped GQDs (F-GQDs) by an oxidative cutting method and using fluorinated graphite as raw material. As shown in Fig. 1a and 1b, the as-synthesized F-GQDs present an average size of 2.1 nm with the fluorine doping amount of 1.43 %. The F-GQDs emit green fluorescence at 365 nm excitation and the relative fluorescence quantum yield achieves 13.72%. Moreover, the cytotoxicity was tested by a MTT assay using HepG2 cell line as a model, the results reveal that the F-GQDs have a very low cytotoxicity (Fig. 1c). Further studies using electron spin resonance spectroscopy (EPR) find that the F-GQDs can generate high production of singlet oxygen (<sup>1</sup>O<sub>2</sub>) under a visible light irradiation, while taking 2,2,6,6-tetramethylpiperidien (TEMP) as a scavenger (Fig. 1d). It is expected that the F-GQDs can be potentially applied in the biomedical area such as fluorescence imaging and photodynamic therapy.

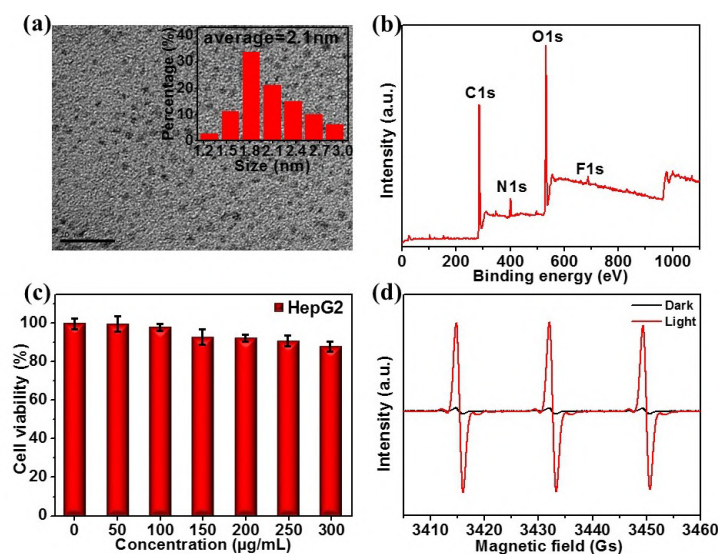


Fig.1. (a) TEM image of F-GQDs (Inset: the corresponding size distribution histogram). (b) XPS survey spectrum of F-GQDs. (c) MTT result of HepG2 cells viabilities after co-incubation with the different concentrations of F-GQDs for 24 h. (d) EPR spectra of photo-induced <sup>1</sup>O<sub>2</sub> generation by TEMP + F-GQDs (0.2 mg/mL). Samples were irradiated with a LED light (400-700 nm, 40 mW cm<sup>-2</sup>) for 12 min.

### References

1. W. S. Kuo, et al. *Biomaterials* (2017) **120** 185-194.
2. J. C. Ge, et al. *Nat. Commun.* (2014) **5** 4596-4603.

## Toxicity of nanodiamonds and its composites in relation to cancer cells, fungus and plants

*Chernysheva M.G.*<sup>1</sup>, *Mysanikov I.Yu.*<sup>2</sup>, *Klein O.I.*<sup>3</sup>, *Melik-Nubarov N.S.*<sup>1</sup>, *Grozdova I.D.*<sup>1</sup>, *Kulikova N.A.*<sup>1,3</sup>, *Badun G.A.*<sup>1</sup>

*chernysheva@radio.chem.msu.ru*

<sup>1</sup> Lomonosov Moscow State University, Moscow, Russia

<sup>2</sup> Vernadsky Institute of Geochemistry and Analytical Chemistry of Russian Academy of Sciences, Moscow, Russia

<sup>3</sup> Federal Research Center "Fundamentals of Biotechnology", Bach Institute of Biochemistry, RAS, Moscow, Russia

Detonation nanodiamonds possess high capacity to adsorption of different compounds and so this material can find an application in different areas of science and industry including bio- and medical fields. Despite of a rapidly growing and developing interest to nanodiamonds the question concerning its toxicity in the relationship to different objects is currently relevant.

In the presentation we summarized the results obtained for nanodiamonds and adsorption composites of nanodiamonds with toxic and non-toxic compounds. Adsorption complexes of nanodiamonds were obtained with benzyldimethyl-myristoylamine-propylammonium chloride monohydrate (Myramistin) that shows high toxic effect as free compound in the relationship to the adhesive epithelial-like MCF-7 cells and fungi namely *Aspergillus niger*. The other nanodiamonds adsorption composites were obtained with coal humic acids, that can be uptake by plants and fungi, but do not show toxic effects. The composition of the composites was determined using radiotracer method: in the adsorption study we used tritium labeled Myramistin and coal humic substances obtained by means of tritium thermal activation method.

In the case of nanodiamond-myramistin complex we have observed the decrease in myramistin toxicity in the relationship to MCF-7 cells but binding efficiency of both nanodiamonds and myramistin was preserved in the case of the formation of the composite [1].

It was shown that nanodiamonds in the suspension can be uptake by plants and penetrate into the green shoots through the roots [2]. Humic substances can adsorb on nanodiamonds with formation of the composite with different penetration ability in the relationship to plant. Noted that both nanodiamonds and nanodiamonds-humic acids adsorption composites do not inhibit the photosynthesis process, but were slightly toxic to wheat plants under excessive light.

Being adsorb on nanodiamonds humic substances together with Myramistin do not affect on the action of Myramistin inhibition of the growth and development of the fungus *Aspergillus niger*. Noted that the inhibition of *A. niger* growth by nanodiamond-Myremistin composite is depends on nanodiamond initial zeta potential. Peculiarity of nanodiamond effects will be discussed in the presentation.

This work was supported by Russian Foundation for Basic Research (17-03-00985, 18-33-20147)

### References

1. G. Chernysheva, N.S. Melik-Nubarov, I.D. Grozdova, I.Yu. Myasnikov, V.N. Tashlitsky, G.A. Badun, *Mendeleev Communications* (2017) **27**, 421.
2. G. Chernysheva, I.Yu. Myasnikov, G.A. Badun, D.N. Matorin, D.T. Gabbasova, A.I. Konstantinov, V.I. Korobkov, N.A. Kulikova, *J. Soils Sediments* (2018) **18**, 1335.

## **Nanodiamonds-film as a modifier for improving heart valve biological prostheses materials**

*Chernysheva M.G.*<sup>1</sup>, *Chaschin I.S.*<sup>2</sup>, *Sinolits A.V.*<sup>1</sup>, *Vasil'ev V.G.*<sup>2</sup>, *Popov A.G.*<sup>1</sup>, *Badun G.A.*<sup>1</sup>, *Bakuleva N.P.*<sup>3</sup>

*chernysheva@radio.chem.msu.ru*

<sup>1</sup> Lomonosov Moscow State University, Moscow, Russia

<sup>2</sup> Nesmeyanov Institute of Organoelement Compounds, RAS, Russia

<sup>3</sup> A.N. Bakulev National Medical Research Centre of Cardiovascular Surgery, Russia

Xenogenic biological prostheses of the heart valves based on bovine pericardium are intensively used in the world of cardiac surgery practice because it is sufficiently strong and elastic material that is rich in collagen connective tissue. The valve also should have a high biocompatibility to eliminate toxic effects on the human body. In present study we applied nanodiamond coverage of bovine pericardium to provide pericardium tissue additional strength.

To prepare nanodiamond film on the surface of bovine pericardium matrix was stirred in the aqueous suspension of nanodiamonds. The thickness of the film was determined with the help of tritium labeled nanodiamonds that were obtained using tritium thermal activation method [1]. The obtained material was characterized by scanning electron microscopy. To characterize coated matrix mechanical properties, the collagen samples were initially cut into rectangular pieces with lateral sizes of approximately  $7 \times 0.5 \text{ cm}^2$  were coated with NDs and stress-strain curves were recorded with a universal testing machine 5 kN load cell LLOYD Instruments LR5R. Modification of the matrix with nanodiamonds results in the increase of both final values of Young modules and tensile strength. Moreover, it was found, that premodification of nanodiamonds with chitosan results in further increase of both values.

The preparation of matrix and observed effects will be discussed in the presentation.

This work was supported by Russian Foundation for Basic Research (grants № 17-03-00985, 17-03-00362, 18-33-20147). Electron microscopy characterization was performed in the Department of Structural Studies of Zelinsky Institute of Organic Chemistry, Moscow.

## Aqueous dispersion of fullerene C<sub>60</sub> anti-HCMV and anti- HSV1 activity

Shershakova N.<sup>1</sup>, Klimova R.<sup>2</sup>, Momotyuk E.<sup>2</sup>, Demidova N.<sup>2</sup>, Andreev S.<sup>1</sup>, Fedorova N.<sup>2</sup>, Chernoryzh Y.<sup>2</sup>, Yurlov K.<sup>2</sup>, Baraboshkina E.<sup>1</sup>, Turetskiy E.<sup>1</sup>, Kushch A.<sup>2</sup>, Khaitov M.<sup>1</sup>, Gintsburg A.<sup>2</sup>

nn.shershakova@nrcii.ru

<sup>1</sup> NRC Institute of Immunology FMBA of Russia, Moscow, Russian Federation

<sup>2</sup> N. F. Gamaleya Federal Research Center for Epidemiology & Microbiology, Moscow, Russian Federation

**Background:** Herpes simplex viruses type 1 (HSV-1) and type 2 (HSV-2) and human cytomegalovirus (HCMV) are common pathogens in the human population. Well-known antiviral drugs have a number of drawbacks including toxicity and resistance to viral neutralization with prolonged use. Previously it was shown a fullerene adducts possess an inhibiting activity against herpes simplex virus (HSV1), however such activity has not been studied for the aqueous dispersion of unmodified fullerene. In connection with the development of biocompatible and scalable method for obtaining a concentrated aqueous fullerene C<sub>60</sub> solution (AFS), we evaluated the anti-HSV and anti-HCMV activities of AFS using *in vitro* and *in vivo* tests.

**Methods:** The AFS (1 mg of C<sub>60</sub>/ml) was produced by novel method using a lab setup for tangential ultrafiltration. The antiviral activities was evaluated in Vero cells, infected with HSV1, and in HF cells, infected with HCMV, by a standard plaque reduction assay. The IC<sub>50</sub> and selectivity index (SI) were calculated. HSV1 experimental model *in vivo* was induced in Balb/c mice by the epicutaneous HSV1 suspension application in scarified areas. After 24 h, mice were treated with AFS, and parallel for comparison ACV (Acyclovir) ointment or PBS, one time daily for 3 days. Therapeutic effects were assessed by the severity of the development of virus-specific skin lesions.

**Results:** *In vitro* antiviral study has shown that the AFS suppressed HSV1-infection with SI>100. In pre-treatment assay, maximal inhibition effect was shown for AFS (93±6.2%) and minimal for ACV (37±2.6%). In post-treatment assay, inhibition of HSV1-infection was 93±5.6% for ACV and 60±4.4% for AFS. In virucidal assay, AFS displayed the high inhibitory activity: 98.2±1.8%. Skin damage was minimal in animals treated with AFS and ACV. However, the first showed effect 24 h earlier and at molar concentration 500-fold lower than the ACV. At concentrations 50 and 10 µg/ml, AFS produced anti-HCMV effect prior to 82±4.6% and 57±1%, respectively, and 80±2.6% and 27±1% after infection. In the tested concentrations AFS displayed no virucidal activity. IC<sub>50</sub> determined by linear regression was 8.0±0.7 µg/ml for prior-infection and 30±2.8 µg/ml for post-infection assay. Anti-HCMV activity of AFS was dose-dependent both in pre- and post-treatment assays. The cytotoxicity of AFS was not observed even at the maximum studied concentration.

**Conclusion:** The results suggest that AFS exhibits a pronounced therapeutic activity against HSV1- and HCMV-infection and it is a promising candidate for a new antiviral drug.

## 2D NANOCARBONES AS THE BASE OF COMBINED MICROBIAL FORMULATION

*Voznyakovskii A.P.*<sup>1,2</sup>, *Novikova I.I.*<sup>3</sup>, *Boikova I.V.*<sup>3</sup>, *Neverovskaya A. Yu.*<sup>1</sup>, *Voznyakovskii A.A.*<sup>4</sup>, *Ganin P.G.*<sup>5</sup>

*voznap@mail.ru*

<sup>1</sup> Lebedev Research Institute for Synthetic Rubber, Saint-Petersburg, Russia

<sup>2</sup> State Institute of Technology, Saint-Petersburg, Russia

<sup>3</sup> Institute of plant protection, Saint-Petersburg, Russia

<sup>4</sup> Ioffe Institute, Saint-Petersburg, Russia

<sup>5</sup> State chemical and pharmaceutical university, Saint-Petersburg, Russia

Nanotechnology, as an interdisciplinary discipline, unites the efforts of research groups working, it would seem, in incompatible areas. Thus, interest has arisen in studies devoted to the study of the functional features of microbial cells located on the surface of 2D graphene structures. Perhaps such interest is since at present biological science is moving from the traditional concept of microbial cells as strictly individual organisms to the concept of microbial communities as integral structures that regulate their behavioral responses depending on changes in living conditions. However, despite the shown efficiency of using graphene in biology, up to the present its use has not been included in the daily practice of laboratories. This fact is due to the need to have a method of synthesis of graphene in quantities that provide real needs of the microbiological industry.

To solve this problem we using 2D carbon structures (multilayer graphene - MG), which we synthesized by the original method of carbonization of biopolymers under the conditions of the process of solid-flame combustion. The specificity of the structure of a graphene sheet makes it possible to form a significant amount of hydrogen bonds along a planar surface. The latter circumstance determines the possibility of reliable adsorption of microbial cells on the surface of graphene sheets.

This work is devoted to the study of the viability and oil-oxidizing activity of strains - hydrocarbon destructors when microorganism cells are applied to MG particles obtained by carbonization of lignin under the conditions of the process of solid-flame combustion.

The results indicate a good survival rate and high activity of the studied cultures on samples of nanocarbon and the possibility of creating drugs based on oil-oxidizing microorganism and graphene strains. It was shown that this result can be associated with good protection of cells and their metabolites by MG particles from solar insolation, drying, and oxidation [figure 1], which will increase the shelf life and duration of action of bioinorganic preparations.

The work was supported by the RFBR grant №19-29-05248.

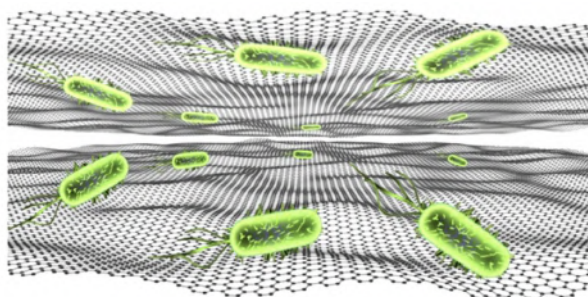


Figure 1. The pattern of distribution of microorganisms on the surface of graphene sheets.

## Application of adaptive data analysis methods for monitoring of carbon nanocomposites in biological medium

*Sarmanova O.E.*<sup>1</sup>, *Burikov S.A.*<sup>1</sup>, *Dolenko S.A.*<sup>2</sup>, *Efitorov A.O.*<sup>2</sup>, *Isaev I.V.*<sup>2</sup>, *Laptinskiy K.A.*<sup>1,2</sup>, *Filippova E.A.*<sup>1</sup>, *Dolenko T.A.*<sup>1</sup>

*oe.sarmanova@physics.msu.ru*

<sup>1</sup> Lomonosov Moscow State University, Moscow, Russia

<sup>2</sup> Skobeltsyn Institute of Nuclear Physics, Lomonosov Moscow State University, Moscow, Russia

The concept of a therapy-accompanying diagnostics has gained a great popularity and turned into a rapidly evolving field of study. Plenty of nanocomposite designs have been suggested and some of them have been already clinically approved<sup>1</sup>. Nanographene oxide (nGO) is one of the most promising object to be utilized as fluorescent biomarker and drug carrier due to its photostable fluorescent properties and high biocompatibility. In this study, nGO + copolymer PEG-PEI (Cop) + folic acid (FA) nanocomposites and their components were used as the objects of the study. It is crucial to control the nanocomposite excretion from the organism, since its accumulation in the body can lead to delayed toxicity effect. In our study, one should consider that nanocomposites degrade as they fulfil their functions, therefore, initial composites and their degraded components can be present in urine. As long as all the nanocomposite's components demonstrate high fluorescence properties, fluorescent spectroscopy is an optimal method for their excretion control. Moreover, it is non-invasive and cheap technique. However, it has one major drawback - autofluorescence, originating from biological tissue fluorophores, prevents one from extracting nanocomposite fluorescence signal. It occurs because the fluorescent bands of both the nanocomposite's components and the tissue fluorophores substantially overlap. Thus, identification and determination of the nGO nanocomposites' concentration excreted from the body represents a multiparameter inverse problem.

In this study we propose a new approach to the solution of such problem of monitoring of the removal of luminescent nanocomposites based on carbon dots and their components with urine using artificial neural networks (ANN). The database consisting of 1459 fluorescence spectra of carbon nanomaterials suspensions with 8 combinations of classes {nGO+Cop+FA}, {nGO+Cop}, {FA}, {nGO+Cop+FA, nGO+Cop}, {nGO+Cop+FA, FA}, {nGO+Cop, FA}, {nGO+Cop+FA, nGO+Cop, FA}, {urine without nanoparticles} was obtained. At the first stage the obtained spectra were visualized with Kohonen self-organizing maps. On the basis of the obtained maps k-means clusterization procedure was performed. Finally, a complex multiparametric problem of optical nanoparticle imaging in a biomaterial was solved with the help of perceptrons, which were used on a full set of spectra and within the selected clusters. In results it was determined which nanoparticles - the nanocomposites themselves and/or its components - and in what quantity are removed from the body with human urine. The advantages and disadvantages of all used adaptive data analysis methods are discussed in the report.

The study was supported by the grant of Russian Foundation for Basic Research (project No. 18-32-00779\_mol\_a) and by Foundation for the Advancement of Theoretical Physics and Mathematics "BASIS" (project No.18-2-6-198-1). The authors are sincerely grateful to O.Shenderova for providing carbon dots and to N. Prabhakar, D. Sen Karaman and J.M.Rosenholm for the synthesis of nanocomposites.

### References

1. Azzouzi A.R., Vincendeau S., Barret E., Cicco A., Kleinclaus F., van der Poel H.G., Stief C.G., Rassweiler J., Salomon G., Solsona E. Padeliporfin vascular-targeted photodynamic therapy versus active surveillance in men with low-risk prostate cancer (CLIN1001 PCM301): An open-label, phase 3, randomised controlled trial. *Lancet Oncol.* (2017)**18**, 181.

## Intermolecular interaction of phi29 DNA polymerase with carbon nanostructures and buffer solution in process of single-molecular DNA sequencing: molecular modeling

Zakharov A.A.<sup>1</sup>, Plastun I.L.<sup>1</sup>, Naumov A.A.<sup>1</sup>

wolfserk@mail.ru

<sup>1</sup> Yuri Gagarin State Technical University of Saratov, Saratov, Russia

The aim of present work is analysis by numerical modeling of phi29 DNA polymerase intermolecular interaction with carbon nanostructures and buffer solution in process of single-molecular DNA sequencing [1]. Buffer solution include a following substance: TRIS(hydroxymethyl)aminomethane hydrochloride (TRIS), hydrogen chloride, magnesium chloride, ammonium sulfate. Also the buffer solution includes the carbon nanostructures - alkanes. In polymerisation process molecules of DNA polymerase phi29 coupled on molecular complex HO-EG3-C11-S-S-C11-EG6-NHCO-Maleimide (named alkane) and they interaction are registered by sensors in the sequencer.

Molecular modeling is based on simulation by Material Studio software package. Basic numerical method is DFTB (Density Functional based Tight Binding) [2].

Figure 1 shows the simulated molecular complex of buffer solution with phi29 DNA polymerase and its calculated Raman spectrum.

The numbers in Figure 1 (b) indicate the frequencies characteristic of the components of the molecular complex: 1 ( $134\text{ cm}^{-1}$ ) - magnesium chloride, 2 ( $2319\text{ cm}^{-1}$ ), 3 ( $2630\text{ cm}^{-1}$ ), 4 ( $2946\text{ cm}^{-1}$ ), 5 ( $3657\text{ cm}^{-1}$ ), - TRIS, 6 ( $3836\text{ cm}^{-1}$ ) - ammonium sulfate.

It can be seen from the spectrum that the main substance involved in the formation of hydrogen bonds is TRIS, since its peaks lie in the field of the formation of hydrogen bonds. If it is necessary to create strong supramolecular compounds that improve the quality of sequencing, it is necessary to increase the concentration of TRIS.

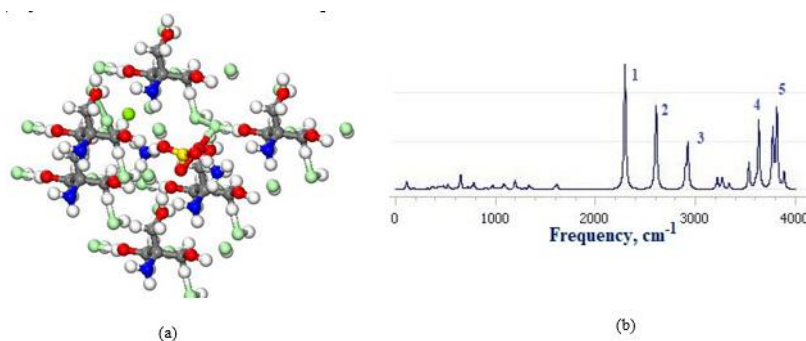


Fig.1. Structure (a) and Raman spectrum (b) of the molecular complex TRIS (hydroxymethyl) aminomethane - hydrogen chloride — magnesium chloride — ammonium sulfate.

### References

1. E.D. Akhunov, V.A. Vakhitov, A.V. Chemeris, DNA sequencing. - M.: Science, 1999. - 427 p. (In Russian).
2. Filik, J.N. Harvey, N.L. Allan, P.W. May, J.E. P. Dahl, L. Shenggao and R. M. K Carlson, Spectrochim. Acta. Part A: Molecular and Biomolecular Spectroscopy (2006), **Volume 64, Issue 3**, P. 681-692.



# Full Contents

<b>Invited Lectures</b>	5
<b>I-01 Sabirov Denis</b> Dipole polarizability of fullerene compounds: Numerical estimates and their applications	6
<b>I-02 Tristan Petit</b> Spectroscopic insights on the nanocarbon-water interface	7
<b>I-03 Shenderova O.A.</b> Fluorescent Diamond Particles: Synthesis, Properties, and Applications	8
<b>I-04 Jackman R.B.</b> Lateral Diamond Nanowires with exceptionally high current density; properties and applications	9
<b>I-05 Bi Hong</b> Synthesis, Structure and Novel Applications of Heteroatoms-Doped Carbon Quantum Dots	10
<b>I-06 Matsumoto K.</b> Sugar Chain Modified Graphene FET for High Sensitive & Selective detection of Influenza Virus	11
<b>I-07 Zhu H.W.</b> Graphene-on-surfaces: structural design and multifunctional applications	12
<b>I-08 Choi Suk-Ho</b> Graphene-based low-dimensional hybrid heterostructures and device applications	13
<b>I-09 Tascon J.M.D.</b> Electrochemically exfoliated graphene: strategies to avoid graphene oxidation	14
<b>I-10 Peter J.F. Harris</b> Formation of carbon nanotubes from graphite	15
<b>I-11 Nasibulin Albert G.</b> Carbon Nanotubes: From Synthesis to Applications	16
<b>I-12 Ohno Y.</b> Highly-stretchable carbon nanotube devices for wearable electronics applications	17
<b>I-13 Nesvizhevsky V V</b> Fluorinated nanodiamond as unique neutron reflector	18
<b>I-14 Vikharev A.L.</b> CVD diamond: technology, properties and applications	19
<b>I-15 Bukalov S. Sergey</b> RAMAN SPECTROSCOPY AS A BASIC TECHNIQUE FOR IDENTIFICATION OF VARIOUS MODIFICATIONS OF CARBON	20
<b>I-16 Brzhezinskaya M.</b> Synchrotron based study of advanced carbon nanostructures	21
<b>I-17 Shvidchenko A.V.</b> Analysis of nanoparticles sizes in sols by dynamic light scattering (DLS) technique	22
<b>I-18 P.M. Tolstoy</b> NMR spectroscopy of weakly ordered nanostructures: capabilities, techniques, examples	23
<b>I-19 Ber Boris</b> Secondary Ion Mass Spectrometry (SIMS) and its Applications for the Characterization of Carbon-Based Material	24
<b>Oral Presentations</b>	25
<b>Or-01 ORI Ottorino</b> Fullerene stability. A topological approach	26
<b>Or-02 Amusia M.Ya.</b> Intershell correlations in endohedral atoms	27

<b>Or-03 Krylov D.S.</b>	Magnetic studies of endohedral fullerenes	28
<b>Or-04 Kuznetsov N.M.</b>	DETONATION NANODIAMOND HYDROSOLS: RHEOLOGY AND STRUCTURE	29
<b>Or-05 Usoltseva L.O.</b>	Thermal conductivity of nanodiamond aqueous dispersions by thermal lensing and heat flow techniques	30
<b>Or-06 Kudryavtsev O.S.</b>	Luminescent properties of Si- and N-doped nanodiamonds synthesized from adamantane	31
<b>Or-07 Osipov V.Yu.</b>	Photoluminescence from NV centers in 5 nm detonation nanodiamonds: identification and large sensitivity to magnetic field	32
<b>Or-08 Vervald A.</b>	Relationship between the type of hybridization of carbon nanoparticles and their fluorescence.	33
<b>Or-09 Shames A.I.</b>	Paramagnetic defects in e-beam irradiated Ib type HPHT micro- and nano-diamonds: effects of variable fluence and annealing	34
<b>Or-10 Orlanducci Silvia</b>	Gold and nanodiamond: new jewels for sensing, imaging, diagnostic and drug delivery.	35
<b>Or-11 Kulvelis Yu.V.</b>	Composite proton-conducting membranes with nanodiamonds	36
<b>Or-12 Alexander C Pakpour-Tabrizi</b>	Lateral boron doped diamond nanowires, properties, performance and prospects for quantum technologies.	37
<b>Or-13 Okotrub A.V.</b>	Microcapacitors based on fluorinated graphene films	38
<b>Or-14 Bairamukov V.Yu.</b>	Carbon-metal endohedral structures synthesized by pyrolysis	39
<b>Or-15 Zinin P. V.</b>	Two photon fluorescence of the hollow spherical carbon nitride nanostructures	40
<b>Or-16 Forro Laszlo</b>	Charge transport in composites with 2D, 1D and 0D carbon nanostructure fillers	41
<b>Or-17 Eletsii A.V.</b>	Percolation phenomena in nanocarbon composites	42
<b>Or-18 Yablokov M.Yu.</b>	Raman study of gradient polypropylene composites filled with carbon black	43
<b>Or-19 Piotrovskiy L.B.</b>	The biodegradation of fullerene C <sub>60</sub> by human enzyme myeloperoxidase	44
<b>Or-20 Garashchenko B.L.</b>	Carbon nanoparticles as carriers for medical radionuclides	45
<b>Or-21 Palmieri Elena</b>	Nanodiamond and cellulose: a technological liaison for restoration methodologies	46
<b>Or-22 Lebedev V.T.</b>	Hybrid molecular structures with nanodiamonds for biomedicine	47
<b>Or-23 Ktitorov S.A.</b>	Complex conductivity of monolayer graphene and zitterbewegung	48
<b>Or-24 Radovic L.R.</b>	On the mechanism of the oxygen reduction reaction at graphene surfaces: insights from computational quantum chemistry	49
<b>Or-25 Aristov V.Yu.</b>	Graphene on the (001) Surface of Cubic-SiC Epilayers: Growth Mechanism and Electronic Properties	50
<b>Or-26 Rabchinskii M.K</b>	Functionalized graphenes: from synthesis to applications	51

<b>Or-27 Stanislav A. Evlashin</b>	52
Nitrogen incorporation in carbon structures by plasma post treatment.	
<b>Or-28 Shevelev V.O.</b>	53
Influence of molecular oxygen on oriented and mismatched graphene on Co(0001)	
<b>Or-29 Talyzin Alexandr V.</b>	54
Swelling of graphene oxide membranes in alcohols: effects of molecule size and ageing.	
<b>Or-30 Dimiev Ayrat</b>	55
Harnessing the Mechanism of Graphene Oxide Formation. The Role of Water.	
<b>Or-31 Stolyarova S.G</b>	56
Hot pressing synthesis of MoS <sub>2</sub> /perforated graphene materials for efficient Li-ion batteries	
<b>Or-32 Kuznetsova V.R.</b>	57
Impact structure of carbon nanotubes on their electrochemical properties	
<b>Or-33 Tambasov I.A.</b>	58
Thermoelectric properties of single-wall carbon nanotube thin films obtained by vacuum filtration	
<b>Or-34 Grebenko A.K.</b>	59
AFM Ultradensification of SWCNT network. Optical and mechanical properties.	
<b>Or-35 Kharlamova M.V.</b>	60
Electronic properties of filled single-walled carbon nanotubes	
<b>Or-36 Mkrtchyan A. A.</b>	61
Multiregime pulse fiber laser based on electrochemically gated carbon nanotube saturable absorber	
<b>Or-37 Bezrodny A.E.</b>	62
New Frontiers in Single-walled Carbon Nanotubes Applications	
<b>Or-38 Shashkov S.N.</b>	63
Characterization of Carbon Materials with Confotec® MR200 Confocal Raman Microscop	
<b>Or-39 Yagubov V.S.</b>	64
Studying the effect of weight concentration of CNTs on the heat release mode in self-regulating heaters	
<b>Or-40 Men'shchikov I.E.</b>	65
Carbon adsorbents of high density with precision nanoporous structure for adsorption storage systems of methane	
<b>Or-41 Vozniakovskii A.P.</b>	66
CARBON NANOMATERIALS BASED ON PLANT BIOPOLYMERS AS SORBENTS OF RADIONUCLIDES	
<b>Poster session 1: Fullerenes. Nanodiamond Particles.</b>	67
<b>P1-01 Bogdanov V.P.</b>	68
Electrophilic trifluoromethylation of fullerene anions: simple, selective, efficient.	
<b>P1-02 Kinzyabaeva Zemfira S.</b>	69
Selective synthesis of dioxane monoadducts of the C <sub>60</sub> and C <sub>70</sub> fullerenes with α-diols in heterogeneous conditions under ultrasonication	
<b>P1-03 Okolzina A.I.</b>	70
Aromatic conjugated fullerenes for organic electronics	
<b>P1-04 Kulbachinskii V.A.</b>	71
Superconductivity in Alkali-Doped Fullerenes with Wood's metal and heterofullerenes with two different alkali metals A <sup>(1)</sup> A <sup>(2)</sup> MC <sub>60</sub>	
<b>P1-05 K. P. Meletov</b>	72
The photopolymerization rate and activation energy of C <sub>60</sub> rotations in fullerene and its molecular complexes.	
<b>P1-06 Tropin T.V.</b>	73
Investigations of polystyrene-fullerene nanocomposites by neutron and X-ray reflectometry	
<b>P1-07 Lebedev V.T.</b>	74
Mechanisms of supramolecular ordering of water-soluble derivatives of fullerenes in aqueous media	

<b>P1-08 Faradzheva M.P.</b>	75
Superconducting properties of nanostructure based on C <sub>60</sub> /YBCO.	
<b>P1-09 Amusia M.Ya.</b>	76
Time delay in electron-fullerene elastic scattering	
<b>P1-10 Kosaya M.P.</b>	77
Double-caged fullerene derivatives with long alkyl moiety for solar cells	
<b>P1-11 Pykhova A.D.</b>	78
Difluoromethylation of trimetallic nitride endohedral fullerenes	
<b>P1-12 Dudnik A.I.</b>	79
Process control of fullerene synthesis by the influence of a magnetic field on the plasma of a high-frequency carbon arc	
<b>P1-13 Gimaldinova M.A.</b>	80
Stability of small nitrogen clusters inside the carbon cage: Molecular dynamic study	
<b>P1-14 Dudnik A.I.</b>	81
Fullerene formation in plasma at different rates of temperature and electron concentration change	
<b>P1-15 Kulvelis Yu.V.</b>	82
Aggregation of C <sub>70</sub> fullerene in an o-xylol solution. The features revealed by the dynamic light scattering methods	
<b>P1-16 Safyannikov N.M.</b>	83
Cryometry data and excess thermodynamic functions in the binary systems: adduct of fullerene C <sub>60</sub> , fullerene C <sub>70</sub> - H <sub>2</sub> O	
<b>P1-17 Vysochanskaya O.N.</b>	84
Skeletal transformations of buckminsterfullerene upon chlorination	
<b>P1-18 Kuzmenko M.O.</b>	85
Fullerenes for medical purposes: from active bioagent to drug-delivery system	
<b>P1-19 Nikolaev D.N.</b>	86
Chromatography-free synthesis of mono-adducts of fullerene C <sub>60</sub> .	
<b>P1-20 Sinitza A. S.</b>	87
Possible role of sp-defect migration in an odd fullerene shell in selection of abundant isomers of fullerenes	
<b>P1-21 Lebedev V.T.</b>	88
Comparative study of endofullerenols with magnetic atoms in aqueous solutions by neutron scattering and NMR	
<b>P1-22 Turetskiy E. A.</b>	89
Characterizing size and composition of fullerene nanoparticles in aqueous dispersions	
<b>P1-23 Tomchuk A.A.</b>	90
Fullerene-based colloids for biomedical applications: Structural study by scattering techniques	
<b>P1-24 Kuzmin A. V.</b>	91
High pressure behavior of the crystal structure of the fullerene molecular complex with ferrocene C <sub>60</sub> *{Fe(C <sub>5</sub> H <sub>5</sub> ) <sub>2</sub> } <sub>2</sub> .	
<b>P1-25 Galimov D.I.</b>	92
Luminescence switching properties of fullerene[60]-containing spiropyrans, a promising light-controlled molecular switches	
<b>P1-26 Popov V.V.</b>	93
Magnetic properties of a fullerene composite	
<b>P1-27 Andreev S.M.</b>	94
Comparative thin-layer chromatographic profile of water dispersions of C <sub>60</sub>	
<b>P1-28 Konarev D.V.</b>	95
Metallic and antiferromagnetic states with strong spin frustration in fullerene radical-anion salts with triangular lattices	
<b>P1-29 Urintsev D.I.</b>	96
Electrochemical study of S <sub>6</sub> -C <sub>60</sub> (CF <sub>3</sub> ) <sub>12</sub> : a new general methodology for low-soluble fullerene derivatives	

<b>P1-30 Pirogova M.O.</b>	Luminescence properties of fullerene C <sub>60</sub> in aqueous media	97
<b>P2-01 Badun G.A.</b>	Adsorption of alkyltrimethylammonium bromides on nanodiamonds	98
<b>P2-02 Simunin M.M.</b>	Application of aluminum oxide nanofibers as a carrier for nanodiamonds.	99
<b>P2-03 Dolmatov V. Yu.</b>	Obtaining of diamonds from detonation of individual explosives.	100
<b>P2-04 Nozhkina A.V.</b>	Influence of physico-chemical environment to get nano-size surface roughness in machining of diamond single crystals	101
<b>P2-05 Dolmatov V. Yu.</b>	Influence of explosives power density the yield of detonation nanodiamonds.	102
<b>P2-06 Ivanov M.G</b>	Formulation and properties of a novel perfluoropolyether based fluid containing nanodiamonds	103
<b>P2-07 Savin S.S.</b>	The new method of purification of detonation nanodiamond and obtaining its stable aqueous suspensions	104
<b>P2-08 Leshchev D.V.</b>	Sensitivity analysis of gas-phase chemistry leading to the formation of carbon nanoparticles	105
<b>P2-09 Soboleva O.A.</b>	Autoradiography study of nanodiamonds distribution in the composite polymeric films	106
<b>P2-10 Soboleva O.A.</b>	Mechanical properties of the composite films based on nanodiamonds and polyvinyl alcohol: influence of nanoparticle modification, thermal annulations, and liquid media	107
<b>P2-11 I.I. Kulakova</b>	Regularities of the detonation nanodiamond surface chlorination	108
<b>P2-12 Breev I.D.</b>	ODMR study in diamonds microcrystals synthesized from detonation nanodiamonds under HPHT conditions without metal catalyst.	109
<b>P2-13 Palmieri Elena</b>	Nanodiamond cellulose composites for printed energy storage devices on paper substrates	110
<b>P2-14 Spitsyn B.V.</b>	To the diamond nanooctahedra thermochemistry	111
<b>P2-15 Laptinskiy K.A.</b>	Electronic effects on the interface "nanodiamond surface groups - water molecules"	112
<b>P2-16 Laptinskiy K.A.</b>	Luminescence of detonation nanodiamonds with different functionalization in ordinary and heavy water	113
<b>P2-17 Vervald A.</b>	The influence of surfactants on the fluorescence of nanodiamonds	114
<b>P2-18 Eidelman E.D.</b>	Quantifying absorption and scattering contributions to light attenuation by nanodiamonds	115
<b>P2-19 Razgulov A.A.</b>	Pressure effect on electron-phonon coupling in GeV centres in diamond.	116
<b>P2-20 Popov V.A.</b>	Non-agglomerated nanodiamonds inside metal matrix	117
<b>P2-21 Yudina E.B.</b>	Structural properties of stabilized colloidal nanodiamonds grafted by rare earth metals	118
<b>P2-22 Vereshchagin A.L.</b>	CALORIMETRY OF LOW-TEMPERATURE LIQUID-PHASE OXIDATION OF CARBON NANOPARTICLES	119
<b>P2-23 Vereshchagin A.L.</b>	Use of nanodiamond for absorption of aerosol particles	120

<b>P2-24 Dolmatov V.Yu.</b>	Development of technology for producing chromium-diamond coatings using dry diamond-containing compounds.	121
<b>P2-25 Lychagin E.V.</b>	Nano-diamond powder as reflector for slow neutrons	122
<b>P2-26 Aleksenskii A.E.</b>	Deagglomeration of shock-compressed synthesis nanodiamond	123
<b>P2-27 D.M.Samosvat</b>	Size effect in the spectra of electron paramagnetic resonance of impurity centers in diamond nanoparticles	124
<b>P2-28 Rubtsov I.A.</b>	Dynamic and static investigation of explosion nanodiamonds	125
<b>P2-29 Sigalaev S.K.</b>	Hexagonal diamond is in detonation nano and microdiamonds	126
<b>P2-30 Popov V.A.</b>	Use of nanodiamonds for in situ synthesis of TiC reinforcing nanoparticles in MMC	127
<b>P2-31 Davydov V.A.</b>	HPHT synthesis of ultranano-sized diamonds with colour centres	128
<b>P2-32 Besedina N.A.</b>	Ultrafine nanodiamond fractionation by ultracentrifugation	129
<b>P2-33 Vlasov I.I.</b>	Broadband photoluminescence of nanodiamonds: intrinsic feature or another carbon phase?	130
<b>P2-34 Tomchuk O.V.</b>	SANS analysis of aqueous dispersions of Eu- and Gd-grafted nanodiamond particles	131
<b>P2-35 Belousov S.I.</b>	DIELECTRIC PROPERTIES OF DETONATION NANODIAMOND SUSPENSIONS IN POLYDIMETHYLSILOXANE	132
<b>P2-36 Tomchuk O.V.</b>	Composite aqueous dispersions of graphene oxide – detonation nanodiamond by small-angle scattering	133
<b>P2-37 Yelisseyev A.P.</b>	Lonsdaleite effect on optical properties of impact diamonds	134
<b>P2-38 Yelisseyev A.P.</b>	Thermoluminescence in diamonds of different genesis and types	135
<b>P2-39 Kagan M.S.</b>	Poole-Frenkel' Effect in Boron-Doped Diamond	136
<b>P2-40 Vins V.G.</b>	UHT annealing of brown centers and radiation defects in CVD diamond	137
<b>P2-41 Fomina I.G.</b>	Novel hybrid nanomaterials based on iron containing diamonds	138
<b>P2-42 Utesov O.I.</b>	New theory of crystalline nanoparticles Raman spectra	139
<b>P2-43 Spitsyn B.V.</b>	The effect of the detonation nanodiamond modification on its functional properties	140
<b>P2-44 Shakhov F.M.</b>	Green N-V-N luminescence of diamond obtained by sintering of polycrystalline nanodiamonds at high pressure	141
<b>P2-45 Shestakov M.S.</b>	Advanced oxidation process for detonation nanodiamond purification and surface modification	142
<b>P2-46 Shakhov F.M.</b>	Gamma-radiation effect on the photoluminescence of the polymer composite MEH-PPV / detonation nanodiamond	143

<b>P2-47 Kochetkov F.M.</b>		
	Diamond crystals synthesized from graphite with a nickel catalyst and aluminum as a nitrogen getter at HPHT	144
<b>Poster session 2: Carbon Nanostructures. School for Young Scientists.</b>		145
<b>P3-01 Lugvishchuk D.S.</b>		
	Natural gas partial oxidation process as a way to synthesize graphitized carbon soot	146
<b>P3-02 Kazachenko V.</b>		
	Structure, properties, and carbon component evolution in nanocomposite TiN-C coating	147
<b>P3-03 Mitberg E.B.</b>		
	Characterization of graphitized carbon formed as a byproduct of partial oxidation of natural gas	148
<b>P3-04 Posrednik O.V.</b>		
	On the N <sub>2</sub> and NH <sub>3</sub> adsorption on silicon carbide	149
<b>P3-05 Kashkarov A.O.</b>		
	Extended structures of detonation soot of HES	150
<b>P3-06 Orlova T.S.</b>		
	Nickel nanoparticles - biomorphic carbon composite for energy storage devices	151
<b>P3-07 Sovyk D.N.</b>		
	Periodically Ordered Opal Nano-Structures Embedded in Single Crystal Diamond: a route to 2D and 3D photonic crystals	152
<b>P3-08 Torok Gy.</b>		
	Structural investigation of aluminum-carbon nanocomposite	153
<b>P3-09 Moshnikov I.A.</b>		
	Biomodification of natural nanostructured shungite carbon and related electrophysical properties	154
<b>P3-10 Kharisov Boris Ildusovich</b>		
	Synthesis of metal-decorated micro- and nanoporous carbons via pyrolysis of ZIF- and HKUST-type MOFs.	155
<b>P3-11 Nechaev Yu.S.</b>		
	On the kinetic analysis of the hydrogen thermal desorption spectra for graphite and advanced carbon nanomaterials	156
<b>P3-12 Kulakova I.I.</b>		
	Effect of structure and oxidation state of carbon nanomaterials on the conversion of propanol-2	157
<b>P3-13 Andronenko S.I.</b>		
	A X- and W-band EPR study of carbon related dangling bonds in SiCN and SiCN/Fe ceramics	158
<b>P3-14 Kozlov V.S.</b>		
	Spectroscopy and TEM of Fe-carbon nanoclusters synthesized in electric arc	159
<b>P3-15 Kashkarov A.O.</b>		
	Detonation method for synthesis of bimetallic nanoparticles	160
<b>P3-16 Fazlitdinova A.G.</b>		
	Features of the use of X-ray diffraction analysis to study the fine structure of carbon fibers	161
<b>P3-17 Sedov V.S.</b>		
	Photo- and X-ray luminescent diamond composites with embedded nanoparticles of rare-earth element fluorides	162
<b>P3-18 Tikhomirova G.V.</b>		
	PHASE TRANSITIONS IN CARBON MATERIALS AT HIGH PRESSURES	163
<b>P3-19 Nelson D.K.</b>		
	Polarization study of carbon nanodots photoluminescence	164
<b>P3-20 Zinin P. V.</b>		
	Synthesis, Characterization of Elastic, Optical and Electrical Properties of Diamond-Like BC <sub>x</sub> Nano-Phases Synthesized under High and Low Pressures	165

<b>P3-21 Kharissova Oxana V.</b>	Low-temperature transformations of carbon allotropes in the theraphthal - ascorbic acid system.	166
<b>P3-22 Siklitskaya A.</b>	Hybrid sp <sup>2</sup> -sp <sup>3</sup> bonds in carbon spirooids: energetical issues	167
<b>P3-23 Voznyakovsky A.P.</b>	Detonation synthesis of 2D carbon structures	168
<b>P3-24 Rossi M.C.</b>	Stress modulation, graphitic nanoclusters and electronically-active defects in laser irradiated bulk-diamond	169
<b>P3-25 Chekulaev Maxim</b>	Optical properties of carbon spiroid C <sub>300</sub>	170
<b>P3-26 Brzhezinskaya M.</b>	Characterization of amorphous hydrocarbon CD <sub>x</sub> films for energy storage applications	171
<b>P3-27 Filonenko V.P.</b>	The transformation of the structure of nanoscale amorphous carbon during the thermobaric treatment	172
<b>P3-28 Proklova A.A.</b>	Physicochemical properties of crystalline carbon/metal nanoflakes	173
<b>P3-29 Rodin E.A.</b>	Emission properties of carbon nanobelts	174
<b>P3-30 Zhurkin A.M.</b>	Low-threshold field emission of electrons and anomalous photosensitivity of carbon quantum dots on the surface of oxidized silicon	175
<b>P3-31 Pasternak D.G.</b>	Characterization of individual SiV-luminescent nanodiamonds grown by CVD on various seeds.	176
<b>P3-32 Shkolin A.V.</b>	Modelling of supramolecular structures based on carbon nanotubes and cyclic/aromatic hydrocarbons for methane and hydrogen storage	177
<b>P3-33 Vedyagin A.A.</b>	Segmented carbon nanofibers: catalytic synthesis, formation mechanism and possible applications	178
<b>P3-34 Ozerin A.N.</b>	A study of process of electroconductive nanofiller particles migration to polymer composite melt boundaries	179
<b>P3-35 Iurchenkova A.A.</b>	Effect of thermal treatment of reduced graphite oxide on its performance in Li-ion battery.	180
<b>P3-36 Ivanova M.K.</b>	Hyperbranched polyglycerol modified carbon nanomaterials	181
<b>P3-37 Vozniakovskii A.A.</b>	Graphene nanostructures synthesized by self-propagating high-temperature synthesis and their application as an additive in polymer and metal composites.	182
<b>P3-38 Nechaev Yu.S.</b>	On manifestation & physics of the Kurdjumov and spillover effects in carbon nanostructures, under intercalation of high density hydrogen	183
<b>P3-39 Kidalov S.V.</b>	Composite material aluminum-carbon nanotubes with high hardness and controllable thermalconductivity.	184
<b>P3-40 Simunin M.M.</b>	Features of ethanol pyrolysis for synthesis of carbon nanostructures	185
<b>P3-41 Tascon J.M.D.</b>	Highly active, MOF-derived nickel/carbon catalysts for nitroarene reduction	186
<b>P3-42 Arkhipov A.V.</b>	Low-field electron emission from carbon cluster films: combined thermoelectric/hot-electron model of the phenomenon	187



<b>P3-43 Dyachkova T.P.</b>	Study of the surface of polymer composites based on carbon nanostructures using the Raman mapping method	188
<b>Y-01 Nikiforov A.A.</b>	Electrochemical synthesis of graphene in supercritical electrolyte	189
<b>Y-02 Shiyanova K.A.</b>	Polymer composites with high electrical conductivity filled by reduced graphene oxide/carbon nanoparticle (CNT, carbon black) blends	190
<b>Y-03 Trofimuk A.D.</b>	Morphology of aerogels based on graphene oxide and detonation nanodiamonds composites	191
<b>Y-04 Anosov A.A.</b>	Electrical resistance analysis of aerogels based on reduced graphene oxide during compression	192
<b>Y-05 Slyusarenko M.A.</b>	Hydrodynamic behavior of complexes of metallofullerenes Fe @ C60 with biocompatible polymers in aqueous media	193
<b>Y-06 Rabchinskii M.K.</b>	The role of edge moieties in electronic properties of graphene layers	194
<b>Y-07 Kozlachkov D. V.</b>	Electric arc synthesis and study of mesoporous carbon with packing tin nanoparticles and their use as an anode material in Li-ion batteries	195
<b>Y-08 Kuznetsova V.R.</b>	Application of tungsten-cobalt molecular cluster for CCVD synthesis of CNTs	196
<b>Y-09 Lobanova E.Yu.</b>	Electronic structure of cobalt-intercalated graphene on silicon carbide	197
<b>Y-10 Zhirov M.S.</b>	Heat treatment of the microwave exfoliated graphite oxide (MEGO) by Knudsen Effusion Mass Spectrometry (KEMS)	198
<b>Y-11 Mingaleva A.E.</b>	NEXAFS study of catalytic system based multiwalled carbon nanotubes	199
<b>Y-12 Ivanov A.V.</b>	Correlation between gas permeability of graphite foil, microstructure of exfoliated graphite and its preparation conditions	200
<b>Y-13 Baskakova K.I.</b>	Impedance spectroscopy analysis and equivalent circuit modeling of polystyrene composites with carbon nanohorns	201
<b>Y-14 Cheretaeva A.O.</b>	On the treatment and identification of deuterium thermal desorption spectra for graphite exposed to high flux plasma at high temperatures	202
<b>Y-15 Zolotaya P.S.</b>	The impact of graphene-like carbon on the properties of MAO-coatings on the AK5M2 alloy	203
<b>Y-16 Iskandarova D.O.</b>	Structure formation of AK12M2MgN alloy modified by carbon nanotubes jointly with copper	204
<b>Y-17 Tataurov M.V.</b>	Influence of fullerene(C <sub>60</sub> )-containing star macromolecules on pervaporation efficiency of membranes for fuel desulfurization	205
<b>Y-18 Pavlova J.A.</b>	Preparation of magnetic sorbent based on exfoliated graphite containing cobalt ferrite for selective sorption of oil from the water surface	206
<b>Y-19 Sokolovsky D.N.</b>	Effect of high pressure on the thermoelectrical properties of fullerene C <sub>70</sub>	207
<b>Y-20 Sinolits A.V.</b>	Chitosan adsorption on nanodiamonds: composite stability and mechanism	208

<b>Y-21 Parfimovich I.D.</b>	209
Structural characterization of carbon nanomaterials by electron microscopy	
<b>Y-22 Bunyaev V.A.</b>	210
Comparison analysis of graphene oxide reduction methods	
<b>Y-23 Larkina A.A.</b>	211
Hybrid macromolecular fullerene(C <sub>60</sub> )-containing stars incorporated polyphenyleneisophthalamide membranes for n-butanol dehydration	
<b>Y-24 Palamarchuk K.V.</b>	212
Colloidosomes with a shell of detonation nanodiamonds	
<b>Y-25 Babenya J.S.</b>	213
Carbon Nanomaterials Modification by Oxidation and Reduction Reactions	
<b>Y-26 Borisenko D.P.</b>	214
Using graphene like buffer layer for PA-MBE of III-nitrides on different amorphous substrates	
<b>Y-27 Iurchenkova A.A.</b>	215
Reduced graphite oxide and polypyrrole nanocomposites for supercapacitor applications.	
<b>Y-28 Fedosova A.A.</b>	216
Characterization and purification of phosphorus filled single-wall carbon nanotubes	
<b>Y-29 Markin G.V.</b>	217
Bis(arene)chromium 1-((2-((2-methoxyphenoxy)methoxy)phenoxy)methyl)-1-hydrofullerides	
<b>Y-30 Belyavin V.A.</b>	218
Colloidal dispersions of nanostructured carbon, silicon and silicon carbide	
<b>Y-31 Rudakova D.A.</b>	219
Novel fullerene(C <sub>60</sub> )-containing membranes with high selectivity: pervaporation and neutron scattering studies in separation of water- acetic acid mixture	
<b>Y-32 Grebenkina M.A.</b>	220
Temperature dependence of water intercalated graphite oxide at heating	
<b>Y-33 Stolyarova S.G.</b>	221
Hot pressing synthesis of P-doped carbon onions as anode material for sodium-ion batteries	
<b>Y-34 Gurova O.A.</b>	222
Sulfur filling and structure of TUBALL™ nanotubes	
<b>Poster session 3: Graphene. Related Materials + Carbon Nanotubes. Biomedical applications.</b>	223
<b>P4-01 Shavelkina M.B</b>	224
Graphene synthesis in plasma jet with ethanol	
<b>P4-02 Vorobiev A.Kh.</b>	225
Nature of paramagnetic centers in graphite oxide according to EPR spectroscopy and DFT calculations	
<b>P4-03 Gudkov M.V.</b>	226
Superhydrophobic aerogels based on reduced graphene oxide and ultra-high molecular weight polyethylene	
<b>P4-04 Zavarinskii V.I</b>	227
Investigation of the mechanical and thermal properties of the composite material of the composition of aluminum-graphene nanoplatelets.	
<b>P4-05 Koval V.S.</b>	228
Graphene aerogel modification with various polymers and electroconductive fillers	
<b>P4-06 Ktitorov S.A.</b>	229
Extraction of the short-range defect potential parameters from available experimental data on the graphene resistance	
<b>P4-07 Komarov I.A.</b>	230
Binding of short DNAs to the surface of reduced graphene oxide for electronic applications	

<b>P4-08 Kononenko O.V.</b>	Observation of resonance effects in the Raman spectra of twisted bilayer graphene	231
<b>P4-09 Konobeeva N.N.</b>	Graphene vs. germanene as a sensor material	232
<b>P4-10 Rybkin A.G.</b>	Spin-orbit and exchange coupling induced in graphene under contact with heavy and magnetic metals	233
<b>P4-11 Rybkina A.A.</b>	Synthesis, ARPES and STM study of quasi-freestanding graphene on Pt <sub>x</sub> Gd alloy	234
<b>P4-12 Moshkalev S. A.</b>	Thermal annealing of defects in graphite nanoplatelets	235
<b>P4-13 Babkin A.V.</b>	A Nanostructured Composite Polyhydroquinone/Graphene Oxide Sorbent: Synthesis and Physical-Chemical Properties	236
<b>P4-14 Neskromnaya E.A.</b>	Development of Sorption Materials Based on Iron(III)-Chloride-Modified Graphene oxide for Selective Removal of Organic Pollutants from Aquatic Media	237
<b>P4-15 Kononenko O.V.</b>	Synthesis of twisted multilayer graphene by the low-pressure chemical vapor deposition with a single injection of acetylene	238
<b>P4-16 Leshchev D.V.</b>	The mechanism of spillover of hydrogen on sp <sup>2</sup> -carbon surface	239
<b>P4-17 Ziatdinov A.M.</b>	The influence of adsorbates on edge zero modes in few-layer nanographenes	240
<b>P4-18 Butko A.V.</b>	Quasistatic phenomena in electrical transport in solution gated graphene transistor structures	241
<b>P4-19 Tarasov A.V.</b>	A new multi-structural approach to photoelectron holography of 2D materials and interfaces	242
<b>P4-20 Nikolaeva M.N.</b>	Low resistance of reduced graphene oxide in polystyrene-based composites with various molecular weights	243
<b>P4-21 Boyko E.V.</b>	The influence of the copper crystallites orientations on the efficiency of graphene transfer	244
<b>P4-22 Alexander A. Lebedev</b>	Investigation of the of Graphen films grown on 4H-SiC.	245
<b>P4-23 Skokan E.V.</b>	Effect of heat treatment on the composition and structure of the microwave exfoliated graphite oxide	246
<b>P4-24 Razanau I.</b>	Low-temperature exfoliation/functionalization of graphite using quaternary ammonium cation salts	247
<b>P4-25 Rebrikova A.T.</b>	Swelling of Graphite oxide in polar liquids: the model to account for sorption and internal structure	248
<b>P4-26 Bokai K.A.</b>	h-BN-Graphene lateral heterolayers on lattice-matched surfaces	249
<b>P4-27 Kislenko V.A.</b>	Influence of defects on heterogeneous electron transfer rate at the basal plane of graphene	250
<b>P4-28 Chumakova N.A.</b>	EPR and NMR study of molecular mobility of polar liquids in the inter-plane space of graphite oxide	251

<b>P4-29 Baryshnikov K.A.</b>	Terahertz transitions between Landau levels in graphene with different concentrations of electrons	252
<b>P4-30 Pavlov S.V.</b>	Graphene edge as an electrocatalyst for the oxygen reduction reaction.	253
<b>P4-31 Danilov E.A.</b>	Transparent conductive few-layered graphene-based Langmuir-Blodgett films	254
<b>P4-32 Marko Radovic</b>	Cost efficient processing of GO for sensing applications	255
<b>P4-33 Rozhkova N.N.</b>	Shungite carbon nanoparticles as modifiers of ZnS:Cu electrophosphor study based on ESR of Mn impurity ions	256
<b>P4-34 Sedlovets D. M.</b>	Graphene-like film CVD on e-beam exposed SiO <sub>2</sub> /Si by the pyrolysis of different organic precursors	257
<b>P4-35 Kobets A.A</b>	Alkaline treatment of reduced graphite oxide	258
<b>P4-36 Mitina A.A.</b>	Charge pre-modified substrates for graphene-like film CVD	259
<b>P4-37 Malkin N.A.</b>	Graphene modified BiVO <sub>4</sub> anode material for high-performance lithium-ion batteries.	260
<b>P4-38 Eliseyev I.A.</b>	Transformation of the buffer layer grown on 4H-SiC to single-layer graphene by hydrogen intercalation	261
<b>P4-39 Grebenkina M.A.</b>	Influence of functional composition and intercalated water on dielectric properties of graphite oxide	262
<b>P4-40 Korobov M.V.</b>	Graphene oxide: synthesis, properties and applications	263
<b>P4-41 Amel'chuk D.G.</b>	Surface morphology control of the SiC (0001) substrate during the graphene growth by sublimation.	264
<b>P4-42 Gogina A. A.</b>	Dirac cone manipulation by bismuth and oxygen intercalation underneath graphene on Re(0001)	265
<b>P4-43 Struchkov N.S.</b>	Uniform graphene oxide thin films deposition via spray-coating	266
<b>P4-44 Potorochin D.V.</b>	Covalent functionalization of graphene by organic dyes via diazonium chemistry approach	267
<b>P4-45 Grebenko A.K.</b>	Self-limiting ambient pressure hydrogen free synthesis of single crystal monolayer graphene.	268
<b>P5-01 Ilina M.V.</b>	Carbon nanotubes as a promising material for nanopiezotronics	269
<b>P5-02 Lobiak E.V.</b>	Electrochemical performance of hybrid materials based on carbon nanotubes/porous carbon	270
<b>P5-03 Kharlamova M.V.</b>	Growth dynamics of inner tubes inside metallocene-filled single-walled carbon nanotubes	271
<b>P5-04 Nazarova A.</b>	Carbon nanostructures for drug delivery systems	272
<b>P5-05 Ilin O.I.</b>	Development a complex model of the catalytic centers formation for carbon nanotubes growth	273

<b>P5-06 Kremlev K.V.</b>	Synthesis of new hybrid materials based on multi-walled carbon nanotubes and nanoscale coatings of copper oxide and tungsten oxide	274
<b>P5-07 Blokhin A.N.</b>	Polymer composites based on epoxy resin with added carbon nanotubes	275
<b>P5-08 Maslov M.M.</b>	Carbon vs silicon polyprismanes: A density functional theory study	276
<b>P5-09 Revenko V.</b>	Synthesis of pyrocatalysts on the basis of different carbon carriers and their application in the alyumovozdushnykh of EHG	277
<b>P5-10 Burakova E.A.</b>	Effect of heat treatment on the characteristics of the catalyst for the synthesis of carbon nanostructured materials	278
<b>P5-11 Kunakovskaya K.D.</b>	Investigation of the effect of carbon nanotube surface modification with various functional groups and their use in catalysts for the O <sub>2</sub> electroreduction reaction.	279
<b>P5-12 Yablokov M.Yu.</b>	Electromagnetic interference shielding of carbon nanotube-fluoropolymer elastomer composites with layered structure	280
<b>P5-13 Brzhezinskaya M.</b>	Effect of carbon nanotubes on structure and properties of the antifriction coatings	281
<b>P5-14 Tsykareva Yu.V</b>	Doping of carbon nanotubes with functional groups	282
<b>P5-15 Matyushkin Y.E.</b>	On chip carbon nanotube tunnelling spectroscopy	283
<b>P5-16 Chichkan A.S.</b>	Preparation of C-C composites from anthracene	284
<b>P5-17 Sokolovsky D.N.</b>	Effect of high pressure on the thermoelectrical properties of carbon nanotubes	285
<b>P5-18 Kremlev K.V.</b>	Synthesis of hybrid materials based on multi-walled carbon nanotubes, decorated with nanosized TiC or WC coatings for use as reinforcing fillers in aluminium alloys	286
<b>P5-19 Karaeva A.R.</b>	Double-walled carbon nanotubes with controlled bundle size	287
<b>P5-20 Rodionova E.V.</b>	Emission properties of carbon nanotubes	288
<b>P5-21 Khaskov M.A.</b>	Modification of sealants with long carbon nanotubes	289
<b>P5-22 Guryanov A.V.</b>	Investigation of the surface potential of deformed carbon nanotubes	290
<b>P5-23 Fedosova A.A.</b>	Synthesis, characterization and the sensor properties of phosphorus filled single-wall carbon nanotubes	291
<b>P5-24 Danilov E.A.</b>	Carbon nanotube oxidation in the presence of phase transfer catalyst and qualitative evaluation of the product	292
<b>P5-25 Grishakov K.S.</b>	Carbon nanotubes for stabilization of nitrogen nanostructures	293
<b>P5-26 Mitina A.A.</b>	The influence of the way of catalyst preparation on the morphology and properties of carbon nanotubes obtained from ethanol vapor	294
<b>P5-27 Neverovskaya A.Yu.</b>	Single-walled carbon nanotubes cleaning via solid-flame combustion process	295
<b>P5-28 Konobeeva N.N.</b>	Influence of nonlinear absorption on the ultrashort optical pulse propagation in carbon nanotubes	296

<b>P5-29 Gurova O.A.</b>	Purification of carbon nanotubes by acid and magnetic separation combination	297
<b>P5-30 Levin D.D.</b>	Conductivity improvement of spray deposited CNT network	298
<b>P6-01 Badun G.A.</b>	Carbon-based nanomaterials as a support for peptides and proteins tritium labelling	299
<b>P6-02 Zakharov A.A.</b>	Supramolecular interaction of modified nanodiamonds, biomolecules and drugs: molecular modeling	300
<b>P6-03 Naumov A.A.</b>	Molecular modeling of graphene oxide intermolecular interaction with DNA nitrogenous bases adenine and thymine	301
<b>P6-04 Razanau I.</b>	Nanosize coatings on the base of diamond-like carbon doped with copper with enhanced antibacterial activity	302
<b>P6-05 Kharissova Oxana Vasilievna</b>	Multiwall carbon nanotubes based optical biosensor for L-Dopa	303
<b>P6-06 Yakovlev R.Y.</b>	Biodistribution of nanodiamond for potential anti-tuberculosis drug delivery systems	304
<b>P6-07 Rozhkova N.N.</b>	Hybrid carbon-metal nanoparticles: structure, functions and processing	305
<b>P6-08 Bi Hong</b>	Synthesis of Fluorine-doped Graphene Quantum Dots with High Singlet Oxygen Production	306
<b>P6-09 Chernysheva M.G.</b>	Toxicity of nanodiamonds and its composites in relation to cancer cells, fungus and plants	307
<b>P6-10 Chernysheva M.G.</b>	Nanodiamonds-film as a modifier for improving heart valve biological prostheses materials	308
<b>P6-11 Shershakova N.</b>	Aqueous dispersion of fullerene C <sub>60</sub> anti-HCMV and anti- HSV1 activity	309
<b>P6-12 Voznyakovskii A.P</b>	2D NANOCARBONES AS THE BASE OF COMBINED MICROBIAL FORMULATION	310
<b>P6-13 Sarmanova O.E.</b>	Application of adaptive data analysis methods for monitoring of carbon nanocomposites in biological medium	311
<b>P6-14 Zakharov A.A.</b>	Intermolecular interaction of phi29 DNA polymerase with carbon nanostructures and buffer solution in process of single-molecular DNA sequencing: molecular modeling	312

# Author Index

## A

Abaturov M.A. - 140  
Abbasi Z.S. - 32  
Aborkin A.V. - 286  
Acosta T. - 40  
Afanasiev V.P. - 134  
Agafonov V.N. - 128  
Ageev O.A. - 269, 290  
Agrinskaya N.V. - 245  
Akhatov I.S. - 52  
Aksenov V.L. - 90, 131, 133  
Aladinskii A.A. - 184  
Alaferdov A.V. - 235  
Aleksenskii A.E. - 118, 123, 131, 133  
Alexandrov E.V. - 298  
Alexandrova N.M. - 156, 183  
Alexenko A.E. - 140  
Altukhov I.V. - 136  
Amel'chuk D.G. - 264  
Amirov R.H. - 224  
Amusia M.Ya. - 27, 76  
Andreev P.V. - 274, 286  
Andreev S.M. - 89, 90, 94, 309  
Andronenko S.I. - 158  
Anisimov A.N. - 109  
Anokhin A.S. - 172  
Anosov A.A. - 190, 192, 226, 228  
Antipova O.M. - 230  
Arhipov V.E. - 297  
Aristov V.Yu. - 50, 267  
Arkhipov A.V. - 187  
Artemiev A.N. - 88  
Arutyunyan A.V. - 82  
Askenov V.L. - 73  
Astvatsaturov D.A. - 225  
Avdeev M.V. - 73, 90, 131, 133  
Avramenko N.V. - 30, 248

## B

Babnikov S.V. - 50  
Babenya J.S. - 181, 213  
Babin D.M. - 286  
Babkin A.V. - 236, 237  
Badun G.A. - 98, 106, 208, 210, 299, 307, 308  
Baidakova M.V. - 51, 194, 267  
Bairamukov V.Yu. - 39  
Bakuleva N.P. - 308  
Balabas O.A. - 159

Balakhnina A.V. - 120  
Baldycheva A. - 32  
Baltenkov A.S. - 76  
Baraboshkina E. - 309  
Baranov P.G. - 109  
Barash I.S. - 264  
Baryshnikov K.A. - 252  
Baskakova K.I. - 201  
Bauman Y.I. - 178  
Bayramukov V.Yu. - 36  
Bedin S.A. - 190  
Belonenko M.B. - 232, 296  
Belousov S.I. - 29, 132  
Belova A.I. - 263  
Belyaev A.D. - 88  
Belyavin V.A. - 218  
Ber B. - 24  
Berezkin V.I. - 93  
Besedina N.A. - 51, 115, 129, 142  
Bezrodny A.E. - 62  
Bezrukova M.A. - 243  
Bi Hong - 10, 306  
Blinkov A.E. - 137  
Blokhin A.N. - 275  
Bobrinetskiy I. - 255  
Bocharov G.S. - 42  
Bocharova I.V. - 304  
Bogachev V.V. - 230  
Bogdanov K.V. - 141  
Bogdanov V.P. - 68  
Bogomolov A. - 40  
Boikova I.V. - 310  
Bokai K.A. - 53, 249  
Bokarev A.N. - 112, 300, 301  
Bolshakov A.P. - 136, 152  
Bondar V.S. - 99  
Borisenko D.P. - 214  
Borisova A.G. - 305  
Borodina T.I. - 224  
Boulanger Nicolas - 54  
Boyko E.V. - 244  
Bozhko S.I. - 238  
Breev I.D. - 109  
Brevnov P.N. - 226  
Brotsman V.A. - 77, 84  
Brunetti F. - 110  
Brunkov P.N. - 194, 267  
Brylev K.A. - 218  
Brzhezinskaya M. - 21, 171, 281  
Bugrov A.N. - 243  
Bukalov S.S. - 20  
Bukreeva T.V. - 212  
Bulat P.V. - 245  
Bulatov K.M. - 165

Bulusheva L.G. - 38, 56, 57, 196, 201, 216, 220, 221, 222, 262, 270, 291, 297  
Bulychev B.M. - 71  
Bunyaev V.A. - 210, 299  
Burakov A.E. - 181, 213, 236, 237  
Burakova E.A. - 188, 278  
Burakova I.V. - 181, 213, 236, 237  
Burikov S.A. - 112, 113, 311  
Burkat G.K. - 121  
Butko A.V. - 241  
Butko V.Y. - 241  
Buyanov A.D. - 230  
Bychin N.V. - 119  
Bykov A.A. - 165

## C

Canesqui M.A. - 235  
Chaika A.N. - 50, 267  
Charykov N.A. - 83  
Chaschin I.S. - 308  
Chaykun A.M. - 289  
Chekulaev M. - 170  
Cheretaeva A.O. - 156, 183, 202  
Chernoryzh Y. - 309  
Chernysheva L.V. - 27  
Chernysheva M.G. - 98, 106, 208, 210, 299, 307, 308  
Chesnokov V.V. - 284  
Chichkan A.S. - 284  
Chilingarov N.S. - 246  
Chizhik V.I. - 88  
Choi Suk-Ho - 13  
Chudoba D.M. - 272  
Chulkov E.V. - 233  
Chumakov R.G. - 51  
Chumakova N.A. - 251  
Churilov G.N. - 79, 81  
Chvalun S.N. - 29, 132  
Cicero C. - 46  
Ciobanu A. - 267  
Conte G. - 169

## D

Da Silva R.R. - 235  
Dai Bing - 152  
Danilov E.A. - 254, 292  
Dashapilov G.R. - 160  
Davydov S.Yu. - 149  
Davydov V.A. - 128

Davydov V.Y. - 241, 245  
Dementev P.A. - 261, 264  
Demidova N. - 309  
Dideikin A.T. - 51, 122, 133,  
142, 243  
Dimiev A. - 55  
Dmitrieva V.A. - 68  
Dolenko S.A. - 112, 311  
Dolenko T. - 33, 112, 113,  
114, 130, 311  
Dolmatov V.Yu. - 100, 102,  
121, 168  
Dorokhov A.O. - 100, 102,  
121  
Dubois M. - 122  
Dudnik A.I. - 79, 81  
Dvorak A. - 147, 302  
Dyachkova T.P. - 188, 275,  
278  
Dyakonov P.V. - 52  
Dyakov S.A. - 152  
Dzhemilev U.M. - 92

## E

Eder D. - 60  
Efitorov A.O. - 311  
Egorov A.V. - 98  
Egorova T.B. - 98  
Eidelman E.D. - 29, 115,  
129, 187  
Ekimov E.A. - 31, 116  
Eletskii A.V. - 42  
Eliseev A.A. - 263  
Eliseyev I.A. - 241, 261, 264  
Eremenko I.L. - 138  
Ershov A.P. - 150  
Estyunin D.A. - 234, 265  
Eurov D.A. - 164  
Evlashin S.A. - 52  
Evsevskaya N.P. - 58  
Ezdin B.S. - 218  
Ezhikov N.S. - 71

## F

Faddeenkov V.V. - 137  
Faradzheva M.P. - 75  
Fazlitudinova A.G. - 161  
Fedorov G.E. - 283  
Fedorov P.P. - 162  
Fedorov V.E. - 218  
Fedorova N. - 309  
Fedorovskaya E.O. - 180,  
195, 215, 258  
Fedosova A.A. - 216, 221,  
291  
Fedotov A.A. - 273  
Fedyushin N.A. - 224  
Filipovich S. - 247  
Filippova E.A. - 311

Filonenko V.P. - 165, 172  
Firsova N.E. - 48, 229  
Fomina I.G. - 138  
Fominski V.Y. - 165  
Fomkin A.A. - 65, 177  
Forro L. - 41

## G

Gabdullin P.G. - 187  
Galimov D.I. - 92  
Galunin E.V. - 278  
Galushko T.B. - 140  
Ganin P.G. - 310  
Gapon I.V. - 73  
Garamus V.M. - 74  
Garashchenko B.L. - 45,  
181, 213  
Gavrilov Y.V. - 292  
Gerasimov E.Yu. - 160  
Gimaldinova M.A. - 80, 276  
Gintsburg A. - 309  
Gladush Y.G. - 61  
Gofman I.V. - 36  
Gogina A.A. - 265  
Golovina E. - 107  
Goltsman G.N. - 283  
Golubev V.G. - 164  
Goodilin E.A. - 138, 263  
Gorbachev V.A. - 126  
Gorbunov A.M. - 140  
Gorenberg A.Ya. - 190, 228  
Gorodetskii D.V. - 38  
Gorshkova Yu.E. - 73  
Goryunkov A.A. - 77  
Goryunov A.S. - 305  
Grebenkina M.A. - 220, 262  
Grebenko A.K. - 59, 268  
Grechikhina A.M. - 140  
Grigorenko A.M. - 63  
Grigorieva A.V. - 210  
Grishakov K.S. - 80, 276,  
293  
Gromilov S.A. - 134  
Grozдова I.D. - 307  
Gudkov M.V. - 190, 191,  
192, 226, 228  
Gurova O.A. - 216, 222, 297  
Guryanov A.V. - 269, 290  
Gusel'nikov A.V. - 201, 220,  
262  
Guselnikova T.Ya. - 297  
Gusev A.S. - 214  
Gusev S.A. - 199, 274  
Gus'kov A.V. - 98  
Gutfreud Ph. - 122  
Gutnik I.V. - 188, 278  
Gvozdev A.A. - 63

## H

Harris P.J.F. - 15  
Hirani M. - 137  
Hogan B.T. - 32  
Hu Xiaolong - 306

## I

Iakunkov A. - 54  
Ievlev A.V. - 88  
Ilin O.I. - 269, 273  
Ilina M.V. - 269, 290  
Imshennik V.K. - 138  
Ioffe I.N. - 78  
Isaev I.V. - 311  
Iskandarova D.O. - 204  
Itkis D.M. - 263  
Iurchenkova A.A. - 180, 215  
Ivanchev S.S. - 36  
Ivanenko A.V. - 61  
Ivankov O.I. - 85, 90  
Ivanov A.V. - 200, 206  
Ivanov D.M. - 103  
Ivanov M.G. - 103  
Ivanova M.K. - 181, 213  
Ivanova M.N. - 218

## J

Jackman R.B. - 9, 37  
Jazdzewska M. - 272  
Jentgens C. - 141

## K

Kadomtseva A.V. - 199  
Kagan M.S. - 136  
Kai Li - 302  
Kalinnikov A.N. - 230  
Kapitanova O.O. - 189, 263  
Kapustin S.N. - 282  
Karaeva A.R. - 148, 287, 289  
Kargin N.I. - 214  
Karmanov A.P. - 66  
Karpets M.L. - 73  
Kashkarov A.O. - 125, 150,  
160  
Kashnik I.V. - 218  
Kataev E.Yu. - 263  
Katayeva E.R. - 101  
Katin K.P. - 80, 276, 293  
Kaurova N.S. - 283  
Kaverin B.S. - 199, 274, 286  
Kazachenko V. - 147, 302  
Kazakov V.A. - 126  
Kazennov N.V. - 287  
Keskinov V.A. - 83  
Keskinova M.V. - 83  
Ketkov S.Yu. - 217  
Khabashesku V. - 40  
Khabushev E.M. - 61  
Khaitov M. - 309  
Khaitov M.R. - 89



- Khalilov L.M. - 70  
 Khannanov A. - 55  
 Kharisov B.I. - 155, 166  
 Kharissova O.V. - 155, 166, 303  
 Kharitonov A.P. - 275  
 Kharlamova M.V. - 60, 271  
 Khasanov S.S. - 91, 95  
 Khaskov M.A. - 289  
 Khavrel P.A. - 246  
 Khmelnitskiy R.A. - 136  
 Khodos I.I. - 238  
 Khomich A.A. - 130, 152  
 Khuzin A.A. - 92  
 Khvalkovskiy N.A. - 136  
 Kidalov S.V. - 66, 93, 104, 109, 182, 184, 227  
 Kiisk V. - 134  
 Kinzyabaeva Z.S. - 69, 92  
 Kirichenko A.N. - 148  
 Kirilenko D.A. - 51, 129, 151  
 Kiselev M.R. - 140  
 Kiseleva E.A. - 279  
 Kislelev M.N. - 100, 102  
 Kislenco S.A. - 250, 253  
 Kislenco V.A. - 250  
 Kizima E.A. - 47  
 Klein O.I. - 307  
 Klimova R. - 309  
 Klimovskikh I.I. - 233, 234, 265  
 Knizhnik A.A. - 87  
 Knotko A.V. - 246  
 Knyazev G.A. - 88  
 Knyazev M.A. - 257, 259  
 Kobernik N.V. - 281  
 Kobets A.A. - 258  
 Kobtsev S.M. - 61  
 Kochetkov F.M. - 144  
 Kocheva L.S. - 66  
 Kokhanovskiy A.Y. - 61  
 Kol'tsova T.S. - 184  
 Komarov A.I. - 203, 204  
 Komarov F.F. - 209  
 Komarov I.A. - 230  
 Komissarov I.V. - 214  
 Komolkin A.V. - 74  
 Kompan T.A. - 235  
 Konarev D.V. - 91, 95  
 Kondratenko M.S. - 189  
 Kondratiev S.V. - 235  
 Koniakhin S.V. - 115, 129, 139  
 Konkov O.I. - 75  
 Konobeeva N.N. - 232, 296  
 Kononenko O.V. - 231, 238  
 Kononenko T.V. - 169  
 Kopachevsky V.D. - 63  
 Kopelevich Ya.V. - 235  
 Kopylova D.S. - 61  
 Korepanov V.I. - 259  
 Korlyukov A.A. - 138  
 Korneev D.V. - 178  
 Korobkov V.I. - 106  
 Korobov M.V. - 30, 97, 248, 251, 263  
 Korobov M. - 54  
 Koroteev V.O. - 56, 216  
 Kosaya M.P. - 77, 96  
 Kosiachkin Ye.M. - 73  
 Kostogrud I.A. - 244  
 Koval V.S. - 190, 192, 228  
 Kovalchuk A.A. - 305  
 Kovalevski V.V. - 154  
 Kozhikhova K.V. - 89, 94  
 Kozlachkov D.V. - 195  
 Kozlov A.S. - 100, 102  
 Kozlov V.S. - 82, 159  
 Kramberger C. - 60, 271  
 Krasilin A.A. - 144  
 Krasnikov D.V. - 268  
 Kremenko S.I. - 125, 160  
 Kremlev K.V. - 199, 274, 286  
 Krivchenko V.A. - 263  
 Krylov D.S. - 28  
 Ksenofonov A.L. - 299  
 Ktitorov S.A. - 48, 229  
 Kucherik A.O. - 305  
 Kudryakov A.V. - 63  
 Kudryashova O.B. - 120  
 Kudryavtsev O.S. - 31, 33, 130, 176  
 Kuklin A.I. - 36  
 Kulakova I.I. - 98, 108, 157  
 Kulbachinskii V.A. - 71  
 Kulenova N.A. - 83  
 Kulikova L.F. - 128  
 Kulikova N.A. - 307  
 Kulnitskiy B.A. - 148, 287, 289  
 Kulvelis Yu.V. - 36, 47, 74, 82, 88, 118  
 Kumzerov Y.A. - 241  
 Kunakovskaya K.D. - 279  
 Kurdyukov D.A. - 152, 164  
 Kurnosov D.A. - 236  
 Kuropatov V.A. - 217  
 Kushch A. - 309  
 Kutuza I.B. - 165  
 Kuzmenko M.O. - 85  
 Kuzmin A.V. - 91  
 Kuznetsov M.V. - 242  
 Kuznetsov N.M. - 29, 132  
 Kuznetsov S.V. - 162  
 Kuznetsova V.R. - 57, 196, 270  
 Kyzyma E.A. - 74  
 Kyzyma O.A. - 85, 90  
 Lanuti A. - 110  
 Laptinskiy K.A. - 112, 113, 311  
 Larionova T.V. - 142  
 Larkina A.A. - 211  
 Lebedev A.A. - 241, 245, 264  
 Lebedev A.M. - 171  
 Lebedev O.V. - 43, 179  
 Lebedev S.P. - 241, 245, 261, 264  
 Lebedev V.T. - 36, 39, 47, 74, 88, 159, 193, 219  
 Lebedeva I.V. - 87  
 Leksikov A. - 165  
 Lepekha L.N. - 304  
 Leshchev D.V. - 105, 239  
 Levashov V.I. - 238  
 Levin D.D. - 266, 298  
 Li Zhenzhen - 306  
 Liopo V.A. - 104, 227  
 Lisichkin G.V. - 98  
 Litasova E.V. - 44  
 Lobanova E.Yu. - 197  
 Lobarev A.I. - 137  
 Lobiak E.V. - 57, 196, 222, 270  
 Locatelli A. - 50  
 Lopatin M.A. - 217  
 Lugvishchuk D.S. - 146, 148  
 Lunin R.A. - 71  
 Lunin V.V. - 157  
 Lyapin S.G. - 116, 172  
 Lychagin E.V. - 122  
 Lyubovskaya R.N. - 95  
**M**  
 Makarova A.A. - 249  
 Maksimkin A.A. - 275  
 Maksimkin A.V. - 188  
 Maksimov Y.M. - 52  
 Maksimov Yu.V. - 138  
 Maksimova N.V. - 200, 206  
 Malakho A.P. - 200  
 Malkin N.A. - 260  
 Mamonova D.V. - 173  
 Mankelevichc Y.A. - 52  
 Manshina A.A. - 173  
 Marchenko D.E. - 50, 249, 267  
 Markin G.V. - 217  
 Martinez-Alonso A. - 14, 186  
 Martin-Jimeno F.J. - 186  
 Martyanov A.K. - 162  
 Maslakov K.I. - 52  
 Maslov M.M. - 80, 276, 293  
 Matsko M.A. - 178  
 Matsumoto K. - 11  
 Matveev V.N. - 238  
 Matyushkin Y.E. - 283  
 Mazur A.S. - 23  
**L**  
 Labunov V.A. - 214  
 Lachko A. - 33

Meletov K.P. - 72, 91  
Melezhyk A.V. - 181, 213, 237  
Melik-Nubarov N.S. - 307  
Melnik N.N. - 140  
Melnikov V.P. - 190, 192, 226, 228  
Men'shchikov I.E. - 65, 177  
Menshikov K.A. - 171  
Mentes T.O. - 50  
Mercuri F. - 46  
Mikheev I.V. - 97  
Mikheev R.S. - 281  
Mikhlina E.V. - 99  
Milchanin O.V. - 209  
Milikisiyants S. - 34  
Minakov A.V. - 185  
Mingaleva A.E. - 199  
Mishakov I.V. - 178  
Mishnev M.O. - 185  
Misra A. - 40  
Misra S.K. - 158  
Mitberg E.B. - 146, 148  
Mitina A.A. - 259, 294  
Mkrtchyan A.A. - 61  
Mkrtchyan E.S. - 237  
Molodtsov S.L. - 267  
Molodtsova O.V. - 50, 267  
Momotyuk E. - 309  
Mordkovich V.Z. - 146, 148, 287, 289  
Moroz B.L. - 160  
Moshkalev S.A. - 235  
Moshnikov I.A. - 154  
Mukhortov L.A. - 43, 179, 280  
Munuera J.M. - 14  
Musikhin S.F. - 143  
Muzychka A.Yu. - 122  
Myasnikov I.Yu. - 106  
Mylymaki V. - 100, 102, 121  
Mysanikov I.Yu. - 307

## N

Nagdaev V.K. - 188  
Nasibulin A.G. - 16, 59, 61, 268  
Naumov A.A. - 300, 301, 312  
Navarro Tellez Ana de  
Monserrat - 155  
Nazarova A. - 272  
Nechaev Yu.S. - 156, 183  
Nekhaev G.V. - 122  
Nekipelov S.V. - 199  
Nekrasov N. - 255  
Nelson D.K. - 164  
Neskoromnaya E.A. - 236, 237  
Nesvizhevsky V.V. - 18, 122

Neverovskaya A.Yu. - 295, 310  
Nezvanov A.Yu. - 122  
Nikiforov A.A. - 189, 218  
Nikolaev D.N. - 86  
Nikolaev N.S. - 79  
Nikolaeva M.N. - 243  
Novikau U. - 247  
Novikov A.P. - 116  
Novikov P.V. - 81  
Novikova I.I. - 310  
Novokshonova L.A. - 226  
Nozhkina A.V. - 101  
Nunn N. - 34  
Nyushkov B.N. - 61

## O

Obiedkov A.M. - 199, 274, 286  
Odinokov A.S. - 36  
Ogorodnikov I.I. - 242  
Ohno Y. - 17  
Okolzina A.I. - 70  
Okotrub A.V. - 38, 56, 57, 196, 201, 216, 220, 221, 222, 262, 270, 291, 297  
Oliva G.C.M. - 155  
Onoprienko E.A. - 230  
Orda D.V. - 204  
ORI O. - 26  
Orlanducci S. - 35, 46, 110  
Orlov M.A. - 230  
Orlova T.S. - 151  
Osipov V.S. - 187  
Osipov V.Yu. - 32, 124, 141, 143, 144  
Osipova I.V. - 79, 81  
Osova O.I. - 273, 290  
Otrokov M.M. - 233  
Otsuka A. - 95  
Ovchinnikov E.V. - 104, 227  
Ovchinnikov-Lazarev M.A. - 111  
Ozerin A.N. - 43, 179, 280

## P

Pakpour-Tabrizi A.C. - 9, 37  
Palamarchuk K.V. - 212  
Palmieri E. - 46, 110  
Panin G.N. - 263  
Panteleev V.N. - 261  
Paprotskiy S.K. - 136  
Paredes J.I. - 14, 186  
Parfimovich I.D. - 209  
Pasternak D.G. - 31, 176  
Pavlov A.A. - 52  
Pavlov S.I. - 51  
Pavlov S.V. - 253  
Pavlova J.A. - 206  
Pena M.Y. - 155  
Peters G.S. - 125

Petrosyan T.K. - 163  
Petrov E.A. - 119, 120  
Petrov Yu.V. - 173  
Petrova O.V. - 199  
Pettinato S. - 169  
Petukhov A.E. - 233  
Petukhov D.I. - 263  
Petukhova G.A. - 65  
Pichler T. - 271  
Piotrovskiy L.B. - 44, 86  
Pirogova M.O. - 97  
Pisarev A.A. - 156  
Plastun I.L. - 112, 114, 300, 301, 312  
Plyusnin P.E. - 178  
Polikarpov Yu.A. - 298  
Polino G. - 110  
Polokhin A.A. - 303  
Polotskaya G.A. - 211, 219  
Polotskaya G.I. - 205  
Polushin N.I. - 140  
Ponomarev D.A. - 151  
Ponyaev A.I. - 102  
Popov A.A. - 28  
Popov A.G. - 98, 208, 210, 308  
Popov A.M. - 87  
Popov V.A. - 117, 127  
Popov V.V. - 93  
Popova E.V. - 127  
Porodenko E.V. - 107  
Posokhina E.D. - 99  
Posrednik O.V. - 149  
Potorochin D.V. - 50, 267  
Predtechensky M.R. - 62  
Prikhodko A.V. - 75  
Primachenko O.N. - 36  
Proklova A.A. - 173  
Pronin I.I. - 197  
Proskurnin M.A. - 30, 97  
Pruuel E.R. - 125, 160  
Pudikov D.A. - 234  
Pulyalina A.Yu. - 205, 211, 219  
Pykhova A.D. - 78

## R

Rabchinskii M.K. - 51, 115, 191, 194, 243, 266, 267  
Rachkova N.G. - 66  
Radovic L.R. - 49  
Radovic M. - 255  
Ralchenko V.G. - 136, 152, 162, 169  
Ramazanova S.A. - 101  
Razanau I. - 147, 247, 302  
Razbegayev A.Y. - 101  
Razgulov A.A. - 116  
Rebrikova A.T. - 54, 248, 251

Redkin A.N. - 294  
Reshetov V.I. - 164  
Revenko V. - 277  
Reznikov E.N. - 137  
Rizakhanov R.N. - 126  
Roamov R.I. - 165  
Rodin E.A. - 174, 288  
Rodionov N.B. - 136  
Rodionova E.V. - 174, 288  
Rodriguez J. - 166  
Romanov N.M. - 143  
Romanyuk A.S. - 203, 204  
Romashkin A.V. - 266, 298  
Romshin A.M. - 31, 176  
Ronzhin N.O. - 99  
Rossi M.C. - 169  
Rozhkov S.P. - 256  
Rozhkov S.S. - 305  
Rozhkova N.N. - 235, 256, 305  
Rubtsov I.A. - 125, 150  
Rudakova D.A. - 219  
Rudenko D.V. - 121  
Rudneva Yu.V. - 178  
Rudyk N.N. - 273  
Rybkin A.G. - 233, 234  
Rybkina A.A. - 233, 234  
Ryzhkov I.I. - 99, 185  
Ryzhkov S.A. - 51

## S

Sabirov D.Sh. - 6, 92  
Safyannikov N.M. - 83  
Saito T. - 271  
Sala A. - 50  
Salvatori S. - 169  
Samoilov V.M. - 254  
Samosvat D.M. - 124  
Sarmanova O.E. - 311  
Satonkina N.P. - 150  
Savilov S.V. - 157  
Savin S.S. - 104  
Savu R. - 235  
Schick C. - 73  
Schmelzer J.W.P. - 73  
Sedelnikova O.V. - 201, 222, 297  
Sedlovets D.M. - 257, 259  
Sedov V.S. - 162, 176  
Selvas Aguilar Romeo de Jesus - 303  
Semenkin A. - 94  
Semenov K.N. - 83  
Semenov N.M. - 199, 274, 286  
Semenov V.G. - 159  
Semivrazhskaya O.O. - 78  
Serrano Q.T.E. - 155  
Shaimardanov Z.K. - 83  
Shaimardanova B.K. - 83

Shakhov F.M. - 32, 122, 141, 143, 144  
Shakhov M.A. - 245  
Shames A.I. - 34, 124  
Sharenkova N.V. - 93  
Sharipov G.L. - 69  
Sharma S. - 40  
Sharonova L.V. - 115  
Shashkov S.N. - 63  
Shatilov A.A. - 89  
Shavelkina M.B. - 224  
Shavyrin A.S. - 217  
Shayderov A.I. - 161  
Shchegolikhin A.N. - 43  
Shchegolkov A.V. - 64, 209  
Shenderova O.A. - 8, 33, 34, 103, 113, 130  
Shershakova N.N. - 89, 90, 94, 309  
Shestakov M.S. - 47, 142  
Shevchenko N.V. - 126  
Shevchenko V.G. - 280  
Shevelev V.O. - 53, 249  
Shikin A.M. - 233, 234, 265  
Shiozawa H. - 271  
Shiryayev A.A. - 65  
Shiyanova K.A. - 190, 192, 226, 228  
Shkolin A.V. - 65, 177  
Shnitov V.V. - 51, 142, 194  
Shomysov N.N. - 199  
Shu G. - 152  
Shubin Y.V. - 178  
Shukhina K. - 55  
Shulga Y.M. - 246  
Shumilov F.F. - 295  
Shurygina N.A. - 156, 183  
Shvidchenko A.V. - 22, 29, 36, 115, 118, 123, 129, 142  
Sigalaev S.K. - 126  
Siklitskaya A. - 167, 170  
Sildos I. - 134  
Simunin M.M. - 99, 185  
Sinita A.S. - 87  
Sinolits A.V. - 98, 208, 308  
Sivkov D.V. - 199  
Sivkov V.N. - 199  
Skokan E.V. - 246  
Skvortsov D.S. - 232  
Slyusarenko M.A. - 193  
Smirnov A.I. - 34  
Smirnov A.N. - 241, 245  
Smirnov V.V. - 89  
Smovzh D.V. - 244  
Soboleva O.A. - 106, 107  
Sokolov A.V. - 44  
Sokolovsky D.N. - 207, 285  
Soldatova V.I. - 174  
Sovyk D.N. - 152  
Spitsyn A.A. - 151  
Spitsyn B.V. - 111, 140  
Stankevich V.G. - 171

Starukhin A.N. - 164  
Stepanova E.A. - 94  
Stepkina M.Yu. - 120  
Stolyarov R.A. - 275  
Stolyarova S.G. - 56, 216, 220, 221, 262, 291  
Strelkov A.V. - 122  
Struchkov N.S. - 255, 266  
Suarez-Garcia F. - 186  
Suetin N.V. - 52  
Suhorukov A.K. - 275  
Sukhanov L.P. - 171  
Sukhanova T.E. - 295  
Sun J. - 54  
Svechnikov N.Yu. - 171  
Svetogorov R.D. - 138  
Svir K.A. - 121  
Sysoev V.I. - 38, 222, 291

## T

Takai K. - 32  
Talanov A.A. - 256  
Talyzin A.V. - 54, 248  
Tambasov I.A. - 58  
Tambasova E.V. - 58  
Tamburri E. - 110  
Tarasov A.V. - 242  
Tascon J.M.D. - 14, 186  
Tatarskiy D.A. - 199, 274  
Tataurov M.V. - 205  
Tebekov A.V. - 163  
Ten K.A. - 125  
Tikhodeev S.G. - 152  
Tikhomirova G.V. - 163  
Timofeeva A.V. - 89  
Titov S.A. - 165  
Titov V.M. - 125  
Tkachev A.G. - 184, 188, 209, 236, 278  
Tkachev Ya.V. - 251  
Tolstoy P.M. - 23  
Tomchuk A.A. - 90  
Tomchuk O.V. - 90, 131, 133  
Tomilin O.B. - 174, 288  
Torelli M.D. - 34  
Torok Gy. - 153, 219  
Tovpenec T.Yu. - 154  
Trenikhin M.V. - 172  
Treussart F. - 32  
Tristan Petit - 7  
Trofimuk A.D. - 47, 122, 123, 191  
Tropin T.V. - 47, 73, 74, 85  
Troyanov S.I. - 84  
Tsykareva Yu.V. - 282  
Tugolukov E.N. - 188, 278  
Tuktarov A.R. - 70, 92  
Tulyabaev A.R. - 70

Turetskiy E.A. - 89, 90, 94,  
309  
Tveritinova E.A. - 157  
Tyumentsev V.A. - 161  
Tyurin D.P. - 83

## U

Ubeyvovk E.V. - 159  
Ulin N.V. - 267  
Urintsev D.I. - 96  
Usachov D.Yu. - 53, 242,  
249  
Usoltseva L.O. - 30  
Utesov O.I. - 139  
Utsal V.A. - 44  
Uzbekov R.E. - 128

## V

Valentini V. - 169  
Varga L.K. - 153  
Vasil'ev V.G. - 308  
Vavilov S.V. - 52  
Vdovichenko A.Yu. - 132  
Vedyagin A.A. - 178  
Vehanen A. - 100, 102, 121  
Veligzhanin A.A. - 125  
Vereshchagin A.L. - 119,  
120  
Vershinina E.V. - 127  
Vervald A. - 33, 113, 114  
Vikharev A.L. - 19  
Vilkov I.V. - 274, 286  
Vilkov O.Yu. - 53, 233, 249  
Villar-Rodil S. - 14  
Vinogradova L.V. - 205, 211,  
219  
Vins V.G. - 135, 137  
Visotina E.A. - 126  
Vlasov I. -  
Vlasov I.I. - 31, 33, 101, 113,  
130, 176  
Volkov D.S. - 30, 97  
Volkova Ya.Yu. - 163, 207,  
285  
Volodin V.V. - 137  
Vorobiev A.Kh. - 225, 251  
Voronin A.S. - 58, 74  
Voronina E.N. - 52  
Voronov B.M. - 283  
Vovk M.A. - 23  
Voznyakovskii A.A. - 66, 104,  
168, 182, 184, 227, 310  
Voznyakovskii A.P. - 66, 104,  
168, 182, 295, 310  
Vul' A.Ya. - 29, 36, 51, 109,  
118, 124, 131, 132, 133  
Vul' S.P. - 142  
Vyatkin A.S. - 185  
Vysochanskaya O.N. - 77, 84

Zolotaya P.S. - 203  
Zubavichus Ya.V. - 125

## W

Walls B. - 267  
Wang C. - 178  
Wang Dong - 306  
Woloszczuk S. - 272  
Wu B. - 36

## X

Xu X. - 189, 263

## Y

Yablokov M.Yu. - 43, 280  
Yagubov V.S. - 64, 188  
Yakimov E.E. - 294  
Yakovlev R.Y. - 45, 181, 213,  
304  
Yakushev I.A. - 138  
Yamochi H. - 95  
Yashenkin A.G. - 139  
Yashina L.V. - 263  
Yastrebov S.G. - 167, 170  
Yelisseyev A.P. - 134, 135,  
137  
Yevlampieva N.P. - 193  
Yudina E.B. - 29, 118, 123,  
138, 142  
Yunin P.A. - 199  
Yurlov K. - 309  
Yusupov D.I. - 224

## Z

Zabrodina G.S. - 274, 286  
Zaikovskii A.V. - 195  
Zakharchenko T.K. - 263  
Zakharov A.A. - 300, 301,  
312  
Zammit U. - 46  
Zavarinskii V.I. - 227  
Zavatskii E.I. - 82  
Zavedeyev Y.A. - 101  
Zdanovich A.A. - 178  
Zegrya G.G. - 124  
Zenova E.V. - 52  
Zhernenkov K.N. - 122  
Zhevnenko S.N. - 111  
Zhirov M.S. - 198, 246  
Zhitnev.Yu.N. - 157  
Zhu H.W. - 12  
Zhu Jiaqi - 152  
Zhukov S.V. - 59  
Zhurkin A.M. - 175, 187  
Zhurkovich I.K. - 44  
Ziatdinov A.M. - 240  
Zibrov I.P. - 172  
Zinin P.V. - 40, 165

**SOL**  
instruments

## CONFOCAL RAMAN IMAGING

### Confotec® Product Line



Confocal Raman Imaging with  
uncompromising performance in speed, sensitivity & resolution

- True confocal 3D imaging microscope equipped with hardware adjustable pinhole, independent Rayleigh channel
- Diffraction limited lateral and axial resolution (XY: 200 nm, Z: 500 nm)
- Ultra-fast Raman imaging: up to 1000 spectra/sec with EMCCD detection and up to 330,000 points/sec with PMT detection
- Enhanced sensitivity due to ultra-high throughput spectrometer and optimizing optical scheme
- Fully automation. Auto calibration and validation system
- Powerful and user-friendly software "NanoSP"
- Raman polarization measurements
- Ultrafast CARS imaging configuration with ps or fs excitation. Simultaneous detection F-CARS, E-CARS and P-CARS signals
- TERS ready! AFM/SNOM + Raman combination on request



#### GET IN TOUCH

sales@solinstruments.com  
www.solinstruments.com

+ 375 17 290 07 17  
+ 375 17 237 35 58

P.O. Box 235 Minsk 220005  
Minsk, Belarus

25  
years  
Innovation  
& Quality



## **FUND FOR INFRASTRUCTURE AND EDUCATIONAL PROGRAMS**

RUSNANO Group

<http://www.fiop.site>

### **Fund for Infrastructure and Educational Programs (part of RUSNANO Group)**

A non-profit organization that promotes the creation of infrastructure for the Russian nanotechnology industry and is part of the "innovation lift" system of Russian development institutions. The Fund is financed by the Russian federal budget.

#### **The Fund works in seven main areas:**

- (1) Development of technology infrastructure.
- (2) Building human resources for the nanoindustry.
- (3) Development of the market for innovative products.
- (4) Standardization, certification and safety assessment of nanotechnology products.
- (5) Metrological support for the nanoindustry.
- (6) Improvement of legislation in the innovation sphere.
- (7) Popularization of nanotechnologies.

*10a Prospect of the 60th Anniversary of October, Moscow, 117036, Russia,*

*Telephone: +7 (495)988 53 88*

*E-mail: [info@rusnano.com](mailto:info@rusnano.com)*

***[www.fiop.site](http://www.fiop.site)***